Cyclotron production of short-lived radionuclides and labelled compounds for use in biomedical research and clinical diagnosis

John Charles Clark

CYCLOTRON PRODUCTION OF SHORT-LIVED RADIONUCLIDES AND LABELLED COMPOUNDS FOR USE IN BIOMEDICAL RESEARCH AND CLINICAL DIAGNOSIS

John C Clark BSc (Durham)
Submission for the Degree of DSc in the University of Durham 1994.

ABSTRACT

The works submitted in this thesis cover the development of methods for the production in a cyclotron of a variety of radionuclides and their incorporation in radio-labelled compounds for use in biomedical research. In addition, papers are included which describe biomedical applications of such radio-tracers. My co-authorship of these publications reflects my interest in the design and execution of experiments in the realm of interdisciplinary research. The original contributions to science embodied in the publications submitted include examples of novel radiochemistry applied in the areas of cyclotron production of short half-life radionuclides and their radiochemical purification. In many cases the use of these radionuclides in biomedical research has added new information to the body of medical scientific knowledge.

Novel radiolabelling strategies using very short half-life radionuclides are included. These have necessitated the development of rapid radio-organic syntheses, several of which have been achieved using automated microchemical engineering process plants of my design. I have also developed novel systems for the administration of radionuclides and radio-labelled compounds of pharmaceutical quality, widely acknowledged to be "World Firsts." My invention of the $^{81}Kr^{m}$ radionuclide generator resulted in publications covering a wide range of medical applications. These are included with the thesis. The device is now produced in many countries around the world for use both in routine clinical diagnosis and in research, particularly in lung disease. More recently, I have created an automated bedside infuser of $H_2{}^{15}O$, which has revolutionised measurements of regional cerebral blood flow using the technique of Positron Emission Tomography for *in vivo* regional mapping of brain activity.

CYCLOTRON PRODUCTION OF SHORT-LIVED RADIONUCLIDES AND LABELLED COMPOUNDS FOR USE IN BIOMEDICAL RESEARCH AND CLINICAL DIAGNOSIS

in

TWO VOLUMES

VOLUME I

John Charles Clark

Submission for the Degree of DSc

in the University of Durham

1994

TABLE OF CONTENTS

DECLARATION

None of the material included in this thesis has previously been submitted for a degree in either the University of Durham or any other University. My contributions to the joint publications enclosed within this thesis are clearly indicated beside each reference in the list of publications submitted.

STATEMENT OF COPYRIGHT

INTRODUCTION

The publications within these volumes and the appended book represent the development of cyclotron methods for the production of a variety of radionuclides and radio-labelled compounds for use by biomedical researchers to address biological and medical scientific questions with the goal of achieving a better understanding of disease, its diagnosis and and the effect of treatment, in order to develop rational therapies.

In addition publications are included which describe biomedical applications of such radio-tracers. My co-authorship of these publications reflects my profound interest in experimental design and execution in the realm of interdisciplinary research.

ORIGINAL CONTRIBUTIONS TO SCIENCE

The original contributions to science embodied in the publications submitted include examples of novel radiochemistry applied in the areas of cyclotron production of short half-life radionuclides and their radiochemical purification (2, 3, 4, 12, 14, 15, 17, 18, 19, 20, 48, 54). In many cases the use of these radionuclides in biomedical research has led to original contributions to medical scientific knowledge (1, 5, 6, 7, 8, 16, 28, 33, 41, 46, 52, 53, 55, 56, 63, 76, 77).

Novel radiolabelling strategies using very short half-life radionuclides which have necessitated the development of rapid radio-organic syntheses are included (21, 22, 23, 43, 44, 57, 59, 65, 72, 78). Several of these have been

achieved using automated microchemical engineering process plants of my design (57, 65, 72, 78).

I have also developed novel delivery systems for radionuclides and radio-labelled compounds of pharmaceutical quality, widely acknowledged to be "World Firsts." The First is my invention of the $^{81}Kr^{m}$ radionuclide generator (27, 36). A wide range of medical applications of these $^{81}Kr^{m}$ generators are included (9, 10, 13, 30, 31, 35, 37, 38, 39, 40, 42, 47). The device is now produced in many countries around the world for use in routine clinical diagnosis particularly in lung disease. The Second is the automated bedside infusor of $H_2{}^{15}O$ (71, 78).

The availability of the $H_2{}^{15}O$ infuser has revolutionised measurements of regional cerebral blood flow (RCBF) using the technique of Positron Emission Tomography (PET) (63, 76, 77). Many centres around the world are now either commissioning my manufacture of the device or assembling devices to my design.

FORMAT

Refereed Journal publications within these volumes are clearly marked (RJ) in the reference list. Interspersed with these in chronological order are articles which represent contributions to books, reviews and conference proceedings. Published abstracts of scientific presentations have been included where the published input did not of itself justify a full paper, but which formed the basis upon which studies by other groups were founded.

The book "Short-lived Radioactive Gases for Clinical Use" which contains a wealth of information has been in constant demand since it was published in 1975. Although now out of print I continue to receive requests for copies to be released from my now rapidly dwindling stock. It is perhaps timely that a revised edition be prepared.

Some of the publications presented take the form of reviews which have more often than not been commissioned as part of a teaching commitment (32, 34, 45, 40, 67, 68, 73, 78) .

PERSONAL CONTRIBUTION

Most of the publications presented here are the result of multi author endeavours. My contribution to these papers is shown clearly in the reference list. Two figures are given : the first indicates the fraction (percent) of the radiochemistry, for which I personally was responsible, and the second the fraction (percent) for the whole work. In many cases I was the only chemist involved, this my contribution to the radiochemistry is shown as 100%

PERSONAL SCIENTIFIC RESUME

My 3 year undergraduate chemistry studies in Durham were followed by a further year of post graduate studies in the Londonderry Laboratory for Radiochemistry with Graham Martin, then Reader in Radiochemistry. The use of radioisotopes as a tool for medical research became a great attraction to me and I eagerly expanded my skills both in the theory and practice of radiochemistry which quickly led me into an involvement in biological applications of the radiotracer methodology. During the course of my

postgraduate training I was re-acquainted with one of Graham's former PhD students who had recently returned from Brookhaven National Laboratory to join the Medical Research Council team at Hammersmith Hospital. I was intrigued to hear from him the plans at Hammersmith to use a cyclotron to produce radionuclides with short half-lives for use in biomedical research. I was fortunate in being able to join the Hammersmith team myself in 1961. I found the team very receptive to many new concepts I introduced for the use of the cyclotron to produce radionuclides. The opportunities of working with interdisciplinary teams of researchers was mutually rewarding.

The teams include basic scientists and clinical scientists who at Hammersmith particularly have a long established tradition of interdisciplinary research. I found myself working alongside mechanical, electrical and electronic engineers, medical and nuclear physicists, biochemists, pharmacologists, pharmacists, neuroscientists, physiologists and cell biologists in the basic sciences.

In the clinical sciences I work with radiotherapists, radiologists, respirologists, paediatricians, obstetricians and gynaecologists, cardiologists, neurologists, surgeons, endocrinologists, gastroenterologists and psychiatrists.

The publications on the applications of radionuclide tracers will be seen to be co-authored by members of these diverse teams.

EVOLUTION OF THE USE OF RADIONUCLIDES IN BIOMEDICINE

Although the first radionuclides to be used for biomedical research had been made using a cyclotron before the 1939-45 war the advent of the nuclear reactor with its prolific neutron flux enabled the production of many more radiotracers in the post war years. They were for the most part neutron rich radionuclides with half-lives commensurate with the need to be able to ship them from the few accessible reactors to the users. This usually meant that only tracers with half-lives greater than a few days were available. The Medical Research Council foresaw the potential for the re-introduction of the cyclotron for radiotracer production close to the site of use, thus opening up the exciting possibility of using neutron deficient tracers with half-lives of only minutes. This opened up the intriguing possibility of using multiple doses of radiotracer in test and retest biomedical experimental protocols as the tracer could be allowed to decay between measurements. In the early days we made these measurements using discrete fixed external radiation detectors (probes) located close to the organ or region of interest. At the birth of medical imaging using radionuclides, probes were mechanically driven to "scan" the region of interest and the radiation events collected and recorded simultaneously on a two dimensional display. The externally detectable gamma rays were "focused" by the probes either by the use of heavy lead collimators or by exploiting the coincidence detection of positron annihilation radiations (2 x 511 KeV photons with 180° correlation) using opposed pairs of detectors set electronically only to produce a signal where the two photons were detected in time coincidence. As many of the tracers produced with the cyclotron were neutron deficient and decayed by positron (β^+) emission,

positron radionuclide imaging could be exploited in many of the Hammersmith pioneering biomedical studies.

The use of simple chemical forms of the positron emitting tracers eg $^{15}O_2$ was soon expanded to the radiolabelling of much more complex molecules with Carbon-11 (half life 20 mins) and fluorine-18 (half life 110 mins) which in many cases involved the design and execution of rapid organic radiosyntheses and purifications to achieve the desired goal of radiolabelled metabolic substrates such as ^{11}C-glucose, pharmaceuticals such as ^{11}C-methylspiperone and related compounds such as ^{18}F-fluoro amino acids and ^{18}F labelled chlorofluorocarbon propellants for drug inhalers.

The ability to exploit positron emitting radiotracers was revolutionised with the advent of Positron Emission Tomography (PET) imaging systems. These systems still exploit the coincidence detection technique referred to above but due to the large number of detectors employed (typically around 2500 pairs) large data sets of coincident events can be collected. Using computer reconstruction algorithms these data can be processed for display as quantitative functional images of living subjects in cross section sometimes referred to as *in vivo* autoradiographs. The pioneering work by teams at Hammersmith, in bringing together these new exciting concepts, has contributed to a world wide expansion of specialist PET centres which employ a small cyclotron and PET scanners to apply these techniques to a wide variety of research studies and clinical diagnostic tests.

ACKNOWLEDGEMENTS

Several hundred of my colleagues have played a part in bringing many of these works to fruition. To name them individually would be a daunting task. There are however a few key individuals who were highly supportive in the endeavours reported in these volumes. I hope all will become aware of my gratitude to them as I come to the point of submitting these works for consideration for the degree of DSc.

Of the few I would like to thank Mr D D Vonberg CBE, the Director of the Cyclotron Unit throughout most of the period covered in these volumes and Dr D J Silvester and Dr T Jones, my close scientific colleagues and friends who have challenged and supported me through thick and thin. I would also like to convey my sincere thanks to my two research assistants and sometimes co-authors Mr P D Buckingham and the late Mr P L Horlock whose enthusiasm and skills so often contributed to steering a productive course.

Finally I would like to acknowledge the untiring support of Dr Hazel A Jones, my partner sometimes co-author and mother of our two boys, for providing me with continuing education in biomedicine and for her moral support.

Finally I would like to acknowledge the University of Durham for my undergraduate and post graduate training which prepared me well for the years of exciting and productive scientific endeavours culminating in the reports in these volumes.

International Links

An integral part of my commitment to science has always been my eagerness to collaborate with scientists internationally and in some of the submitted works my international co-authors will be found as follows:

Mr Roman	Bucharest Romania	(21, 23)
F Skrabal	Innsbruck Austria	(8, 11)
F Fazio	Pisa, Italy	(25)
R D Finn et al	Miami, USA	(31, 45, 48)
G L Lenzi	Sierra, Italy	(28, 33)
P Buranapong	Bangkok, Thailand	(39)
H A O'Brien et al	Los Alamos Nat. Lab. USA	(47, 49, 53)
F Oberdorfer	Heidelberg, Germany	(51)
R E Forster	Philadelphia USA	(52)
I Kanno	Akita, Japan	
H Tochon-Danguy	Geneva, Switzerland and Melbourne, Australia	(63, 71)
J Link	Seattle, USA	(73)
T Ruth	Vancouver, Canada	(73)
D A Silbersweig & E Stern	New York, USA	
J-L Morelle	Louvain la Neuve, Belgium	
G Firnau	Hamilton, Canada	(59)

In addition I have had continuous commitment to an EEC initiative for PET chemistry which can be found in refs. 61, 64, 74, 75.

PUBLICATIONS SUBMITTED

			% of Chemistry	% of Total
1.	Matthews CME., Dollery CT., Clark JC and West JB., Radioactive gases. Radioactive Pharmaceuticals: ed Andrews WS., RM Kinsley and HN Wagner. U.S.A.E.C. Division of Technical Information, Oak Ridge, Tennessee., 1966. pp. 567-592.		100	20
2.	**Clark JC., Glass HI and Silvester DJ. In vitro labelling of red cells with carbon-11. Proc 2nd Int Conf. on methods of preparing and storing labelled compounds., Brussels, 1966: pp 603-609.**		**70**	**30**
3.	**Clark JC and Silvester DJ. A cyclotron method for the production of fluorine-18. Int J Appl Radiat Isotopes., 1966: 17: 151-154**	RJ	**70**	**70**
4.	**Clark JC., Matthews CME., Silvester DJ and Vonberg DD. Using cyclotron-produced isotopes at Hammersmith Hospital., Nucleonics. 1967: 25: 54.**	RJ	**50**	**30**
5.	Glass HI., Brant A., Clark JC., De Garreta AC and Day LG. Measurement of blood volume using red cells labelled with radioactive carbon monoxide. J Nucl Med., 1968: 9: 571-575	RJ	100	20
6.	Glass HI., Jacoby J., Westerman B., Clark JC., Arnott RN and Dixon HG. Placental localisation by inhalation of radioactive carbon monoxide. J Nucl Med., 1968: 9: 468-470	RJ	100	15
7.	Glass HI., Edwards RHT., de Gareta AC and Clark JC. ^{11}CO red cell labelling for blood volume and total haemoglobin in athletes: effect of training. J Appl Physiol., 1969: 26: 131-134.	RJ	100	20
8.	Skrabal F., Glass HI., Clark JC., Jeyasingh K and Joplin GF. A simplified method for simultaneous electrolyte studies in man utilising potassium-43. Int J Appl Radiat Isotopes., 1969: 20: 677-681	RJ	100	20
9.	Clark JC., Jones T and Mackintosh A. 81mKr an ultra short lived inert gas tracer for lung ventilation and perfusion studies with the scintillation camera. Radioaktive Isotope in Klinik und Forschung: 9th Int Symposium: Bad Gastein, 1979. Ed. F Fellinger and R Höfer. Munich, Urban & Schwarzenberg., 1970: 9: 444-450.		100	40

10.	Arnot RN., Glass HI., Clark JC., Davies JA., Schiff D and Picton-Warlow CG. Methods of measurement of cerebral blood flow in the newborn infant using cyclotron produced isotopes. Radioactive Isotope in Klinik und Forschung. 9th Int Symposium. Gad Bastein, 1979. Ed K Fellinger and R Höfer, Munich, Urban & Schwarzenberg., 1970: 9: 60-74.		100	25
11.	Skrabal F., Arnot RN., Clark JC., Helus F., Glass HI., Joplin GF. Electrolyte and body fluid investigations in endocrine diseases using Cyclotron produced Isotopes. Radioaktive Isotope in Klinik und Forschung: 9th Int Symposium Bad Gastein 1970. Ed K Fellinger and R Höfer: 1970: 9: 76 - 83.		50	25
12.	**Vonberg DD., Baker LC., Buckingham PD., Clark JC., Finding K., Sharp J and Silvester DJ. Target systems for radioisotope production on the Medical Research Council cyclotron. The uses of cyclotrons in chemistry, metallurgy and biology: Proc of a Conference, Oxford 1969. Ed. C B Amphlett. London: Butterworths, 1970. 258-269.**		**60**	**20**
13.	Jones T and Clark JC. , Hughes JMB and Rosenzweig DY. ^{81m}Kr generator and its uses in cardiopulmonary studies with the scintillation camera. J Nucl Med., 1970: 11: 118-124		100	30
14.	**Jones T., Clark JC., Kocak N., Cox AG and Glass HI. Measurement of gastric emptying using the scintillation camera and ^{129}Cs. Brit J Radiol., 1970: 43: 537-541.**	**RJ**	**100**	**25**
15.	**Thakur ML., Clark JC and Silvester DJ., The production of ^{117}Sb labelled potassium antimonyl tartrate for medical use. Int J Appl Radiat Isotopes., 1970: 21: 33-36.**	**RJ**	**30**	**30**
16.	Galasko CSB., Coombs RRH and Clark JC. The use of carbon-11 dioxide for skeletal scintigraphy. Brit J Radiol., 1970: 43: 670-1.		100	40
17.	**Clark JC and Buckingham PD. The preparation of carbon-11 labelled carbon monoxide and carbon dioxide. Radiochem Radioanal., Letters: 1971: 6: 281-286.**	**RJ**	**100**	**50**

18.	Clark JC and Buckingham PD. The preparation and storage of carbon-11 labelled gases for clinical use. Int J Appl Radiat Isotopes., 1971: 22: 639-646.	RJ	100	50
19.	Buckingham PD and Clark JC. Nitrogen-13 solutions for research studies in pulmonary physiology. Int J Appl Radiat Isotopes., 1972: 23: 5-8.	RJ	100	50
20.	Clark JC., Thakur ML and Watson IA. The production of potassium-43 for medical use. Int J Appl Radiat Isotopes., 1972: 23: 229-335.	RJ	50	30
21.	Palmer AJ., Clark JC.,Goulding RW and Roman M. Preparation of ^{18}F labelled DL-3-Fluorotyrosine labelled radiopharmaceuticals. Proc of Symposium on Radiopharmaceuticals and Labelled Compounds. Copenhagen, 1973. Vienna, I.A.E.A. ST1/PUB/344: Vol 1, pp 291-302.		30	30
22.	Clark JC., Goulding RW and Palmer AJ. Preparation of ^{18}F-labelled fluorocarbons for use in pharmacodynamic studies. Proc of Symposium on Radiopharmaceuticals and Labelled Compounds. Copenhagen, 1973. Vienna, I.A.E.A. ST1/PUB/344: Vol 1, pp 411-421.		50	40
23.	Clark JC., Goulding RW., Roman M and Palmer AJ. The preparation of fluorine-18 labelled compounds using a recirculatory neon target. Radiochem Radioanal. Letters. 1973: 14: 101-108.	RJ	50	40
24.	Williams FM., Draffan GH., Dollery CT., Clark JC., Palmer AJ and Vernon P. Use of 18F-labelled fluorocarbon-11 to investigate the fate of inhaled fluorocarbons in man and in the rat. Thorax., 1974: 29: 99-103.	RJ	70	20
25.	Fazio F., Clark JC., Buckingham PD., Rhodes CG., Hudson FR., Jones HA., Jones T and Hughes JMB. An external counting method for regional measurements of extravascular lung water. Prog Resp Res., 1975: 9: 249-253.	RJ	100	15
26.	Clark JC and Buckingham PD: Short-lived Radioactive Gases for Clinical Use. Butterworth 1975: ISBN 0 407 39770 1	Book	100	50

26a	Clark JC and Buckingham PD: Short-lived Radioactive Gases for Clinical Use. Butterworth 1975: Review by N Trott Medical and Biological Engineering, Nov. p. 763. 1975			
26b	Clark JC and Buckingham PD: Short-lived Radioactive Gases for Clinical Use. Butterworth 1975: Review by D M Ackery. Brit J of Radiol: 49: No. 578: p 160. 1976.			
26c	Clark JC and Buckingham PD: Short-lived Radioactive Gases for Clinical Use. Butterworth 1975: Review by N Veall. Physics in Med. and Biol. Vol 20: No.6 p 1038 1975.			
26d	Clark JC and Buckingham PD: Short-lived Radioactive Gases for Clinical Use. Butterworth 1975: Review by Y Murakami Atomic Power Industry in Japan Vol: 21. No.11 p8 1975 (in Japanese)			
27.	**Clark JC., Horlock PL and Watson IA. Krypton-81m Generators. 1976: Radiochem Radioanal Lett: 25 245-254.**	**RJ**	**80**	**30**
28.	Jones T., McKenzie CG., Moss S., Buckingham PD and Clark JC. The non-invasive use of oxygen-15 for studying regional brain function in patients with cerebral tumours. 12th Int Symp on Radioactive Isotopes in Clinical Medicine and Research. Bad Gastein, 1976. pp 517-523.		100	20
29.	Clark JC. The Medical Research Cyclotron at Hammersmith Hospital: A status report 1976: Prog nucl Med: Vol 4: 140-145 (Karger, Basel).			
30.	Amis TC., Giofetta G., Clark JC., Hughes JMB., Jones HA and Pratt TA. Effect of posture on distribution of pulmonary ventilation and perfusion studied with $^{81}Kr^{m}$ and $^{85}Kr^{m}$. Proc Physiological Society. 1977: 81-2.	Abstract	100	20

31.	Kenny PJ., Watson DD., Clark JC., Finn RD and Gilson AJ. Pulmonary ventilation and perfusion measurements using $^{81}Kr^{m}$; basic methodology. J Nucl Med., 1977: 18: 626.	Abstract	100	20
32.	Palmer AJ., Clark JC and Goulding RW. The preparation of fluorine-18 Labelled Radiopharmaceuticals. Int J Appl Radiat Isotopes., 1977: 28: 53-65.	RJ	30	30
33.	Lenzi GL., Jones T., McKenzie CG., Buckingham PD., Clark JC and Moss S. Study of regional cerebral metabolism and blood flow relationships in man using the method of continuously inhaling oxygen-15 and oxygen-15 labelled carbon dioxide. J Neurology, Neurosurgery and Psychiatry., 1978: 41: 1-10.	RJ	100	20
34.	Clark JC. "Radioactive gases of short half-life for Brain, Heart and Lung Studies". Radiochemistry in Medicine. Proc Analyt Div Chem Soc., Oct 1978: 287-9.	Teaching		
35.	Selwyn AP., Jones T., Turner JH., Clark JC and Lavender JP., Continuous assessment of regional myocardial perfusion in dogs using $^{81}Kr^{m}$. Circulation Research., 1978: Vol 42: No.6: 771-777.	RJ	100	15
36.	**Clark JC., Horlock PL and Watson IA. Krypton-81m generators for ventilation and perfusion. Brit Institute of Radiology. 1978: Special report No. 15. Experimental and Clinical Applications of Krypton-81m. p 7-15. Proc meeting held at Hammersmith Hospital, June 1977.**		80	30
37.	Jones T., Clark JC., Rhodes CG., Heather J and Tofts P. Combined use of Krypton-81m and 85m in ventilation studies. Brit J Radiol., Special Report No. 15. 1978: 46-51.		100	20
38.	Amis TC., Ciofetta G., Clark JC., Hughes JMB., Jones HA and Pratt TA. Use of Krypton-81m and 85m for measurement of ventilation and perfusion distribution within the lungs. Brit J Radiol., Special Report No. 15, 1978. 52-59.		100	20

39.	Arnot RN., Sykes MK., Clark JC., Herring AN., Chakrabarti MK and Buxanapong P. Measurement of total lung ventilation in anaesthetized dogs using Kryton 81m and Nitrogen-13. Brit J Radiol. Special Report No. 15, 1978. 69-79		100	20
40.	Selwyn AP., Steiner RE., Clark JC., Raphael MJ and Forse G. Clinical applications of krypton-81m in the assessment of regional myocardial perfusion. Brit J Radiol. Special Report No. 15. 1978. 171-175.		100	15
41.	Segal AW., Clark JC and Allison AC. Tracing the fate of oxygen consumed during phagocytosis by human neutrophils with $^{15}O_2$. Clinical Science and Molecular Medicine., 1978: 55: 413-415.	RJ	40	30
42.	Selwyn AP., Welman E., Pratt TA., Clark JC., MacArthur C and Lavender JP. The interpretation of thallium-201 sentigrams: studies in experimental ischaemic heart disease. Circulation Research., 1978: 43: 287-293.	RJ	100	20
43.	**Goulding RW and Clark JC. ^{18}F-L and DL-Fluoraryl amino acids. Present status. J Labelled Compounds and Radiopharmaceuticals., 1979: 16: 145-147**		50	50
44.	**Palmer AJ., Clark JC., Horlock PL and Buckingham PD. Incorporation of fluorine-18 into perhalo compounds using the ^{20}Ne (d,α)^{18}F reaction. J Labelled Compounds and Radiopharmaceuticals 1979: 16: 150-151**		30	20
45.	Clark JC. "Accelerators for radionuclide production" in Nuclear Cross Sections for Technology. National Bureau of Standards (US) Special Publication 594. Eds Fowler JL & Johnson CH. 1980: 458-463.		Teaching Review	
46.	Ginsberg MD., Lockwood AH, Busto R., Finn RD., and Clark JC. Measurement of Regional cerebral blood flow (rCBF) by PositronEmissionTomography using ^{15}O-water: validation of an in vivo autoradiographic paradigm. American Academy of Neurology, Annual Meeting (1980)		70 Abstract	20

47.	Arnot RN., Clark JC., Herring AN., Chakrabarti MK and Sykes MK. Measurements of regional ventilation using nitrogen-13 and krypton-81m in mechanically ventilated dogs. Clin Phys Physiol Meas., 1981: 2: 183-196.	RJ	100	20
48.	**Horlock PL., Clark JC., Goodier IW., Barnes JW., Bentley GE., Grant PM and O'Brien HA. The preparation of a rubidium-82 radionuclide generator. J Radioanalytical Chemistry., 1981: 64: 257-265.**	**RJ**	**15**	**15**
49.	Finn R., Vora M., Boothe T., Campbell J., Carroll S and Clark J. Radiation-induced defects as illustrated by the 81Rb-81Krm target system. Int J Appl Radiat Isotopes., 1982: 33: 349-353.	RJ	50	15
50.	Selwyn AP., Allan RM., L'Abbate A., Horlock PL., Camici P., Clark JC., O'Brien HA and Grant P. Relation between regional myocardial uptake of rubidium-82 and perfusion: absolute reduction of cation uptake in ischaemia. Am J Cardiol., 1982: 50: 112-121.	RJ	20	20
51.	Clark JC and Oberdorfer F. Thermal characteristics of the release of fluorine-18 from an inconel-600 gas target. J Labelled Compounds and Radiopharmaceuticals., 1982: 19: 1337-1339.		50	50
52.	Jones HA., Clark JC., Davies EE., Forster RE and Hughes JMB. Rate of uptake of carbon monoxide at different inspired concentrations. J Appl Physiol., 1982: 52 (1): 109-113.	RJ	70	20
53.	Jones HA., Stradling JR., Clark JC., Davies EE and Rozkovec A. Quantitative measurement of intrapulmonary and extrapulmonary right-to-left shunt. J Appl Physiol., 1983: 54: 1434-1438.	RJ	72	20
54.	**Waters SL., Butler KR., Clark JC., Horlock PL., Kensett MJ., Goodier IW., Makepeace J., Smith D., Woods MJ., Barnes JW., Bentley GE., Grant PM and O'Brien HA. Radioassay problems associated with the clinical use of Rb-82 radionuclide generator. Int J Nucl Med Biol., 1983: 10: 2/3, 69-74.**	**RJ**	**10**	**10**
55.	Kanno I., Lammertsma AA., Heather JD., Gibbs JM., Rhodes CG., Clark JC and Jones T. Measurement of cerebral blood flow using bolus inhalation of $C^{15}O_2$ and Positron Emission Tomography : Description of the	RJ	70	10

Method and its Comparison with the $C^{15}O_2$ Continuous Inhalation Method. J Cerebral Blood Flow and Metabolism., 1984: 4: 224-234.

56. Spinks TJ., Bateman JE., Flesher AC., Clark JC., Hopkins NFG and Jones T. Blood flow in the feet of diabetic patients measured with a MWPC positron camera and inhalation of $C^{15}O_2$. Phys Med Biol., 1984: 29: 873-879. RJ 100 30

57. Pike VW., Horlock PL., Brown C and Clark JC. The remotely-controlled preparation of a ^{11}C-labelled radiopharmaceutical - [1-^{11}C]Acetate. Int J Appl Radiat Isotopes. 1984: 35: 623-627. **RJ 30 25**

58. Herold S., Leenders KL., Turton DR., Kensett MJ., Pike VW., Clark JC., Brooks DJ., Crow TJ., Owen F., Cooper S., Johnstone EC. Dopamine receptor binding in Schizophrenic patients as measured with ^{11}C methyl-spiperone and PET. J Cerebral Blood Flow and Metabolism. 1985. Vol: 5: Suppl 1. S191-2 10 Abstract 10

59. Leenders KL., Palmer AJ., Quinn N., Clark JC., Firnau G., Garnett ES., Nahmias C., Jones T and Marsden CD. Brain dopamine metabolism in patients with Parkinson's Disease measured with positron emission tomography. J Neurology, Neurosurgery, Psychiatry., 1986: 49: 853-860. **RJ 10 10**

60. Clark JC. Positrons from generators. 67-84 In: Progress in Radiotherapy. Eds Cox PM et al. Martinus Nijhoff, Netherlands, 1986. Teaching Review

61. Clark, JC., Crouzel C., Meyer GJ and Strijckmans K. Current Methodology for Oxygen-15 production for Clinical Use., Appl Radiat Isot: 38.8 1987: 597-600. RJ 30 25

62. Jones AJ., Rhodes CG., Law MNP., Becket JM., Clark JC., Boobis AR., and Taylor GW. Rapid analysis for metabolites of 11C-labelled drugs: fate of [11C]-S-4-(tert-butylamino-2-hydroxypropoxy)- benzimidazol-2-one in the dog. J. Chromatography., 1991: 570, 361-370. RJ 10 20

63. Colebatch JG., Adams L., Murphy K., Martin AJ., Lammertsma AA., Tochon-Danguy HJ., Clark JC., KJ Friston and Guz A. Regional Cerebral Blood Flow during Volitional Breathing in Man. J Physiology., 1991: 443, 91-103. RJ 50 15

64.	Guillaume M., Luxen A., Nebeling B., Argentini M., Clark JC and Pike VW. Recommendations for fluorine-18 production. Appl Radiat Isot., 42.8: 1991: 749-762.	RJ	20	20
65.	**Brady F., Luthra SK., Tochon-Danguy HJ., Steel CJ., Waters WL., Kensett MJ., Landais P., Shah F., Jaeggi KA., Drake A., Clark JC and Pike VW. Assymetric synthesis of a precursor for the automated radiosynthesis of S-(3'-t-Butylamino-2'- hydroxypropoxy)-benzimidazol-2-[^{11}C] one (S-[^{11}]CGP 12177) as a preferred radioligand for β -Adrenergic Receptors. Appl Radiat Isot., 1991: 42.7: 621-628.**	**RJ**	**10**	**10**
66.	Ranicar ASO., Williams CW., Schnorr L., Clark JC., Rhodes CG., Bloomfield PM and Jones T. The on-line monitoring of continuously withdrawn arterial blood during PET studies using a single BGO/ photomultiplier assembly and non-stick tubing. Medical Progress through Technology: 1991: 17: 259-264, 1991.	RJ		25
67.	Clark JC. Production and Application of Oxygen-15. Radiopharmacy aspects. Progress in Radiopharmacy (1992) 91-107: Eds Schubiger PA and Westera G. Kulwer Academic Publishers.	Teaching		100
68.	Clark JC. (1992) Production of Radiopharmaceuticals for PET. Proceedings of the 1992 Advanced School on Medical Physics. Physica Medica Vol 13: Suppl 1: 1992: 43-47.	Teaching		100
69	Clark JC. Morelle J-L. An Oxygen-15 Generator: Early Experience with the IBA Cyclone-3 Proceedings of the IVth International Workshop on Targetry and Target Chemistry: PSI-Proceedings ISSN 1019-6447. August 1992. pp 34-35. Ed Regin Weinreich. Paul Scherrer Institut, 1992.		50	50
70.	Clark JC. Status report from Hammersmith. Proceedings of the IVth International Workshop on Targetry and Target Chemistry: PSI-Proceedings ISSN 1019-6447. pp 237-241. Ed Regin Weinreich. Paul Scherrer Institut, 1992.	Status report		
71.	Clark JC and Tochon-Danguy H., "R2D2", A Bedside [Oxygen-15] Water Infuser. Proceedings of the IVth International Workshop on Targetry and Target Chemistry:		70	70

PSI-Proceedings ISSN 1019-6447. pp 234-235.
Ed Regin Weinreich. Paul Scherrer Institut, 1992.

72 Clark JC and Dowsett K. Automated Carbon-11 Radiopharmaceutical Production.
Proceedings of the IVth International Workshop on Targetry and Target Chemistry:
PSI-Proceedings ISSN 1019-6447. pp 207-209.
Ed Regin Weinreich. Paul Scherrer Institut, 1992.
70 50

73. Link JM., Clark JC and Ruth TJ., Introduction: State of the Art in Automated Syntheses of Short-Lived Radiopharmaceuticals.
Proceedings of the IVth International Workshop on Targetry and Target Chemistry:
PSI-Proceedings ISSN 1019-6447. pp pp 174-185.
Ed Regin Weinreich. Paul Scherrer Institut, 1992.
40 Chair persons Review 40

74. Qaim SM., Clark JCC., Crouzel C., Guillaume M, Helmeke HJ., Nebeling B., Pike VW and Stöcklin G. PET radionuclide production. Radiopharmaceuticals for Positron Emission Tomography - Methodologica l Aspects. Kluwer Academic Publs. 1993. pp 1 - 44.
EEC Chapter

75. Crouzel C., Clark JC., Brihaye C., Langstrom B., Lemaire C., Meyer G-J., Nebeling B and Stone-Elander S.
Radiochemistry automation for PET.
Radiopharmaceuticals for Positron Emission Tomography - Methodological Aspects.
Kluwer Academic Publs. 1993: pp 45 - 90.
EEC Chapter

76. Ramsay S C., Murphy K., Shea SA., Friston KJ., Lammertsma AA., Clark JC., Adams L., Guz A and Frackowiak RSJ. Changes in global cerebral blood flow in humans: Effect on regional cerebral blood flow during a neural activation task.
J of Physiology 1993: 471: pp 521-534
RJ 100 20

77. Silbersweig DA., Stern E., Frith CD., Cahill C., Schnorr L., Grootoonk S., Spinks T., Clark JC., Frackowiak RSJ and Jones T.
Detection of Thirty-Second Cognitive Activations in single subjects with positron emission tomography: A new low-dose $H_2{}^{15}O$ regional cerebral blood flow three-dimensional imaging technique.
J Cerebral Blood Flow and Metabolism 1993:
13: pp 617-629.
RJ 100 20

78. Clark JC. The Hammersmith Philosophy for PET Chemistry Automation to be published in American Chemical Society monograph 1994. "Chemist views of Imaging Centers" Symposium held at ACS fall meeting Chicago, August 1993. Teaching

Chapter 31

RADIOACTIVE GASES

C. M. E. MATTHEWS, Ph. D., B.A., B. Sc.; C. T. DOLLERY, M.B., B. Sc., M.R.C.P.; J. C. CLARK, B. Sc.; and J. B. WEST, M.D., Ph. D.
Medical Research Council, Cyclotron Unit, and Department of Medicine, Postgraduate Medical School, Hammersmith Hospital, London, England

ABSTRACT

The following radioactive gases can be produced by the Medical Research Council cyclotron at Hammersmith Hospital: $^{15}O_2$, $C^{15}O_2$, $C^{15}O$, $^{11}CO_2$, ^{11}CO, and $^{13}N_2$. Oxygen-15, ^{11}C, and ^{13}N are all pure positron emitters with very short half-lives. They have been used for studies of lung function and of body CO_2 stores. Reactor-produced ^{133}Xe is also used.

For lung-function studies, the radioactivity in a region of lung is measured with external scintillation counters. The measured counting rate depends on radioactivity in both alveolar air and blood. For many gases the slope of this counting-rate curve is a complex function of alveolar clearance and blood clearance of the radioactive gas. Alveolar clearance is limited by blood flow and solubility for most of the gases, but for labeled carbon monoxide it is probably limited by diffusion. It is unfortunately not possible at present to obtain an accurate measure of diffusion with this gas. The uptake of $C^{15}O_2$ into the blood is very rapid because it exchanges with the water space, through the equilibrium with carbonic acid. It can be used to measure regional blood flow and to detect cardiac shunts. $^{11}CO_2$ exchanges rapidly with an extracellular CO_2 pool. $^{13}N_2$ is much less soluble than ^{133}Xe, and so it is more suitable for measurement of ventilation and lung volume.

This paper is a review of some of the work done with the radioactive gases at the Medical Research Council Cyclotron Unit at Hammersmith Hospital by many different people, involving collaboration among clinicians, physiologists, physicists, chemists, engineers, and technicians. Radioactive gases provide a method for studying regional lung function which gives information that cannot be obtained in other

ways. Oxygen-15 is the only practical radioactive isotope of oxygen, and ^{11}C is the only available isotope of carbon emitting gamma rays. These isotopes offer possibilities for studies of metabolism that have not yet been fully explored. Owing to their short half-lives of 2 min for ^{15}O and 20 min for ^{11}C, they can only be used close to the cyclotron.

The first radioactive gas to be used for lung-function studies was reactor-produced ^{133}Xe, introduced by Knipping[1] in 1957; $^{15}O_2$ was first used in biological investigation by Ter-Pogossian and Powers[2] in 1958. The use of ^{15}O for lung-function studies was developed by Dyson et al.[3]; this isotope was produced by bombardment of nitrogen with deuterons from the Medical Research Council cyclotron. Initially, the isotope was used as molecular oxygen, and, since ^{15}O emits positrons in 100% of its disintegrations, coincidence counting can be used. Later ^{11}C was also produced; this is also a pure positron emitter.

At present the following radioactive gases are available from the Medical Research Council cyclotron: ^{15}O-labeled molecular oxygen, carbon dioxide, and carbon monoxide; ^{11}C-labeled carbon dioxide and carbon monoxide; and $^{13}N_2$. Reactor-produced ^{133}Xe is also used extensively for the measurement of regional ventilation and blood flow. The use of this gas was developed by Bates and coworkers.[4]

Although ^{133}Xe is more convenient in some ways owing to its longer half-life of 5.3 days and the lower energy (80 and 30 kev) of the gamma and X rays emitted, it has disadvantages that will be discussed.

The cyclotron-produced radioactive gases that are most used at present are $C^{15}O_2$ for detection of cardiac shunts and $^{11}CO_2$ for studies of body CO_2 stores. It is planned to use $^{13}N_2$, another pure positron emitter, for the measurement of regional ventilation and blood flow in the future.

PRODUCTION METHODS

The production of radioactive gases is fully described by Buckingham and Forse[5] and will only be briefly outlined here.

Oxygen-15 is produced by bombardment of nitrogen with 4-Mev deuterons from the reaction $^{14}N(d,n)^{15}O$. The target box has a 1-mm-thick magnesium window that reduces the energy of the 15-Mev deuterons and at the same time produces ^{22}Na from the reaction $^{24}Mg(d,\alpha)^{22}Na$. The yield of ^{15}O increases by only 50% if the deuteron energy is increased from 4 to 15 Mev, and the proportion of other isotopes produced, ^{11}C and ^{13}N, is much greater at the higher energy.

The flow system for molecular $^{15}O_2$ is shown at the top of Fig. 1. Four percent oxygen carrier in nitrogen is dried by passing it through silica gel absorbers, and then it passes through the target box. More absorbers then remove water, ozone, and oxides of nitrogen. The

primary gas is diluted about 10 times with air to give the required concentration of radioactivity, which is measured by passing the gas through a half-liter glass bulb in an ionization chamber.

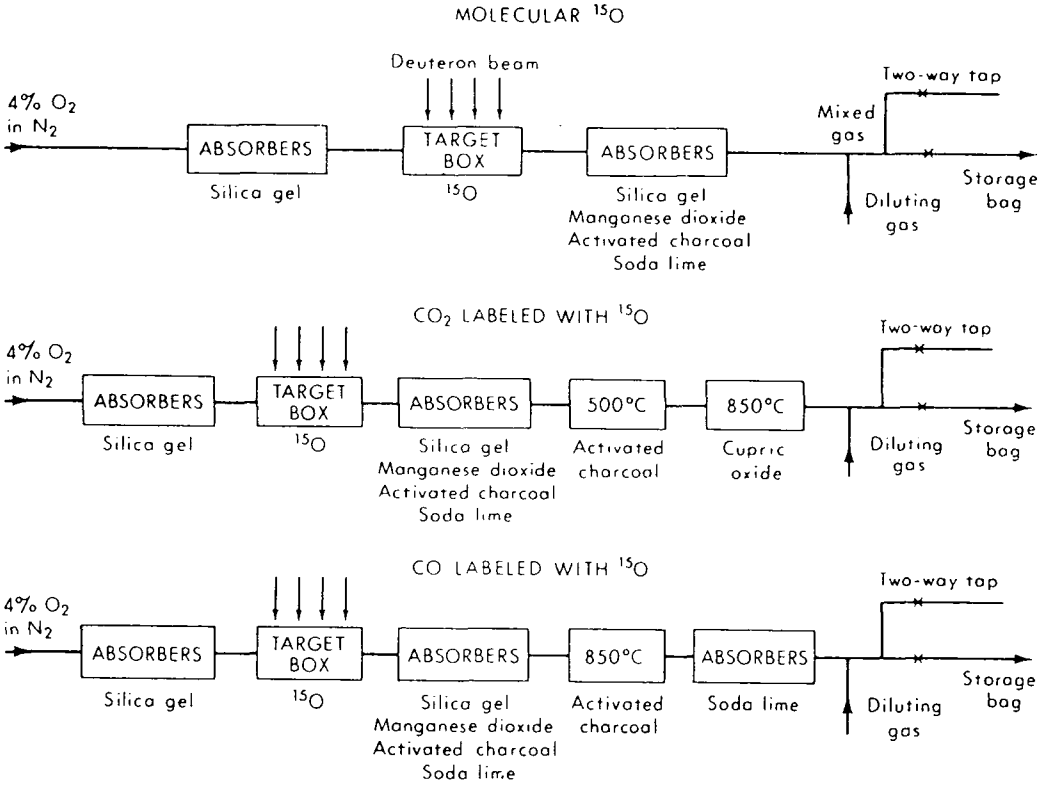

Fig. 1—Flow system for production of gases labeled with ^{15}O.

When carbon dioxide labeled with ^{15}O is required, the gas from the target box, after being passed through the usual absorbers, is passed over activated charcoal at 500°C to convert oxygen to carbon dioxide plus some carbon monoxide (Fig.1). The carbon monoxide is then oxidized to carbon dioxide by passing it over cupric oxide at 850°C.

For ^{15}O-labeled carbon monoxide, activated charcoal at 850°C converts most of the oxygen to carbon monoxide with some carbon dioxide, which is absorbed by soda lime (Fig. 1).

Carbon-11 is produced by bombarding boron with 15-Mev deuterons. The reactions are $^{10}B(d,n)^{11}C$ and $^{11}B(d,2n)^{11}C$. The target consists of boric oxide, which is kept molten in the beam. Five percent carbon monoxide or carbon dioxide carrier gas in argon passes through silica gel absorbers into the target box (Fig. 2). Both ^{11}CO and $^{11}CO_2$ are formed in the target box. If ^{11}C-labeled carbon monoxide (^{11}CO) is required, the $^{11}CO_2$ is absorbed in soda lime. If ^{11}C-labeled carbon dioxide ($^{11}CO_2$) is required, the ^{11}CO is oxidized by cupric oxide at 850°C (Fig. 2). Recently we changed the primary gas for CO_2 produc-

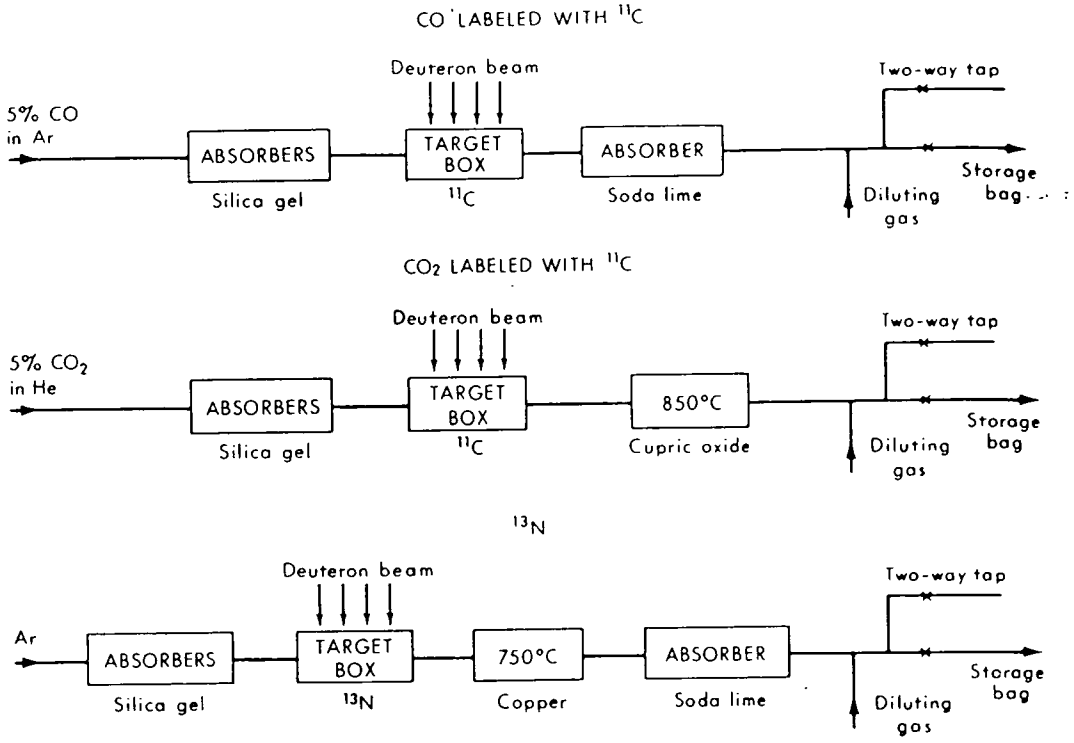

Fig. 2—Flow system for production of gases labeled with ^{11}C and ^{13}N.

tion to 5% CO_2 in helium instead of in argon since this eliminates the ^{41}Ar contaminant.

Nitrogen-13 is produced by bombarding carbon with 15-Mev deuterons by the reaction $^{12}C(d,n)^{13}N$. Argon has been used as the primary gas (Fig. 2). The target box contains coarsely granulated activated charcoal retained by graphite rods. These rods replace the stainless-steel mesh used previously since they do not melt or become so radioactive.

The flow of gas through the different furnaces and absorbers is controlled from the clinical-investigation room by remotely operated valves. The furnaces and absorbers are situated in a concrete hut outside the building, considerably reducing the dose to the operator.

A new method of producing ^{13}N is being developed so that solutions of the gas can be obtained in very high concentrations of radioactivity required for measurement of blood flow with $^{13}N_2$. The advantages of $^{13}N_2$ compared with ^{133}Xe are due to the much lower solubility of $^{13}N_2$.

The small-volume closed-circuit system shown in Fig. 3 is filled with methane. The $^{13}N_2$ concentration is allowed to build up for a few minutes; then the methane is displaced from the closed circuit through a copper oxide furnace at 800°C, converting the methane to carbon dioxide. The dose rate at the outlet of the furnace is monitored with a cadmium sulfide photoconductive cell,[6] and the CO_2 containing $^{13}N_2$ is collected in a syringe. Saline is then injected into the syringe and

shaken vigorously under compression. The carbon dioxide dissolves rapidly and thus increases the partial pressure of the $^{13}N_2$ in the remaining bubble and drives it into solution.

With this method activity levels of 500 μc per 10 ml of saline have been achieved.

It is hoped to obtain a much higher concentration of radioactivity by using pure hydrogen as a carrier gas and converting it to water vapor by suitable oxidation. A system similar to that shown in Fig. 4 is under development. The water vapor containing $^{13}N_2$ is collected in a syringe containing saline. The partial pressure of the $^{13}N_2$ should be very high if all permanent gases are excluded from the system.

Xenon-133 is obtained from the Radiochemical Centre, Amersham, in a glass tonometer connected to a mercury reservoir for dispensing. The whole tonometer and associated taps are enclosed in a gastight lead-covered steel box with a lead-glass front. Batches of about 700 mc are usually obtained.

YIELDS

Typical yields for a primary gas flow of 0.4 liter/min at a 30-μa deuteron beam current are 100 mc/liter for $^{15}O_2$, 16 mc/liter for $C^{15}O$, and 19 mc/liter for $C^{15}O_2$, all after dilution to 3 liters/min total flow. Yields of the ^{11}C-labeled gases and of $^{13}N_2$ are 10 mc/liter for

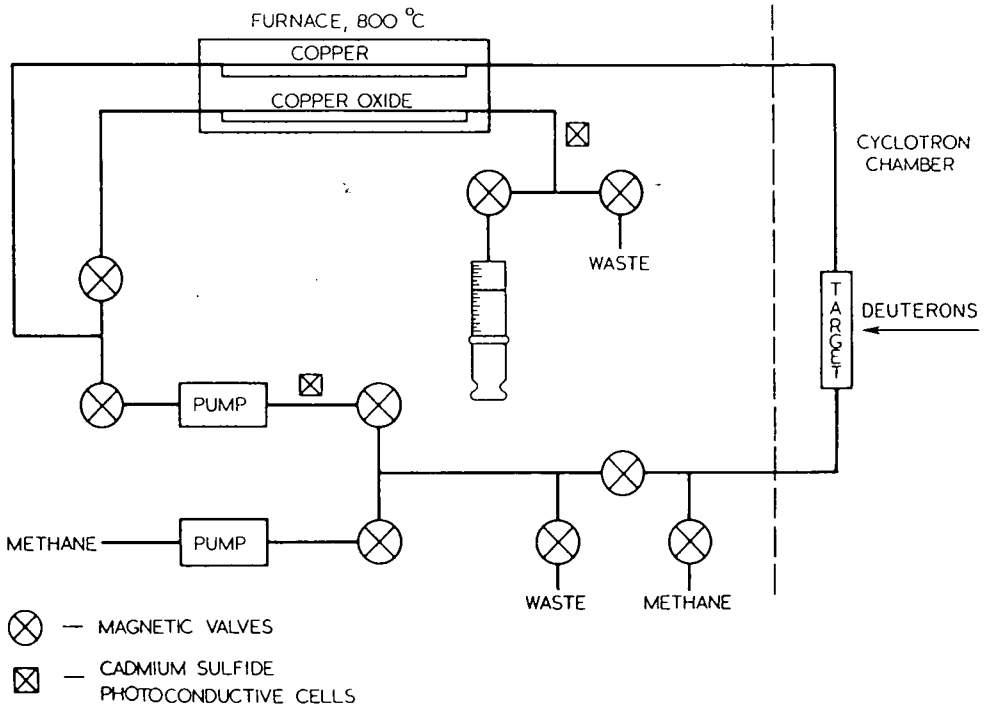

Fig. 3—Flow system for production of $^{13}N_2$ solutions using methane flow gas.

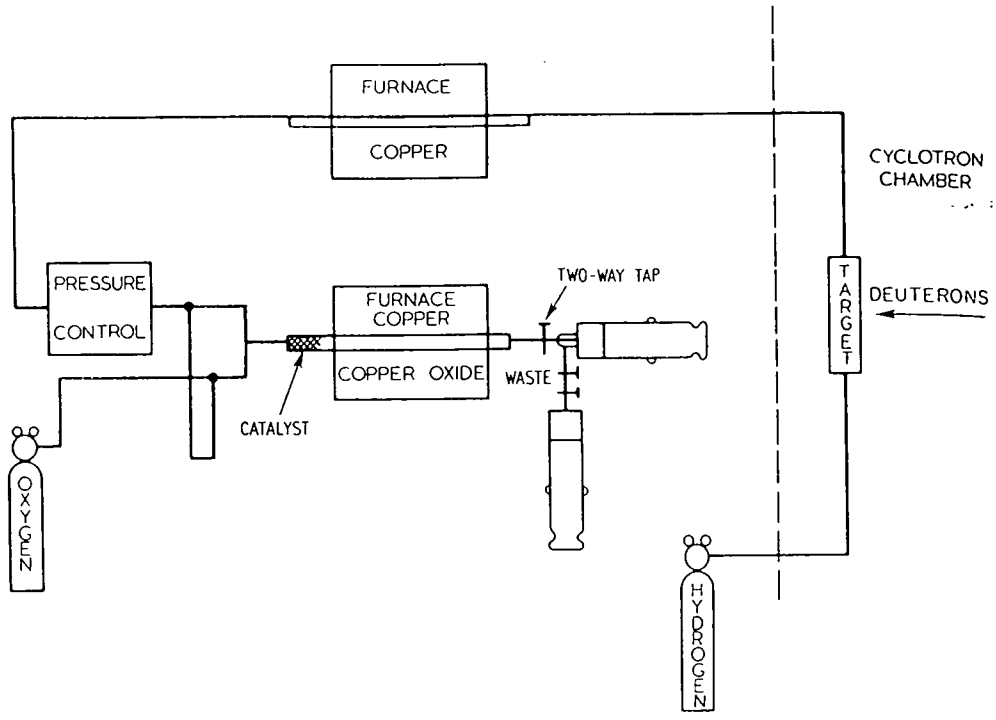

Fig. 4—Flow system for production of $^{13}N_2$ solutions using hydrogen flow gas.

^{11}CO or $^{11}CO_2$ and 60 mc/liter for $^{13}N_2$, all undiluted. After the activated-charcoal absorber is changed, the yield of $C^{15}O_2$ goes down to 5 to 7 mc/liter and then gradually increases with use.

CONTAMINANTS

The radioactive contaminants were determined by decay-curve analysis and gamma-ray spectroscopy. For ^{15}O-labeled gases, they are 0.03 to 2% of ^{13}N and 0.0001 to 0.01% of ^{41}Ar. For ^{11}C-labeled gases they are 2 to 7% of ^{13}N and ^{15}O and 1 to 3% of ^{41}Ar. The ^{41}Ar is not present when helium is used.

Chemical contaminants were measured with a mass spectrometer and a CO meter. For $^{15}O_2$, the gas contained 4% of O_2, 0.09% of CO, and <0.001% of CO_2; for $C^{15}O$, 4% of CO, <0.1% of O_2, and <0.001% of CO_2; for $C^{15}O_2$, 4% of CO_2, 0.1% of O_2, and 0.005% of CO; for ^{11}CO, 5% of CO, 0.1% of O_2, and 0.08% of CO_2; for $^{11}CO_2$, 5% of CO_2 and 0.1% of O_2; plus 95 to 96% of N_2 or argon in each case.

DOSES

The absorbed doses[3,7] for the ^{15}O- and ^{11}C-labeled gases are shown in Table 1. The dose for $^{11}CO_2$ has been revised since it has been

Table 1 — ABSORBED TISSUE DOSES PER BREATH OF 5 MC FOR 20 SEC

Gas	Millirads			
	Lungs (apex)	Blood	Spleen	Gonads
$^{15}O_2$	63	23	12	5
$C^{15}O$	68	39	20	9
$C^{15}O_2$	80	72	35	18
^{11}CO	128	211	109	61
$^{11}CO_2$	220	55	55	55

found that $^{11}CO_2$ equilibrates with a pool that is much larger than the blood. Originally it was assumed to remain in blood so that the dose is now reduced.

Doses for ^{133}Xe (Ref. 8) and $^{13}N_2$ are given in Table 2.

SCINTILLATION COUNTERS

For the lung-function studies, radioactivity in the lungs is examined with two pairs of external scintillation counters with $1\frac{1}{2}$-in. sodium iodide crystals. Each pair points to a region of the left or right lung; one counter is in front of the chest and the other is behind. In the early work with $^{15}O_2$, coincidence counting was used, but later this was changed to "parallel" counting with the outputs added in each pair.

Table 2 — ABSORBED TISSUE DOSES*

Gas	Millirads					
	Lungs	Fat	Other tissues	Gonads	Lungs† (emphysema patient)	
					¼ lung	¾ lung
	Single breath or injection of 1 mc for 30 sec					
^{133}Xe	14			0.1 to 0.3	57	28
$^{13}N_2$	35		0.1 to 0.5	0.1 to 0.5	330	200
	Rebreathing of 1 mc/liter for 2 min					
^{133}Xe	56 to 58	17 to 19	3 to 4	2 to 3	210 to 220	120 to 130
$^{13}N_2$	136		0.5 to 2	0.5 to 2	400	280

*The lower doses assume 5% of fat by weight on the body; the higher doses assume 50% of fat.

†Wash-out half-life of 4 min is assumed for one-fourth of lung and of 2 min for three-fourths of lung. These are taken from some measured values of ^{133}Xe and may be too large for $^{13}N_2$.

With the collimators used this gives a much higher counting rate than coincidence counting, and the resolution is quite adequate. At present two types of collimator are used for clinical work. One is conical with a field of view about 9 cm in diameter at 15 cm from its end. The other is a slit collimator, which views a slab of lung about 4 cm thick and 17 cm wide at 15 cm from the end of the collimator. A short multihole collimator is used for ^{133}Xe for experimental work. Pulse-height analysis is used for ^{133}Xe, and the 30-kev X ray is cut out. For the positron emitters only a single discriminator bias is used; it is set to include the whole spectrum for coincidence but only the photoelectric peak for parallel counting.

At present the same counters are used for both the positron emitters and ^{133}Xe, a system that is not ideal for either; in the future it is planned to use two different counting systems.

For profile scanning the counters are moved up the lung by means of an electrically driven hydraulic pump.

UPTAKE, DISTRIBUTION, AND FATE OF RADIOACTIVE GASES IN THE BODY

There are five stages in the fate of the radioactive gases in the body. First, the initial uptake of the gas in a region of lung after a single breath will depend on the ventilation to that region. Next, during a subsequent breath-holding period, the radioactivity will be removed from the alveolar air by the blood. The extent to which this occurs may be limited by diffusion or by solubility and blood flow. Third, the radioactivity is removed from the lungs by the blood flow. Fourth, it may exchange with tissue pools in the systemic capillaries. Finally, radioactivity returns to the lungs in the venous blood and may be expired.

The calculation of the different clearances may be applied to a region of lung or to the whole lung if it is uniform.

Initial Uptake

The initial uptake, which depends on ventilation, will be similar for all gases, but, for those rapidly cleared by the blood, this initial uptake will be difficult to measure.

Alveolar Clearance

The alveolar clearance can be defined as the fraction of radioactivity in alveolar air removed per unit time by the blood during breath holding. If it is assumed that during a short breath-holding period a negligible amount of radioactivity returns in the venous blood, then alveolar clearance, A, is given by the expression

$$A = \frac{\text{Rate of removal of stable gas by arterial blood (liters per unit time)}}{\text{Initial liters of stable gas in alveolar air} \pm \text{liters of stable gas added or removed}}$$

$$A = \frac{\dot{Q} \cdot C}{V_A F} = -\frac{1}{X_A}\frac{dX_A}{dt} \qquad (1)$$

where $\dot{Q}$ = blood flow
V_A = alveolar volume
F = fraction of stable gas in alveolar air at time t
= alveolar partial pressure ÷ (barometric pressure − pressure of water vapor)
C = concentration of stable gas in arterial blood
X_A = radioactivity in alveolar air

For gases whose uptake is limited by solubility and blood flow, C is the concentration for equilibrium with alveolar air.

In general, F will be a function of time, but for very short times it may be approximately constant.

Molecular Oxygen Dyson, Sinclair, and West[9] derived a similar expression for $^{15}O_2$ alveolar clearance and demonstrated the rapid uptake of $^{15}O_2$ compared with $^{16}O_2$ in the lung. This more rapid uptake is simply explained by the fact that all the $^{15}O_2$ starts in the lung, and so initially none is coming back in the venous blood. Dyson et al. simplify the expression for alveolar radioactivity by assuming that the ratio of $^{15}O_2$ to $^{16}O_2$ partial pressure is constant (i.e., X_A/F = constant) so that alveolar radioactivity decreases linearly with time. A better approximation is probably to assume that uptake of $^{16}O_2$ by the arterial blood is negligible for a breath-holding period of about 10 to 15 sec; so that F and therefore A are constant, and alveolar $^{15}O_2$ decreases exponentially with time.

Dyson, Sinclair, and West[9] also investigated the variation of $^{15}O_2$ concentration along the lung capillary by means of a stepwise calculation. They found that equilibration between blood and alveolar air was not quite reached at the end of the capillary except when a high-oxygen mixture was being breathed. With $^{16}O_2$, equilibration fails to occur only when 1% of O_2 in nitrogen is being breathed. Thus the foregoing equation, which assumes equilibration, is not quite correct for $^{15}O_2$, but the error is small.

Oxygen-15-labeled Carbon Dioxide West and Dollery[10] found that the alveolar clearance of ^{15}O-labeled carbon dioxide was at least four times faster than that for carbon dioxide labeled with ^{11}C. This is due to the exchange of the ^{15}O label with oxygen in water through the equilibrium between carbon dioxide plus water and carbonic acid. Thus $C^{15}O_2$ exchanges with the entire water volume, although this does not occur until the $C^{15}O_2$ reaches the blood since the presence of carbonic anhy-

drase is required to accelerate the reaction. Hence the rate of uptake of $C^{15}O_2$ is very rapid owing to the high solubility, and possibly uptake is limited by diffusion rather than by blood flow and solubility.[10]

Carbon-11-labeled Carbon Dioxide It has been found[11] that $^{11}CO_2$ exchanges very rapidly with the extracellular fluid CO_2, and so the concentration C in Eq. 1 will now represent mean concentration in blood plus extracellular fluid in the lung.

Nitrogen-13 and Xenon-133 For the inert gases the ratio of blood concentration to alveolar air fraction is simply equal to the solubility, which is a constant.

Hence

$$A = \frac{\dot{Q}\alpha}{V_A} = -\frac{1}{X_A}\frac{dX_A}{dt} \tag{2}$$

where α is the solubility. Thus uptake is exponential as long as return of radioactivity in the venous blood is negligible. The solubility of nitrogen in blood is 0.013, and so little uptake of $^{13}N_2$ occurs even if the gas is rebreathed for several minutes. For ^{133}Xe, on the other hand, the solubility is about 0.16, the exact value depending on the hematocrit.[12,13] For a single breath with a breath-holding period of about 10 sec, the uptake will still be small; but, if the gas is rebreathed for a few minutes, a considerable uptake will occur; so it is no longer correct to assume that a negligible amount of radioactivity returns in the venous blood.

Carbon Monoxide Labeled with Oxygen-15 or Carbon-11 The alveolar clearance of this gas is probably limited by diffusion, and therefore the alveolar clearance is given by the equation

$$A = \frac{DP_B}{V_A} = -\frac{1}{X_A}\frac{dX_A}{dt} \tag{3}$$

where D is the diffusing capacity (ml/mm Hg/unit time) and P_B is the barometric pressure minus the pressure of water vapor. Here again A is constant and uptake is exponential.

Approximate calculated or measured values of the alveolar clearances for the various radioactive gases for a short period of breath holding are given in Table 3.

Blood Clearance

The blood clearance is important since it affects the fall in radioactivity in a region of lung measured by external counters. The simplest treatment is to assume that the radioactive gas in the blood and tissue

Table 3—ALVEOLAR (A), BLOOD (B), AND COUNT RATE (S) CLEARANCES

	Fraction/min					
	A		B		S (2 sec)	
Gas	Calculated	Measured	Calculated	Measured	Calculated	Measured
$C^{15}O_2$		>60 (Ref. 10)	7.7	5 to 25 (Ref. 26)	7.7	3 to 15 (Ref. 26)
$^{11}CO_2$		13 (Ref. 10)	11		4	1.5 to 8 (Ref. 26)
$C^{15}O$ or ^{11}CO	6.9		19* (15)†		3* (2.5)†	0.5 to 5 (Ref. 27)
$^{15}O_2$	2.6	2.8 (Ref. 9)	17* (15)†		1* (1)†	0.3 to 1.6 (Ref. 26)
^{133}Xe	0.38		7.7		0.38	
$^{13}N_2$	0.031		7.7		0.031	

Calculated values are for cardiac output of 6 liters/min, alveolar volume of 2.5l, diffusing capacity of 24 ml/mm Hg/min, lung water volume of 780 ml, lung extracellular volume of 540 ml, and lung blood volume of 390 ml. Calculations give values clearance would have if distribution of perfusion and alveolar clearance in lung were uniform. Measured values show variation from apex to base.

*Using Eq. 5.

†Assuming rapid mixing in blood pool.

in the lung has a uniform concentration as in a well-mixed tank. The rate of clearance is then given by the expression

$$B = \frac{\dot{Q}\, C_B}{V_s\, C_s} = -\frac{1}{X_B}\,\frac{dX_B}{dt} \tag{4}$$

where $\dot{Q}$ = blood flow from region of lung being studied
C_B = concentration of gas in arterial blood in lung
C_s = concentration of gas in space in which gas is distributed
V_s = volume of this space
X_B = radioactivity in blood in lung region

The blood clearance, B, is defined as the fraction of radioactivity in the blood plus tissue removed from the region per unit time.

Oxygen-15-labeled carbon dioxide equilibrates rapidly with the water volume in the lung, V_w; thus C_B is equal to C_s, V_s is equal to V_w, and B is equal to Q/V_w.

It has been shown experimentally in the isolated dog lung[14] that the clearance as measured with external counters is proportional to blood flow (Fig. 5). Also, the ratio of $C^{15}O_2$ clearance to flow was found to decrease with increasing edema in the lung.

For ^{11}C-labeled carbon dioxide, which equilibrates rapidly with extracellular CO_2, Eq. 4 might apply, although this has not been investigated experimentally. Here C_s is the mean concentration of gas in blood plus extracellular fluid and V_s is the volume of extracellular fluid including blood.

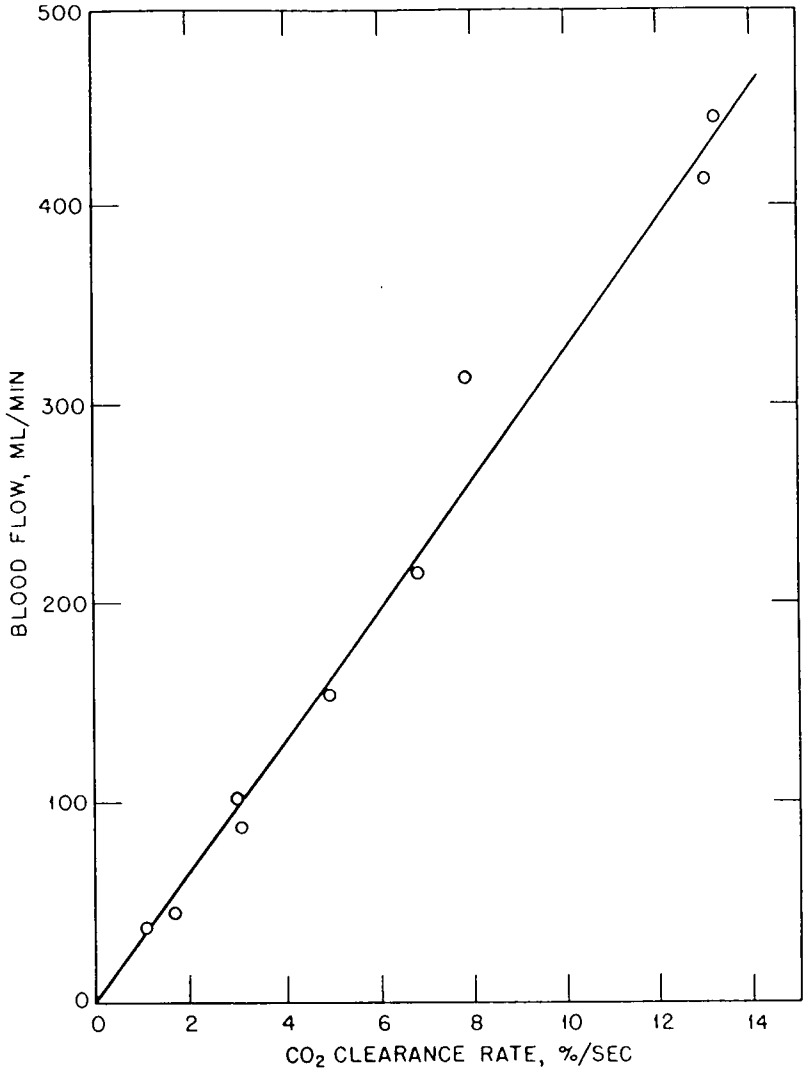

Fig. 5—Counting-rate clearance for $C^{15}O_2$ plotted against blood flow in an isolated dog lung.

For ^{133}Xe and ^{13}N, which equilibrate rapidly with tissue spaces, Eq. 4 may also be applicable. However, the blood clearance will not be an important factor here since the much slower alveolar clearance will be the limiting factor.

Both molecular $^{15}O_2$ and carbon monoxide (labeled with either ^{15}O or ^{11}C) remain in the blood bound to hemoglobin. West et al.[15] assumed that Eq. 4 was applicable to these gases, but, in fact, there is certainly not complete mixing in the blood pool.

An alternative expression for a small region of lung which may be a little closer to reality can be derived as follows. It is assumed that radioactivity travels along the venules as a square front until it leaves the lung region that is being considered and that the effect of all the separate venules is equivalent to a single "average" venule (see Fig. 6). It is also assumed that the velocity of flow is constant along

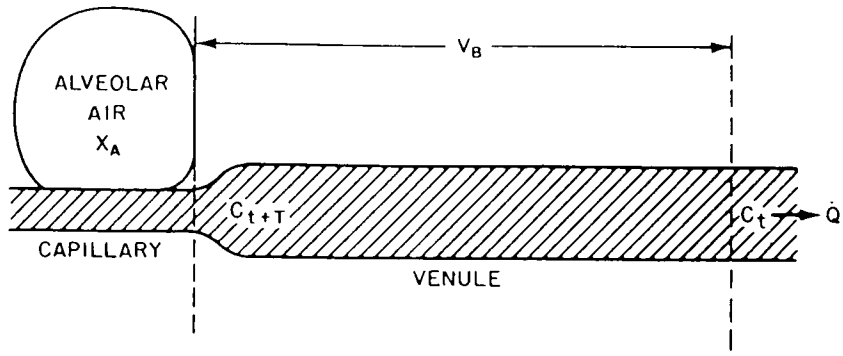

Fig. 6—Model for development of equation for blood clearance.

the venule, that the alveolar clearance is exponential, and that the volume of capillary blood is negligible compared with total volume of blood in the region considered.

If we let T represent the mean time for blood to flow through volume V_B ($T = V_B/\dot{Q}$, where $\dot{Q}$ is blood flow), C_t represent concentration of radioactivity in blood leaving the region, C_{t+T} represent concentration of radioactivity in blood leaving the capillaries, and use the other symbols as previously defined, then for time t after the radioactive front has reached the edge of the lung region,

$$-\frac{dX_A}{dt} = AX_A = \dot{Q}\,C_{t+T}$$

$$-\frac{dX_B}{dt} = \frac{dX_A}{dt} + BX_B$$

$$-\frac{d(X_A + X_B)}{dt} = \dot{Q}C_t$$

Therefore

$$X_A = (X_A)_0\, e^{-At}$$

and

$$C_t = \frac{A}{Q}(X_A)_0\, e^{AT}\, e^{-At}$$

By integrating along the venule, we find that

$$X_B = (X_A)_0\, e^{-At} \cdot e^{AT}\,(1 - e^{-AT})$$

and therefore

$$B = \frac{A}{1 - e^{-AT}} \tag{5}$$

Hence B is constant and independent of time and therefore blood clearance is exponential; however, it is a function of alveolar clearance.

Another possible model is to consider that clearance from the blood is exponential owing to an exponential distribution of passage times along the venules from the capillary to the edge of the region considered. Thus $C_t = C_0 e^{-B(t-t_0)}$ if the radioactivity is instantaneously taken up by the blood. If t_0 is very small, it can be shown that the equations are the same as for two well-mixed pools but with $t - t_0$ substituted for t.

Table 3 shows approximate calculated or measured values for blood clearances for the radioactive gases.

Exchange with Tissue Pools and Return in Venous Blood

Carbon monoxide labeled with ^{15}O or ^{11}C remains bound to hemoglobin with very little exchange with the tissues.

On the other hand, when molecular $^{15}O_2$ taken up by the blood reaches the systemic capillaries, it will take part in metabolism and some will return to the blood as ^{15}O-labeled water. Ter-Pogossian et al.[16] studied the kinetics of uptake and desaturation of $^{15}O_2$ in red cells and the rate of appearance of labeled water in plasma in the dog. These authors and Dollery and West[17] showed that the plasma radioactivity was in the form of water and not carbon dioxide.

Oxygen-15-labeled carbon dioxide exchanges with the entire water pool, as has already been mentioned. Hence the radioactivity returning in the venous blood is negligibly small since it is so diluted. However, if there is a shunt in the heart through which radioactivity can return more rapidly to the lungs without much dilution, a secondary recirculation peak can be seen when counting rate over the lungs is recorded.

Fowle, Matthews, and Campbell[11] used ^{11}C-labeled carbon dioxide to investigate the distribution of carbon dioxide in body stores. The $^{11}CO_2$ was rebreathed from a small bag for about a quarter of a minute, and arterial samples were taken at short intervals. Within half a minute from the end of administration, the radioactivity in arterial blood was already diluted in a pool that was much larger than the blood CO_2 and approximately equal to extracellular CO_2. Subsequently the $^{11}CO_2$ exchanged much more slowly with another pool that corresponded approximately with intracellular CO_2. Figure 7 shows the radioactivity in arterial blood plotted vs. time. The distribution of tritiated water was also consistent with very rapid exchange with the extracellular pool and slower exchange with the intracellular pool. With this hypothesis of slow extracellular–intracellular exchange of CO_2, it was possi-

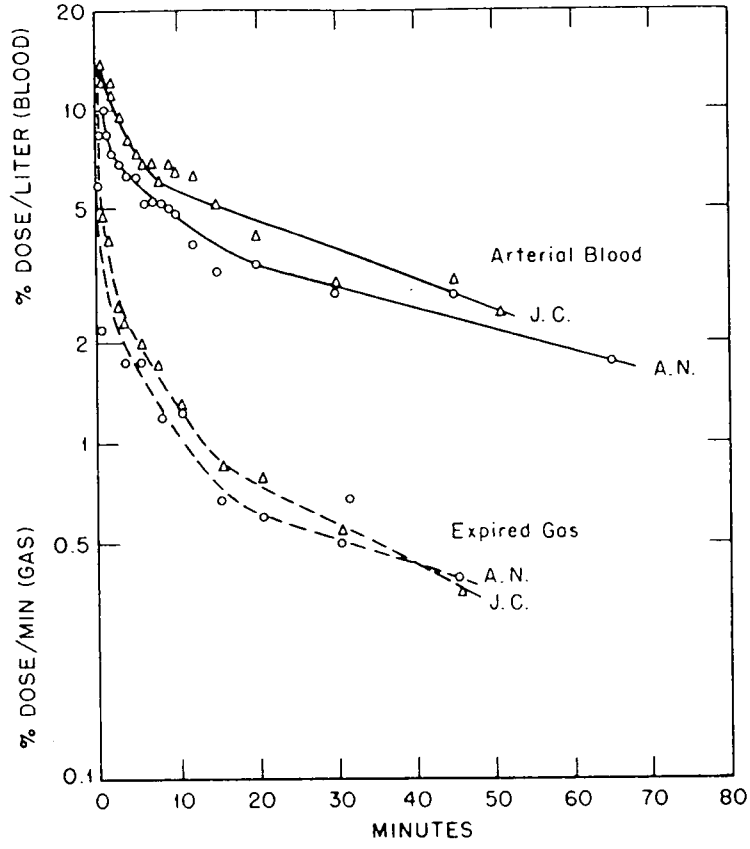

Fig. 7—Disappearance of radioactivity from arterial blood after administration of $^{11}CO_2$ to normal subjects. [From A. S. E. Fowle, C. M. E. Matthews, and E. J. M. Campbell, Clinical Science, *27: 51 (1964).]*

ble to explain the rate of rise of lung P_{CO_2} during rebreathing from a small bag.[11] This rise was inconsistent with models of CO_2 stores in which exchange rates are limited only by blood flow.

It is usually assumed that the inert gases ^{133}Xe and $^{13}N_2$ exchange instantaneously with the entire tissue space in an organ when they reach the capillaries.[18-20] Thus their distribution is determined by blood flow and solubility. Xenon-133 is twenty times more soluble in fat than in water, but, since blood flow to fat is low, the concentration does not build up appreciably for a short period of breathing ^{133}Xe.

Matthews and Dollery[21] used an analog computer to investigate the effect of blood and tissue uptake of ^{133}Xe on lung wash-in and wash-out rate in normal subjects and in patients rebreathing ^{133}Xe in a closed circuit. They also investigated $^{13}N_2$. Radioactivity in arterial and venous blood as well as counting rate over the lung were measured with external scintillation counters. Results were consistent with a model with two tissue pools (Fig. 8), one of about 30 to 40 liters with a blood flow of 2.5 to 4.4 liters/min and the other of about 0.3 to 2 liters with a blood flow of 2.4 liters/min. These correspond fairly well

with Mapleson's[22] two pools, a rapidly exchanging visceral one and a slowly exchanging "lean" pool consisting mainly of muscle and skin. Figure 9 shows analog-computer curves and experimental points for radioactivity in the different pools for a normal subject for ^{133}Xe and

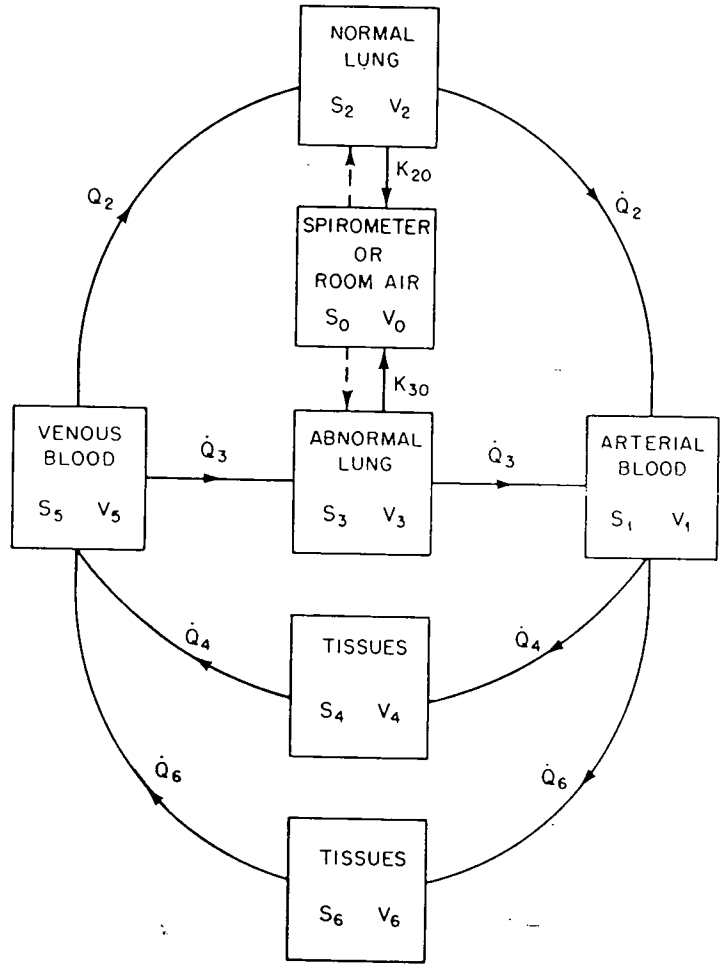

Fig. 8—Pool system used for analog simulation of lung and arterial- and venous-blood radioactivity curves during and after rebreathing of ^{133}Xe. $\dot{Q}$, blood flow; V, volume; K, fractional ventilation; and S, concentration of radioactivity. [From C. M. E. Matthews and C. T. Dollery, Clinical Science, *28: 573 (1965).]*

$^{13}N_2$ rebreathed for 2 min. The slow wash out of ^{133}Xe in the upper zone is probably due to radioactivity in the chest wall.

The return of radioactivity in the venous blood was found to vary little for different subjects for a given rebreathing time. This enabled the analog-computer program to be considerably simplified.

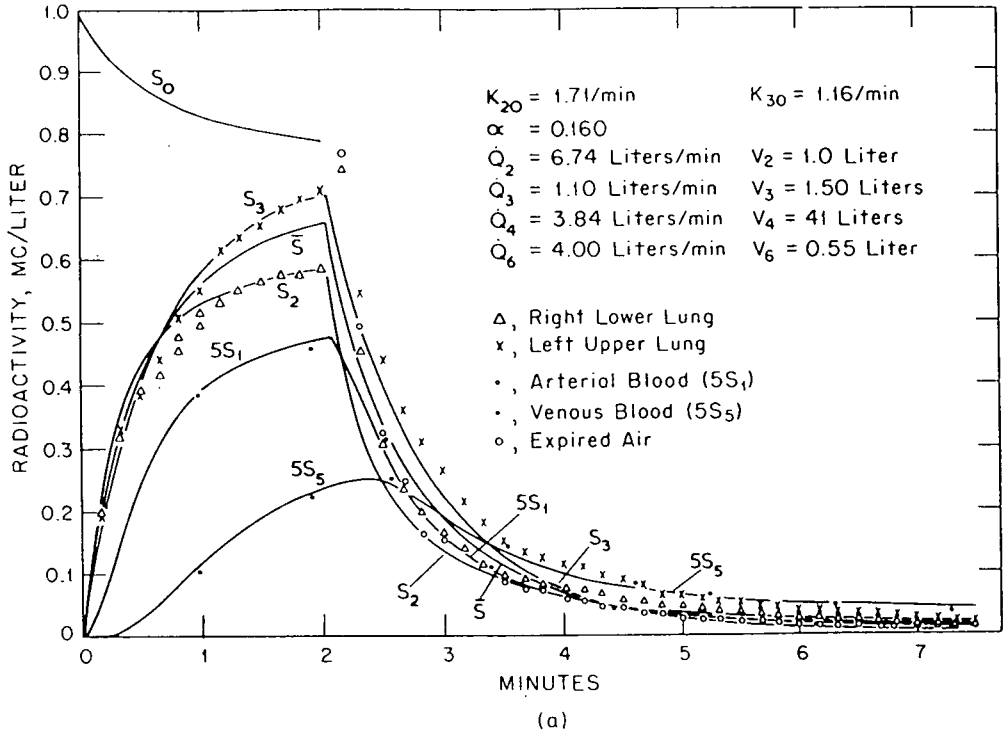

(a)

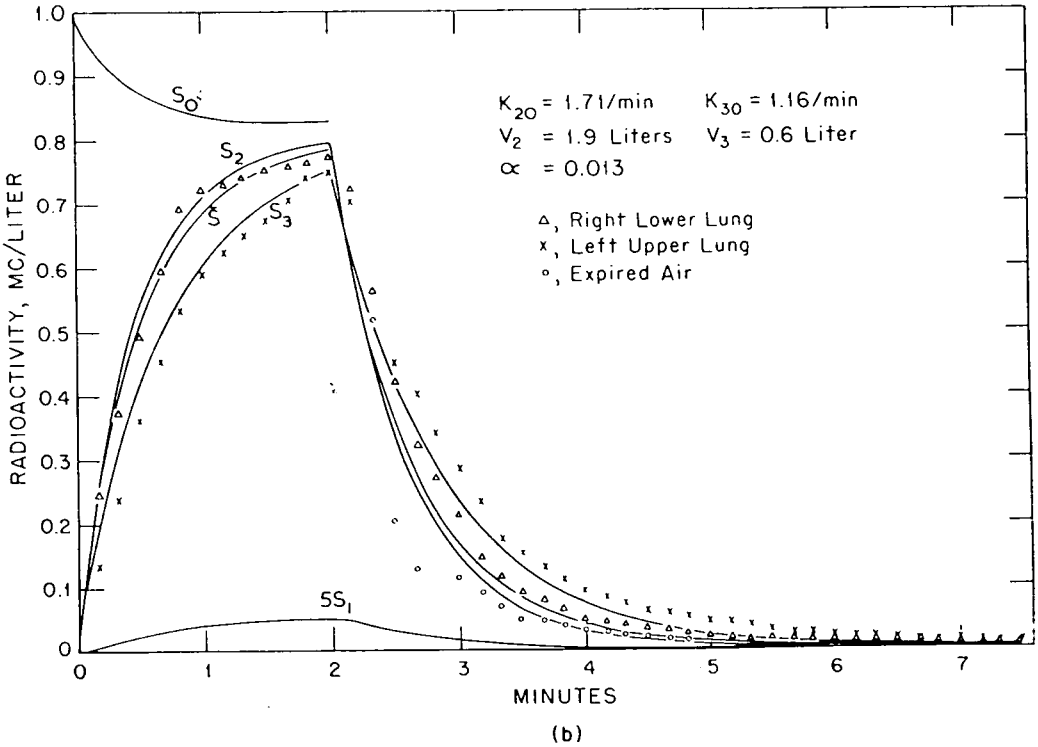

(b)

Fig. 9—Analog-computer curves and experimental points for a normal subject rebreathing (a) ^{133}Xe and (b) ^{13}N. $\dot{Q}$, blood flow; V, volume; S, concentration of radioactivity in millicuries per liter ($\bar{S}$, mean for whole lung); K_{20} and K_{30}, ventilations of two lung zones as fractions per minute; and α, solubility coefficient. (For numbering of pool system see Fig. 8.) [From C. M. E. Matthews and C. T. Dollery, Clinical Science, *28: 573 (1965).]*

METHODS OF USE

Counting-rate Clearance

The use of the external scintillation counters is complicated by the fact that measured counting rate will depend on radioactivity in both alveolar air and blood. Thus counting-rate clearance will, in general, be a complex function of both alveolar clearance and blood clearance. Counting-rate clearance may be defined as the fractional rate of change of counting rate recorded by scintillation counters pointing at the lung during a breath-holding period. The following equation for the counting-rate clearance or the exponential slope, S, of the counting-rate curve at time t has been derived[15]:

$$S = \frac{A\,B(e^{-At} - e^{-Bt})}{B\,e^{-At} - Ae^{-Bt}} \qquad \text{for } A \neq B$$

$$S = \frac{A^2 t}{1 + At} \qquad \text{for } A = B \tag{6}$$

where A is the alveolar clearance and B is the blood clearance as before. This assumes exponential alveolar and blood clearances.

For ^{15}O-labeled carbon dioxide, A is so much greater than B that the slope S becomes equal to B, and hence the clearance during breath holding of $C^{15}O_2$ can be used as a measure of blood flow. At the other extreme A is negligibly small for $^{13}N_2$, and S is equal to 0. For ^{133}Xe, B is much greater than A, and thus S is equal to A.

For the other radioactive gases, molecular ^{15}O, ^{11}C-labeled carbon dioxide, and carbon monoxide labeled with ^{15}O or ^{11}C, A and B are comparable, and so S has no simple significance. Counting-rate clearance curves for the different gases labeled with ^{15}O are shown in Fig. 10.

Measurement of Regional Diffusing Capacity

The slope of the counting-rate curve cannot be used as a simple measure of regional diffusing capacity. An attempt was made to work out a method of measuring diffusing capacity in the isolated dog lung (C. T. Dollery, P. Heimburg, C. M. E. Matthews, and J. B. West, unpublished results, 1963). Blood flow, blood volume, and slope of the counting-rate curve were measured. Alveolar clearance was also measured directly by taking samples of alveolar air in tonometers. Alveolar clearances were calculated and compared with the directly measured values. Although there was some correlation, there was considerable scatter of the points. It was found that an extra delay was introduced owing to an increase in blood volume on inspiration which temporarily

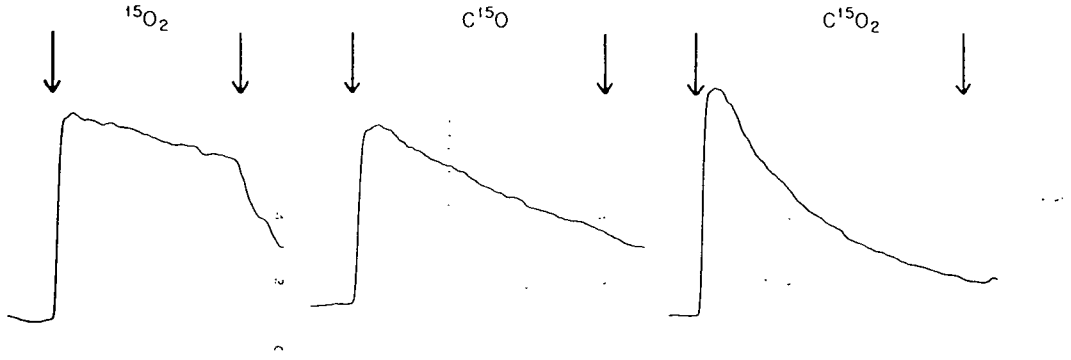

Fig. 10—Fall in counting rate over the lungs for three different gases labeled with ^{15}O. The first arrow shows the time of inspiration, and the second one shows the end of the breath-holding period, about 10 sec later.

reduced blood flow. This probably accounts for the erratic results obtained and means that diffusing capacity cannot be accurately measured by this method. A method based on the difference in the clearance curves of radioactive carbon monoxide and a radioactive substance, which was very rapidly absorbed by the blood and which remained in the blood, might be possible if a suitable substance could be found.

Table 3 shows approximate calculated and measured values for counting-rate clearances.

Measurement of Regional Blood Flow

Regional blood flow has been measured by the following methods:

1. $^{15}O_2$ counting-rate clearance during breath holding
2. $C^{15}O_2$ counting-rate clearance during breath holding
3. ^{133}Xe arrival
4. $^{13}N_2$ arrival

Method 1 does not give a true measure of blood flow since S is a complex function of flow.

Method 2 is normally satisfactory. However, it actually measures blood flow per unit water volume (see p. 576), and so the result obtained will be affected by the presence of edema.

Figure 11 shows $^{15}O_2$ and $C^{15}O_2$ clearance curves for a normal subject and for a patient with mitral-valve disease.

In method 3, ^{133}Xe is dissolved in saline and injected intravenously. The ^{133}Xe is first mixed with carbon dioxide and then shaken with saline. The carbon dioxide dissolves rapidly and thus increases the partial pressure of ^{133}Xe in the remaining bubble and drives it into solution. After injection the subject holds his breath, and the counting rate is measured over a region of lung. When the injected ^{133}Xe reaches

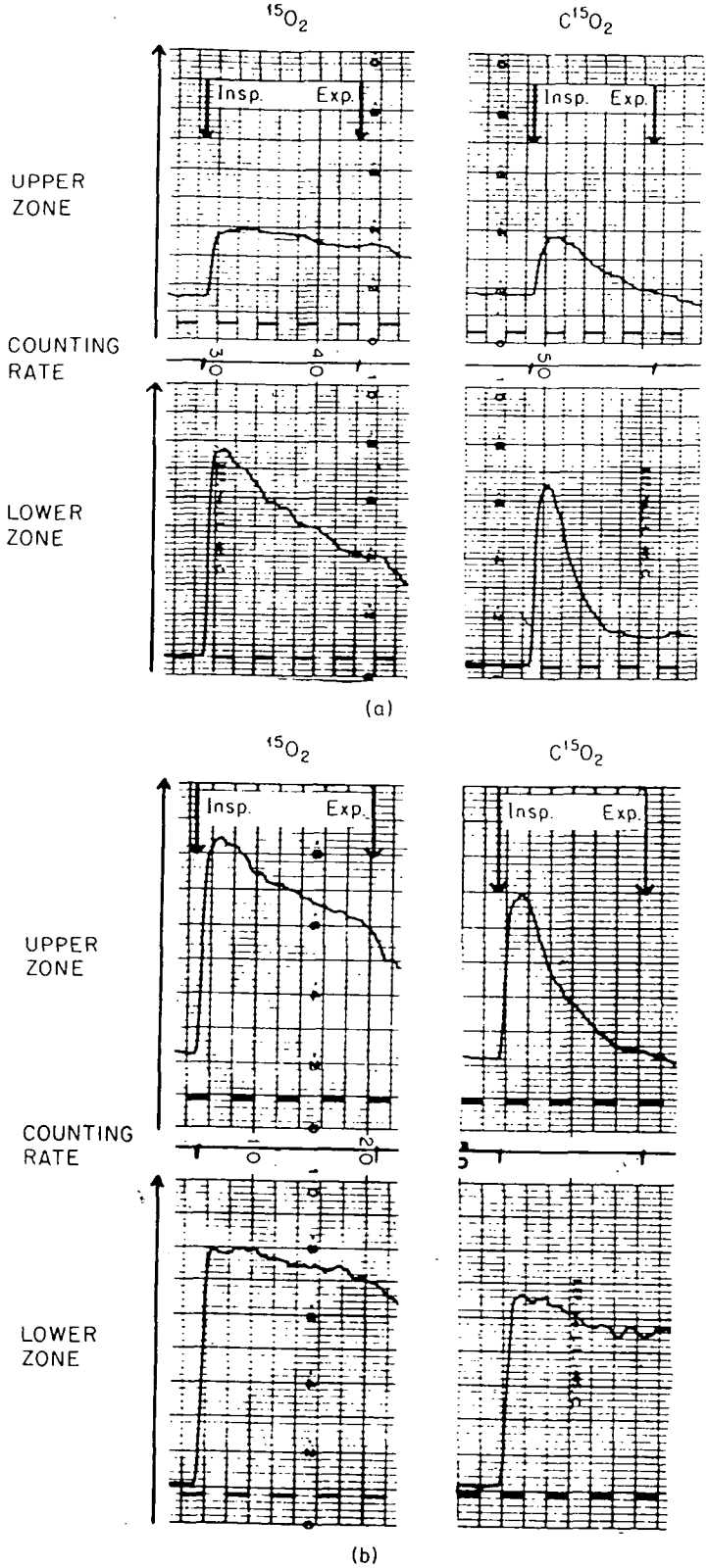

Fig. 11—Counting-rate clearance curves for $^{15}O_2$ and $C^{15}O_2$ for upper and lower zones (a) for a normal subject and (b) for a patient with mitral-valve disease. In the normal subject the clearance is greater in the lower zone because of the much higher blood flow in this zone. For the patient, this pattern is reversed, and the clearance is greater in the upper zone because of a higher blood flow. [From C. T. Dollery et al., Sonderbände zur Strahlenbehandlung, *53: 88 (1963).]*

the lung capillaries, it is nearly all evolved into the alveolar air; thus the radioactivity arriving in a region of lung is proportional to the blood flow to that region as a fraction of cardiac output. This method gives slightly different information from that given by method 2 since it depends on cardiac output. However, when blood flow in two regions is to be compared, this difference is immaterial.

This method, introduced by Ball et al.,[4] has been used to investigate the distribution of blood flow in the isolated lung in relation to vascular and alveolar pressures.[23] It is also used routinely in patients.[24]

Method 4 is exactly the same as method 3 except that $^{13}N_2$ is used. Since the breath-holding period is so short, very little uptake of ^{133}Xe by the blood occurs; thus similar results should be obtained with ^{133}Xe and $^{13}N_2$.

Detection of Cardiac Shunts

The method for detecting cardiac shunts has already been mentioned. The counting rate over the lung is recorded after a breath of $C^{15}O_2$. The presence of a shunt gives rise to a second peak due to recirculation. Figure 12 shows an example of $C^{15}O_2$ curves for upper and lower zones before and after operation for closure of the shunt.

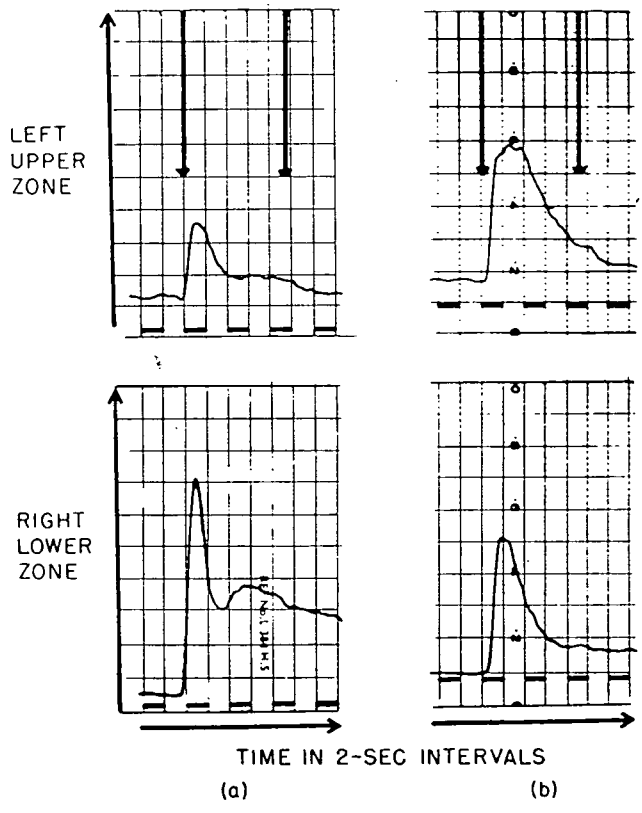

Fig. 12—Counting-rate curves for $C^{15}O_2$ during breath holding for a patient with a ventricular septal defect (a) before and (b) after operation for closure of the defect. The recirculation peak disappears after the operation.

Measurement of Regional Ventilation Per Unit Lung Volume

The following methods have been used to study regional ventilation:

1. Single breath of $^{15}O_2$
2. Single breath of ^{133}Xe
3. Single breath of $^{13}N_2$
4. Wash in and wash out of ^{133}Xe
5. Wash in and wash out of $^{13}N_2$

Regional ventilation measured by the single-breath method must be related to regional lung volume, and this has been measured by rebreathing either ^{133}Xe or $^{13}N_2$ in a closed circuit for a few minutes and taking the counting rate over a region to be proportional to lung volume in that region. In practice, however, equilibration may not occur with ^{133}Xe owing to the uptake in blood which, with an alveolar clearance rate of about 38%/min, is certainly not negligible during 2 min rebreathing. On the other hand, for $^{13}N_2$ with an alveolar clearance of only about 3%/min, the uptake will be small even for several minutes of rebreathing. With an analog computer[21] it was found that, although the error with ^{133}Xe was probably small in normal subjects, it could be considerable in patients, and volume could be underestimated by about 45%. This is illustrated in Fig. 13 for a patient with bullous emphysema where concentration in the different regions of the lung did not reach the spirometer concentration even after 4 min rebreathing.

Another disadvantage of the single-breath method is that in regions of low ventilation there is little uptake of the radioactive gas, and so it is difficult to obtain a quantitative measure of the reduction in ventilation. The results obtained by the wash-out method are much more sensitive to small proportions of badly ventilated alveoli and also give ventilation per unit volume directly. The wash-in method is less sensitive than the wash-out method. Here again $^{13}N_2$ is much better than ^{133}Xe because of its lower solubility. The ^{133}Xe wash out is distorted by radioactivity in the chest wall (Fig. 9) and by uptake of ^{133}Xe in arterial blood and return in venous blood. Nevertheless, ^{133}Xe can be used to give a rough indication of reduced ventilation. Figure 14 shows a wash-out curve after rebreathing of ^{133}Xe and after injection in a patient with emphysema. The reduced ventilation in the lower zone is clearly shown, although the lower trace shows that this zone is perfused.

Scanning Profile scanning has been used with ^{133}Xe and the single-breath method to show the distribution of ventilation and with the injection method to show the distribution of perfusion.[25]

Body CO_2 Stores and Control of Ventilation

The use of $^{11}CO_2$ for investigation of body CO_2 stores has already been mentioned. This work is now being extended to cover control of

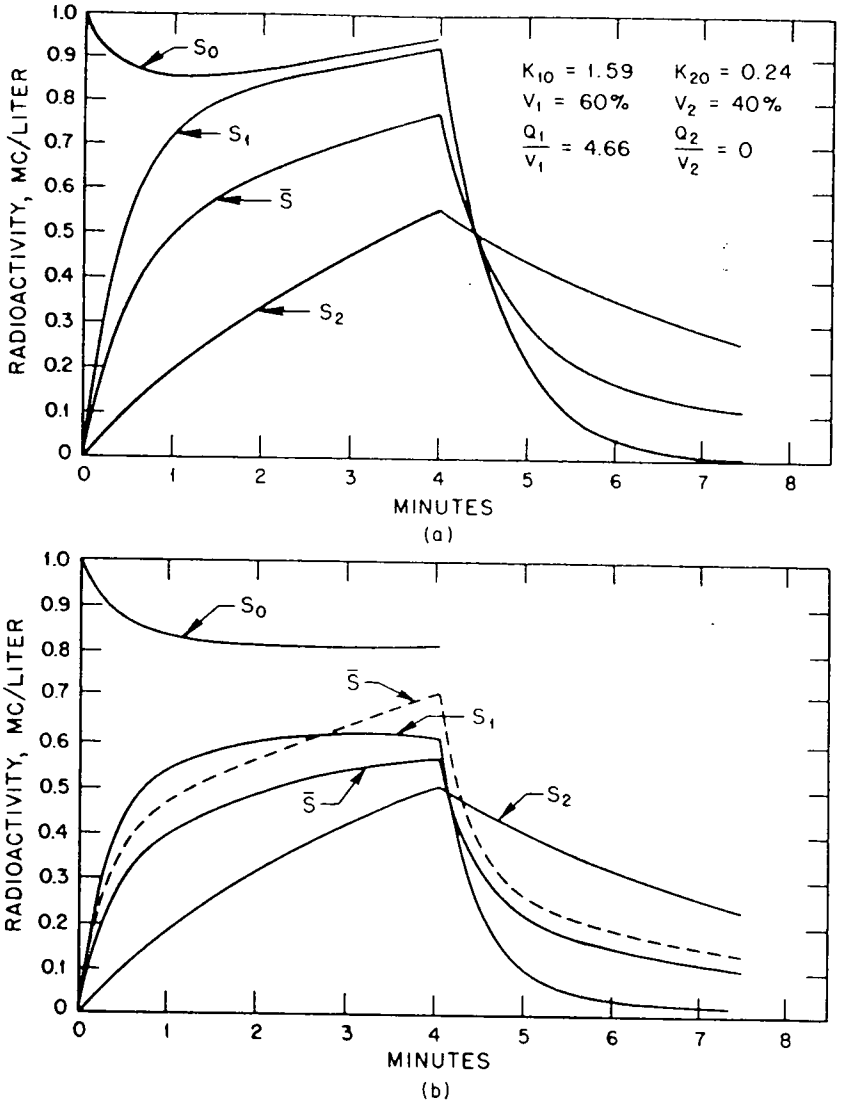

Fig. 13—Analog-computer curves for concentration of radioactivity in two different lung regions, S_1 and S_2, for a patient with bullous emphysema rebreathing (a) $^{13}N_2$ and (b) ^{133}Xe for a period of 4 min. $\bar{S}$ is the mean concentration and S_0 is the spirometer concentration. The curves matched the experimental points reasonably well. For ^{133}Xe, the concentrations in both lung regions are much lower than in the spirometer at the end of rebreathing. [From C. M. E. Matthews and C. T. Dollery, Clinical Science, *28: 573 (1965).]*

ventilation from changes in brain CO_2 with the use of an analog computer. Further experiments are being carried out with $^{11}CO_2$ to determine whether or not fractional exchange rates between the pools vary with the level of P_{CO_2}.

Measurement of Blood Volume

Carbon-11-labeled carbon monoxide could be used for labeling red cells and hence for measuring blood volume. The advantage over other

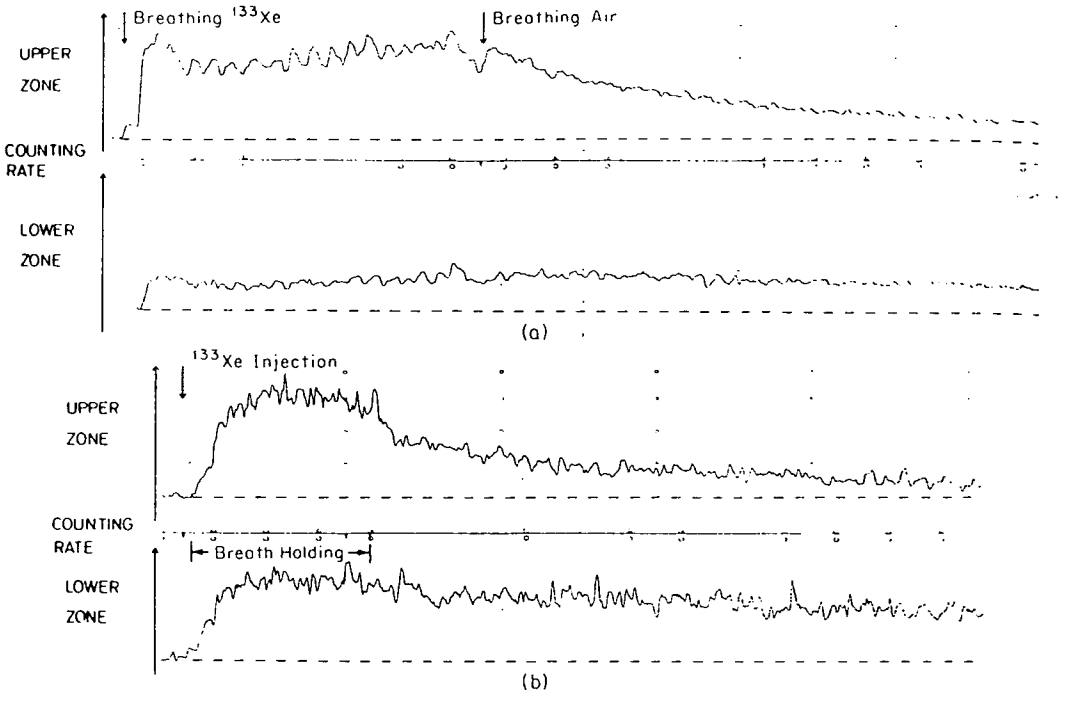

Fig. 14—Wash out of ^{133}Xe measured with scintillation counters over upper and lower zones (a) after rebreathing ^{133}Xe and (b) after an injection of ^{133}Xe for a patient with emphysema with bullous areas in the lower zones. This lower zone had very little ventilation but only slightly reduced perfusion.

methods would be the short half-life, which would allow repeated measurements to be made with a very low dose to the patient. The uptake is limited by the presence of the carbon monoxide carrier gas since the red cells rapidly become saturated, but a concentration of about 50 μc/ml can be obtained, which is adequate. The method has been tried in rabbits (Priolisi, unpublished results).

REFERENCES

1. H. W. Knipping, W. Bolt, H. Valentin, H. Venrath, and P. Endler, Regionale Funktionsanalyse in der Kreislauf-und Lungen-Klinik mit Hilfe Isotopenthroakographie und der selektiven Angiographie der Lungengefässe; Beitrag zur präoperativen Funktionsanalyse in der Thorax-chirurgie, *München. Med. Wochensch.*, 99: 46-47 (1957).
2. M. Ter-Pogossian and W. E. Powers, The Use of Radioactive Oxygen 15 in the Determination of Oxygen Content in Malignant Neoplasms, *Proceedings of the First UNESCO International Conference of Radioisotopes in Scientific Research, Paris, 1957,* Vol. 3, pp. 625-636, Pergamon Press, New York, 1958.
3. N. A. Dyson, P. Hugh-Jones, G. R. Newbery, and J. B. West, The Preparation and Use of Oxygen-15 with Particular Reference to Its Value in the Study of Pulmonary Malfunction, in *Proceedings of the Second United Nations International Conference on the Peaceful Uses of Atomic Energy, Geneva, 1958,* Vol. 26, pp. 103-115, United Nations, New York, 1958.

4. W. C. Ball, Jr., P. B. Stewart, L. G. S. Newsham, and D. V. Bates, Regional Pulmonary Function Studied with Xenon^{133}, *J. Clin. Invest.*, 41: 519-531 (1962).
5. P. D. Buckingham and G. R. Forse, The Preparation and Processing of Radioactive Gases for Clinical Use, *Int. J. Appl. Radiat.*, 14: 439-445 (1963).
6. L. C. Baker and P. D. Buckingham, Cadmium Sulphide D.C. Conductivity Cells for Gamma Ray Detection, *Phys. Med. Biol.*, 10: 201-208 (1965).
7. C. T. Dollery, J. F. Fowler, P. Hugh-Jones, C. M. E. Matthews, and J. B. West, The Preparation and Use of Radioactive Oxygen, Carbon Monoxide, and Carbon Dioxide for Investigation of Regional Lung Function, and Their Comparison with Xenon-133, *Strahlentherapie, Sonderbände*, Pt. 5, 53: 88-103 (1963).
8. C. M. E. Matthews, J. F. Fowler, and P. C. R. Turner, Absorbed Doses from ^{133}Xe M.R.C. Cyclotron Unit, *Tech. Mem.*, No. 84. Rev. (1963).
9. N. A. Dyson, J. D. Sinclair, and J. B. West, A Comparison of the Uptakes of Oxygen-15 and Oxygen-16 in the Lung, *J. Physiol.*, 152: 325-336 (1960).
10. J. B. West and C. T. Dollery, Uptake of Oxygen-15-labeled CO_2 Compared with Carbon-11-labeled CO_2 in the Lung, *J. Appl. Physiol.*, 17: 9-13 (1962).
11. A. S. E. Fowle, C. M. E. Matthews, and E. J. M. Campbell, The Rapid Distribution of ^3H_2O and $^{11}CO_2$ in the Body in Relation to the Immediate Carbon Dioxide Storage Capacity, *Clin. Sci.*, 27: 51-65 (1964).
12. W. H. Isbister, P. F. Schofield, and H. B. Torrance, Measurement of the Solubility of Xenon-133 in Blood and Human Brain, *Phys. Med. Biol.*, 10: 243-250 (1965).
13. N. Veall and B. L. Mallett, The Partition of Trace Amounts of Xenon Between Human Blood and Brain Tissues at 37°C, *Phys. Med. Biol.*, 10: 375-380 (1965).
14. C. T. Dollery, P. Heimburg, and P. Hugh-Jones, The Relationship Between Blood Flow and Clearance Rate of Radioactive Carbon Dioxide and Oxygen in Normal and Oedematous Lungs, *J. Physiol.*, 162: 93-104 (1962).
15. J. B. West, R. A. B. Holland, C. T. Dollery, and C. M. E. Matthews, Interpretation of Radioactive Gas Clearance Rates in the Lung, *J. Appl. Physiol.*, 17: 14-20 (1962).
16. M. Ter-Pogossian, J. S. Spratt, Jr., S. Rudman, and A. Spencer, Radioactive Oxygen 15 in Study of Kinetics of Oxygen of Respiration, *Amer. J. Physiol.*, 201: 582-586 (1961).
17. C. T. Dollery and J. B. West, Metabolism of Oxygen-15, *Nature*, 187: 1121 (1960).
18. C. A. Tobias, H. B. Jonès, J. H. Lawrence, and J. G. Hamilton, Symposium on Radioactive Isotopes; Uptake and Elimination of Krypton and Other Inert Gases by the Human Body, *J. Clin. Invest.*, 28: 1375-1385 (1949).
19. H. B. Jones, Respiratory System: Nitrogen Elimination, in *Medical Physics*, Vol. 2, O. Glasser (Ed.), pp. 855-871, Year Book Publishers, Inc., Chicago, 1950.
20. S. S. Kety, The Theory and Applications of the Exchange of Inert Gas at the Lungs and Tissues, *Pharmacol. Rev.*, 3: 1-41 (1951).
21. C. M. E. Matthews and C. T. Dollery, Interpretation of ^{133}Xe Lung Wash-in and Wash-out Curves Using an Analogue Computer, *Clin. Sci.*, 28: 573-590 (1965).
22. W. W. Mapleson, An Electric Analogue for Uptake and Exchange of Inert Gases and Other Agents, *J. Appl. Physiol.*, 18: 197-204 (1963).
23. J. B. West, C. T. Dollery, and A. Naimark, Distribution of Blood Flow in Isolated Lung; Relation to Vascular and Alveolar Pressures, *J. Appl. Physiol.*, 19: 713-724 (1964).
24. C. T. Dollery, P. Hugh-Jones, and C. M. E. Matthews, Use of Radioactive Xenon for Studies of Regional Lung Function, *Brit. Med. J.*, 2: 1006-1016 (Oct. 20, 1962).

25. C. T. Dollery and P. M. Gilliam, The Distribution of Blood and Gas Within the Lungs Measured by Scanning After Administration of ^{133}Xe, *Thorax*, 18: 316-325 (1963).
26. J. B. West, C. T. Dollery, and P. Hugh-Jones, The Use of Radioactive Carbon Dioxide to Measure Regional Blood Flow in the Lungs of Patients with Pulmonary Disease, *J. Clin. Invest.*, 40: 1-12 (1961).
27. C. T. Dollery, N. A. Dyson, and J. D. Sinclair, Regional Variations in Uptake of Radioactive CO in the Normal Lung, *J. Appl. Physiol.*, 15: 411-417 (1960).

DISCUSSION

INGHAM: We have been using ^{135}Xe at McMaster for pulmonary function studies and wonder if you have any comments on this radionuclide.

MATTHEWS: Xenon-135 would have the advantage of a shorter half-life than ^{133}Xe and thus a lower dose but would be less convenient and would have the same disadvantages, owing to blood solubility, as ^{133}Xe.

Radioactive Pharmaceuticals

x760

Proceedings of a symposium held at the
Oak Ridge Institute of Nuclear Studies,
an operating unit of
Oak Ridge Associated Universities,
November 1–4, 1965

Editors

Gould A. Andrews, M.D.
Ralph M. Kniseley, M.D.
Henry N. Wagner, Jr., M.D.

Technical Editor

Elizabeth B. Anderson, M.S.

April 1966

U.S. ATOMIC ENERGY COMMISSION / Division of Technical Information

IN VITRO LABELLING OF RED CELLS WITH CARBON-11

J.C. CLARK, H.I. GLASS (*) and D.J. SILVESTER
Medical Research Council Cyclotron Unit, and
(*) Department of Medical Physics, Postgraduate Medical School,
Hammersmith Hospital, London, W.12, England

Abstract

The ready availability of ^{11}C-labelled carbon monoxide from the Medical Research Council's cyclotron has led to the development of a routine technique for labelling red cells with this isotope.

The method of producing the labelled gas and of labelling the cells will be described, and preliminary results of a comparison with the conventional ^{51}Cr labelling procedure will be presented.

INTRODUCTION

Before the stable isotope ^{13}C and the long-lived radioisotope ^{14}C became available as isotopic tracers for carbon, a remarkable volume of useful work [1] was achieved using short-lived ^{11}C, which was made without much difficulty—though in small yield—with early cyclotrons. Not surprisingly, in view of its 20-minute half-life, ^{11}C has found few practical applications since. In recent years it has again proved valuable, however, particularly in the form of labelled carbon dioxide gas, for a number of physiological studies [2]. The purpose of this paper is to report another useful application of this isotope (this time one in which it is incorporated into a high-molecular weight compound), where its short half-life is a positive advantage.

The measurement of circulating blood volumes is important in medicine, and is conventionally achieved by labelling red cells with ^{51}Cr and performing what is, in effect, a classical isotope dilution analysis. However, the long physical and biological half-lives of ^{51}Cr preclude its use in, for example, infants and expectant mothers, where the radiation dose would be too high, and in patients where serial measurements at short intervals are required. For such applications a short-lived label is desirable.

The affinity of haemoglobin for carbon monoxide is well known, and indeed non-radioactive carbon monoxide has been used as a red cell label [3-6]. Since carbon monoxide labelled with ^{11}C is readily available from the Medical Research Council's cyclotron, a routine technique for labelling red cells with this isotope has been developed.

PREPARATION OF ^{11}C-LABELLED CARBON MONOXIDE (*)

Carbon-11 is produced by the bombardment of boron, as boric oxide, with deuterons, the reactions being $^{10}B(d,n)^{11}C$ and ^{11}B $(d,2n)^{11}C$. Some nitrogen-13 is produced simultanéously by the reaction $^{16}O(d,\alpha n)^{13}N$, but these are the only reactions that need be considered for present purposes. The target vessel is shown in fig. 1, and consists essentially of a brass box containing a wedge

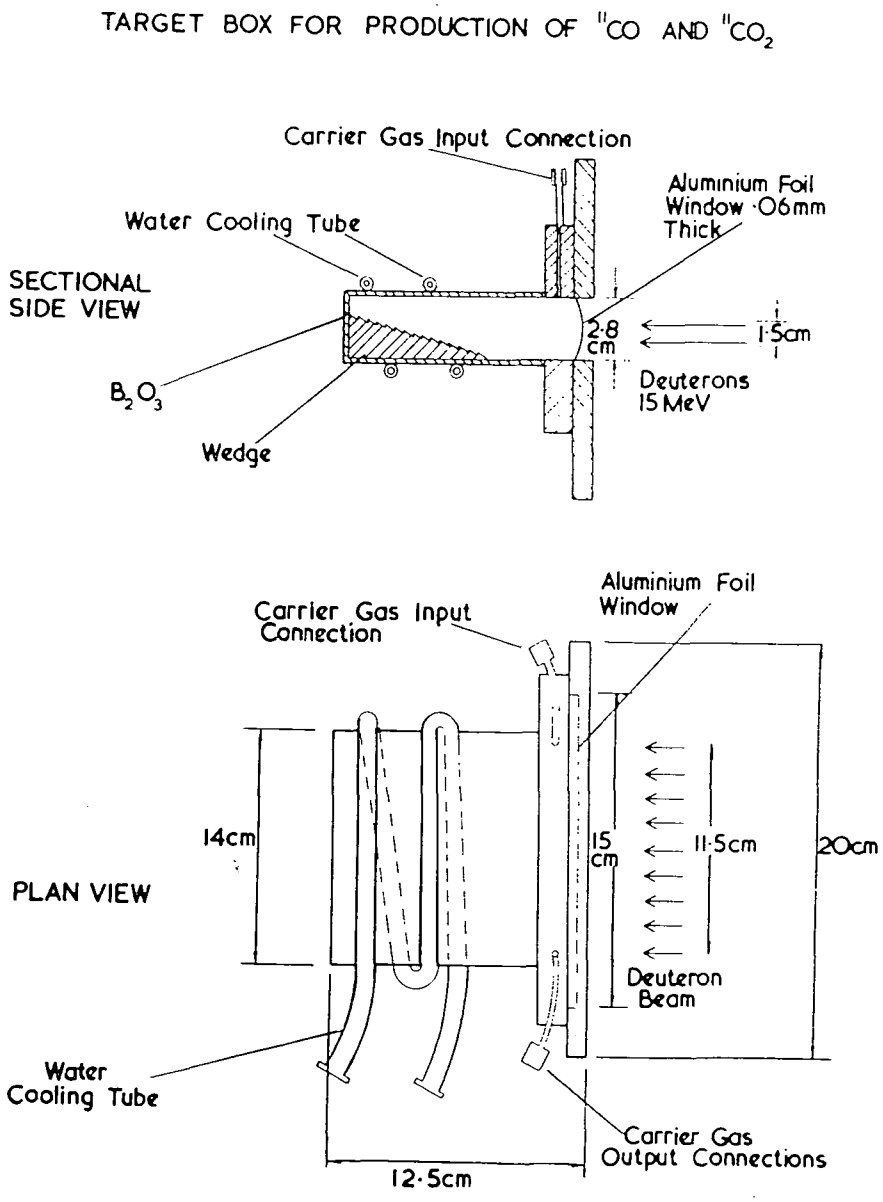

Figure 1

Cyclotron Target for production of ^{11}CO and $^{11}CO_2$.

(*) This method has been developed from that previously used in our laboratories, and described by Buckingham and Forse [7].

which supports a thin layer of boric oxide (B_2O_3) on its serrated surface. The deuteron beam enters the box through a thin aluminium foil window.

The power dissipated by the beam (which amounts to 450 W for a 30 μA beam of 15 MeV deuterons) melts the B_2O_3, and a mixture of gases labelled with ^{11}C and ^{13}N is releated from the melt. These radioactive products are swept out of the target vessel in a stream (50 ml/min) of carrier gas, which consists of 1 % carbon monoxide in helium. We cannot say what intermediate products may be formed inside the target vessel, but chromatographic analysis of the gas swept out shows that the ^{11}C leaves the vessel only in the form of carbon monoxide (95 %) or dioxide (5 %), and the ^{13}N (about 16 % of the total activity) only as molecular nitrogen. The labelled carbon dioxide is reduced to monoxide by passing the gas over "active" carbon at 900° C; it then flows through a soda-lime trap to remove any residual traces of CO_2, as shown schematically in fig. 2.

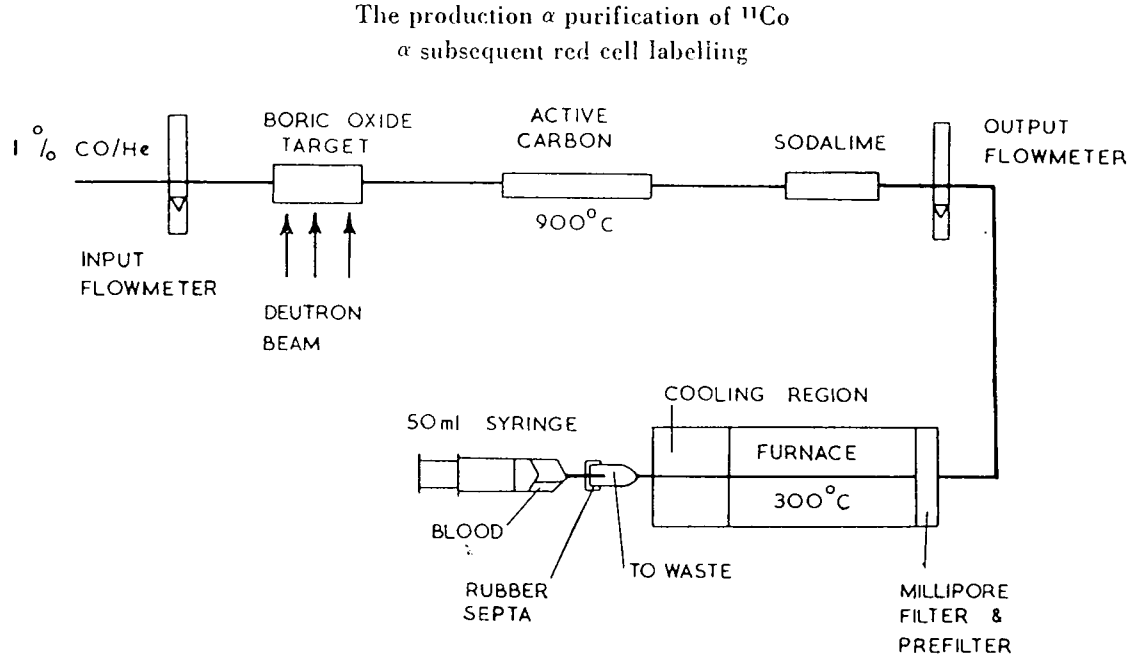

Figure 2

Flow sheet for the production and purification of ^{11}CO, and red cell labelling.

The gas to be used for labelling red cells must be sterile and pyrogen-free. Sterility is achieved by millipore filtration, whilst the risk of possible pyrogen contamination is considerably reduced by passing the gas through a small-bore silica tube at 300° C in which any protein fragments would be denatured. From this tube the gas flows to waste through a small sterile vessel from which samples can be withdrawn when required by piercing its soft rubber cap with

a hypodermic needle. Under typical operating conditions (beam current 30 μA, gas flow 50 ml/min) the specific activity of the CO at the sampling point (which incidentally is some 100 feet from the target vessel) is about 200 mC/mM.

RED CELL LABELLING TECHNIQUE

Samples of "whole blood", usually between 5 and 15 ml, are drawn into a sterile 50 ml syringe to which a little anticoagulant has previously been added. The syringe is then filled to capacity with the radioactive gas extracted from the sampling vessel, and is sealed with a sterile cap. Blood and gas are next mixed by rotating the syringe on its axis at 10 r.p.m. for 10 minutes. This method of mixing is suitably efficient (about 50 % of the CO is absorbed into the red cells in 10 minutes) and causes very little haemolysis compared with that produced, for example, by bubbling the gas through the blood, or by more violent agitation.

After mixing, the activity remaining in the gas phase is expelled to waste. Because of its very low solubility the ^{13}N-labelled nitrogen is completely removed by this and the subsequent washing steps. The red cells are now centrifuged to separate them from the plasma in which a very small amount of CO dissolves, and, after washing three times with isotonic saline, they are ready for clinical use. A typical preparation would give 50 μC of ^{11}C in 5 ml of red cells at this time.

For one series of experiments, blood samples were labelled simultaneously with both ^{11}C and ^{51}Cr simply by adding ^{51}Cr-labelled sodium chromate to the syringe before drawing in the radioactive gas and mixing. Fig. 3 shows the result obtained when a sample of such double-labelled red cells was haemolysed, and a fraction of the haemolysate was run through a column of Sephadex G-75. The ^{51}Cr was distributed between high and low molecular weight fractions, where the first corresponded with haemoglobin. This result was in agreement with the observation of Prins [8], whose suggestion that the low molecular weight substance to which the ^{51}Cr was bound was glutathione was later endorsed by Koutras *et al.* [9]. As was expected, however, the ^{11}C elution corresponded entirely with the haemoglobin.

RESULTS AND DISCUSSION

Carbon-11 labelled red cells have been used at Hammersmith Hospital in a number of clinical studies, the results of which will be reported in detail elsewhere. In this paper, however, we wish to draw attention to the result of a series of blood volume measurements that was made using cells labelled with both ^{11}C and ^{51}Cr by the method just described.

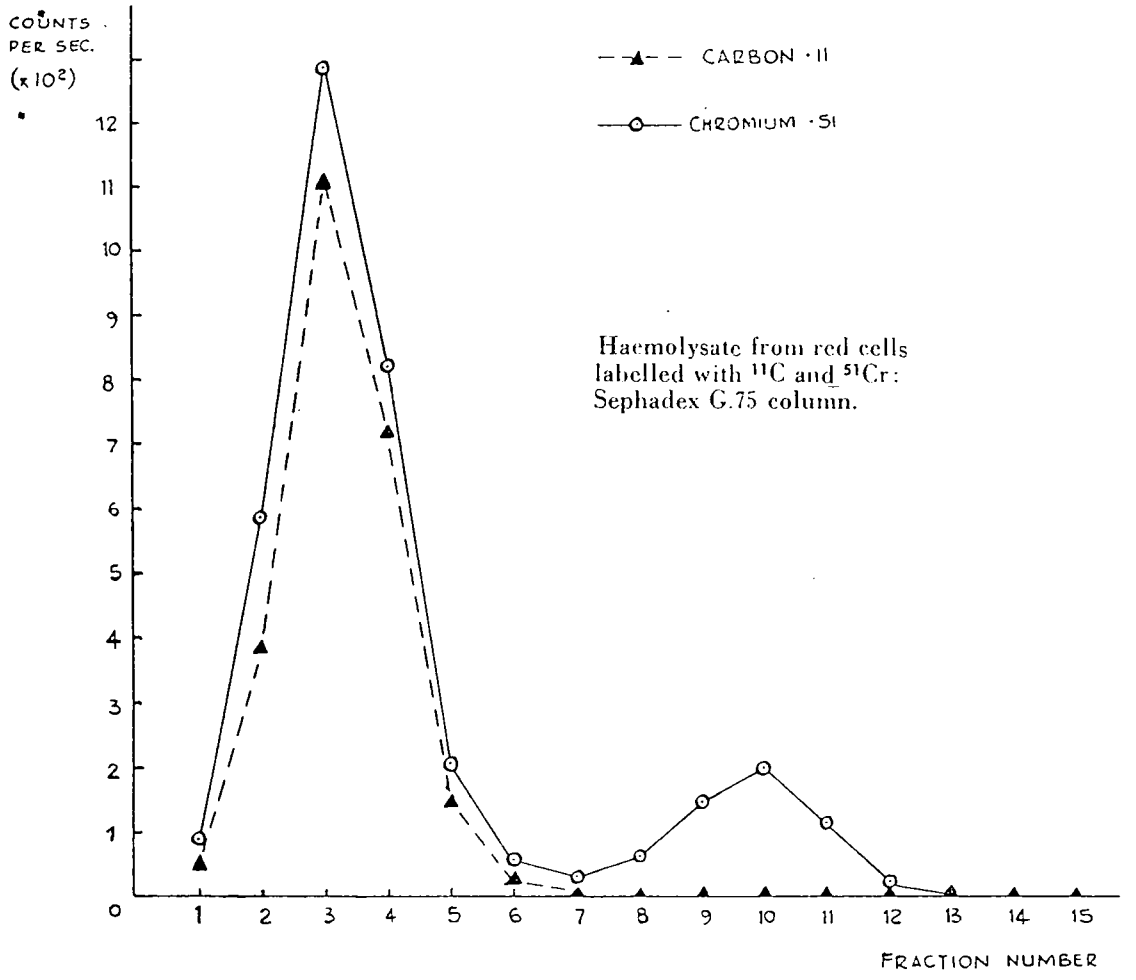

Figure 3

Elution curve for haemolysate obtained from doubly labelled red cells.

The dilution volume of ^{11}C has been found to be consistently higher than that of ^{51}Cr. Table I summarises the results of measurements made on twenty-one subjects, and shows that the average difference in dilution factor was 9.99 %, with a probable error of ± 5.8 %. Approximately ± 3 % of this error can be accounted for by counting statistics. This would therefore suggest that the method is potentially useful in practice, since the error in a blood volume measured by ^{11}C alone would certainly be less than ± 5.8 % if corrected by -9.99 %, on the assumption that the blood volume measured with ^{51}Cr-labelled red cells is correct. This is a strikingly similar result to that observed by those groups of workers [3–6] who have compared dilution volumes of non-radioactive CO (administered by a breathing technique) with those of cells labelled with ^{32}P, ^{51}Cr or ^{55}Fe.

Table I

Subject	Average difference in Dilution Factor (%)
1	9.2
2	13.8
3	20.0
4	18.4
5	6.0
6	6.5
7	9.1
8	11.1
9	10.4
10	5.65
11	9.26
12	8.87
13	10.69
14	3.28
15	12.72
16	6.95
17	22.4
19	6.45
18	8.35
20	11.8
21	11.4
Overall average	= 9.99
Probable error	= ± 5.8

$$\text{Difference in Dilution Factor \%} = \frac{^{11}\text{C vol.} - {}^{51}\text{Cr vol.}}{^{51}\text{Cr vol.}} \times 100$$

It is worth pointing out that the figures shown in column 2 of Table I are the average values of three separate dilution measurements for each subject, made over a period of about 8 to 15 minutes after the injection of the doubly labelled cells. The fact that the difference between the dilution volumes for ^{11}C and ^{51}Cr does not appear to increase during this period suggests that it is not due simply to continuous dissociation of labelled carboxyhaemoglobin. A more likely explanation has been offered by Wennesland *et al.* [9], who found that in rabbits and dogs CO accumulated in red skeletal muscle and heart muscle in amounts sufficient to account for the discrepancy. The implication is [10] that CO equilibrates rapidly between haemoglobin and myoglobin, and this is currently being investigated in our laboratories.

REFERENCES

(1) (a) BUCHANAN, J.M. and HASTINGS, A.M., *Physiol. Rev.*, 26, 120 (1946).
(b) KAMEN, M.D., "Isotopic Tracers in Biology", Chapter 10, Academic Press, New York (1957).

(2) (a) WEST, J.B. and DOLLERY, C.T., *J. Appl. Physiol.*, **17**, 9 (1962).
(b) FOWLE, A.S.E., MATTHEWS, C.M.E. and CAMPBELL, E.J.M., *Clin. Sci.*, **27**, 51 (1964).
(3) ROOT, W.S., ALLEN, T.H. and GREGERSEN, M.I., *Am. J. Physiol.*, 175, 233 (1953).
(4) NOMOF, N., HOPPER, J., BROWN, E., SCOTT, K. and WENNESLAND, R., *J. Clin. Invest.*, **33**, 1382 (1954).
(5) NICKERSON, J.L., SHARPE, L.M., ROOT, W.C., FLEMING, T.C. and GREGERSON, M.I., *Fed. Proc.*, **9**, 94 (1950).
(6) WENNESLAND, R., NOMOF, N., BROWN, E., HOPPER, J. and BRADLEY, B. *Proc. Soc. Exper. Biol. and Med.*, **96**, 655 (1957).
(7) BUCKINGHAM, P.D. and FORSE, G.R., *Int. J. Appl. Rad. Isotopes*, 14, 439 (1963).
(8) PRINS, H.K., *Vox. Sang. (Basel)*, **7**, 370 (1962).
(9) KOUTRAS, G.A., HATTORI, M., SCHNEIDER, A.S., EBAUGH, F.G. Jr., and VALENTINE, W.M., *J. Clin. Invest.*, **43**, 323 (1964).
(10) HALDANE, J. and SMITH, J.L., *J. Physiol.*, **25**, 331 (1899).

International Journal of Applied Radiation and Isotopes, 1966, Vol. 17, pp. 151–154. Pergamon Press Ltd. Printed in Northern Ireland

A Cyclotron Method for the Production of Fluorine-18

J. C. CLARK and D. J. SILVESTER
Medical Research Council Cyclotron Unit, Hammersmith Hospital, London

(*First received* 9 *June* 1964 *and in revised form* 18 *August* 1965)

Fluorine-18 is produced, with yields of up to 40 mc/hr, by the bombardment of water contained in a suitable target held in the external α-particle beam of a 30 MeV cyclotron: a method is described which is in routine use to produce samples for medical research purposes.

UNE METHODE EMPLOYANT UN CYCLOTRON POUR PRODUIRE DU FLUOR-18

Le fluor-18 se produit, avec des rendements de jusqu'à 40 mc/hr, par le bombardement de l'eau contenue dans une cible située dans le faisceau extérieur de particules α d'un cyclotron de 30 MeV: on décrit une méthode qui est en usage régulier pour la production d'échantillons destinés à la recherche médicale.

ЦИКЛОТРОННЫЙ МЕТОД ДЛЯ ПОЛУЧЕНИЯ ФТОРА-18

Фтор-18 получается с выходом до 40 мк/час посредством облучения воды, заключенной в специальной мишени, установленной во внешнем луче α-частиц 30 мегаэлектронвольтного циклотрона. Описывается метод уже использованный для получения образцов в целях медицинских исследований.

EINE ZYKLOTRONMETHODE FÜR DIE ERZEUGUNG VON FLOUR-18

Fluor-18, mit Erträgen bis zu 40 mc/Stunde, ist erzeugt bei der Bombadierung von Wasser, enthalten in einer Aufprallfläche und festgehalten in dem äusseren α-Massenteilchenstrahl eines 30 MeV Zyklotrons: eine Methode wird beschrieben welche im normalen Gebrauch ist, um Proben für Medizinische Versuchszwecke zu erzeugen.

INTRODUCTION

FLUORINE-18 is essentially a pure positron-emitting isotope which, with a half-life of 109·7 min,[1] is the longest-lived radioisotope of the element. It was first reported as a product of various cyclotron-induced nuclear reactions in 1937[2–5] and the first tracer studies with F^{18} were carried out with cyclotron produced material.[6,7]

That F^{18} could also be made in a nuclear reactor, by the irradiation of salts containing lithium and oxygen, was first reported by KNIGHT *et al.*[8] Since then numerous papers [9–19] have appeared from reactor centres in many parts of the world describing a variety of techniques which may be adopted to isolate it, either "carrier-free" or otherwise, from the irradiated material and contaminating activities.

The yields of F^{18} obtained by these techniques are generally substantially higher than those which have been achieved by previously reported methods using accelerators.[20–24] In fact, however, even higher yields can be obtained very conveniently with an accelerator under suitable conditions. The investigations for which this isotope is at present produced in the Medical Research Council's Cyclotron Unit require that it should be supplied to the clinician concerned in a high specific activity solution, either as fluoride or fluoroborate, suitable for clinical injection: the purpose of this paper is to describe the latest developments in a method of

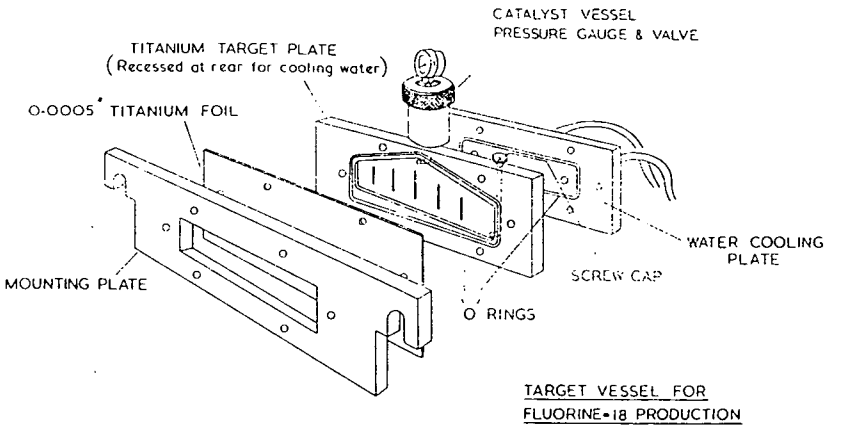

FIG. 1. Target vessel for F^{18} production.

production which has been in routine use since early 1963.

METHOD AND DISCUSSION

Fluorine-18 is made on the MRC Cyclotron by bombardment of water in the external 30 MeV α-particle beam; 10 ml of water are contained in a specially designed titanium vessel, an exploded view of which can be seen in Fig. 1. The α-beam passes through a thin (0·0005 in.) titanium foil on the front of the target, striking the water which is held in a shallow depression (the overall dimensions of which are 5·25 in. × 2 in. × 0·062 in.) in the main titanium target plate. The back of this plate is water-cooled, and the front foil is air-cooled, to carry away the thermal power, about 900 W, dissipated by the beam. The water is injected into the vessel, and removed after bombardment, through a hole which is sealed with a screw cap during bombardment, by means of a syringe fitted with a tap and a needle which is long enough to reach to the lowest point inside the vessel.

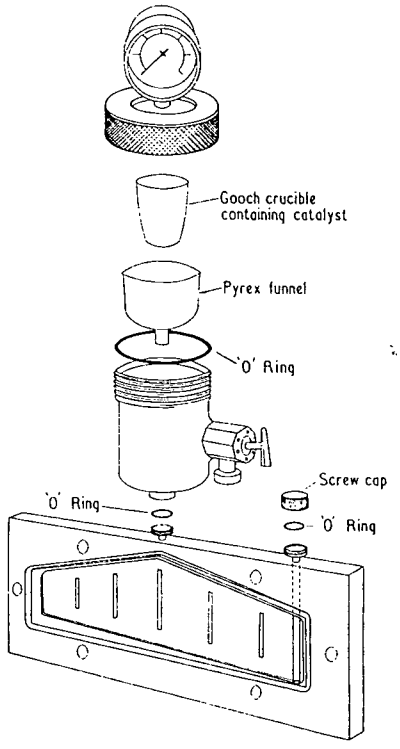

FIG. 2. Target plate and catalyst vessel.

The intensity of the ionising radiation produced by the beam causes partial decomposition of the water, and hydrogen and oxygen are liberated. These radiolytic gases are recombined, within the sealed target system, by means of the catalyst (Deoxo catalyst, Model D, supplied by Engelhard Industries Ltd., Baker Platinum Division) contained in the vessel shown in detail in Fig. 2. Before the water is put into the target, the whole assembly is flushed with oxygen and pressure-tested up to 40 lb/in^2 by connecting an oxygen cylinder to the valve on the catalyst vessel. During bombardment, the pressure inside the target is indicated by means of the gauge on top of the catalyst vessel (which can be viewed from the cyclotron control room by closed-circuit television). Starting from atmospheric pressure, it

rapidly increases to 10–15 lb/in^2 when the beam is brought on, remains at about that value throughout bombardment, fluctuating with beam current, and drops to 3–4 lb/in^2 after bombardment. This excess pressure must be released by opening the valve before the screw cap is opened to withdraw the water.

Fluorine-18 is the product of the nuclear reactions $O^{16}(\alpha, pn)$ and $O^{16}(\alpha, d)$ for which the threshold energies are 23·2 MeV and 20·4 MeV respectively, and for which the total cross section is about 100 mbarns at 30 MeV.[25] In practice, using the target described, a 1-hr bombardment at a beam current of 35 μA yields about 40 mc of F^{18}. Without the catalyst in the sealed system, the radiolytic gas pressure builds up rapidly and soon causes the thin titanium foil to burst. When a simple splash trap was used in place of the catalyst vessel, and the target was bombarded at atmospheric pressure by permitting the radiolytic gases to escape, yields were only—at most—a quarter of those which are obtained with catalyst in a sealed vacuum.

Immediately after bombardment, the active solutions are usually left in the target vessel for about 20 min to allow any very short-lived contaminating species to decay. The longest-lived of these has been identified as O^{15}, which has a 2-min half-life and could result from $O^{16}(\alpha, \alpha n)$ and $O^{16}(n, 2n)$ reactions. The only other radioactive contaminants to have been found in the samples are traces of V^{48} (16·1 days) and Cr^{51} (17·8 days), identified by chemical separation and γ-spectroscopy after the F^{18} had decayed. These contaminants result from recoils following nuclear reactions occurring in the titanium foil, but their activity amounts to not more than about 1 μc at the end of bombardment.

In early experiments on this method of production the target vessel used was made of aluminium, in which less long-lived activity accumulates than in titanium. However, it was found that much of the F^{18} which was produced remained adsorbed on the aluminium surfaces when the active solution was removed from this vessel. This loss could be prevented by using a sodium bicarbonate buffer solution (pH = 8, 394 mg $NaHCO_3$/l.) instead of pure water, but then substantial quantities (about 50 μg/ml) of aluminium were found in the solutions after bombardment. Using a titanium vessel and pure water, the F^{18} losses through surface adsorption are negligible, and less than 1 μg titanium/ml (the limit of detection for the ring-oven test we used) has been found in solution after bombardment.

If the subsequent use of the isotope requires it, all radioactive and inactive contaminants can be readily removed by a simplified version of the method described by STRANKS,[18] whereby concentrated H_2SO_4 is added to the active target solution in a Polythene apparatus and, on warming, aqueous HF^{18} is distilled into a trap in a stream of nitrogen gas. In the clinical work for which the isotope has so far been required, however, this purification step has not proved necessary.

The F^{18} present in the target solution after bombardment is, of course, carrier-free. Various paper-electrophoresis and chromatography experiments have indicated that it is not in the form of simple fluoride ions, but is complexed in some as yet undetermined manner. The same experiments have also shown, however, that the complexed F^{18} very readily exchanges with a few micrograms of inactive fluoride ions, giving solutions of high specific activity ^{18}F-fluoride.

In preparing F^{18}-fluoroborate solutions the method used is based on that described by ASKENASY *et al.*[26] The target solution (10 ml) is reduced to about 2 ml by evaporation in a small beaker under a radiant heater. The solution is transferred to a test-tube containing 4 mg KBF_4 and is acidified with 0·1 ml 4 M HCl. The tube is placed in a boiling water-bath for 20 min, during which time isotopic exchange takes place, and then the solution is neutralized by addition of a few drops of 1 M $NaHCO_3$. Fluoride ions are removed by passing the solution through a small column of chromatographic alumina (approx. 1·5 × 0·25 in.). Using this technique, about 70 per cent of the F^{18} appears as labelled fluoroborate. The entire operation can be carried out within about an hour from the end of bombardment, so that samples having activities of up to 20 mc can readily be obtained.

Acknowledgments—It is a pleasure to acknowledge the extensive preliminary work on F^{18} production

carried out in this Unit by Dr. FRANCOIS, Dr. MATTHEWS and Mr. TURNER, and the assistance of Mr. SHARP and Mr. FINDING in the design of the present target. Our thanks are also due to the Director of the Unit, Mr. D. D. VONBERG, for his advice and for permission to publish this paper.

REFERENCES

1. MAHONY J. D. and MARKOWITZ S. S. *J. inorg. nucl. Chem.* **26,** 907 (1964).
2. SNELL A. H. *Phys. Rev.* **51,** 143 (1937).
3. DUBRIDGE L. A., BARNES S. W. and BUCK J. H. *Phys. Rev.* **51,** 995 (1937).
4. POOL M. L., CORK J. M. and THORNTON R. L. *Phys. Rev.* **52,** 239 (1937).
5. YASAKI T. and WATANABE S. *Nature, Lond.* **141,** 787 (1938).
6. VOLKER J. F., HODGE H. C., WILSON H. J. and VOORHIS S. N. VAN *J. biol. Chem.* **134,** 543 (1940).
7. VOLKER J. F., SOGNNAES R. F. and BIBBY B. G. *Am. J. Physiol.* **132,** 707 (1941).
8. KNIGHT J. D., NOVEY T. B., CANNON C. V. and TURKEVICH A. *Radiochemical Studies: The Fission Products*, Bk. 3, pp. 1916–1923, McGraw-Hill, New York (1951).
9. BERNSTEIN R. B. and KATZ J. J. *Nucleonics* **11,** (10) 46 (1953).
10. BANKS H. O., JR. *Nucleonics* **13,** (12) 62 (1955).
11. ANBAR M. *Production and Use of Short-Lived Radioisotopes from Reactors*, Vol. II, p. 227, IAEA, Vienna (1963).
12. BALCARCZYK L. and LANZEL E. *Atomkernenergie* **8,** 404 (1963).
13. BEG K. and BROWN F. *Int. J. appl. Radiat. Isotopes* **14,** 137 (1963).
14. BRESESTI M., DEL TURCO A. M. and OSTIDICH A. *Radiochim. Acta* **2,** 49 (1963).
15. FELIX F. W., PARRWITZ D. and SZABO DE BULS, E. *Production and Use of Short-Lived Radioisotopes from Reactors*, Vol. I, p. 105, IAEA, Vienna (1963).
16. NAGY G. A. and BEREI K. *J. inorg. nucl. Chem.* **26,** 659 (1963).
17. STANG L. G., JR. *Production and Use of Short-Lived Radioisotopes from Reactors*, Vol. I, p. 3, IAEA, Vienna (1963).
18. STRANKS D. R. *Inorganic Syntheses*, Vol. VII, p. 150, McGraw-Hill, New York (1963).
19. THOMAS C. C., JR., SONDEL J. A. and KERNS R. C. *Int. J. appl. Radiat. Isotopes* **16,** 71 (1965).
20. GARRISON W. M. and HAMILTON J. G. *Chem. Rev.* **49,** 258 (1951).
21. MYERS H. M., HAMILTON J. G. and BECKS H. *J. dent. Res.* **31,** 743 (1952).
22. MURIN A. N., NEFEDOV V. D. and YUTLANDOV I. A. *Usp. Khim.* **24,** 527 (1955).
23. CARLSON C. H., SINGER L., SERVICE D. H. and ARMSTRONG W. D. *Int. J. appl. Radiat. Isotopes* **4,** 210 (1959).
24. HARDWICK J. L., FREMLIN J. H. and MATHIESON J. *Br. dent. J.* **104,** 47 (1958).
25. SAITO K., NOZAKI T., TANAKA S., FURUKAWA M. and CHENG H. *Int. J. appl. Radiat. Isotopes* **14,** 357 (1963).
26. ASKENASY H. M., ANBAR M., LAOR Y., LEWITUS Z., KOSARY I. Z. and GUTTMANN S. *Am. J. Roentg.* **88,** 350 (1962).

Using cyclotron-produced isotopes at Hammersmith Hospital

by J. C. Clark, C. M. E. Matthews, D. J. Silvester and D. D. Vonberg
Medical Research Council Cyclotron Unit, Hammersmith Hospital, London, England

At Hammersmith Hospital we have been using the Medical Research Council cyclotron to explore a wide variety of accelerator-produced radionuclides for new applications in nuclear medicine. So far we have studied some 36 radionuclides, and thirteen are currently being produced (see Table 1). In addition, we are using the cyclotron to produce charged-particle beams for radiobiological studies as well as a fast-neutron beam for radiotherapy.

There are various reasons for preferring accelerator-produced isotopes to the more usual reactor-produced isotopes of the same element (*1*). For example, accelerators open up a broad new range of isotopes to the medical community—increasing the chance of obtaining isotopes with acceptable physical properties for the problem in hand. In addition, the ideal half-life for an isotope for many medical purposes is inconveniently short for transport from producer to remote user. A cyclotron which produces short-lived isotopes directly in a hospital offers an excellent solution.

The Hammersmith cyclotron

The cyclotron at Hammersmith (*2, 3*) has a higher energy (16-Mev deuterons) than those now gaining popularity in the United States (6–8 Mev deuterons), but of course it is larger and more costly. The machine forms part of the equipment of the Medical Research Council Cyclotron Unit which provides radiation and radioisotopes for medical research, diagnosis and therapy. Two other accelerators—an 8-Mev electron linear accelerator and a 2-Mev Van de Graaff machine—provide additional radiation sources for radiobiological studies but are of course too low in energy for isotope production. The cyclotron runs for about two-thirds of its time on isotope production; the remaining one-third provides radiation for radiobiological work and for radiotherapy with fast neutrons which has started recently.

Although the staff is mainly nonmedical, there is close collaboration with medical workers at Hammersmith and other centers for developing isotope applications. In addition to collaborative projects, the isotope section of the unit is also engaged on an internal program of improving detection instrumentation with camera and scanning devices and interpreting tracer experiments using an analog computer.

Christine Matthews, who is senior isotope physicist at Hammersmith, joined the Unit in 1959 after spending 5 years at the National Institute for Medical Research. She received her Ph.D. from Trinity College in Dublin as well as a B.Sc. in physiology from London University. David J. Silvester, senior radiochemist, joined the Unit in 1959 after a year as research associate at Brookhaven. Both he and John C. Clark, who came to the group in 1961, previously did postgraduate work in radiochemistry at the Univ. of Durham. Derek D. Vonberg, Director of the Cyclotron Unit since 1962, graduated in electrical engineering from London Univ., did postgraduate work in radioastronomy at Cambridge after the war and joined the Unit design team in 1949.

Production program. For production purposes radionuclides fall into two categories. The first consists of those materials that have such short half-lives that they are processed continuously "on line" during production and then piped from the accelerator to the user. The second group includes radionuclides with longer half-lives which are produced by batch methods.

This latter group can be subdivided into those radionuclides which must be used on the day they are made and those which will "keep" for several days. How long they will "keep" depends on either the loss of total activity or the rise in the proportion of long-lived contaminants.

At Hammersmith the machine running schedule is largely shaped by half-life considerations. Between 5 and 10 a.m. the machine usually makes isotopes to be processed and used later the same day (F^{18} and Fe^{52}). During the day isotopes processed and used "on line" are produced (O^{15}, N^{13} and C^{11}) alternating with radiation; research on new production methods is also carried out. In the evening, between 6 and 10 p.m., longer-lived materials are made for processing on a later day (I^{123}, Y^{87}, Cs^{129}, etc.).

Short-lived gases "on line"

In the earliest clinical work with radioisotopes from our cyclotron we used radioactive gases only for lung-function studies. More recently, however, we have also been using the gases for investigating carbon dioxide pools and for blood-volume and flow measurements. The labeled gases include

Table 1—Isotopes in demand at Hammersmith

Radioactive Substance		Decay mode and main radiation emitted (γ energy)	Method of production	Medical application	Comments
CO_2^{15}	2.0 m	β^+	$N^{14}(d,n)O^{15}$	Detection of heart shunts and measurement of regional lung blood flow	Very high solubility in blood. Label exchanges with OH^- in water.
N_2^{13}	10.0 m	β^+	$C^{12}(d,n)N^{13}$	Regional lung ventilation and blood flow	Solubility 0.013 (cf Xe^{133} — 0.16)
$C^{11}O_2$	20.5 m	β^+	$B^{10}(d,n)C^{11}$ $B^{11}(d,2n)C^{11}$	CO_2 pools and control of ventilation	Can be used in humans because dose is very low
$C^{11}O$	20.5 m	β^+	$B^{10}(d,n)C^{11}$ $B^{11}(d,2n)C^{11}$	Blood volume	Very low dose measurement can be repeated
F^{18}	1.83 h	β^+	$O^{16}(\alpha,pn)F^{18}$	Detection of bone lesions	More rapidly cleared from blood than Sr^{87m}
Sr^{87m}	2.9 h	I.T., γ (0.388 Mev)	Milked from Y^{87} (q.v.)	Detection of bone lesions	
KBF_4^{18}	1.83 h	β^+	$O^{16}(\alpha,pn)F^{18}$	Brain scanning	
Nb^{90}	14.6 h	E.C., β^+, γ (0.14 — 2.3 Mev)	$Zr^{90}(d,2n)Nb^{90}$	Possible detection of tumors	Concentrates in stomach High uptake in rat transplanted tumors
Cs^{129}	32.4 h	E.C., γ (0.385 Mev)	$I^{127}(\alpha,2n)Cs^{129}$ $I^{127}(\alpha,n)Cs^{130}$	Coronary flow and heart scanning	
Cs^{130}	29.1 m	E.C., β^+			
Rb^{81}	4.7 h	E.C., β^+, γ (0.45, 1.1 Mev)	$Br^{79}(\alpha,2n)Rb^{81}$ $Br^{79}(\alpha,n)Rb^{82}$		Rb^{81} parent of 13-sec Kr^{81m} (q.v.)
Rb^{82m}	6.3 h	E.C., β^+, γ (0.55, 0.78 Mev)			
K^{43}	22 h	β^-, γ (0.63, 0.37 Mev)			Longer half-life useful for longer K metabolic studies
I^{123}	13 h	E.C., γ (0.16 Mev)	$Sb^{121}(\alpha,2n)I^{123}$	Thyroid scanning	
Cr^{51}	27.8 d	E.C., γ (0.32 Mev)	$V^{51}(d,2n)Cr^{51}$	Ultra-high specific activity for lymphoid cell labelling	Reduces radiation dose
Cu^{64}	12.8 h	E.C., β^+, β^-, γ (1.34 Mev)	$Zn^{64}(d,\alpha)Cu^{64}$	High specific activity	
Ga^{68}	68 m	E.C., β^+	Milked from Ge^{68} (q.v.)		
Ge^{68}	275 d	E.C.	$Zn^{68}(\alpha,2n)Ge^{68}$		Parent of Ga^{68} (q.v.)
I^{124}	4.2 d	E.C., β^+, γ (0.60–2.26 Mev)	$Sb^{121}(\alpha,n)I^{124}$ $Sb^{123}(\alpha,3n)I^{124}$		
I^{125}	57 d	E.C., γ (0.035 Mev)	$Sb^{122}(\alpha,2n)I^{125}$		
Kr^{79}	33 h	E.C., β^+, γ (0.26 Mev many others)	$Br^{79}(d,2n)Kr^{79}$		
Kr^{81m}	13 s	I.T., γ (0.19 Mev)	Milked from Rb^{81} (q.v.)	Inert gas solution for blood flow studies	Daughter of Rb^{81}. Low solubility and very low radiation dose
Mn^{52}	5.6 d	E.C., β^+, γ (0.73 Mev)	$Cr^{52}(d,2n)Mn^{52}$		
Mn^{54}	291 d	E.C., γ (0.84) Mev)	$Fe^{56}(d,\alpha)Mn^{54}$		
Fe^{52}	8 h	E.C., β^+, γ (0.16 Mev)	$Cr^{50}(\alpha,2n)Fe^{52}$	Fe uptake in organs and marrow scanning	
Y^{87}	80 h	E.C., β^+, γ (0.48 Mev)	$Rb^{85}(\alpha,2n)Y^{87}$		Parent of Sr^{87m} (q.v.)
			OCCASIONAL DEMAND		
Ag^{110m}	253 d	β^-, γ (0.66, 0.94 Mev)	$Pd^{110}(\alpha,2n)Ag^{110m}$		
As^{72}	26 h	E.C., β^+, γ (0.63, 0.84 Mev)	$Ga^{69}(\alpha,n)As^{72}$	Brain scanning	
As^{74}	17.5 d	E.C., β^+, γ (0.6 Mev)	$Ge^{74}(d,2n)As^{74}$ $Ge^{73}(d,n)As^{74}$	Brain scanning	
Be^7	53 d	E.C., γ (0.48 Mev)	$Li^7(d,2n)Be^7$		γ standard
Bi^{206}	6.4 d	E.C., γ (many)	$Pb^{206}(d,2n)Bi^{206}$		
Ce^{139}	140 d	E.C., γ (0.166 Mev)	$La^{139}(d,2n)Ce^{139}$		γ standard
Cd^{109}	470 d	E.C. to Ag^{109m}, γ (0.88 Mev)	$Ag^{109}(\alpha 2n)Cd^{109}$		γ standard, Ag^{109m}
Rb^{83}	83 d	E.C., γ (0.53 Mev)	$Kr^{83}(d,2n)Rb^{83}$ or $Br^{81}(\alpha,2n)Rb^{83}$	Coronary flow and heart scanning	
Rb^{84}	33 d	E.C., β^+, γ (0.89 Mev)	$^{84}Kr(d,2n)Rb^{84}$ or $Br^{81}(\alpha,n)Rb^{84}$		
Se^{72}	8.4 d	E.C.	$Ge^{70}(\alpha,2n)Se^{72}$		Parent As^{73} (q.v.) potential cow system
Se^{75}	127 d	E.C., γ (0.27, 0.14 Mev)	$As^{75}(d,2n)Se^{75}$		
Sr^{85}	65 d	E.C., γ (0.51 Mev)	$Rb^{85}(d,2n)Sr^{85}$		
V^{48}	16.1 d	E.C., β^+, γ (0.99, 1.31 Mev)	$Ti^{46}(d,2n)V^{48}$		
Zn^{65}	245 d	E.C., β^+, γ (1.12 Mev)	$Cu^{65}(d,2n)Zn^{65}$		γ standard

O_2^{15}, CO_2^{15}, CO^{15}, $C^{11}O$ and N_2^{13} (*4–8*) as well as reactor-produced Xe^{133}. We expect N_2^{13} to partly replace Xe^{133} in the future.

The counting system for lung-function studies with all the radioactive gases consist of two pairs of scintillation counters—one pair for each lung—with one crystal behind and one in front of the chest. In each pair the outputs of the two counters are summed so that counts are recorded from a section of lung between the counters. Two different types of collimators are used: with one type the section of lung is cylindrical and with the other it is a horizontal slab. Although coincidence counting was used in the early work, this method gives too low a counting rate for accurate results in this application, and we have abandoned it. Profile scanning of the lungs is also used (*9*).

CO_2^{15} for regional blood flow and detecting cardiac shunts. When a patient takes a breath of carbon dioxide labeled with O^{15} (2.0-min half-life), there is an initial rise in counting rate over the chest followed by a rapid fall as the radioactive gas is

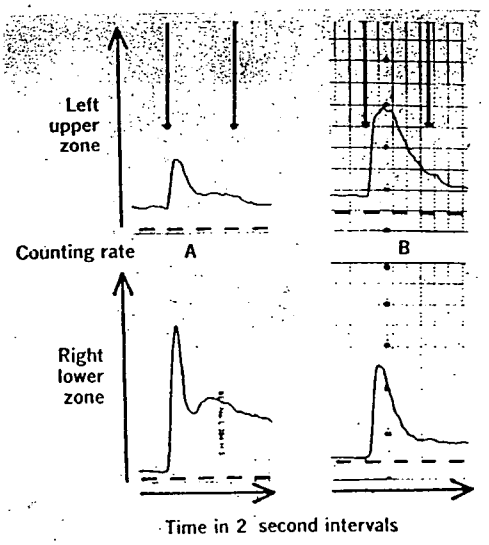

FIG. 1. To detect cardiac shunts radioactive blood (after breath of CO_2^{15}) that returns to lungs through shunt is measured. Counting rates over left upper and right lower zones are measured (A) before and (B) after operation for closure of left-to-right cardiac shunt. In (A) second peak due to recirculation of radioactive blood can be seen. More rapid blood flow in lower zone gives more rapid clearance of radioactivity than in upper zone (*8*)

absorbed from the alveolar air by the blood and removed from the counting field. The uptake by the blood is very rapid because of the high solubility of the gas—a solubility which is increased by the exchange of the O^{15} label with OH^- ions in water through the equilibrium with bicarbonate and carbonic acid. Therefore the counting rate over the chest is almost entirely due to radioactivity in the blood, and the rate of clearance from the counting field depends only on blood flow.

It has been shown experimentally in the isolated dog lung that the exponential slope of the counting-rate curve is proportional to blood flow for a given lung water volume (*10*). Therefore this slope can be used as a measure of regional blood flow. However, the slope is reduced in the presence of edema because of the increased water volume. An advantage of this method of measuring regional blood flow is that no venepuncture is needed.

If a left-to-right cardiac shunt is present, some radioactive blood will return to the lungs through the shunt more rapidly than blood that recirculates by the normal route. When this happens, a second peak occurs on the counting-rate curve because of the rapid recirculation (Fig. 1). This method of detecting shunts can be used to evaluate the success of operations for closure of the shunt (*11, 12*).

The O^{15} used in these studies is produced from the $N^{14}(d,n)O^{15}$ reaction by bombarding nitrogen with 4-Mev deuterons. The target box has a 1-mm-thick magnesium window which reduces the energy of the 15-Mev deuterons and at the same time produces Na^{22} by the $Mg^{24}(d,\alpha)Na^{22}$ reaction. The O^{15} yield only increases by 50% if the maximum available deuteron energy is used, but the proportion of other isotopes produced—mainly N^{13} and C^{11}—is greatly increased.

In the gas-flow system 4% oxygen carrier in nitrogen is passed through the target box at a flow rate of ~400 ml/min. The gas issuing from the target box is freed from the ozone and oxides of nitrogen by absorbers.

Carbon dioxide labeled with O^{15} is produced by passing the labeled molecular oxygen over heated active carbon. Carbon monoxide produced at the same time is converted to carbon dioxide with heated cupric oxide. Provision is made for diluting the product gas with air, and the diluted gas passes through a bulb in an ionization chamber for measurement. Yields of 240 mc/min at a specific activity of 255 mc/mM result at a flow rate of 700 ml/min and a beam current of 35 μa.

Xe^{133} and N_2^{13} for regional ventilation and blood-flow measurements. Reactor-produced Xe^{133} (5.7-day half-life) was the first radioactive gas used for lung-function studies (*13, 14*). To measure regional blood flow using either Xe^{133} or N_2^{13} (10-min half-life) the radioactive gas is dissolved in saline and injected intravenously. When it reaches the lungs, nearly all the gas is evolved into the alveolar air so that the counting rate over a region of lung is proportional to the amount of radioactivity carried to that region and therefore to its blood flow. This method gives relative regional blood flow as a fraction of the cardiac output whereas the CO_2^{15} method gives flow per unit volume of lung water.

Regional ventilation has been measured in a number of different ways. For example, in the single-breath method, the peak counting rate over the lungs is recorded after a rapid single inspiration of radioactive gas. In the wash-in and wash-out method, on the other hand, the radioactive gas is rebreathed in a closed circuit for a few minutes after which the subject breathes room air normally. The counting rate curves during wash in and wash out of the gas are then analyzed to obtain regional ventilation.

The radioactive gas used to measure ventilation must have a low solubility in blood. Otherwise the peak counting rate will be reduced in the single-breath method because of the rapid uptake of the gas by the blood, and the shape of the wash-in and wash-out curves will depend not only on ventilation but also on the removal of radioactivity by the arterial blood and its return in the venous blood.

The solubilities of both Xe^{133} and N_2^{13} are low enough for the single-breath method. But in the wash-in and wash-out method the Xe^{133} uptake in the blood and its return from the tissues can cause serious errors; moreover the counting rate over the chest is affected by radioactivity in the chest wall (*15*). Therefore N_2^{13}, which has only about a tenth of the solubility of Xe^{133}, is much more suitable for this method. N_2^{13} is also more suitable for the single-breath method because the measurement must be related to lung volume in the counting field which cannot be accurately determined with Xe^{133} (*15*). Therefore we plan to change to N_2^{13} as soon as we can produce solutions of this gas routinely.

The single-breath method will give no values for ventilation for poorly ventilated regions because little gas will enter these regions in a single breath; but the other method will give the proportion of alveoli with different ventilations per unit volume in the region examined. Moreover, the method has the advantage that the measurements are made under conditions of normal breathing.

Both CO_2^{15} and Xe^{133} can be used to measure blood flow. In normal subjects in the sitting position blood flow per unit lung volume increases

from apex to base of the lung whereas in patients with severe mitral stenosis this pattern is reversed (*16, 17*). The physiology of the distribution of lung blood flow has been worked out in detail using the isolated perfused dog lung (*18*). The absorbed doses for lungs and gonads are shown in Table 2 for the radioactive gases (*5, 6, 8, 19*). The dose from a series of tests is normally of the same order of magnitude as from a chest x-ray.

The N^{13} is produced by bombarding carbon with deuterons by the $C^{12}(d,n)N^{13}$ reaction. The target material is a layer of active carbon granules supported in the external deuteron beam by a graphite grid. This replaces the nichrome grid which was used to produce gaseous N_2^{13} by Nicholas, Silvester and Fowler (*20*) in studying nitrogen fixation in bacterial cells and their extracts.

Carrier gas is passed through the target to sweep out the volatile N^{13} compounds released from the active carbon. Any oxides of nitrogen are reduced to nitrogen with heated copper. Various carrier gases have been used including argon, methane and hydrogen. Argon gives high yields but also contributes the long-lived A^{41} contaminant. Hydrogen, on the other hand, gives lower yields but has the advantage of being readily removed from the gas phase by conversion to water, giving a large increase in specific activity.

When solutions of N_2^{13} are needed, the active carbon is outgased under vacuum before use, and a carrier gas of high-purity hydrogen is used. With a carrier gas flow of 50-ml/min hydrogen and a deuteron beam current of 35 μa, gas samples with a specific activity of 5 curies/liter are obtained after the hydrogen is oxidized with cupric oxide at 700°C. If this gas is then mixed with water or normal saline, solutions are produced containing 100–150 μc/ml of N_2^{13}. A typical sample of 1 mc N_2^{13} in 10 ml of saline takes 10 min to prepare. This solution is sterile and pyrogen free because it is the product of a high-temperature combustion. The output of the furnace has a sterile demountable assembly.

$C^{11}O_2$ for studying body CO_2 pools. We have used $C^{11}O_2$ (20-min half-life) to study body CO_2 in normal volunteers (*21*). The radioactive gas was administered during ¼–½ min of rebreathing, and radioactivity in arterial blood samples was measured at intervals up to ~1 hr after injection. The results indicate that there is a rapid exchange between blood and extracellular CO_2 and a slower exchange with an intracellular pool. This hypothesis explains the rate of rise of P_{CO_2} (partial pressure of CO_2 in blood) during rebreathing which could not be explained by models in which the rate of exchange of CO_2 throughout the body was limited only by blood flow.

We are now extending these experiments using an improved technique in which radioactivity and CO_2 in expired air are measured continuously. Since ~0.5 mc is given, the doses are one tenth of those shown in Table 2. Results are being analyzed with an analog computer using a model that includes rate limitations due to both blood flow and extracellular-intracellular exchange.

The control of ventilation is also simulated with this model (*22*), and we find that a number of different experiments can all be matched with the same value for pool sizes and exchange rates in a given subject. This new model includes separate pools for dissolved CO_2 and bicarbonate and takes into account the interchange with buffer anions. We hope that this model will help us understand the control of the acid-base balance in the body.

The C^{11} is produced by the $B^{10}(d,n)C^{11}$ and $B^{11}(d,2n)C^{11}$ reactions by bombarding boron with deuterons. The target material is boric oxide which is kept in the molten state by the power dissipated by the beam (450 watts at 30 μa) and is prevented from running off the wedge by surface tension. A mixture of carbon monoxide and carbon dioxide labeled with C^{11} together with some N_2^{13} is released from the molten boric oxide.

When C^{11}-labeled carbon dioxide is needed, a flow of 100 ml/min of 5% CO_2 in helium is used as a carrier sweep gas, and the C^{11}-labeled carbon monoxide is oxidized to carbon dioxide with heated cupric oxide. The N^{13}-labeled nitrogen is removed in batches by trapping the carbon dioxide at −196°C.

$C^{11}O$ for red-cell volume measurements. To measure circulating red-cell volumes one conventionally uses an isotope dilution technique with red cells labeled with Cr^{51}. But the long half-life of Cr^{51} precludes its use in infants and expectant mothers because the radiation dose would be too high and in patients when serial measurements at short intervals are required. For these applications a short-lived label must be used.

The affinity of hemoglobin for carbon monoxide is well known, and because this gas labeled with short-lived C^{11} is readily available from our cyclotron, we have developed a routine method for labeling red cells with this isotope (*23*).

The target arrangement and bombardment conditions are the same as for $C^{11}O_2$ but when we need $C^{11}O$ we use a flow of 50 ml/min of 1% carbon monoxide in helium as carrier sweep gas. The carbon dioxide is reduced to carbon monoxide using active carbon at 900°C. The gas then flows through a soda lime trap to remove the last traces of CO_2.

For red-blood-cell labeling high specific activity is needed. This is achieved by using small carrier concentrations, low flow rates and high beam currents. The gas must also be sterile and pyrogen-free. We therefore use Millipore filtration and bake the gas in a small silica tube furnace. The gas is then removed by a sterile septum straight into a 50 ml disposable syringe which contains the "whole-blood" sample. About 15 ml of blood are then mixed with 35 ml of the C^{11}-labeled 1% carbon monoxide/helium mixture by gently rotating the syringe on its axis at 20 rpm for 10 min. Because the N^{13}-labeled molecular nitrogen has a very low solubility, it does not interfere with the radiochemical

Table 2—Absorbed tissue doses from isotopes

Isotopes	Absorbed dose (millirads) to: Lungs	Gonads
Single breath 5 mc for 20 sec		
$C^{11}O_2$	80 (apex)	18
CO_2^{11}	220 (apex)	55
Single breath or injection 1 mc for 30 sec		
Xe^{133}	14	0.1→0.3
N_2^{13}	35	0.1→0.5
Rebreathing 1 mc/l for 2 min		
Xe^{133}	57	2→3
N_2^{13}	136	0.5→2

purity of the red cells. Yields of 7 mc/min are obtained in the gas phase with a specific activity of 250 mc/mM at a beam current of 35μa at ~14 Mev.

Batch isotopes: F^{18} and Sr^{87m}

The longer-lived radioisotopes used at Hammersmith are produced by batch methods. F^{18} fluoride and Sr^{87m} citrate are used for detecting bone lesions—sometimes letting one see the lesions on the scan before they become visible on the x-ray (*24–26*). As Monte Blau of Roswell Park Memorial Institute has pointed out, F^{18} fluoride is more rapidly cleared from the blood than Sr^{87m} and is more suitable; however, because of its short half-life, it can only be used close to a cyclotron or reactor. Sr^{87m}, on the other hand, has the advantage that it can be milked from its longer-lived parent Y^{87} (80-hr half-life).

The dose from both F^{18} and Sr^{87m} is considerably smaller than that from the longer-lived Ca^{47} and Sr^{85} which are more often used. For example, Blau calculates the dose from F^{18} to the whole body as only 0.23 rads/mc (*24*) while we calculate it as 0.41 rads/mc allowing a factor of five for nonuniform distribution in bone. The doses from Ca^{47} and Sr^{85} are several rads per investigation.

Both osteolytic and osteoblastic lesions show an increased uptake of these isotopes compared with normal bone. The uptake is rapid and is probably due to exchange with salts of the bone crystal and not to metabolism; thus increased uptake may be due to a larger available area of crystal. Budy discusses the uptake mechanism of a number of different isotopes in bone (*27*).

The distribution of F^{18} in the body has also been considered to depend on blood flow. Using the positron camera Van Dyke and his colleagues have visualized the distribution of this uptake for the whole body and have studied the variation in uptake pattern in various diseases (*28*).

We make F^{18} in 40–60-mc batches twice a week and dispatch them to several London hospitals that are interested in bone scanning. More distant parts of the country are supplied with Y^{87} cows which are also made on a regular schedule.

Twenty-one patients have now been scanned with F^{18} by R. Morrison and J. Davey at Hammersmith. These patients either have known or suspected neoplastic changes on x-ray or have symptoms that suggest bone involvement although their x-rays are normal. Good scans have been obtained in all patients, and four positive scans were found when the x-rays were entirely normal.

For example, Fig. 2 shows a F^{18} scan of a 64-year-old patient who had a history of carcinoma of the cervical stump in May 1965 and was treated with supervoltage irradiation. She was well and free of recurrence for 1 year when she presented with severe pain in the left arm and some tenderness over the head of the left humerus. The x-rays, as Fig. 2 shows, were normal. We gave 1 mc of F^{18} intravenously and scanned the patient 1 hr later. As the scan shows, increased uptake resulted compared with the expected uptake in normal subjects, and despite the normal x-ray finding the patient was considered to have a secondary deposit in the head of the humerus. She was given a course of palliative irradiation to this secondary deposit and 5 months later was free of pain.

R. McCready of the Royal Marsden Hospital has given 1–2-mc intravenous injections of F^{18} to 47 patients. Of 15 cases with positive x-rays, 14 gave positive scans. In a further 8 positive scans, the x-rays were negative. Of the remaining cases, 19 showed negative scans and x-rays while 5 gave equivocal results. McCready has also used Sr^{87m} and finds that the bone uptake is similar to that for F^{18}. Moreover he finds that both F^{18} and Sr^{87m} give better scans in a shorter time than Sr^{85}. Since a high percentage of the scans are negative, much time is wasted if each scan takes a long time so this is an important advantage of these short-lived isotopes.

We make F^{18} by irradiating water held in a titanium vessel in the external alpha beam of the cyclotron (*29*). The essential nuclear reaction is $O^{16}(\alpha,pn)F^{18}$ for which the threshold energy is ~20 Mev. Recently we have installed an infrared TV camera which lets us observe the distribution of the beam on the target during bombardment. If the beam is kept well spread, up to 60 mc of F^{18} can be obtained from a 1-hr bombardment at 40 μa.

For purposes such as bone-lesion scanning the cyclotron target solution can be administered directly to the patients without further treatment other than sterilization because contaminating activities are negligible (only traces of Cr^{51} and V^{48} which recoil from the walls of the target vessel) and the solutions have been shown to be pyrogen free. Reactor produced F^{18}, on the other hand, must be separated from the lithium salt from which it is made and from the large quantities of tritium that are made simultaneously (*30, 31*).

The Y^{87} for the Sr^{87m} generator is produced by the $Rb^{85}(\alpha,2n)Y^{87}$ reaction. Rubidium chloride is used as the target, melted onto a copper plate which is water cooled during bombardment. The separation procedure has been described by Hillman and his group (*32*). After bombardment the rubidium chloride is removed from the target plate by dissolution in dilute hydrochloric acid containing a few milligrams of yttrium carrier. Yttrium hydroxide is precipitated and purified and finally applied in citric acid solution to an anion exchange resine column in the carbonate form.

The column consists of a 1-ml bed of amberlite CG.400 resin followed by a 4-ml bed of IRA 400 mounted in a 10-ml disposable syringe. The Sr^{87m} daughter is milked by allowing 5 ml of sterile 0.005% citric acid to flow through the resin column. The milkings are then sterilized by autoclaving or Millipore filtration. The cow system will produce pyrogen-free solutions if the milking procedure is carried out carefully.

Production yields of Y^{87} at 30 Mev are ~340 μc/μAh at the end of bombardment after chemistry. This gives a Sr^{87m} yield on milking of 240 μc/μAh at the end of bombardment. We found that the average milking efficiency for seven cows was 72%. Occasionally we find very high milking efficiencies of around 90%. Yttrium contamination of the milkings never amounts to more than 0.05% of the Sr^{87m} content at the time of milking.

KBF.[18] for brain scanning. Previously two groups have used KBF.[18] (1.8-hr half-life) for brain scanning (*33, 34*). At Hammersmith we use the F^{18} produced by alpha bombardment of water to label fluoroborate using a method similar to that described by Ashkenasy and his group (*33*).

To compare labeled fluoroborate with other radioactive substances used for brain scanning, some criterion for comparison is needed. Since many substances used for brain scanning are distributed approximately uniformly in extracellular fluid (*35*, *36*), these all give the same tumor-to-brain concentration ratio, and none of them has any particular biological advantage. Therefore the choice of the best radionuclide depends mainly on physical characteristics. In some cases it may be difficult to decide which of two radioactive substances will be best because one may have better biological properties while the other has better physical properties. Various figures of merit have been used to compare nuclides and counting systems for brain scanning (*4*, *37–40*).

It is assumed that the "best" nuclide is the one that will enable the smallest tumor to be detected with a given statistical significance in a given time. Then the over-all figure of merit for the nuclide counting-system combination can be split up into two factors, *A* and *B* (*40*). *A* depends on the biological and physical properties of the nuclide while B depends on the physical properties in relation to the counting system. The minimum volume of tumor that can be detected with a given statistical significance is inversely proportional to A x B.

The two groups of nuclides likely to give the best results are low-energy gamma emitters (70–300 or 400 kev) and positron emitters. If high-energy gamma rays are also emitted and if coincidence counting is not used, the problems of penetration through septa and side shielding will be difficult to overcome. For each of these groups of nuclides the *B* factor will not vary greatly so that nuclides within each group can be compared approximately by means of the *A* factor alone. This factor is greater for KBF_4^{18} than for other positron emitters (*40*) because of its short half-life.

Unfortunately, however, Turner and Matthews at Hammersmith have recently found that KBF_4^{18} concentrates in the stomach although this was not reported by other workers. Fig. 3 is a positron camera picture of a rat given KBF_4^{18} which clearly shows the high concentration in the stomach. Presumably the mechanism is similar to that for iodide because fluoroborate

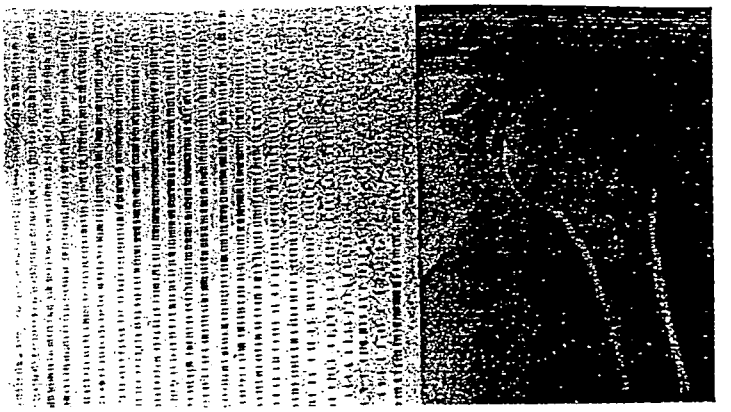

FIG. 2. F^{18} scan made 1 hr after intravenous injection of 1 mc F^{18} shows secondary deposit in head of humerus although x-ray of patient was normal (Reproduced from results of R. Morrison and J. Davey)

behaves rather like iodide in the body. It is possible to block the stomach uptake to some extent by giving perchlorate before injecting the KBF_4^{18}, and we are now investigating the effectiveness of this method.

The main advantage of KBF_4^{18} over other substances is its short half-life which—if the stomach uptake can be effectively blocked—lets one give larger amounts for the same radiation dose. Previous workers (*33*, *34*) have only given similar amounts to those used for longer-lived radioactive substances so the value of KBF_4^{18} for brain scanning cannot be properly assessed from their results.

Nb^{90} for tumor detection

Of a number of radioactive substances which we compared for their uptake in transplanted tumors in rats (*35*) Nb^{95} oxalate gives the highest concentration in the tumor. Therefore we thought that radioactive niobium might be useful for localization of tumors anywhere in the body. Nb^{95}, for example, appears to concentrate specifically in the tumor in contrast to isotopes usually used for brain-tumor localization which are merely excluded by brain and not by tumor.

For the animal experiments it was convenient to use reactor-produced Nb^{95}. But this material is unsuitable for clinical use because it has a long half-life (35 days) and emits hard gamma rays which are difficult to collimate. Cyclotron-produced Nb^{90} is better suited to work with patients because it has a short half-life of 14.8 hr and emits positrons in addition to gamma rays; therefore the annihilation radiation can be collimated by coincidence methods.

The distribution of niobium isotopes in rats has been measured by Matthews and Gartside (*41*). Uptake per gram is highest in transplanted tumors, plasma, spleen, kidney and marrow. The rate of clearance from the blood is similar to that of I^{131}-labeled fibrinogen in the blood. This may possibly explain the high tumor uptake because there is some evidence that tumors tend to concentrate fibrinogen (*42*, *43*). We hope to investigate the uptake in human tumors shortly.

The Nb^{90} is produced when zirconium is bombarded with 15-Mev deuterons. The most serious contaminant is Nb^{95} (10-day half-life) which is present in amounts ~5% that of Nb^{90} at the end of bombardment. But other niobium isotopes including Nb^{95} occur in smaller amounts (not exceeding 1% at the end of bombardment).

Our targets consist of a thin layer (~0.05 mm) of zirconium metal sprayed onto a copper plate. After bombardment the zirconium can be easily etched off the backing with strong hydrofluoric acid. The niobium isotopes are then recovered from the solution, and after excess hydrofluoric acid has been removed by a series of solvent extraction steps (*44*). the isotopes are finally prepared in a solution of 0.05% oxalic acid. The Nb^{90} yield is ~2mc/μAh at the end of bombardment.

Cs and Rb isotopes

Rb^{86} has been used in various ways for measuring coronary flow and for heart scanning. For example, Donato and others (*46*) have used a method for measuring coronary flow with Rb^{86} which gives good agreement with re-

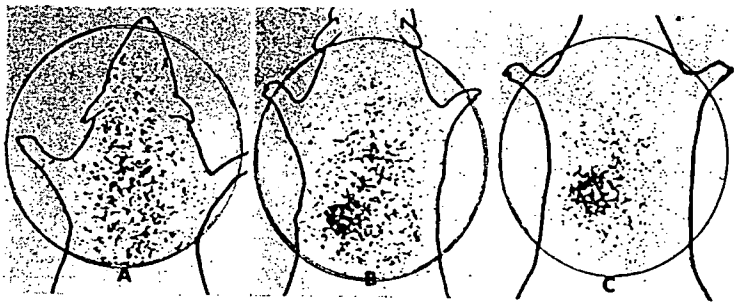

FIG. 3. Positron camera pictures of KBF_4^{18} distribution in rat (A) 8–11 min, (B) 64 min, and (C) 113 min after injection show that material concentrates in stomach

sults obtained with N_2O in normal subjects and in patients with heart disease. In addition Cs^{131} has been investigated for these applications (*45*).

But neither Rb^{84} nor Cs^{131} have very suitable physical properties for collimation and scanning, and both nuclides give rather high radiation doses. It should be possible to improve the method considerably by using one of the cyclotron-produced isotopes Cs^{129} (32 hr), Cs^{130} (29 min), Rb^{81} (4.7 hr) and Rb^{82m} (6.3 hr). The short half-lives of these nuclides lead to reduced radiation dose, and either positron or gamma rays of reasonably suitable energy are emitted.

R. Caldwell, I. Gabe, P. Kibby and C. Matthews at Hammersmith have carried out preliminary experiments in dogs with these isotopes. They find a high uptake of cesium in kidney which limits the dose that can be given. The uptake in heart muscle varies from ~3 to 7% for cesium and rubidium isotopes. Clearance from the blood is rapid, but it is somewhat slower for cesium isotopes. B. Westerman has made gamma camera pictures with Cs^{129} in patients with heart disease but the energy of the main gamma ray is rather high for the camera and the resolution is not good. Possibly better pictures of the heart can be made using Cs^{130} and the positron camera.

The reason why coronary flow can be calculated from the myocardial uptake of these isotopes does not seem to be clearly understood. It is sometimes explained on the basis of the "extraction ratio" for heart muscle having the same value as the average extraction ratio for the whole body. The extraction ratio is usually defined as the difference between arterial and venous concentration of the isotope divided by arterial concentration—or the integrated value of this ratio from time 0 to time t. Clearly this quantity is a function of time and might also be expected to be itself a function of flow and to vary for different organs. In fact, it will be the same for different organs only if the ratio of blood flow to potassium content is the same for each organ (*47*) which seems unlikely. However, it may be that the extraction ratio only *appears* to be constant. As L. A. Sapirstein has pointed out, there will only be a small amount of isotope returning to the venous blood because of the large size of the organ potassium pool with which the isotope is assumed to exchange.

The Cs^{129} and Cs^{130} are made in the cyclotron by the $I^{127}(\alpha,2n)Cs^{129}$ and $I^{127}(\alpha,n)Cs^{130}$ reactions using powdered sodium iodide as the target material. By covering the target with sufficiently thick aluminum-absorber foils, the alpha beam energy can be reduced to less than the 15-Mev threshold of the former reaction so that Cs^{130} can be obtained entirely free from Cs^{129} contamination. The yield of Cs^{130} under these conditions is ~0.5 mc/μAh at the end of bombardment or ~5 mc from a 30-min run at 20 μA. On the other hand, by bombarding the target at maximum energy (~30 Mev) and allowing the Cs^{130} to decay, pure Cs^{129} can be obtained with yields of ~0.2 mc/μAh.

After bombardment the sodium iodide is dissolved in sodium citrate buffer solution (pH = 5.5) to which a little thiosulfate is added to reduce free iodine. The radiocesium is extracted into a solution of sodium tetraphenylboron in amyl acetate (*48*). No carrier is added; indeed, the presence of carrier or traces of alkali metals other than sodium results in the formation of a precipitate at this stage which reduces the efficiency of the chemical separation. Therefore target material of highest purity is desirable. The organic phase is washed with dilute alkali, and the radiocesium is back-extracted into dilute HCl.

This extraction cycle is repeated, and the final HCl solution is thoroughly washed with ether to remove other organic reagents. The residual ether is then removed by evaporation, sodium bicarbonate is added to neutralize the HCl and the solution is taken to dryness.

When dry, the residue is baked to ensure the breakdown on any pyrogenic material which may be present. It is then dissolved in pyrogen-free water and sterilized by Millipore filtration. The only contamination detected in these samples is a trace of Na^{22} from $Na^{23}(\alpha,an)Na^{22}$ reactions, some of which will follow cesium through the separation procedure. This has been found only in the Cs^{129} samples where it amounts to <1 part in 10^7 of Cs^{129} at the end of bombardment.

The same production technique is used to prepare the rubidium isotopes Rb^{81} and Rb^{82m}, except that of course sodium bromide is used as the target material. We are currently studying the relative yields of these two isotopes and their contaminants, Rb^{83} and Rb^{84}, at various bombarding energies.

I^{123} for thyroid uptake

I^{123} decays almost entirely by emitting 160-kev gamma radiation. This property would make the pure isotope the ideal tracer for iodine in many clinical studies because of its low radiation dose per millicurie compared with, say, I^{131}. But in practice the isotope is invariably contaminated with other iodine isotopes which add somewhat to the radiation dose.

We are presently supplying I^{123} for thyroid-uptake measurements in patients. The pure isotope would give a dose to the thyroid of 0.015 rads/μc; even when it contains up to 10% I^{124}, H. I. Glass finds that the dose is only 0.075 rads/μc compared with 18 rads/μc for I^{131}.

I^{123} together with relatively small amounts of the longer-lived I^{124}, I^{125} and I^{126} is made by alpha bombardment of antimony; targets consist of a thin layer of antimony sprayed on a copper backing. If the targets are

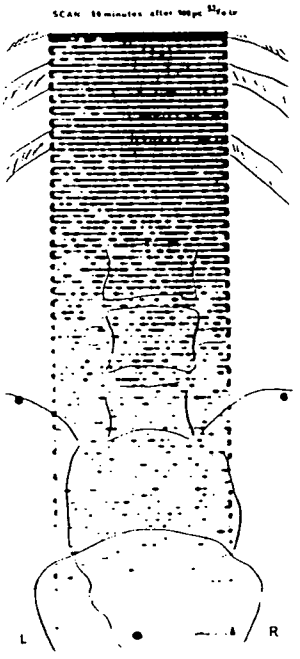

FIG. 4. Fe^{52} scan shows reduction in iron uptake in lower lumbar region after deep x-ray therapy to abdominal grands involved by cancer (R. McCready)

placed inside the dee-box of the machine where the beam strikes them at grazing incidence, they become effectively thick targets, and the I^{124} content (which is the most serious contamination from the point of view of dose to patients) will be ~5% of the I^{123} content at the end of bombardment. The yield of the I^{123} in this case is ~200μc/μAh. If, however, the targets are placed normal to the external beam and covered with enough aluminum foil to reduce the incident beam energy of 25 Mev, the I^{124} content is reduced to ~0.5% of the I^{123}; but the yield of I^{123} drops to ~20 μc/μAh.

After bombardment the antimony layer is removed from its copper backing with a remotely controlled milling machine, and the turnings are dissolved in a sulfuric acid nitrite mixture to which ~50 μg of iodide carrier are added. When this mixture is warmed, the iodide is distilled into an alkaline trap. Solvent extraction steps—all remote controlled—further purify the iodine, and the final solution consists of radiodine plus carrier in the form of iodide in 0.9% saline.

For purposes such as thyroid-uptake measurements the radioiodine is used in this form. But we are also using it to prepare labeled human serum albumin. The iodination technique is similar to that described by Rosa (*49*), but the labeled product is separated from non-protein-bound iodine by passing it through a column of Sephadex-G25.

Fe^{52} in tracer studies

Fe^{52} (8.2-hr half-life) was first used in 1957 at Hammersmith by L. Szur and others to study the distribution of erythropoietic tissue along the femur in patients with a wide variety of hematological disorders (*50*). The nuclide decays by positron emission, and the detection system uses coincidence counting.

Using a large positron scintillation camera (*51*) H. O. Anger and his colleagues at the Univ. of California have used Fe^{52} to study the whole-body patterns of marrow hypertrophy and atrophy in man (*52*) and intestinal iron absorption (*53*). The short half-life lets one make the serial measurements necessary to investigate the effects of cytotoxic agents and ionizing radiation on marrow function. Figure 4 is a scan made by R. McCready showing the reduction in iron uptake in the lower lumbar region following deep x-ray therapy to abdominal glands involved by cancer.

Fe^{52} is made by bombarding chromium targets in the internal alpha beam of the cyclotron where currents up to 300 μa are routinely used. The targets consist of a thin (0.05 mm) layer of natural chromium on an aluminum backing plate. They are placed at grazing incidence to the beam so that they become in effect infinitely thick. Details of the solvent-extraction technique used in isolating the radioiron in carrier-free form from the irradiated targets are given elsewhere (*54*).

The reaction that yields Fe^{52} is $Cr^{50}(\alpha,2n)Fe^{52}$. Because Cr^{50} is only ~4% abundant in natural chromium, the yield is rather low; a 1-hr bombardment at 300 μa produces only ~0.15 mc. Higher yields can obviously be obtained if enriched Cr^{50} is used as the target material, and the feasibility of doing this is at an advanced stage of investigation.

The produce is contaminated only by small amounts (<5% at end of bombardment) of Fe^{55}, but this has not proved an embarrassment to its clinical use because Fe^{55} is a long-lived x-ray emitter. This contamination, however, should be reduced by using an enriched Cr^{50} target.

K^{43} for tracer studies

K^{43} has been used to study the rate of transport of potassium across the membrane of red blood cells at Donner Laboratory (*53*) and to investigate the total exchangeable potassium in patients for a longer period than is possible with the 12-hr half-life reactor-product K^{42} at Hammersmith.

We obtain carrier-free K^{43} from the cyclotron by the $A^{40}(\alpha,p)K^{43}$ reaction by allowing the particle beam to enter a vessel containing argon (*56–58*).

If the argon is rapidly circulated through the target vessel and the exit gas is passed through a borosilicate fiber filter, more than 70% of the available activity is recovered on the filter. After bombardment the activity can be removed from the filter with 10 ml of 0.001 *N* hydrochloric acid without adding a carrier. If we use an alpha-particle energy of 13 Mev during bombardment, the K^{43} yield is 18μc/μAh and the K^{42} contamination is 3%. When high chemical purity of the sample is needed, the carrier-free K^{43} is purified by extracting the tetraphenyl boron compound into ethyl acetate at *p*H 5.7–6.0, followed by a back extraction into 0.1 HCl.

Summing up

There are a number of reasons why these accelerator-produced isotopes are preferable to reactor-produced isotopes of the same element. For example accelerator-produced O^{15} and N^{13} are the only isotopes of these elements which can be used in practice because the others have even shorter half-lives. C^{11} on the other hand, is preferred to C^{14} for certain work in humans because the much shorter half-life reduces the radiation dose. Moreover, the annihilation gamma radiation lets one use *in vivo* counting methods that would be impossible with C^{14}.

F^{18} and Sr^{87m} are preferred for bone scanning because of shorter half-life and lower dose than reactor-produced strontium or calcium isotopes. Nb^{97} has rather too short a half-life for general tumor localization, but reactor-produced Nb^{95} is too long lived and emits unsuitable radiation. The cesium and rubidium isotopes in Table

l are more suitable than reactor-produced ones both because of their more useful radiation and shorter half-lives. K^{42}, however, is more useful because of its longer half-life. The radiation emitted by I^{123} has almost ideal properties for *in vivo* measurements and for some applications the short half-life is also an advantage. Fe^{52} is useful because of its short half-life which lets one make serial measurements with it.

In practice we do not choose cyclotron-produced isotopes at Hammersmith over reactor-produced because they are positron emitters or have high specific activities. However, in some cases, if specific activity were too low the material would be unsuitable. We do not think that coincidence counting with positrons is necessarily an advantage since better efficiency can be obtained for the same resolution with a low-energy gamma-emitting nuclide and focusing collimators (*60*). If no suitable low-energy gamma emitter is available, however, coincidence counting may certainly be preferable to the use of focusing collimators with high-energy gamma rays.

So far little use has been made of cyclotron-produced isotopes for labeling molecules more complex than simple inorganic salts. For example, C^{11} or F^{18} might be used to label a wide variety of substances of physiological interest if the difficulties of carrying out the labeling process in a short time can be overcome. Some of the most interesting developments of the future may lie in this direction.

References

1. M. M. Ter-Pogossian, A new look at the cyclotron for making short-lived isotopes, NUCLEONICS *21*, No. 10, 50 (1966)
2. J. W. Gallop et al, A cyclotron for medical research, *Proc. I.E.E. 104B*, 452 (1957)
3. D. D. Vonberg, J. F. Fowler, The cyclotron unit: Medical Research Council, *Nature 198*, 827 (1963)
4. M. Ter-Pogossian, W. E. Power, "Proc. 1st (UNESCO) Internat. Conf. on Radioisotopes in Scientific Research," vol. III (Pergamon Press, Paris, 1957)
5. N. A. Dyson, et al, "Proc. 2nd U.N. Conf. on Peaceful Uses of Atomic Energy," Paper 278, (Pergamon Press, London, 1959)
6. C. T. Dollery, et al, The preparation and use of radioactive oxygen, carbon monoxide, and carbon dioxide for investigation of regional lung function, and their comparison with xenon-133, *Sonderbande zur Strahlenbehandlung, 63*, 88 (1963)
7. P. D. Buckingham, G. R. Forse, The preparation and processing of radioactive gases for clinical use, *Int. J. Appl. Radn. and Isotopes 14*, 439 (1963)
8. C. M. E. Matthews et al, Radioactive gases in "Radioactive Pharmaceuticals". (U.S.AEC, Oak Ridge, 1966)
9. C. T. Dollery, P. M. S. Gillam, The distribution of blood and gas within the lungs measured by scanning after administration of xenon-133. *Thorax, 18*, 316 (1963)
10. C. T. Dollery, P. Heimburg, P. Hugh-Jones, The relationship between blood flow and clearance rate of radioactive carbon dioxide and oxygen in normal and odematous lungs. *J. Physiol. 162*, 93 (1962)
11. C. T. Dollery, P. Hugh-Jones, Distribution of gas and blood in the lungs in disease. *Brit. Med. Bull. 19*, 59 (1963)
12. C. T. Dollery et al, Regional pulmonary blood flow in patients with circulatory shunts. *Brit. Heart Journal 25*, 225 (1961)
13. H. W. Knipping et al, Funktionsanalyse in der Kreislauf- und Lungen-Klinik mit Hilfe der Isotopenthorakographie und der selectiven Angiographie der Lungengefasse; Beitrag zur praoperativen Funktionsanalyse in der Thorax-Chirurgie. *Münch. Med. Wschr. 99*, 46 (1957)
14. W. C. Ball et al, Regional pulmonary function studies with xenon-133. *J. Clin. Invest. 41*, 519 (1962)
15. C. M. E. Matthews, C. T. Dollery, Interpretation of ^{133}Xe lung wash in out curves using an analogue computer. *Clin. Sci., 28*, 573 (1965)
16. J. B. West, C. T. Dollery, P. Hugh-Jones, The use of radioactive carbon dioxide to measure regional blood flow in the lungs of patients with pulmonary disease. *J. Clin. Invest., 11*, 1006 (Oct. 26, 1962)
17. C. T. Dollery, P. Hugh-Jones, C. M. E. Matthews, "Use of radioactive xenon for studies of regional lung function." *Brit. Med. J., ii*, 1006 (Oct. 20, 1962)
18. J. B. West, C. T. Dollery, "Distribution of blood flow and the pressure-flow relations of the whole lung." *J. Appl. Physiol. 20*, 175 (1965)
19. C. M. E. Matthews, J. F. Fowler, P. C. R. Turner, Absorbed doses from xenon-133 in M. R. C. Cyclotron Unit, Tech. Mem. No. 84, (1963)
20. D. J. D. Nicholas, D. J. Silvester, J. F. Fowler, Use of radioactive nitrogen in studying nitrogen fixation in bacterial cells and their extracts. *Nature, 189*, 634 (1961)
21. A. S. E. Fowle, C. M. E. Matthews, E. J. M. Campbell, The rapid distribution of ^2H_2O and $^{11}CO_2$ in the body in relation to the immediate carbon dioxide storage capacity. *Clin. Sci., 27*, 51 (1964)
22. E. J. M. Campbell, C. M. E. Matthews, D. Read, Analogue computer simulation of CO_2 stores and control of ventilation. *J. Physiol. 184*, 55p. (1966)
23. J. C. Clark, H. I. Glass, D. J. Silvester, "Proc. of Second. Internat. Conf. on Methods of Preparing and Storing Labelled Compounds," (Brussels, 1966)
24. M. Blau, W. Nagler, M. A. Bender, Fluorine-18, a new isotope for bone scanning. *J. Nucl. Med., 3*, 332 (1962)
25. M. Blau, Y. Laor, M. A. Bender, Clinical experience with F-18 and Sr-87m for bone scanning. *J. Nucl. Med., 4*, 193 (1963)
26. W. G. Myers, M. Olejar, Radiostrontium-87m in studies of healing bone fracture. *J. Nucl. Med. 4*, 202 (1963)
27. A. M. Budy, The use of radioisotopes in orthopaedics, Part II, *J. Bone and Jt. Surg., 45-A*, 1073 (1963)
28. D. Van Dyke et al, Bone blood flow shown with F-18 and the positron camera, *Amer. J. Physiol. 209*, 65 (1965)
29. J. C. Clark, D. J. Silvester, A cyclotron method for the production of fluorine-18. *Int. J. Appl. Radn. and Isotopes, 17*, 151 (1966)
30. M. Anbar, "Production and Use of Short Lived Radioisotopes from Reactors." Vol. 2, (IAEA, Vienna, 1963)
31. H. H. Dworkin, P. D. LaFleur, Fluorine-18; production by neutron activation and pharmacology in "Radioactive Pharmaceuticals." (U.S.AEC, Oak Ridge, 1966)
32. M. Hillman et al, Production of Y^{87} and a Sr^{87m} generator, *Int. J. Appl. Radn. and Isotopes, 17*, 9 (1966)
33. H. M. Ashkenazy et al, The localization of intracranial space occupying lesions by fluoroborate ions labelled with fluorine-18. *Amer. J. Roentgenol. 88*, 35 (1962)
34. W. Entzian et al, Evaluation of fluorine-18 as a scanning agent for intracranial tumours in "Medical Radioisotope Scanning." Vol. 2 (IAEA, Vienna, 1964)
35. C. M. E. Matthews, G. Molinaro, "A study of the relative value of radioactive substances used for brain tumour localization and of the mechanism of tumour:brain concentration. Uptake in transplantable fibrosarcoma, brain and other organs in the rat. *Brit. J. Exp. Path., 44*, 260 (1963)
36. F. Mundinger, H. Gerhard, Untersuchungen über die Verteilung der zur Hirntumordiagnostik verwendeten Radioisotope in der Blutbahn in experimentellen Tumoren und menschlichen Hirngeschwulsten. *Acta Neurochirurgica, 11*, 398 (1963)
37. W. C. Dewey, W. K. Sinclair, Criteria for evaluating collimators used *in vivo* distribution studies with radioisotopes. *Int. J Appl. Radn. and Isotopes, 10*, 1 (1961)
38. R. N. Beck, A theoretical study of brain scanning systems. *J. Nucl. Med. 2*, 314 (1961)
39. R. N. Beck, A theory of radioisotope scanning systems, in "Medical Radioisotope Scanning," Vol. I (IAEA, Vienna, 1964)
40. C. M. E. Matthews, Comparison of isotopes for scanning. *J. Nucl. Med., 6*, 155 (1965)
41. C. M. E. Matthews, J. M. Gartside, Tumour uptake and distribution of niobium isotopes in rats. *Brit. J. Cancer, 19*, 551 (1965)
42. E. D. Day, J. A. Plannisek, D. Pressman Localization in vivo of radioiodinated anti-rat-fibrin antibodies and radioiodinated rat fibrinogen in the Murphy rat lymphsarcoma and on other transplantable rat tumours. *J. Nat. Cancer Inst. 22*, 413 (1959)
43. G. Monasterio, M. F. Becchini, N. Riccioni, Radioiodinated (^{131}I and ^{125}I) fibrinogen for detection of malignant tumours in man, in "Medical Radioisotope Scanning." Vol. 2 (IAEA, Vienna, 1964)
44. H. L. Scherff, A. Herrman, Comparative examination of the solvent extraction of Pa Ta, Nb and Zr from strong hydrochloric acid." *Zeitschrift für Electrochemie, 64*, 1022 (1960)
45. E. A. Carr, Pharmacology of radioactive caesium salts, in "Radioactive Pharmaceuticals" (U. S. AEC, Oak Ridge, 1966)
46. L. Donato et al, Measurement of coronary blood flow by enternal counting with radioactive rubidium. Critical appraisal and validation of the method. *Circ. 33*, 708 (1966)
47. L. A. Sapirstein, Regional blood flow by fractional distribution of indicators. *Amer. J. Physiol. 193*, 161 (1958)
48. H. L. Finston, M. T. Kinsley, The radiochemistry of cesium. *N.A.S.-N.S. 3035 U. S. AEC 60* (1961)
49. U. Rosa et al, Labelling of human fibrogen with ^{131}I by electrolytic iodination. *Biochim. Biophys. Acta, 86*, 519 (1964)
50. P. E. Francois, L. Szur, Use of Iron-52 as a radioactive tracer. *Nature, 181* 1665 (1958)
51. H. O. Anger, Human bone narrow distribution shown in vivo by iron-52 and the positron scintillation camera. *Science, 142* 1587 (1964)
52. D. Van Dyke, H. O. Anger, Patterns of marrow hypertrophy and atrophy in man. *J. Nucl. Med., 6*, 109 (1965)
53. R. A. Fawwas et al, Intestinal iron absorption studies using ^{52}Fe and Anger positron camera. *J. Nucl, Med. 7*, 569 (1966)
54. D. J. Silvester, J. Sugden, Production of carrier-free iron-52 for medical use. *Nature 210*, 1282 (1966)
55. H. K. Awvvad, A. W. G. Goolden, The uptake of radioactive potassium by red cells in various thyroid states. *Clin. Sci. 20*, 115 (1961)
56. R. Overstreet, L. Jacobson, On the existence of a calcium isotope with an 8.5 day period *Phys. Rev., 72*, 349 (1947)
57. R. Overstreet, L. Jacobson, P. R. Stout, Evidence for a new isotope of potassium. *Phys Rev., 76*, 231 (1949)
58. T. Lindqvist, A. C. G. Mitchel, Disintegration of K-43. *Phys. Rev., 95*, 444 (1949)
59. N. A. Dyson, P. E. Francois, The preparation of potassium-43 using an interrupted cyclotron beam. *Int. J. Appl. Radn. and Isotopes, 7* 150 (1959)
60. C. M. E. Matthews, Comparison of coincidence counting and focusing collimators with various isotopes in brain tumour detection. *Brit. J. Radiol. 37*, 531 (1964)

MEASUREMENT OF BLOOD VOLUME USING RED CELLS LABELED WITH RADIOACTIVE CARBON MONOXIDE

H. I. Glass, A. Brant, J. C. Clark, A. C. de Garetta and L. G. Day

Hammersmith Hospital, London, England

In the early 1940's, blood volume was measured by inhaling a gas mixture containing carbon monoxide (*1*). By measuring the concentration of carbon monoxide in the blood and by knowing the amount extracted from a closed-circuit breathing system, one can calculate the blood volume. A modification of this method, in which no blood samples are withdrawn, was described by Sjöstrand (*2*), but some of the assumptions on which his method is based have been questioned (*3*). It has been consistently demonstrated, however, that the dilution volume measured by inhaling carbon monoxide averages 12–16% more than the volume measured with cells labeled with radioactive phosphorus, chromium or iron (*4–7*).

Root and his co-workers (*8*) have shown that a similar difference is found with splenectomized dogs intravenously injected with red cells labeled *in vitro* with stable carbon monoxide. This work can be criticized, however, because the insensitivity of the chemical methods used means the amount of blood removed for labeling must range from 50 to 80 ml in dogs with blood volumes of between 200 and 350 ml. A second possible criticism is that a correction for the disappearance of the carbon monoxide label from the blood may not have been applied, although a disappearance rate of 36%/hr is quoted in the paper. Tobias *et al* (*9*), who used radioactive ^{11}C-carbon monoxide-labeled red cells to study the elimination of carbon monoxide from the body, have stressed the importance of this disappearance-rate measurement if reliable estimates of blood volume are to be made. If radioactive ^{11}C-carbon monoxide-labeled red cells are used to measure blood volume, the amount of labeled blood used is less than 5 ml in subjects with blood volumes of about 5,000 ml. The correction factor applied to account for the loss of ^{11}C activity from the blood can be determined easily.

The purpose of the present investigation was to obtain an accurate estimate of the clearance rate of ^{11}C-carbon monoxide from the blood and an accurate estimate of the difference in dilution space measured with ^{51}Cr-labeled red cells and ^{11}C-carbon monoxide-labeled red cells. As a further study of the possible usefulness of this method in practice, repeated measurements of blood volume using ^{11}C-carbon monoxide-labeled red cells were made in two volunteers.

METHODS

Production of ^{11}C-carbon monoxide. ^{11}C was produced by bombarding boron as boric oxide with 15-MeV deuterons from the Medical Research Council cyclotron (*10*). The nuclear reactions that occur are ^{10}B(d,n)^{11}C and ^{11}B(d,2n)^{11}C (*11,12*). Some ^{13}N is produced simultaneously by the ^{16}O(d,αn)^{13}N reaction. These reactions are the only ones that need to be considered for our purposes. The target vessel consisted essentially of a brass box containing a wedge that supports a thin layer of boric oxide (B_2O_3) on its serrated surface. The deuteron beam entered the box through a thin aluminum foil window. The radioactive products were swept out of the target vessel in a stream (50 ml/min) of carrier gas which consisted of 1% carbon monoxide in helium. The ^{11}C left the vessel only in the form of carbon monoxide or carbon dioxide, and the ^{13}N (about 16% of the total activity) left only as molecular nitrogen. The labeled carbon dioxide was reduced to monoxide by passing the gas over "active" carbon at 900°C; it then flowed through a soda-lime trap to remove any residual traces of carbon dioxide. The

Received May 22, 1967; revision accepted Jan. 30, 1968.

For reprints contact: H. I. Glass, Dept. of Medical Physics, Hammersmith Hospital, DuCane Rd., Shepherds Bush, London, W. 12, England.

TABLE 1. DISAPPEARANCE RATE OF ^{11}C ACTIVITY FROM BLOOD

Patient	^{11}CO dilution space (ml)	Fractional loss rate (min^{-1})
AH	3,635 ± 120	0.00535 ± 0.00115
MF	3,776 ± 94	0.00530 ± 0.00095
EB	3,919 ± 157	0.00369 ± 0.00134
PC	1,917 ± 63	0.00433 ± 0.00122
AT	6,469 ± 115	0.00485 ± 0.00078
RE	4,638 ± 71	0.00304 ± 0.00046
JG	3,766 ± 127	0.00304 ± 0.00146
LC	3,045 ± 128	0.00564 ± 0.00158
MP	3,438 ± 113	0.00355 ± 0.00128
Weighted mean	—	0.00394 ± 0.00114
Average coefficient of variation (%)	3.03	—

composition of the final gas mixture used for labeling was checked with a gas chromatograph. Sterility was assured by Millipore filtration while the risk of possible pyrogen contamination was virtually eliminated by passing the gas through a small-bore silica tube at 300°C to denature any protein fragments. From this tube the gas flowed to waste through a small sterile vessel from which samples were withdrawn by piercing its soft rubber cap with a hypodermic needle.

Labeling procedures. To label the red cells with ^{11}C-carbon monoxide, 5 ml of venous blood were withdrawn into a 50-ml syringe containing 1.5 ml of acid citrate dextrose anticoagulant (ACD). Forty-five milliliters of ^{11}C-carbon monoxide plus helium carrier gas mixture were drawn into the syringe which was then rotated at 10 rpm for 10 min. The excess gas was expelled. Because of the high radioactivity per milliliter of blood achieved by this method (75 μCi/ml), there was adequate time to prepare standards and doses. The amount of ^{11}C-carbon monoxide contained in the plasma was less than 0.01%. Therefore it was not necessary to wash the plasma from the red cells after labeling.

To label the red cells with ^{11}C-carbon monoxide and ^{51}Cr, 10 ml of venous blood were withdrawn into a 50-ml syringe containing 1.5 ml of ACD. Less than 100 μCi of ^{51}Cr (as sodium chromate) was added to this syringe under sterile conditions. Forty milliliters of the ^{11}C-carbon monoxide gas mixture (containing 500 μCi of activity) was drawn into the syringe. The syringe was rotated for 10 min at 10 rpm. The excess gas was expelled, and the red cells were washed three times with isotonic saline (four centrifugations at 3,000 rpm) for 5 min each time. The amount of ^{51}Cr activity contained in the washing was checked. Virtually no activity (less than 0.01%) remained in the supernatant after the washing procedure. The washed labeled red cells were resuspended in saline up to the original volume of 10 ml.

RADIATION DOSIMETRY

^{11}C has a physical half-life of 20.34 min and emits positrons with a maximum energy of 0.97 MeV which yield 0.51-MeV annihilation photons. The k-factor (specific gamma-ray emission) is 5.8 R/hr/mCi at 1 cm. Assuming a body weight of 65 kg and a height of 160 cm, the average geometrical factor (*13*) is 126 and the geometrical factor at the center of the body is 180. Instantaneous mixing and uniform distribution within the body is assumed. The effective half-time clearance from the blood is 18 min since the biological half-life is 161 min (see below). The average beta dose is 0.0059 mrads/μCi and the gamma dose is 0.0049 mrads/μCi, giving a total dose of 0.011 mrads/μCi. An injected dose of 30 μCi gives a whole-body dose of 0.33 mrads. The total-body dose from an injection of 30 μCi of ^{51}Cr is 7.3 mrads.

RESULTS

Clearance of ^{11}C-carbon monoxide from the blood. One hundred microcuries of ^{11}C-carbon monoxide-labeled autologous red cells was administered to nine normal female patients, and five samples were taken at approximately 10-min intervals from 8 min up to 50 min after injection. The blood clearance rate was estimated by fitting a single exponential function to the data using the computer program devised by Marquardt (*14*). This program also yields estimates of the errors in the calculated parameters. The results are shown in Table 1. The average fractional loss rate is 0.0039 ± 0.0011 min^{-1} which corresponds to a clearance half-time of 176 min; i.e., the rate of disappearance from the blood is 25%/hr. This is identical with the value of 0.0039 previously reported by Pace *et al* (*15*) in five women following inhalation of stable carbon monoxide. Although these authors report a difference in carbon monoxide clearance rate between men and women, our own results on 11 male athletes (*16*) do not confirm this difference when a small quantity of ^{11}C-carbon monoxide-labeled cells is used.

Comparison of blood volume measured with ^{11}C-carbon monoxide- and ^{51}Cr-labeled red cells. Approximately 2 ml of the labeled red cells were taken up into each of two 5-ml syringes. Three syringes were necessary if two standards were to be used for an occasional check. Each syringe contained 30 μCi

of ^{11}C-carbon monoxide and 20 μCi of ^{51}Cr. One of the syringes was used to make up a standard by injecting the contents directly into a plastic vial containing 0.2 ml of saturated saponin solution and 0.5 ml of liquid paraffin. We used paraffin originally as a control to investigate whether any loss of ^{11}C-carbon monoxide occurred when the red cells were hemolyzed with saponin. No detectable loss occurred, but because the paraffin prevented the blood from being trapped near the stopper of the plastic vial during mixing, we continued to use it. The volume of the standard was made up to 5 ml with water. The contents of the remaining 5-ml syringe were injected intravenously into the patient and washed in by drawing back the venous blood four times. The residual activity in the syringe was less than 0.01% of the injected dose. The total time between removing the patient's blood and reinjecting the labeled blood was always less than 1 hr.

Venous blood samples were taken into plastic syringes containing three drops of heparin solution (5,000 units/ml) from a vein in the opposite arm approximately 8, 10 and 12 min after injection. These were immediately put into plastic counting vials containing 0.5 ml of saturated saponin solution and 0.5 ml of paraffin. The exact amount placed in each vial was not measured because the amount does not affect the ratio of the dilution volumes measured by the two isotopes and is only important if actual volumes are of interest. The samples and standard were then mixed on a rotary mixer for 10 min and counted after letting them stand for 5 min to allow the frothing caused by the saponin to subside. The ^{11}C activity relative to the standard was then calculated. Allowance was made for the decay of ^{11}C activity during the counting time. Using the value of the clearance rate obtained previously, the value of the dilution measured by each sample of ^{11}C-carbon monoxide was corrected to zero time from a knowledge of the exact time at which the sample was taken. The average value of the three samples corrected in this manner was calculated. Twenty-four hours later the ^{51}Cr content of the sample was measured. The difference between the dilution factors measured with ^{11}C-carbon monoxide and ^{51}Cr was expressed as a percentage of the factor measured with ^{51}Cr.

The results of measurements on 21 normal female patients is shown in Table 2. It can be seen that the average value of the dilution space measured with ^{11}C-carbon monoxide is 6.2% larger than that measured with ^{51}Cr, but the variation in this difference—although large—is within useful limits.

Measured accuracy of repeated blood volumes using ^{11}C-carbon monoxide. The relative activities of two syringes containing approximately 2 ml of labeled blood were measured by supporting each syringe over a well counter in a fixed mechanical jig. The contents of one syringe were reinjected into the patient by washing four times with venous blood and the contents of the other syringe were injected into a plastic counting vial containing 0.2 ml of saponin solution. The volume was made up to nearly 5 ml by washing the activity remaining in the syringe into the counting vial and making the final volume up to a mark on the vial. Blood samples were taken at 8, 10 and 12 min. Exactly 5 ml of each sample were pipetted directly into a counting vial containing 0.2 ml of saponin solution. The standard and samples were mixed for 10 min and counted after allowing them to stand for 5 min. The total time between taking the blood and reinjecting it into the patient in this procedure was less than 30 min. The same procedure was repeated for the second and third measurements with intervals of about 90 min between measurements. The activity remaining in the blood from the previous measurement was assessed and was found in all cases to be negligible compared with activity due to the later injection. The values obtained were corrected to zero time using the value for clearance rate determined when the measurement was carried out for the third time and five instead of three samples were taken. The results are shown in Table 3. The measured coefficient of variation is 3.88% in one case and 1.48% in the other.

TABLE 2. COMPARISON OF BLOOD VOLUME MEASURED WITH ^{11}CO- AND ^{51}Cr-LABELED CELLS

Patient	$\left(\frac{^{11}\text{CO dilution factor}}{^{51}\text{Cr dilution factor}} - 1\right) \times 100$
AB	+ 4.40
EG	+ 9.41
LC	+15.24
GJ	+13.00
JW	+ 0.00
MK	+ 1.95
RD	+ 4.43
FG	+13.79
JP	+ 5.03
BT	+ 2.62
PB	+ 4.89
EH	+ 3.38
JC	+ 6.43
PC	+ 0.00
AP	+ 8.14
DJ	+ 3.50
JB	+17.26
MC	+ 3.04
MP	+ 3.74
RP	+ 3.35
AMcH	+ 6.81
Average	6.21
Standard deviation	± 4.89

TABLE 3. REPEATED ESTIMATION OF ^{11}CO BLOOD VOLUME IN TWO PATIENTS

	^{11}CO blood volume (ml)	
	Patient 1	Patient 2
1st estimate (3 samples)	3,701	3,043
2nd estimate (3 samples)	3,501	3,153
3rd estimate (5 samples)	3,386	3,131
Weighted mean	3,503	3,113
Standard deviation	± 136	± 46
Coefficient of variation (%)	3.88	1.48

DISCUSSION

The results in Table 1 indicate that if samples are taken approximately 10 min after injection and if no correction is made for the clearance of ^{11}C-carbon monoxide from the blood, the estimated carbon monoxide dilution space will be approximately 4% too large. Unless extreme accuracy is required, it appears to be unnecessary to carry out blood-clearance estimations on individual patients. Instead it is sufficient to apply the average correction. This has been confirmed by subsequent studies (*16*).

Despite the fact that the ^{11}C-carbon monoxide was administered labeled to red cells, the volume measured is greater than that measured with ^{51}Cr-labeled cells (Table 2). Roughton and Root (*17*) have suggested that the rate of transfer of carbon monoxide from red cells to myoglobin is far faster than is generally supposed, and they have calculated a reaction half-time of 10 sec. The relative amounts of myoglobin to hemoglobin in the body have been estimated to be 15% (*18*), 6.2% (*19*) and 4.4% (*20*). The proportion of carbon monoxide combined with the myoglobin in man has been estimated at about 5% of that combined with hemoglobin (*21*).

The result obtained by us (Table 2) appears to suggest that with ^{11}C-carbon monoxide-labeled red cells the total hemoglobin and myoglobin space in the body is being measured, and the difference of 6.2% between ^{11}C-carbon monoxide- and ^{51}Cr-measured volumes is close to the expected difference of approximately 5%.

It is not easy to account for the larger difference of 12–16% noted by other workers (*4–7*) although part of this may be due to the failure of some previous workers in some cases to correct for the disappearance of carbon monoxide from the blood.

If it is considered necessary to correct the volume measured with ^{11}C-carbon monoxide by the 6.2% factor to obtain a red cell equivalent volume, then, assuming that the error in estimating the dilution space is 3.03% (see below), the error in the blood-volume estimate will increase to ±5.2%. It should be pointed out that the ^{11}C-carbon monoxide dilution spaces measured in this comparison test were all calculated using the average fractional loss-rate correction determined previously. In many clinical situations it is change of blood volume that is important within individual patients, and it is therefore probably not always necessary to apply the 6.2% correction factor with its associated error.

The average coefficient of variation in the method determined by repeated measurements on two patients is 2.68%. This can be compared with an error of ±3.8% claimed for the modified closed-circuit breathing method of Sjöstrand (*22*). The computer program used to fit the five-sample data provides an independent estimate of the accuracy of the method by estimating the error in the intercept. The average coefficient of variation in the measured dilution volume estimated by this method in nine patients is 3.0% (Table 1).

In this investigation whole-blood samples were counted and the hematocrits of the samples were not used to obtain red-cell volume or plasma volume allowing for the difference between venous and whole-body hematocrit. The estimate of hematocrit might itself be expected to be subject to a ±2% error.

In estimating the $^{51}Cr/^{11}C$-carbon monoxide ratio, several simplifying and time-saving procedures were introduced. Labeling was carried out by gentle rotation of the syringe for 5–10 min instead of the more usual 40–60 min. No hemolysis was measurable after labeling by this technique. No washing is necessary when ^{11}C only is used for labeling the red cells and the blood is reinjected into the patient within 30 min after the sample is taken. This insures that the blood is outside the body for only a short time and reduces the likelihood of the red cells becoming damaged. By using counting equipment with a short resolution time (0.7 μsec) and by delaying the time at which counting is carried out, the entire standard can be counted directly. This eliminates the need to make up a separate standard in a dilute form and to count an aliquot of this new standard. It also avoids the additional errors involved in the volumetric manipulations associated with a secondary standard.

CONCLUSIONS

If a cyclotron is available on site, ^{11}C-carbon monoxide-labeled red cells offer a convenient and accurate way of measuring the carbon monoxide dilution space in the body. If a correction is applied, the red cell equivalent volume can be estimated—but this correction introduces an additional error. Using the average clearance rate calculated on a group of nine

normal female patients instead of measuring individual clearance rates does not appear to add significantly to the error. It is probably desirable to measure individual clearances if the greatest possible accuracy is required. The blood volume can therefore be estimated by taking two samples at known times after injection, having allowed approximately 10 min for adequate mixing to take place. The accuracy of the method determined by repeated estimates in two patients is $\pm 2.7\%$, which compares well with the computer-derived estimate of $\pm 3.0\%$ based on measurements on nine patients. For multiple studies and in situations in which it is especially desirable to use minimal radiation doses (such as in pregnancy and in measurements on children), the ^{11}C-carbon monoxide method is of particular value.

ACKNOWLEDGMENTS

The authors wish to acknowledge the support and encouragement of J. F. Fowler, W. McGregor and D. D. Vonberg. They also wish to acknowledge the many helpful discussions and critical comments provided by Miss R. N. Arnot during this investigation and the kind cooperation and assistance of Peter Buckingham. This work was supported by a Clinical Research Grant from Hammersmith Hospital.

REFERENCES

1. HOPPER, J., JR., TABOR, H. AND WINKLER, A. W.: Simultaneous measurement of the blood volume in man and dog by means of Evans blue dye, T-1824, and by means of carbon monoxide. I. Normal subjects. *J. Clin. Invest.* **23**: 628, 1944.

2. SJÖSTRAND, T.: Method for the determination of total haemoglobin in the body. *Acta Physiol. Scand.* **16**:211, 1948.

3. ROOT, W. S. AND ALLEN, T. H.: Determination of red cell volume with carbon monoxide. In *Methods in Medical Research*, Vol. 8. Year Book Publishers, Chicago, 1960, p. 80.

4. HALDANE, J. AND SMITH, J. L.: The mass and oxygen capacity of the blood in man. *J. Physiol.* **25**:331, 1899.

5. NICKERSEN, J. L, SHARPE, L. M., ROOT, W. S., FLEMING, T. C. AND GREGERSEN, M. I.: Simultaneous blood volume determination in dogs with dye (T-1824), carbon monoxide and radioactive iron, ^{59}Fe. *Federation Proc.* **9**: 94, 1950.

6. NOMOFF, N., HOPPER, J. JR., BROWN, E., SCOTT, K. AND WENNESLAND, R.: Simultaneous determinations of the total volume of red cells by the use of carbon monoxide and chromium-51 in healthy and diseased human subjects. *J. Clin. Invest.* **33**:1,382, 1954.

7. DE HEVESY, G.: Red corpuscle content of circulating blood determined by labelling the erythrocyte with radiophosphorus. *Acta Med. Scand.* **116**:561, 1944.

8. ROOT, W. S., ALLEN, T. H. AND GREGERSEN, M. I.: Simultaneous determinations in splenectomised dogs of cell volume with CO and P-32 and plasma volume with T-1824. *Am. J. Physiol.* **175**:233, 1953.

9. TOBIAS, C. A., LAWRENCE, J. H., ROUGHTON, F. J. W., ROOT, W. S. AND GREGERSEN, M. I.: The elimination of carbon monoxide from the human body with reference to the possible conversion of CO to CO_2. *Am. J. Physiol.* **145**: 253, 1945.

10. VONBERG, D. D. AND FOWLER, J. F.: The Cyclotron Unit: Medical Research Council. *Nature*, **198**:827, 1963.

11. CLARK, J. C., GLASS, H. I. AND SILVESTER, D. J.: In-vitro labelling of red cells with carbon-11. In *Proc. Second Intern. Conf. Prep. Storage Labelled Compounds.* Euratom, Brussels, 1966.

12. BUCKINGHAM, P. D. AND FORSE, G. R.: The preparation and processing of radioactive gases for clinical use. *Intern. J. Appl. Radiation Isotopes* **14**:439, 1963.

13. HINE, G. J. AND BROWNELL, G. L.: *Radiation Dosimetry*. Academic Press, New York, 1956.

14. MARQUARDT, D. W.: IBM Share Programme, No. 3094, 1964.

15. PACE, N., STRAJMAN, E. AND WALKER, E. L.: Acceleration of carbon monoxide elimination in man by high pressure oxygen. *Science* **111**:652, 1950.

16. GLASS, H. I., EDWARDS, R. H. T., DE GARRETA, A. C. AND CLARK, J. C. Blood volume and total haemoglobin in athletes measured with ^{11}CO labelled red cells. *J. Appl. Physiol.* In press.

17. ROUGHTON, F. J. W. AND ROOT, W. S.: The fate of CO in the body during recovery from mild carbon monoxide poisoning in man. *Am. J. Physiol.* **145**:239, 1945.

18. WHIPPLE, G. H.: The haemoglobin of striated muscle. *Am. J. Physiol.* **76**:693, 1926.

19. BOTHWELL, T. H. AND FINCH, C. A.: *Iron Metabolism*. J. A. Churchill Ltd., London, 1962.

20. DRABKIN, D. L.: Metabolism of hemin chromoproteins. *Physiol. Rev.* **31**:245, 1951.

21. KILLICK, E. M.: Carbon monoxide anoxaemia. *Physiol. Rev.* **20**:313, 1940.

22. SJÖSTRAND, T.: Volume and distribution of blood and their significance in regulating the circulation. *Physiol. Rev.* **33**:202, 1953.

PLACENTAL LOCALIZATION BY INHALATION OF RADIOACTIVE CARBON MONOXIDE

H. I. Glass, J. Jacoby, B. Westerman, J. C. Clark, R. N. Arnot and H. G. Dixon

Hammersmith Hospital, London, England

Many different radioisotope techniques have been used for placental localization since 1950 when Browne and Veall (*1*) published their results, using ^{24}Na. The usual procedure is to inject intravenously a labeled intravascular substance which is then detected by a scanning procedure. The two intravascular substances which have been used are albumin and red cells. Albumin has been labeled with ^{131}I (*2,3*) ^{132}I (*4–6*), ^{99m}Tc (*7,8*) and ^{51}Cr (*9*). Red cells labeled with ^{51}Cr (*10*) have been used. Recently the use of ^{113m}In (*11*) has been proposed. The relative merits of the various substances are related to two factors: convenience in use and radiation hazard. ^{131}I-HSA and ^{51}Cr-HSA are convenient to use because of their comparatively long half-lives. By using ^{132}I-HSA and ^{99m}Tc-HSA the radiation dose is reduced considerably because of the 2-hr half-life of ^{132}I and the 6-hr half-life of ^{99m}Tc, but their short half-lives also require the albumin to be labeled for use each day. The advantage of ^{113m}In over ^{99m}Tc-HSA is that the former material may be autoclaved. However, some care in adjusting the *p*H during the preparation of the material for injection is required. ^{24}Na has a relatively high radiation dose/μc compared with ^{99m}Tc and is unsuitable for automatic scanning due to the difficulty of collimating high-energy gamma rays (2.75 and 1.37 Mev) and to the rapid clearance of ^{24}Na from the blood. A disadvantage of ^{51}Cr-labeled red cells is the necessity and inconvenience of *in vitro* labeling followed by reinjection into the patient. In this communication we describe the use of ^{11}C-monoxide for placental localization. *In vivo* labeling of the red cells was performed by administering the gas for a brief period by inhalation. The radiation dose is comparable with ^{99m}Tc-HSA.

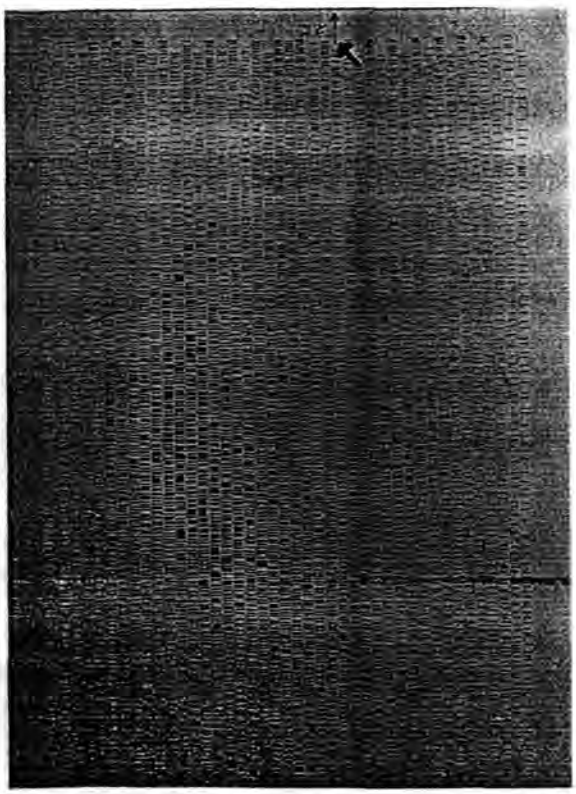

FIG. 1. AP dot scan obtained from color dot scan showing placenta in right lateral position. Xiphisternum is indicated by arrow.

METHOD

^{11}C-monoxide is produced by bombardment of boron as boric oxide with deuterons in the Medical Research Council Cyclotron (*12*). Seven hundred fifty microcuries of the gas are withdrawn into a syringe and after allowing time for the decay of ^{13}N which is also produced as a 16% impurity, 500 μc of ^{11}CO containing 60 μc of ^{13}N are injected into a 3-liter bag containing oxygen. The patient breathes this gas mixture for about half a minute through a well-fitting face mask. The mask and bag are removed and the patient is scanned immediately. Both

Received July 25, 1967; revision accepted Jan. 11, 1968.

a gamma camera (Nuclear Chicago) using an 11-in. diameter × ½-in. thick sodium iodide detector and a dual-detector scanner whose detector crystals are 3½-in. diameter × 3-in. thick sodium iodide have been used for localization of the placenta.

Using the camera, two AP views were taken routinely and one lateral view was also taken, the patient remaining in the supine position. The time for each view was approximately 4 min. A 4½-in.-thick multihole collimator was used to improve resolution (*13*) because of the comparatively high energy of the annihilation radiation emitted by the ^{11}C. The total number of counts recorded on each view was 50,000.

The scanner was operated at a speed of 3 cm/sec with a time constant of 0.3 sec. Two opposed 19-hole high-energy focusing collimators were used, the distance between the collimators being 32 cm. The maximum counting rate was approximately 200 cps. One AP and one lateral scan were performed. The lateral scan was carried out by turning the patient on to the appropriate side to bring the placenta proximal to the lower detector. The total scanning time taken for two views was 25 min. A color dot scan was produced by the scanner.

RADIATION DOSE CALCULATIONS

^{11}C has a physical half-life of 20 min and emits positrons with a maximum energy of 0.97 Mev which yield annihilation gamma rays of 0.51 Mev. The effective half-life of clearance in the blood is 18 min, and the whole-body dose is 0.011 mrads/μc (*14*). Thus the total whole-body dose due to 500 μc ^{11}C-monoxide in the blood is 5.5 mrads. The additional dose to the lungs during rebreathing is 5 mrads. The fetal dose is estimated at 4 mrads, and the dose to the fetal blood as 6 mrads. The fetal whole-body dose is due to gamma radiation received by the mother's trunk in the pelvic region. The dose to the fetal blood is calculated by assuming that one-tenth of the fetal blood is in the placenta. The fetal blood thus received one-tenth of the radiation dose to the placenta as well as nine-tenths of the fetal whole-body dose. A total blood volume of 4 liters, a placental mass of 750 gm and a placental blood volume of 250 ml were assumed in calculating the radiation dose to the placenta.

This radiation dose is approximately equal to that due to the administration of 500 μc of ^{99m}Tc-HSA and is about one-third of that due to the administration of only 8 μc of ^{24}Na.

The additional radiation dose due to the inhalation of 60 μc of ^{13}N along with the 500 μc of ^{11}CO is 0.8 mrads to the maternal lungs and is negligible to the whole body and fetus.

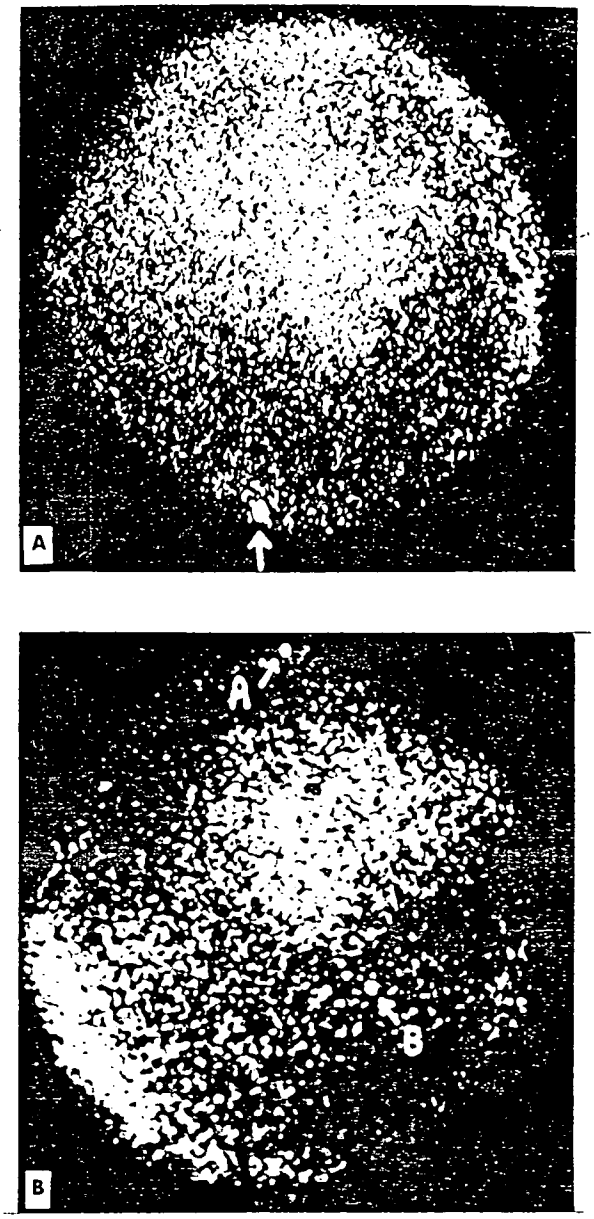

FIG. 2. A: Anterior view of abdomen taken with gamma camera. Placenta is seen in upper part of picture. Pubic symphasis is indicated by arrows. B: Right lateral view of same patient. Umbilicus (A) and iliac crest (B) are marked. Placenta is seen close to anterior wall of abdomen. Increased activity at bottom left of picture is due to liver.

RESULTS

AP and lateral gamma-camera pictures are shown in Fig. 1. The placenta is readily seen and lies in the upper anterior region. A 100-μc ^{57}Co source was used for anatomical marking and is indicated by the arrow. An AP dot scan is shown in Fig. 2.

Successful gamma-camera pictures and scans with ^{11}CO have now been obtained in 50 patients. The technique, involving a low radiation dose, is simple and is performed both as an in-patient and out-patient procedure. Placentas, whether sited anteriorly, posteriorly or laterally were all readily detected by either the camera or the scanner. An advantage of the scanner is that the size of the picture obtained is the same as the area scanned which makes the identification of the placental position more accurate. Lateral views of the abdomen are more easily obtained with the gamma camera because they do not involve changing the position of the patient. However, both methods are very satisfactory, provide the clinician with a permanent and easily interpretable record and are of value in the diagnosis of placenta previa in cases of antepartum hemorrhage. A significant advantage of this technique over the ^{99m}Tc-labeled albumin method is the lack of accumulation of activity in the bladder which may confuse the diagnosis of placenta previa.

CONCLUSIONS

With the availability of small isotope-producing cyclotrons, the use of ^{11}C-monoxide for the localization of the placenta may well have wide application. The combination of low radiation dose, complete absence of handling and labeling problems and the atraumic administration by 30-sec inhalation makes it an attractive alternative to other substances previously used for placental localization.

ACKNOWLEDGMENTS

The authors wish to acknowledge the support and encouragement of J. F. Fowler, J. C. McClure Browne and D. D. Vonberg. They also wish to thank Peter Buckingham, Miss G. Thompson and Miss M. Gallagher for their assistance and other clinical colleagues for their kind cooperation. This work is supported by a grant from the Medical Research Council.

REFERENCES

1. BROWNE, J. C. M. AND VEALL, N.: A method of locating the placenta in the intact human uterus by means of radioactive sodium. *J. Obstet. Gynaecol. Brit. Commonwealth* **57**:566, 1950.

2. WEINBERG, A., SHAPIRO, C. AND BRUHN, D. F.: Isotopic placentography—an evaluation of its accuracy and safety. *Am. J. Obstet. Gynecol.* **87**:203, 1963.

3. MERCHANT, R. J. AND MORAN, J. P.: Routine use of isotope localization of the placenta using ^{131}I. *Obstet. Gynecol.* **23**:72, 1964.

4. HIBBARD, B. M.: Placental localization using RISA. *J. Obstet. Gynaecol. Brit. Commonwealth* **68**:481, 1961.

5. POOL, K. R., LEACH, K. G. AND HAWKINS, L. A.: Placental localization using ^{132}I-labelled human serum albumin. *J. Obstet. Gynaecol. Brit. Commonwealth* **72**:706, 1965.

6. HIBBARD, B. M.: Placental localization using radioisotopes. *Clin. Obstet. Gynecol.* **9**:93, 1966.

7. LARSON, S. M. AND NELP, W. B.: Visualization of the placenta by radioisotope photo-scanning using ^{99m}Tc-albumin. *Am. J. Obstet. Gynecol.* **93**:960, 1965.

8. MCAFEE, J. G., STERN, H. S., FUEGER, G. F., BAGGISH, M. S., HOLTZMAN, G. B. AND ZOLLE, I.: ^{99m}Tc-albumin for scintillation scanning of the placenta. *J. Nucl. Med.*, **5**:936, 1964.

9. JOHNSON, P. M., SCIARRA, J. J. AND STICKLEY, E. E.: A new radiopharmaceutical for placentography. *Radiology* **83**:346, 1964.

10. VRETTOS, A. S., MEGAPANOS, E., COSTAMIS AND BINOPOULOS, D.: Isotopic placentography using ^{51}Cr tagged erythrocytes. *Am. J. Obstet. Gynecol.* **93**:957, 1965.

11. STERN, H. S., GOODWIN, D. A., SCHEFFEL, U. AND WAGNER, H. N.: ^{113m}In for blood-pool and brain scanning. *Nucleonics* **25**:No. 2, 62, 1967.

12. CLARK, J. C., GLASS, H. I. AND SILVESTER, D. J.: In-vivo labelling of red cells: *Proceedings of the Second International Conference on Preparing and Storing Labelled Compounds*. Euratom, Brussels, 1966.

13. WESTERMAN, B. AND GLASS, H. I.: The specification and performance of an 11-in. gamma camera. *J. Nucl. Med.* **9**:24, 1968.

14. GLASS, H. I., BRANT, A., CLARK, J. C., DE GARRETA, A. C. AND DAY, L. G.: Measurement of blood volume with radioactive carbon monoxide labelled red cells. *J. Nucl. Med.* In press.

JOURNAL OF APPLIED PHYSIOLOGY
Vol. 26, No. 1, January 1969. *Printed in U.S.A.*

^{11}CO red cell labeling for blood volume and total hemoglobin in athletes: effect of training

H. I. GLASS, R. H. T. EDWARDS, A. C. DE GARRETA, AND J. C. CLARK
Departments of Medical Physics and Medicine, and Medical Research Council Cyclotron Unit, Royal Postgraduate Medical School, Hammersmith Hospital, London, England

GLASS, H. I., R. H. T. EDWARDS, A. C. DE GARRETA, AND J. C. CLARK. *^{11}CO red cell labeling for blood volume and total hemoglobin in athletes: effect of training.* J. Appl. Physiol. 26 (1): 131–134. 1969.—Blood volume and total hemoglobin were measured in 10 male racing cyclists with a ^{11}CO red cell labeling technique. Venous blood (5 ml) was equilibrated with ^{11}CO and subsequently reinjected. The distribution volume was estimated for each of five timed blood samples, and an empirically selected single exponential function fitted to the data and the instantaneous dilution volume for ^{11}CO-labeled red cells were calculated. The average blood volume of the group was 82.6 ± 4.2 ml/kg and the average total hemoglobin 10.6 ± 0.7 g/kg. The average coefficient of variation in the estimation of the ^{11}CO dilution space was ±3.4%. Estimation from a single timed sample instead of five samples did not significantly increase the error. The error in blood volume was estimated to be ±5.2% and ±6.2% for total hemoglobin. In five subjects after a 2-month intensification of training resulting in improved working capacity there was no significant change in ^{11}CO space, total hemoglobin, or blood volume. This has been attributed to the high degree of physical fitness of the subjects at the start of the study.

TOTAL HEMOGLOBIN and blood volume are important determinants of cardiorespiratory fitness (11, 12). Most measurements of blood volume and total hemoglobin in athletes have been made with Sjöstrand's rebreathing technique with stable carbon monoxide (14, 19, 20). A method has recently been developed by us in which red cells labeled with radioactive carbon monoxide are reinjected intravenously and the dilution volume is estimated from subsequent timed venous blood samples. The exposure to radioactivity is considerably less than the radioactivity dose incurred with other radioactive isotopic methods, making it suitable for studies on normal subjects, especially when repeated measurements are required. In this paper the technique has been used to measure blood volume and total hemoglobin in 10 racing cyclists. In 5 of these subjects, the measurements were repeated after an intensive 2-month training program.

METHODS

The subjects were 10 male athletes, average age 20.6 years. They were studied in the course of a training program, and measurements were repeated on 5 of them following a 2-month intensification of the training regime. The physical working capacity at a heart rate of 170/min (PWC_{170}) was measured with cycle ergometer exercise by the method described by Holmgren (14). The average PWC_{170} of the group at the start of the study was 1,438 kpm/min.

Carbon-11 monoxide-labeled carbon monoxide was produced in the Medical Research Council Cyclotron by bombarding a boric oxide target with deuterons (4). Five milliliters of venous blood were withdrawn into a 50-ml syringe containing 1.5 ml of acid citrate dextrose anticoagulant (ACD). Then 45 ml of helium containing 1% carbon-11-labeled carbon monoxide were drawn into the syringe, which was then rotated at 10 rpm for 10 min. Because of the high radioactivity per milliliter of blood achieved by this method (75 μc/ml), there was adequate time for preparation of standards and doses despite the 20-min half-life of carbon-11. The amount of carbon-11-labeled carbon monoxide contained in the plasma was measured, and this was found to be less than 0.01% (6). It was not, therefore, necessary to wash the plasma from the red cells after labeling.

Two aliquots were taken, each of approximately 2 ml, into two syringes, one of which was used as a standard. After the count rates of the two syringes were measured, the contents of the one syringe were reinjected into the subject. The syringe was flushed by drawing back the venous blood four times. The residual activity in the syringe after such a procedure was found to be less than 0.01% of the injected dose (6). Five blood samples were withdrawn between 9 and 45 min after the injection of the labeled red cells. The blood was lysed with saponin and the activity in 5 ml of lysed whole blood was assayed in a well scintillation counter. The measured activity was counted for a fixed period of 100 sec and was related to the injected activity by comparison with the total contents of the standard syringe counted under identical conditions. The activity in each sample was corrected for decay up to and during the counting periods. This was facilitated by use of a fixed counting time. The whole-body dose due to the injection of 30 μc of ^{11}CO-labeled cells is estimated to be 0.33 mrad.

The dilution volume was estimated for each of the five samples and an empirically selected single exponential function was fitted to the data by a least-squares procedure with the computer program devised by Marquardt (15). The program also calculates the errors in the estimated parameters due to scatter of the data.

Hemoglobin concentration was estimated from duplicate

samples by the cyanomethemoglobin method (4). The total hemoglobin was calculated from the hemoglobin concentration in the venous blood and the carbon monoxide space, corrected for the 6.2% difference between this space and the blood volume measured with ^{51}Cr-labeled cells. This correction factor had been determined previously in 21 normal adults (6), with red cells which had been doubly labeled with ^{51}Cr and ^{11}CO. To calculate blood volume, it was assumed that the total body hematocrit is 0.91 times the peripheral hematocrit (3).

RESULTS

The total body hemoglobin and blood volume have been expressed in terms of body weight to allow comparison with the results obtained by other workers and the average values obtained for these quantities were 10.6 ± 0.7 g/kg and 82.6 ± 4.2 ml/kg, respectively (Table 1). In five of the subjects it was possible to carry out repeat measurements after 2 months (Table 1).

A correction is required in order to estimate the dilution volume at zero time owing to the continuous clearance of activity from the blood. This rate of clearance is of importance when a carbon monoxide space is estimated with a single timed sample. The results of 15 estimations of the clearance of activity from the blood, determined from five samples in each case, yield an average fractional loss rate of activity per minute of 0.00379 with a standard deviation of 0.00140.

The errors introduced by taking a single blood sample at 10 min, using the clearance correction obtained above instead of estimating the clearance rate in each individual, indicate that the average percentage difference between the five-sample and the single-sample methods is only 2.1%, which is within the estimated reliability of the method.

The coefficient of variation of the carbon monoxide space is ±3.4%. This estimate was based on the computer-derived estimates of the error of the intercept on the axis of the fitted monoexponential curve to the five data points for all the subjects who were investigated. This includes one result (*RH*) with an unusually high error of 8.9%. If this is excluded, the error reduces to ±3.0%. The accuracy in estimating the blood volume from the carbon monoxide space after applying a suitable correction factor is ±5.2%. This figure is computed from the coefficient of variation in measuring the carbon monoxide space and the error associated with the 6.2% correction factor for converting from carbon monoxide space to blood volume. This assumes that the correction term relating peripheral to total hematocrit contains no error. The coefficient of variation of the duplicate hemoglobin estimates was ±3.4%. Combining this result with the estimated accuracy in the blood volume, the accuracy of the total hemoglobin estimation is ±6.2%.

DISCUSSION

The need for safe and accurate techniques of estimating blood volume is increasing with the widespread demand for blood volume measurement in surgical and medical practice. The alveolar carbon monoxide method of Sjöstrand (19) in which red cells are labeled with stable carbon monoxide is entirely safe and has been used extensively. Ekelund (5) reported that the coefficient of variation in duplicate determinations of total hemoglobin is less than 4.6 and 6.1% for blood volume estimated by the alveolar CO method. For the ^{11}CO technique the values are 6.2 and 3.4%, respectively.

TABLE 1. *Blood volume, total hemoglobin, and work capacity of individual subjects*

Subj	Weight, kg		PWC_{150},* kpm/min			Carbon Monoxide Space, ml				Blood Volume, ml/kg				Total Hemoglobin, g/kg			
	Before	After	Before	After	Difference	Before	After	Difference	Difference %	Before	After	Difference	Difference %	Before	After	Difference	Difference %
Subjects studied before and after 2-month intensification of training regime																	
FR	67.7		1,320			5,461				81.7				10.9			
RS	73.3		1,460			5,873				82.6				11.0			
RH	63.3		1,360			5,142				84.7				10.3			
AS	73.6		1,580			5,932				83.1				9.4			
PS	69.6		1,410			5,430				80.4				10.7			
MS	71.8	73.5	1,440	1,510	70	5,247	5,362	+115	+2.19	75.4	75.2	−0.1	−0.13	10.0	9.4	−0.6	−6.00
DD	75.3	74.9	1,460	1,760	300	6,449	6,402	−47	+0.67	88.3	89.2	+0.9	+1.02	11.9	11.0	−0.9	−7.56
MB	62.9	64.6	1,320	1,420	20	5,080	5,228	+148	+2.91	83.3	83.4	+0.1	+0.12	10.6	11.0	+0.4	+3.77
AP	74.6	77.5	1,620	1,800	180	6,248	6,104	−144	−2.30	86.3	81.2	−5.1	−5.91	11.2	10.6	−0.6	−5.35
CC	66.4	66.2	1,400	1,500	100	5,400	5,265	−135	−2.50	83.8	82.0	−1.8	−2.15	10.9	10.8	−0.1	−0.91
Average	69.8	71.3	1,430	1,598	134	5,467	5,448	−19	0.19	82.8	82.2	−1.2	−1.41	10.7	10.6	−0.4	−3.21
SD	14.25	5.04	97	153	98	441	464	123	2.24	4.5	4.5	1.72	2.08	0.5	1.07	+0.3	4.13

* PWC$_{150}$ = Physical working capacity at heart rate of 150 beats

Gregersen (7), using an inhalation method, estimated that the carbon monoxide space exceeded the red cell space by 12–16%. A similar difference was observed by Root and his co-workers (17) in splenectomized dogs by intravenous injection of red cells labeled in vitro with stable carbon monoxide. In a previous study (9) with red cells doubly labeled with ¹¹CO and ⁵¹Cr, we have found the dilution space measured with ¹¹CO-labeled red cells to be only 6.2% greater than the space measured with ⁵¹Cr-labeled red cells. Roughton and Root (18) have suggested that the rate of transfer of carbon monoxide from red cells to myoglobin is far faster than is generally supposed and have calculated a half-time of reaction of 10 sec. The ¹¹CO dilution space measured by us has therefore been reduced by 6.2% in our calculations of blood volume.

The question arises whether quoting the blood volume provides any more useful information than the carbon monoxide space, which can be estimated with greater accuracy. When the total hemoglobin is to be estimated, an additional measurement, the blood hemoglobin concentration, is also required.

The average fractional loss rate of activity per minute was 0.00379 with a standard deviation of 0.00140. This compares with a value of 0.0039 previously reported by Pace (16) in five women following the inhalation of stable carbon monoxide. Since applying a correction for clearance from the blood allows the carbon monoxide space to be calculated from one timed blood sample without any significant loss of accuracy, this greatly enhances the scope of application of the method. The single-sample method requires only 10 min for the estimation instead of 45 min required for the stable carbon monoxide method of Sjöstrand, and only three venipunctures.

The blood volumes of 677 males reported in the world literature range from 59.8 to 101.7, with an average of 77.6 ml/kg (9). Our average of 82.6 ± 4.2 ml/kg is thus comparable to this and is close to the values 81.9 ± 8.64 ml/kg and 79 ml/kg in 10 (20) and 20 (12) cyclists measured by the alveolar carbon monoxide method of Sjöstrand (19).

Our values for total hemoglobin are similarly comparable to those quoted in the literature. Holmgren (12) found a value of 11.02 ± 1.02 g/kg in 19 male cyclists of an age and physical working capacity similar to ours. Ekelund (5) quotes 10.4 ± 1.3 g/kg in 26 normal males. Our value of 10.6 ± 0.7 g/kg is close to Ekelund's, but the standard deviation of the average value quoted is smaller. In the present study, no significant change in blood volume and total hemoglobin was observed.

The accuracy of the present method would be expected to demonstrate changes in blood volume and total hemoglobin of the order of magnitude noted by other workers (13). The apparent absence of change greater than 2.9% is probably related to the higher initial fitness (as reflected by the PWC_{170}) of our subjects compared with those of Holmgren. The percentage increase in PWC_{170} observed in our subjects is comparable with values quoted by Holmgren and his co-workers (13). The subjects in the present study would seem to be most comparable to their group of skiers in whom continuous training of an endurance type led to a smaller increase in blood volume in relation to improvement in PWC_{170} than that observed in the group with training of shorter daily duration with varying tempo up to exhaustion. In this study ¹¹CO space, blood volume, and total hemoglobin were not significantly changed in five cyclists with a high initial physical working capacity as a result of a 2-month intensification of the training program. It is possible that these subjects were approaching physiological maxima for ¹¹CO space, total hemoglobin, and blood volume when the first measurements were made. As suggested by Holmgren (13), the increase in physical working capacity in the absence of a corresponding increase in blood volume might be due to a more efficient peripheral circulatory adaptation to muscular work, resulting in a larger utilization of blood oxygen.

The authors wish to acknowledge the encouragement and support of Professor J. F. Fowler and Mr. D. D. Vonberg. Drs R. L. Hughes, E. A. Oppenheimer, R. Knill Jones, and Mr. P. Buckingham gave valuable assistance in the studies, and advice and criticism in the preparation of the manuscript was gratefully received from Drs. E. J. M. Campbell and N. L. Jones.

This work was supported by the Medical Research Council and also by a grant from the Hammersmith Hospital Clinical Research Fund.

Received for publication 11 December 1967.

REFERENCES

1. ÅSTRAND, P. O. *Experimental Studies of Physical Working Capacity in Relation to Sex and Age*. Copenhagen: Munksgaard, 1952.
2. CHAPLIN, H., P. L. MOLLISON, AND H. VETTER. The body/venous hematocrit ratio: its constancy over a wide range. *J. Clin. Invest.* 32: 1309–1316, 1953.
3. CLARK, J. C., H. I. GLASS, AND D. J. SILVESTER. In vitro labelling of red cells with carbon-11. In: *Proceedings of the Second International Conference on the Preparation and Storage of Labelled Compounds*. Brussels: Euratom, 1966.
4. DACIE, J. V., AND S. M. LEWIS. *Practical Hematology* (3rd ed.). London: Churchill, 1963, chapt. 2, p. 36.
5. EKELUND, L. G. Determination of blood volume. *Scand. J. Clin. Lab. Invest.* 17, Suppl. 86: 53–66, 1966.
6. GLASS, H. I., A. BRANT, J. C. CLARK, A. C. DE GARRETA, AND L. G. DAY. The measurement of blood volume with radioactive carbon monoxide labelled red cells. *J. Nucl. Med.* 9: 571–575, 1968.
7. GREGERSEN, M. I., AND R. A. RAWSON. Blood volume. *Physiol. Rev.* 39: 307–342, 1959.
8. GULLBRING, B., A. HOLMGREN, T. SJÖSTRAND, AND T. STRANDELL. The effect of blood volume variations on the pulse rate in supine and upright positions and during exercise. *Acta Physiol. Scand.* 50: 62–71, 1960.
9. HOBBS, J. T. *Total Blood Volume—Its Measurement and Significance*. Amersham, Buckinghamshire, England: United Kingdom Atomic Energy Authority, The Radiochemical Centre 1967, Medical Monograph No. 3.
10. HOLMGREN, A. Circulatory changes during muscular work in man. *Scand. J. Clin. Lab. Invest.* 8, Suppl. 24: 1–97, 1956.
11. HOLMGREN, A. Cardiorespiratory determinants of cardiovascular fitness. *Can. Med. Assoc. J.* 96: 967–702, 1967.
12. HOLMGREN, A., AND ÅSTRAND, P.-O. DL and the dimensions and functional capacities of the oxygen transport system in humans. *J. Appl. Physiol.* 21: 1463–1470, 1966.
13. HOLMGREN, A., F. MOSSFELDT, T. SJÖSTRAND, AND G. STRÖM. Effect of training on work capacity, total hemoglobin, blood volume, heart volume and pulse rate in upright and recumbent positions. *Acta Physiol. Scand.* 50: 72–83, 1960.
14. LAWSON, H. C. The volume of blood—a critical examination of method for its measurement. In: *Handbook of Physiology: Circulation*. Washington, D.C.: Am. Physiol. Soc., 1962, sect. 2 vol. 1, chapt. 3, p. 23–49.

15. MARQUARDT, D. W. *I.B.M. Programme*. No. 3094. White Plains, N.Y., SHARE organization, 1964.
16. PACE, N., E. STRAJMAN, AND E. L. WALKER. Acceleration of carbon monoxide in man by high pressure oxygen. *Science* 111: 652–654, 1950.
17. ROOT, W. S., T. H. ALLEN, AND M. I. GREGERSEN. Simultaneous determinations in splenectomized dogs of cell volume with CO and ^{32}P and plasma volume with T-1824. *Am. J. Physiol.* 175: 233–235, 1953.
18. ROUGHTON, F. J. W., AND W. S. ROOT. The fate of CO in the body during the recovery from mild carbon monoxide poisoning in man. *Am. J. Physiol.* 145: 239–252, 1945.
19. SJÖSTRAND, T. A method for the determination of total hemoglobin content of the body. *Acta Physiol. Scand.* 16: 211–231, 1948.
20. SJÖSTRAND, T. Blood volume. In: *Handbook of Physiology. Circulation*. Washington, D.C.: Am. Physiol. Soc., 1962, sect. 2, vol. 1, chapt. 4, p. 51–62.

International Journal of Applied Radiation and Isotopes, 1969, Vol. 20, pp. 677–681. Pergamon Press. Printed in Northern Ireland

A Simplified Method for Simultaneous Electrolyte Studies in Man Utilizing Potassium-43

F. SKRABAL, H. I. GLASS, J. C. CLARK, K. JEYASINGH and G. F. JOPLIN
Departments of Medicine, Medical Physics and M.R.C. Cyclotron Unit, Royal Postgraduate Medical School, Hammersmith Hospital, London W.12

(*Received* 8 *April* 1969)

A method is presented which enables the exchangeable sodium, potassium and bromide space to be estimated entirely by gamma counting using sodium-24, potassium-43 and bromine-82. The potassium-43 is a cyclotron produced isotope with a 22-hr half-life. The principal gamma radiation is at 370 keV. Duplicate estimations on nine patients indicate that the error in the estimation in exchangeable sodium, exchangeable potassium and bromide space is 4·6, 2·78 and 2·14 per cent respectively. By using a dual channel automatic gamma counter the assay may be completed in a single counting run. This technique permits a more widespread application of these measurements in clinical research and diagnosis.

UNE METHODE SIMPLIFIEE POUR LES ETUDES SIMULTANEES D'ELECTROLYTE CHEZ L'HOMME UTILISANT LE POTASSIUM-43

On présente une méthode qui permet l'estimation du sodium, du potassium et du bromure échangeables entièrement par comptage de gamma en employant le sodium-24, le potassium-43 et le brome-82. Le potassium-43 est un isotope produit du cyclotron ayant une demi-période de 22 heures. Le principal rayonnement gamma est à 370 keV. Des mesures en duplication sur neuf sujets indiquent que les erreurs d'estimation de sodium échangeable, de potassium échangeable et d'espace de bromure serait de 4,6, 2,78 et 2,14 pour cent. En employant un compteur gamma automatique à deux canaux on peut achever le dosage en une seule série de comptes. Cette méthode permet une application plus répandue de ces mesures dans la recherche clinique et dans la diagnostique.

УПРОЩЕННЫЙ МЕТОД ОДНОВРЕМЕННЫХ ЭЛЕКТРОЛИТИЧЕСКИХ ИССЛЕДОВАНИЙ В ЧЕЛОВЕКЕ С ПРИМЕНЕНИЕМ КАЛИЯ^{43}

Приводится метод, дающий возможность полного определения обменных натрия, калия и брома посредством измерения гамма-активности, применяя натрий^{24}, калий^{43} и бром^{82}. Калий^{43} является изотопом с периодом полураспада в 22 часа, полученным с помощью циклотрона; основные гамма-лучи = 370 килоэлектронвольт.

Дублированные определения на девяти пациентах показывают, что погрешности определения обменного пространства для натрия, калия и брома равны 4,6%, 2,78% и 2,14% соответственно. Применяя автоматический гамма-счетчик с 2-мя каналами, можно производить полное определение в один счетный период. Этот метод дает возможность широкого применения таких измерений в клинических исследованиях и диагностике.

EINE VEREINFACHTE METHODE FÜR GLEICHZEITIGE ELEKTROLYT-STUDIEN IM MENSCHEN UNTER VERWENDUNG VON KALIUM 43

Es wird ein Verfahren angegeben zur messung des austauschbaren Natrium, Kalium und Brom, lediglich durch Gammazählung unter Verwendung von Natrium 24, Kalium 43 und Brom-82. Kalium 43 ist ein im Zyklotron hergestelltes Isotop mit einer Halbwertzeit von 22 h. Die Hauptgammastrahlung liegt bei 370 keV. Doppelbestimmungen an neun Patienten deuten an, dass der Fehler in der messung des austauschbaren Natrium-, austauschbaren Kalium- und Brom-Raumes 4,6 bezw. 2,78 und 2,14% beträgt. Wenn ein automatischer Doppelkanal-Gammazähler benutzt wird, kann die Analyse in einem einzigen Zählgang beendet werden. Dieses Verfahren kann zu einer grösseren Verwendung dieser Messungen in der klinischen Forschung und Diagnose führen.

1. INTRODUCTION

THE CHIEF problem in assaying mixtures of isotopes used for the simultaneous determination of exchangeable sodium, potassium and chloride for electrolyte studies in man has been the estimation of the radioactive sodium in the presence of radioactive potassium. Several methods of assay of ^{42}K and ^{24}Na have been described, using chemical separation methods,[1–3] physical methods,[4–7] and physical-physiological methods.[8,9] The last method was also used by BOLING[10] using a plastic phosphor for beta detection instead of the more usual Geiger counter. RÖVNER and CONN[11] used ^{22}Na instead of ^{24}Na and assayed the mixture of this isotope with ^{42}K by differential decay. However, ^{22}Na, because of its long half-life and radiation characteristics, is undesirable for this purpose.

The method described below utilizes cyclotron-produced ^{43}K instead of ^{42}K and this results not only in improved accuracy over previous methods but a greatly simplified technical procedure, since ^{24}Na and ^{43}K can be assayed by gamma counting alone. A dual channel automatic counter allows the ^{43}K and ^{24}Na to be assayed simultaneously and ^{82}Br is conveniently assayed under the same counting conditions following a resin separation. A single channel automatic counter could also be used, but would require repeated counting.

2. PRODUCTION OF ^{43}K

Carrier free ^{43}K was produced in the external beam of the Medical Research Council cyclotron by irradiating argon-40 with 16·4 MeV α-particles. Details of the method of production are presented elsewhere[12]. ^{43}K is produced by the ^{40}A$(\alpha p)^{43}$K reaction which has a threshold of 3·64 MeV. The argon is circulated at a rate in excess of 100 l/min through the target vessel and the exit gas is passed through a borosilicate fibre filter. Between 50 and 80 per cent of the activity is recovered from the filter. The activity is removed from the filter with 5 ml of 0·001 N hydrochloric acid. The yield is 18 μc/μA hr and the contamination with ^{42}K is less than 7 per cent. For the present application, 5 mg/ml of KCl carrier is added to prevent glassware adhesion.

2.1. *Physical characteristics of* ^{43}K

The physical characteristics of ^{42}K and ^{43}K are shown in Table 1. The principal differences between the two isotopes are the lower γ and β energies of the ^{43}K, resulting in a lower radiation dose despite its longer half-life.

TABLE 1. Radiation characteristics of potassium-42 and potassium-43

	^{42}K	^{43}K
Half life	12·4 hr	22 hr
Principal γ-energies	1·52 MeV (18%)	0·37 MeV (85%), 0·61 MeV (81%)
k-factor	1·4	5·6
Average β energy (E_β)	1·45 MeV	0·30 MeV
Whole body radiation dose	0·85 mrad/μc	0·6 mrad/μc

3. METHOD

3.1. *Clinical procedure*

50 μc of ^{43}K and 20 μc of ^{24}Na were administered orally at 9 a.m. after an overnight fast of 10 hr. 10 μc of ^{82}Br were given orally 14 hr later. Normal food and fluids were permitted from 9 a.m. up to 9 p.m. Urine was collected in polythene flasks as follows: 0–24 hr, 24–24·5 hr, and 24·5–25 hr. At 24 hr and 25 hr heparinised blood samples were taken.

3.2. *Radioactive assay*

15 ml of each plasma and urine sample were passed through a moist resin column, 6 mm in dia. and 15 cm long, to remove the ^{82}Br. The resin used was Amberlite Tropor Deacidite FFIP, of a calculated exchange capacity of 5·1 mEq. The first 2 ml of the eluent was discarded, and the remainder assayed for radioactivity and for stable sodium and potassium concentration by flame photometry. Plasma was used for the measurement of exchangeable sodium and the bromide space, while urine was used for the exchangeable potassium.

Standards of the radioactive sodium, potassium and bromide were prepared by diluting an additional dose with distilled water up to 1 l. Aliquots of the standard dilution of ^{24}Na and ^{43}K were transferred directly to counting vials. The standard ^{82}Br was passed through an identical resin column as used for the samples. After washing each of the columns with 200 ml deionised water to remove any cations, the resin was transferred into the counting vials. This procedure resulted in identical sample and standard treatment for the ^{82}Br estimation, and produced identical counting geometry.

All the samples were assayed on a dual channel automatic gamma counter. The ^{82}Br was counted under the same conditions as the ^{43}K and ^{24}Na. This enabled all the samples to be counted in a single run on the automatic counter. This practical advantage outweighed the lower counting efficiency which resulted from assaying bromide under these less optimal conditions. Channels 1 and 2 were arranged to accept energies between 0·135 MeV and 0·415 MeV, between 1·05 MeV and 5·6 MeV respectively. The counting efficiencies for ^{24}Na and ^{43}K on channel 1 were 4·5 and 18·8 per cent respectively, whilst in channel 2 the efficiency was 13·4 and 0·1 per cent respectively. The counting efficiency for ^{82}Br (summed in the two channels) was 21 per cent.

4. RESULTS

4.1. In vitro *test of isotope measurement accuracy*

To establish the accuracy of the method, varying amounts of the ^{24}Na, ^{43}K and ^{82}Br were added to each of 6 flasks containing 100 ml of distilled water. Samples were passed through resin columns, and counted to determine the volume of distribution of each isotope. The results obtained are shown in Table 2.

4.2. *Clinical measurements*

Sodium, potassium and bromide spaces were estimated simultaneously in seven patients, and sodium and potassium spaces in a further two patients. These spaces were estimated at both 24 and 25 hr for ^{43}K and ^{24}Na and at 10 and 11 hr for ^{82}Br. The results are shown in Table 3.

5. DISCUSSION

The results presented in Table 2 indicate that no significant systematic error in the laboratory technique is present. The magnitude of the difference between duplicate estimates as seen in Table 3 are comparable or better than similar estimates of other workers.[13–17] The larger error in estimation of exchangeable sodium is associated with the poorer counting statistics of

TABLE 2. *In vitro* test of distribution volume

	^{24}Na (ml)	^{43}K (ml)	^{82}Br (ml)
	99·56	99·49	102·22
	100·12	100·76	99·12
	99·41	99·31	98·44
	99·99	101·34	100·76
	98·04	98·68	100·90
	100·11	100·66	101·80
Mean	99·54	100·04	100·51
coefficient of variation (%)	±0·79	±0·93	±1·48

The actual volume of distribution for each isotope was 100 ml in all six experiments.

TABLE 3. Results of clinical investigations

Patient number	Exchangeable sodium (mEq) Sampling time 24 hr	25 hr	Diff (%)	Exchangeable potassium (mEq) Sampling time 24 hr	25 hr	Diff (%)	Bromide space (l.) Sampling time 10 hr	11 hr	Diff (%)
1	2968	3143	+5·89	3356	3248	−3·2	21·49	21·59	+0·46
2	2086	2089	+0·14	2215	2222	+0·31	16·31	15·85	−2·82
3	1932	2028	+4·96	1850	1951	+5·46	17·31	17·43	+0·69
4	2148	2178	+1·39	2039	2094	+2·69	16·45	15·83	−3·76
5	4350	4480	+2·98	1723	1707	−0·92	28·29	28·71	+1·48
6	2127	1997	−6·11	1962	1952	−0·16	—	—	—
7	4119	4434	+7·6	2832	2859	+0·95	34·11	34·41	+0·88
8	4311	4264	−1·09	3191	3078*	−3·5	35·89	35·00	−2·47
9	2768	2705	−2·27	2021	2047	+1·28	—	—	—
Mean	2978·7	3035·3	+1·50	2354·3	2350·8	+0·32	24·26	24·11	−0·79
Standard deviation of diffs.			4·6			2·78			2·14

* 48 hr value.

the sodium assay. Approximately 3000 counts/400 sec are obtained for ^{24}Na assay in each plasma sample whereas 15,000/400 sec are usually obtained in the potassium assay from the urine sample. The error in the assay of stable sodium and potassium by flame photometry is estimated to be ±2 per cent. The relatively short time (1 hr) between successive samples makes it unlikely that further equilibration would affect the error estimates shown in Table 3.

The considerable saving of time and effort associated with the use of gamma counting only makes the replacement of ^{42}K by ^{43}K for these space estimations very attractive. The longer half-life of ^{43}K and the reduced radiation dose are additional advantages. The problems of calculating the final results are greatly eased by this procedure since all three isotopes are counted in a single run on a dual channel automatic counter. By loading the samples in a predetermined order, a punch tape record obtained from the counter facilitates the use of a computer programme to estimate the individual space values, allowing for physical decay.

6. CONCLUSION

The use of ^{43}K instead of ^{42}K in the simultaneous estimation of exchangeable sodium, potassium and bromide space results in a lower radiation dose and greatly simplifies the practical procedures. The use of a dual channel automatic gamma counter for estimating the three isotopes eases the computational problems associated with this technique and permits a more widespread application in clinical research and diagnosis.

Acknowledgements—We wish to thank Dr. R. M. HASLAM for her kind co-operation in performing the chemical estimations. This work was supported by a grant to G.F.J. from the Ernest and Minnie Dawson Cancer Trust which is gratefully acknowledged. F. S. gratefully acknowledges an Austrian Government Fellowship.

REFERENCES

1. ARONS W. L., VANDERLINDE R. J. and SOLOMON A. K. *J. clin. Invest.* **33,** 1001 (1954).
2. MCMURRAY J. D., BOLING E. A., DAVIS J. M., PARKER H. V., MAGNUS I. C., BALL M. R. and MOORE F. D. *Metabolism* **7,** 651 (1958).
3. MUNRO D. S., RENSCHLER H. and WILSON G. M. *Phys. med. Biol.* **2,** 239 (1958).
4. TAIT J. F. and WILLIAMS E. S. *Nucleonics* **10,** 47 (1952).
5. JAMES A. H. BROOKS L., EDELMAN I. S., OLNEY J. M. and MOORE F. D. *Metabolism* **3,** 313 (1954).
6. ROBINSON C. V., ARONS W. L. and SOLOMON A. K. *J. clin. Invest.* **34,** 134 (1955).
7. VEALL N. and VETTER H. *Radioistope Techniques in Clinical Research and Diagnosis*, p. 209, Butterworth, London (1958).
8. EKINS R. P. and SLATER J. D. H. *Phys. med. Biol.* **4,** 264 (1960).

9. Belcher E. H., Fraser R., Joplin G. F., Slater J. D. H. and Taylor R. G. S. *Radioaktive Isotope in Klinik und Forschung* Band IV, p. 194, Urban und Schwarzenberg, München (1960).
10. Boling E. A., Rossmeissl E., McLean R., Alpert H., Gardner R., Halpin M. and Lipkind J. B. *J. appl. Physiol.* **18,** 1252 (1964).
11. Rovner D. R. and Conn J. W. *J. lab. clin. Med.* **62,** 492 (1963).
12. Clark J. C. and Silvester D. To be published (1969).
13. Corsa L. Jr, Olney J. M., Steinburg R. W., Ball M. R. and Moore F. D. *J. clin. Invest.* **29,** 1280 (1950).
14. Miller H. and Wilson G. M. *Clin. Sci.* **12,** 97 (1953).
15. James A. H., Brooks L., Edelman I. S., Olney J. M. and Moore F. D. *Metabolism* **3,** 313 (1954).
16. Cox J. R., Platts M. M., Horn M. E., Adams R. and Miller H. E. *J. Endocrinol.* **36,** 103 (1966).
17. Lindholm B. *Acta Endocrinol.* **55,** 212 (1967).

M. R. C. Cyclotron Unit, Hammersmith Hospital,
Department of Radiodiagnosis, Hammersmith Hospital

^{81m}Kr an Ultra Short Lived Inert Gas Tracer for Lung Ventilation and Perfusion Studies with the Scintillation Camera

By

J. C. Clark and T. Jones
and
A. Mackintosh

Abstract

Krypton-81m, halflife 13 secs, is the daughter of cyclotron produced ^{81}Rb, halflife 4.7 hours. Krypton-81m emits 190 KeV photons in 65 % of its transitions and can be readily generated in high radioactiv concentrations both in the gas phase and in sterile water solution. The solution generator is described in detail. The photon emission energy is very suitable for use with a gamma camera, and for lung function studies ^{81m}Kr may have advantages over the widely used ^{133}Xe. Preliminary results of lung ventilation and perfusion studies are presented. Radiation doses are low for high administered activities for example 6 millirads lung dose for a 10 mCi intravenous injection.

Extrait

Le krypton-81m de 13 sec de période, est le fils du rubidium-81 produit de cyclotron de 4,7 heures de période. Le krypton-81m émet des photons de 190 KeV qui représentent 65 % des désintégrations; il peut être facilement produit à une activité élevée, aussi bien sous forme gazeuse qu'en solution aqueuse stérile. Le procédé d'obtention du ^{81m}Kr est décrit en détail. L'énergie d'émission des photons est très favorable à la réalisation d'images à la gamma caméra; pour étudier la fonction pulmonaire, le ^{81m}Kr peut présenter des avantages pa rapport au ^{133}Xe utilisé habituellement. Des résultats préliminaires concernant des études de perfusion et de ventilation pulmonaire sont présentés. Les doses de radiation sont faibles, même après l'administration d'activités élevées; par exemple une dose de 6 millirads est délivrée aux poumons après l'injection intraveineuse de 10 mCi.

Auszug

Krypton-81m mit einer Halbwertszeit von 13 Sekunden ist das Tochterisotop des im Cyclotron erzeugten Rubidium-81 mit einer Halbwertszeit von 4,7 Stunden. Krypton-81m sendet mit einer Häufigkeit von 65 % 190 KeV Photonen aus. ^{81m}Kr kann in einem Generator ohne Schwierigkeit mit hoher radioaktiver Konzentration hergestellt werden, und zwar sowohl in der Gasphase als auch in Lösung mit sterilem Wasser. Der Generator zur Herstellung von wassergelöstem Krypton-81m wird detailliert beschrieben. Die Gammaenergie der ausgesendeten Photonen ist zur Verwendung mit einer Gammakamera besonders gut geeignet und darüberhinaus dürfte Krypton-81m für Untersuchungen der Lungenfunktion Vorteile im Vergleich mit dem meistverwendeten Xenon-131 haben. Es werden vorläufige

Ergebnisse über Untersuchungen der Lungenventilation und Lungenperfusion mitgeteilt. Die Strahlendosis ist äußerst gering, so ergibt sich z. B. bei der i.v. Verabreichung von 10 mCi Krypton-81m eine Lungendosis von nur 6 millirad.

Introduction

Krypton-81m has a 13 second half life and emits 190 keV photons in 65 % of its disintegrations. It is the daughter of ^{81}Rb which has a half life of 4.7 hours. The decay scheme of ^{81}Rb is shown in figure 1. The nuclear reaction used to produce it is also shown. The external alpha particle beam of the M. R. C. Cyclotron is used to irradiate a sodium bromide target (Vonberg et al., 1970). Figure 2 shows the gamma spectra of the equilibrium mixture and separated ^{81m}Kr respectively using a 3 inch by 3 inch NaI (Tl) spectrometer. The krypton can be readily generated in the gas phase, owing to its low solubility in water, by passing a sweep gas through a solution containing ^{81}Rb (Jones et al., in press). Figure 3 shows a schematic diagram of a system capable of delivering 10 litres/min of air labelled with ^{81m}Kr. The generator contains a solution of sodium bromide target material with the unseparated ^{81}Rb, and is usually placed in a lead shield about 5 metres away from the γ camera. ^{81m}Kr can also be generated

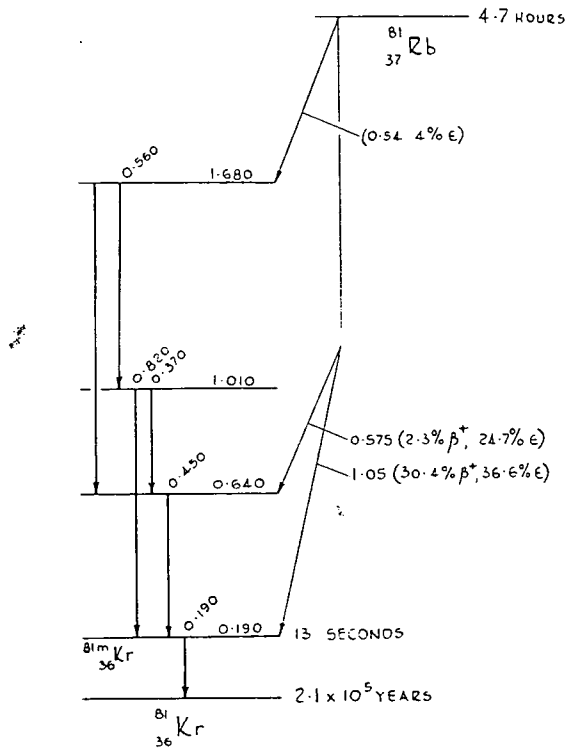

NUCLEAR REACTION FOR THE PRODUCT OF ^{81}Rb

$$^{79}_{35}Br(\alpha,2n)\,^{81}_{37}Rb$$

Fig. 1. Decay scheme for ^{81}Rb/^{81m}Kr nuclear reaction for the production of ^{81}Rb.

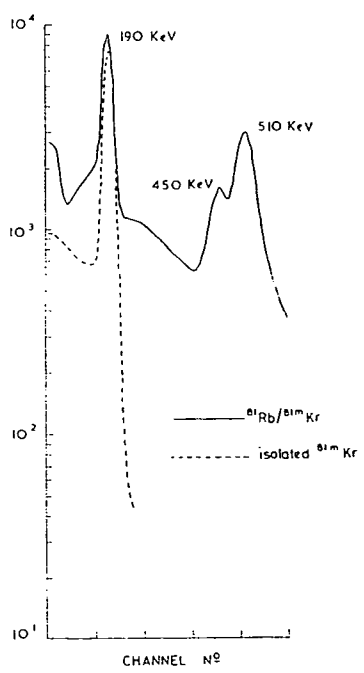

Fig. 2. Gamma spectrum of ^{81}Rb/^{81m}Kr equilibrium mixture on 3 inch by 3 inch NaI (Tl) spectrometer and Gamma spectrum of ^{81m}Kr on 3 inch × 3 inch NaI (Tl) spectrometer.

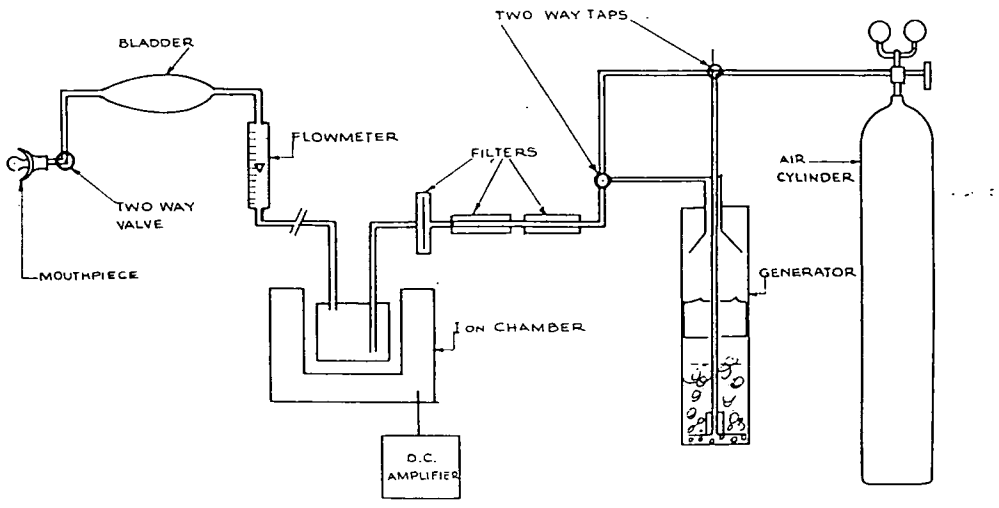

Fig. 3. Schematic diagram of the circuit for the generation of gas phase ^{81m}Kr.

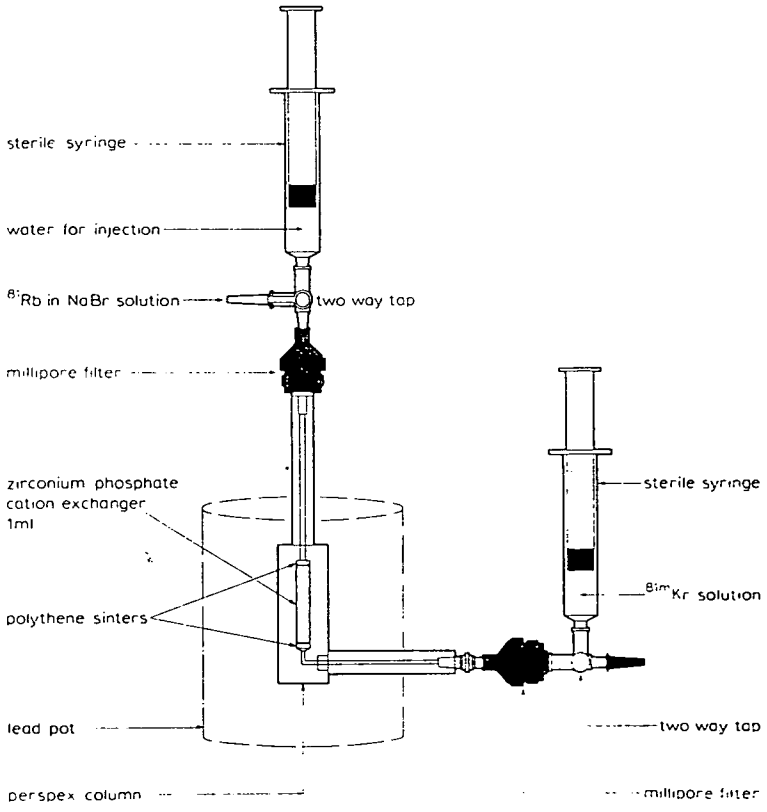

Fig. 4. Schematic diagram of the ^{81m}Kr solution generator.

in solution by rapidly eluting a bubblefree cation exchange column on which the rubidium is absorbed (Jones et al., in press). A schematic diagram of the solution generator is shown in figure 4. The zirconium phosphate cation exchanger provides a chemical separation of the rubidium from the sodium bromide and has a high distribution co-

efficient for rubidium which leads to low rubidium breakthrough values typically 4×10^{-4} % for a 3 ml elution. We use zirconium phosphate prepared in our own laboratory as this gives much higher elution efficiencies than commercial materials (BIO RAD Z P1). This is thought to be due to our material having a crystaline lattice which allows the krypton to diffuse out more rapidly. With a 3 ml elution taking 5 seconds the elution efficiency is typically 65 %, the krypton activity being corrected for decay back to the start of elution.

Lung Function

At present ^{133}Xe is used extensively for lung function studies (West, 1967; Loken and Westgate, 1968; Suprenant et al., 1967; Marks et al., 1968), but it has the disadvantage of emitting low energy photons thus giving relatively poor resolution with the γ camera. ^{81m}Kr on the other hand emits photons of more suitable energy for the

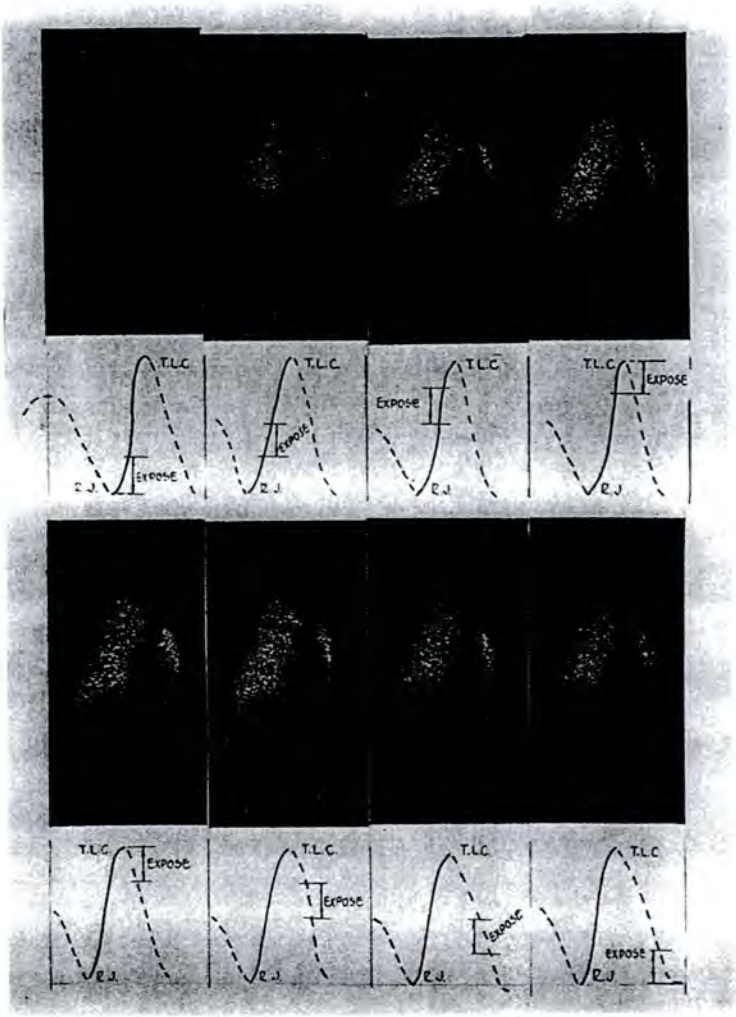

Fig. 5. Dynamic lung ventilation study using ^{81m}Kr and the gamma camera — ^{81m}Kr/air mixture breathed from residual volume up to total lung capacity — right lung anterior view normal.

γ camera. Also the generator systems can produce, more readily than ^{133}Xe dispensing systems, large quantities of isotope with easily controlled radioactive concentrations.

It is possible to study lung ventilation dynamics when high concentrations of ^{81m}Kr air mixtures of the order of 40 mCi litre are administered. Investigations have been made in this field by introducing ^{81m}Kr during specific parts of inspiration. Figure 5 shows the fate of ^{81m}Kr inhaled from residual volume up to total lung capacity, pictures being taken during both inspiration and the following expiration. The procedure illustrated was carried out on a 27 year old normal male volunteer and shows that the filling of the upper zone preceeds the principal filling in the lower zone, a finding which confirms the work of EMILI et al. using ^{133}Xe with multiple probes (MILIC-EMILI et al., 1966). The first picture shows an absence of activity due to inactive gas in the dead space of the inspiration equipment. The dose received is 12 milli rads to the lung per inspiration. Investigations of this type have also been carried out in isolated dog lung preparations in order to study patterns of ventilation under controlled conditions.

Lung Perfusion

Lung perfusion can be illustrated by using an intravenous injection of a solution of an inert gas such as ^{81m}Kr. The solution passes through the heart to the lungs where once it comes into contact with the alveolar spaces, it leaves the blood in which it is very insoluble and accumulates in the air cavities, the air cavities occupying a major part of the lung. Thus the resulting inert gas distribution is dependent on the blood perfusion distribution of the lung.

A comparison made by other workers of the perfusion distributions obtained with an injection of ^{133}Xe solution to that with an injection of ^{131}I labelled macroaggregates (CEDERQUIST et al., 1968) indicates that the lung perfusion patterns are similar but that areas of depressed perfusion are not so prominent with ^{133}Xe as with ^{131}I. This, it is thought, is due to relatively non degraded scatter of the low energy ^{133}Xe photons from the well perfused areas of the lungs into the low activity regions, thus effectively reducing the detectability for cold areas. This defect would not be so great for the 190 keV γ ray of ^{81m}Kr.

Lung perfusion studies were first carried out in dogs. Figure 6 shows serial photographs taken after an intravenous injection of 10 mCi of ^{81m}Kr into a catheter placed in the femoral vein, the bolus of activity entering the heart through the inferior vena cava. A significant lung perfusion picture can clearly be obtained.

Lung perfusion studies have also been carried out on volunteer patients. The preliminary results are shown in figure 7.

Figure 7 shows an anterior scintigraph taken with a Nuclear Chicago Pho Gamma II with a diverging collimator designed for ^{99m}Tc (LOWE and COTTRALL, 1969). 9 mCi of ^{81m}Kr in 3 ml of water were injected into the antecubital vein of the left arm followed by a 10 ml saline flush. The patient held his breath for 10 to 15 seconds after the tracer had left the heart, data being acquired during this period. (A region of reduced perfusion can be seen in the right lung.) Since the radiation dose from such an investigation is only 6 mr the procedure can be repeated several times without significant radiation hazard.

Several patients can be conveniently studied in an afternoon's scintigraphy session with a generator delivering 20 mCi of krypton-81m at 12,00 noon, the limiting factor only being the time required to position the patients.

It is conceivable that using higher radioactive concentrations, studies of the dynamics of lung perfusion could be carried out thus fully exploiting the γ camera, as an instrument for dynamic study.

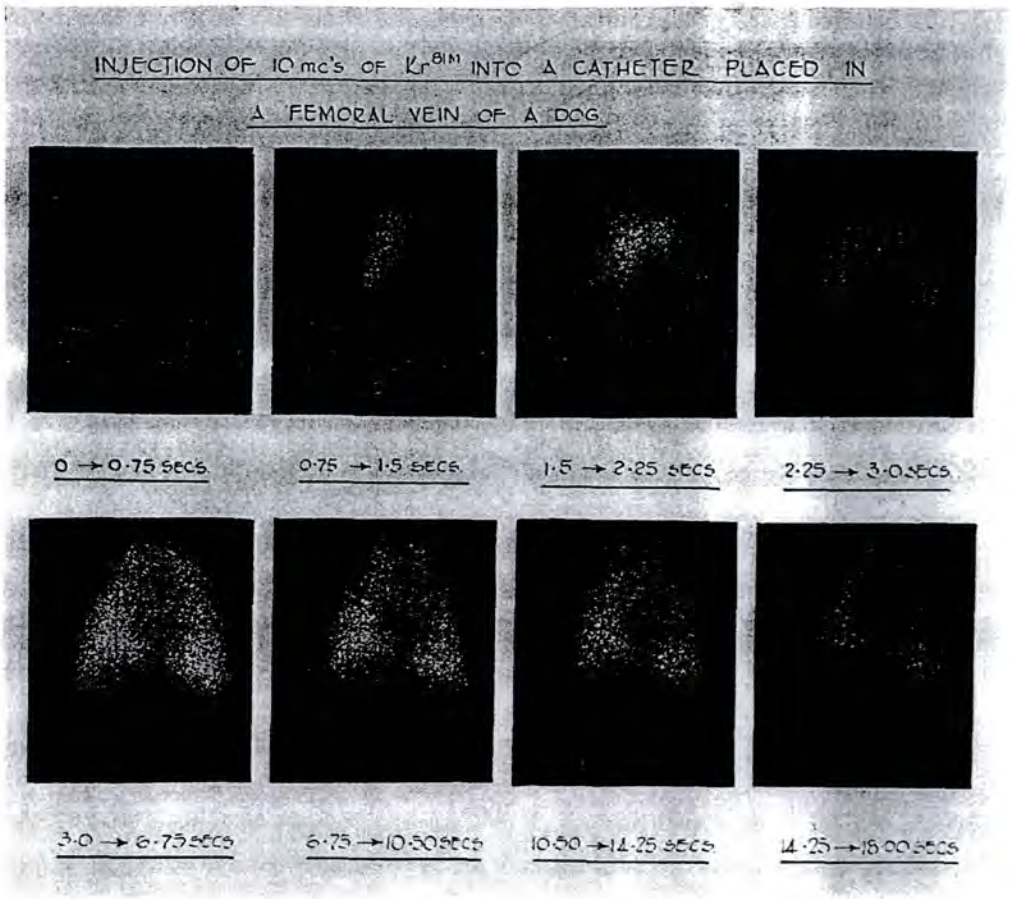

Fig. 6. Injection of 10 mCi of ^{81m}Kr into a catheter placed in a femoral vein of a dog.

Fig. 7. Anterior view of lung after the intravenous injection of 9 mCi of ^{81m}Kr solution using the gamma camera with a diverging collimator designed for ^{99m}Tc, showing a region of diminished perfusion in the right lung.

Conclusion

With the increasing use of the γ camera in medicine its ability to carry out both static and dynamic studies of short duration is important.

Thus specific isotopes are required to play a complementary role with the camera. Such isotopes must be available in sufficient activities to make short duration studies statistically feasible and yet they must have the physical characteristics to meet the requirements of high resolution and low absorbed dose to the patient (YANO and ANGER, 1968).

It is believed that in this context ^{81m}Kr generators have a useful role to play in medicine, in association with gamma cameras.

Acknowledgements

We thank Mr. D. D. Vonberg, the Director of our Unit, for his permission to present this paper and his continued encouragement. We thank Mr. Sharp and the cyclotron team for preparing the targets and carrying out the irradiations. The cooperation of the medical physics department in the use of the gamma camera was appreciated.

References

Cederquist, E., Y. Naversten, and T. White: Comparative Study of Regional Lung Function with Intravenous Injection of ^{131}I-Labelled Macroaggregated Albumin and ^{133}Xe. SM-108/143 I. A. E. A. Symposium on Medical Scintigraphy, Salzburg 1968.

Jones, T., J. C. Clark, J. M. Hughes, and D. Y. Rosenzweig: A ^{81m}K Generator and its uses in Cardiopulmonary Studies with the Scintilation Camera. J. Nucl. Med. Vol. II (1970), 118—124.

Loken, M. K., and H. O. Westgate: Evaluation of Pulmonary Function Using Xenon-133 and the Scintillation Camera. J. nucl. Med. 9 (1968), 45—50.

Lowe, J. E., and M. Cottrall: A Diverging Collimator for use with Gamma Camera. Personal Communication (1969).

Marks, A., I. Cervony, R. Lankford, E. M. Smith, A. J. Gilson, and W. Smoak: Ventilations-Perfusion Relations in Humans Measured by Scintillation Scanning. J. nucl. Med. 9 (1968), 450—456.

Milic-Emili, J., J. A. M. Hederson, M. B. Dolovich, D. Trop, and K. O. Kane: Regional Distribution of Inspired Gas in the Lung. J. appl. Physiol. 21 (1966), 749—759.

Suprenant, E. L., L. R. Bennet, M. M. Webber, and A. F. Wilson: Measurements of Regional Pulmonary Ventilation with Radio Xenon and the Anger Camera. J. nucl. Med. 8 (1967), 343—344.

Vonberg, D. D., L. C. Baker, P. D. Buckingham, J. C. Clark, K. Finding, J. Sharp, and D. J. Silvester: Target Systems used for Radioisotope Production on the Medical Research Council Cyclotron. Proc. of Int. Conference on the use of cyclotrons in chemistry, metallurgy and biology, Oxford 22/23 Sept. 1969. Butterworths, London 1970.

West, J. B.: Pulmonary Function Studies with Radioactive Gases. Ann. Rev. Med. 18 (1967), 459—70.

Yano, Y., and H. O. Anger: Ultrashort-lived radioisotopes for visualising blood vessels and organs. J. nucl. Med. 9 (1968), 2—6.

Diskussion zum Vortrag Clark

W. Adam, Ulm:

Das ^{81m}Kr ist zweifellos eine ausgezeichnete Substanz für Perfusionsuntersuchungen der Lungen, zumal man ja wegen der kurzen Halbwertszeit mehrere Untersuchungen am selben Patienten unter gleichen Bedingungen (zur Gewinnung von Mittelwert und Varianz) oder unter variierten Bedingungen durchführen kann.

Die geringe Halbwertszeit dürfte sich aber nachteilig bei Ventilationsuntersuchungen bemerkbar machen, es sei denn, man beschränkt sich auf die „single breath"-Methode und verzichtet auf die Informationen, die man mit ^{133}Xe bekommen kann („Wash-in", „Wash-out"-Kurven, evtl. Vitalkapazität und Tiffeneau bezogen auf Lungenteilbereiche, Residualkapazität). Glauben Sie überhaupt, unter Berücksichtigung der zeitaufwendigen Vorbereitungen der Ventilationsuntersuchungen, daß nach Abschluß der Inhalation die Aktivität in beiden Lungen noch groß genug ist, um eine quantitative Bestimmung der Radioaktivitätsverteilung zu ermöglichen?

Department of Medical Physics,
Medical Research Council Cyclotron Unit
and Neonatal Research Unit, Institute of Child Health,
Hammersmith Hospital, London

Methods of Measurement of Cerebral Blood Flow in the Newborn Infant using Cyclotron Produced Isotopes

By

R. N. Arnot, H. I. Glass, J. C. Clark, J. A. Davis, D. Schiff and C. G. Picton-Warlow

Abstract

Two methods for the measurement of cerebral blood flow in the newborn infant are described. The first uses red blood cells labelled with carbon-11 monoxide to obtain total cerebral blood flow by measuring mode transit time and cerebral blood volume. The red cells are injected via the umbilical artery. The second method uses inhalation of krypton-81m and krypton-85m in succession to obtain perfusion rate of a section of cerebral tissue. The krypton-81m measurement gives the total blood flow through the section, and the krypton-85m inhalation is required to relate this value to the mass of brain tissue within the field of view of the detector. A method for measuring short term changes in cerebral blood flow is also described. This uses two inhalations. Radiation doses are small. The theory, physical results, and clinical procedures for each method are described.

Extrait

Deux méthodes de mesure du débit sanguin cérébral chez le nouveau-né sont décrites. La première utilise des hématies marquées au carbone-11 monoxyde pour obtenir le débit sanguin cérébral total en mesurant le temps moyen de passage et le volume sanguin cérébral. Les hématies sont injectées dans l'artère ombilicale. La seconde méthode utilise l'inhalation successive de ^{81m}Kr et ^{85m}Kr pour mesurer la vitesse de perfusion à travers une partie de tissu cérébral. La mesure du ^{81m}Kr donne le débit sanguin total à travers cette partie de tissu et l'inhalation du ^{85m}Kr est nécessaire pour mettre cette valeur en relation avec la masse du tissu cérébral qui se trouve dans le champ du détecteur. Une méthode de mesure des variations rapides du débit sanguin cérébral est également décrite. Elle utilise deux inhalations de krypton-81m. Les doses de radiation sont faibles. La théorie, les résultats physiques et l'application clinique sont décrits.

Auszug

Es werden zwei Methoden zur Messung der Gehirndurchblutung beim Neugeborenen angegeben. Bei der ersten werden mit Kohlenstoff-11-Monoxyd markierte rote Blutkörperchen verwendet, um die totale Gehirndurchblutung aus mittlerer Transitzeit und zerebralem Blutvolumen zu berechnen. Die Injektion der roten Blutkörperchen erfolgt dabei in die Umbilikalarterie. Die zweite Methode bedient sich der Inhalation von Krypton-81m

und Krypton-85m zu aufeinander folgenden Zeitpunkten, um die Perfusionsrate eines Abschnittes von Gehirngewebe zu erhalten. Die Messung der Krypton-81m-Aktivität ergibt den totalen Blutfluß durch den Gehirnabschnitt, während die Krypton-85m-Inhalation notwendig ist, um diesen Wert für den Blutfluß zu der vom Detektor gesehenen Masse an Gehirn in Beziehung zu setzen. Es wird noch eine Methode zur Messung kurzzeitiger Veränderungen der Gehirndurchblutung beschrieben. Bei dieser Methode werden zwei Inhalationen verwendet. Die Strahlenbelastung ist gering. Theorie, physikalische Ergebnisse und der klinische Vorgang für jede Methode werden beschrieben.

Introduction

In recent years, paediatricians have become increasingly concerned with the problem of hypoglycaemia in the immediate neonatal period, together with the possible sequela to such an insult. The incidence of this problem is of the order of 0.5 % of all live births. Now that the predisposing factors have been catalogued, so that susceptible infants can be monitored from birth, it has become clear that a large number of infants exhibiting one or two blood glucose recordings of less than 20 mg% do not develop any symptoms and that clinical illness as a rule only follows a fairly prolonged period of severe glucose deprivation albeit that the prognosis in such cases is bad. It would appear therefore that the cerebral activity of newborn infants is in the long, but not in the short term, dependant on supplies of exogenous glucose unless the infant brain possesses, like some animals, a specific glucokinase.

In animals and human adults, it is evident that glucose is the brain's main source of energy. However, EDWARDS (1964) has demonstrated that calves' brains can metabolize lactic acid in the place of glucose and OWEN et al. (1967) have demonstrated that the human adult brain can metabolize beta-hydroxy butyric acid and other ketone bodies. It has been postulated that the newborn infant's brain can similarly make use of substrates other than glucose, such as glycerol, ketones and lactate, especially during the asymptomatic period (SCOPES, 1964; CORNBLATH and SCHWARTZ, 1966), symptoms developing when such substitutes have also been exhausted. Studies related to hypoglycaemia in the newborn period require the knowledge of how much glucose is being utilized by the brain, and what substrates, if any, other than glucose, can the infant's brain use. Arteriovenous samples of blood across the newborn infant's brain are obtainable from an umbilical artery catheter and the posterior sagittal sinus with little stress or danger to the infant, but the interpretation of such arterio-venous differences would be dependent upon a knowledge of the infant's cerebral blood flow at the time.

In the measurement of cerebral blood flow in newborn infants, carotid arterial or jugular venous puncture is unacceptable and handling of the infant and radiation dose must be kept to a minimum.

Cerebral clearance has been measured following inhalation of a radioactive inert gas using external detectors (MALLETT and VEALL, 1963). This method requires continuous monitoring of the expired air (VEALL and MALLETT, 1966; OBRIST et al., 1967) or a timed sampling of venous cerebral blood (ZIERLER, 1965), which are not usually possible in measurements on babies. Nearly all previous methods using intravenous injections of radioactive tracers (SAPERSTEIN, 1962; STEINER et al., 1962; FEDORUK and FEINDEL, 1960) are impractical in newborn babies. OLDENDORF (1962) measured the mode transit time of plasma through the adult brain following an intravenous injection of ^{131}I hippuran, which together with a measurement of cerebral blood volume, allowed the total cerebral blood flow to be calculated (OLDENDORF, 1963; KATSUKI et al., 1964).

We have adapted OLDENDORF's method, using red blood cells labelled with ^{11}CO administered via an umbilical arterial catheter. External monitoring was used and a blood sample was collected from the posterior sagittal sinus.

MATTHEWS (1967) suggested that if krypton-81m (half life 13 seconds) is inhaled continuously until the activity in the brain is constant, then this activity would be proportional to the cerebral blood flow. The flow in the tissue in the field of view of an external counter may be calculated if the arterial concentration is known. To avoid the necessity of viewing the whole head, a modification to this principle was introduced, which enabled the measured blood flow in a specific quantity of tissue to be estimated using, in addition, krypton-85m (half life 4.4 hours) to estimate the mass of tissue being viewed.

Also, successive measurements with krypton-81m alone over the same region were used to measure short term changes in flow. In both methods, inhalation and external monitoring were required for short periods only, and blood sampling to assess the inflow concentration was performed via an umbilical arterial catheter.

The radiation doses to the patient were small (see below).

Physical Characteristics of Isotopes and Radiation Dosage

Carbon-11 has a half life of 20 minutes and is a pure positron emitter with annihilation radiation energy of 511 KeV. The whole body radiation dose to a baby from 10 $\mu Ci^{11}CO$ labelled red blood cells varies from 2.5 to 6.5 mrads (weight varying from 2.5 to 0.8 kg).

Krypton-81m has a half life of 13 secs and emits a single gamma energy of 190 keV which is 35 % internally converted. The radiation dose to the lungs due to breathing 20 mCi/litre for 2.5 minutes is 48 mrads. The whole body dose is negligible.

Krypton-85m has a half life of 4.4 hours. It has gamma energies of 150 keV (78 %) and 305 keV (13.5 %) and a beta radiation of 830 keV. The radiation dose to the lungs due to breathing 0.2 mCi/litre for 15 minutes is 42 mrads, which is largely due to the β radiation. The whole body dose is 1 mrad.

In comparison, the whole body radiation dose received by a foetus during a single X-ray film of the maternal pelvis in late pregnancy is from 100 to 300 mrads (REEKIE et al., 1967).

Method Using ^{11}CO Red Blood Cells

Theory and Assumptions

When a bolus of a non diffusible tracer is introduced into the brain it spreads throughout the vascular system, and a graph of the tracer concentration in the outflowing blood against time gives the spectrum of transit times of the tracer through the system. With external monitoring, the countrate is directly proportional to the activity in the volume viewed by the detector provided its sensitivity is uniform throughout that volume. If $C_i(t)$ and $C_o(t)$ are the concentrations of isotope in the inflowing and outflowing blood respectively, then the countrate R (t) is given by

$$R(t) = SF \int_o^t C_i(t)dt - SF \int_o^t C_o(t)dt$$

where S is the sensitivity of the detecting system and F is the rate at which blood enters and leaves the volume seen by the detector. Since $C_i(t)$ passes through a maximum at the point when inflowing isotope concentration is greatest, the rate of change

of R(t) at this time is a maximum and a point of inflection occurs. A second point of inflection occurs when $C_o(t)$ reaches a maximum.

The period of time between the two inflections is the mode transit time of blood through the volume viewed (OLDENDORF, 1962).

This theory assumes that no activity has left the viewed volume before the most concentrated part of the bolus enters, and that entry of activity has ceased before $C_o(t)$ reaches a maximum. It is also assumed that no activity enters the field of view more than once and that the detecting system views the whole brain and no other tissues containing significant activity.

Blood flow through a system is equal to V/t, where V is the volume through which a radioactive tracer is distributed when uniformly mixed within the system, and t is the mean transit time of the tracer through the system (MEIER and ZIERLER, 1954). Provided the spectrum of transit times through the system is not considerably asymmetrical, the mode transit time approximates closely to the mean transit time. Total cerebral blood flow may therefore be found by measurement of the mode transit time and the total cerebral blood volume (OLDENDORF, 1963).

Equipment

The requirements of the detecting system for the transit time measurement in babies are high sensitivity and precise collimation, and for the measurement of the brain blood volume, good uniformity of response. Two $4^1/_4$" diameter × 2" thick NaI crystals were used. Their outputs were summed and a pulse height analyser was used to select the 511 keV photopeak. The dilution curve was recorded simultaneously on a pen recorder and on magnetic tape (KEMPLAY and VERNON, 1967). The magnetic tape recording was used in case the optimum range and time constant had not been selected on the ratemeter.

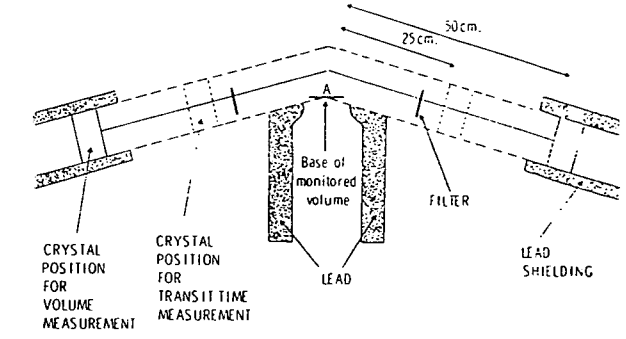

Fig. 1. Diagram showing arrangement of detectors and shields used for measurement of total cerebral blood flow using ^{11}CO labelled red blood cells.

The detectors, shielded by lead 2" thick, were arranged as shown in figure 1. The central axes of the crystals were at an angle of 150°, and the distance between their point of intersection and the crystal faces was 25 cm for the transit time measurement and 50 cm for the blood volume measurement. The detectors could be easily moved between the two positions.

The baby rested on an adjustable padded support and radiation from all parts of the body except the upper part of the head was excluded by a specially shaped shield of 2" lead bricks. The angulation of the detector and of the shield ensured that the response of the detectors decreased rapidly to activity within the shield. Thin lead filters were used to obtain uniform response, in a way similar to that of OLDENDORF (1963).

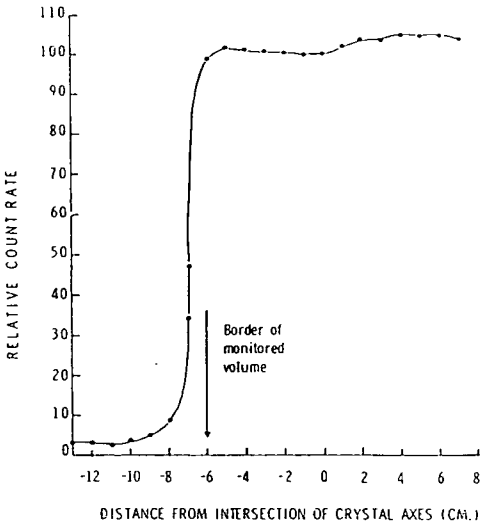

Fig. 2. Graph showing the point-source response of the ^{11}C detecting system, measured along the inferno-superior axis of the patient's head at the level of the crystal axes.

The point source response of the system was measured in a water tank with the crystals in the volume measurement position. The response along the infero-superior axis of the patient and at the level of the crystal axes, is shown in figure 2. The response is uniform to ± 3 % over 13 cm, and drops from 99 % to 10 % in 2 cms outside the volume of interest. The border of the volume to be measured is shown. Point source measurements made along other axes showed the response within a 10 cm sphere to be uniform to ± 6 %.

The variation of sensitivity with volume was found by measuring spherical flasks of ^{11}C activity with the detectors in both positions. Spheres varying from 6 cm to 12.5 cm diameter were used. Over the range of head size encountered (8 to 10 cm) the sensitivity was constant to ± 1½ %. The result was almost identical in the other detector position.

The absolute sensitivities to an 8.5 cm diameter flask filled with solution containing ^{11}CO were 440 c/s/μCi and 120 c/s/μCi in the two detector positions.

Production of ^{11}CO and Labelling of Red Blood Cells

^{11}CO was produced on the Medical Research Council cyclotron at Hammersmith Hospital. The target material, boric oxide, was supported on a wedge, inclined at 10° to the horizontal beam plane, in a gas-tight brass target box which was flushed continuously with commercial hydrogen at 80 ml/min. No carriers were added. With 40 μA of 15 MeV deuterons spread over 7.5 cm^2 at the beam exit-window, the beam power (600 watts) is sufficient to melt the boric oxide and release the volatile radioactive products. These products are ^{11}CO, $^{11}CH_4$, $^{13}N_2$ and $^{11}CO_2$, the percentages being 81, 16, 0.3 and 2 respectively.

Under these conditions, the rate of production and radioactive concentration of ^{11}CO as measured at the target outlet are 3.3 mCi/min and 50 μCi/ml respectively. The specific activity of the ^{11}CO is greater than 900 mCi/mMole. For clinical use, the sweep gas containing the ^{11}CO is normally fed to a point 100 metres from the cyclotron chamber through 1.5 mm stainless steel tubing. A schematic diagram of the flow system is shown in figure 3.

2 ml of heparinised blood were transferred to a sterile 50 ml syringe. Sterile hydrogen containing ^{11}CO was drawn into the syringe, which was capped and rotated

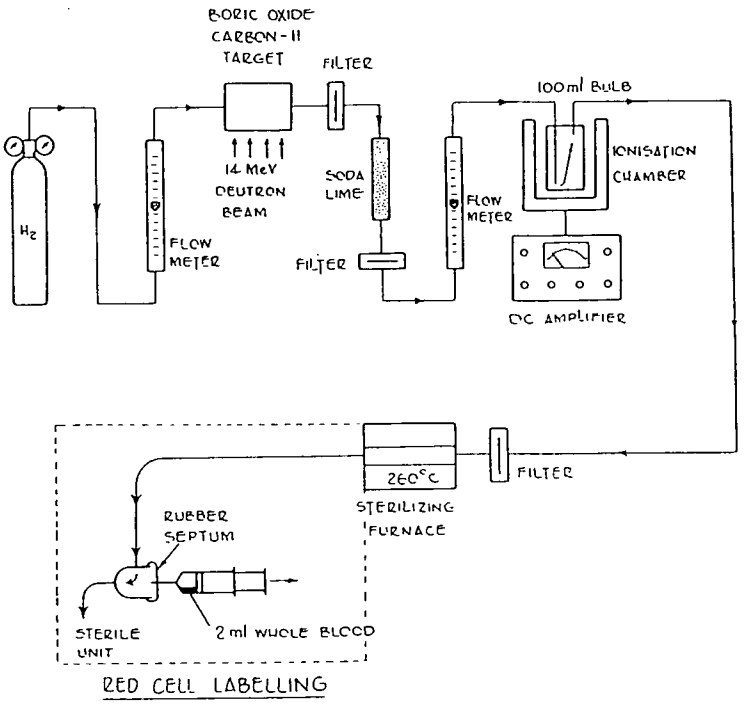

Fig. 3. Flow system for the production of sterile ^{11}CO for use in red cell labelling.

axially at 20 r.p.m. for 10 minutes. The hydrogen and any remaining ^{11}CO were ejected and the activity in the blood measured (CLARK et al., 1966).

Clinical Procedure and Calculations

Fourteen infants were studied. All these infants had required umbilical artery catheterization as part of the routine clinical management for their basic problem, e.g. asphyxia neonatorum, respiratory distress syndrome, and were infants predisposed to develop hypoglycaemia or who had already done so. At the time of inveigation, they had recovered to the extent that no hazard was introduced by the little handling that was necessary for the measurements. In all cases, the umbilical artery catheter was inserted well into the thoracic cage (18—21 cm from the umbilical cord), aiming at a position above the ductus arteriosus and near the left carotid artery takeoff. This manoeuvre was not performed under fluoroscopic control. At the completion of the test, the catheter was pulled back into an intra-abdominal position.

2 mls of venous blood were withdrawn from the patient via the umbilical catheter and were labelled with ^{11}CO. A standard and doses of 0.3 to 1 ml were withdrawn into sterile syringes and the ratios between the activities were measured by counting them between the detectors. The baby was positioned with the line joining the outer canthus to the external auditory meatus placed vertically and 1.5 cm beyond the edge of the lead shielding, i.e. at the level of point A in figure 1. The midplane of the head was at the level of the crystal axes. A dose containing 10 μCi was injected via the arterial catheter.

Approximately five minutes afterwards, the patient was repositioned and two 20 second counts were made to estimate the cerebral blood volume. The standard, diluted with water to 500 mls in a spherical flask of 10.5 cm diameter, was counted. A 1 ml sample of blood was taken from the sagittal sinus and counted in a well counter. 1 ml of the 500 ml standard was counted in the same way.

The rate of change of count rate on the dilution curve was plotted by using time increments of $^5/_{16}$ sec on the upward part of the curve and $^5/_8$ sec on the downpart, and plotting the change in count rate at the midpoint of the increments. The mode transit time was then estimated.

Standard countrates were corrected for decay back to the relevant measurements on the patient, and the countrate obtained with the 10.5 cm diameter flask was corrected for the actual size of the baby's head. The total cerebral blood volume (V) is then given by

$$V = \frac{H}{F} \times \frac{S}{B} \times 500 \text{ mls}$$

where H is the countrate of the head, F is the corrected countrate of the 500 ml standard, S is the corrected countrate of the 1 ml standard, and B is the countrate of 1 ml blood.

The total body blood volume is given by $\frac{S \times R \times 500}{B}$ ml where R is the ratio of activity in the patient's dose to that in the standard.

Results

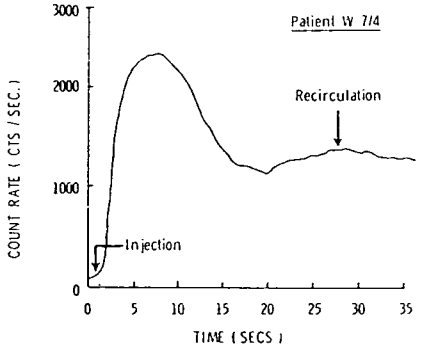

Fig. 4. Dilution curve measured over the head of a patient following intra-arterial injection of 10 μCi of ^{11}CO labelled red blood cells.

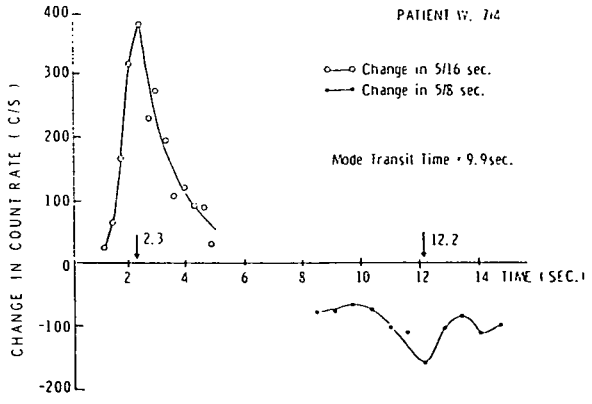

Fig. 5. Graph of the rate of change in countrate obtained from the dilution curve shown in figure 4.

From the fourteen investigations, five satisfactory blood flow results were obtained. A dilution curve of one such patient is shown in figure 4 and the plotted graph of the rate of change of countrate is shown in figure 5. The mode transit time in this case was 9.9 secs. The brain blood volume of this patient was 26.2 mls, and the total cerebral blood flow 189 mls/min. The results of the five successful investigations are shown in table 1. The total blood volume and the percentage of this in the brain are also shown.

The remaining 9 investigations failed since satisfactory transit time curves were not obtained. In some cases, the countrate rose sharply at first but then flattened or continued to rise slowly. The countrate sometimes rose slowly after a delay whilst in other cases the arrival of more than one bolus of activity in the field of view was apparent, and the curve was unusable to measure transit time.

Table 1: Results of Measurements Using ^{11}CO Labelled Red Blood Cells

Patient	Gestational Age (weeks)	Age (hours)	Weigth (gm)	Clinical Condition	Lowest Blood Glucose (mg/100 ml)	Total Blood Vol (ml)	% in Brain	Brain Blood Vol (ml)	Mode Transit Time (sec)	C. B. F. (ml/min)
1	$35^{5}/_{7}$	12	2420	Born early	20	139	14.8	20.6	10.0	126
2	38	27	1180	Small for dates, respiratory distress syndrome, hypoglycaemia	Below 5	119	31.1	26.2	9.9	189
3	$39^{3}/_{7}$	38	1620	Small for dates, birth asphyxia	25	101	29.0	29.1	8.0	218
10	$42^{6}/_{7}$	$28^{1}/_{2}$	3030	Birth asphyxia	52	274	13.0	35.7	6.6	327
11	$40^{3}/_{7}$	30	4100	Birth asphyxia, transient hypoglycaemia	Below 10	254	10.2	26.0	8.4	186

Method Using Krypton-81m and Krypton-85m

Theory

If air or oxygen containing a constant concentration of ^{81m}Kr, which has a 13 second half life, is inhaled, the concentration of radioactivity in the arterial blood rapidly reaches a constant value. This value decreases with distance from the heart, owing to the appreciable decay which occurs with this isotope. If the transit time through the brain is more than 5 half lives, a negligible amount of radioactivity leaves the system in venous blood.

When equilibrium in the brain is established,

Rate of inflow of activity = Rate of decay of activity

$$FC = A\lambda$$

where F = blood flow (ml sec^{-1})
C = concentration of activity in inflowing arterial blood ($\mu Ci\ ml^{-1}$)
A = activity in brain (μCi), and
λ = decay constant of ^{81m}Kr (sec^{-1})

C and A can be measured. A calibration factor to relate the blood well counter and brain external counting systems is required. Then,

if R_e = external detector countrate (c/s)
R_w = countrate per ml of blood in well (c/s)
S_e = sensitivity of external detector to ^{81m}Kr (c/s/μCi)
S_w = sensitivity of well to ^{81m}Kr (c/s/μCi)
and $S = S_w/S_e$,
we have:

$$F = A\lambda/C$$

$$= \frac{R_e/S_e \cdot \lambda}{R_w/S_w}$$

$$= R_e S\lambda/R_w \text{ ml/sec} \ldots\ldots\ldots (1)$$

This technique is useful only if the whole cerebral region can be monitored. However 190 keV gamma radiation is scattered through large angels, which makes it difficult to measure the activity in the brain of small babies without interference from the high activity in the mouth, throat and lungs. If only a part of the brain is monitored, it is necessary to estimate the mass of tissue viewed by the detector.

The mass of tissue being monitored was estimated by inhalation of ^{85m}Kr. As is seen below, this eliminates the variable detector calibration factor S of equation (1), which varies between patients and between different cerebral regions. After the ^{81m}Kr measurement is completed, ^{85m}Kr gas is inhaled until the concentration of radioactivity in the cerebral tissue is constant. In this condition, for ^{85m}Kr,

if A' = activity viewed by detector (μCi)
M = mass of brain tissue viewed by detector (gm)
C' = concentration of activity in the blood (μCi ml^{-1})
P = equivalent volume of blood contained in 1 gm cerebral tissue (ml gm^{-1})
R'_e = external detector countrate (c/s)
R'_w = countrate per ml of blood in well (c/s)
S'_e = sensitivity of external detector to ^{85m}Kr (c/s/μCi)
S'_w = sensitivity of well to ^{85m}Kr (c/s/μCi)
and $S' = S'_w/S'_e$,
we have:

$$M = A'/C'P = R'_e/S'_e \cdot \frac{1}{R'_w/S'_w} \cdot \frac{1}{P} = R'_e S'/R'_w P \text{ gm} \quad \ldots\ldots\ldots (2)$$

The perfusion rate is obtained by combining (1) and (2):

$$\text{Perfusion rate} = \frac{F}{M} = \frac{R_e}{R_w} \cdot \frac{R'_w}{R'_e} \cdot \frac{S}{S'} \cdot \lambda P \text{ ml/sec/gm} \quad \ldots\ldots\ldots (3)$$

The ratio S/S' was found to be constant owing to the similar energies of ^{81m}Kr and ^{85m}Kr (190 keV and 150 keV + 17 % of 305 keV respectively). Its value depends only on the counting conditions and is independent of the geometry and composition of the region viewed by the external detector. The cerebral perfusion rate can thus be obtained from two external counts and two blood sample counts.

The fractional change in flow was measured using ^{81m}Kr only since it is necessary only to measure change in the ratio of A/C under the different physiological conditions being investigated. This technique has the further attraction that it does not depend on the blood sampling being carried out at a point exactly equivalent in distance from the aortic valve to the carotid arteries, since any error is eliminated when the successive results are compared with each other.

Detecting System. Reduction of Scatter Contribution

The external detector consisted of a 1/2" diameter × 1/2" thick NaI crystal, and a 1/2" thick lead shield and 2" long cylindrical collimator which was cut off at an angle of 45°. A single channel analyser was used to select energies from 170 keV to 256 keV when counting ^{81m}Kr and from 138 keV to 198 keV for ^{85m}Kr. The lower gates corresponded to 85 % and 92 % of the photopeak energies of ^{81m}Kr and ^{85m}Kr

respectively. These settings and the angled position of the collimator were chosen to minimise the effect of scatter.

To investigate scatter, a 10 cm diameter flask of inactive water representing a baby's head was suspended above a litre bag which contained a constant activity of ^{81m}Kr and was surrounded by scattering material. The scattered radiation was substantially reduced when the detector was at an angle of 45° below the horizontal, under the counting conditions chosen. The energy spectra with the detector in this position, in the horizontal position and viewing the source directly through the flask are shown in figure 6. Using 170 keV to 256 keV (channels 69 to 99 in figure 6), the countrates in the horizontal and 45° positions were 0.9 and 0.06 % respectively of that in the vertical position. If the full photopeak is counted (155 keV to 227 keV, channels 59 to 99), these values rise to 2.0 % and 0.4 %. Although these are small values, total activity in the mouth and nose is so much greater than in the brain that a scatter contribution of this magnitude could be significant.

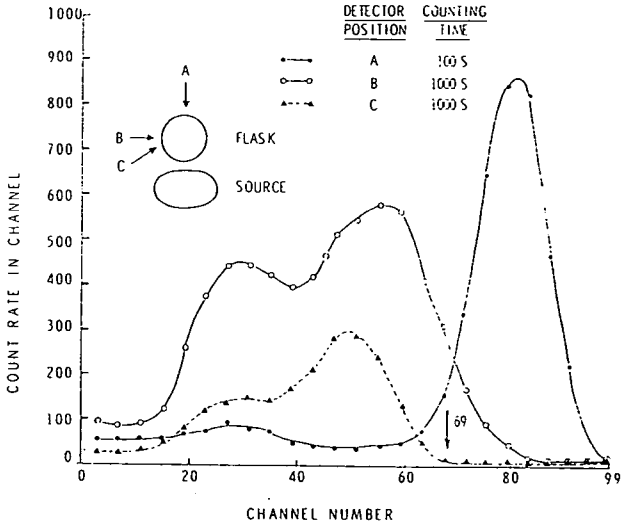

Fig. 6. Energy spectra obtained using a multichannel analyser, when viewing from 3 positions a flask of inactive water placed over an extended source of ^{81m}Kr. Channel 69 corresponds to the lower discriminator used, 170 keV.

Measurements were made on the head of a baby who was inhaling ^{81m}Kr in order to confirm that the scatter contribution was negligible using these conditions. The detector was first directed through the top of the patient's head viewing the air

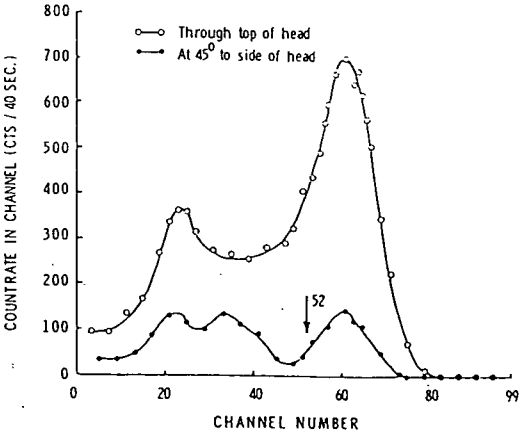

Fig. 7. Energy spectra obtained using a multichannel analyser, when viewing from two positions the head of an infant inhaling ^{81m}Kr. Channel 52 corresponds to the lower gate of 170 keV.

passages and lungs, then at 45° to the side of the skull just above the ear. The spectra obtained are shown in figure 7. The contribution from scatter (0.06 % of the countrate in the first position) was estimated on two successive measurements to be 0.4 % and 0.9 % of the total countrate obtained when viewing at 45°.

The experiment with flask and gas bag was repeated using ^{85m}Kr. The relative contribution of scatter using ^{85m}Kr was greater than that using ^{81m}Kr due to the 305 keV gamma radiation of ^{85m}Kr as well as to the slightly greater scattering effect at 150 keV, and the lower gate was required to be set higher (92 % of photopeak value compared with 85 %).

Production of Krypton-81m Generator and of Krypton-85m

Krypton-81m was generated continuously in the gas phase by passing air or air-oxygen mixtures through a solution containing ^{81}Rb, half life 4.7 hr. A schematic diagram of the generator is shown in figure 8. ^{81}Rb was prepared by irradiating sodium bromide with 30 MeV alpha particles in the external beam of the M.R.C. cyclotron, the nuclear reaction being ^{79}Br (α, 2n) ^{81}Rb. The yield of ^{81}Rb for a 1 hr bombardment at 35 μA is 90 mCi.

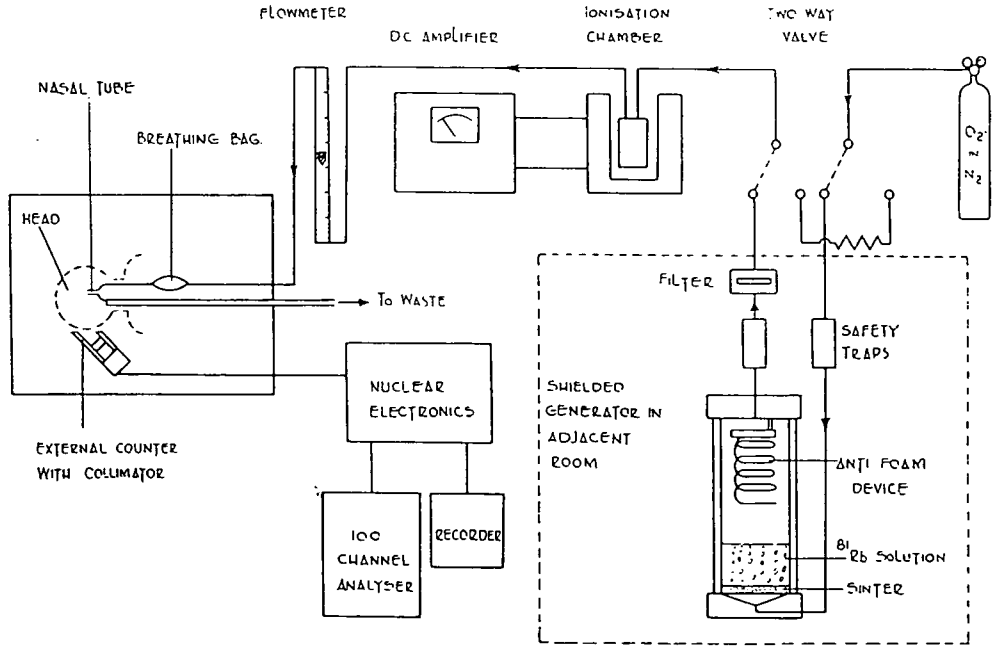

Fig. 8. Schematic diagram of the circuit used to supply ^{81m}Kr to infants, and of the detecting system.

Krypton-85m was produced by irradiating krypton gas with 15 MeV deuterons, the nuclear reaction being ^{84}Kr (d, p) ^{85m}Kr. Contaminants ^{87}Kr, 1.27 hr, and ^{79}Kr, 1.45 d, are also produced by (d, p) reactions on ^{86}Kr and ^{78}Kr respectively. The ^{87}Kr was allowed to decay for 14 hours before the gas was used clinically. The levels of these contaminants at time of use were 1 % ^{87}Kr and 2.5 % ^{79}Kr.

The irradiation was carried out in a 45 cm long water cooled target box filled with 2.5 litres of krypton at a pressure of 0.7 kgm cm^{-2}. A typical yield of ^{85m}Kr at end of bombardment was 60 mCi for a 2 hour bombardment with a deuteron beam current

of 35 μA. Assay was carried out by γ spectrometry using a 15 cc Ge(Li) spectrometer. Reliable assays could not be carried out using ionisation chambers due to interference from ^{79}Kr and traces of ^{87}Kr.

Clinical Procedure

The infants investigated had all had umbilical artery catheters inserted for the monitoring of gas tensions or metabolites. The babies remained in their incubators during the investigation. The gas with which the radioactivity was mixed was chosen according to the breathing requirements of the individual patient. The external detector was positioned on the side of the patient's head just above the ear.

Blood samples were taken rapidly from the umbilical arterial catheter by means of a three way tap. In the case of ^{81m}Kr, timing for the purpose of decay correction was measured from the beginning of the withdrawal of blood. The 0.5 ml sample was removed into a weighed syringe whose dead space was filled with heparin. The capped syringe was counted directly in the well.

The circuit used for ^{81m}Kr is shown schemetically in figure 8. The generator was sited in a lead shield in an adjacent room. A filter and traps were fitted close to the generator to ensure no ^{81}Rb escaped and a two way valve system allowed switching between active and inactive gas. The yield from the generator was measured continuously by a high pressure ionisation chamber containing a bulb of known volume. The gas flow was monitored before passing to the patient via a miniature breathing bag and nasal tube. The excess gas and expired gas was led to waste through a large bore tube. In some cases the circuit was modified to allow the patient to remain on a respirator. Flow rates between 600 ml/min and 4000 ml/min were used, the high flow rates being necessary when the patient was being ventilated with a respirator.

For ^{85m}Kr a rebreathing circuit was used, as shown in figure 9. The circuit was filled with a known volume of krypton containing ^{85m}Kr at a known specific activity.

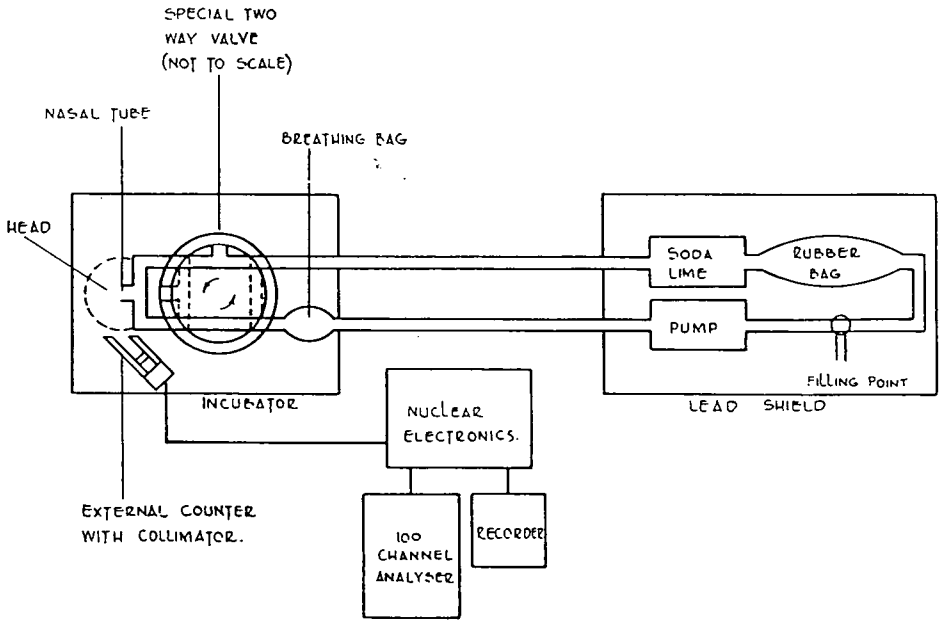

Fig. 9. Schematic diagram of the rebreathing circuit used to supply ^{85m}Kr to infants, and of the detecting system.

Oxygen was then added until the oxygen concentration was at the desired level for the particular patient under investigation. The patient was allowed to breathe normally or on the closed circuit by means of the large bore two-way tap.

The radioactive concentrations of activity used were 20 mCi/litre for ^{81m}Kr and 200 μCi/litre for ^{85m}Kr, the low concentration of ^{85m}Kr being necessary to reduce the radiation dose. A constant countrate over the head was obtained after inhalation of ^{81m}Kr for 30 to 60 secs, when the countrate varied from 5 c/s to 15 c/s above a background of 0.6 c/s. Time for equilibration of ^{85m}Kr was about 6 min. The countrate was 1 to 2 c/s above a background of 0.6 c/s.

Two investigations were made using both gases and three investigations with ^{81m}Kr only. The baby breathed ^{81m}Kr for a total of 160 seconds. 60 seconds after the beginning of inhalation, a 100 sec count over the head was started. A blood sample was taken 50 sec after beginning the head count, and counted immediately. The baby then breathed ^{85m}Kr for a total of 15 minutes. After inhalation for 9 minutes, the head was counted for 400 sec, a blood sample being taken at the midtime of this count. A background measurement was made for each isotope with the gas circuit full and with the detector in the normal position, but with a lead plug in the collimator. The sampling syringes were weighed and the pO_2 and pCO_2 of the blood was measured.

The ^{81m}Kr well countrates were corrected for decay during both counting time and the time between sampling and the beginning of the count. The countrate/gm of blood was found for each well measurement. The relative blood flow was found from the repeat ^{81m}Kr measurements by calculating the ratio of the head countrate to the countrate/gm of blood, and normalising to the highest value of the ratio.

Results

The low countrate obtained with ^{85m}Kr made results obtained with this method unreliable. A flow rate of 96 mls/min/100 gm was obtained for one patient. The results of the repeat measurements with ^{81m}Kr are shown in table 2, together with clinical data.

Table 2: Results of Repeated Measurements Using Krypton-81m

Patient	Gestational Age (weeks)	Age (hours)	Weight (gm)	Clinical Condition	Relative Flow	pO_2	pCO_2
1	33	39	2060	Respiratory distress syndrome, born early	1.00	90	30
					0.67	65	35
					0.74	65	38
2	32	16	1800	Respiratory distress syndrome, born early	1.00	99	36
					0.97	97	36
3	32	35	1800	Respiratory distress syndrome born early, birth asphyxia	1.00	60	25
					0.82	30	23.5

Discussion

The method using ^{11}CO labelled red blood cells provides an atraumatic method for the measurement of total cerebral blood flow in the newborn infant. If it were

possible to position the catheter tip using an image intensifier, it is likely that successful measurements could always be carried out, but there would be a significant increase in radiation dose.

The studies were performed at a time when the infant's circulatory system was undergoing a change from a foetal-type circulation to an adult-type circulation, and thus early re-circulation of the bolus of the ^{11}CO red blood cells, particularly through the ductus arteriosus could explain the failure of the method in 9 of the infants studied. It would seem that critical placement of the catheter tip above the ductus arteriosus, specifically in the ascending part of the aorta, is essential.

In the 5 successful cases, the cerebral blood flow found was slightly higher than one would have expected. The variation in the blood flow from infant to infant may be accounted for by the different clinical conditions of the infants, some having developed a greater degree of acidosis and hypercapnea than others.

The method using both ^{81m}Kr and ^{85m}Kr is potentially useful, but was not usable with babies owing to the limitation on ^{85m}Kr concentration due to radiation dosage. It could be used for measurements on adults where a higher radiation dose may be acceptable. The positioning of the arterial sampling catheter to give a concentration comparable to that in the carotid arteries would have to be carefully chosen.

Repeat measurements using ^{81m}Kr proved useful in investigating the effect of change in pO_2 and pCO_2 in babies. The lowering of blood flow with a decrease in pO_2 in the patients investigated was unexpected.

This method can only be accurate if successive measurements are made without any movement of the patients or detector. Any relative movement changes the region monitored and also the ratio of the counter sensitivities. Long term changes in blood flow therefore cannot be investigated in this way.

The investigation of the contribution of scatter to countrates mesaured over the heads of patients inhaling radioactive gas are of interest. The results indicate that measurements on adults using low energy radiation and large collimators and counting the full photopeak will include a substantial number of counts from scattered radiation.

Conclusion

Three methods are described for the measurement of cerebral blood flow in the newborn infant. The method measuring total cerebral blood flow using ^{11}CO labelled red blood cells is dependent upon the precise placement of the catheter tip in the aorta above the ductus arteriosus. With this method, 5 successful estimations of cerebral blood flow were made. The method employing ^{81m}Kr and ^{85m}Kr was not reliable with the concentrations of ^{85m}Kr used. The method using repeated measurements with ^{81m}Kr alone was useful in assessing the dependence of the brain perfusion rate on pO_2.

Acknowledgements

We are grateful to Dr. J. Rundo of the A.E.R.E., Harwell who loaned us the two large crystals to make possible the work with ^{11}C, and to the Sir William Coxen Trust Fund for provision of laboratory facilities. We wish to thank all staff and users of the M.R.C. cyclotron who co-operated in enabling schedule changes to be made at short notice in order to allow the production of these isotopes as required, shortly after the birth of the patients. We appreciate the encouragement given by Professor J. F. Fowler and Professor J. P. M. Tizard.

References

Clark, J. C., H. I. Glass, and D. J. Sylvester: In vitro Labelling of Red Cells with Carbon-11. Proc. 2nd Int. Conference on Methods of Preparing and Storing Labelled Compounds. Brussels, Nov. 28—Dec. 3, 1966.

Cornblath, M., and R. Schwartz: Disorders in Carbohydrate Metabolism in Infancy. Major Problems in Clinical Paediatrics, Vol. 3. W. B. Saunders Co., Philadelphia and London 1966.

Edwards, A. V.: Resistance to Hypoglycaemia in the Newborn Calf. J. Physiol. (Lond.) 171 (1964), 46.

Fedoruk, S., and W. Feindel: Measurement of Brain Circulation by Radioactive Iodinated Albumin. Canad. J. Surg. 3 (1960), 312.

Katsuki, S., H. Uzawa, K. Tanaka, K. Fukiyama, M. Fujishima, and I. Omae: Brain Circulation Studies by External Counting of Intravenously Injected RISA. Jap. Heart J. 5 (1964), 127.

Kemplay, J. R., and P. Vernon: An Efficient Method of using an Audio Magnetic Tape Recorder for Storing Random Pulses. J. sci. Instrum. 44 (1967), 566.

Mallett, B. L., and N. Veall: Investigation of Cerebral Blood Flow in Hypertension, using Radioactive Xenon Inhalation and Extracranial Recording. Lancet I (1963), 1081.

Matthews, C. M. E.: Personal communication, 1967.

Meier, P., and K. L. Zierler: On the Theory of the Indicator-Dilution Method for Measurement of Blood Flow and Volume. J. appl. Physiol. 6 (1954), 731.

Obrist, W. D., H. K. Thompson jr., C. H. King, and H. S. Wang: Determination of Regional Cerebral Blood Flow by Inhalation of Xenon-133. Circulat. Res. 20 (1967), 124.

Oldendorf, W. H.: Measurement of the Mean Transit Time of Cerebral Circulation by External Detection of an Intravenously Injected Radioisotope. J. nucl. Med. 3 (1962), 382.

Oldendorf, W. H.: Measuring Brain Blood Flow with Radioisotopes. Nucleonics 21 (1963), 87.

Owen, O. E., A. P. Morgan, H. G. Kemp, J. M. Sullivan, M. G. Herrera, and G. P. Cahill: Brain Metabolism during Fasting. J. clin. Invest. 46 (1967), 1589.

Reekie, D., M. Davison, and J. K. Davidson: The Radiation Hazard in Radiography of the Female Abdomen and Pelvis. Brit. J. Radiol. 40 (1967), 849.

Saperstein, L. A.: Measurement of Cephalic and Cerebral Blood Flow Fractions of Cardiac Output in Man. J. clin. Invest. 41 (1962), 1429.

Scopes, J. W.: Discussion of Hypoglycaemia. Proc. roy. Soc. Med. 57 (1964), 1065.

Steiner, S. H., K. Hsu, L. Oliner, and R. H. Behnke: Measurement of Cerebral Blood Flow by External Isotope Counting. J. clin. Invest. 41 (1962), 2221.

Veall, N., and B. L. Mallett: Regional Cerebral Blood Flow Determination by ^{133}Xe Inhalation and External Recording: the Effect of Arterial Recirculation. Clin. Sci. 30 (1966), 353.

Zierler, K. L.: Equations for Measuring Blood Flow by External Monitoring of Radioisotopes. Circulat. Res. 16 (1965), 309.

Diskussion zum Vortrag Arnot

S. Grebe, Gießen:

In welcher Größenordnung liegt die Strahlenbelastung bei diesen Neugeborenen und bedeuten sie kein Risiko für diese Patienten?

R. Arnot, London:

The radiation dose to the whole body from 10 μC of ^{11}C labelled red blood cells varies from 2,5 to 6,5 mrads depending on the weight of the patient. The administration of Krypton-81m (20 mC/active for 2,5 minutes) gives a dose of 48 mrads to the lungs and a negligeable whole body dose. For Krypton-85m (0,2 mC/active for 15 minutes) the lung dose is 42 mrads and the whole body dose 1 mrad. In comparison the whole body dose to the foetus from a single x-ray film of the maternal pelvis in late pregnancy is from 100 to 300 mrads.

Department of Medicine, Universitäts Klinik, Innsbruck

Department of Medical Physics, Medical Research Council Cyclotron Unit and Department of Medicine, Hammersmith Hospital, London

Electrolyte and Body Fluid Investigations in Endocrine Diseases using Cyclotron Produced Isotopes

By

F. Skrabal, R. N. Arnot, J. C. Clark, F. Helus, H. I. Glass and G. F. Joplin

Abstract

The different gamma energies of ^{24}Na, ^{43}K and ^{77}Br allow mixtures of the three isotopes that contain normal quantities of activity to be analyzed with an error of less than 1.5 % by gamma counting of previously untreated samples. A computer programme is used to perform the calculations.

This method was used to investigate the relation between Na space and Br space in 20 normals and in 46 patients with various endocrine or metabolic diseases.

The mean value for the Na space/Br space ratio in normals was found to be 1.13 ± 0.07 (± 2 S.D.). 39 % of the patients were found to have values for the Na space/Br space ratio which were outside the 95 % confidence limits for the normal group. The possibility of detecting cellular Na gain or loss on a whole body basis is discussed.

Extrait

Des quantités normales de ^{24}Na, ^{43}K et ^{77}Br contenues dans un même échantillon peuvent être séparées par spectrométrie γ et mesurées par une méthode non destructive avec un pourcentage d'erreur inférieur à 1,5 %. Un programme de calculateur est utilisé pour obtenir les résultats.

Cette technique a été employée pour étudier le rapport entre l'espace Na et l'espace Br chez 20 sujets normaux et chez 46 patients atteints d'affections endocrines ou métaboliques diverses. La valeur moyenne du rapport espace Na/espace Br a été trouvée égale à $1,13 \pm 0,07$ (± 2 S.D.) chez les sujets normaux.

Chez 39 % des malades, la valeur de ce rapport se trouve en dehors des limites de confiance à 95 % établies pour le groupe normal. La possibilité de détecter par cette méthode une accumulation ou une perte de Na intracellulaire par l'organisme est discutée.

Auszug

Durch die Einführung zweier im Cyclotron hergestellter Isotope, Brom-77 und Kalium-43 wurde es möglich, Mischungen dieser beiden Isotope mit Natrium-24 erstmals ohne vorherige Trennverfahren zu analysieren, indem man die unterschiedliche Gammastrahlung der drei Isotope unter verschiedenen Zählbedingungen mißt. Die Ergebnisse werden mit Hilfe eines Computers errechnet.

Kombiniert mit einer Bestimmung von tritiummarkierten Wassers wurde diese Methode für die gleichzeitige Messung des austauschbaren Natriums, austauschbaren Kaliums, extra-

zellulären Raumes und des Körperwassers bei 20 Gesunden und 46 Patienten mit endokrinen Störungen angewendet. Spezielles Interesse lag auf der Bestimmung der Fraktion des austauschbaren Natriums, die außerhalb der extrazellulären Flüssigkeit liegt.

Das Durchschnittsverhältnis Natriumraum: Bromidraum betrug bei Gesunden $1{,}13 \pm 0{,}07$ (± 2 S.D.). 39 % der Patienten mit endokrinen Störungen lagen außerhalb der Vertrauensgrenzen für gesunde Kontrollobjekte. Die Möglichkeit, Veränderungen des intrazellulären Natriumgehaltes an einer Ganzkörperbasis festzustellen, wird diskutiert.

Introduction

To investigate electrolytes and body water in humans, several methods are available. Tissue analysis may be used to investigate the composition of a single tissue, or balance studies may be used to examine net gains or losses from the body. However, neither method gives information about the distribution of electrolytes in the body or the total body stores. This information can be obtained by use of the isotope dilution technique.

The simultaneous measurement of exchangeable Na (Na_E), exchangeable K (K_E), extra cellular fluid volume (ECFV) and total body water (TBW) permits the calculation of distribution of sodium, potassium and water between the extra cellular and intra cellular spaces (Veall and Vetter, 1958).

In spite of the obvious advantage of using four isotopes simultaneously, the few reported clinical studies have indicated the inaccuracies and difficulties in separating isotopes in the same sample by chemical or physical separation procedures.

The use of two cyclotron-produced isotopes, ^{43}K (Skrabal, Glass et al., 1969) and ^{77}Br (Skrabal, Arnot et al., 1969) made it possible to analyse by gamma counting mixtures of these two isotopes together with ^{24}Na as untreated plasma and urine samples. A computer programme is used to perform the calculations and includes an allowance for decay of the isotopes during the counting time. Tritiated water may be estimated on the same samples after decay of the other three isotopes.

When it became possible to measure the dilution of ^{24}Na and ^{77}Br accurately on the same untreated samples (and in the presence of ^{43}K), the question arose whether it might now be possible to detect smaller differences between these two very similar physiological spaces. Various workers (McMurray et al., 1958; Crooks et al., 1959; Moore et al., 1963) have measured both spaces simultaneously, yet alterations in the ratio between the two spaces in any disease do not appear to have been demonstrated.

Whe have investigated the possibility of detecting an excess or a deficit of exchangeable sodium outside the bromide space and this paper presents our findings in 66 clinical studies.

Material and Methods

Production of ^{43}K

^{43}K is produced by the ^{40}A (α, p) ^{43}K reaction in the external beam of the Medical Research Council cyclotron. The argon is circulated at a rate in excess of 100 l/min through the target vessel and bombarded with 16.4 MeV α particles. The exit gas is passed through a borosilicate fiber-glass filter which extracts $50 - 80$ % of the activity from the gas phase. The activity is removed from the filter using 5 ml of 0.001 N hydrochloric acid. This solution is then evaporated to dryness and baked in the presence of 5 mgm KCl carrier. The residue is taken up in 5 ml of isotonic saline and filtered through a millipore filter. The yield of ^{43}K is 18 μCi/μA hr and the

^{42}K contamination at end of bombardment is less than 7 per cent (CLARK and WATSON, 1969).

Production of ^{77}Br

^{77}Br is produced by the ^{75}As (α, 2 n) ^{77}Br reaction in the external beam of the M.R.C. cyclotron. The target material, As_2O_5, is bombarded with α particles of approximately 28 MeV, the yield of ^{77}Br being about 3 mCi for a 1 hour bombardment at 20 μA. The As_2O_5 is then dissolved in hot water and after adding concentrated H_2SO_4 and $K_2Cr_2O_7$, the bromine is distilled, without the addition of carrier, into an ice-cooled water trap. The pH of this solution is then adjusted to 9 and the bromine is reduced to bromide by adding NH_2OH. HCl solution. The solution is evaporated to dryness and the residue is heated to about 400° C to decompose any possible pyrogenic contaminants, then dissolved in water for injection. The resulting solution is adjusted to pH 6–7 and filtered (HELUS, 1969).

^{24}Na and ^{3}H

The ^{24}Na was received in the form of sterile NaCl in isotonic solution from the Radiochemical Centre, Amersham. Sterile tritiated water was obtained from the same suppliers.

Patients Studied

20 normal subjects and 46 patients suffering from various endocrine diseases were investigated. The patients were classified as follows: untreated acromegaly (8), treated acromegaly (pituitary implantation of yttrium-90) (9), Cushing's disease (5), and 10 hypopituitary subjects. There were 14 patients with various other endocrine or metabolic diseases.

Clinical Procedures

20 μCi of ^{24}Na and 50 μCi of ^{43}K were administered intravenously at 9 a.m. 12 hours later 30 μCi ^{77}Br and 250 μCi $^{3}H_2O$ were injected. Doses for injection were prepared in counting vials and after injection, the residue in the syringe was washed into the dose vial and made up to 10 mls for subsequent counting. Normal meals were permitted from 9 a.m. to 8 p.m. after which no fluids or food was taken until 10 a.m. on the following day. Urine was collected in polythene bottles as follows: 0–24 hours, 24–25 hours, 25–26 hours. Heparinised blood samples were taken at 24 hours and 25 hours.

The concentration of stable sodium and potassium in the plasma was estimated on an auto-analyser and in the urine samples on a flame photometer.

Radioactive Assay and Calculations of Results

A dose of each isotope, identical to that given to the patient was used to prepare three standard solutions in siliconed glass flasks by diluting each dose with distilled water up to 1 litre. Duplicate 10 ml samples of each standard solution and 10 ml of each plasma and urine sample, together with a background sample of water, were transferred into counting vials. All samples were counted twice on a two channel automatic counter, equipped with a punched paper tape output. The first time, the

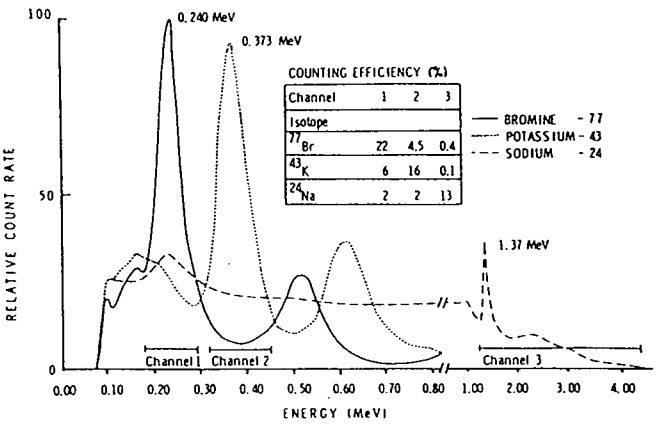

Fig. 1. Energy spectra of ^{77}Br, ^{43}K and ^{24}Na, showing the channels used and the counting efficiencies for each isotope.

channels were arranged to accept energies between 320 KeV and 447 KeV (^{43}K), and between 1.2 MeV and 4.5 MeV (^{24}Na) respectively. The samples were counted again either immediately or up to two days later using one channel arranged to accept energies between 190 KeV and 275 KeV (^{77}Br). Spectra of the three isotopes are shown in figure 1. A computer programme was used to calculate the quantity of each isotope in each sample. Details of the equations used and of the computer programme are given elsewhere (SKRABAL, ARNOT et al., 1969). A factor of 0.9 was used to correct the bromide space for serum water and Donnan equilibrium. For the calculation of the Na space it was assumed that the corrections for serum water and Donnan equilibrium cancel each other.

We have shown that using this method, mixtures of ^{24}Na, ^{43}K, ^{77}Br in the proportions encountered in space measurements, can be analysed with an error of less than 1.5 % (SKRABAL, ARNOT et al., 1969).

Results

The individual results for Na_E, K_E, ECFV and TBW and the calculated values for intracellular K concentration are given elsewhere (SKRABAL, ARNOT et al., 1969; SKRABAL et al., in preparation). The Na space/Br space ratio in 20 normal subjects was found to be 1.13 $\pm$ 0.07 ($\pm$ 2 S.D.). Figure 2 shows the Na space/Br space ratio for normal subjects calculated from data in the literature compared with the results of this series. The Na space/Br space ratio for our normals (95 % confidence limits) and the ratio for 46 patients with various endocrine or metabolic diseases are shown in figure 3. It can been seen that 28 patients (61 %) out of the 46 patients are within the normal range. 13 patients (28 %) were found to have higher values (range 1.2 to 1.35) and 5 patients (11 %) had a ratio closer to unity (range 1.04 to 1.00).

Discussion

To investigate cellular sodium only a few methods are available. The only cells easily separated from the extra cellular fluid with its large Na content are the blood cells, and red blood cells have been used to measure the amount of intra cellular sodium (RIECKER et al., 1963; BEILIN, 1966). Since red cells are the only cells without nuclei in the human body and are known to have a low metabolic rate, alterations in red cell sodium do not necessarily imply that the sodium content of other body cells is also altered.

Tissue analysis has also been used by LITCHFIELD and GADDIE (1958), to measure cellular sodium, but conflicting results have been reported by FLEAR (1965), presumably due to the difficulties in correcting for the large amount of extra cellular sodium.

It has been shown that the amount of sodium in cells (FLEAR et al., 1960; Dow and IRVINE, 1967) and bone (EDELMAN et al., 1954) is significantly bigger than the chloride content of these tissues. The fact that the Na space after equilibration is found to be greater than the bromide space confirms that the excess Na in cells and bone is at least partly exchangeable. The exchangeable sodium outside the ECFV has been referred to simply as the residual sodium, since the exact anatomical site of this space is not certain. The calculation of residual Na needs the isotopic measurement of radioactive sodium and bromide as well as the chemical estimation of stable Na in the plasma. Furthermore, the size of this space is as dependent on body height and weight as the total exchangeable Na. To establish values of residual Na for normal subjects, we have chosen the Na space/Br space ratio, which depends only on the isotopic measurement.

Fig. 2. Mean values for the Na space/Br space ratio calculated from data in the literature compared with the results of this series.

Figure 2 shows that various workers using different methods have found mean values for the Na space/Br space ratio ranging from 1.21 to 1.13. These differences may be due to systematic errors introduced by the methods and to the use of elaborate calculations for deriving the ECFV (MCMURRAY et al., 1958; MOORE et al., 1963).

The problem in measuring mean whole body intracellular sodium and potassium concentration is the lack of a suitable tracer for ECFV. Tracers such as inulin which do not penetrate into all compartments of the ECFV, underestimate the amount of extracellular ions and therefore lead to high calculated values for intracellular (exchangeable) sodium.

Bromide is known to measure the whole ECF and in addition to penetrate the cells to some degree. Therefore, it also is not a true measure of extracellular fluid. Moreover, the ECF is not an exactly defined physiological space. A review of the problems in extimating the ECFV is given by WALSER (1967).

Our mean ratio of 1.13 for normal subjects implies that about 300 to 400 mEq Na are placed outside the bromide space in cells and bone. Using the difference between TBW (as measured with tritiated water) and the Br space as a measure for intracellular water, we derived an intracellular concentration of Na of about 10 mEq/litre. This agrees well with the reported values obtained from tissue analysis. Since it is

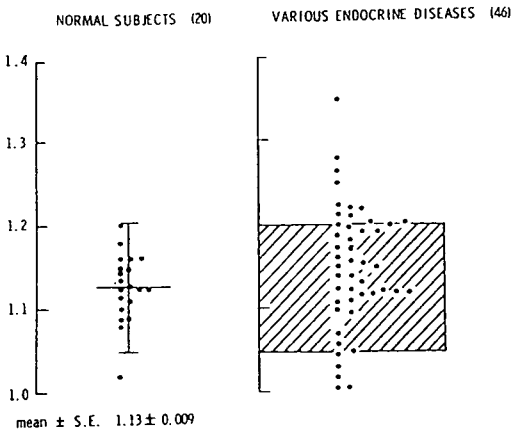

Fig. 3. Na space/Br space ratio in 20 normal subjects and in 46 patients with various endocrine and metabolic diseases.

known that isotopic Na exchanges also with the bone crystals (EDELMAN et al., 1954), the values for the true cellular Na concentration after subtraction of the Na exchanged in bone would be considerably lower.

Figure 3 shows a disturbed Na space/Br space ratio in 39 % of the patients with various endocrine diseases. The high ratio in 28 % of the patients would indicate either an excess of exchangeable Na outside the extracellular fluid or gradual elimination of bromide from the cells. The removal of bromide from the cells is the consequence of an active transport mechanism. It seems unlikely that this would occur in disease states. It is not possible to draw conclusions about the absolute amount of increased "cellular" sodium, since simultaneous shifts of bromide may occur. The low ratio in 11 % of the patients could imply that Na moves out of the cells or that bromide penetrates the cells in some conditions to a greater extent than sodium.

It is known that after 24 hours the specific activity of Na in tissues other than bone is constant and equal to the specific activity in plasma. The same applies to bromide after 12 hours. Increase in "cellular" sodium therefore does not represent an increased exchangeability of Na in the cells. It is likely to reflect either a true gain of intracellular sodium in excess of bromide, on a whole body basis, or in some conditions an increased exchangeability of Na in bone. It will be of interest, to compare the results of cell or tissue analysis in conditions in which cellular sodium gain is known to occur (e.g. the red cell sodium in uraemia) with the whole body measurements.

Conclusion

The results indicate that alterations in the exchangeable fraction of body Na outside the bromide space occur in various endocrine or metabolic disorders and are detectable with this method. Similar changes of residual sodium were found in patients suffering from endocrine disorders as well as in patients with metabolic bone disease. The exact anatomical site of the alterations in residual Na remains an open question for further investigation.

Acknowledgements

We wish to thank Professor RUSSELL FRASER for his continued support. The ^{24}Na and some equipment were purchased with a grant to G. F. J. from the ERNEST and MINNIE DAWSON Cancer Trust. F. S. gratefully acknowledges a Fellowship from the Austrian Government.

References

Beilin, L. J., G. J. Knight, A. D. Munro-Faure, and J. Anderson: The Measurement of Sodium Concentration in Human Red Blood Cells. J. gen. Physiol. 50 (1966), 61.

Clark, J. C., and I. A. Watson: The Preperation of ^{43}K for Medical Use. Radiochem. Radioanalyt. Letters (Submitted 1970).

Crooks, J., M. M. Bluhm, and F. P. Muldowney: The Interrelation between Total Exchangeable Sodium, Potassium and Chloride, and Lean Body Mass in Man. Clin. Sci. 18 (1959), 175.

Dow, J. W., and R. O. H. Irvine: Determination of the Chloride Content of Small Muscle Samples. Clin. Chim. Acta 15 (1967), 199.

Edelman, I. S., A. H. James, H. Baden, and F. D. Moore: Electrolyte Composition of Bone and the Penetration of Radiosodium and Deuteriumoxide into Dog and Human Bone. J. clin. Invest. 33 (1954), 122.

Flear, C. T. G., R. F. Crompton, and D. M. Matthews: An In Vitro Method for the Determination of the Inulin Space of Skeletal Muscle with Observations on the Composition of Human Muscle. Clin. Sci. 19 (1960), 483.

Flear, C. T. G., R. G. Carpenter, and I. Florence: Variability in the Water, Sodium, Potassium and Chloride Content of Human Skeletal Muscle. J. clin. Path. 18 (1965), 74.

Helus, F.: The Production of ^{77}Br for Medical Use. Radiochem. Radioanalyt. Letters (In press 1970).

Litchfield, J. A., and R. Gaddie: The Measurement of the Phase Distribution of Water and Electrolytes in Skeletal Muscle by the Analysis of Small Samples. Clin. Sci. 17 (1958), 483.

McMurray, J. D., E. A. Boling, J. M. Davis, H. V. Parker, I. C. Magnus, M. R. Ball, and F. D. Moore: Body Composition: Simultaneous Determination of Several Aspects by the Dilution Principle. Metabolism 7 (1958), 651.

Moore, F. D., K. H. Olesen, J. D. McMurray, H. V. Parker, M. R. Ball, and C. M. Boyden: The Body Cell Mass and its Supporting Environment. p. 532. W. B. Saunders Company, Philadelphia: London 1963.

Riecker, G., H. J. Gurland, H. Edel, H. D. Balte, J. Eigler, E. Renner, und E. Buchborn: Neue Methoden zur Erkennung von Störungen der intra-extracellulären Wasser- und Elektrolytverteilung bei Niereninsuffizienz. Verh. dtsch. Ges. inn. Med. 69 (1963), 707.

Skrabal, F., H. I. Glass, J. C. Clark, K. Jeyasingh, and G. F. Joplin: A Simplified Method for Simultaneous Electrolyte Studies in Man Utilizing Potassium-43. Int. J. appl. Radiat. 20 (1969), 677.

Skrabal, F., R. N. Arnot, F. Helus, H. I. Glass, and G. F. Joplin: A Method for Simultaneous Electrolyte Investigations in Man using Bromine-77, Potassium-43 and Sodium-24. Int. J. appl. Radiat. (In press 1970).

Skrabal, F., R. N. Arnot, and G. F. Joplin: Body Composition Studies in Acromegaly, Mb. Cushing, Primary Hyperaldosteronism and Insulinoma. (In preperation).

Veall, N., and H. Vetter: In: Radioisotope Techniques in Clinical Research and Diagnosis, p. 209. Butterworth, London 1958.

Walser, M.: Compartments, Pools and Spaces in Medical Physiologie. p. 241. U.S. Atomic Energy Commission 1967. Conf. 661010.

Diskussion zum Vortrag Skrabal

B. Francois, Lyon:

Je voudrais évoquer deux points.

En premier lieu, je ne mésestime pas l'intérêt pour les études du métabolisme hydrominéral de l'utilisation de ces nouveaux radionuclides produits par un cyclotron. Je signale simplement que chaque semaine, depuis 8 ans, nous utilisons des techniques conventionnelles qui donnent toute satisfaction: séparation $^{22}Na - ^{82}Br$ ou $^{24}Na - ^{82}Br$ par des équations de décroissance radioactive, séparation de l'eau tritiée d'avec le sodium et le brome par distillation par le vide du sérum.

Le deuxième point est une question. L'orateur a fait état d'une valeur de sodium résiduel représentant 10 % du sodium échangeable et d'une position intra cellulaire de ce sodium résiduel. J'avais la notion que le sodium intra cellulaire n'exédait pas 3 % du sodium échangeable et que le sodium résiduel était essentiellement squelettique. L'auteur donne-t-il au sodium résiduel une signification véritablement cellulaire?

F. SKRABAL, Innsbruck:

Ich selbst halte Natrium-22 auf Grund der langen Halbwertszeit und Strahlungscharakteristik nicht für wünschenswert für diese Studien, speziell da Wiederholungen innerhalb kürzester Zeit von Interesse sind.

Die Halbwertszeiten von 56 Stunden für Brom-77, 22 Stunden für Kalium-43 und 15 Stunden für Natrium-24 erlauben eine Wiederholung der Studien innerhalb einer Woche, andererseits sollten sie die Durchführung der Untersuchung auch an Kliniken ermöglichen, die über kein eigenes Cyclotron verfügen.

Zur zweiten Frage:

Ich glaube, wir stimmen in dem Punkt überein, daß es prinzipiell nicht möglich ist, mit dieser Methode zwischen intrazellulärem und im Knochen austauschbarem Natrium zu unterscheiden. Wir haben gleichsinnige Veränderungen des Na/Br-Raumverhältnisses sowohl bei Patienten mit Nebennierenrindeninsuffizienz gefunden als auch bei Patienten mit Knochenerkrankungen. Bei der ersten Gruppe kam es zum Anstieg des Residualnatriums innerhalb weniger Tage. Die gleichzeitig erfolgende zelluläre Hydration würde für eine intrazelluläre Anreicherung des Natrium sprechen Überdies ist der Austausch von Elektrolyten im Knochen hauptsächlich abhängig von der aktiven Knochenoberfläche, d. h. Resorptionsfläche. Es erscheint mir unwahrscheinlich, daß diese sich innerhalb kürzester Zeit ändern würde.

N. TELFER, Los Angeles:

Did you measure the exchangeable potassium at 24 and 48 hours? Did you find any abnormalities in the intracellular concentration of potassium?

F. SKRABAL, Innsbruck:

To answer your first question: We have measured the exchangeable K beginning from 24 hours up to 48 hours and we found in agreement with other workers an increase in exchangeable potassium. This increase was fairly constant in all patients and as we were not certain as to how much this increase was due to newly ingested K, we have chosen the 24 hours equilibration period.

To your second question: In the particular group of patients studied we did not find a change in intracellular potassium concentration. Since residual or "intracellular" Na increased the cellular hydration which occurred in some of the patients would be explained by the increasing amount of intracellular ions.

C. CONSTANTINIDES, Athen:

When you measure the Na Space/Br Space ratio, do you consider the fraction of Na which goes to bone? Because this may introduce an error into your calculations.

F. SKRABAL, Innsbruck:

I think we have covered that point partly already in the discussion with Prof. FRANCOIS. It is certainly not possible to calculate absolute figures for the intracellularily located sodium. Therefore we have chosen the Na/Br ratio.

Target systems for radioisotope production on the Medical Research Council cyclotron

D. D. Vonberg, L. C. Baker, P. D. Buckingham, J. C. Clark, K. Finding, J. Sharp, and D. J. Silvester

Medical Research Council, Cyclotron Unit, Hammersmith Hospital, Ducane Road, London, W.12, England

ABSTRACT

Target systems used for short-lived radioisotope production on the M.R.C. Cyclotron are described in detail and the factors affecting efficient production discussed. Choice of target material, target cooling, radioisotope recovery, suitable beam energy and target thickness for optimum yield of the required isotope, are all considered. The problems of power dissipation in the internal target using beam currents up to 300 μA are fully discussed. Reasons for using the static 'grazing incidence' target in preference to rotary or vibratory target systems are stated and methods of internal target preparation described.

Beam extraction through a thin vacuum-retaining foil permits a range of external targets to be bombarded using beams of low power density and also allows the use of energy-degrading foils. A method is described of indicating the external beam distribution during bombardment and details are given of external targets using solid, liquid and gaseous target materials. Recently-developed targets for radioactive gas production are described and typical performance figures quoted.

INTRODUCTION

The Medical Research Council cyclotron,[1,2] which was designed and built between 1950 and 1955, operates for 14 h daily on five days a week. About one third of each day is used for experimental radiobiology or fast neutron radiotherapy; the remainder is devoted to producing radioisotopes for medical use, which often but not invariably because of their short half-life cannot be obtained commercially. Much has been published on the uses of these isotopes,[3,4] and sometimes the methods of producing them have been included, but with very few exceptions the cyclotron target systems have not been described in detail. This paper discusses the factors that have to be considered in designing suitable

targets for efficient isotope production, and describes some of those currently in use on the M.R.C. machine.

In general, four main factors must be considered:

(1) The physical properties and chemical purity of the target material, which may be solid, liquid or gas.

(2) The provision of adequate cooling to control the temperature rise of the target surface.

(3) The method for recovery of the required radioisotope from the target during or after bombardment.

(4) The selection of a beam energy and target thickness that will maximise the yield of the required radioisotope and minimise the yield of possible impurities.

The M.R.C. machine is a fixed-energy, classical cyclotron capable of accelerating deuterons to 16 MeV and α-particles to 32 MeV. Internal beam currents up to 500 μA and extracted beams up to 100 μA can be obtained without special tuning. In practice however, the internal and external beam currents normally used are rarely greater than 300 μA and 50 μA respectively, because of the target limitations to be discussed.

The four external target positions are shown in Fig. 1. A beryllium target on beam 1 provides the fast-neutron beam used in an adjacent room for radiotherapy and activation analysis, and beam 2 is used for radiobiology experiments in the same room. Beams 3 and 4 are used in the cyclotron chamber for isotope production, as is the internal target position shown in Fig. 2. An automatic changing device

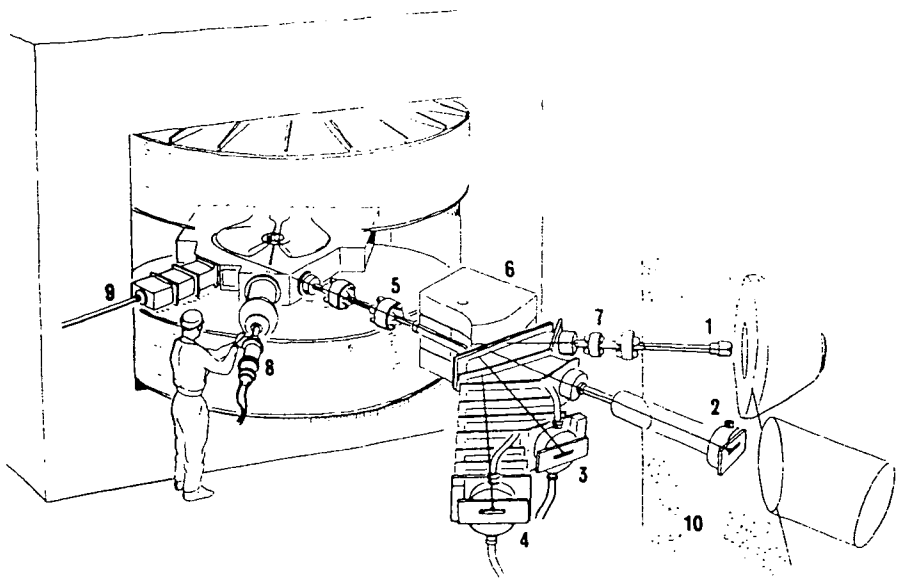

Fig. 1. M.R.C. Cyclotron–External Target Arrangements:
1. Be *target producing fast neutrons beam for radiotherapy, radiobiology and activation analysis)*
2. Beam 2: (Charged particles for radiobiology and activation analysis)
3. Beam 3: (for isotope production)
4. Beam 4: (for isotope production)
5. Beam shaping magnets
6. Beam bending magnet
7. Beam 1 focusing magnets
8. Ion source equipment
9. Internal target equipment
10. Wall dividing cyclotron chamber and 'radiation room'

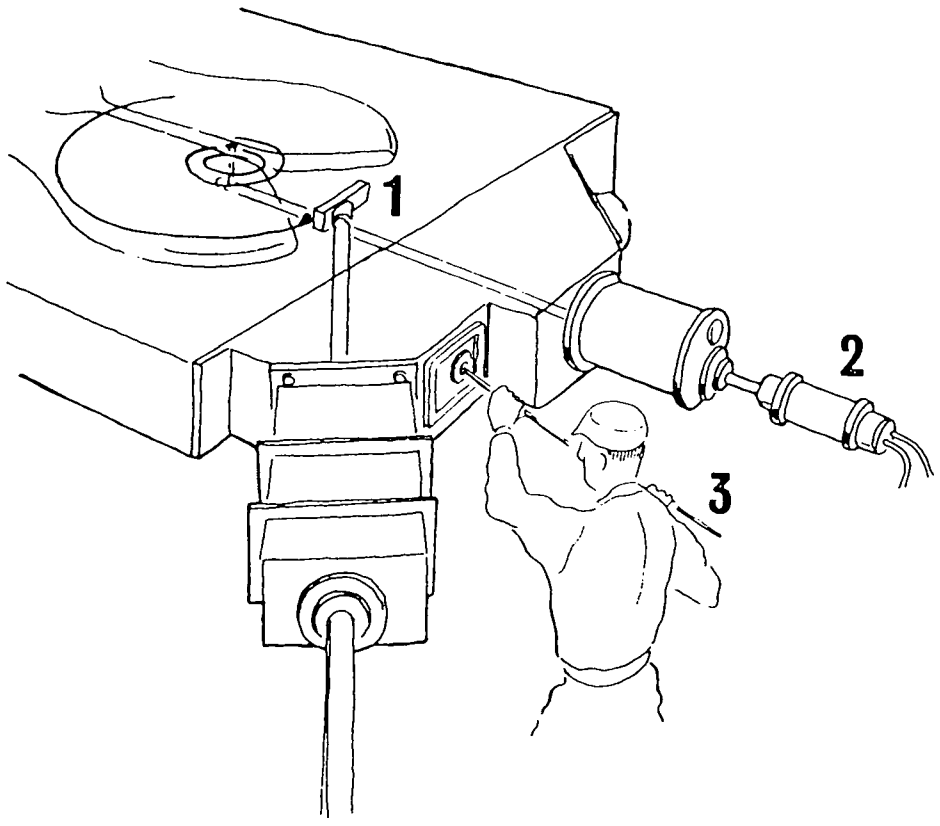

Fig. 2. M.R.C. Cyclotron–Internal Target Arrangement:
1. Grazing incidence target assembly on support tube
2. Ion source equipment
3. Manual probe for maintenance of dee-chamber

enables each of two alternative targets to be selected remotely for bombardment on beam 3, while all internal targets may be loaded and unloaded automatically without the need for personnel to enter the cyclotron chamber. The latter facility is to be extended to beam 3 in the near future.

INTERNAL TARGETS

The internal beam is normally intercepted by the target at approximately 60 cm radius, beyond which the beam current falls rapidly. At this point the beam is in the form of a ribbon 1 cm high × 3 mm wide. In order to use the high beam currents up to 500 μA regularly available in the internal beam, the target must be designed to dissipate the high power density of the beam. At 15 MeV a 500 μA beam of dimensions 1 cm × 3 mm has a power density of 20 kW cm^{-2}. Almost all the power reaching the target appears as a rise in temperature of the target coolant. The temperature differential between the front surface struck by the beam and the cooled back surface depends on the thermal conductance of the target and the power density in the beam.

In a copper target of thermal conductivity 0·92 cal cm^{-1} s^{-1} deg C^{-1}, a surface power density of 20 kW cm^{-2} results in a temperature gradient of 5 × 10^{3}°C cm^{-1}. In a poorly-conducting metal the gradient would be much higher, e.g. over 20 times higher for antimony. Non-metals generally have thermal conductivities

much lower still, resulting in temperature gradients of the order of 1000 times higher than that in copper.

The hottest surface of the target must be kept below the temperature at which the vapour pressure of the target material rises sufficiently to allow appreciable evaporation either of the target itself, or of the products of the nuclear reaction. If it is assumed that the back of the target is kept between 100 and 150°C by cooling water at a pressure of ~7 kg cm^{-2}, then at 20 kW cm^{-2} melting would occur if the thickness exceeded 2 mm for copper or 0·1 mm for antimony. Target construction therefore would present serious mechanical problems except for materials of high conductivity like copper. Moreover, the thickness of 0·1 mm is less than the particle range at 15 MeV, and this would affect the production efficiency in some cases.

Perhaps a more serious problem would be that of water cooling. At thicknesses of this order the power density at the cooled surface will be similar to that in the beam itself. However, the maximum power which could be removed by water cooling under conditions of surface boiling was found in experimental tests to be only about 4·5 kW cm^{-2}. On several counts, therefore, targets perpendicular to the internal beam of the M.R.C. cyclotron are not practicable.

The two methods commonly employed to reduce the power density at the target surface and at the cooled surface are either to present the target to the beam at grazing incidence, as depicted in Fig. 2, or to move the target or the beam continuously.

Rotating targets have been used at Hammersmith, but have been abandoned because of the complicated mechanism required to provide:

(a) the high rotational speed necessary to avoid mechanical stresses from thermal cycling, and

(b) sufficient mechanical power to overcome the eddy current drag on the target assembly in the magnetic field.

Since these two requirements are in direct opposition, and since such targets are inherently more expensive to produce than their static counterparts, rotating or vibrating target systems have not been developed. Thus the M.R.C. machine uses a grazing or oblique incidence target in the form of a flat plate arranged tangentially to the beam. From purely thermal considerations, since the power density is reduced by a factor of $1/\cos\theta$ (Fig. 3), such oblique incidence targets can be thinner than perpendicular incidence targets by a factor of $\cos\theta$, where θ

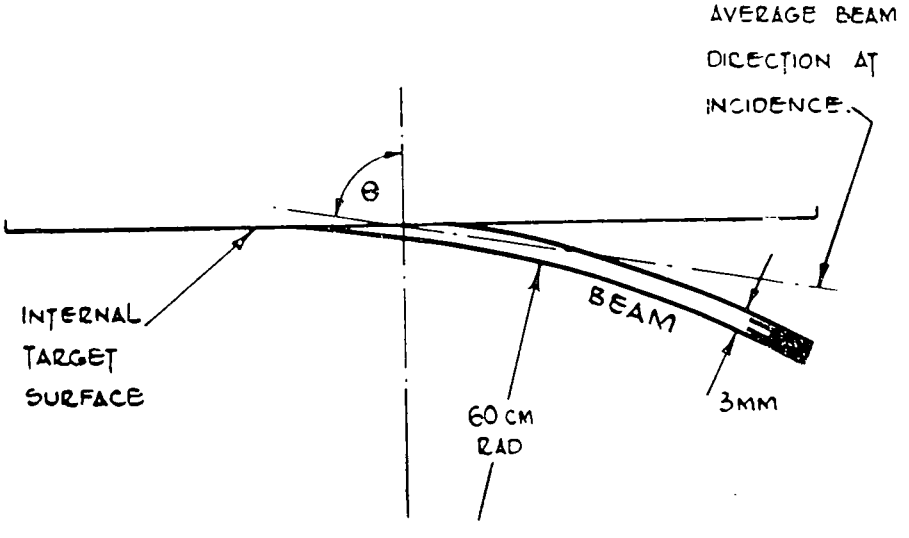

Fig. 3. Internal target geometry

is the angle between beam direction and the normal to the target face. The effective thickness of the target presented to the beam is increased by $1/\cos\theta$ and the former becomes a thick target in the nuclear sense in practical cases.

Since the beam has a finite radial width, θ is not the same for all particles. If the inner edge of the beam is tangential to the target the average value of $1/\cos\theta$ is about 10 in the M.R.C. machine.

For chemical processing the smaller the amount of target material present the better; in practice target thicknesses between 0·025 and 0·050 mm are found to give good yields on the grazing incidence target.

Clearly a target 0·050 mm in thickness needs mechanical support to retain the coolant; this is provided by a target backing plate which is in intimate thermal contact with both the target material and the coolant. The plate is of high thermal conductivity, copper or aluminium being chosen according to the chemical process to be employed in separation, for some of the backing plate material usually appears as a contaminant.

The target back is smooth for optimum cooling, and a water velocity of 4 m s^{-1} is obtained by narrowing the waterway at the back of the target plate to 0·25 mm. The direction of flow is perpendicular to the long dimension of the beam strike area. Because the effectiveness of the cooling depends on a high water velocity, it is essential to avoid distortion of the target plate, which would widen the gap and reduce the velocity. In practice copper or aluminium target plates need to be at least 2 mm thick to avoid distortion under the combined effect of heat and water pressure.

A thin target plate (1·5 mm) permits a high heat transfer rate through the plate, but affords little cooling due to conduction parallel to its surface. Conversely, a thick plate (6·5 mm) has a low heat transfer rate through the plate but a high cooling capacity due to conduction parallel to its surface. Maximum heat dissipation is therefore achieved at an optimum target plate thickness. Experimental measurements on copper target plates show this to be about 5 mm for applied power densities between 0·3 and 5 kW cm^{-2}. However, 3 mm was

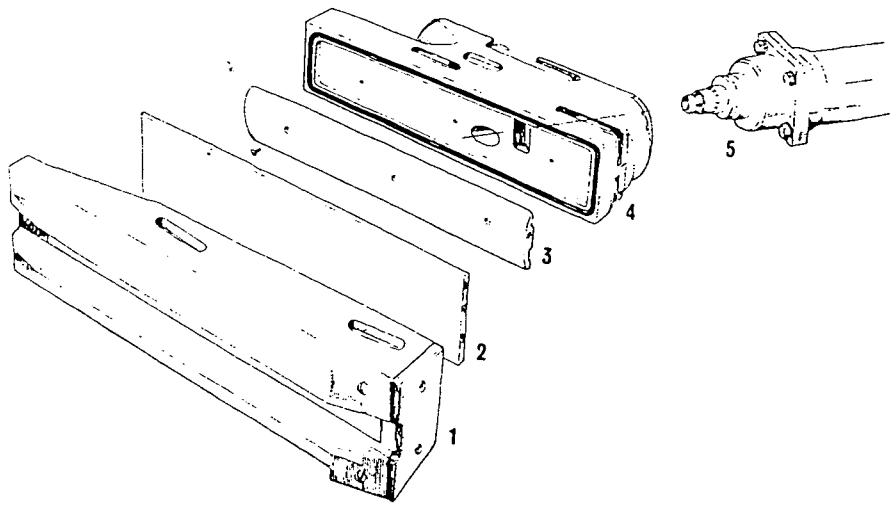

Fig. 4. Internal Target Head:
1. Target plate clamp with carbon blocks
2. Target plate carrying target material
3. Water flow spoiler
4. Target head block with 'O' ring and water ways
5. Support tube with water connections

finally chosen to simplify handling and reduce cost, without serious reduction in effectiveness.

Fig. 4 shows in exploded view the final form of the target assembly incorporating the features described above. Several other features have been added as a result of practical operating experience over a period of seven years. For example, as the machine tuning is adjusted the centre of curvature of the beam moves and the strike area moves along the plate. If the edge of the beam should approach either end of the target it strikes a carbon block, causing it to glow, giving visible warning on a CCTV monitor. As mentioned above, a remote automatic handling machine removes the target assembly from the vacuum system, detaches it from its water supplies, and transfers it by railway to a distant processing cell where the assembly is dismantled. The target plate is then removed and machined or chemically treated to remove the target layer, from which the required isotope is then extracted. The total bombardment on each target in μA h is recorded by a device which integrates the rise in water temperature against time.

In preparing targets for bombardment, a layer of target material 0·025–0·050 mm thick is applied to the target plate by a method selected to provide the optimum bonding. For example chromium (for ^{52}Fe production) is electroplated on aluminium, nickel (for ^{62}Zn production) is deposited by metal spraying, whilst lead (for ^{206}Bi production) is fused onto copper in a vacuum furnace.

EXTERNAL TARGETS

(a) General. Clearly, internal targets for high beam currents can be prepared only from a limited range of materials with suitable physical properties. The M.R.C. cyclotron has the design restriction that such targets can only be bombarded at maximum beam energy and, as has been shown, are necessarily thick in the nuclear sense. Fortunately these limitations can be overcome by using the extracted beam, albeit at the expense of lower maximum currents.

Once extracted from the dee-chamber, the particle beam is defocused by quadrupole magnets and can be made to cover a relatively large area (5–10 cm wide and 1 cm high) at the external target positions on beams 3 and 4. Having reduced the power density in this way, targets can be presented normal to the beam instead of at grazing incidence, and it is then possible to vary the thickness of target material which is bombarded. The energy of the beam incident on the target surface may also be varied by interposing energy-degrading foils of the appropriate thickness. These two variables can be very important; for example, in ^{123}I production from natural antimony the incident α-particle energy is reduced to 25 MeV, and the energy lost in the antimony is restricted to 2 MeV by limiting its thickness to 0·025 mm. This minimises contamination of the ^{123}I produced by an (α, 2n) reaction by ^{124}I from (α, n) and (α, 3n) reactions.[5]

Although it is not always desirable to degrade the beam energy, it is usually necessary to interpose a thin foil between the incoming beam and the target material in order that the latter, if it be a powder, liquid or gas, should be contained. Similarly, a foil is needed at the end of the external beam tube to maintain the vacuum. In principle a single foil could combine both these functions, but in practice target foils are often found to be very vulnerable to corrosion by hot target materials, and so separate foils are used. On the M.R.C. machine, 0·025 mm titanium is used on the beam tube, as this has high mechanical strength

and thermal conductivity. Target foils are usually of aluminium or copper, unless there are special reasons for avoiding these materials. Both foils must be efficiently cooled, or they may be perforated by the beam; this is achieved by circulating cooled dry air between them and by water-cooling their supporting frames. A grid of 25 0·2 mm diam. tungsten wires having a 5 mm spacing is supported 2·6 cm on the vacuum side of the titanium foil, and a CCTV system is used to show the beam distribution indicated by incandescence of the wires intercepting the beam. Since all external targets are mounted in such a way that they are electrically insulated from the cyclotron and its beam tubes, beam currents can be measured using a microammeter and simultaneously integrated.

(b) Solids. The standard target plate used to support solid target materials during bombardment in the external beam is similar to that used for internal bombardment, and they may be prepared in the same way, e.g. antimony (for ^{123}I production) is electroplated on copper. However, many alternative methods of preparation are

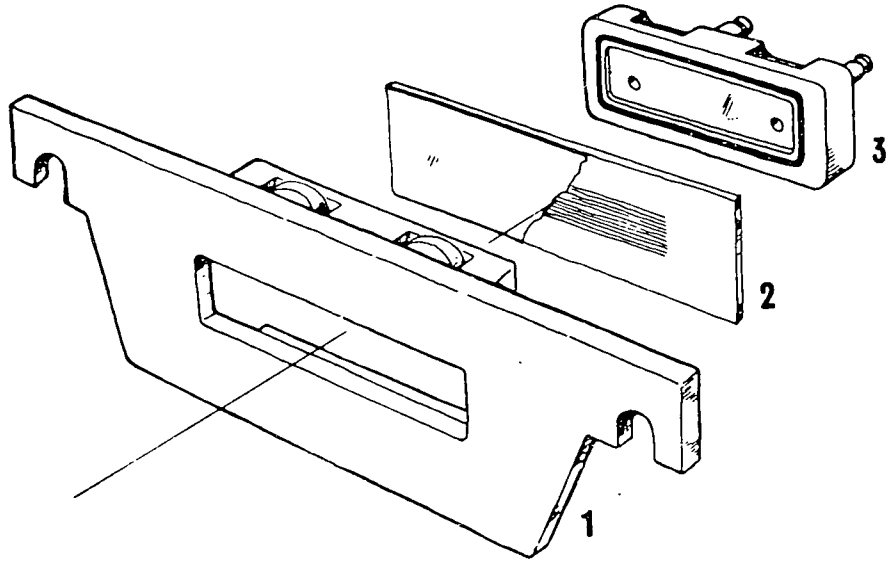

Fig. 5. External Target for Solid Materials:
1. Target mounting plate
2. Target plate carrying target material with target foil shown cut away
3. Target cooling block with 'O' ring

available; for instance, a thin metal foil (such as indium for ^{117}Sb production) may simply be clamped to the target plate, or a salt (such as NaBr for ^{81}Rb production) may be pressed firmly or melted into grooves cut in the plate. A typical target of this type is shown in Fig. 5, which also shows the method of applying water cooling to the back of the target plate.

Variations on the standard pattern of solid external targets are used in preparing radioactive gases incorporating ^{11}C or ^{13}N. Carbon-11 is produced by the reactions ^{10}B(d, n)^{11}C and ^{11}B(d, 2n)^{11}C; the target material is B_2O_3, which is bombarded with deuterons of ~14 MeV in the target system shown in Fig. 6. A layer of B_2O_3 1-2 mm thick, is melted on to the wedge. The deuteron beam passes through the 0·050 mm aluminium window and strikes the surface of the B_2O_3 at grazing incidence. With a defocused beam of ~40 μA the power density is 10-20 watts cm^{-2} on the surface of the wedge, which is deliberately in poor thermal contact with the surrounding box.

This power density is sufficient to melt the B_2O_3, releasing ^{11}C-labelled gases

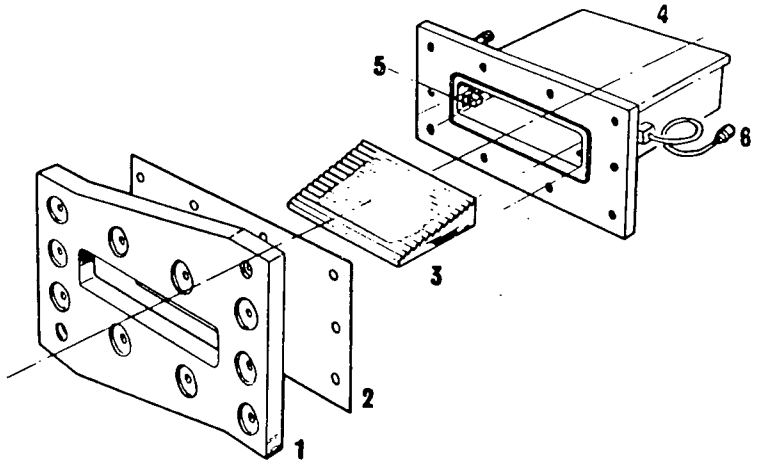

Fig. 6. External Target for ^{11}C Production:
1. Target mounting plate (water cooling not shown)
2. Foil window
3. Brass wedge supporting B_2O_3
4. Gas-tight target box
5. Wedge locating pins
6. Gas connections

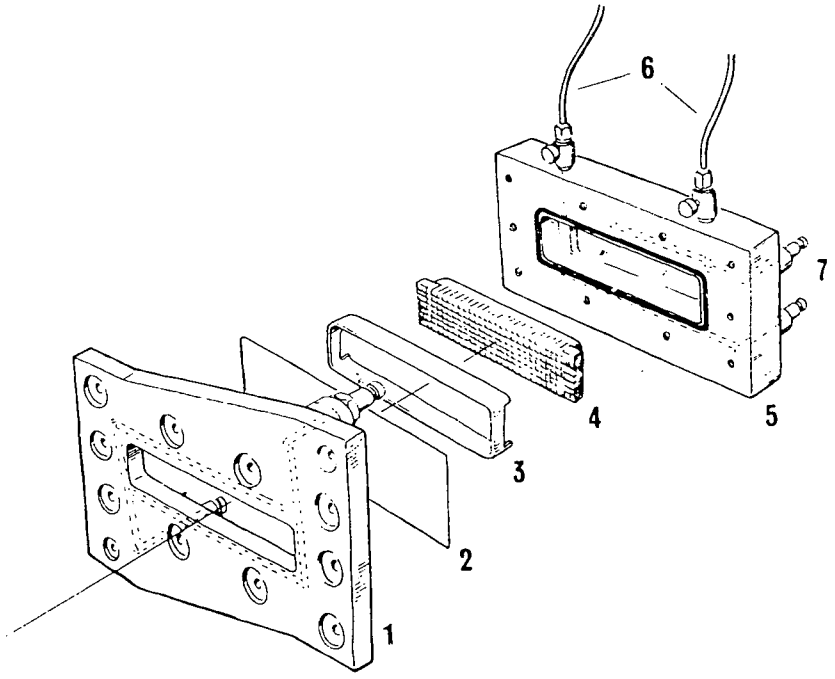

Fig. 7. External Target for ^{13}N Production:
1. Target mounting plate
2. Foil window
3. Spacer
4. Graphite block
5. Gas-tight target box
6. Gas connections
7. Cooling water connections

into a stream of carrier gas passing through the box at ~50 ml min^{-1}. When pure hydrogen is used as carrier gas ^{11}C appears as ^{11}CO and $^{11}CH_4$; when helium containing a little CO is used ^{11}CO, $^{11}CO_2$ and $^{13}N_2$ are produced.[6] The volume of the target box is kept small (~200 cm^3) to maximise the specific activity of the effluent gas.

The normal working pressure is about 0·1 kg cm^{-2} above atmospheric pressure. The ^{11}C target is used on an open-circuit system, a typical yield being 0·1 mCi ml^{-1} measured in a 100 ml bulb in an ionisation chamber approximately 100 m from the target. After about 12 h bombardment the B_2O_3 migrates from the area of the beam strike causing a loss of yield, necessitating re-coating of the wedge.

Nitrogen-13 is produced by the $^{12}C(d, n)^{13}N$ reaction in the target system shown in Fig. 7. Graphite is used as the target material when very high specific activity $^{13}N_2$ is required for making solutions of $^{13}N_2$ for physiological research.[7] Activated charcoal, the target material previously reported,[8] has proved to be unsuitable for this purpose owing to difficulties encountered in removing the

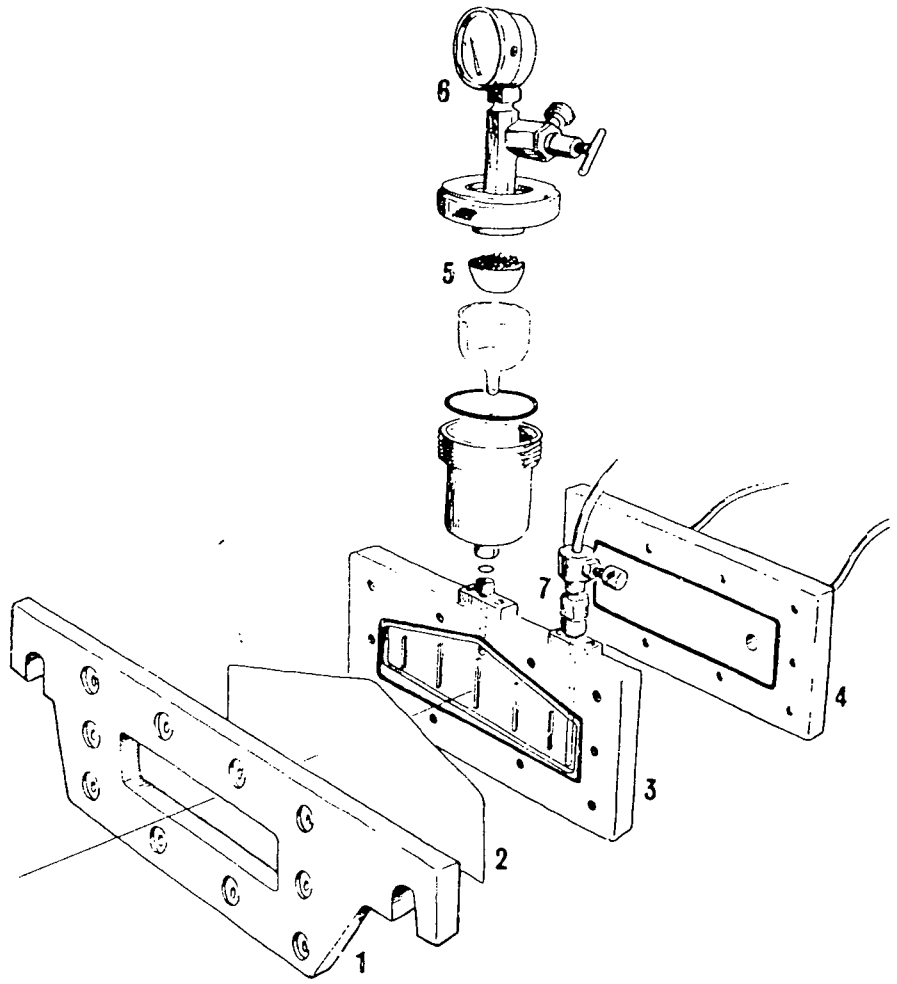

Fig. 8. External Target for ^{18}F Production
1. Target mounting plate
2. Foil window
3. Target plate with target water cavity
4. Target cooling block with 'O' ring
5. Catalyst in container
6. Pressure gauge
7. Tube and valve for filling/emptying cavity with target water

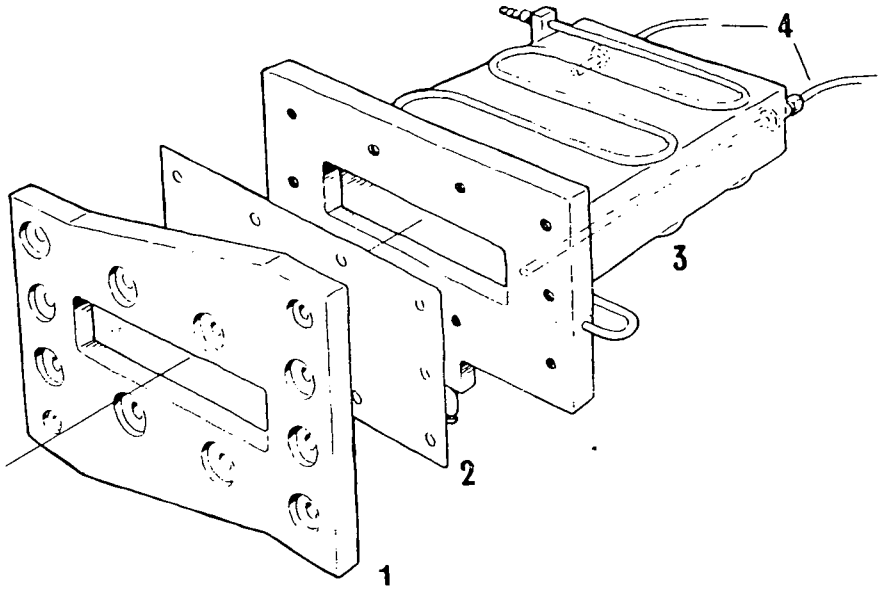

Fig. 9. External Target for ^{15}O Production
1. Target mounting plate
2. Foil window
3. Water-cooled gas-tight target box
4. Gas connections

adsorbed gases before irradiation. In an atmosphere of He, Ar or H_2 only small amounts of $^{13}N_2$ are released from the irradiated graphite. However, in the presence of carbon dioxide, the graphite (which is raised to a temperature above 1450°C by the beam power, typically about 100 W cm^{-2} at 50 μA) is eroded continuously as the following reaction occurs: $C + CO_2 \longrightarrow 2CO$. The purpose of cutting the graphite target material into a matrix, as depicted in Fig. 7, is to minimise the heat loss from the area struck by the beam. In this way the release of nitrogen-13 from the target has been greatly increased. The useful life of such a target is about 8 h.

This continuous erosion releases $^{13}N_2$ previously trapped in the graphite lattice. The yield from this target system is quite sensitive to power density; at high power densities erosion is more rapid. The target effluent, a mixture of CO_2 and CO of variable composition, is normally passed over heated copper oxide and the resulting CO_2 removed batch-wise. This leaves $^{13}N_2$ in the accumulated residual permanent gases found in the system. Typical specific activities achieved are ~7mCi ml^{-1}, which on mixing with physiological saline yields solutions of $^{13}N_2$ containing up to 150 μCi ml^{-1}. The major problem in using this type of target system has been to find a beam entry window which would retain its strength at elevated temperatures. Stainless steel foil (EN58B) 0·025 mm thick has proved to be very reliable at beam currents up to 70 μA.

(c) Liquids. In practice, the only liquid target material at Hammersmith is water, which is bombarded by the α-particle beam to produce ^{18}F through the reaction ^{16}O (α, pn). The target system is shown in Fig. 8. Its construction is similar to that for external solid targets in that a layer of water, thick enough to stop 30 MeV α-particles, is sandwiched between a thin air-cooled titanium foil (through which the beam enters) and a specially shaped water-cooled titanium target plate.[9]

The target is sealed, and during bombardment the pressure builds up to

about 1·1 kg cm^{-2} above atmospheric due to the formation of radiolytic H_2 and O_2. This increases the boiling point of the target water, and thereby helps to retain it in the beam so that good yields of ^{18}F are achieved (normally in excess of 1 mCi μA^{-1} h^{-1} for a 1 h bombardment). A catalyst in the chamber above the level of the water recombines the radiolytic gases which would otherwise build up sufficient pressure to burst the target foil. This target will withstand beam currents up to 80-100 μA without risk, provided the beam is spread over an area not less than about 5 cm^2.

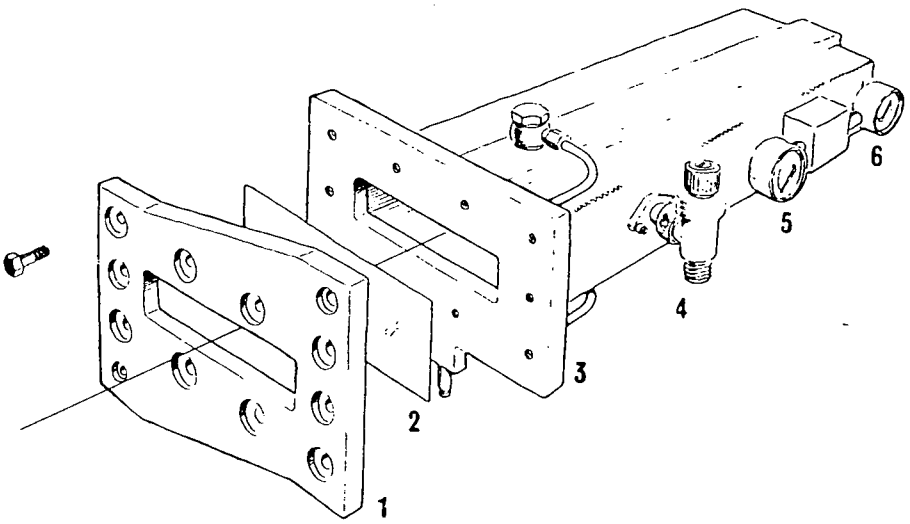

Fig. 10. External Target for ^{85m}Kr Production
1. Target mounting plate
2. Foil window
3. Water-cooled gas-tight target box
4. Gas connection
5. Pressure gauge
6. Vacuum gauge

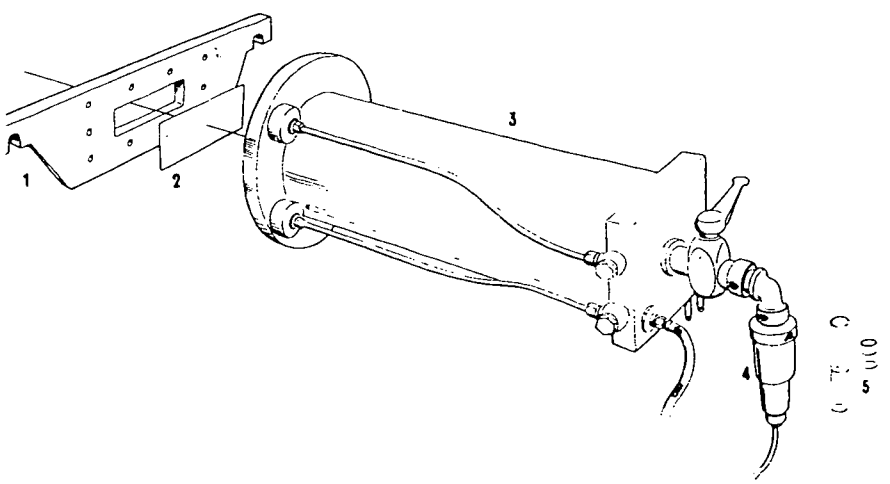

Fig. 11. External Target for ^{43}K Production
1. Target mounting plate
2. Foil window
3. Water-cooled gas-tight target box
4. Filter assembly
5. Sintered glass filter stick, glass-fibre filter paper and glass retaining ring

(d) Gases. Essentially, such a target is simply a water-cooled metal box filled with gas, and having a thin foil window for beam entry. The thickness of this window, its material, the target box dimensions and its operating pressure are all interdependent as discussed below.

Three such targets are in regular use. The first is shown in Fig. 9 and is used to prepare molecular oxygen labelled with ^{15}O. This is produced by the reaction ^{14}N (d, n) ^{15}O, using nitrogen as the target gas, to which 4% O_2 is added. The oxygen acts as a carrier for the ^{15}O; if it is absent the yield of ^{15}O as O_2 is very small. The target beam entry window is 1 mm magnesium, which reduces the beam energy from 15 to 5 MeV. This has the effect of reducing the contaminants otherwise produced by the reactions ^{14}N (d, nα) ^{11}C and ^{16}O (d, nα) ^{13}N.[8]

The length of the box is sufficient to stop the 5 MeV deuteron beam with the target gas at about 0·5 kg cm^{-2} above atmospheric pressure. Using 35 μA of 5 MeV deuterons and a target gas flow rate of 0·7 l min^{-1}, the yield of $^{15}O_2$ is typically 120 mCi l^{-1} measured in a 500 ml bulb in an ionisation chamber 90 m from the target.

A target similar in design (Fig. 10) is used to produce ^{85m}Kr by the ^{84}Kr(d, p) reaction. The 45 cm long target box is filled with krypton to a pressure of 0·7 kg cm^{-2} above atmospheric, ideally sufficient to stop the deuteron beam. This pressure rises to about 1·75 kg cm^{-2} during bombardment at 30 μA. The target box is therefore rigidly constructed, and is fitted with a 0·025 mm titanium foil window which readily withstands the pressure and temperature differential. After bombardemnt, krypton is recovered from the target by sorption on molecular sieve in a trap cooled by liquid nitrogen.

Finally, the target used for the production of ^{43}K is shown in Fig. 11. Argon is the target gas, and when this is bombarded in the α-particle beam ^{43}K results from the $^{40}Ar(\alpha, p)$ reaction. The target box is filled to a pressure of 0·7 kg cm^{-2} above atmospheric, and is fitted with a foil window which reduces the incident beam energy to 15 MeV, which is approximately the threshold for the $^{40}Ar(\alpha, pn)$ ^{42}K reaction. This foil window consists of 0·025 mm titanium which, as in the krypton target, has the required mechanical strength, backed by a 0·2 mm aluminium foil, to degrade the beam energy.[10]

During bombardment, the argon is recirculated through the target box at about 100 l min^{-1} by oil-free diaphragm pumps. On leaving the target box the gas passes through a glass-fibre filter paper supported on a coarse sintered glass disc, which traps more than 70% of the ^{43}K produced. At the end of bombardment the activity is readily recovered by washing the filter with a few ml of dilute hydrochloric acid.

REFERENCES

1. Gallop, J. W., Vonberg, D. D., Post, R. J., Powell, W. B., Sharp, J., and Waterton, P. J., *Proc. I.E.E.* **104 B**, 452, (1957).
2. Vonberg, D. D. and Fowler, J. F., *Nature* **198**, 827, (1963).
3. Clark, J. C., Matthews, C. M. E., Silvester, D. J., and Vonberg, D. D., *Nucleonics* 25, 54, (1967).
4. Glass, H. I. and Silvester, D. J., submitted to *Brit. J. Radiol.* (1969).
5. Silvester, D. J., Sugden, J., and Watson, I. A., *Radiochemical and Radioanalytical Letters*, in press (1969).
6. Clark, J. C. and Buckingham, P. D., submitted to *Radiochemical and Radioanalytical Letters* (1969).
7. Clark, J. C. and Buckingham, P. D., to be published.
8. Buckingham, P. D. and Forse, D. J., *Int. J. Appl. Radn. and Isotopes* 14, 439, (1963).
9. Clark, J. C. and Silvester, D. J., *Int. J. Appl. Radn. and Isotopes* 17, 151, (1966).
10. Clark, J. C., submitted to *Radiochemical and Radioanalytical Letters* (1969).

^{81m}Kr GENERATOR AND ITS USES IN CARDIOPULMONARY STUDIES WITH THE SCINTILLATION CAMERA

T. Jones and J. C. Clark

Medical Research Council, Cyclotron Unit, Hammersmith Hospital, London, England

J. M. Hughes* and D. Y. Rosenzweig†

Royal Postgraduate Medical School, Hammersmith Hospital, London, England

The radionuclide ^{81}Rb can be readily produced by bombarding bromine, in the form of sodium bromide, with 30-MeV alpha particles ($^{79}_{35}$Br(α,2n) $^{81}_{37}$Rb) from the Medical Research Council's Cyclotron. Rubidium-81 has a 4.7-hr half-life and decays to ^{81m}Kr which in turn decays with a 13-sec half-life to ^{81}Kr emitting a 190-keV gamma ray which is 35% internally converted.

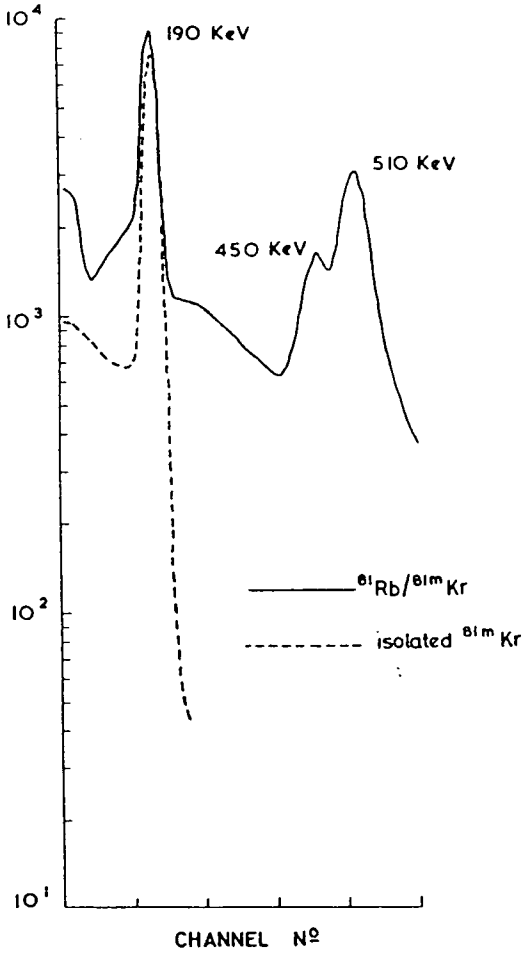

FIG. 1. Gamma-ray spectrum of ^{81}Rb and ^{81m}Kr in radioactive equilibrium, together with isolated ^{81m}Kr.

Figure 1 shows the gamma spectrum of ^{81}Rb and ^{81m}Kr in radioactive equilibrium. This figure also shows the isolated ^{81m}Kr, illustrating its monoenergetic 190-keV gamma ray.

The following are some of the points which make ^{81m}Kr suitable for certain clinical investigations:

1. Krypton is an inert gas and can therefore play the same biological role in medical scintigraphy as ^{85}Kr and the widely used ^{133}Xe.

2. ^{81m}Kr emits a single 190-keV gamma ray and thus provides a clean spectrum for analysis. Photons of this energy are not subjected to as much low degraded scatter of the primary photons as the 80-keV and 30-keV photons from ^{133}Xe. The energy is not high enough to cause difficulties from septa penetration in the collimator. In fact it falls within the energy range considered suitable for the gamma camera and provides a resolution diameter using the ^{99m}Tc collimator of about 18 mm full width at half maximum height at a depth of 10 cm in water.

3. Since ^{81m}Kr has a short physical half-life (13 sec) and a short biological half-life (inert gas), one can administer large activities which are necessary for certain short-duration gamma-camera studies and still keep the radiation dose to a tolerable level. One millicurie of ^{81m}Kr administered by inhalation or injection results in a total lung dose of 0.6 mrad. With these short physical and biological half-lives it would be practical to repeat the administration of this isotope without significant health hazard. The repetition could be made after a few minutes, without interference from the previous administrations.

Received April 15, 1969; revision accepted Nov. 5, 1969.

For reprints contact: T. Jones, Medical Research Council, Cyclotron Unit, Hammersmith Hospital, Ducane Road, London W. 12, England.

* Present address: Dept. of Physiology, Harvard School of Public Health, 655 Huntington Ave., Boston, Mass.

† Present address: Dept. of Medicine, Marquette School of Medicine, 8700 W. Wisconsin Ave., Milwaukee, Wis.

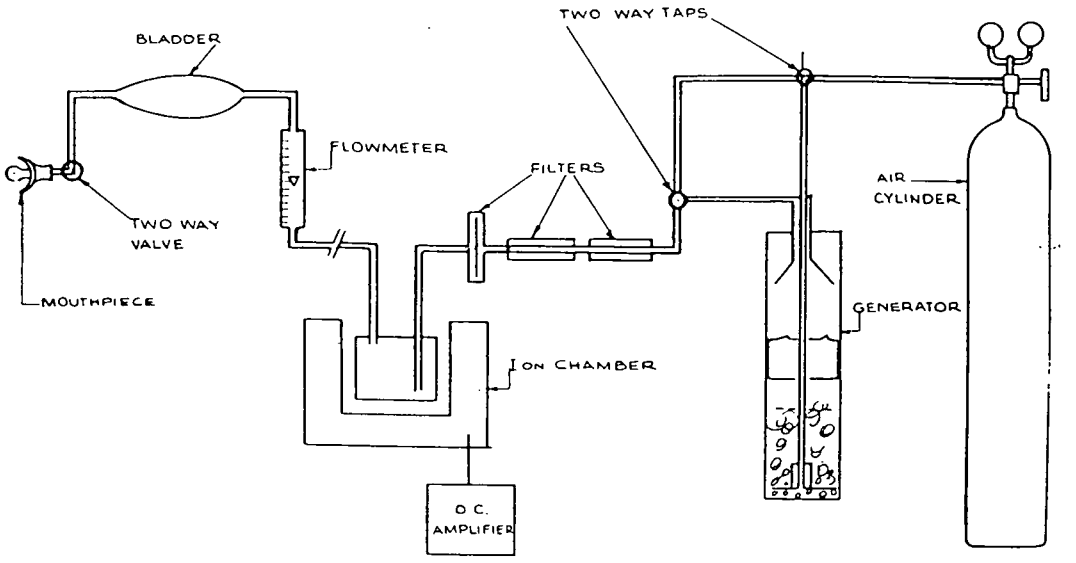

4. Unlike many of the other radionuclides obtained from generators used in medical scintigraphy, ^{81m}Kr can be generated more or less continuously from its rubidium parent.

5. Because the ^{81}Rb parent has a 4.7-hr half-life, the generator could be readily used in institutions other than where it is manufactured. For example, ^{18}F (110-min half-life) is supplied by the Medical Research Council's Cyclotron Unit to 16 hospitals up to a range of 20 miles.

6. Because the parent radionuclide has a 4.7-hr half-life and the daughter a 13-sec half-life, waste-disposal problems with this generator are minimal.

With these particular merits of ^{81m}Kr in mind, investigations were made into the feasibility of preparing ^{81}Rb-^{81m}Kr generators which could provide, in the gas and solution phase, ^{81m}Kr for convenient clinical use (*1*).

PREPARATION OF MATERIAL

Production of ^{81}Rb. Sodium bromide is used as target material. This is melted onto a grooved copper plate by eddy-current heating in a hydrogen atmosphere.

The external alpha beam of the cyclotron is used. The target is covered with aluminum foil 0.0025 cm thick. At 30 μA, a typical operating current, the power dissipated is 450 watts. Water cooling is applied to the back of the copper plate to carry away the beam power. After bombardment the ^{81}Rb is recovered by washing the target with 10 ml of water. This is carried out in a special machine in a shielded cell. The yield of ^{81}Rb is 2 mCi/μA-hr.

FIG. 2. Schematic diagram of circuit for generation of gas-phase ^{81m}Kr.

Generation of ^{81m}Kr in the gas phase. To date the principal method of generating ^{81m}Kr in the gas phase has been to bubble air through the crude target solution, thus washing out ^{81m}Kr continuously because of its low solubility in water. The ^{81}Rb and the sodium bromide stay in solution in the generator. Figure 2 shows the schematic circuit for producing gas-phase ^{81m}Kr.

The mixture of ^{81m}Kr and air passes through a centrifugal antispray device installed in the generator and then through a series of filters to ensure that no ^{81}Rb is carried out of the generator into the rest of the circuit. The flow continues through a bulb in an ion chamber for yield determination. Since it is important to keep the transit time from the generator to the point of examination to a minimum, 1.5-mm-dia nylon tubing is used. An air cylinder provides a supply of carrier gas, and pressures of approximately 3.5 kg/cm^2 are required to provide a flow rate of 5–6 liters/min at the point of examination.

The ^{81m}Kr yield is shown as a function of flow rate through the generator in Fig. 3.

The generator is housed in a lead castle with 4-in.-thick walls. The dose rate on the outside is 1 mrad/hr when a generator capable of producing 19 mCi of ^{81m}Kr/liter at a flow rate of 5 liters/min is then placed inside.

The generator is installed at a distance of approxi-

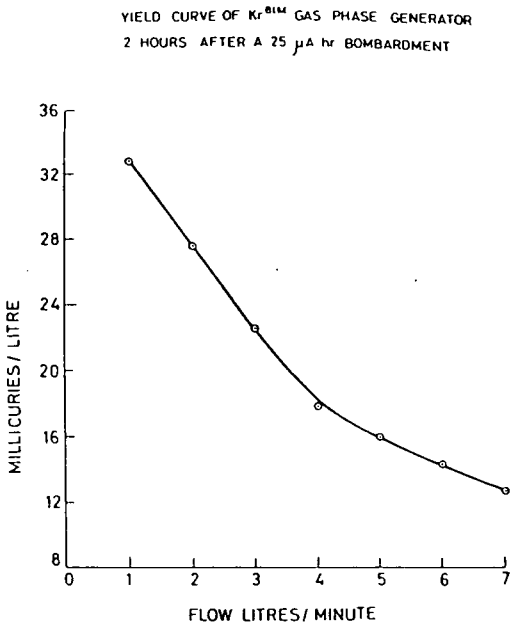

FIG. 3. Yield curve of gas-phase ^{81m}Kr generated from ^{81}Rb–^{81m}Kr solution 2 hr after 25-μA-hr bombardment.

mately 15 ft from the point of investigations, usually in an adjacent room.

Generation of ^{81m}Kr in solution. The aqueous sodium bromide solution containing ^{81}Rb is passed through a zirconium phosphate cation exchange column.

The column is then exhaustively washed with water to remove all the sodium bromide, leaving the ^{81}Rb strongly bound to the zirconium phosphate. A schematic diagram of the ^{81m}Kr solution generator is shown in Fig. 4.

If the column is eluted rapidly with a few milliliters of bubble-free water, the ^{81m}Kr, which is dissolved in the water remaining in the column at equilibrium, will be eluted into a bubble-free syringe at the outlet of the column.

The generator is contained in a lead shield. For a 2-ml elution, the elution efficiency is 65% and the ^{81}Rb contamination is less than 0.03% at the end of elution. A 44-μA-hr cyclotron bombardment taking 90 min produced a generator capable of providing an administered activity of 10.0 mCi of ^{81m}Kr in 2 ml of water 3 hr after the end of the bombardment. At least 1 min of "re-equilibration" time is allowed between elutions.

APPLICATIONS

Preliminary clinical studies have been made with these ^{81m}Kr generators to assess their potential in conjunction with a gamma camera.

Lung function. At present ^{133}Xe is used extensively for lung-function studies (*2–5*), but it has the disadvantage of emitting low-energy photons, thus giving relatively poor resolution with the gamma camera. ^{81m}Kr on the other hand emits gamma rays of more suitable energy for the gamma camera. Also the generator system can produce, more readily than ^{133}Xe dispensing systems, large quantities of isotope with easily controlled specific activity.

Lung ventilation. A 30-μA-hr bombardment taking 1 hr will produce a ^{81m}Kr generator of sufficient activity to supply ^{81m}Kr air mixtures with activities of the order of 19 mCi/liter at 2 hr after bombardment. Such activities are sufficient to produce significant gamma-camera pictures of lung-ventilation distribution taken using a 10-sec exposure after a single inhalation; from residual volume up to total lung capacity about 70,000 counts are accumulated. Illustrations of the ventilation distribution in the right lung of a normal 25-year-old male are shown in Figs. 5A and B. Unlike the normal Polaroid dis-

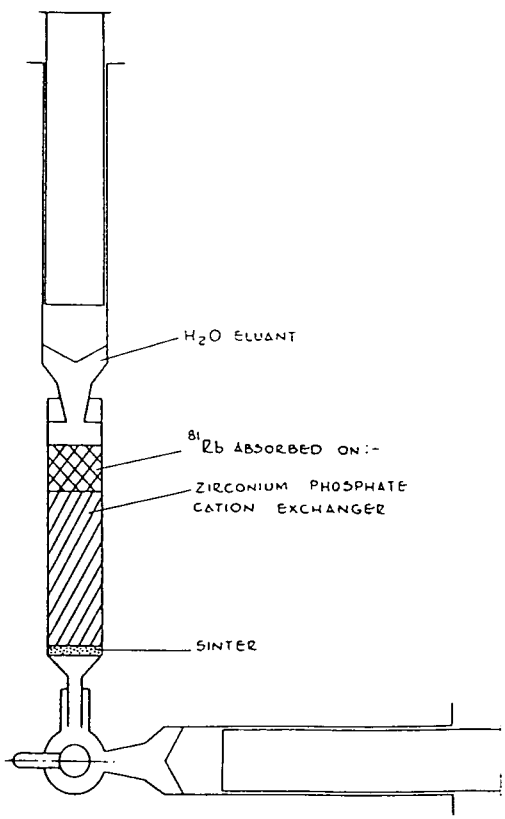

FIG. 4. Schematic diagram of the ^{81m}Kr solution generator.

play the images shown are diffused pictures on 12.5 × 10-cm sheet film (Tri-X Ortho).

As can be seen, the size of the gamma-camera field of view using a parallel-holed ^{99m}Tc collimator is such that it is not possible to visualize both lungs simultaneously. However, this size restriction would be eliminated if a diverging collimator was used.

The radiation dose to the lungs per inspiration necessary for pictures of good definition is 6 mrad (10 mCi inhalation). This technique of obtaining gamma-camera pictures of lung ventilation has the following advantages over the labeled aerosol method (*6*):

1. Inhalation of air with trace amounts of an inert gas is more physiological than inhaling a labeled aerosol.

2. Much shorter measuring time is needed with ^{81m}Kr; this is due to the administered activity restrictions in the aerosol case.

3. Poorer resolution would be encountered with the aerosol technique, unless a respiratory gating device is used due to the blurring effect caused by the subject breathing.

4. Several variable factors are introduced in the aerosol technique such as particle size, air flow, respiratory rate and tidal volume, all of which influence the deposition of the aerosol.

5. It is not as feasible to repeat the aerosol procedure.

It is possible to study lung-ventilation dynamics when higher concentrations of ^{81m}Kr air mixtures of the order of 40 mCi/liter (leaving the generator) are used. Using this level of activity ^{81m}Kr has been introduced into specific parts of inspiration. Figure 6 shows the fate of ^{81m}Kr inhaled from residual volume up to total lung capacity; pictures were taken during both inspiration and the following expiration. The procedure illustrated was carried out on a normal 27-year-old male volunteer and shows that the filling of the upper zone precedes the principal filling in the lower zone, a finding which confirms the work of Emili *et al* using ^{133}Xe with multiple probes (*7*). The first picture shows an absence of activity due to inactive gas in the dead space of the inspiration equipment. The dose received is 12 mrad to the lung per inspiration. Investigations of this type have also been carried out in isolated dog lung preparations in order to study patterns of ventilation under controlled conditions.

The photographic sequence shown in Fig. 6 was obtained by storing the gamma-camera data on magnetic tape and subsequently replaying it at slower speeds. The x and y pulses were recorded using the

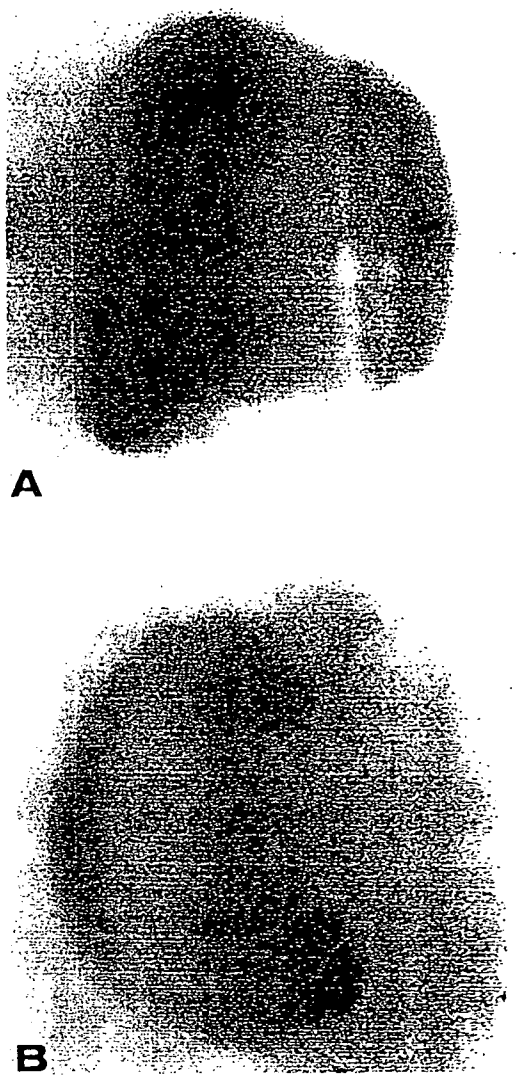

FIG. 5. A shows lung ventilation distribution in right lung front view. B shows lung ventilation distribution in right lung back view.

frequency modulation mode and the z pulses using direct modulation (*8*).

One generator resulting from a 40-μA-hr bombardment taking 80 min received at midday would be sufficient for a complete afternoon of lung-ventilation studies. The practical limit to the number of patient studies is dictated by the setting-up time of each patient. (Such a generator would provide an average lung count of 99,000 counts/10 sec at 4.30 pm).

Lung perfusion. Lung perfusion can be illustrated by using an intravenous injection of a solution of

an inert gas such as ^{81m}Kr. The principle of this method rests on the insolubility of the inert gas which, once it reaches the lung capillaries, leaves the blood and accumulates in the air cavities. Therefore the resulting distribution of inert gas in lung depends on the lung's distribution of blood flow.

A comparison made by other workers of the perfusion distributions obtained with an injection of ^{133}Xe solution to that with an injection of ^{131}I-labeled macroaggregate (9) indicates that the lung-perfusion patterns are similar but that areas of depressed perfusion are not so dominant with ^{133}Xe as with ^{131}I. This, it is thought, is due to relatively lower degraded scatter of the photons of ^{133}Xe from the well-perfused areas of the lungs into the low-activity regions, thus effectively reducing the detectability for cold areas. This defect would not be as great for the 190-keV ^{81m}Kr gamma ray.

To date lung-perfusion studies with ^{81m}Kr have only been carried out on dogs. Figure 7 shows serial photographs taken after intravenous injections of 2 ml of solution (containing approximately 10 mCi of ^{81m}Kr), into a catheter placed in the femoral vein, the bolus of activity entering the heart through the inferior vena cava. The injection was followed by a 10-ml flush with saline. The anesthetized dog was respiring slowly during this procedure.

It can be seen from Fig. 7 that photographic exposures between 4 and 10 sec post-injection produced significant pictures of lung-perfusion distributions.

Since the radiation dose from such an injection

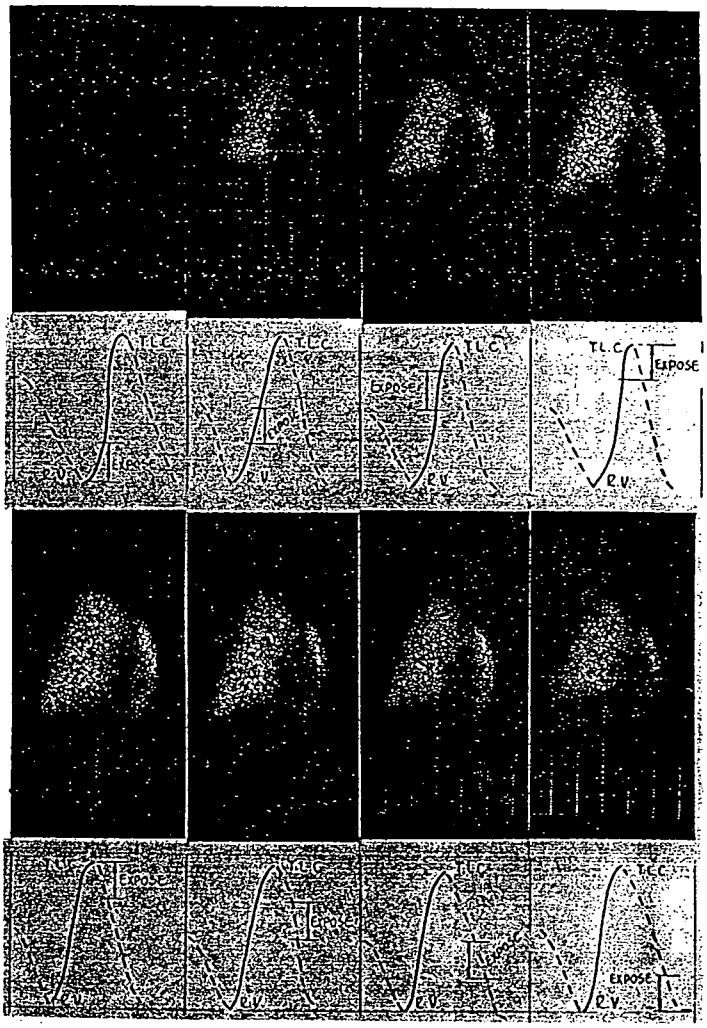

FIG. 6. Dynamic lung ventilation study in which ^{81m}Kr air mixture was breathed from residual volume up to total lung capacity. Figure shows right lung front view of normal male.

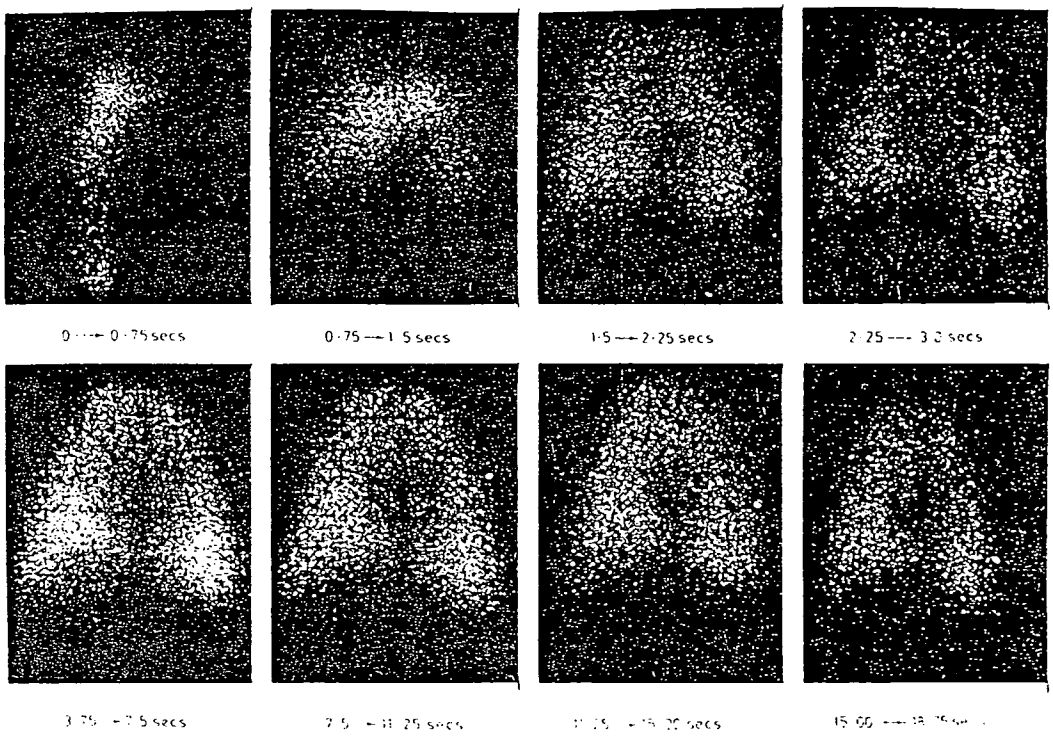

FIG. 7. Lung perfusion study in dog using ^{81m}Kr solution.

is 6 mrad, the procedure can be repeated several times without significant radiation hazard.

Radiocardiology. After the lung-perfusion studies had been completed and the data recorded on magnetic tape, we found that we could follow the injected bolus as it passed through the right side of the heart. Recently interest has been shown in using the gamma camera for radiocardiographic studies (*10,11*) as the camera has an advantage over single probes in accuracy of localization. Thus attempts were made to obtain radiocardiograms from the recorded lung-perfusion data.

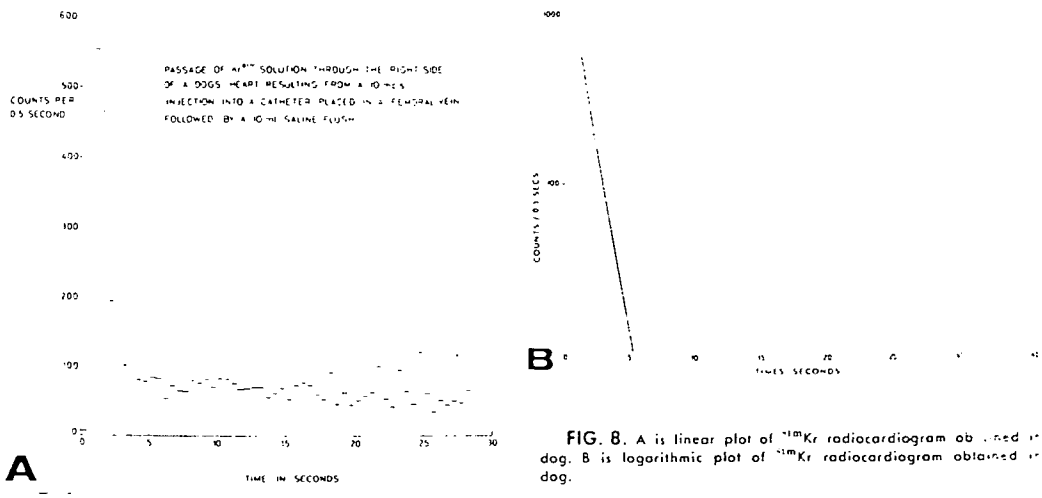

FIG. 8. A is linear plot of ^{81m}Kr radiocardiogram obtained in dog. B is logarithmic plot of ^{81m}Kr radiocardiogram obtained in dog.

It was possible to obtain the quantitative time course of the ^{81m}Kr as it passes through the heart by simply masking off on the oscilloscope screen all regions other than the right side of the heart, as depicted by the photographs, then replaying the tape and counting the dots as they appear on the screen with a photomultiplier (*8,11–13*). Figures 8A and B show a linear and logarithmic plot of a right heart radiocardiogram resulting from an injection through a catheter placed in a femoral vein.

It can be seen that there is a tail on the radiocardiagrams due, it is thought, to some lung tissue overlying the heart as well as some scatter from the adjacent lung areas into the heart region.

It is thought legitimate to extrapolate the falling portions of the curve to the base line on semilog paper, thus describing the full radiocardiogram. From this a mean transit time can be obtained for the passage through the right heart. The curves shown have been corrected for decay.

The advantages of this radionuclide over others used to date for gamma-camera radiocardiographic studies, e.g. ^{99m}Tc (*10,11*), are:

1. The absorbed dose is much lower because the isotope is only present long enough for the examination. A 10-mCi injection of ^{81m}Kr results in an absorbed dose of 6 mrad to the lungs (critical organ), whereas a 10-mCi injection of ^{99m}Tc results in 960 mrad to the upper large intestine (critical organ) (*14*).

2. High specific activities are readily available from the ^{81}Rb parent.

3. The test can be repeated without significant hazard.

4. Being an inert gas ^{81m}Kr does not return from the lungs to the left heart as ^{99m}Tc does. Therefore there is no interference in the radiocardiogram due to activity in the left heart.

This last point, although advantageous in the context of the right heart, is a disadvantage in that a left heart radiocardiogram cannot be obtained as in the ^{99m}Tc case. Even when it is obtained, these composite heart profiles are not easy to analyze.

CONCLUSION

The properties of the gamma camera make it an important instrument for physiological studies of short duration. Thus specific isotopes are required to play a complementary role with the camera in these investigations. Such isotopes must be available in sufficient activities to make short duration studies statistically feasible, and yet they must have the physical characteristics to meet the requirements of high resolution and low absorbed dose to the patient (*15*).

It is believed that it is in this context that the ^{81}Rb-^{81m}Kr generator has a useful role to play in medicine in association with gamma cameras.

ACKNOWLEDGMENT

The authors wish to acknowledge the support of D. D. Vonberg and J. B. West and the helpful discussion of D. K. Bewley, D. J. Silvester, J. F. Fowler and H. I. Glass. Thanks are also expressed for the cooperation of the Medical Physics Department, in particular B. Westerman, and for the technical assistance of A. S. O. Ranicar and W. Verney together with the Cyclotron Team for their excellent service.

REFERENCES

1. JONES, T. AND CLARK, J. C.: A cyclotron produced ^{81}Rb-^{81m}Kr generator and its uses in gamma camera studies. *Brit. J. Radiol.* **42**:237, 1969.

2. WEST, J. B.: Pulmonary function studies with radioactive gases. *Ann. Rev. Med.* **18**:459, 1967.

3. LOKEN, M. K. AND WESTGATE, H. O: Using xenon-133 and the scintillation camera to evaluate pulmonary function. *J. Nucl. Med.* **9**:45, 1968.

4. SUPRENANT, E. L., BENNETT, L. R., WEBBER, M. M. AND WILSON, A. F.: Measurement of regional pulmonary ventilation with radioxenon and the Anger camera. *J. Nucl. Med.* **8**:343, 1967.

5. MARKS, A., CHERVONY, I., LANKFORD, R., SMITH, E. M., GILSON, A. J. AND SMOAK, W.: Ventilation-perfusion relationship in humans measured by scintillation scanning. *J. Nucl. Med.* **9**:450, 1968.

6. PIRCHER, F. J.: The aerosol scan in the assessment of lung disease. In *Proceedings of the Symposium on Nuclear Activation Techniques in the Life Sciences*, vol. 2, IAEA, Vienna, 1969.

7. MILIC-EMILI, J., HEDERSON, J. A. M., DOLOVICHU, M. B., TROP, D. AND KANE, K. O.: Regional distribution of inspired gas in the lung. *J. Appl. Physiol.* **21**:749, 1966.

8. HOLROYD, A. M. AND JONES, T.: A simple method for obtaining dynamic quantitative information from the gamma camera. *Phys. Med. Biol.* **14**:631, 1969.

9. CEDERQUIST, E., NAVERSTEN, Y. AND WHITE, T.: Comparative study of regional lung function with intravenous injection of ^{131}I-labelled macroaggregated albumin and ^{133}Xe. In *Proceedings of the Symposium on Nuclear Activation Techniques in the Life Sciences*, vol. 1, IAEA, Vienna, 1968.

10. ANGER, H. O., GOTTSCHALK, D. C., YANO, Y. AND SCHAER, L. R.: Scintillation camera in diagnosis and research. *Nucleonics* **23**:No. 1, 57, 1965.

11. ADAM, W. E., SCHENCK, P., KAMPMANN, H., LORENZ, W. J., SCHNEIDER, W. C., AMMAN, W. AND BILANIUK, L.: Investigations of cardial dynamics using scintillation camera and computer. In *Proceedings of the Symposium on Nuclear Activation Techniques in the Life Sciences*, vol. 1, IAEA, Vienna, 1968.

12. ADAM, W. E. AND LORENZ, W. J.: Ein Einfaches Verfahren zur analogen Auswertung funktionsszintigraphischer Messungen mit der Szintillation-Kamera. *Atompraxis* **13**:4, 1967.

13. LORENZ, W. J. AND ADAM, W. E.: Digitale und analoge Auswertung von Aufnahmen mit de Szintillation Kamera. *Nucl. Med.* **6**:367, 1967.

14. SMITH, E. M.: Internal dose calculation for ^{99m}Tc. *J. Nucl. Med.* **6**:231, 1965.

15. YANO, Y. AND ANGER, H. O.: Ultrashort-lived radioisotopes for visualizing blood vessels and organs. *J. Nucl. Med.* **9**:2, 1968.

1970, *Br. J. Radiol.*, *43*, 537–541

Measurement of gastric emptying using the scintillation camera and ^{129}Cs

By T. Jones, M.Sc. and J. C. Clark, B.Sc.
Medical Research Council, Cyclotron Unit, Hammersmith Hospital, London, W.12
N. Kocak, M.D. and A. G. Cox, M.D., F.R.C.S. (E).
Department of Surgery, Royal Postgraduate Medical School, Hammersmith Hospital, London, W.12
and H. I. Glass, M.A., A.Inst.P.
Department of Medical Physics, Royal Postgraduate Medical School, Hammersmith Hospital, London, W.12

(*Received October, 1959 and in revised form February, 1970*)

Measurement of the rate of gastric emptying is a difficult clinical problem to which the best current solution is external detection of a meal labelled with a radioactive tracer substance. This basic method has the advantages that it does not require nasogastric intubation and the results can be easily quantified.

The main problem in such a technique is accurate localisation of the stomach and continuous detection of all its radioactive contents. A radioisotope scanner can be used to outline the stomach and estimate the activity by adding up the counts within a defined area (Griffiths, Owen, Campbell and Shields, 1968; Williams, Glass, Arnot and De Garreta, 1968). The main disadvantage of the scanning technique is that detailed changes in stomach emptying may be missed because of the time taken to scan the stomach. Gross inaccuracies are inevitable when stomach emptying is rapid.

We have used the Anger scintillation camera to measure activity in the whole stomach. Quantitation has been achieved by a relatively simple and inexpensive technique, modified from one developed previously for quantifying gamma-camera data (Holroyd and Jones, 1969). In this method a photomultiplier counts light scintillations within the area of interest on the oscilloscope display of the gamma-camera. ^{51}Cr in the form of sodium chromate has been used by workers who have measured gastric emptying by radioisotopic scanning techniques (Griffiths *et al.*, 1968). We have used cyclotron-produced ^{129}Cs absorbed on a suspension of zirconium phosphate.

Physical Characteristics of ^{129}Cs

1. *Production of ^{129}Cs and its incorporation into a suitably inert medium for gastric emptying measurements.*

^{129}Cs is produced on the Medical Research Council's cyclotron by bombarding iodine with 30 MeV α particles ^{127}I $(\alpha,2n)$ ^{129}Cs. The target is prepared by pressing powdered sodium iodide (analytical grade) into a grooved aluminium plate. The target material is then covered with aluminium foil to prevent contamination and loss of powder during irradiation. The back of the target is water cooled during irradiation to carry away the beam power, 450 watts at 30 μA. The yield of ^{129}Cs is approximately 170 μCi/μAh. After bombardment the sodium iodide is removed from the target plate by washing it with water. To the resulting sodium iodide solution containing ^{129}Cs is added approximately 1 g of zirconium phosphate cation exchanger (B10-RAD ZP-1 100-200 mesh). The ^{129}Cs is absorbed rapidly on to the zirconium phosphate. The slurry of ^{129}Cs-labelled zirconium phosphate is then separated from the sodium iodide by repeated washing and centrifugation, discarding the supernate. The high distribution coefficient for caesium between zirconium phosphate and aqueous solutions (caesium activity per gram of zirconium phosphate/caesium activity per gram of solution) has been confirmed by various workers (Maeck, Kussy and Rein 1963; Amphlett, McDonald, Burgess and Maynard 1959). This high affinity of zirconium phosphate for caesium together with its insolubility over the pH range of 0–13 (2×10^{-6} M/100 g in 10 M HCl) (Amphlett, 1964) led us to choose this agent, rather than an ionic solution of ^{51}Cr the gastric chemistry of which may be subject to variation. Zirconium phosphate at the mesh sizes used is thought to be more suitable, due to possible sedimentation in the stomach, for administration with a solid rather than a liquid meal.

2. *Physical half-life of ^{129}Cs*

This is 32·1 hours which is relatively short and therefore prevents unnecessary irradiation of the intestine, but still is convenient for general use. The practical minimum half-life of an isotope for

TABLE I

RADIATION CHARACTERISTICS OF ^{129}Cs*

Principal γ-ray emission	Probability of γ-ray emission per disintegration
40 keV	0·02
280 keV	0·03
320 keV	0·04
370 keV	0·48
410 keV	0·25
545 keV	0·05

Specific γ-ray constant = 2·28 R cm^2/mCi.h.
Mean β energy per disintegration: 21 keV.
*Nuclear data from: Lederer, Hollander and Perlman (1967).

this study is dictated by the need to administer the tracer at breakfast for the sake of physiological consistency.

3. *Radiation characteristics of* ^{129}Cs

These are shown in Table I. Most of the γ rays emitted from ^{129}Cs are distributed between 370 and 410 keV photons. By counting both these γ rays a suitable compromise is achieved between collimator septal penetration and depth response, an important consideration when only one detector is used. The half-value thickness in tissue for ^{129}Cs is 9·3 cm.

4. *Radiation dosimetry*

The absorbed dose to the lower large intestine, which is the critical organ, is 3·7 mrads per μCi of ^{129}Cs administered. The corresponding dose to the ovaries from activity in the lower large intestine, considered as a point source 3·7 cm away (Macintyre, Crespo and Christie, 1963; Smith 1965), is 1·58 mrads per μCi administered.

These absorbed dose values were calculated using the ICRP (1959) data for normal gastrointestinal transit (total time spent in the stomach, small intestine, upper large intestine, lower large intestine = 1, 4, 8 and 18 hours respectively). The dose to the critical organ calculated using these data is half that which would result if an activity of ^{51}Cr were administered which gave a comparable external count rate. Gastro-intestinal transit is frequently much slower than the values given by the ICRP (Davenport, 1966), and this further favours ^{129}Cs with its much shorter half-life (32·1 hours compared with 27·8 days for ^{51}Cr).

METHOD

A solid meal into which has been mixed 100 μCi of ^{129}Cs-zirconium phosphate suspension is eaten by the subject. The gamma-camera is then manoeuvred over the supine patient until the whole stomach, as depicted by the tracer, lies centrally in the field of view displayed on the oscilloscope. An 11·4 cm thick, 1,090-hole collimator is used (Westerman and Glass, 1963). Using a Polaroid camera, a photograph is taken of the display which includes an illuminated graticule to which the stomach can be related. With the aid of the photograph, an outline of the stomach is cut out of a piece of light-proof paper on which an identical graticule has been ruled. This masking paper is then superimposed on the oscilloscope face and the graticules aligned. This procedure delineates the stomach within the field of view of the gamma-camera. A photomultiplier tube mounted to view the oscilloscope screen is then used to count light pulses on the exposed part of the oscilloscope screen. The output pulses from the photomultiplier are amplified, analysed and counted using standard equipment. The magnitude of the pulses is adjusted by varying the intensity control of the oscilloscope. As a result of the method used to locate the stomach accurately and to construct the oscilloscope mask it was not normally possible to begin measurements before 15 minutes after completion of the meal. In practice two display oscilloscopes are used, one for counting and the other for serial photography. However, the development of a semi-silvered mirror system could eliminate the need for one of these. The count rate from the stomach resulting from a 100 μCi administration is about 20 counts per second. Counts are integrated over 100 second periods to obtain reasonable counting statistics. This is an acceptable period since the emptying rate of the stomach is long relative to this counting interval. Measurements are usually continued for about 90 minutes after the mid-time of the meal.

RESULTS

The technique described has been used specifically in investigations of stomach emptying in patients who have undergone vagotomy. The purpose of this study was to measure gastric motility in patients soon after vagotomy. The full clinical implications of these investigations will be published elsewhere (Tinker, Kocak, Jones, Glass and Cox, 1970).

Figures 1 and 2 show respectively the mean results in five normal subjects and in five patients within a few weeks of vagotomy. Comparison of these figures suggests that the rate of gastric emptying is decreased early after vagotomy. Figure 3 shows the photographic sequence of stomach emptying in a patient before and after vagotomy. Figure 4 shows

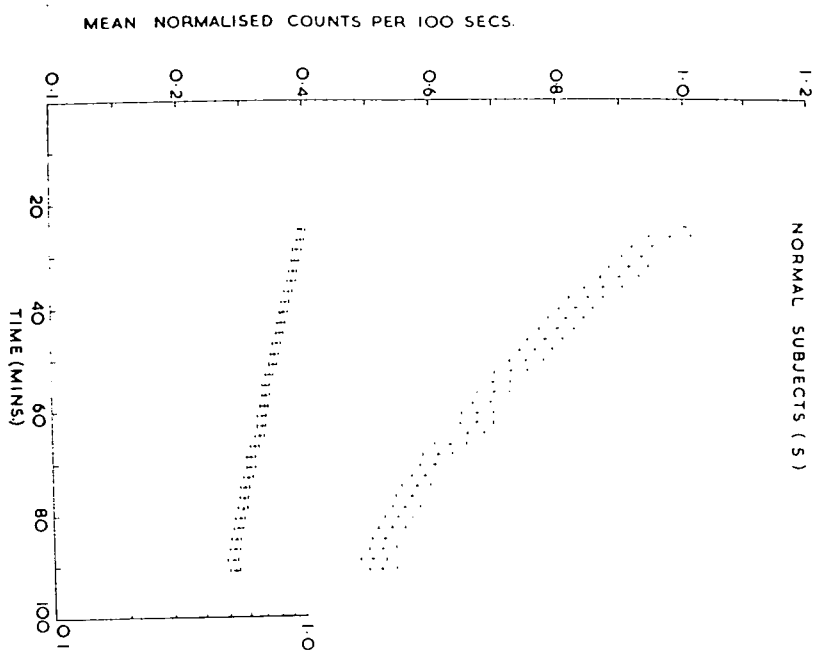

FIG. 1.

Mean linear (upper) and logarithmic (lower) plot in five normal subjects of stomach activity against time after the mid-point of the meal (standard error of the mean limits).

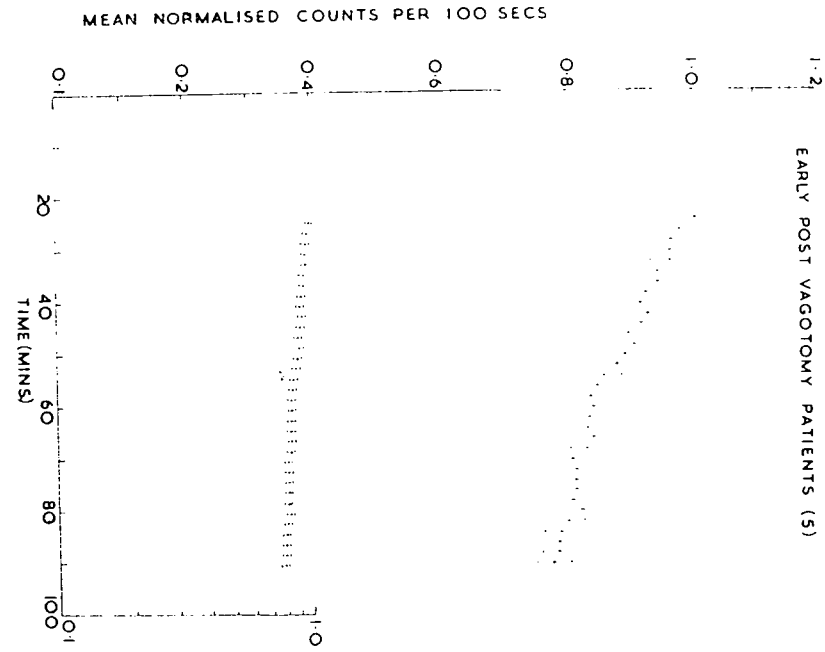

FIG. 2.

Mean linear (upper) and logarithmic (lower) plot in five patients, within a few weeks of vagotomy, of stomach activity against time after the mid-point of the meal (standard error of the mean limits).

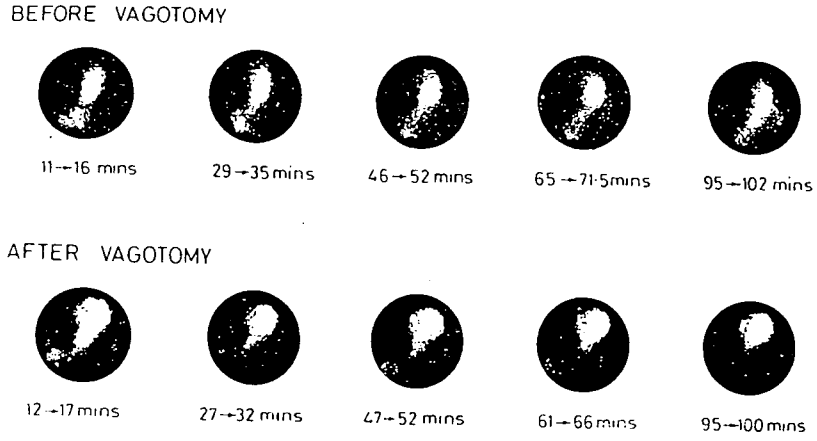

FIG. 3.

Photographic sequence of stomach emptying in a patient before and after vagotomy.

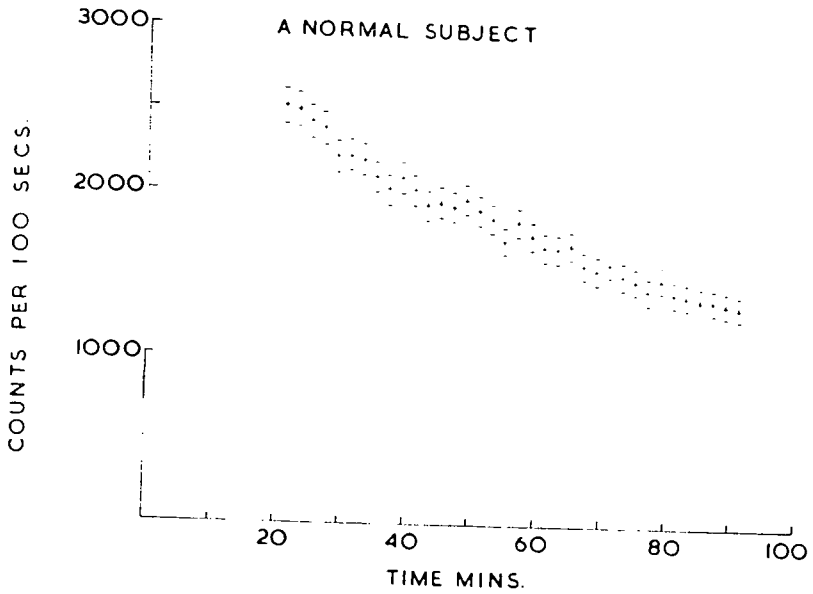

FIG. 4.

Stomach emptying in a single normal subject against time after the mid-point of the meal (two standard deviation limits).

the results from a single normal subject. This suggests a steplike pattern which may reflect the true nature of gastric emptying more accurately than the simple curve seen when conventional scanning is used. The difference may be attributed to the ability of the gamma-camera to make relatively faster counts of the whole stomach and thereby detect the "fine details" of gastric emptying.

This steplike pattern is seen in all subjects but is inevitably obliterated when the results of a number of patients are grouped together as was done for Figs. 1 and 2.

DISCUSSION

A technique has been developed for measuring stomach emptying with the scintillation camera in combination with ancillary equipment and a radionuclide of a relatively short half-life which is still

convenient for general use. The method is simple and can be carried out by relatively unskilled personnel.

The radioactive tracer used is cyclotron-produced ^{129}Cs bound to insoluble zirconium phosphate. This ensures no loss of radioactive marker through absorption by the gastrointestinal tract. ^{129}Cs which has a 32·1 hour half-life has advantages in reduced dose to the patient over other longer-lived radionuclides used for stomach emptying measurements, particularly in patients with delayed motility. The useful γ rays emitted by ^{129}Cs (370 and 410 keV) facilitate a reasonable compromise between depth response and septal penetration. Other workers have used moving detector scanners for gastric emptying, but the camera has the advantage of measuring the whole of the stomach simultaneously. This eliminates the main inaccuracies associated with the use of scanners. Since the scanner only observes one portion of the stomach at any time, movement of activity within the stomach or from that part of the stomach which is not being monitored, will introduce inaccuracies in the estimate of gastric emptying, especially if the activity is not uniformly distributed throughout the stomach. Furthermore, the finite time taken to scan in order to obtain suitable statistics increases the time error in the measurement.

The main disadvantage of the camera relative to a double-headed scanner system is the inherently poorer depth response of a single detection system. A further disadvantage of this technique rests in the time delay between the mid-point of the meal and the onset of counting the stomach contents. This delay is probably not important when a solid meal is administered but might be with a liquid meal. Significant reduction in this delay could be achieved by magnetic tape recording of the gamma camera data and subsequent analysis. When patients are lying supine, the gastric antrum frequently overlies the duodeno-jejunal flexure and thus the technique measures some activity which has passed beyond the pylorus. Whilst this does not invalidate the method, if this has occurred the effect has not been apparent on the observed curves.

The simplicity of the method relies on the patient remaining in one position during the whole of the procedure and this may meet with certain physiological criticisms. However, the technique has been specifically developed for comparative studies of stomach emptying. Examples of the use of this technique are illustrated by the emptying patterns in groups of normal subjects and patients after vagotomy. The basic quantitating system developed for stomach emptying may also be used for other studies, which must, however, have rate constants long enough to permit localisation of the area of interest before counting actually begins. Alternatively, the technique could be used for faster studies if a preliminary dose of tracer, possibly of a lower energy, is administered to delineate initially the region of interest.

ACKNOWLEDGMENTS

The authors wish to acknowledge the support of Mr. D. D. Vonberg, Director of the Medical Research Council Cyclotron Unit, and the useful comments of Dr. D. K. Bewley. Thanks are given to Mr. P. L. Horlock for preparing the isotopic tracer and Mr. K. S. J. Wilson and Mr. K. R. Butler for computer assistance.

ABSTRACT

A simple technique is presented for directly measuring gastric emptying using an Anger scintillation camera in conjunction with readily available nucleonic equipment. Cyclotron-produced ^{129}Cs is the radioisotopic marker which is mixed with the patient's meal. It has a 32·1 hour half-life and principally emits 370 and 410 keV photons, which provide a half-value thickness in tissue of 9·3 cm. The ^{129}Cs is bound to insoluble zirconium phosphate to prevent absorption from the stomach. Illustrations of the use of this method are given with normal subjects and patients after vagotomy. The "step like" emptying pattern of the stomach contents is sometimes apparent when this technique is used. The relative merits of the camera and the scanner for this type of study are discussed.

REFERENCES

AMPHLETT, C. B., 1964, *Inorganic Ion Exchanges* (Elsevier Publishing Co., New York).

AMPHLETT, C. B., MCDONALD, L. A., BURGESS, J. S., and MAYNARD, J. C., 1959, *J. Inorg. Nucl. Chem.*, *10*, 69.

DAVENPORT, H. W., 1966, *Physiology of the Digestive Tract*, 216 (Year Book Medical Publishers Inc., Chicago).

GRIFFITHS, G. H., OWEN, G. M., CAMPBELL, P. H., SHIELDS, R., 1968, *Gastroenterology*, *54*, 1.

HOLROYD, A. M., and JONES, T., 1969, *Phys. med. Biol.*, *14*, 631.

LEDERER, C. M., HOLLANDER, J. M., and PERLMAN, I., 1967, *Table of Isotopes*, 6th edn. (John Wiley, New York).

MACINTYRE, W. J., CRESPO, G. G., and CHRISTIE, J. H., 1963, *Am. J. Roentg.*, *93*, 315.

MAECK, W. J., KUSSY, M. E., and REIN, J. E., 1963, *Analytical Chemistry*, *35*, 2086.

Recommendations of the International Commission on Radiological Protection. Report of Committee II on Permissible Doses for Internal Radiation, 1959 (Pergamon Press, New York).

SMITH, E. M., 1965, *J. nucl. Med.*, *6*, 231.

TINKER, J., KOCAK, N., JONES, T., GLASS, H. I., and COX, A. G., 1970, *Gut* (in press).

WESTERMAN, B. R., and GLASS, H. I., 1963, *J. Nucl. Med.*, *9*, 24.

WILLIAMS, E. D., GLASS, H. I., ARNOT, R. N., and DE GARRETA, A. C., 1968, in *Medical Radioisotope Scintigraphy*, Vol. 1, p. 665 (I.A.E.A. Vienna).

International Journal of Applied Radiation and Isotopes, 1970, Vol. 21, pp. 33–36. Pergamon Press. Printed in Northern Ireland

The Production of ^{117}Sb-labelled Potassium Antimonyl Tartrate for Medical Use

(*Received* 11 *June* 1969)

Introduction

SEVERAL antimony compounds have uses in medicine. Amongst them, potassium antimonyl tartrate (hereinafter referred to as PAT) is used in the treatment of schistosomiasis.[1] It has recently been suggested[2] that this substance, labelled with ^{117}Sb, might prove to be a useful agent for liver scanning, and samples are now in production in our laboratory for clinical trials.

Antimony-117 has a half-life of 2·8 hr and decays chiefly by electron capture (97 per cent) followed by emission of a 158 keV γ-ray; only 3 per cent decays by positron emission.[3] It can be made conveniently by α-bombardment of indium[4], through the reaction ^{115}In(α, $2n$)^{117}Sb.

Experimental

(1) *Cyclotron targets and bombardment*

Targets of natural indium foil (96 per cent ^{115}In), 50 × 10 × 0·125 mm, weighing about 400 mg, are bombarded in the external α-particle beam of the Medical Research Council's cyclotron. They are covered by an air-cooled aluminium foil (0·025 mm) and backed by a water-cooled copper plate, but because indium metal melts at only 155°C the beam current is restricted to 20 μA. The energy of the α-particles incident on the indium is about 29 MeV, and the energy loss in the target is about 12 MeV.

Under these conditions a 30-min bombardment (10 μAh) yields about 35 mCi of ^{117}Sb. At the same time, some ^{118m}Sb (half-life 5·1 hr) is produced by the ^{115}In (α, n) reaction and its activity amounts to about 6 per cent of the ^{117}Sb activity at the end of bombardment. Yields of the shorter-lived ^{115}Sb and ^{116}Sb from reactions with ^{113}In (3 per cent) are negligible.

(2) *Dissolution of indium targets and recovery of radioantimony*

The apparatus used to dissolve the indium targets after bombardment and to recover the radioantimony is shown schematically in Fig. 1. It consists of four small glass vessels connected in series and flushed continuously by a slow stream of nitrogen.

In vessel A, the indium target is dissolved in 5 ml concentrated hydrochloric acid, assisted by mild heating. This takes about 10 min, and during this step about 65 per cent of the radioantimony is liber-

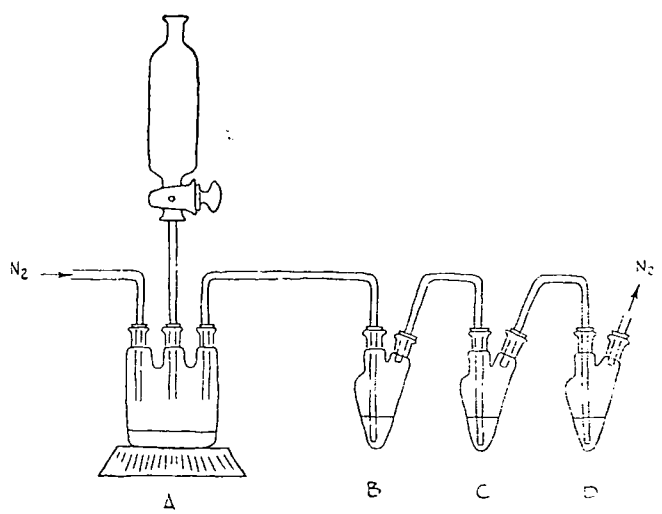

FIG. 1. Apparatus used to dissolve indium targets and recover radioantimony.

ated into the gas stream as stibine, affording an excellent method of isolating it from the highly toxic indium when samples for clinical injection have to be prepared. The remainder is oxidised to the 5-valent state and stays in solution. Work still in progress is aimed at increasing the efficiency of stibine formation.

Subsequent recovery of radioantimony could be achieved by means of the classical Marsh reaction whereby stibine is decomposed by passage through a heated silica tube, and antimony is deposited on cold regions of the tube.[5,6] However, we found this to be an inefficient and inconvenient method since a high proportion of the "carrier-free" radioactive stibine passed through the tube without decomposition and recovery of the deposited radioantimony was slow and difficult to manage.

Instead, we permit the stibine to react with excess silver nitrate according to the following equations:[7]

$$SbH_3 + 3\,AgNO_3 \rightarrow Ag_3Sb + 3\,HNO_3 \quad (1)$$

$$4\,Ag_3Sb + 12\,AgNO_3 + 6\,H_2O \rightarrow Sb_4O_6 + 24\,Ag + 12\,HNO_3 \quad (2)$$

Vessel B contains water to remove acid spray from the gas stream, and vessels C and D each contain about 3 ml of a 0·1% aqueous solution of silver nitrate. More than 99 per cent of the radioactive stibine is decomposed in vessel C; the remainder is decomposed in vessel D but this activity is not generally recovered. Experiments in which ^{113m}In was used as a tracer have shown that less than 1×10^{-4} per cent of the indium target material reaches vessel C.

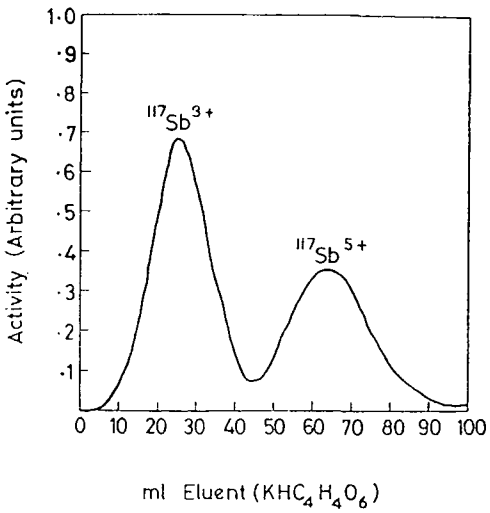

FIG. 2. Elution curve for radioantimony (Column: Amberlite IR-120, 14-52 mesh, 200 mm × 15 mm. Element: 0·1% $KHC_4H_4O_6$, 5 ml/min).

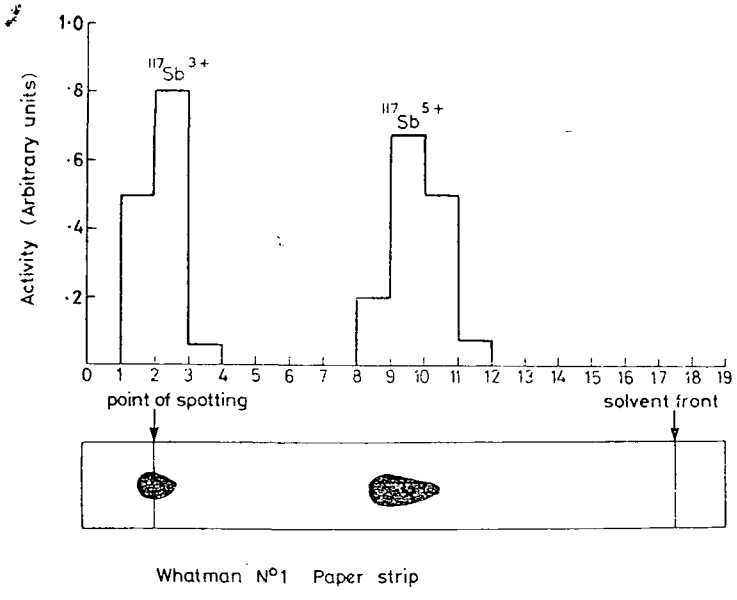

FIG. 3. Paper chromatographic separation of Sb^{5+} from Sb^{3+}. Solvent: TBP:5 M acetic acid:acetone = 1:1:3).

About two min after the indium target has completely dissolved, the solution from vessel C is transferred to a centrifuge tube. Concentrated HCl, 2 ml, is then added, when the radioantimony is converted to $SbCl_3$, and all the silver is precipitated as AgCl to be removed by centrifugation. The loss of radioantimony due to adsorption on AgCl at this step has been found to be quite negligible.

The supernatant solution from this step is taken down to dryness, heating gently to avoid loss of $SbCl_3$ (b.p. 223°C), and this is repeated after 2 ml conc. HCl have been added to destroy all traces of nitric acid. The resulting residue is readily dissolved in 5 ml 0·05 *M* HCl and a clear solution is obtained with a pH $\simeq$ 1.

The separation of indium from other elements by cation exchange has been described.[8,9] We obtain very effective further purification of carrier-free radioantimony from indium using Amberlite IR-120 resin (14–52 mesh) and 0·1% potassium hydrogen tartrate, $KHC_4H_4O_6$, as the eluting agent. The resin column is 200 × 15 mm and is conditioned by washing first with conc. HCl and then with about 100 ml 0·05 *M* HCl. The solution as described above, in which the radioantimony is 3-valent, is loaded on this column and washed with 5 ml 0·05 *M* HCl. Upon eluting the column with 0·1% $KHC_4H_4O_6$ at a flow rate of approximately 5 ml/min, 95 per cent of the radioantimony can be collected in a 25 ml fraction which is subsequently used for the preparation of PAT for clinical injection (see 3 below).

When samples are not required for clinical use, so that a slight risk of contamination with indium can be tolerated, the 5-valent radioantimony present in the original indium target solution may also be recovered. To do this, the solution from vessel A is reduced to dryness (avoiding strong heat which leads to loss of $SbCl_5$, b.p. 141°C); the residue is taken up in 0·05 *M* HCl and loaded on to the ion exchange column, at the same time as the solution of 3-valent radioantimony. In these circumstances, an elution curve such as that shown in Fig. 2 is obtained. Confirmation of the valence-states of the radioantimony in the elution peaks has been obtained by means of paper chromatography, using n-Tributylorthophosphate, 5 *M* acetic acid, and acetone (1:1:3)[10] as the solvent and the results are shown in Fig. 3.

Indium may subsequently be removed from the column by eluting with 0·5 *M* HCl, but tracer studies using ^{113m}In have shown that even when loaded with 400 mg In, less than 10 μg (0·0025 per cent) are eluted from the column with the radioantimony by the 0·1 per cent $KHC_4H_4O_6$ solution.

(3) *Preparation of labelled PAT for clinical injection*

Following elution from the cation exchange column, the solution containing the radioantimony is essentially tartaric acid. It is therefore titrated to pH 4 with KOH solution, and then contains $KHC_4H_4O_6$ equivalent to that present in the original 25 ml 0·1% solution used for the elution (i.e. 25 mg). To this solution is added exactly 19·4 mg Sb_2O_3 (stoichiometrically equivalent to the $KHC_4H_4O_6$) and on boiling a solution of PAT is thereby obtained.[11] If required, the PAT concentration may be adjusted either by dilution or by reducing the volume of solution by evaporation. As a final step, the solution is passed through a "Millipore" filter, prior to dispensing, to remove "bits" which are occasionally present.

Paper chromatography is used to check that the final solution contains a negligible fraction (always less than 3 per cent) of radioantimony that is not present as PAT. Using Whatman No. 1 paper, and water as solvent, PAT has $R_f = 0{\cdot}95$, whilst uncombined radioantimony has $R_f = 0{\cdot}05$.

Discussion

The entire procedure for the production of clinical samples of PAT takes less than one half-life of ^{117}Sb to work through, and losses of activity at each step other than the first are so small than one may reasonably expect the final PAT solution to contain at least 30 per cent of the starting (i.e. end-of-bombardment) activity. Most of the chemical manipulations can be carried out by simple remote handling techniques, so that radiation doses to the hands may be minimised.

When preparing samples for clinical use we use reagents of the highest purity commercially available, and solutions are freshly prepared in "water for injection B.P.". Observing these precautions, we have prepared samples that have been shown to be free from contamination by pyrogens. Solutions of PAT may be sterilised by autoclaving without decomposition.

Medical Research Council
Cyclotron Unit
Hammersmith Hospital
London, W.12, England

M. L. Thakur
J. C. Clark
D. J. Silvester

References

1. Todd R. C. (editor), *Extra Pharmacopoeia*, p. 125. 25th Edn. The Pharmaceutical Press, London (1967).

2. CHAUDHRI M. A. and ROWLAND H. A. K. private communication (1968).
3. LEDERER C. M., HOLLANDER J. M. and PERLMAN I. *Table of Isotopes*, 6th Edn, p. 263. Wiley, New York (1967).
4. TEMMER G. M. *Phys. Rev.* **76,** 424 (1949).
5. GREENDALE A. E. and LOVE D. L. *Analyt. Chem.* **35,** 632 (1963).
6. TOMILSON L. *Analyt. Chim. Acta* **31,** 547 (1964).
7. VOGEL A. I. *Qualitative Chemical Analysis*, 3rd Edn, p. 175. Longmans, Green, London (1947).
8. KLEMENT R. and SANDMAN H. *Z. Analyt. Chem.* **145,** 325 (1955).
9. KIMURA K., SAITO N., KAKIHARA H. and ISHIMORI T. *J. chem. Soc. Japan, Pure Chem. Section* **74,** 305 (1953).
10. THAKUR M. L. to be published (1969).
11. TAYLOR F. S. *Inorganic Theoretical Chemistry*, 9th Edn, p. 589. William Heineman, London (1952).

1970, *Br. J. Radiol.*, *43*, 670–671

Correspondence

(The Editors do not hold themselves responsible for opinions expressed by Correspondents.)

THE EDITOR—SIR,

THE USE OF CARBON 11 DIOXIDE FOR SKELETAL SCINTIGRAPHY

There is now much evidence to show that scintigraphy is more accurate than radiology for the detection of skeletal metastases (Galasko, Westerman, Li, Sellwood and Burn, 1968; Galasko, 1969a). Opinions differ, however, as to the choice of the isotope. ^{47}Ca, ^{85}Sr, $^{87}Sr^{m}$ and ^{18}F have been the isotopes most commonly used. Of these ^{18}F is probably the isotope of choice (Galasko, 1969b). Recently, it has been suggested that ^{11}C, in the form of carbon dioxide, is the isotope of choice for skeletal scintigraphy (Myers and Hunter, 1967; 1969). As the carbon dioxide can be inhaled, the problems of sterility and pyrogenicity associated with intravenous injections need cause little concern. ^{11}C has a half-life of only 20·3 minutes and, therefore, can be given in large doses, producing high count rates and a rapid scintigram, with the patient still receiving only a low dose of irradiation.

Myers and Hunter (1967; 1969) have reported on the use of ^{11}C in studying spontaneous osteosarcomata in the limbs of dogs. We have studied the usefulness of $^{11}CO_2$ for the detection of skeletal metastases from mammary cancer and have compared it with ^{18}F. There has been no previous report on its use, in man, for the detection of skeletal metastases.

Patients and methods

Six patients with suspected skeletal metastases were examined with a gamma-camera (Pho—Gamma Mk II—Nuclear Chicago). In this study the camera was used with a 4·5 in. collimator, which was obtained by bolting together the 3 in. and 1·5 in. multichannel collimators, since both ^{18}F and $^{11}CO_2$ have a relatively high emission energy of 0·511 MeV. Two separate studies were made on each patient, one after an intravenous injection of ^{18}F and the other after inhalation of $^{11}CO_2$. The dose of ^{18}F was 1·5 mCi and that of $^{11}CO_2$ was 30 mCi.

In three patients the scintigram with ^{18}F was carried out first and in the other three patients the scintigram with $^{11}CO_2$ was first. The interval between the two examinations was two to six days.

The ^{18}F scintigrams were started 90 minutes after the injection of ^{18}F (Galasko, 1969a). The $^{11}CO_2$ was administered close to an extractor fan to remove $^{11}CO_2$ from the room in which it was administered. The patient breathed the air from a cylinder, through a rubber tube to which an expiratory valve and a rebreathing bag had been attached. There was no soda-lime absorber included in the circuit. After breathing normally for one to two minutes the patient took four to six deep breaths with the expiratory valve open. The valve was then closed, 30 mCi of $^{11}CO_2$ were injected into the tubing and five or six deep breaths were taken by the patient. The face-mask was then removed and the patient walked to an adjacent room where the gamma-camera was situated. Regions previously shown to contain metastases were then examined, with the camera, at intervals of 15 minutes until the count-rate became too low for scintigraphy to be practical.

High specific activity ^{11}C-labelled carbon dioxide was prepared by the irradiation of boric oxide in the external deuteron beam of the Medical Research Council Cyclotron (Vonberg, Baker, Buckingham, Clark, Finding, Sharp and Silvester, 1969; Buckingham and Clark, 1970). The $^{11}CO_2$ was continuously removed from the target by a helium sweep gas and recovered in a laboratory 100 m from the cyclotron by freezing in a cold trap at −196°C. The $^{11}CO_2$ was then dispensed by allowing the cold trap to warm to room temperature and was then flushed with air into a 30 ml. syringe until the required dose was accumulated.

TABLE I

RESULTS OF THE $^{11}CO_2$ AND ^{18}F SCINTIGRAMS IN THE PATIENTS STUDIED

Pt. No.	Sites of lesion	^{18}F scintigram	$^{11}CO_2$ scintigram
1	Prox. femur	Lesions present	Lesions not present
	Cerv. spine	Lesions present	Lesions not present
2	Lumbar spine	Lesions present	Lesions not present
	Dorsal spine	Lesions present	Lesions not present
	Cerv. spine	Lesions present	Lesions not present
	Ilium	Lesions present	Lesions not present
	Skull	Lesions present	Lesions not present
3	Ribs	Lesions present	Lesions not present
	Dorsal spine	Lesions present	Lesions not present
	Prox. femur	Lesions present	Lesions not present
4	Lumbar spine	Lesions present	Lesions not present
	Dorsal spine	Lesions present	Lesions not present
	Pelvis	Lesions present	Lesions not present
5	Cerv. spine	Lesions present	Lesions not present
	Dorsal spine	Lesions present	Lesions not present
	Lumbar spine	Lesions present	Lesions not present
6	Cerv. spine	Lesions present	Lesions not present
	Dorsal spine	Lesions present	Lesions not present
	Lumbar spine	Lesions present	Lesions not present
	Rib cage	Lesions present	Lesions not present

Results

The results on the six patients are shown in Table I. Although permission was obtained from the Medical Research Council to study eight patients, the investigation was abandoned after six patients had been studied as the $^{11}CO_2$ had not been concentrated in any metastases. The regions examined included the skull, cervical, dorsal and lumbar spine, rib cage, pelvis and proximal femora.

High count rates were obtained, initially, over regions distant from the lungs indicating that the $^{11}CO_2$ had been absorbed. After two to two and a half hours the count rate had become too low for scintigraphy to be practical.

The scintigrams indicated that the $^{11}CO_2$ had been taken up generally by the tissues as the body outline was demonstrated (Fig. 1). With ^{18}F all metastases were seen.

Correspondence

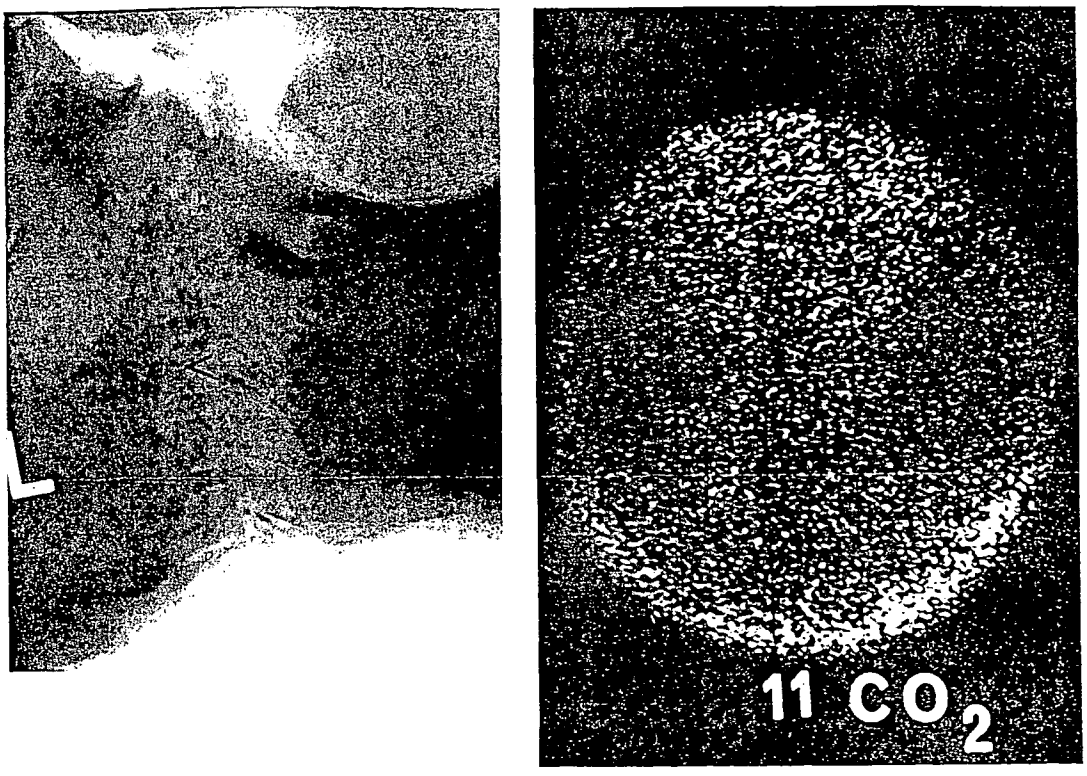

A FIG. 1. B

(A) A lateral X-ray of the cervical spine. A lesion (arrowed) can be seen in the 3rd cervical vertebra.

(B) The $^{11}CO_2$ scintigram of the same region. Although the outline of the neck can be seen the ^{11}C has not concentrated in bone nor in the metastasis.

Discussion

This study indicated that $^{11}CO_2$ is unsuitable for skeletal scintigraphy. The results suggest that it is evenly distributed through the body tissues and this is not surprising since carbon is an essential component of all biological material. The larger the bulk of tissue the greater the uptake and, therefore, it is suggested that its concentration in spontaneous osteosarcomata of dogs (Myers and Hunter, 1967; 1969) may have been due solely to the increased bulk of that limb.

Yours, etc.,

C. S. B. GALASKO, Ch.M., F.R.C.S., F.R.C.S.E.
R. R. H. COOMBS, M.A., M.B., B.Ch.
Breast Unit and Department of Surgery,
Royal Postgraduate Medical School and
Hammersmith Hospital.

J. C. CLARK, B.Sc.
M.R.C. Cyclotron Unit,
Hammersmith Hospital, London.

REFERENCES

BUCKINGHAM, P. D., and CLARK, J. C., 1970, *Inter. J. applied Rad.* (to be published).

GALASKO, C. S. B., 1969a, *Br. J. Surg.*, *56*, 757; 1969b, Ch.M. thesis, Univ. Witwatersrand.

GALASKO, C. S. B., WESTERMAN, B., LI, J., SELLWOOD, R. A., and BURN, J. I., 1968, *Br. J. Surg.*, *55*, 613.

MYERS, W. G., and HUNTER, W. W., jun., 1967, *J. nucl. Med.*, *8*, 305; 1969, in *Medical Radioisotope Scintigraphy*, Vol. II, p. 43 (I.A.E.A., Vienna).

VONBERG, D. D., BAKER, L. C., BUCKINGHAM, P. D., CLARK, J. C., FINDING, K., SHARP, J., and SILVESTER, D. J., 1969, Paper presented to the International Conference on the Use of Cyclotrons in Chemistry, Metallurgy and Biology, Oxford. Proceedings in press (Butterworths, London).

RADIOCHEM.RADIOANAL.LETTERS 6 /5/ 281 - 286 /1971/

THE PREPARATION OF CARBON-11 LABELLED CARBON MONOXIDE AND CARBON DIOXIDE

J.C.Clark, P.D.Buckingham

Medical Research Council Cyclotron Unit,
Hammersmith Hospital, London, W.12, U.K.

Received 15 March 1971
Accepted 20 March 1971

A target system is described for the production of ^{11}CO and $^{11}CO_2$ by the deuteron bombardment of B_2O_3. The radiochemical composition of the gas at the target output is given for a range of target sweep gases using a fixed flow rate and beam current. Values are also given for the production rate and radioactive concentration of the ^{11}C labelled products, together with values for the overall ^{11}C target extraction efficiency. The use of various target sweep gases is discussed and sweep gas compositions are given for the direct production of ^{11}CO and $^{11}CO_2$.

INTRODUCTION

Carbon monoxide and carbon dioxide both labelled with ^{11}C are in routine production for clinical studies at Hammersmith Hospital[1] and elsewhere. The present paper describes the systems currently in use for the production of carbon monoxide and carbon dioxide labelled with ^{11}C. The most notable improvement over previous systems[2,3] is in the use of hydrogen as a target sweep gas, which makes the production of ^{11}CO virtually carrier-free, whilst inhibiting the formation of significant amounts of $^{13}N_2$ /^{13}NN/.

TARGET DESIGN

^{11}C has a 20.3 min half-life and decays by the emission of 0.96 MeV positrons. The target material generally used for

^{11}C production in a cyclotron is boron in the form of boron trioxide. When bombarded with 14 MeV deuterons, the following reactions take place:

$$^{10}B/d,n/^{11}C \quad \text{and} \quad ^{11}B/d,2n/^{11}C$$

The target box is shown in Fig.1. The B_2O_3 powder is melted onto the wedge in an electric furnace to a thickness of 1-2 mm. The deuteron beam, defocussed to cover an area approx. 5 cm^2, passes through the 0.05 mm aluminium foil window and strikes the surface of the B_2O_3 at grazing incidence. With a beam of 40 μA the power density is approx. 20 W cm^{-2} on the surface of the wedge which is deliberately in poor thermal contact

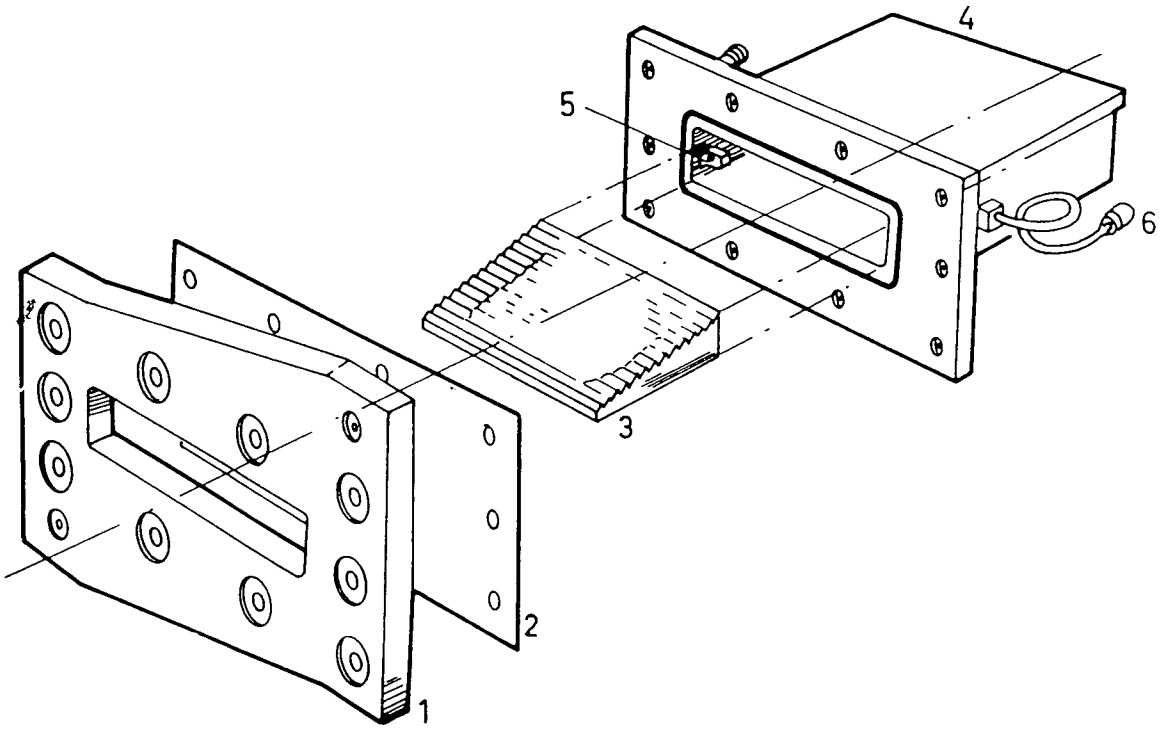

Fig.1. External target for ^{11}C production.
1 - target mounting plate, 2 - beam entry window foil, 3 - brass wedge supporting B_2O_3, 4 - gas tight target box, 5 - wedge locating pins, 6 - sweep gas connections

with the surrounding box. This power density is sufficient to melt the B_2O_3 /MP ≈ 400 ^{o}C/ releasing labelled gases into a stream of sweep gas passed through the box at about 80 ml min^{-1}. The molten B_2O_3 is prevented from rapid movement down the wedge by the step shape.

The swept volume of the target box is kept small /about 200 ml/ to maximise the radioactive concentration of the effluent gas. Its normal working pressure is approx. 0.007 kg cm^{-2} above atmospheric pressure.

TARGET SWEEP GASES AND YIELDS

The nature and composition of the target sweep gas are of critical importance. The yield is expressed as the rate of production of activity in mCi min^{-1} continuously monitored by a 200 ml container, in an ionisation chamber approx. 10 m from the target. Table 1 shows the effect of varying the composition of the sweep gas at a flow rate of 80 ml min^{-1} and a beam current of 40 μA, the values being obtained by radio-gas chromatography and the use of a calibrated ionisation chamber system. The target efficiency values were obtained by comparing the yield of ^{11}C induced in a similar wedge under conditions where there were no losses of volatile products, decay curve analysis being necessary to extract the ^{11}C component.

The precise nature of the chemical and radiolytic reactions which take place in the target during irradiation is not fully known. However, it is thought that ^{11}CO is the primary product of the reaction between the ^{11}C atoms and the oxygen atoms in the B_2O_3. In the absence of any oxygen radical scavenger the

TABLE 1

Carbon-11: solid target: B_2O_3 /wedge/: $^{10}B/d,n/^{11}C/d$, $2n/^{11}C$

Target sweep gas	% of total recovered yield at target output				^{11}C recovery at target output		target ^{11}C extraction efficiency %
	^{11}CO	$^{11}CO_2$	$^{11}CH_4$	^{13}NN	mCi min^{-1}	mCi ml^{-1} 20 °C 760 mm Hg	
Helium	1.0	83	<0.1	16	17	0.21	52
1% CO in He	52	36	<1	11	16	0.20	50
5% CO in He	72	19	<1	8.2	16	0.20	50
1% CO_2 in He	<1	88	<0.1	11	14	0.17	44
5% CO_2 in He	<1	83	<0.1	16	16	0.20	50
1% H_2 in He	60	21	9.0	10	13	0.17	42
5% H_2 in He	56	15	22	7.0	12	0.15	37
Hydrogen	86	8.7	5.2	< 1	14	0.17	43
Tolerances	>60% ..... ±10%						
	11-60% ..... ±20%					±10%	±20%
	<10% ..... ±50%						

Particle	Deuteron
Current	40 μA
Energy	15 MeV
Energy incident on target material	≈14 MeV
Window material and thickness	Al 0.05 mm /.002"/
Energy loss in window	≈1 MeV
Beam distribution dimensions	3-4 cm wide 1-1.5 cm high
Target dimensions	12.7 cm wide 2.2 cm high 10 cm deep /gas vol. 200 ml/
Target pressure	0.007 kg cm^{-2} /0.1 lb in^{-2}/ gauge
Sweep gas flow rate	80 ml min^{-1}

^{11}CO is largely radiolysed to $^{11}CO_2$. Thus when helium is used as the sweep gas most of the ^{11}C activity in the target effluent is $^{11}CO_2$; the addition of CO_2 carrier having little effect upon the recovered yield. When stable CO is added to the helium less $^{11}CO_2$ is made, the CO acting as a scavenger for oxygen radicals and protecting the ^{11}CO. As more CO is added this protection is seen to increase.

When a sweep gas of helium containing a small amount of hydrogen is used it also acts as a radical scavenger giving some recovery of ^{11}CO without added carrier. If however hydrogen is used alone, a much higher recovery of ^{11}CO is achieved, also without added carrier.

It should be noted that there is a significant recovery of $^{13}N_2$ with all sweep gases except hydrogen. Presumably the ^{13}N atoms are scavenged by hydrogen to form non volatile products. The absence in the target effluent of a possible volatile product, $^{13}NH_3$, has been demonstrated both chemically and gas chromatographically.

The only detected ^{11}C labelled contaminant is $^{11}CH_4$ formed by the combination of ^{11}C and H radicals within the target during irradiation. This, as would be expected, is only present in significant amounts when H_2 is used in the sweep gas.

CONCLUSION

In the production of ^{11}CO and $^{11}CO_2$ by the deuteron bombardment of B_2O_3, the chemical form of the product nuclei recovered from the target is largely determined by the target sweep gas composition. The use of hydrogen inhibits the forma-

tion of $^{11}CO_2$ and $^{13}N_2$ resulting in virtually carrier free ^{11}CO production. The use of helium or 1% CO_2 in He results in the production of a high proportion of $^{11}CO_2$, but with no suppression of the $^{13}N_2$.

Thus the choice of an appropriate target sweep gas results in the preferential production of either ^{11}CO or $^{11}CO_2$.

x

We wish to thank Mr.P.L.Horlock for valuable technical assistance.

REFERENCES

1. J.C.Clark, C.M.E.Matthews, D.J.Silvester, D.D.Vonberg, Nucleonics, 25 /1967/ 54.

2. P.D.Buckingham, G.R.Forse, Int.J.Appl.Radiation and Isotopes, 14 /1963/ 439.

3. M.J.Welch, M.M.Ter-Pogossian, Rad.Res., 36 /1968/ 580.

International Journal of Applied Radiation and Isotopes, 1971, Vol. 22, pp. 639–646. Pergamon Press. Printed in Northern Ireland

The Preparation and Storage of Carbon-11 Labelled Gases for Clinical Use

J. C. CLARK and P. D. BUCKINGHAM
Medical Research Council Cyclotron Unit, Hammersmith Hospital, London W12, England

(*Received* 30 *April* 1971)

The target systems used for the production of carbon monoxide and carbon dioxide, both labelled with carbon-11, in the Medical Research Council Cyclotron at Hammersmith Hospital are described. The radiochemical composition of the gas at the target output is given for a range of target sweep gases using a fixed flow rate and beam current. Values are also given for the production rate and radioactive concentration of the ^{11}C labelled products, together with values for the ^{11}C target extraction efficiency. Reasons are stated for the present routine use of hydrogen as a target sweep gas and its advantages discussed.

Systems are described for the production of ^{11}CO and $^{11}CO_2$ for routine clinical use and details given of storage devices for these gases.

LA PREPARATION ET LE MAGASINAGE DES GAZ MARQUES AU CARBONE-11 POUR EMPLOI DANS LA CLINIQUE

On décrit les systèmes de cibles qui servent à la production du monoxyde de carbone et du bioxyde de carbone, marqués tous les deux de carbone-11, dans le cyclotron du Conseil de Recherche Médical à l'Hôpital de Harrersmith. On présente la composition radiochimique du gaz au débit de la cible pour une gamme de gazbalayeurs de cible en employant un taux d'écoulement et un courant de faisceau fixes. On donne aussi des valeurs pour le taux de production et pour la concentration radioactive des produits marqués au ^{11}C, ainsi que des valeurs pour l'efficacité d'extraction du ^{11}C de la cible. On précise des raisons pour l'emploi couramment habituel de l'hydrogène comme gaz-balayeur de cible et on discute ses avantages.

On décrit des systèmes pour la production du ^{11}CO et du $^{11}CO_2$ pour emploi régulier dans la cliniqueet on détaille des appareils pour l'emmagasinage de ces gaz.

ПРИГОТОВЛЕНИЕ И ХРАНЕНИЕ ГАЗОВ, МЕЧЕННЫХ УГЛЕРОДОМ C^{11}, ДЛЯ ПРИМЕНЕНИЯ В КЛИНИКЕ

Описаны мишенные системы производства CO, CO_2, меченных углеродом C^{11}, в циклотроне Совета медицинских исследований у больницы Гаммерсмита в Лондоне. Дан радиохимический состав газа на выходе мишени для области газов развертки мишени, используя постоянную скорость потока и постоянный ток пучки. Также даны значения интенсивности производства и радиоактивной концентрации продуктов, меченых углеродом C^{11}, вместе с значениями для эффективности экстракции мишени C^{11}. После обоснования установившейся практики применения водорода в качестве газа развертки мишени обсуждаются преимущества этого газа.

Описаны системы для производства CO^{11}, $CO_2{}^{11}$ для установившейся практики в клинике, представлены данные о устройствах для хранения этих газов.

DIE ZUBEREITUNG UND LAGERUNG VON ^{11}C MARKIERTEN GASEN

Die Treffplattensystems für die Herstellung von Kohlenmonoxyd und Kohlensäure, beide mit einer ^{11}C Markierung, im Zyklotron des Medical Research Council im Krankenhaus Hammersmith werden beschrieben. Die radiochemische Zusammensetzung des Gases am Treffplattenausgang wird für eine Reihe von Treffplattenspülgasen bei Benutzung einer

festen Durchflussmenge und Strahlstromstärke angegeben. Werte werden auch vorgelegt für die Produktionsgeschwindigkeit und die radioaktive Konzentration der ^{11}C markierten Produkte, zusammen mit Werten für die ^{11}C Treffplattenextraktionsausbeute. Es werden Gründe angegeben für die derzeitige laufende Verwendung von Wasserstoff als Treffplattenspülgas, und seine Vorteile werden besprochen.

Einrichtungen für die Produktion von ^{11}CO und $^{11}CO_2$ zur laufenden klinischen Verwendung werden bexchrieben und Einzelheiten werden angegeben für Lagerungsvorrichtungen für diese Gase.

INTRODUCTION

CARBON monoxide and carbon dioxide both labelled with ^{11}C are in routine production for clinical studies at Hammersmith Hospital.[1] The principal uses are in serial blood volume estimations,[2,3] lung function investigations[4] and organ visualisation using a gamma camera[5] or scintiscanner.[6] Ease of administration and a low radiation dose to the patient make ^{11}C an attractive nuclide for this work. A further advantage is that the 20 min half-life is sufficiently long to make ^{11}C storage systems a practical proposition. Such systems allow the use of the nuclide away from the site of production, and make for more efficient use of cyclotron running time.

The present paper describes the systems currently in use for the production and storage of carbon monoxide and carbon dioxide labelled with ^{11}C. The most notable improvement over previous systems[7,8] is the use of hydrogen as a target sweep gas, which makes the production of ^{11}CO virtually carrier-free, whilst inhibiting the formation of significant amounts of $^{13}N_2$ (^{13}NN).

EXPERIMENTAL

Target design

Carbon-11 has a 20.3 min half-life, decays by the emission of 0.96 MeV positrons and is the product of several nuclear reactions as shown in Table 1.

The target is shown in Fig. 1. The B_2O_3 powder is melted onto the wedge in an electric furnace to a thickness of 1–2 mm. The 14 MeV deuteron beam, defocussed to cover an area approximately 5 cm^2, passes through the 0.05 mm aluminium foil window and strikes the surface of the B_2O_3 at grazing incidence. With a beam current of 40 μA the power density is approximately 20 W cm^{-2} on the surface of the wedge which is deliberately in poor thermal contact with the surrounding box. This power density is sufficient to melt the B_2O_3 (M.P. $\approx$ 400°C) releasing ^{11}C labelled gases into a stream of sweep gas passed through the box at about 80 ml min^{-1}. The molten B_2O_3 is prevented from rapid movement down the wedge by the step shape.

TABLE 1. Some nuclear reactions used for the production of carbon-11

Nuclear reaction	Threshold energy (MeV)	Reference
$^{10}B(d, n)^{11}C$	1.70	(7) (8)
$^{11}B(d, 2n)^{11}C$	5.89	(7) (8)
$^{14}N(p, \alpha)^{11}C$	3.13	(9) (10)
$^{11}B(p, n)^{11}C$	3.01	(10)
$^{14}N(d, \alpha n)^{11}C$	5.88	(11)

The volume of the target box is kept small (about 200 cm^3) to maximise the radioactive concentration of the effluent gas. Its normal working pressure is approximately 0.007 kg cm^{-2} (0.1 lb in^{-2}) above atmospheric pressure. Brass is used for all parts of the target except the front plate and window which are aluminium and water cooled. The gas inlet and outlet connections are made using $\frac{1}{16}$ in vacuum fittings.

During bombardment the molten B_2O_3 slowly migrates from the area of the beam strike causing a loss of yield. This process takes about 12 hr after which the wedge has to be re-coated. Since B_2O_3 is hygroscopic, wedges are always stored in a desiccator until required for use.

Target sweep gases and yields

The nature and composition of the target sweep gas are of critical importance. The range of gases which we have used is listed in

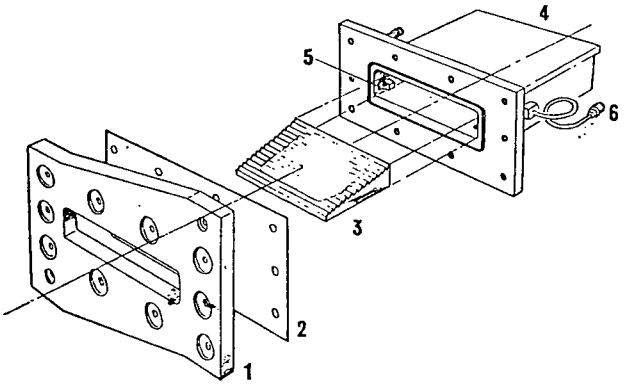

FIG. 1. External target for ^{11}C production. (1) Target mounting plate (Beam entry window 2·5 cm × 12·7 cm) (2) Beam entry window foil (3) Brass wedge supporting B_2O_3 (4) Gas tight target box (5) Wedge locating pins (6) Sweep gas connections.

TABLE 2. Carbon-11: Solid target: B_2O_3 (wedge): $^{10}B(d, n)^{11}C$ $^{11}B(d, 2n)^{11}C$

Particle	Deuteron
Current	40 μA
Energy	15 MeV
Energy incident on target material	$\cong$14 MeV
Window material and thickness	Al 0.05 mm (0.002 in.)
Energy loss in window	$\simeq$1 MeV
Beam distribution dimensions	3–4 cm wide 1–1.5 cm high
Target dimensions	12.7 cm wide 2.2 cm high 10 cm deep (gas vol. 200 ml)
Target pressure	0.007 kg cm^{-2} (0.1 lb in.$^{-2}$ gauge)
Sweep gas flow rate	80 ml min^{-1}

Target sweep gas	Per cent of total recovered yield at target output				^{11}C Recovery at target output		Target ^{11}C extraction efficiency per cent
	^{11}CO	$^{11}CO_2$	$^{11}CH_4$	^{13}NN	mCi min^{-1}	mCi ml^{-1} 20°C 760 mm Hg	
Helium	1.0	83	<0.1	16	17	0.21	52
1% CO in He	52	36	<1	11	16	0.20	50
5% CO in He	72	19	<1	8.2	16	0.20	50
1% CO_2 in He	<1	88	<0.1	11	14	0.17	44
5% CO_2 in He	<1	83	<0.1	16	16	0.20	50
1% H_2 in He	60	21	9.0	10	13	0.17	42
5% H_2 in He	56	15	22	7.0	12	0.15	37
Hydrogen	86	8.7	5.2	<1	14	0.17	43
Tolerances (%)		>60 · · · ± 10 11–60 · · · ± 20 <10 · · · ± 50			±10		±20

Table 2 which also shows the effect on the radiochemical composition of varying the composition of the sweep gas at a fixed beam current of 40 μA and fixed flow rate of 80 ml min^{-1}. The gas flow system, shown schematically in Fig. 2, is an open circuit design.

The precise nature of the chemical and radiolytic reactions which take place in the target during irradiation is not fully known. However, it is thought that ^{11}CO is the primary product of the reaction between the ^{11}C atoms and the oxygen atoms in the B_2O_3. In the

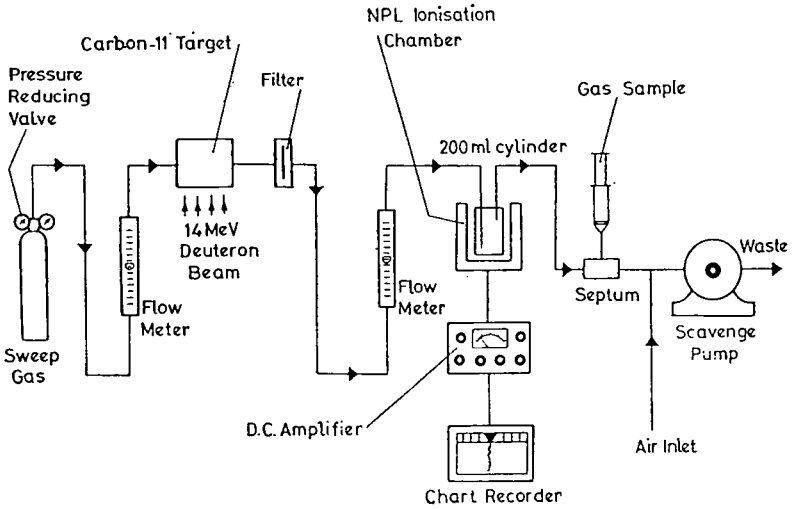

FIG. 2. ^{11}C experimental gas flow system.

absence of any oxygen radical scavenger the ^{11}CO is largely radiolysed to $^{11}CO_2$.[8] Thus when helium is used as the sweep gas most of the ^{11}C activity in the target effluent is $^{11}CO_2$, the addition of CO_2 carrier having little effect upon the recovered yield. When stable CO is added to the helium less $^{11}CO_2$ is made, the CO acting as a scavenger for oxygen radicals and protecting the ^{11}CO. As more CO is added this protection is seen to increase.

When a sweep gas of helium containing a small amount of hydrogen is used it also acts as a radical scavenger giving some recovery of ^{11}CO without added carrier. If however hydrogen is used alone, a much higher recovery of ^{11}CO is achieved, also without added carrier.

It should be noted that there is a significant recovery of $^{13}N_2$ with all sweep gases except hydrogen. Presumably the ^{13}N atoms are scavenged by hydrogen to form non volatile products. The absence in the target effluent of a possible volatile product, $^{13}NH_3$, has been demonstrated both chemically and gas chromatographically.

The only detected ^{11}C labelled contaminant is $^{11}CH_4$ formed by the combination of ^{11}C and H radicals within the target during irradiation. This, as would be expected, is only present in significant amounts when H_2 is used in the sweep gas.

The parameters affecting the total yield recovered from the carbon-11 target may be listed as follows:

(a) Target material nuclear cross section
(b) Beam current
(c) Beam energy
(d) Target material thickness
(e) Sweep gas flow rate
(f) Sweep gas composition
(g) Beam distribution
(h) Target material water content
(i) Target material temperature.

These parameters may be divided into those affecting the activity produced within the target, and those affecting the recovery of activity from the target. Thus (a–d) largely determine the activity produced, whilst (e–i) tend to determine the amount of recovered activity and its chemical composition. With the recovery of the activity depending upon so many factors, the yield is never constant from day to day or even during a run of say, 3 hr duration. However, it is possible to determine the relationship between some of the parameters by running for long periods and taking mean values of beam current, yield and analyses of samples.

Activity assay

Table 2 shows the radioactive products that have been detected in ^{11}C experimental bombardments. The analysis of these products was

carried out using a Pye Series 104 gas chromatograph, modified so that the effluent gas passed through a β-counter connected to an amplifier, ratemeter and second recording channel. It was thus possible to detect both stable and radioactive gases. Three 1.5 m × ≈ 4.5 mm bore columns were used: molecular sieve (type 5A), silica gel and "poropak Q" all of 80–100 mesh. Helium was used as the chromatograph carrier gas.

The target efficiency values were obtained by comparing the yield of ^{11}C induced in a similar wedge under conditions where there were no losses of volatile products, decay curve analysis being necessary to extract the ^{11}C component. The activity of the target effluent was measured using a calibrated ionisation chamber system shown schematically in Fig. 2. The calibration was performed by taking a 1 ml sample from the input of the monitored volume and measuring it in a calibrated gamma spectrometer.

PRODUCTION

Routine production of ^{11}CO

For the production of ^{11}CO for routine clinical use, either H_2 (commercial grade) or 1% CO in He may be used as the sweep gas. Usually H_2 is to be preferred since the target effluent gas then contains very little $^{11}CO_2$, obviating the need of a reducing furnace. The $^{11}CH_4$ contaminant does not interfere with red cell labelling and one has the advantage of a very low $^{13}N_2$ contaminant level.*

When 1% CO in He is used the $^{11}CO_2$ is reduced to ^{11}CO by passing the gas over activated charcoal. At 800°C the following reaction takes place:

$$^{12}C + {}^{11}CO_2 \xrightarrow{800°C} {}^{11}CO + {}^{12}CO.$$

Heated zinc can be used as an alternative reducing agent:[12]

$$Zn + {}^{11}CO_2 \xrightarrow{400°C} ZnO + {}^{11}CO$$

We find that for sweep gas flow rates of approximately 80 ml min^{-1} a pyrex glass furnace tube 5 cm long and 2.5 cm dia. filled with zinc powder maintained at 400°C ± 10°C to avoid melting, is satisfactory.

Any unconverted $^{11}CO_2$ is absorbed in a soda lime column 60 cm long and 2 cm dia. The use of 1% CO in He as a sweep gas for clinical production bombardments does have limitations. The presence of CO carrier lowers the specific activity of the target effluent gas, causes inefficient red cell labelling, restricts the volume of gas used when it is administered by inhalation and causes inefficient trapping of ^{11}CO in the storage system to be described. Moreover, the $^{13}N_2$ contaminant level is often unacceptably high.

The ^{11}C labelled gases are used at two sites: experimentally, in an area approximately 10 m from the cyclotron target, and clinically in a measuring and dispensing area approximately 100 m from the target. Gas transmission pipes of 1.5 mm bore stainless steel are used between the target and the experimental area. The pipes between the target and the clinical area are 1.5 mm bore stainless steel and 1.9 mm bore nylon.

At a target pressure of about 0.05 kg cm^{-2} above atmospheric pressure (necessary when using the long gas transmission pipes) and a sweep gas flow rate of 50 ml min^{-1}, the transit time from the target to the clinical area is approximately 8 min.

^{11}CO storage system

The storage systems described in this paper work on the principle of trapping the labelled gas using low temperature techniques. ^{11}CO may be trapped either on activated charcoal at −196°C, or on a molecular sieve at −85°C. We have found the latter to be more reproducible.

The molecular sieve ^{11}CO storage system is shown schematically in Fig. 3, and consists of a 27 cm length of 0.6 cm ID copper tubing filled with $\frac{1}{16}$ in. pellets of type 13 × molecular sieve (Linde Air Products, USA). The gas is passed through it to waste for 20 min, the trap being cooled to −85°C in an acetone "Dricold" bath.† Trapping efficiency is about 85 per cent.

* When H_2 containing ^{11}CO is administered by rebreathing[4,5] a maximum volume of 15 ml is diluted to 3 l. with air or oxygen thus giving a 0.5% maximum H_2 mixture which is 10 times lower than the explosive limit for air/O_2 mixtures.[13]

† "Dricold": solid CO_2 supplied by Distillers Co. Ltd.

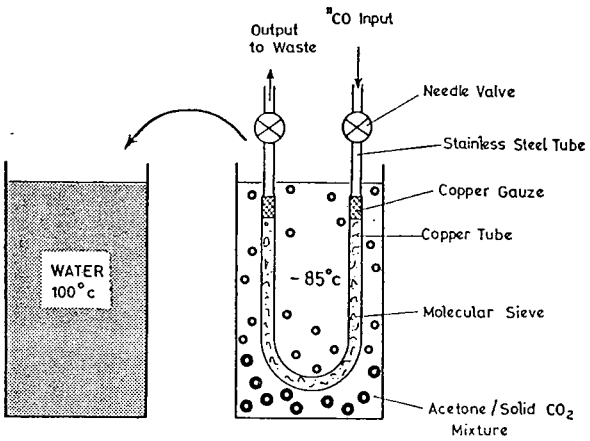

FIG. 3. ^{11}CO storage system.

With an ^{11}CO production rate of about 12 mCi min^{-1}, a typical trapped activity is 150 mCi of which approximately 95 per cent is released on heating the trap to 90°C. Since some of the residual oxygen or nitrogen in the system is trapped at −85°C, the volume of the released gas is about 7 ml. This is transferred to the low pressure storage unit shown in Fig. 4 by flushing the trap with 40 ml of air or helium. Alternatively, if about 40 ml of air is introduced into the trap during the first 2 min of trapping, flushing becomes unnecessary since upon heating, the air together with about 90 per cent of the ^{11}CO is released directly into the low pressure storage unit. An indication of the volume of stored gas is given by a simple water displacement indicator. When sterile samples are required they are dispensed through a millipore filter. Before use, the molecular sieve is outgassed at 200°C for about 12 hr and will retain its adsorbing characteristics providing it remains dry.

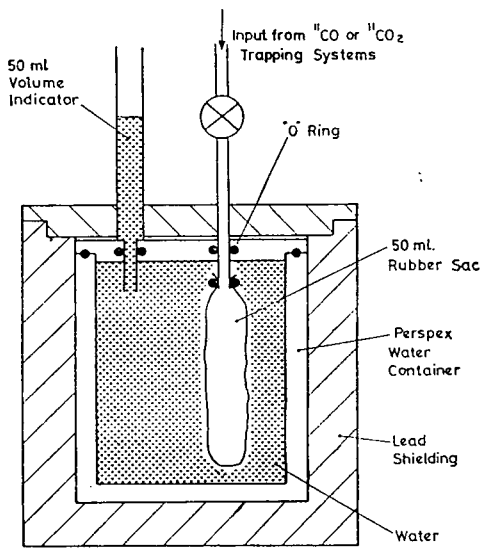

FIG. 4. Low pressure storage unit.

Routine production of $^{11}CO_2$

$^{11}CO_2$ may be produced continuously without the use of a furnace, by using the B_2O_3 target with a sweep gas of either pure He or a mixture of 1 % CO_2 in He. Such a system produces a significant amount of $^{13}N_2$ contaminant (Table 2) which for some applications may have to be removed. The $^{11}CO_2$ storage system to be described does this effectively.

Occasionally ^{11}CO and $^{11}CO_2$ are required simultaneously. Under these circumstances $^{11}CO_2$ is supplied batch-wise using the apparatus depicted in Fig. 5 which is used to oxidise the ^{11}CO to $^{11}CO_2$. To prepare a batch of $^{11}CO_2$ a charge of ^{11}CO is first trapped in the storage system described previously. The output of the trap is then connected to the input of the conversion unit and the ^{11}CO flushed through the cupric oxide furnace for 3–4 min at about 10 ml min^{-1}, to be collected in the tonometer at the furnace output as $^{11}CO_2$. To collect the $^{11}CO_2$ a 50 ml syringe is connected to the tonometer output and the gas collected by the displacement of mercury. $^{11}CO_2$ radioactive concentrations of about 3 mCi ml^{-1} are readily obtained.

Since the trapped ^{11}CO contains a little hydrogen, traces of water, which tend to dissolve the $^{11}CO_2$, are formed in the CuO furnace during conversion. To remove this water, and thereby reduce absorption, a drying agent, magnesium perchlorate, is added at the furnace tube output.

$^{11}CO_2$ *Storage system*

The trap for $^{11}CO_2$ shown in Fig. 6 consists of a 3.6 m length of empty copper tube ≈3 mm OD, 1.7 mm bore, formed into a closely wound spiral approximately 4.5 cm dia. and 7.3 cm long. When used in conjunction with a system using He as the sweep gas it is possible to trap

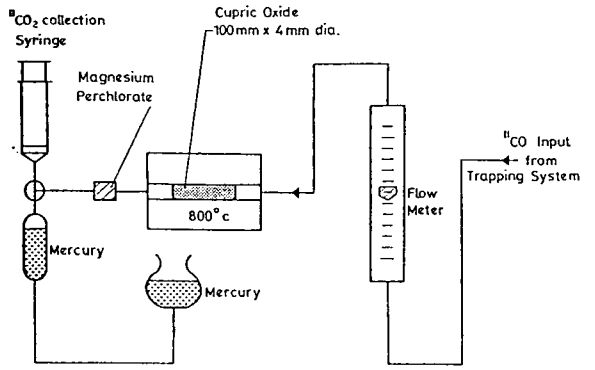

FIG. 5. Apparatus for batch-wise conversion of ^{11}CO to $^{11}CO_2$.

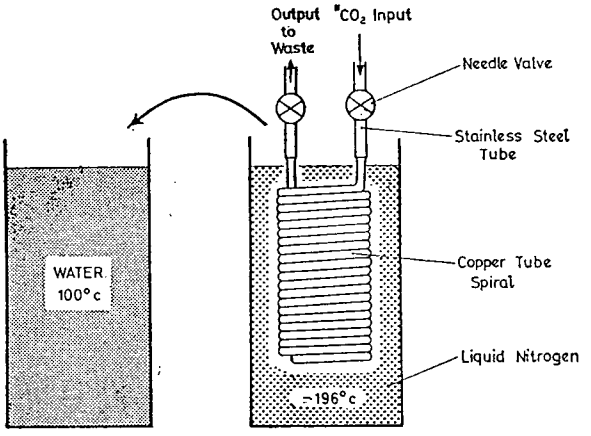

FIG. 6. $^{11}CO_2$ storage system.

$^{11}CO_2$ of high specific activity. In use it is similar to the ^{11}CO storage systems already described. The target effluent gas is passed for 20 min through the trap which is placed in liquid nitrogen, and the $^{11}CO_2$ condensed in the tube. A typical $^{11}CO_2$ trapped activity is 220 mCi of which more than 95 per cent is recoverable on heating the trap to approximately 90°C. The released gas is flushed with 20 ml He into a low pressure storage unit as used with the ^{11}CO molecular sieve trap.

A notable feature is that although the yield may contain as much as 16 per cent $^{13}N_2$, the stored activity contains less than 1 per cent of this nuclide. It is however essential to ensure the trap is dry before use.

CONCLUSIONS

^{11}CO and $^{11}CO_2$ are produced for routine clinical use using well proven cyclotron target systems. The chemical form of the product nuclei recovered from the target is largely determined by the target sweep gas composition. Hydrogen is now used for ^{11}CO production since it results in a yield which is virtually carrier-free, and has practically no $^{13}N_2$ contamination. A typical ^{11}CO production rate and radioactive concentration at the target output is 12 mCi min^{-1} and 0.15 mCi ml^{-1} respectively.

When $^{11}CO_2$ is required continuously either helium or 1 % CO_2 in He is used as the target sweep gas, a typical production rate and radioactive concentration at the target output being 17 mCi min^{-1} and 0.2 mCi ml^{-1} respectively. Under these conditions however there is significant $^{13}N_2$ contamination. This contaminant is virtually absent if the $^{11}CO_2$ is supplied batch-wise by oxidising ^{11}CO which has previously been stored. A charge of $^{11}CO_2$ produced batch-wise typically contains about 100 mCi in 35 ml of helium.

Both ^{11}CO and $^{11}CO_2$ may be stored in suitable trapping systems with high trapping and release efficiencies. Typical trapped activities are 150 mCi of ^{11}CO and 220 mCi of $^{11}CO_2$, the radioactive concentrations on release being approximately 3.5 mCi ml^{-1} and 10 mCi ml^{-1} respectively. The storage systems will supply up to seven 500 μCi patient doses at 20-min intervals from a single 100 mCi charge. This results in ^{11}CO and $^{11}CO_2$ being available either to a larger number of patients locally or to a more limited number at several miles' radius from the cyclotron.

Acknowledgement—We wish to thank Mr. P. L. Horlock for valuable technical assistance.

REFERENCES

1. Clark J. C. and Buckingham P. D. *Short lived Radioactive Gases for Clinical Use.* Butterworth, London (1972).
2. Clark J. C., Glass H. I. and Silvester D. J. Proc. Second International Conference on Methods of Preparing and Storing Labelled Compounds. Euratom, Brussels (1966).
3. Glass H. I., Edwards R. H. T., De Garreta A. C. and Clark J. C. *J. appl. Physiol.* **26,** 131 (1969).
4. West J. B. and Dollery C. T. *J. appl. Physiol.* **17,** 9 (1962).
5. Glass H. I., Jacoby J., Westerman B., Clark J. C. Arnott R. N. and Dixon H. G. *J. nucl. Med.* **9,** 468 (1968).
6. Glass H. I., De Garreta A. C., Lewis S. M., Grammaticos P. and Szur L. *Lancet* **1,** 669 (1968).
7. Buckingham P. D. and Forse G. R. *Int. J. appl. Radiat. Isotopes* **14,** 439 (1963).
8. Welch M. J. and Ter-Pogossian M. M. *Radiat. Res.* **36,** 580 (1968).
9. Finn R. D., Christman D. R., Ache H. J. and Wolf A. P. To be published in *Int. J. appl. Radiat. Isotopes.*
10. Barkas W. H. *Phys. Rev.* **56,** 287 (1939).
11. Way K. *et al. Nuclear Data Sheets,* **A2,** Nos. 5 and 6, 449. Academic Press, New York (1966).
12. Huston H. L. and Norrish T. H. *J. Am. chem. Soc.* **70,** 1968 (1948).
13. Macintosh R., Mushin W. W. and Epstein H. G. *Physics for the Anaesthetist* (including a section on explosions) 2nd Ed., p. 325. Blackwell, Oxford (1958).

International Journal of Applied Radiation and Isotopes, 1972, Vol. 23, pp. 5–8. Pergamon Press. Printed in Northern Ireland

Nitrogen-13 Solutions for Research Studies in Pulmonary Physiology

P. D. BUCKINGHAM and J. C. CLARK
MRC Cyclotron Unit, Hammersmith Hospital, London W12 OHS, England

(*Received* 14 *June* 1971)

Techniques are described in detail for producing saline solutions of nitrogen-13 suitable for clinical use. The target system, cyclotron irradiation conditions and gas handling system are fully described.

LES SOLUTIONS DE NITROGENE-13 POUR LES ETUDES DE RECHERCHE DANS LA PHYSIOLOGIE PULMONAIRE

On décrit en détail les techniques pour la production des solutions salines de nitrogène-13 convenables à l'emploi dans la clinique. On explique complètement le système de cible, les conditions de l'irradiation dans le cyclotron et le système pour la manipulation du gaz.

РАСТВОРЫ АЗОТЫ-13 ДЛЯ ИССЛЕДОВАНИЙ В ЛЕГОЧНОЙ ФИЗИОЛОГИИ

Дано подетальное описание приемов для производства соленых растворов азоты-13 пригодных для использования в клинике. Полно описаны мишенная система, условия облучения в циклотроне, система для улавливания выделяющихся газов.

N-13 LÖSUNGEN FÜR FORSCHUNGSSTUDIEN IN DER LUNGENPHYSIOLOGIE

Arbeitsweisen werden im einzelnen beschrieben zur Herstellung von Salzlösungen mit zur klinischen Verwendung geeignetem Stickstoff-13. Das Treffplattensystem, die Bedingungen der Zyklotronbestrahlung und das System der Gasbehandlung werden eingehand beschrieben.

INTRODUCTION

NITROGEN-13 ($T_{1/2} = 9.96$ min) labelled molecular nitrogen $^{13}N_2(^{13}NN)$ has been produced for research studies in pulmonary physiology at Hammersmith Hospital using the Medical Research Council's cyclotron.[1–4] Recently sterile solutions labelled with $^{13}N_2$ have become routinely available.[5,6] Many lung ventilation and perfusion studies have been carried out using ^{133}Xe ($T_{1/2} = 5.3$ days) which is widely available commercially. However inaccuracies in these measurements can arise due to the solubility of xenon.[7–10] MATTHEWS and DOLLERY[11] have shown that the use of N_2, the solubility of which is 12 times less than that of xenon under similar conditions, should reduce these inaccuracies. A further advantage of $^{13}N_2$ over ^{133}Xe is that the 511 keV annihilation radiation is not so readily scattered as the 80 keV and 30 keV photons emitted by ^{133}Xe. The higher energy of ^{13}N also affords better depth response characteristics than ^{133}Xe. However, the production of ^{13}N requires the use of a cyclotron in the vicinity of the clinical facility and at present this precludes its use at many centres.

TARGET SYSTEM AND IRRADIATION CONDITIONS

The MRC cyclotron is a fixed energy classical machine capable of accelerating deuterons to 16 MeV and alpha particles to 32 MeV. Nitrogen-13 is produced by the bombardment of carbon with deuterons having an energy of $\approx$14 MeV, the nuclear reaction being $^{12}C(d, n)^{13}N$. The target material used for the production of $^{13}N_2$ for use in the gas phase is activated charcoal.[1] However, carbon is this physical form is quite unsuitable for making $^{13}N_2$ for labelling solutions, since it is extremely difficult to remove all the adsorbed gases before irradiation.

When making $^{13}N_2$ for use in solution, it is imperative that unwanted gases are excluded

from the cyclotron target, its "sweep" gas and the gas handling system. If these unwanted gases are insoluble they will have the undesired effect of reducing the radioactive concentration and thus the proportion of $^{13}N_2$ dissolving in the final solution. Hence, the target material we use is carbon in the form of graphite,* the adsorbed gas content of which is much lower than that of activated charcoal.

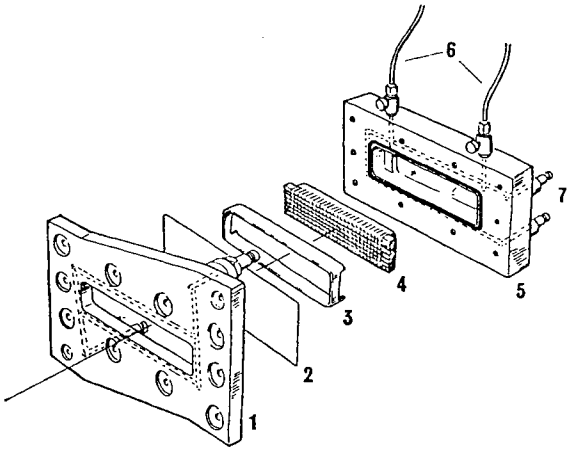

FIG. 1. External target for ^{13}N production
(1) target mounting plate
(Beam entry window 2.5 cm × 12.7 cm)
(2) beam entry window foil
(3) spacer
(4) graphite block
(5) gas tight target box
(6) sweep gas connections
(7) cooling water connections.

The complete target is shown in Fig. 1. The $^{13}N_2$ is removed from the target during irradiation by a suitable sweep gas, the choice of which is important. In an atmosphere of 99.9% helium, 99.99% argon or 99.9% hydrogen, only small amounts of $^{13}N_2$ are released from the graphite. However, in the presence of carbon dioxide,† the graphite, which is raised to a temperature in excess of 1450°C by the beam power, typically 170 W cm^{-2} at 60 μA, is eroded continuously as the following reaction occurs

$$C + CO_2 \rightarrow 2\,CO.$$

This continuous erosion leads to the release of volatile ^{13}N labelled molecules previously trapped in the graphite lattice. Of particular importance is the release of $^{13}N_2$.

The purpose of cutting the graphite into a matrix as shown in Fig. 1 is to minimise the heat loss by conduction from the area struck by the beam. This increases the release of $^{13}N_2$ from the target.

The yield from this target system is quite sensitive to beam power density; at high power densities erosion is more rapid. Under normal cyclotron operating conditions the beam strike area is approx 5 cm^2, the life of the graphite matrix being about 8 hr.

The extraction efficiency for the graphite matrix target system is about 6 per cent. This value is obtained by comparing the yield of ^{13}N recovered from the graphite matrix with that induced in a solid block of graphite having the same dimensions as that used in the target, under conditions where there are no losses of ^{13}N labelled molecules.

A major problem in using this type of target system is to find a beam entry window which will retain its strength at elevated temperatures. Stainless steel foil (EN58B) 0.025 mm thick is very reliable at beams currents up to 70 μA (200 W cm^{-2}). In the present target design both air and water cooling are employed, air for the beam entry foil and water for the target back plate and 'O' ring.

GAS HANDLING, MEASUREMENT AND SOLUTION PREPARATION

The complete target and gas handling system is shown schematically in Fig. 2. It may be considered in three sections: the target which is described above, the measuring and processing equipment, and the sterile assembly. In practice the target is situated about 40–50 m from the rest of the apparatus and is connected to it by 1.5 mm bore stainless steel tubing.

The measuring and processing equipment consists of the following: flowmeters (5–150 ml min^{-1}); an air-filled re-entrant ionisation chamber and associated d.c. amplifier; a furnace containing a vertical column of copper oxide 23 cm × 2.5 cm dia. at a temperature of 700°C, the copper oxide being formed *in situ* by the oxidation of a roll of copper gauze.

* General purpose extruded graphite grade EY9 (Supplied by Morganite Carbon Ltd.).

† Analytical grade containing 10–50 vpm of residual gases (Supplied by Distillers Co. Ltd.).

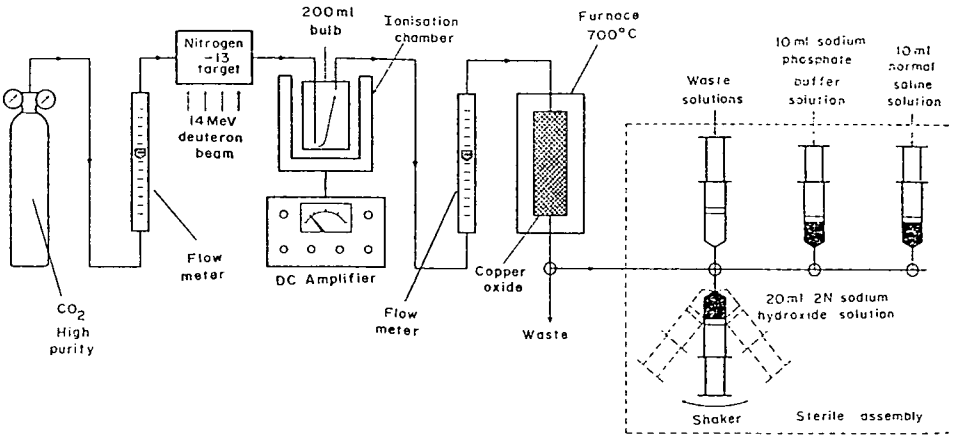

FIG. 2. Gas flow system for the production of $^{13}N_2$ solutions.

The sterile assembly consists of a small frame on which are mounted four syringes connected by a suitable arrangement of taps. The frame is so constructed that it will attach to a unit containing a small variable speed shaking machine which will oscillate the lower syringe (Fig. 2). Several such assemblies are in use; all are prepared under sterile conditions using disposable syringes, taps and solutions. Great care is taken to exclude all gas bubbles.

Ancillary equipment consists of a cylinder of high purity carbon dioxide, a shaking machine, and a second ionisation chamber and d.c. amplifier for solution dose measurements.

$^{13}N_2$ solutions are prepared as follows. Carbon dioxide sweep gas is passed to the target through a two-stage regulator and flow meter. The normal input flow rate is approx 45 ml min^{-1}, the target gas pressure being approx 0.1 kg cm^{-2} above atmospheric pressure. The target is then bombarded with deuterons at a beam current of 60 μA and the nuclear and chemical reactions described above take place. The target effluent, a mixture of approx 98% CO and 2% CO_2, together with the $^{13}N_2$ molecules, is piped back to the preparation room where its radioactive concentration, expressed in mCi ml^{-1} is continuously monitored by passing it through a 200 ml cylindrical bulb in the ionisation chamber.[12] On leaving the bulb, the gas passes through a second flow meter to the copper oxide furnace which both sterilises it and oxidises the CO to CO_2. After leaving the furnace through a removable sterile fitting, the CO_2 and $^{13}N_2$ mixture may be either passed to waste, or to the sterile assembly for $^{13}N_2$ solution production.

A minimum concentration of 0.25 mCi ^{13}N ml^{-1} gas is required for the reliable production of solutions having a concentration of 100 μCi ml^{-1}. A typical concentration under the above irradiation and flow rate conditions is about 0.5 mCi ml^{-1} gas.

To prepare 10 ml of $^{13}N_2$ labelled 0.9% NaCl solution the furnace effluent is passed to the syringe containing 20 ml of 2*N* sodium hydroxide, which absorbs the CO_2 at a rate depending upon the speed of oscillation of this syringe; by adjusting the rate of shaking, the absorption rate may be kept sensibly constant for 5 min. At the end of this time all the CO_2 sweep gas delivered will have been removed, leaving the $^{13}N_2$ in the accumulated residual permanent gases found in the system. Since the volume of the residual gas bubble can be as low as 1 ml, the radioactive concentration can be very high; a typical bubble contains approx 20 mCi.

This bubble is then transferred to the 10 ml of sodium phosphate buffer solution which neutralises any traces of sodium hydroxide which may also have been transferred. The buffer is next passed into the sodium hydroxide, leaving the bubble to be finally transferred into the syringe containing 10 ml of NaCl solution. This syringe and its tap are then removed and measured in an ionisation chamber prior to shaking vigorously for 90 sec to obtain optimum

solution activity. After allowing the phases to separate the bubble is ejected and a solution containing between 100 and 300 μCi ml^{-1} is obtained.

QUALITY CONTROL

The pH of the labelled solution is always tested to ensure that it has remained unchanged, using a suitable indicator paper. The solution must also remain sterile, pyrogen free and isotonic.

For reliable physiological measurements at least 99 per cent of the solution activity must be present as nitrogen-13 labelled molecular nitrogen. This is confirmed by making a typical $^{13}N_2$ solution and recording its activity as the $^{13}N_2$ is washed out of solution by bubbling nitrogen through it at about 250 ml min^{-1}, as shown in Fig. 3. If no contamination is present the washout curve falls to the base line. In practice it falls to between 0.01 per cent and 0.1 per cent of the original solution activity. Gamma ray spectrometry and decay curve analysis of this contaminant show that it contains ^{13}N and ^{11}C labelled soluble compounds.

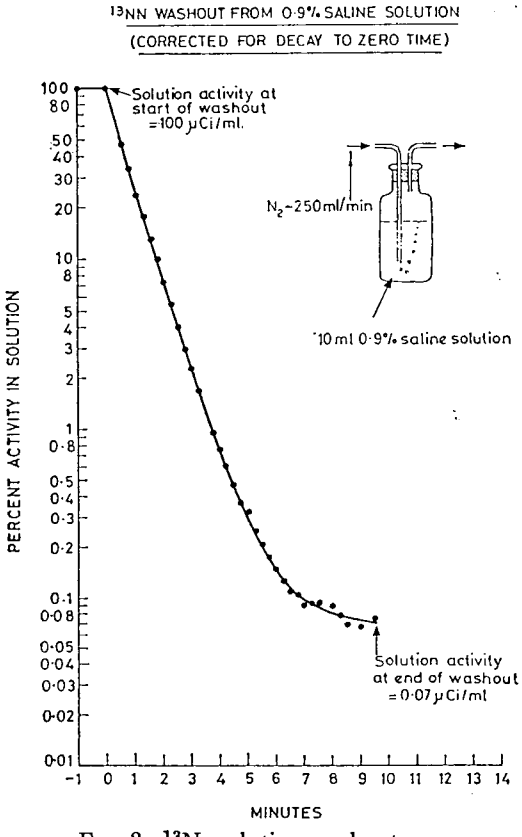

FIG. 3. $^{13}N_2$ solution washout curve.

Regular checks are made on the gas phase composition using a Pye series 104 gas chromatograph having both thermal and radioactive detectors. The composition of the gas bubble is shown to be nitrogen and oxygen with traces of CO_2.

CONCLUSION

The above system has been in frequent use for over 1 yr, during which time a total of 43 $^{13}N_2$-labelled solutions were prepared for clinical use. Its performance has proved reliable and has been little affected by day to day changes in cyclotron operating conditions, typical solution radioactive concentrations of up to 300 μCi ml^{-1} being readily obtained using a 14 MeV deuteron beam current of 60 μA.

Acknowledgement—The authors wish to thank Mr. P. L. HORLOCK for valuable technical assistance.

REFERENCES

1. BUCKINGHAM P. D. and FORSE G. R. *Int. J. appl. Radiat. and Isotopes* **14,** 439 (1963).
2. CLARK J. C., MATTHEWS C. M. E., SILVESTER D. J. and VONBERG D. D. *Nucleonics* **25,** 54 (1967).
3. WEST J. B. *The use of radioactive materials in the study of lung function.* The Radiochemical Centre, Amersham (1966).
4. MATTHEWS C. M. E., DOLLERY C. T., CLARK J. C. and WEST J. B. Radioactive Pharmaceuticals, Symposium Series, No. 6, 567 (U.S.A.E.C., Washington 1966).
5. VONBERG D. D. *et al. Uses of Cyclotrons in Chemistry, Metallurgy and Biology* (Edited by C. B. AMPHLETT) Butterworth, London (1970).
6. CLARK J. C. and BUCKINGHAM P. D. *Short-lived Radioactive Gases for Clinical Use.* Butterworth, London (1972).
7. CONN H. L. *J. appl. Physiol.* **16,** 1065 (1961).
8. SCHOENBORN B. P. *Nature, Lond.* **208,** 760 (1965).
9. VEALL N. and MALLETT B. L. *Phys. Med. Biol.* **10,** 375 (1965).
10. YEH S.-Y. and PETERSON R. E. *J. appl. Physiol.* **20,** 1041 (1965).
11. MATTHEWS C. M. E. and DOLLERY C. T. *Clin. Sci.* **28,** 573 (1964).
12. CLARK J. C. and BUCKINGHAM P. D. *Int. J. appl. Radiat. Isotopes* **22,** 639 (1971).

International Journal of Applied Radiation and Isotopes, 1972, Vol. 23, pp. 329–335. Pergamon Press. Printed in Northern Ireland

The Production of Potassium-43 for Medical Use

J. C. CLARK, M. L. THAKUR and I. A. WATSON
MRC Cyclotron Unit, Hammersmith Hospital, Ducane Road, London W12 OHS, England

(*Received* 3 *February* 1972)

A dynamic argon gas target system is described for the production of potassium-43 and the method for recovery of the activity is stated. The influence of the incident alpha particle beam energy on the relative yield of potassium-42 and potassium-43 is reported. The effects were investigated of other parameters, such as gas pressure and gas flow rate on the yields. The results are discussed.

LA PRODUCTION DU POTASSIUM-43 POUR EMPLOI MÉDICAL

On décrit un système de cible dynamique à gaz d'argon pour la production du potassium-43 et on précise la méthode pour le recouvrement de l'activité. On rend compte de l'influence de l'énergie du faisceau incident de particules alpha sur le rendement rélatif de potassium-42 et de potassium-43. On regarda les effets d'autres paramètres tels que la tension du gaz et le taux d'écoulement du gaz sur les rendements. On présente une discussion des résultats.

ПРОИЗВОДСТВО КАЛИЯ-43 ДЛЯ ИСПОЛЬЗОВАНИЯ В МЕДИЦИНСКИХ ЦЕЛЯХ

Описана динамическая аргоновая газовая мишенная система для производства калия-43, дается и метод для восстановления активности. Сообщено влияние энергии падающего пучка альфа-частиц на относительный выход калия-42, калия-43. И исследованы влияния других параметров, например, давление газа и расход газа.

DIE HERSTELLUNG VON KALIUM-43 FÜR MEDIZINISCHE ZWECKE

Ein dynamisches Treffplattensystem von Argongas für die Herstellung von Kalium-43 wird beschrieben und ein Verfahren wird angegeben für die Wiedergewinnung der Aktivität. Der Einfluss der Einfallstrahlenergie eines Alphateilchens auf die relative Ausbeute an Kalium-42 und Kalium-43 wird festgestellt. Die Wirkungen von anderen Parameter wie z.B. Gasdruck und Gasgeschwindigkeit auf die Ausbeuten wurden untersucht. Die Ergebnisse werden besprochen.

INTRODUCTION

THERE are several ways in which radioactive potassium may be of value in medical investigations. For example the presence of ^{40}K in naturally occurring potassium has enabled estimation of the body content of potassium by means of whole body counting.[1] Isotope dilution analysis enables *in vivo* estimation of total body concentrations and measurement of the exchangeable potassium.[2–5] Comparison of the physiological behaviour of potassium with that of rubidium and caesium has been carried out with the aid of radioactive potassium[6] and in particular their accumulation in muscle tissue.[7] The labelling of red cells with radioactive potassium has been carried out successfully and used in the measurement of blood volume.[8] It has also been used for imaging the heart[9] and in myocardial perfusion studies.[10] One further application has been found in the localisation of brain tumours.[11,12] Of the seven radioactive isotopes

TABLE 1

Characteristics	^{42}K	^{43}K	Ref.
Half life	12·4 h	22·6 h	13, 14
γ energies	1·524 MeV (18%)	373 keV (87·8%) 618 keV (81%)	13, 14
β^- energies	3·52 MeV (max)	830 keV (max)	13
Whole body radiation dose	0·85 m rad μCi^{-1}	0·6 m rad μCi^{-1}	4
K factor	1·4	5·6	4

of potassium there are only two which permit satisfactory use in clinical investigations. These are ^{42}K and ^{43}K.

^{42}K has been used most extensively in medical work as it is readily available from a reactor irradiation. It is produced by the reaction $^{41}K(n, \alpha)^{42}K$, $^{42}Ca(n, p)^{42}K$ and $^{45}Sc(n, \alpha)^{42}K$. The half life of ^{42}K is relatively short, 12·4 hr, but its principal γ-ray energy and β^- end point energy are high, 1·524 MeV and 3·52 MeV respectively, making it unsuitable for some medical applications. On the other hand ^{43}K has abundant γ-rays with energies of 373 keV and 618 keV, and β^- end point energies of 830 keV and 460 keV, making this isotope more suitable for medical use. These physical characteristics of ^{42}K and ^{43}K are shown in Table 1.

Potassium-43 can be prepared by the reactions $^{40}Ar(\alpha, p)^{43}K$ and $^{44}Ca(p, 2p)^{43}K$ using accelerators or by the $^{43}Ca(n, p)^{43}K$ reaction using highly enriched ^{43}Ca[15] (natural abundance 0·145 per cent) for a reactor irradiation with fast neutrons.

In 1959 DYSON and FRANCOIS[16] described an electrostatic method of recovering ^{43}K from an argon gas-phase target in which some of the potassium ions were collected on a stainless steel rod held at a negative potential of about 1 kV.

The method described was inherently inefficient as it was found to be necessary to interrupt the alpha particle beam with a 50 per cent duty cycle in order to establish a high electric field to collect the ^{43}K ions. Although a more powerful source of high voltage may be used to overcome this problem, the recovery of the ^{43}K from a long stainless steel rod was not attractive.

In the first publication describing the discovery of ^{43}K[17] it was found that as the argon was allowed to flow out of the target chamber through a glass wool filter plug some of the ^{43}K was carried as far as the filter in the gas phase and could be removed by a warm water wash. However, the majority of the ^{43}K was recovered by washing the walls of the irradiation vessel with water. The present work describes efforts to increase the proportion of ^{43}K recovered on a small, easily washed filter and other factors influencing the yield and purity of the final product.

TARGET SYSTEM AND PREPARATION FOR CLINICAL USE

The target chamber consists of an aluminium tube, 46 cm long, 14 cm dia., 3·18 mm wall thickness, onto both ends of which are welded 1·25 cm thick aluminium plates which are water cooled. The front plate has a rectangular aperture 12·5 cm × 2·5 cm for beam entry over which is mounted a beam entry window consisting of an 0·025-mm titanium foil and two 0·10-mm aluminium foils. This reduces the 30-MeV external alpha beam of the Medical Research Council (MRC) cyclotron to about 17 MeV. As a result about 500 W are dissipated in the foils. This heat is removed by a combination of front plate water cooling, air cooling blast on the foil[18] and transfer in the recirculating argon to the rest of the system. The back plate of the target chamber has two gas connections, a 6·4-mm gas inlet with delivery tube and a 19·2-mm outlet. The target is connected to a gas flow system shown in Fig. 1 and schematically in Fig. 2. It is of closed circuit design and uses oil-free diaphragm pumps (Compton oil-free compressors, type 4D, supplied by Dawson McDonald and Dawson Ltd., Ashbourne, Derbyshire) to circulate the gas. A flow meter and pressure gauge are provided for monitoring purposes during filling

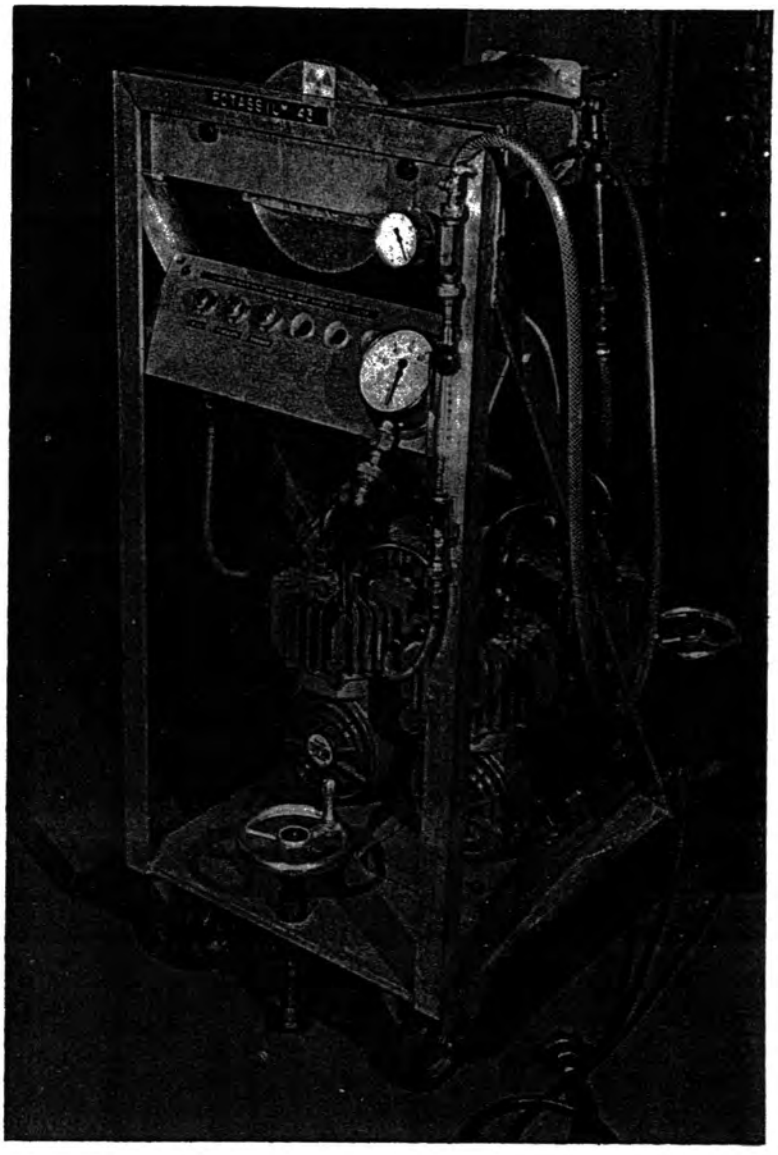

FIG. 1. The target and gas flow system assembly.

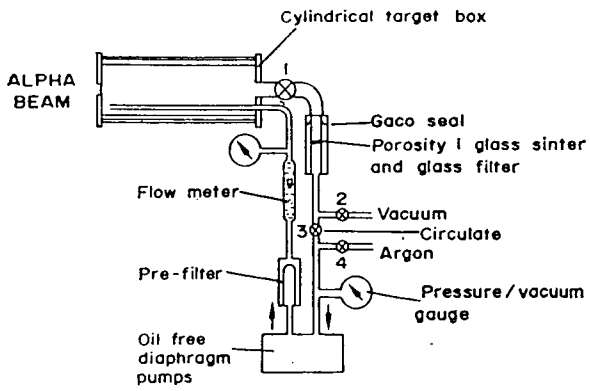

FIG. 2. Potassium-42/43 gas flow circuit.

and irradiation. A borosilicate glass fibre filter paper (Whatman GF/A 3·4 cm diameter) is supported on a glass sinter filter tube, porosity 1, which is in turn supported in a brass pressure vessel placed close to the target outlet. The system is evacuated to approx 1 mm Hg before filling with argon to 0·73 kg cm^{-2} (10 lb in^{-2}). During bombardment at beam currents of around 35 μA the gas is circulated at approx 118 l. min^{-1}.

About 70–80 per cent of the total activity produced is recovered on the filter. A single filter is able to retain more than 95 per cent of the activity carried up to the filter in the gas stream. After bombardment the argon is released to waste and the filter tube together with the filter paper is removed and washed with about 5 ml of 0·001 *M* HCl which removes more than 99 per cent of the activity without added carrier. The yield of ^{43}K at the end of bombardment, based on the activity recovered, varies between 40 and 60 μCi μAh^{-1}. Potassium-42 contamination amounts to 8–10 per cent.

To prepare the solution for i.v. injection it is boiled to dryness in a 50-ml silica glass centrifuge tube and baked for a few minutes to decompose any pyrogenic material which may be present. The residue is then taken up in isotonic saline, isotonic KCl or water for injection depending on the intended application. The solution is sterilised before injection by filtration through a 0·22 μ millipore filter or by autoclaving.

EXPERIMENTAL

A series of investigations have been carried out in order to establish the optimum beam energy, target pressure and gas circulation flow rate for this target system. The aim was to produce ^{43}K in the highest possible yield but with minimal ^{42}K contamination.

(a) *Yields of* ^{42}K *and* ^{43}K *as a function of incident* α *particle energy*

The 30-MeV external α-particle beam of the MRC cyclotron can be degraded using aluminium foils of various thicknesses. Several bombardments were carried out each with a different incident particle beam energy entering the gas target, but with a constant conveniently selected gas pressure of 0·73 kg cm^{-2} (10 lb in^{-2}) and the maximum flow rate of 118 l. min^{-1}. As far as possible the beam intensity distribution was kept constant for all bombardments. At the end of each bombardment measurements of activity on the filter were carried out by γ-spectroscopy using a 3 in. × 3 in. NaI(Tl) detector and 100-channel pulse height analyser. Experimentally determined geometry and crystal efficiency factors were used in the calculation of the yields of the two isotopes. The 591/618 keV combined photopeak was used to measure the ^{43}K activity and the 1524 keV photopeak to measure the ^{42}K activity both of which decayed with the correct half lives of 22·6 h and 12·4 h respectively. In all measurements corrections for decay during bombardment have been neglected, since the bombardment times were short relative to the half lives of the two isotopes, and yields have been expressed as μCi μAh^{-1} at the end of bombardment (E.O.B.).

The yields are plotted as a function of energy in Fig. 3 and the relative yields in Fig. 4. The former curves show that the ^{43}K activity recovered from the $^{40}Ar(\alpha, p)$ reaction starts at about 8 MeV reaching a maximum at about 26 MeV whilst ^{42}K recovery from the $^{40}Ar(\alpha, pn)$ reaction starts at a beam energy of 15 MeV and is still increasing at 30 MeV. The latter curves show that in order to reduce the ^{42}K contamination to less than 1 per cent of ^{43}K the beam energy must be kept below 17 MeV. It should be noted that these measurements were carried out with a low beam and for a

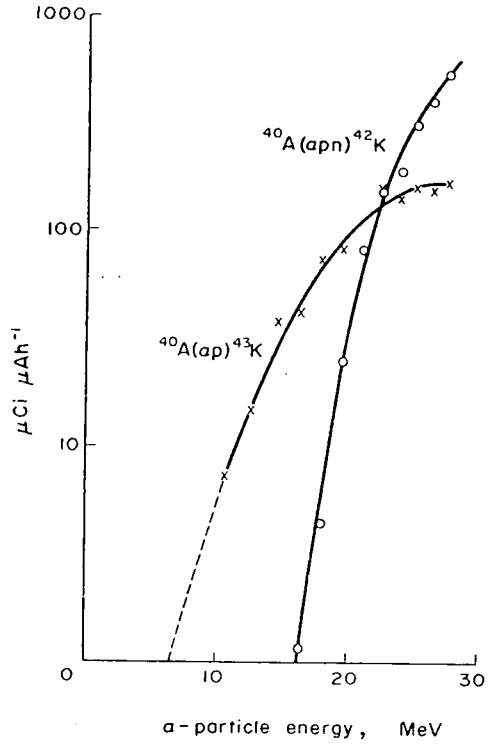

FIG. 3. Yields of ^{42}K and ^{43}K.

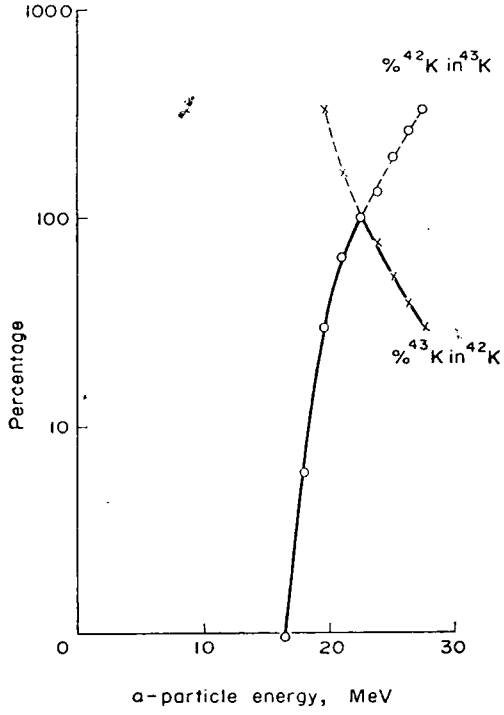

FIG. 4. Contamination of ^{42}K by ^{43}K and of ^{43}K by ^{42}K (Measurements at E.O.B.).

short time; production runs use a higher beam current often for up to 2 h with the result that ^{42}K contamination can amount to 8 per cent or more. This is probably caused by "thinning" of the target foil window by beam heating, with consequent increase in the incident particle energy.

(b) *Yields of ^{42}K and ^{43}K as a function of argon pressure*

Bombardments of the argon gas target were carried out with 17-MeV α-particles using a combination beam entry foil consisting of 0·025-mm Ti and two 0·10-mm Al foils. The gas flow was the maximum obtainable and the gas pressure was raised from zero above atmospheric pressure to 1·5 kg cm^{-2} (20 lb in^{-2}) above atmospheric pressure in equal steps. In these and all subsequent experiments the

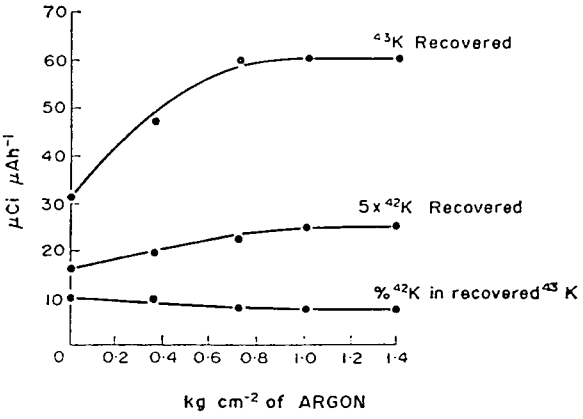

FIG. 5. Yields of ^{42}K and ^{43}K as a function of argon pressure.

activities were measured using a 15-cm^3 Ge(Li) detector coupled to a 4000-channel pulse height analyser. The higher resolution of this detector enabled the 618-keV photopeak alone to be used to measure the ^{43}K activity. Once again experimentally determined geometry and crystal efficiency factors were used to calculate the activities and yields were expressed in μCi μAh^{-1} at the end of bombardment. The yields of ^{42}K and ^{43}K are both plotted as a function of pressure in Fig. 5.

The ^{43}K yield curve from the (α, p) reaction reaches a maximum at 0·73 kg cm^{-2} indicating that at this pressure the target gas thickness reduces the beam energy to the reaction

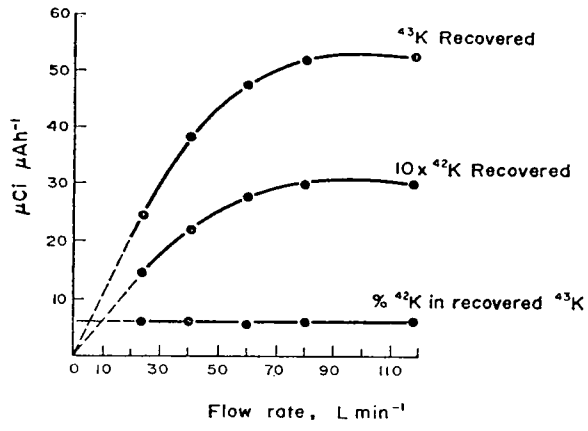

FIG. 6. Yields of ^{42}K and ^{43}K as a function of flow rate of argon.

threshold energy of about 8 MeV. Only a small change in the ^{42}K yield is noted, the increase with pressure being difficult to explain satisfactorily on account of the many other variables in this system. However, for routine production purposes it is clear that there is no advantage in increasing the argon pressure above 0·73 kg cm^{-2}.

(c) *Yields of ^{42}K and ^{43}K as a function of rate of flow of argon*

Since it is the gas stream which carries the produced activity to the filter the influence of the flow rate on the recovered activity was studied. The rotameter flow meter was calibrated against a gas meter calibrated by United Gas Industries (London). The flow was controlled by an adjustable valve inserted in the circulation system between valve No. 3 and the pump (Fig. 2). Bombardments were carried out with 17-MeV α-particles and with a gas pressure of 0·73 kg cm^{-2}. Activities were measured using the Ge(Li) detector and the yields, corrected to E.O.B., were plotted as a function of flow rate in Fig. 6. These curves show that no increase in recovery can be obtained with flow rates in excess of 100 l. min^{-1} and the relative yields remain, as expected, unchanged at all flow rates. Activity lost at the lower flow rates is deposited on the inside surface of the target chamber. For routine production purposes therefore the maximum attainable flow rate of 118 l. min^{-1} is used.

(d) *Activity losses on the target chamber at a fixed energy and pressure*

In order to see the ^{43}K yield distribution within the target chamber, bombardments were carried out in a static system at a pressure of 0·73 kg cm^{-2} with 17-MeV α-particle beams of 35 μA. The target was lined with aluminium foil which after bombardment was removed and cut into cylinders 5 cm tall. Each piece of foil therefore represents a different depth in the target. The ^{43}K activity was then measured on each cylinder using the 15-cm^3 Ge(Li) detector. The percentage of the total activity on each strip was calculated and the results are plotted as a histogram in Fig. 7. These measurements were then repeated with the dynamic system with the maximum gas flow rate. The results, expressed as the percentage of the total activity produced during the static run, are also plotted in Fig. 7. The dotted curves are the total integrated activity in each case. The differences between the two histograms represent the activity swept from the target chamber. In the static system 65–70 per cent of the activity is produced in the first 15 cm of the chamber and adheres to the wall. In the dynamic system two thirds of this activity is removed from the target and collected on the

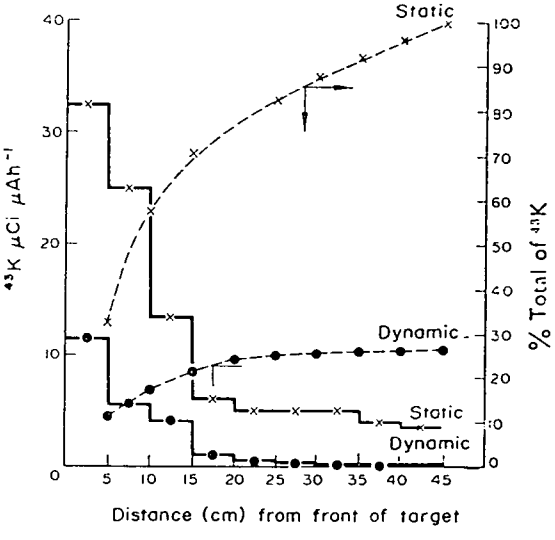

FIG. 7. Formation and losses of ^{43}K activity inside the target chamber.

glass fibre filter, but still one third of the total activity produced is left on the target walls.

An attempt was made to reduce these losses of activity by changing the flow path of the gas in the target. The flow was arranged across the front section of the chamber and under these conditions the total recovery increased by about 15–20 per cent reducing the total loss to about 10 per cent. ^{42}K contamination in the recovered activity also decreased to about 2 per cent. However, as before, the ^{42}K contamination was found to be very sensitive to changes in the incident particle energy. A 1-MeV increase raised the ^{42}K in the recovered activity to about 15 per cent. This system has not yet been adopted for routine production as a suitable target has not yet been constructed.

DISCUSSION

The maximum attainable external α particle beam current from the MRC cyclotron is 100 μA. The target foil system described in this paper permits a maximum continuous beam current of only 35 μA. Even at this beam current the loss of energy in the foil is equivalent to about 500 W. If beam currents greater than this are employed, particularly if the beam defocusing is inadequate, then the present cooling system of air blown onto the foil face and water cooling around the edges of the foil window becomes insufficient, resulting very quickly in puncture of the foil.

Several different foil materials have been tried including tantalum, titanium and stainless steel (EN58B) of a thickness which reduces the beam energy to 17-MeV, but none proved better than the present titanium/aluminium combination. A graphite window, uncooled, of 0·25-mm was tried, protected from pressure and oxidation by a 0·025-mm titanium foil. This proved satisfactory for bombardments at beam currents up to 70 μA. However, the yield of ^{43}K per μAh dropped by about 30 per cent below the yield at 35 μA. This is probably explained by local density reduction of the gas in the target chamber along the path of the beam as a result of the heat produced by the beam. Increasing the pressure to 1·5 kg cm^{-2} (20 lb in^{-2}) did not improve the yield. The overall result of operating the system at 70 μA with a Ti/graphite window combination was to raise the rate of production from 2 mCi h^{-1} to 3 mCi h^{-1} but with a decrease in reliability due to foil window failures. This method has not therefore been used for regular production of this isotope.

The measurements described in this paper were made wholly to obtain practical data for the target system described. Factors such as the shape and size of target, geometry of the gas inlet and outlet all make the target system unique. Variation in beam distribution also results in considerable variation in yields and contamination levels. However the system, although perhaps not ideal, can be operated reliably and reasonably reproducibly under the conditions described.

Acknowledgement—The authors wish to thank Dr. D. J. Silvester for his comments.

REFERENCES

1. Anderson E. C. and Langham W. H. *Science* **130,** 713 (1959).
2. James J. A. and Robertson J. S. *Am. J. Dis. Child.* **93,** 217 (1953).
3. Corsa L. *J. Clin. Invest.* **29,** 1280 (1950).
4. Skrabal F., Glass H. I., Clark J. C., Jeyasingh K. and Joplin G. F. *Int. J. appl. Radiat. Isotopes* **20,** 677 (1969).
5. Johnson J. E., Hartsuck J. M., Zollinger R. M. and Moore F. D. *Metabolism* **18,** 663 (1969).
6. Relman A. S. *J. Biol. Med.* **29,** 248 (1956).
7. Relman A. S., Lambic A. T. and Burrow B. A. *J. clin. Invest.* **36,** 8 (1957).
8. Hevesy G. and Hylin G. *Acta Physiol. Scand.* **24,** 285 (1952).
9. Hurley P. J., Cooper M., Reba R. C., Poggenburg K. J. and Wanger H. N. *J. nucl. Med.* **12,** 518 (1971).
10. Holman B. L., Poggenburg K. J., Adams D. F., Erdh P. and Adelstein S. J. *J. nucl. Med. Abstract* **12,** 366 (1971).
11. Susen A. F., Small W. T. and Moore F. D. *Surg. Forum of Am. Coll. Surgeons, 36th Congress,* p. 362 (1952).
12. Silverstone B., Sweet W. H. and Ireton R. S. *Surg. Forum of Am. Coll. Surgeons, 36th Congress,* p. 371 (1952).

13. LEDERER C. M., HOLLANDER J. M. and PERLMAN I. *Table of Isotopes* (6th edn), p. 14. Johnson and Wiley, New York.
14. WATERS S. L. *Radiochimica Acta*, in press.
15. O'BRIAN H. A. and HUPF H. B. *J. nucl. Med. Abstract* **9**, 340 (1968).
16. DYSON N. A. and FRANCOIS P. E. *Int. J. appl. Radiat. Isotopes* **7**, 150 (1959).
17. OVERSTREET R., JOCOBSON L. and STOUT P. L. *Phys. Rev.* **75**, 231 (1949).
18. VONBERG D. D., BAKER L. C., BUCKINGHAM P. B., CLARK J. C., FINDING K., SHARP J. and SILVESTER D. J. *Uses of Cyclotrons in Chemistry, Metallurgy and Biology*, p. 258. Butterworths, London (1970).

IAEA-SM-171/8

PREPARATION OF ^{18}F-LABELLED DL-3-FLUOROTYROSINE

A.J. PALMER, J.C. CLARK, R.W. GOULDING, M. ROMAN*
MRC Cyclotron Unit, Hammersmith Hospital,
London,
United Kingdom

Abstract

PREPARATION OF ^{18}F-LABELLED DL-3-FLUOROTYROSINE.

A method of preparing ^{18}F-labelled DL-3-fluorotyrosine is described. ^{18}F is produced by the cyclotron bombardment of neon via the ^{20}Ne (d, α) ^{18}F reaction using a glass-lined target vessel. The ^{18}F is recovered in aqueous solution by remote washing of the glass liner, by rotation of the liner with 20 ml of water in it. Detailed operation of the system is described. The ^{18}F activity is introduced into a diazonium tetrafluoroborate derivative of the amino-acid by an exchange reaction in aqueous acetone/acetonitrile solution. The preparation of this diazonium salt, 4-methoxy-3-(2',2'-dicarbethoxy-2'-acetamidoethyl)-phenyl diazonium tetrafluoroborate (I) starting from p-methoxybenzyl chloride is fully described. Pyrolysis of the labelled diazonium salt (I) yields ^{18}F-diethyl 3-fluoro-4-methoxybenzylacetamidomalonate (Schiemann Reaction) which is then hydrolysed to ^{18}F-3-fluorotyrosine by red phosphorus and hydriodic acid. A similar synthesis, starting from L-phenylalanine, has been investigated with a view to preparing ^{18}F-L-phenylanine. Experimental details of the labelling procedure are described and quality control methods for ^{18}F-labelled amino-acids are also discussed.

INTRODUCTION

Following the success of the organometallic compounds chlormerodrin and BMHP (^{197}Hg), and the purely organic compounds selenomethionine (^{75}Se), rose bengal and sodium iodohippurate (^{123}I, ^{125}I, ^{131}I) as scanning agents, it has been generally thought desirable to try to prepare organic compounds containing short-lived gamma-emitting radionuclides in which some of the limitations of the scanning agents in use at the present time, namely reliability of distribution, loss of label from the form in which it is administered, and radiation dose, are minimized. In the past few years several organic compounds containing the firmly bound ^{18}F label ($T_{\frac{1}{2}}$ 110 min, β^+) have been prepared, prominent among which are the monofluoro-derivatives of two natural aromatic aminoacids, phenylalanine [1, 2] and tryptophan [2]. A description will here be given of the preparation of ^{18}F-DL-3-fluorotyrosine, a previously unreported ^{18}F-labelled aromatic amino-acid.

The monofluoro aromatic amino-acids have attracted interest because of their well-documented pharmacological properties. They are incorporated into proteins [3], show anti-tumour properties [4] and are anti-metabolites of the natural amino-acids [5]. These properties and the utility of ^{75}Se-selenomethionine indicate a potential for these materials when labelled

* On leave from Laboratory of Labelled Compounds, Institute of Atomic Physics, Bucharest, Romania.

with ^{18}F, as organ scanning agents, especially for the pancreas [6]. The success of a compound in this application depends critically upon the pancreas-to-liver ratio, which must be as high as possible if good pancreas images are to be obtained. The ratio varies with the structure of the compound concerned [7], so that it is essential to test as many different compounds as possible in order to maximize this ratio.

Two other important points must also be considered since they are directly related to the synthetic method used at present for making ^{18}F-labelled amino-acids. These compounds show varying toxicities. The most toxic, including 3-fluorotyrosine [8], have an LD_{50} in the range 5-10 mg kg^{-1} and consequently must be prepared with the highest possible specific activities. Also, all natural amino-acids belong to the L-series and it is only possible, at the present state of knowledge, to prepare the DL-racemates of compounds labelled with ^{18}F.

GENERAL CONSIDERATIONS FOR ^{18}F-LABELLING

The carbon-fluorine bond has a very high dissociation energy ($\sim$ 110 kcal $mole^{-1}$), and consequently stability problems are less likely to be encountered with ^{18}F-labelled compounds than, for example, iodine-labelled compounds. However, this fact means that some of these compounds are difficult to prepare in the short periods of time available, the half-life of the radionuclide being 110 min. Long reaction times and large molar excesses of the fluorinating agent are used in many fluorination reactions, consequently radiochemical yields would be extremely low if such reactions were adopted as labelling procedures. Because of the high specific activities often required, difficulties in handling small amounts of material efficiently are also encountered.

To prepare ^{18}F-labelled 3-fluorotyrosine it was necessary to devise a synthesis in which the ^{18}F activity could be introduced into a precursor which would then be rapidly transformed into the product. Unlabelled 3-fluorotyrosine has been previously synthesized by condensation of 3-fluoro-4-methoxy- or 3-fluoro-4-ethoxybenzaldehyde, with hippuric acid and subsequent hydrolysis and reduction [9]. It has also been prepared from m-fluorophenylalanine by nitration, reduction and finally decomposition of the corresponding diazonium salt on refluxing the aqueous solution [9]. Neither of these two methods is feasible as a route to the ^{18}F-labelled material because of the excessively long times required.

In the previously reported preparation of ^{18}F-labelled p-fluorophenylalanine, the ^{18}F was introduced into 4-(2',2'-dicarbethoxy-2'-acetamidoethyl)-phenyl diazonium tetrafluoroborate [1]. Thermal decomposition of this diazonium salt gave the corresponding fluoro-ester, and then the amino-acid function was generated from the diethyl acetamidomalonate side chain by acid hydrolysis. ^{18}F-3-fluorotyrosine has now been prepared in an analogous manner from ^{18}F-2-methoxy-5-(2',2'-dicarbethoxy-2'-acetamidoethyl)-phenyl diazonium tetrafluoroborate, the ring hydroxyl group being protected as the methyl ether. In all syntheses of this type certain functional groups (for example OH, NH_2, aliphatic COOH) must be protected in order not to interfere with the production of the diazonium salt and/or the subsequent Schiemann reaction.

SYNTHETIC CHEMISTRY

The synthetic route adopted for the preparation of the diazonium tetrafluoroborate precursor is shown in Fig.1. Diethyl p-methoxybenzyl-acetamidomalonate (I) is prepared by condensation of p-methoxybenzyl chloride with diethyl acetamidomalonate. Careful nitration of (I) with a one molar equivalent of fuming nitric acid in acetic anhydride at 0°C yields diethyl 3-nitro-4-methoxybenzylacetamidomalonate (II), the structure of which was confirmed by its ^1H NMR spectrum (aromatic region $H_A\delta$ = 7.05 (singlet) $H_B\delta$ = 7.15 (doublet J = 2 Hz) $H_c\delta$ = 7.7 (doublet J = 2 Hz). This compound has been previously prepared by reaction of 3-nitro-4-methoxybenzyl chloride with diethyl acetamidomalonate [10]. The 3-nitro derivative is reduced to diethyl 3-amino-4-methoxybenzylacetamidomalonate (IV) using 10% Pd/C catalyst in glacial acetic acid at a hydrogen pressure of 1 atm. The amine (IV) may be diazotized, and the diazonium tetrafluoroborate (Va) isolated in the normal way. This material is stored and used in the radioactive synthesis as required. For the reduction, and the subsequent diazotization step to proceed satisfactorily, it is essential that the diethyl p-methoxybenzylacetamidomalonate is purified by vacuum distillation as described in the experimental section below.

Thermal decomposition of the diazonium salt (Va or b) gives diethyl 3-fluoro-4-methoxybenzylacetamidomalonate (VI), and this is hydrolysed to 3-fluorotyrosine (VII) by hydriodic acid and red phosphorus (Fig.2). This is the standard reagent for the reductive demethylation of methoxy groups, and it is also very effective for hydrolysis of the diethyl acetamido-malonate group to give the amino-acid function. Passage of the hydrolysed

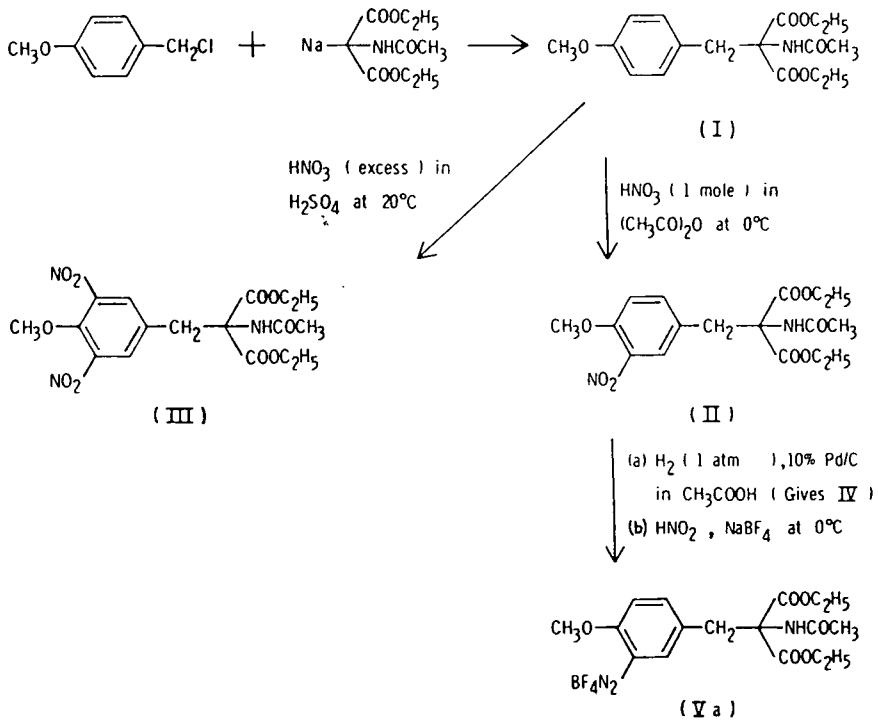

FIG. 1. Preparation of 2-methoxy-5-(2',2'-dicarbethoxy-2'-acetamidoethyl)-phenyl diazonium tetrafluoroborate.

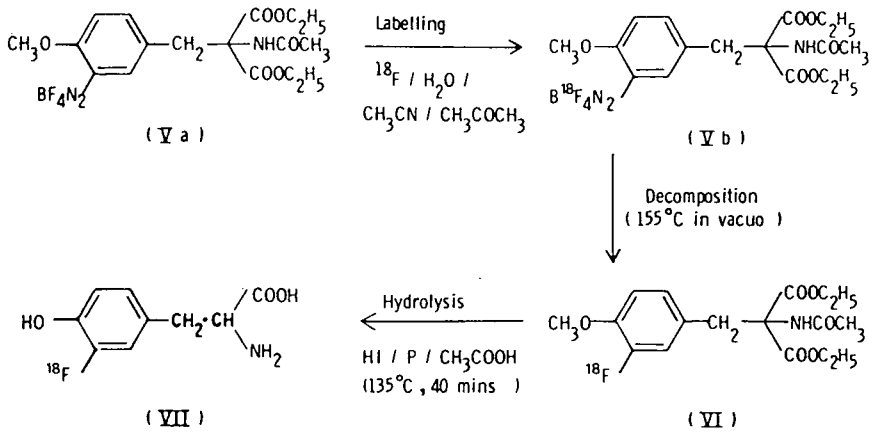

FIG. 2. Preparation of ^{18}F-labelled DL-3-fluorotyrosine.

solution down a column of IR4B (OH^-) resin removes hydriodic acid and phosphoric acid, but the product may contain traces of acetic acid which may be neutralized with a few drops of dilute sodium hydroxide solution.

The preparation of other fluorine substituted tyrosine derivatives was also attempted. Nitration of (I) with excess nitric acid produced diethyl 3,4-dinitro-4-methoxybenzylacetamidomalonate (III), the structure of which was also confirmed by ^1H NMR spectroscopy (aromatic region $2H_A\delta = 7.71$ (singlet)). This cannot be used to prepare 3,5-difluorotyrosine since the equivalent diazonium tetrafluoroborate derivative (which may be easily prepared in the normal way) yields < 0.2% diethyl 3,4-difluoro-4-methoxybenzylacetamidomalonate on pyrolysis. It might be possible to prepare this compound in labelled form if the synthetic route for 3-fluorotyrosine is followed, but using 3-fluoro-4-methoxybenzyl chloride as starting material.

Diethyl 2-nitro-4-methoxybenzylacetamidomalonate has been prepared from the corresponding benzyl chloride [11], but this cannot be reduced to the 2-amino compound because an alternative reaction takes place [12]. Thus it is not possible to prepare 2-fluorotyrosine by this route.

EXPERIMENTAL

Diethyl p-methoxybenzylacetamidomalonate (I)

p-Methoxybenzyl chloride was prepared by the reaction of thionyl chloride in chloroform on the corresponding alcohol, the crude product being purified by vacuum distillation (b.p. 85°C/5 mm Hg). Sodium metal (1.70 g, 0.077 g atom) was dissolved in anhydrous ethanol (105 ml) and diethyl acetamidomalonate (16.7 g, 0.077 mole) was added. This solution was stirred under reflux and a solution of p-methoxybenzyl chloride (12.2 g, 0.083 mole) in ethanol (30 ml) was added over 10 min under anhydrous conditions. The mixture was refluxed for a further 2 h, cooled, and stirred into crushed ice and water (500 ml). The white solid so produced was filtered off and purified by vacuum distillation (b.p. 180°C/5 mm Hg)

followed by crystallization from 70% ethanol/water to produce a colourless crystalline solid (10.0 g, 38%) m.p. 98° - 99°C (Lit. 101°C [13]) λ $(EtOH)_{max}$ = 277 nm, $\nu_{NH(KBr)}$ = 3270 cm^{-1}, ν_{CO} = 1750, 1650 cm^{-1}.

Diethyl-3-nitro-4-methoxybenzylacetamidomalonate (II)

The compound (I) (2.95 g, 8.8 mmole) was dissolved in acetic anhydride (10 ml) cooled to between -5° and 0°C, and a solution of fuming nitric acid (0.40 ml, 9.0 mmole) in acetic anhydride (10 ml) (prepared at 0°C) was added over 5 min with efficient stirring. The resultant yellow solution was stirred for a further 10 min, then poured on to crushed ice and stirred, a yellow sticky solid being produced. This was extracted into chloroform, the organic phase was dried over calcium chloride, and the solvent removed in vacuo. Several recrystallizations from aqueous ethanol gave a pale yellow crystalline solid (1.95 g, 58%) identified as diethyl 3-nitro-4-methoxybenzyl-acetamidomalonate, m.p. 165°-168°C, by ^1H NMR spectroscopy, $\lambda_{max\,(EtOH)}$ = 260, 330 nm, (ϵ 3240, 2270), ν_{NO_2} = 1510, 1370 cm^{-1}.

Diethyl 3-amino-4-methoxybenzylacetamidomalonate (IV)

The compound (II) (0.50 g, 1.3 mmole) was hydrogenated at 1 atm in glacial acetic acid (20 ml) in the presence of 10% Pd/C (0.1 g). After absorption of hydrogen had ceased (about 30 min), the solution was filtered off from the catalyst and evaporated in vacuo leaving a grey crystalline solid, diethyl 3-amino-4-methoxybenzylacetamidomalonate (0.44 g, 96%), m.p. 185°-189°C (Lit.191.5°-93°C[10]), $\nu_{NH(KBr)}$ = 3450, 3370, 1620 cm^{-1}.

2-Methoxy-5(2',2'-dicarbethoxy-2' acetamidoethyl)-phenyl diazonium tetrafluoroborate (Va)

The amine (IV) (0.44 g, 1.25 mmole) was dissolved in a mixture of concentrated hydrochloric acid (0.35 ml, 3.7 mmole) and water (1 ml). The resulting suspension of the hydrochloride was cooled to 0°C, and a solution of sodium nitrite (0.085 g, 1.25 mmole) in water (0.7 ml) added dropwise with stirring. When the addition was complete a solution of sodium fluoroborate (0.3 g, 2.7 mmole), in water (0.7 ml, previously cooled to 0°C), was added. The product was obtained as a dark oil which slowly solidified to a yellow-grey crystalline solid, 2-methoxy-5-(2',2'-dicarbethoxy-2' acetamidoethyl)-phenyl diazonium tetrafluoroborate (0.40 g, 71%) m.p. 125°C-130°C (dec.), (found: C, 45.5; H, 4.9; N, 9.15; $C_{17}H_{22}N_3\,BF_4O_6$ requires: C, 45.25; H, 4.9; N, 9.3%), $\nu_{N=N(KBr)}$.= 2250 cm^{-1}.

Diethyl 3-fluoro-4-methoxybenzylacetamidomalonate (VI)

This compound was prepared as described below (m.p. 117°-119°C); (found: C, 57.8; H, 6.5; N, 4.3; $C_{17}H_{22}NFO_6$ requires: C, 57.5; H, 6.2; N, 3.9%), $\lambda_{max(EtOH)}$ = 274, 320 nm (ϵ 1600, 220).

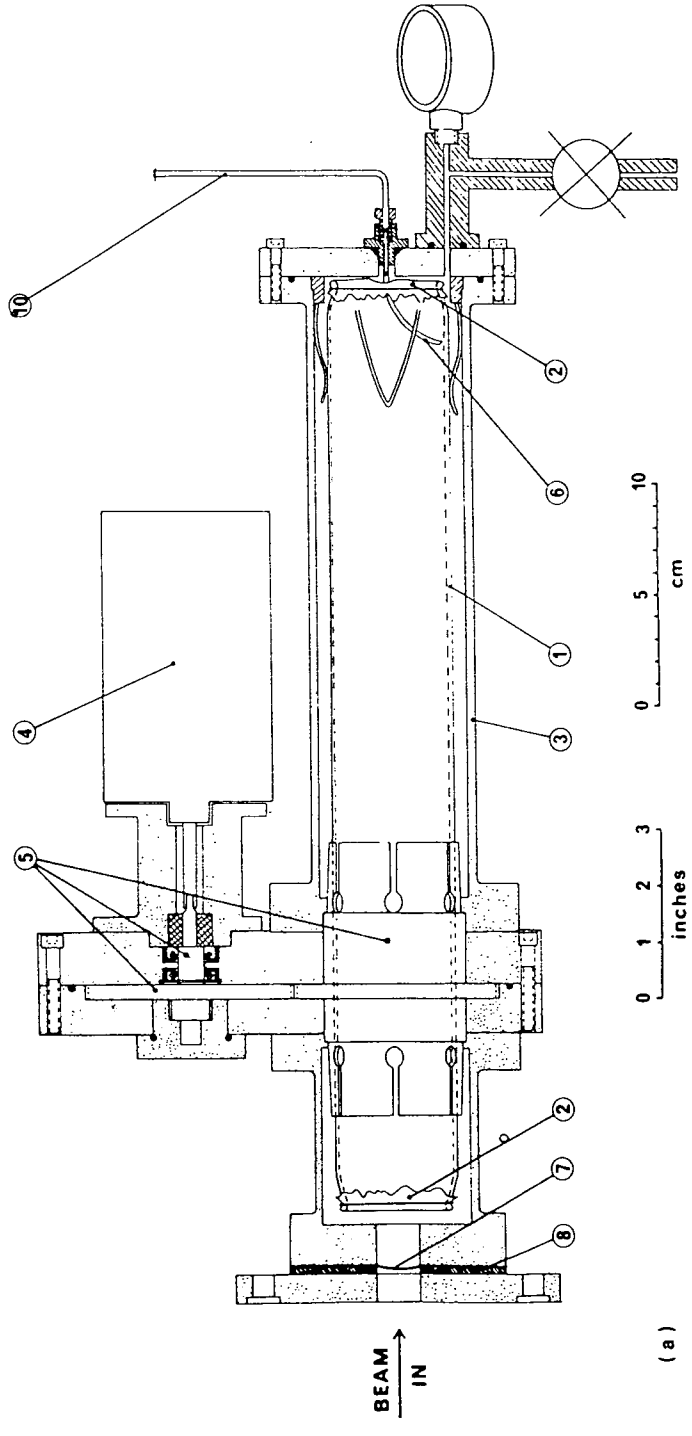
10
2
6
1
4
3
5
2
7
8
BEAM IN
0 5 10
cm
0 1 2 3
inches
(a)

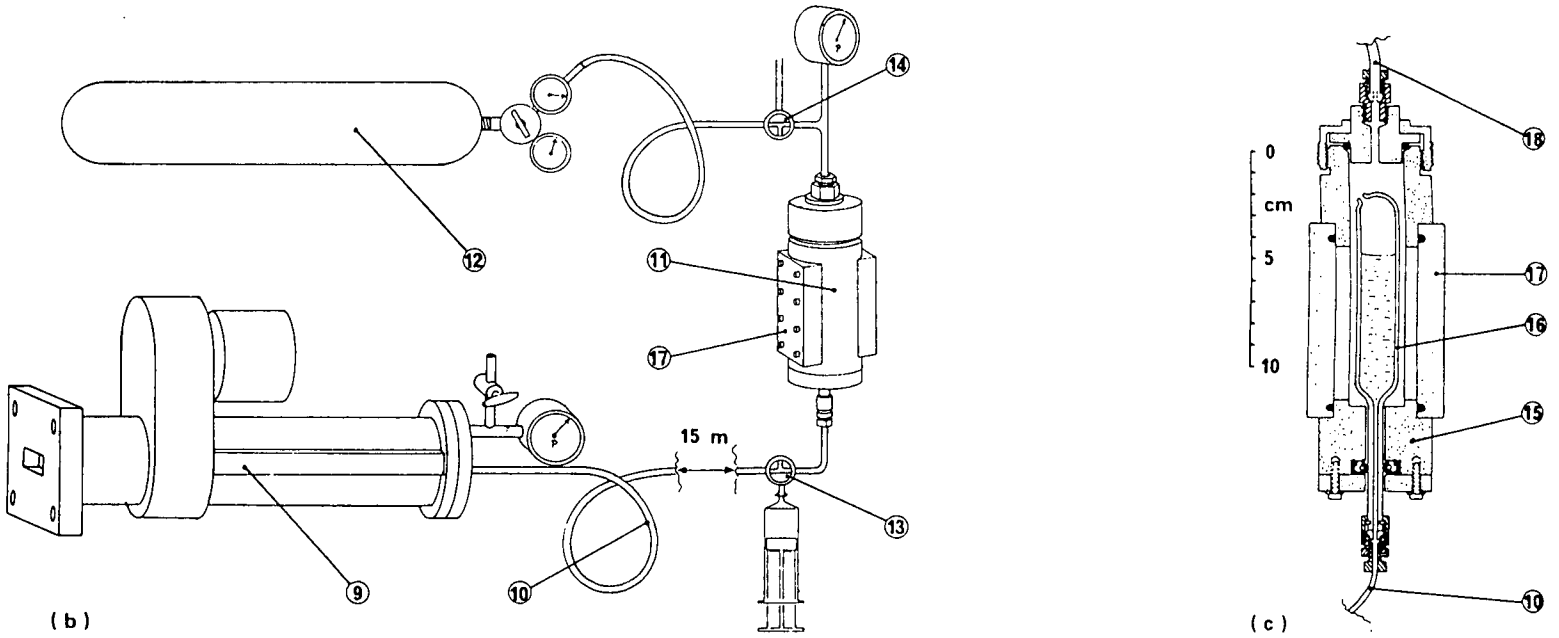

FIG. 3. Production of aqueous ^{18}F: (a) target assembly; (b) schematic diagram of target and recovery system; (c) solution recovery vessel.

(1) Borosilicate glass liner 56 mm o.d., 2.5 mm wall.
(2) Titanium foil windows 0.025-mm thick.
(3) Aluminium pressure vessel.
(4) Driving motor 10 rev/min.
(5) Gear box including driving shaft, gear wheels and collet drive to glass liner.
(6) Stainless-steel water pick-up tube.
(7) EN58B stainless-steel beam entry window 0.050-mm thick.
(8) Target mounting plate and insulator.
(9) Complete target assembly.
(10) Polyethylene tubing 1.5-mm bore, 15-m long.
(11) Complete solution recovery vessel (located in a small hot cell outside the cyclotron chamber).
(12) Cylinder and regulator, c.p. neon.
(13) Three-way valve for liquid transfer.
(14) Three-way valve for venting and pressurizing solution recovery vessel.
(15) Aluminium pressure container.
(16) Glass liner.
(17) Perspex viewing windows.
(18) Neon inlet tube.

DL-3-Fluorotyrosine (VII)

This compound was also prepared as described below and was shown to be identical with an authentic sample by i.r. and u.v. spectroscopy, λ_{max} (H_2O, pH 7) 274 nm.

THE PREPARATION OF ^{18}F

Operational principles of the target system

^{18}F is produced by the ^{20}Ne (d,α)^{18}F reaction. Neon (CP grade, supplied by British Oxygen Co., Ltd.), at 7 kgf/cm^2 gauge is irradiated with 13-14 MeV deuterons in a 45-cm long target vessel shown schematically in Fig.3. The outer aluminium pressure vessel (Fig.3.3), houses a 56-mm o.d., 2-mm wall, borosilicate glass liner (Fig.3.1). The glass liner, which has thin titanium windows (Fig.3.2) crimped on to each end, may be rotated by the motor (Fig.3.4) and the gear box (Fig.3.5) at 10 rev/min. Irradiations are currently carried out at up to 30 μA when the neon pressure rises to 10 kgf/cm^2 gauge. Most of the ^{18}F produced is caught by the glass liner. Of the ^{18}F caught on the liner, 60-65% may be recovered by washing its inner surface with 15-20 ml of water. This is achieved remotely by transferring the water from the recovery vessel (Fig.3.11) to the target under pressure, rotating the glass liner for 5 min, then, after a draining period of 2 min allowing the solution to return by reducing the pressure with the three-way valve (Fig.3.14), in the recovery vessel. The solution is finally transferred to a suitable container, e.g. a 50 ml syringe or 50 ml boiling tube via the three-way valve for liquid transfer (Fig.3.13).

The following features are important for the successful operation of this system. A strong target window and a well-distributed deuteron beam are essential for high mechanical reliability. For a 4 cm × 2 cm beam aperture a 0.050-mm EN58B stainless-steel foil (supplied by Goodfellows Metals Ltd, Esher, Surrey, England) has proved to be very reliable at beam currents and pressures of up to 30 μA and 10 kgf/cm^2 respectively. The 0.025-mm-thick titanium windows on the glass liner are necessary to reduce "diffusion" losses to the walls of the aluminium pressure vessel. These windows are crimped on to a rim formed on the liner ends so that no adhesives are required. Adhesives may be degraded during irradiation and give rise to organic chemical contamination of the wash solution. A small hole, 3-4 mm in diameter, is left in the rear window to allow entry of the stainless-steel water pick-up tube (Fig.3.6) and for pressure equalization. The target must, of course, be quite level to avoid spillage of solution from these unsealed ends and to ensure efficient pick-up of the solution. The glass liner must be easily wetted so that washing and recovery of the wash solution is efficient. This simply means careful cleaning of the liner with, for example, "Pyroneg" (Diversy (UK) Ltd, Barnet, Herts, England) followed by an exhaustive rinse with distilled water. The choice of material and diameter of the liquid transport tube (Fig.3.10) is also important if efficient transfers are to be achieved. It is best if the tubing is not wetted and that the solution forms into columns

rather than droplets in the tube bore. Polyethylene tubing, 1.5 mm bore, 2.7 mm o.d., 15 m long, has proved to be very satisfactory in this respect.

Target system performance

Many irradiations have been carried out under various conditions up to maximum filling pressures and beam currents of 7 kgf/cm^2 and 45 μA. A preliminary irradiation of 2 μAh at 20 μA and 3.5 kgf/cm^2 yielded 28 mCi/μAh at the end of bombardment, of ^{18}F on the glass liner. The liner was assayed using a large re-entrant ionization chamber. By washing on the bench with 20 ml of water, 65% of this ^{18}F was recovered in 19 ml, thus giving a recovered yield of 17.8 mCi/μAh. Two further irradiations under similar conditions but with remote washing and recovery yielded 17.5 mCi/μAh and 17.0 mCi/μAh for a dry and a "wet" liner respectively. Thus it is possible to carry out repetitive irradiation/recovery cycles without drying the target or significant loss of the neon filling. To maintain these yield figures at 30 μA it was necessary to increase the filling pressure to 7 kgf/cm^2, the design limit for the present system. Above 35 μA at this pressure the yield begins to fall through thinning of the target gas by the beam power. The longest irradiation carried out to date was 20 μAh at 30 μA and a pressure of 7 kgf/cm^2. 318 mCi of ^{18}F, at end of bombardment, in 19 ml of water were recovered. This corresponded to a yield of 15.9 mCi/μAh. The only radiochemical impurities detected in the ^{18}F solutions from this system are ^{22}Na 3.0×10^{-4}%, ^{48}V 6.7×10^{-5}% and ^{7}Be 2.3×10^{-5}%, all values being the maximum observed and corrected to end of bombardment.

Preparation of ^{18}F-DL-3-fluorotyrosine (VII)

The ^{18}F solution is first reduced in volume to approximately 0.5 ml by boiling in a 50 ml centrifuge tube while nitrogen is slowly bubbled in through a fine glass capillary. The diazonium tetrafluoroborate (Va) (130-150 mg) is then added to the solution (after cooling) followed by the minimum amount of 50% acetone/acetonitrile solution necessary to dissolve the salt completely ($\sim$ 1 ml). The solution is then left to exchange at room temperature for about 1 h. After this time sufficient anhydrous sodium sulphate is added to take up the water present and the solution is left for a further 5 min.

Part of the solution is then removed using a Pasteur pipette and added to dry diethyl ether (45 ml) in a 50-ml centrifuge tube causing precipitation of the labelled diazonium salt (Vb). The precipitate is separated by centrifugation, and more diethyl ether (45 ml) is added followed by the remaining acetone/acetonitrile solution and further acetone ($\sim$ 1 ml) to wash the sodium sulphate. The combined precipitate is then centrifuged off.

The labelled diazonium salt (Vb) is dried in vacuo at room temperature and then decomposed to the fluoro ester by heating under vacuum in an oil bath at 155°C. The dark brown tarry residue is extracted with hot toluene (2×2 ml) and this solution is chromatographed on a column of basic alumina (grade 1) (4×1.3 cm) eluting with 10% chloroform in toluene.

After elution and evaporation of the solvent, the ^{18}F-diethyl 3-fluorobenzylacetamidomalonate (VI) is left as a white solid. This is dissolved in a little acetone and transferred to a 2-ml flask. The acetone is then evaporated and the flask is fitted with a reflux condenser. Red phosphorus (~ 10 mg) is added followed by acetic anhydride (0.3 ml) and the flask is heated by immersion in an oil bath at 135°C. When refluxing has begun 55% Analar hydriodic acid (0.6 ml) is added dropwise through the condenser and refluxing is continued for a further 40 min.

After cooling the solution is diluted to 3 ml with water for injection, and passed down an Amberlite IR4B (OH^- form)[1] ion exchange column (6 × 1 cm) which has been previously prepared in and eluted with water for injection. The fraction containing the activity is collected, neutralized if necessary with a few drops of 2N sodium hydroxide, and passed through a Millipore filter into a sterile vial.

Analysis

The product is analysed by ion exchange chromatography. In this case a 30 μCi sample is applied to a 24 × 1.3-cm column of AG50W-X8 (Na^+ form) 200-400 mesh resin eluting with a McIlvanes standard citrate/phosphate buffer at pH 7.6. The column output is connected via 0.15 mm i.d. ptfe tubing to a Cecil instruments CE 212 UV monitor (270 nm) and then to a measuring cylinder. The connecting tubing is viewed by a shielded NaI(Tl) scintillation counter (Nuclear Enterprises Edinburgh Series). The output signals of both instruments are displayed on a dual pen recorder, thus a continuous record of the mass concentration of the product and the radioactive concentration in the eluent is obtained.

The mass concentration of the amino-acid in the final solution is determined by an absorbance measurement at 270 nm (after a 100-fold dilution), by comparison with the absorbance of a standard solution.

DISCUSSION

The times and radiochemical efficiencies for two typical preparations are given in Table I. The thermal decomposition of the diazonium tetrafluoroborate (Vb) to the corresponding fluoro-ester (VI) occurs with low chemical yield because substantial tar formation takes place as in other reactions of this type, particularly when the decomposition temperature is high. Also, the maximum possible radiochemical yield in this stage is 25% because the activity is divided between the aryl fluoride and the other product, boron trifluoride, in the ratio of 1:3. Both factors combine to give a very low radiochemical yield of about 3.5% (corrected for decay) for the desired product. However, the low chemical yield does not affect the specific activity of the final product which is about 75 μCi mg^{-1} (starting from 100 mCi ^{18}F). This is substantially higher than specific

[1] Before use the resin must be regenerated in the OH^- form by washing with 2N sulphuric acid, 2N sodium hydroxide solution and finally de-ionized water until the eluant is neutral. This serves to remove soluble impurities from the resin.

TABLE I. RADIOCHEMICAL YIELDS FOR ^{18}F-3-FLUOROTYROSINE PREPARATION

Weight (Va) (mg)	Starting ^{18}F activity (mCi)	Radiochemical yields (%) [a]			Specific activity of (VII) (μCi mg^{-1}) [b]
		Exchange	Decomposition	Hydrolysis	
150	58	26.5	3.1	83	19.4
130	102	48.5	3.6	86	76.8

[a] Corrected for decay.
[b] At time of despatch.

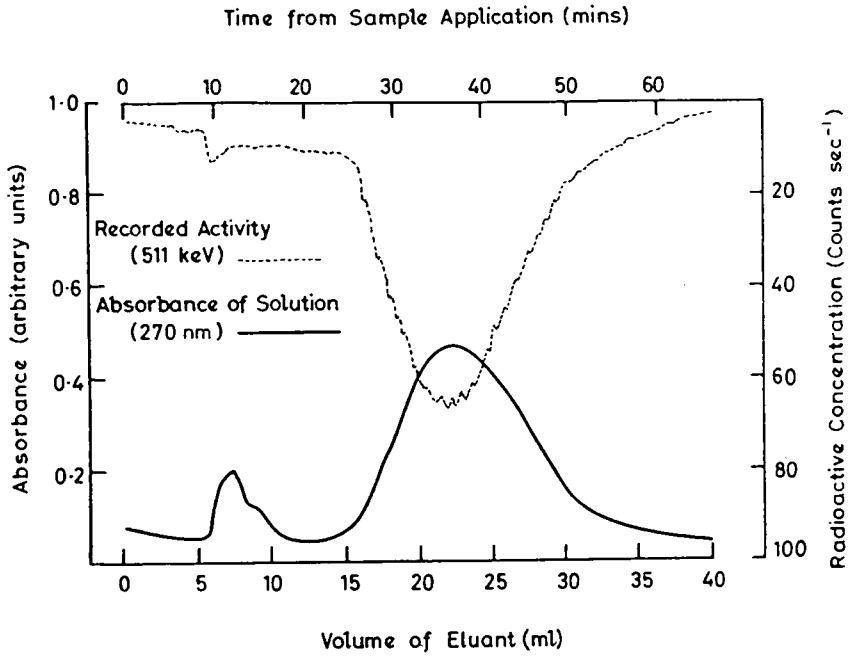

FIG. 4. Elution behaviour of DL-3-fluorotyrosine on a 24 x 1.3-cm column of AG50W-X8 (Na^+-form) 200-400 mesh resin.

activities hitherto reported for other ^{18}F-labelled amino-acids, and there is probably room for further improvement. The proportion of activity incorporated in the diazonium salt (Vb) appears to vary between 25 and 50% when a period of 1 h and 130-150 mg of material are used. The total time required for the preparation (after delivery of the ^{18}F solution) is approximately 210 min.

Amino-acids may be conveniently analysed on cationic [14] or anionic [15] ion exchange columns, and this method is valuable when working with short-lived radionuclides. A typical chromatogram obtained by the technique described in the experimental section is given in Fig.4. This shows a major peak in both the activity and mass traces at an elution volume of 22 ml corresponding to 3-fluorotyrosine. A smaller multiple peak ~ 5% is also present in each trace at 7 ml from the partially hydrolysed intermediates. The u.v. spectrum of the product is identical with

that of an authentic sample. If the time for hydrolysis is reduced to 20 min the peaks of low retention time account for about 50% of the activity present.

The method described produces a DL-mixture of the amino-acid since the asymmetric centre is generated in the hydrolysis stage. Resolution of the isomers in a sufficiently short time is not at present practicable, but advances in liquid chromatography might change this in future, for example by the use of suitable optically active stationary phases [16, 17].

ACKNOWLEDGEMENTS

The authors wish to thank D.J. Silvester for his interest in this work. One of us (M.R.) also thanks the Royal Society, London, for the award of a Fellowship held over the period April to December 1972.

REFERENCES

[1] GOULDING, R.W., PALMER, A.J., The preparation of fluorine-18 labelled p-fluorophenylalanine for clinical use, Int. J. Appl. Radiat. Isotopes 23 (1972) 133.

[2] HOYTE, R.M. et al., Organic radiopharmaceuticals labelled with short-lived nuclides: III. ^{18}F-labelled phenylalanines, J. Nucl. Med. 12 (1971) 280; V. ^{18}F-labelled 5- and 6-fluorotryptophan, J. Nucl. Med. 13 (1972) 713.

[3] PREVIC, E.P., BINKLEY, S.B., Slow exponential growth of E. coli in presence of p-fluorophenylalanine; effect of analogue on aromatic biosynthesis, Biochim. Biophys. Acta 87 (1964) 277.

[4] MAY, H., LITZKA, G., Inhibition of tumour growth by 3-fluorotyrosine, Z. Krebsforsch. 48 (1939) 376.

[5] MEISTER, A., Ch. 3, Biochemistry of the Amino Acids 1, Academic Press, New York (1965).

[6] FOWDEN, L., "Fluoroamino acids and protein synthesis", Carbon-Fluorine Compounds (A Ciba Foundation Symposium), Associated Scientific Publishers, Amsterdam (1972) 141.

[7] BLAU, M., MANSKE, R.F., The pancreas specificity of ^{75}Se-Selenomethionine, J. Nucl. Med. 2 (1961) 102.

[8] NIEMANN, C., RAPPORT, M.M., The toxicity of 3-fluoro-D- and L-tyrosine, J. Amer. Chem. Soc. 68 (1946) 1671.

[9] SCHIEMANN, G., WINKELMULLER, W., Fluorinated amino acids and their derivatives, J. Prakt. Chem. 135 (1932) 101.

[10] DEGUTIS, J., STRAUKAS, I., Synthesis of m-[bis(2-chloroethyl)amino] -o-methyl-DL-tyrosine, Zh. Obshch. Khim. 32 (1962) 1255.

[11] DAVIS, A.L. et al., 2-Aminotyrosine, an analogue of tyrosine, J. Med. Chem. 9 (1966) 828.

[12] DAVIS, A.L. et al., The synthesis and biological activities of o-aminophenylalamine and related compounds, Arch. Biochem. Biophys. 102 (1963) 48.

[13] BERLINGUET, L., Synthesis of 2-amino alcohols, Can. J. Chem. 32 (1954) 31.

[14] MOORE, S., STEIN, W.H., Chromatography of amino acids on sulphonated polystyrene resins, J. Biol. Chem. 192 (1951) 663.

[15] HIRS, C.H.W., MOORE, S., STEIN, W.H., The chromatography of amino acids on ion exchange resins, J. Amer. Chem. Soc. 76 (1954) 6063.

[16] DAVANKOV, V.A., ROGOZHIN, S.V., Stereoselective effects in α-amino acid copper (II) complexes, J. Chromatogr. 60 (1971) 28.

[17] BACZUK, R.J., LANDRAM, C.K., DUBOIS, R.J., DEHM, H.C., Liquid chromatographic resolution of racemic β-3,4-dihydroxyphenylalanine, J. Chromatogr. 60 (1971) 351.

DISCUSSION

C. MĂNTESCU: Did you try to use the fluorination of the diazonium salt in liquid hydrogen fluoride?

A.J. PALMER: No. Hydrogen fluoride is an inconvenient compound to use because of its corrosive nature.

IAEA-SM-171/9

PREPARATION OF ^{18}F-LABELLED FLUOROCARBONS FOR USE IN PHARMACODYNAMIC STUDIES

J.C. CLARK, R.W. GOULDING, A.J. PALMER
MRC Cylotron Unit, Hammersmith Hospital,
London,
United Kingdom

Abstract

PREPARATION OF ^{18}F-LABELLED FLUOROCARBONS FOR USE IN PHARMACODYNAMIC STUDIES.

For many years fluorocarbons, widely used components of aerosol propellents both for domestic and pharmaceutical use and known by a number of proprietary names including "Freon" and "Arcton", were considered to be inert. Recently doubts were cast on this belief and work is being carried out in many centres to investigate the possible causes of the reported toxicity. It was felt that labelled fluorocarbons would be of help in some investigations, and ^{18}F was chosen as having physical properties most suited to the investigations envisaged, namely in-vivo distribution studies using a scinticamera and retention studies using a whole-body counter. ^{18}F-labelled trichlorofluoromethane ("Freon-11") and dichlorodifluoromethane ("Freon-12") were prepared using both silver fluoride $Ag^{18}F$ and silver difluoride $Ag^{18}F_2$. $Ag^{18}F$ and $Ag^{18}F_2$ were both labelled by lining a neon-filled target vessel with carrier AgF or AgF_2. After irradiation with 14 MeV deuterons the neon was removed and the appropriate reactants added to the target vessel by vacuum transfer, the reaction then being carried out at an elevated temperature. The reaction products were removed by vacuum transfer and purified by radio-gas chromatography. The final product was then either diluted with air for rebreathing or transferred by vacuum distillation to aerosol dispensers for placebo administration.

INTRODUCTION

Several chlorofluorocarbons are used as propellents in a wide variety of aerosol generators both for domestic and pharmaceutical use. These propellents are known by a number of proprietary generic names including Freon ® and Arcton ®. For example, the compounds $CCl_{4-n}F_n$ are named in this system as Freon-1n or Arcton-1n. For many years these compounds have been considered to be pharmacologically inert [1, 2], but doubts were recently cast on this belief and work is being carried out in many centres to investigate the pharmacodynamics of these fluorocarbons in man and animals [3-5]. It was felt that labelled fluorocarbons would be of help in some investigations. Fluorine-18 was chosen as having physical properties most suited to the investigations envisaged in man, namely in vivo distribution studies using a scintillation camera and simultaneous retention studies using a whole-body counter. Some work has been reported where ^{38}Cl was used as the label [5] but its high gamma-ray energies of 1.60 and 2.17 MeV make it unsuitable for use with most imaging devices, in particular an Anger-type scintillation camera.

In the present work the method of administration to man was by means of a placebo aerosol drug dispenser of the Riker Medihaler ® type, in order to fully simulate certain clinical situations. Animal experiments were to be carried out using dilute mixtures of labelled fluorocarbons in air.

A direct synthetic route was chosen for the preparation of labelled Freon-11 and -12, CCl_3F and CCl_2F_2, using fluorides of silver [6, 7] as

the fluorinating agent. Preliminary investigations into recoil or hot-atom-labelling techniques using carbon tetrachloride/neon mixtures did not give promising results presumably because of the high radiation dose deposited in the target filling during ^{18}F production.

Fluorine-18 was introduced into the silver fluorides by an indirect method. Neon gas at 3.5 kgf/cm^2 was irradiated with deuterons in a static gas target, the inner walls of which were coated with fluoride. The hot atoms produced by the $^{20}Ne(d,\alpha)^{18}F$ reaction interact with the target walls resulting in the production of appreciable amounts of labelled silver fluorides.

The silver fluoride or difluoride layer was prepared fresh for each bombardment, and to facilitate this the target (Fig. 1) was fitted with a removable copper liner, silver plated on its inner surface. This liner was removed from the target for coating with the fluoride, and then replaced. A quick-release Triclamp ® was used to seal the removable back plate and a gauge was provided so that the pressure conditions inside the target could be continuously monitored during filling, irradiation and subsequent reaction stages.

After the irradiation the target vessel was evacuated and a suitable organic reactant (~2 g) introduced. The sealed vessel was then heated to temperatures of up to 170°C for 40-50 min, when ^{18}F-labelled fluorocarbons were produced by heterogeneous gas phase reaction, chemical yields of up to 90% (based on starting organic compound) and radiochemical yields of up to 40% (based on estimated starting activity) being obtained, as detailed in the following reactions:

$$2Ag^{18}F + CCl_3Br \xrightarrow{70°C} AgBr \cdot Ag^{18}F + CCl_3{}^{18}F \quad (1)$$

$$2Ag^{18}F + CCl_4 \xrightarrow{160-170°C} AgCl \cdot Ag^{18}F + CCl_3{}^{18}F \quad (2)$$

$$2Ag^{18}F_2 + 2CCl_3F \xrightarrow{160-170°C} 2Ag^{18}F + 2CCl_2{}^{18}F_2 + Cl_2 \quad (3)$$

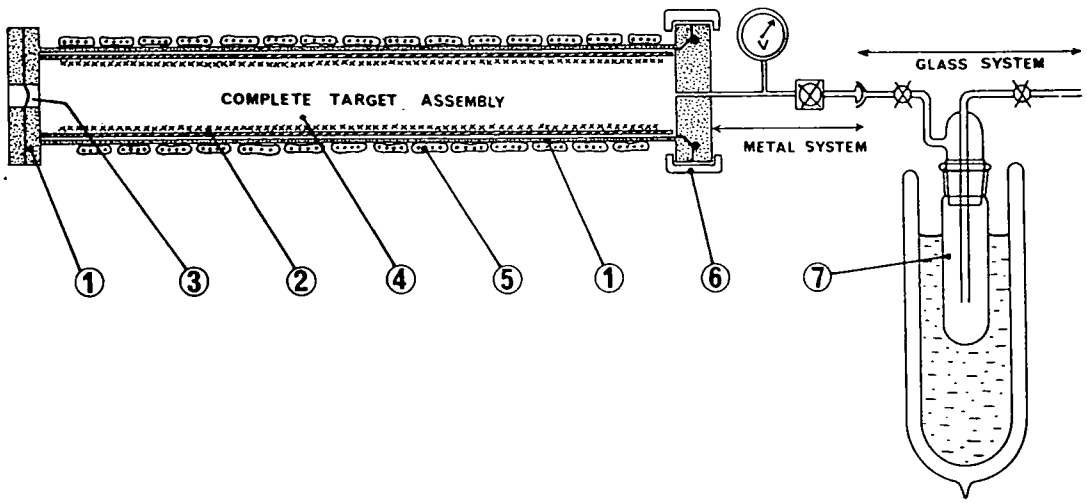

FIG. 1. Apparatus used for chemical reaction: 1. Aluminium pressure vessel, target 45-cm long, 6-cm diameter; 2. Silver-plated copper tube coated internally with silver fluoride or difluoride; 3. Beam entry window, 0.050-mm stainless-steel; 4. Reactant carbon tetrachloride; 5. Electrothermal ® heating tape; 6. Ladish ® quick-release clamp; 7. Product recovery trap.

For the production of Freon-11, reaction (1) has certain disadvantages. Bromotrichlormethane readily decomposes on heating, and significant amounts of the highly toxic compound carbonyl chloride (phosgene) are produced in the reaction. Reaction (2) does not suffer from these disadvantages and so is used routinely for the preparation of Freon-11. Freon-11 does not react under the same conditions at a significant rate with silver fluoride to give Freon-12; therefore the more reactive difluoride, reaction (3), is necessary.

In preliminary studies of these reactions, samples were withdrawn during the course of the reaction and analysed by radio-gas chromatography, so that the optimum reaction times could be determined. For routine production, after allowing the reaction to proceed for 40-50 min, the volatile products were distilled out of the reaction vessel into a cold trap. The desired product was isolated using preparative scale glc, when it was recovered from the helium effluent in a glass trap at -196°C. If necessary it was diluted with carrier on a glass and Teflon ® vacuum line, and a small sample transferred to a tared ampoule for specific activity determination. After this the required mixture of labelled and unlabelled Freons was made up in a modified Riker aerosol dispenser. Finally the dispenser was tested before clinical use.

EXPERIMENTAL

Target system for ^{18}F production

Fluorine-18 was produced from neon by the $^{20}Ne(d, \alpha)^{18}F$ reaction, C. P. Neon being contained in the target vessel shown schematically in Fig. 1. Preliminary irradiations of the target with a glass liner with 0.25 mm aluminium end cover foils and a neon-filling pressure of 3.5 kgf/cm^2 yielded 28 mCi/μAh for a 2 μAh irradiation with 14 MeV deuterons at a beam current of 20-25 μA [8].

A copper liner (Fig. 1.2), electroplated with silver internally to a thickness of 0.1 mm, was used to support the inorganic fluorinating agents which were to be labelled. This liner was introduced into the target from the back and the back plate secured by a quick-release clamp (Fig. 1.6). The target was also used as the reaction vessel, it being heated electrically at this stage.

Silver fluoride preparation

Two methods were used to coat the inside of the silver-plated tube with silver fluoride.

Evaporation of aqueous silver fluoride solutions

This method was used for most of the work when preparing Freon-11. 25% aqueous silver fluoride solution (25 ml) was evaporated under vacuum on to the liner while it was rotated and gradually heated with hot air to 50°-70°C. A schematic layout of this system is shown in Fig. 2. The apparatus consisted of a rotary evaporator with Teflon vapour duct and liquid nitrogen cold trap. The target liner was attached to this apparatus and

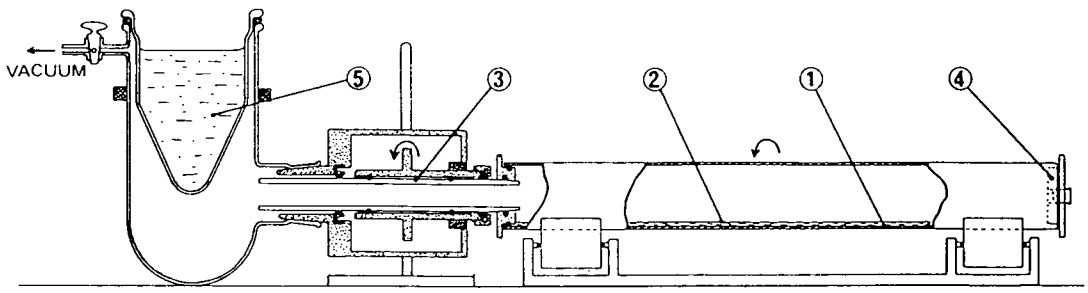

FIG. 2. Apparatus used for coating target liner with silver fluoride: 1. Copper tube (45-cm long, 5-cm diam.), silver-plated internally (0.1-mm thick); 2. 25% Aqueous solution of silver fluoride; 3. Rotary evaporator with Teflon liner; 4. Vacuum-tight end fittings (polythene); 5. Cold trap (liquid N_2).

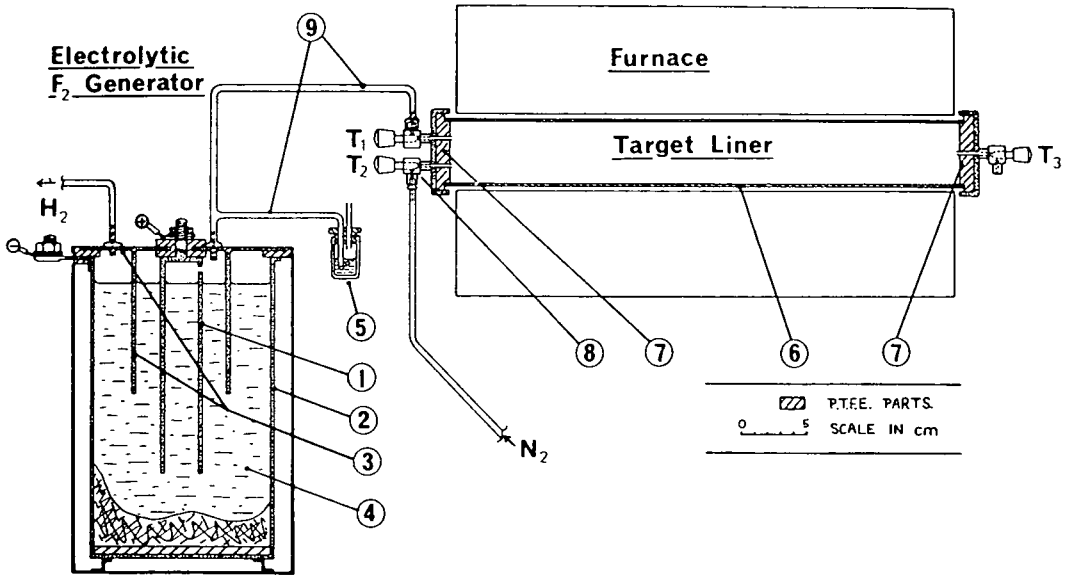

FIG. 3. Apparatus for the preparation of silver fluorides inside the target liner: 1. Anode, nickel; 2. Cathode, and containing vessel, mild steel; 3. Mild steel lid (insulated from both electrodes) and skirt to separate anode and cathode chambers; 4. Electrolyte, KF.2HF, maintained at 80°C; 5. Safety lute filled with KEL-F® oil; 6. Silver-plated copper tube mounted in furnace; 7. Teflon-sealed end caps; 8. Gas control valves, Teflon barrel in copper (modified Rotoflo ® valves); 9. Connecting tubes for fluorine gas, copper 5-mm i.d.

sealed by means of polyethylene plugs with neoprene "O"-rings, and was supported on rollers to facilitate rotation. This method resulted in a non-uniform deposit of silver fluoride of damp appearance, the colour of which varied from yellow to dark brown.

The reaction of heated silver with fluorine

A schematic layout of the system used is shown in Fig. 3. The silver-lined tube was purged with dry nitrogen and a small flow of fluorine then allowed to enter the tube until it was detected strongly at the outlet (moist potassium iodide paper). The fluorine was generated in a small electrolytic cell which had nickel anode and mild steel cathode. Other compo-

nents were steel and Teflon and the electrolyte was the salt KF.2HF maintained in a molten state at 80°C [9, 10]. The fluorine was conducted through 5 mm-bore copper tubing and copper taps with Teflon plugs. After filling the tube it was heated to 150°C, and the contents were sampled occasionally using KI paper by allowing a small volume to be purged by the nitrogen supply. When only traces of fluorine were detectable at the outlet the heating was stopped. The tube was then purged with nitrogen to waste until cool. The resulting silver fluoride appeared as a quite uniform greenish yellow layer. The quantity of the fluoride present, however, was unknown. After preparation the lined tube was handled under nitrogen.

Silver difluoride preparation

The silver-plated target liner was coated with silver difluoride using fluorine in a similar way to the preparation of the monofluoride described above, except that the temperature of the silver was raised to 350°C and the fluorine was passed through slowly until excess reagent was detected strongly at the waste outlet. After preparation the coated liner was handled under nitrogen as above.

Labelling of the silver fluorides with ^{18}F

The coated liner, prepared by any of the above methods, was introduced into the target vessel. In the case of fluorides derived from fluorine this procedure was carried out under dry nitrogen. The target was then evacuated and filled to a pressure of 3.5 kgf/cm^2 with CP Neon. Irradiations of the neon were carried out with 14 MeV deuterons at beam currents of up to 25 μA. No attempt was made to measure the total activity of silver halide produced.

Synthesis of ^{18}F-labelled Freon-11

After irradiation the neon was released, the target evacuated, and heated to 160°-170°C. Spectroscopic grade carbon tetrachloride (1.5 ml) was then transferred via the target valve into the target/reaction vessel. The temperature was maintained for 40 min, and then the reaction vessel was connected to an evacuated trap (Fig. 1.7) which was cooled to -196°C. When most of the target contents had distilled into the trap (1 min) it was opened to vacuum and the trapping-out procedure continued for a further 5 min. The trap was then isolated and the contents carefully melted and refrozen to obtain a concentration at the bottom of the trap. After allowing the pressure to rise in the trap it was dismantled and toluene (0.5 ml) added to simplify further handling procedures.

Synthesis of ^{18}F-labelled Freon-12

A procedure analogous to that adopted for Freon-11 was used, the main differences being the use of labelled silver difluoride and inactive Freon-11 as the starting materials. Although a detailed study of the temperature/time course of the reaction has not been undertaken, labelled Freon-12 was observed as the major condensable reaction product after 30 min at 160°-170°C.

Purification of the ^{18}F-labelled Freons

The compounds were separated from the crude reaction mixture by preparative gas liquid chromatography using a 22 ft × 3/8 in. (6 m × 10 mm) aluminium column of 20% SE 30 on 30-60 mesh chromosorb W operated at 60°C with a helium flow rate of 100 ml/min (injector 150°C, thermal conductivity detector 150°C). The effluent was passed through an unheated length of 2 mm ID Teflon tubing supported over a shielded NaI(Tl) scintillation counter. A simultaneous mass and radioactive concentration record was thus obtained. The crude product at -8°C was taken from the cooled trap (Fig. 1.7) using a 5 ml Hamilton type 1005 "Gas Tight", glass and Teflon syringe, and applied to the glc injector via a tap and large bore dwelling needle. A typical preparative chromatogram is shown in Fig. 4. The Freon-11 and -12 are eluted well before the other components of the mixture, carbon tetrachloride and toluene. The desired product, in this case Freon-11, was recovered by placing a small glass trap (Fig. 5A) at the radiation detector outlet, and cooling it to -196°C as the product was being eluted. Freon-12 may be purified in an analogous fashion although more care is necessary in handling the crude product before and during application to the column, since the boiling point of this compound is lower than that of Freon-11.

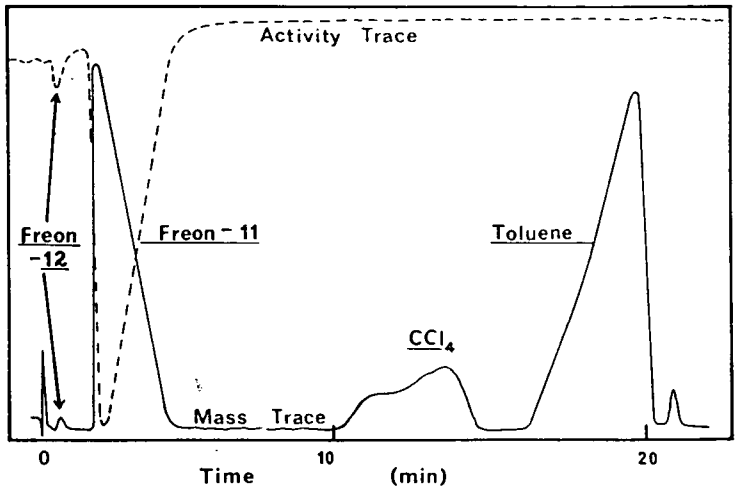

FIG. 4. Separation of ^{18}F-labelled Freon-11 from the crude reaction mixture by preparative gas liquid chromatography (after the addition of 30% toluene carrier, conditions as described in the text).

RADIOCHEMICAL ANALYSIS

Analytical chromatograms were obtained for the crude reaction mixtures and purified products using a 5 ft × 1/8 in (1.5 mm × 3 mm) stainless-steel column of 80-100 mesh Poropak-Q programmed from 160°C to 230°C (injector 160°C, detector 240°C). A typical mass trace of the crude reaction mixture from a Freon-11 preparation (2 μl injected on to the column) is shown in Fig. 6. In preliminary experiments the products were identified by infra-red spectroscopy and analytical glc, by comparison with authentic samples.

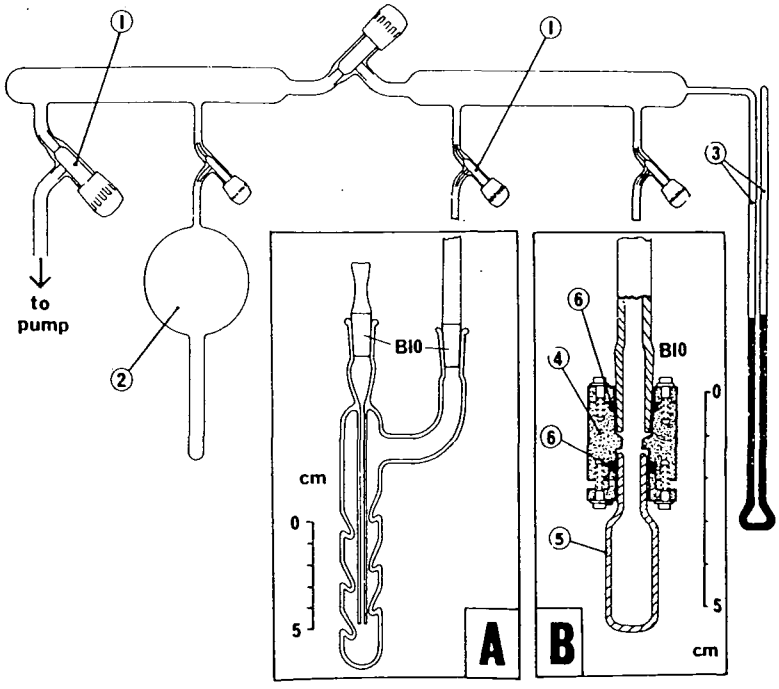

FIG. 5. Vacuum system used for dispensing ^{18}F-labelled Freons: 1. Rotoflo ® taps; 2. Vessel for storing Freon-12; 3. Pressure gauge, 0-400-mm Hg; Inset A: glc trap containing Freons-^{18}F, Inset B: Assembly for filling aerosol vial; 4. Connector from B10-cone to vial neck (stainless-steel); 5. Vial; 6. "O"-ring seals.

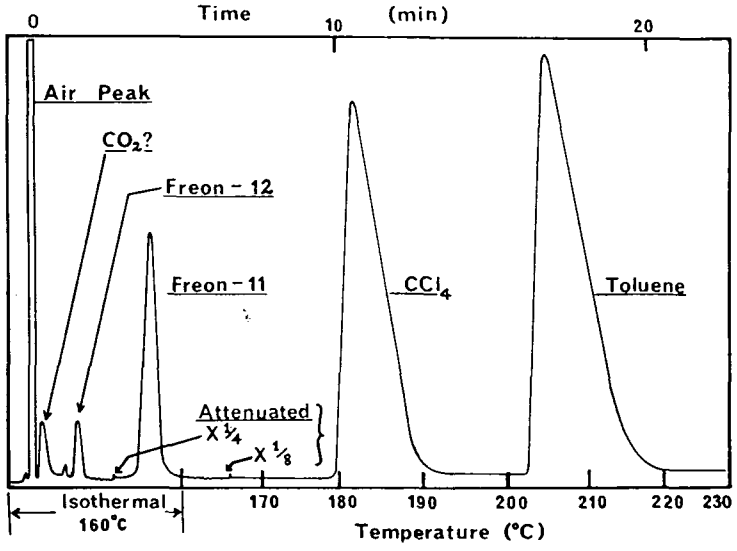

FIG. 6. Analytical gas chromatography of Freons; trace shows a typical crude Freon-11 reaction mixture, conditions as described in the text.

After the desired product had been collected in the trap (Fig. 5A) at the chromatograph output, the trap was quickly transferred to a vacuum line (shown schematically in Fig. 5). A small preweighed ampoule (Fig. 7C) was also attached to the vacuum manifold and a small fraction of the product distilled into it. The radioactive content of this container was then estimated using a calibrated re-entrant high-pressure (20 atm) argon-filled ionization chamber type IG 12. Finally the container was weighed. Thus a direct estimate of the specific activity of the product was obtained.

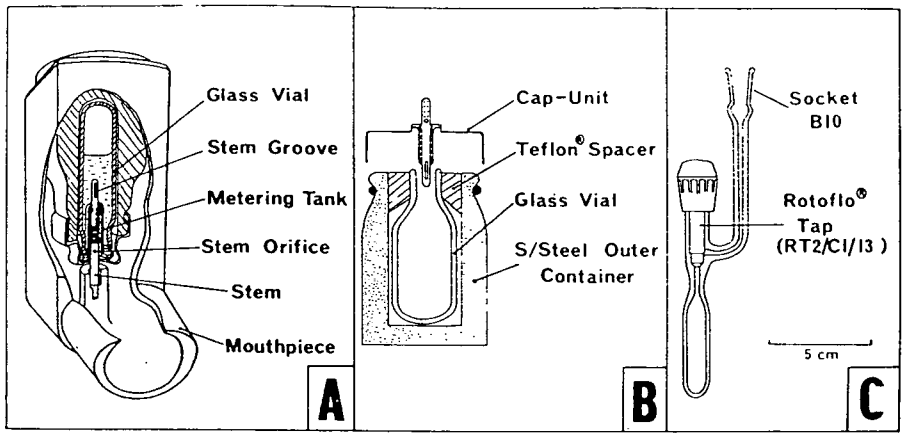

FIG. 7. A. Cross-sectional view of assembled aerosol spray unit containing labelled Freon, inverted for use and with the valve open.
B. The stainless-steel container, vial and valve assembly shown partially assembled.
C. Ampoule used for handling liquid labelled Freons, e. g. for weight determination.

PACKING AND DISPENSING

Animal investigations were carried out using air/fluorocarbon mixtures. These were prepared by evaporating weighed amounts of the fluorocarbon from the ampoule (Fig. 7C) into the chamber in which the animals were being exposed. For the investigations in man it was necessary to fill a clinical aerosol dispenser. The Riker clinical dispenser, the Medihaler Ⓡ, is widely used for the aerosol administration of pharmaceutical products (e. g. Isoprenaline for treatment of asthma), and was chosen for this study.

The main components are a thin-walled aluminium canister, a lid assembly with Spraymiser Ⓡ metering valve and an outer plastic holder/mouthpiece. The valve is contained in a sub-reservoir which ensures that it is charged with liquid Freon. A groove at the upper end of the stem allows the pressurized liquid to pass from the canister via the sub-reservoir into the metering tank which also houses a return spring.

When the canister is pressed into the holder the groove in the stem moves out of the metering tank and thereby isolates its contents (a measured dose) from the canister. This movement at the same time allows the small hole at the lower end of the stem to enter the metering tank. This provides an outlet for the measured dose which passes into the mouthpiece. When downward pressure is released the spring returns the stem to its former position and the tank refills.

In order to administer labelled fluorocarbon mixtures to human volunteers, a container of similar external appearance and operational characteristics was necessary. The thin-walled canister was replaced by a stainless-steel container (Fig. 7A, B) of identical external form. This had a central well in which the small glass vial (Fig. 5. 5 and Fig. 7) closely fitted. A Teflon collar was used to fill the dead space around the neck of the vial. The Spraymiser valve assembly and lid was used to complete the device, but was modified by the omission of the small sub-reservoir.

A recommended filling mixture for such a dispenser is Freon-12 (2 parts) Freon-11 (1 part by gas volume). The filling was carried out on the vacuum line shown in Fig. 5. The manifold section was filled to a suitable pressure with the labelled product which was then condensed into the vial. The amount introduced into the vial was determined from manometer readings. The inactive constituent was introduced by the same process. The vial was then rapidly transferred to the stainless-steel container while the contents were still frozen, and the valve assembly crimped on together with its sealing "O" ring. A leak test was then carried out by immersing the assembly in water, followed by discharge tests into 1-litre flasks with rubber septa. A needle adaptor was temporarily fitted to the Spraymiser valve to achieve this. The labelled fluorocarbon content of the flask was measured using a re-entrant ionization chamber thus giving a close estimate of the activity. This figure together with that for the specific activity enables the mass of fluorocarbon administered to the subject to be determined. In addition, the chemical composition of the mixture inside the aerosol dispenser may be checked by gas chromatography of a sample taken out of the flask.

DISCUSSION

The production rate of ^{18}F from neon by the $^{20}Ne(d, \alpha)^{18}F$ reaction with 15 MeV deuterons is far greater than that using 30 MeV alpha particles in the $^{16}O(\alpha, pn)^{18}F$ reaction. The results obtained suggest that a very large proportion of the ^{18}F product nuclei are caught in the silver fluoride lining and are available for synthetic incorporation.

The volume of 25% aqueous silver fluoride solution used was chosen in order to be sufficient to cover completely the interior of the liner on evaporation, while at the same time providing a reagent of sufficiently high specific activity when it was labelled. Reaction of fluorine with silver metal produces a much smaller amount of uniformly distributed silver fluoride and consequently could be used to produce labelled Freons with higher specific activities although this was not necessary for the present application.

Reaction at 170°C of carbon tetrachloride and silver fluoride produced by evaporation always resulted in the production of small amounts of Freon-12 (< 5%). However it was necessary to use silver difluoride and Freon-11 in order to produce ^{18}F Freon-12 at a satisfactorily high rate at this temperature (near the maximum attainable using the present target/reaction vessel). For repeated use a silver metal tube would be desirable since the silver layer on a plated tube is soon exhausted. In both types of reaction the aluminium vessel served adequately although it was not ideal because of corrosion problems. A nickel target would probably be more satisfactory.

It should be noted that the maximum attainable radiochemical yield in these reactions with silver fluoride is 50%. Silver fluoride forms molecular compounds with other silver halides produced in the reaction with organic halides. These contain and immobilize one equivalent of silver fluoride (reactions 1-3) [7]. The times and radiochemical efficiencies for several preparations of ^{18}F-labelled Freon-11 are given in Table I. All the production runs listed were carried out using silver fluoride produced

TABLE I. RADIOCHEMICAL EFFICIENCIES FOR ^{18}F-FREON-11 PREPARATION

Int. beam current (μAh)	Reaction times (min)	Activity ^{18}F-$CFCl_3$ (mCi) [a]	Radiochem. yield (%)	Specific activity [b] ^{18}F-$CFCl_3$ (μCi mg-1)	Total time for preparation and purification (min)
5	40	17 (67)	18	10.0	121
10	50	50 (81)	30	20.7	129
10	50	45 (89)	41	–	117
15	50	55 (98)	24	23.4	122
20	45	76 (73)	21	35.4	115

[a] The figures in brackets are the time after E. O. B. (min).
[b] After glc purification.

by evaporation of aqueous solution. This resulted in the production of up to 76 mCi of impure ^{18}F Freon-11 (from a 20 μAn bombardment) approximately 70 min after E. O. B. Purification by preparative scale glc took a further 40 min, producing a final product of specific activity ~ 35 μCi mg^{-1} ready for packaging for clinical use.

The chemical conversion of carbon tetrachloride (2.2g) was usually ~80%. Dilution of the product to a volume of ~3 ml with toluene enabled purification to be accomplished by a single preparative glc injection. The trapping efficiency at the glc outlet was ~ 90%, handling losses which did occur being mainly during transfer of the solution from the trap to the syringe. A system of direct transfer from the trap to the glc inlet port would be desirable.

CONCLUSION

The preparative method described above yielded gas chromatographically pure ^{18}F-labelled Freon-11 of specific activity of 20-30 μCi mg^{-1} at time of dispatch for clinical use. This was sufficient to provide satisfactory counting statistics and scintillation camera pictures when measured doses were administered to human volunteers from the modified Riker Medihaler dispenser. The results of investigations in man and rats will be published elsewhere.

The fluorination method described is of general application and could be used to prepare other volatile ^{18}F-labelled compounds. Its use in the preparation of polar involatile ^{18}F compounds, e. g. amino-acids or steroids, would be more difficult. In particular it would be necessary to produce the silver fluorides on a smaller scale and with much higher specific activities.

ACKNOWLEDGEMENTS

The authors wish to thank Professor C. T. Dollery of the Department of Clinical Pharmacology, R. P. M. S., Hammersmith Hospital, for his continuous encouragement throughout this work, and the cyclotron team who carried

out the irradiations. The guidance of W. Massingham of Birmingham University Chemistry Department was greatly appreciated when designing, constructing and commissioning the fluorine cell. We are also indebted to Riker Laboratories for the loan of special tools and supply of the components necessary for the assembly of the modified Medihaler, and to L. W. Brown for the construction of equipment used in this work. Silver plating of the target liners was kindly carried out by Somerville Laboratories Ltd, London.

SOURCES OF MATERIALS

25% Aqueous AgF solution	Hopkin & Williams Ltd
Neon CP grade	British Oxygen Co. Ltd
Quickfit Rotaflo ® valves	J. A. Jobling & Co. Ltd, Stone, Staffordshire
Electrothermal heating tape	Electrothermal Engineering Ltd, London
Triclamp ® type 4	Ladish Co., Triclover Division
High-pressure ionization chamber Type IG12	20th Century Electronics Ltd, Croydon, Surrey
Spraymiser ® metering valve and Medihaler ®	Riker Laboratories
Poropak Q	Waters Associates Ltd

REFERENCES

[1] UNDERWRITERS' LABORATORIES, Underwriters' Laboratories Bulletin, M.H. 2375, Chicago, Ill. (1933).

[2] SAYERS, R.R., YANT, W.P., CHORNYAK, J., SHOAF, H.W., Toxicity of Dichlorodifluoromethane: a New Refrigerant, US Bureau of Mines, Report of Investigations, 3013 (May 1930).

[3] DOLLERY, C.T., DRAFFAN, G.H., DAVIES, D.S., WILLIAMS, F.M., CONNOLLY, M.E., Blood concentrations in man of fluorinated hydrocarbons after inhalation of pressurised aerosols, Lancet ii (1970) 1164.

[4] PATERSON, J.W., SUDLOW, M.F., WALKER, S.R., Blood levels of fluorinated hydrocarbons in asthmatic patients after inhalation of pressurised aerosols, Lancet ii (1971) 565.

[5] MORGAN, A., BLACK, A., WALSH, M., BELCHER, D.R., The absorption and retention of inhaled fluororinated hydrocarbon vapours, Int. J. Appl. Radiat. Isotopes 23 (1972) 285.

[6] LOVELACE, A.M., POSTELNEK, W., RAUSH, D.A., Aliphatic Fluorine Compounds, A.C.S. Monograph No. 138, Reinhold, New York (1958) 3.

[7] HUDLICKY, M., Chemistry of Organic Fluorine Compounds, Pergamon Press, Oxford (1961) 51.

[8] PALMER, A.J., CLARK, J.C., GOULDING, R.W., ROMAN, M., "The preparation of ^{18}F labelled DL-3-fluorotyrosine", these Proceedings, IAEA-SM-171/8.

[9] HUDLICKY, M., Chemistry of Organic Fluorine Compounds, Pergamon Press, Oxford (1961) 45.

[10] LEECH, H.R., Laboratory and technical production of fluorine and its compounds, Quart. Rev. Chem. Soc. 3 (1949) 22.

RADIOCHEM.RADIOANAL.LETTERS 14/2/ 101 - 108 /1973/

THE PREPARATION OF FLUORINE-18 LABELLED COMPOUNDS USING A RECIRCULATORY NEON TARGET

J.C. Clark, R.W. Goulding, Maria Roman*, A.J. Palmer

M.R.C. Cyclotron Unit, Hammersmith Hospital, Ducane Road, London W.12, OHS, U.K.

Received 19 April 1973
Accepted 27 April 1973

A method for the preparation of flurine-18 labelled metal fluorides and organic diazonium tetrafluoroborates is described. ^{18}F is produced using a dynamic neon gas target system. The compound to be labelled is supported on a glass fibre filter paper which is mounted in the gas stream externally to the target vessel. The greatly improved specific activities of the product amino acids which may be obtained using this system are due to two factors. Firstly very much smaller starting amounts of the diazonium tetrafluoroborate may be used compared with previously reported methods. Secondly, the times required for chemistry following irradiation have been substantially reduced.

INTRODUCTION

In recent years considerable effort has been directed towards the synthesis of ^{18}F labelled organic compounds, with a view to their possible use as organ scanning agents. However, no compound has yet been prepared that has yielded encouraging results in clinical trials [1] Amongst the reasons for this are possibly the choice of compound, or insufficiently high specific activity. In addition to other types of compounds, there

*On temporary leave from the Laboratory of Labelled Compounds, Institute of Atomic Physics, Bucharest, Romania

are several references to the preparation of ^{18}F labelled amino acids in the literature[2-5]. Previously reported work has produced ^{18}F labelled amino acids with specific activities of 10-100 μCi mg^{-1} /after chemistry/ using aqueous solutions of ^{18}F produced from either water [2,3] or neon gas targets [4].

We now wish to report some preliminary results obtained from a recirculatory neon gas target system, similar to that used for ^{43}K production [6], in which several non-volatile compounds containing ionic or potentially ionic fluorine atoms have been labelled at high specific activities /5-10 mCi mg^{-1} at end of bombardement, eob/. Potassium fluoride, antimony trifluoride and six aromatic diazonium tetrafluroborates have been successfully labelled.

The inorganic fluorides may be used for introducing ^{18}F into non-aromatic compounds by the nucleophilic displacement of another halogen or a good leaving group /e.g. tosylate/. The reactions are carried out in anhydrous aprotic solvents e.g. DMSO, DMF, acetonitrile and hexamethyl phosphoramide /HMPA/. After about 1 hour reaction at reflux temperature, the mixture is cooled, diluted with water and the organic compounds extracted into ether or chloroform. Model compounds used have included bromocyclohexane and 1-bromoadmantane.

The diazonium salts labelled by this method may be precursors of useful synthetic intermediates e.g. /fluorobenzoyl chloride/, or the fluoro-analogues of useful bio-organic substrates /e.g. amino acids, Table 1/. We have prepared ^{18}F labelled p- and m- fluorophenylalanine /III a,b/, ^{18}F-3-fluorotyrosine /IIIc/, ^{18}F-5- and 6-fluorotyptophan /III d,e/ and ^{18}F-p-fluorobenzoic acid using this target system.

TABLE 1

Preparation of ^{18}F-labelled DL-amino acids

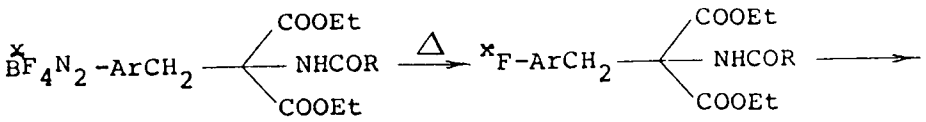

I/a-e/ II/a-e/.

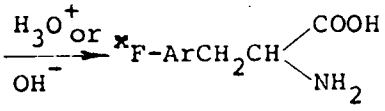

III/a-e/.

Ref.	Precursors /I/	Amino-acids /III/.	Lit.
a,p$^-$ b,m$^-$	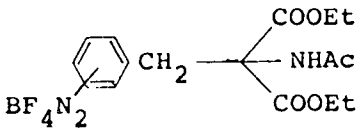	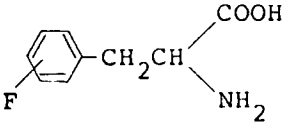	/2,3/
c	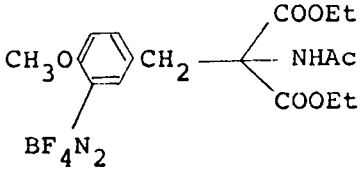	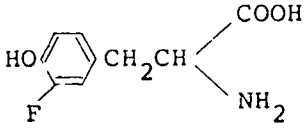	/3/
d,5$^-$ e,6-	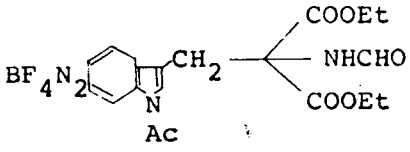	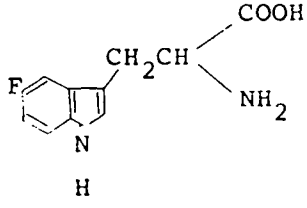	/4/

The diazonium salts are decomposed to give the corresponding fluorocompounds by heating in an inert high boiling solvent such as xylene, dichlorobenzene or diphenyl ether. These latter compounds are purified by adsorption chromatography, and then converted to the desired products by further chemical reactions as necessary.

Target system

Irradiation of C.P. neon with 15 MeV deuterons produces a reactive carrier free ^{18}F- containing species in the gas phase, by the $^{20}Ne/d, \alpha /^{18}F$ reaction. Since air is not rigorously excluded from the system and it has been shown that only compounds containing exchangeable fluorine atoms may be labelled, the activity is probably present as NO_xF or $\cdot O_2F$ and not $\cdot F$. The species has sufficient stability to be transported via ptfe tubing to a filter where a suitable fluoro-compound /5-20 mg/ will incorporate a large proportion of the ^{18}F activity.

The design of the system was dictated by the properties of the ^{18}F species. It is rapidly removed from the gase phase by aluminium; slowly removed by nylon, perspex, brass and glass; and is apparently inert towards ptfe and silver /all at 30-90°C/.

The cylindrial aluminium target vessel /45 x 6 cm, see Fig.1/ has a borosilicate glass liner connected to 2 mm I.D.

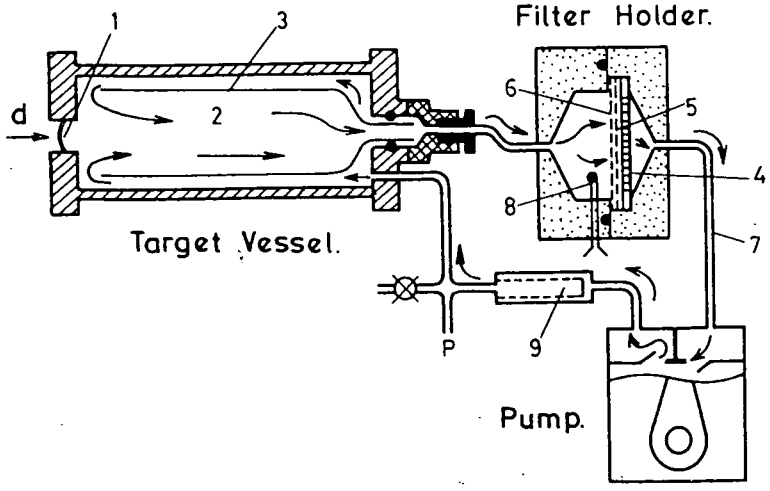

Fig. 1. Schematic diagram of the target system.
/1-Beam inlet, stainless steel 0.05mm, 2-Gas flow, 3-Borosilicate glass liner, 4-Inert supporting disc, 5-GFA backing disc, 6-GFA disc and fluoro-compound, 7-Ptfe lines with brass connectors, 8-Thermocouple probe, 9-Pre-filter for target inlet gas/

ptfe tubing as shown. The system is evacuated to ∿1 mm Hg and then filled with CP-grade neon to a pressure of 4 kgf.cm^{-2} and the gas is circulated at a flow rate of ∿10 litre/min λ / at 4 kgf. cm^{-2}/ by means of a Compton oil-free diaphram pump, type 415 IE* with 0.25 HP motor.

Most irradiations to date have been carried out at beam currents of 5-10 μA. The maximum beam current is determined by two factors, the first of which is the pressure of the neon in the system. It is desirable that the beam is completely attenuated before it reaches the back of the target, favouring a high pressure, but the maximum operating pressure is determined by the pressure rating of the pump. The second is the temperature of the gas entering the filter holder which must be kept below 100°C since diazonium tetrafluoroborates are temperature sensitive compounds.

The compound to be labelled /5-20 mg/ is coated onto a type GFA glass fibre filter paper /Whatman Ltd./, 3-5 cm in diameter. To achieve this the compound dissolved in a suitable solvent/ ∿1 ml/, namely water for potassium fluoride, ethanol f for antimony trifluoride and acetonitrile for the diazonium tetrafluoroborates, is applied to the filter element and the solvent allowed to evaporate. In the case of potassium fluoride the filter is dried at 120°C for 1 day before use. After the bombardement the GFA filter paper is removed from the filter unit and used without elution of the labelled fluoro-compound

* Dawson, Mc. Donald and Dawson Ltd. Ashbourne, Derbyshire, England

TABLE 2

Data for ^{18}F-labelled DL-amino acids, III /a-e/

Compound reference letter /I,II,III/	Weight of diazonium salt /mg/.	Activity collected on filter /mCi at eob/.	Activity of fluoro-ester II/a-e/ /mCi corrected to eob/.	Activity of DL-amino acid III /a-e/ /mCi at time of dispatch/	Specific activity of III/a-e/ /μCi mg^{-1} at dispatch/	Time elapsed from eob to dispatch /mins/.
/a/	11	58.9	4.50	1.18	930	155
/b/	16	47.9	2.10	0.705	800	130
/c/	17	61.0	1.60	0.445	215	140
/d/	11	33.8	2.45	0.560	365	200
/e/	18	151.8*	8.35*	2.58*	860*	160

Integrated beam current 4 μA hr except for /*/ where 12 μA hr was used.
Beam current 10 μA. ^{18}F production rate ~28 mCi/μA hr^{-1}. Neon pressure 4 kgf/cm^2.
For formulae of I,II,III /a-e/ see table 1.

from it. The filter paper is merely crumpled-up and introduced into the reaction mixture.

Preparation of ^{18}F-labelled DL amino acids:

The diazonium tetrafluoroborate /10-20 mg/ is labelled as described above. After bombardement the labelled product, I/a-e/, still on the GFA filter paper, is decomposed in diphenyl ether/biphenyl /Dowtherm A,~3 ml/ at 160-200°C. Decomposition is complete within 10 min and the resulting fluoro-ester, II/a-e/ now in solution, is purified by chromatography on basic alumina, eluting with 10-50% chloroform in toluene. The conditions for the final stage, namely hydrolysis to the free amino acid, III/ /a-e/, depend upon the particular compound. Compounds II/a,b/are heated in 13N sulphuric acid at 170°C for 30 mins[2] and II/c/ is refluxed in hydriodic acid/red phosphorus/acetic acid for 40 mins[4]. Compounds II/d,e/ are refluxed in 2.5N sodium hydroxide for 60 mins, treated with conc. hydrochloric acid to pH 1, and refluxed a further 10 mins.[3]

The final product is deacidified using IR4B/$O\bar{H}$/ resin, or alternatively in cases /a,b,d and e/ desalted using Poropak Q[7]. Radiochemical analysis of the product is by means of the tlc on silica gel[8], or by either high[9] or low[2,4]pressure ion exchange chromatography, and the specific activity determined by ionisation chamber assay and U.V. spectrophotometry[2,4].Data for several typical preparations are given in Table 2.

x

Many of the ideas concerning this target system were based on information supplied by Dr. Nozaki of the Institute of Physical and Chemical Research, Wako Shi, Japan, who has used a similar approach to ^{18}F labelling procedures.

REFERENCES

1. M.F.Cottrall, D.M.Taylor, T.J.McElwain, Brit.J.Radiol., 46 /1973/ 277.

2. R.W.Goulding, A.J.Palmer, Int.J.Appl.Radiation Isotopes, 23 /1972/ 133.

3. H.L.Atkins, D.R.Christman, J.S.Fowler, W.Hauser, R.M.Hoyte, J.F. Klopper, S.S.Lin, A.P.Wolf, J.Nucl.Med.,12 /1971/ 280, ibid,13 /1972/ 713.

4. A.J.Palmer, J.C.Clark, R.W.Goulding, M.Roman, "The preparation of ^{18}F-labelled DL-3-fluorotyrosine", presented at the Symposium on New Developments in Radiopharmaceuticals and Labelled Compounds, Copenhagen, Denmark, 26-30 March, 1973. Proceedings to be published by The International Atomic Energy Agency, Vienna, Austria.

5. G.Firnau, C.Nahmias, S.Garnett, Int.J.Appl.Radiation Isotopes, 24 /1973/ 182.

6. J.C.Clark, M.L.Thakur, I.A. Watson, Int.J.Appl. Radiation Isotopes, 23 /1972/ 329.

7. A. Niederwiesser, P.Giliberti, J.Chromatog.,61 /1971/ 81, ibid 95.

8. C.Haworth, T.A. Walmsley, J.Chromatog., 66 /1972/ 311.

9. A. Mondino, G.Bongiovanni, V.Noe, I. Raffaele, J.Chromatog., 63 /1971/ 411.

Thorax (1974), 29, 99.

Use of ^{18}F labelled fluorocarbon-11 to investigate the fate of inhaled fluorocarbons in man and in the rat

FAITH M. WILLIAMS, G. H. DRAFFAN, and C. T. DOLLERY

MRC Clinical Pharmacology Research Group, Royal Postgraduate Medical School, Du Cane Road, London W12

J. C. CLARK and A. J. PALMER

MRC Cyclotron Unit

P. VERNON[1]

Department of Medical Physics, Hammersmith Hospital, London W12

Williams, Faith M., Draffan, G. H., Dollery, C. T., Clark, J. C., Palmer, A. J., and Vernon, P. (1974). *Thorax*, 29, 99–103. Use of ^{18}F labelled fluorocarbon-11 to investigate the fate of inhaled fluorocarbons in man and in the rat. The distribution and elimination of ^{18}F labelled fluorocarbon-11 has been followed in a group of rats killed after air breathing following six minutes' exposure to ^{18}F fluorocarbon-11. Whole body and individual organ count rates were measured. In four volunteers the fate of ^{18}F labelled fluorocarbon-11 was followed by both whole body counting and gamma camera measurement of the activity in the lung and mouth region after inhalation from a specially loaded aerosol dispenser.

In the rat there was a high initial level in high blood flow organs and in the adrenals and fat: the level in blood and high blood flow organs fell rapidly. Elimination from fat was slow but the adrenal level had fallen within one hour. The fall in whole body count rate was similar to that in fat.

In man, the fall in lung concentration was consistent with rapid uptake into tissues followed by slow elimination; the whole body count rate curve also indicated slow elimination. There was no evidence of deposition of droplets of fluorocarbon in the mouth region after use of the aerosol.

The present investigation was undertaken as part of a series (Draffan, Dollery, Williams, and Clare, 1974) designed to evaluate the hazards that might arise from the fluorocarbon propellants used in pressurized aerosol products for the treatment of asthma. The aim was to determine the absorption, distribution, and elimination of fluorocarbons in man and rat.

The levels of fluorocarbons-11 and -12 (F-11, CCl_3F; F-12, CCl_2F_2) in arterial and venous blood and alveolar air have been measured in man following the use of an aerosol inhaler (Dollery *et al.*, 1970; Paterson, Sudlow, and Walker, 1971; Dollery *et al.*, 1974; Draffan *et al.*, 1974). Immediately after use of the inhaler the concentration of fluorocarbon in arterial blood rose to a peak and then fell again, initially rapidly and then more slowly. The slow phase probably reflected elimination of fluorocarbon concentrated in the tissues and fat deposits. Morgan, Black, Walsh, and Belcher (1972) investigated the retention of ^{38}Cl fluorocarbon after inhalation of the vapour, by counting the expired gas, and drew a similar conclusion.

These studies were made with cyclotron produced ^{18}F fluorocarbon-11. ^{18}F has a radiation (51 KeV) suitable for external detection and a half-life of 110 minutes. The count rate/time curves of the whole body and specific organs in rats exposed to ^{18}F fluorocarbon vapour were measured. In man, distribution and elimination were followed by whole body counting and use

[1]Present address: Department of Nuclear Medicine, Charing Cross Hospital, London

Requests for reprints to: Dr. C. T. Dollery, Royal Postgraduate Medical School, Du Cane Road, London W12

of a gamma camera after inhalation from a specially loaded aerosol dispenser, similar to that used by patients with asthma.

METHODS

PREPARATION OF FLUOROCARBON-11 LABELLED WITH ^{18}F (described in greater detail by Clark, Goulding, and Palmer (1973)) Fluorine-18 was prepared as silver fluoride by the cyclotron irradiation of a vessel filled with neon and lined with carrier silver fluoride. The nuclear reaction used was $^{20}Ne(d,\alpha)^{18}F$. After the irradiation with 15 MeV deuterons the neon was removed and CCl_4 was transferred into the target vessel which was then heated to 170°C when the following reaction proceeded:

$$CCl_4 + 2Ag^{18}F \xrightarrow{170°C} CCl_3\,^{18}F + AgCl\,Ag^{18}F$$

The target contents were removed after a reaction time of 30–40 minutes by vacuum distillation into a trap at −196°C. The contents of the trap were diluted with toluene to raise the boiling point of the mixture and thus simplify the subsequent handling of CCl_3F (boiling point 23°C at 760 mmHg). This mixture was then purified by radio-gas chromatography. Purified samples of fluorocarbon-11 were recovered at the chromatograph outlet by condensation at −196°C, the specific activity being typically 20 μCi/mg at the end of chemistry for a 10 μAhr irradiation.

Fluorocarbon-11 was diluted with air for rebreathing by rats. For studies in human volunteers, it was mixed with stable fluorocarbon-12, CCl_2F_2, and transferred to an aerosol dispenser by vacuum distillation so that one pressure on the dispenser released 50 mg fluorocarbon containing 1 mCi ^{18}F.

DISTRIBUTION OF ^{18}F FLUOROCARBON-11 IN THE RAT Rats (100 g male Wistar under light nembutal anaesthesia) were exposed to an atmosphere of 0·3% v/v ^{18}F fluorocarbon-11 in air in a sealed 20 litre Perspex box fitted with a fan to maintain a uniform atmosphere. The animals were removed after a 6-minute exposure and killed by decapitation at 0, 15 or 60 minutes. (At 0 minutes the animals were killed under anaesthesia while still in the fluorocarbon atmosphere because of its rapid elimination from the blood on breathing air.) Blood and tissue were rapidly removed after death to sealed containers and counted in a NaI (Tl) well scintillation counter. The tissue levels of fluorocarbon-11 at each time were calculated. The whole body fluorocarbon content of a single rat was followed by observing its whole body ^{18}F activity using a 6×4 in NaI (Tl) detector. The rat was retained in a fixed geometry in a container which was ventilated to waste by means of a fan to prevent the accumulation of exhaled activity. From a phantom calibration of the whole body counter the whole body content of fluorocarbon-11 was calculated. In order to estimate the correction necessary due to surface adsorption on the skin and fur a dead rat was simultaneously exposed to the fluorocarbon vapour and the ^{18}F activity was estimated under similar geometric conditions. The skin contribution was less than 1%.

FATE OF ^{18}F FLUOROCARBON-11 IN MAN AFTER NORMAL ADMINISTRATION FROM AN AEROSOL DISPENSER This was investigated in four healthy male volunteers who were free of respiratory disease. The subject was seated and a gamma camera (Nuclear Enterprises Mark III) was placed against the body. On the other side of the subject at approximately 2 metres was a single 6×4 in NaI (Tl) detector used to count radiation from the whole body.

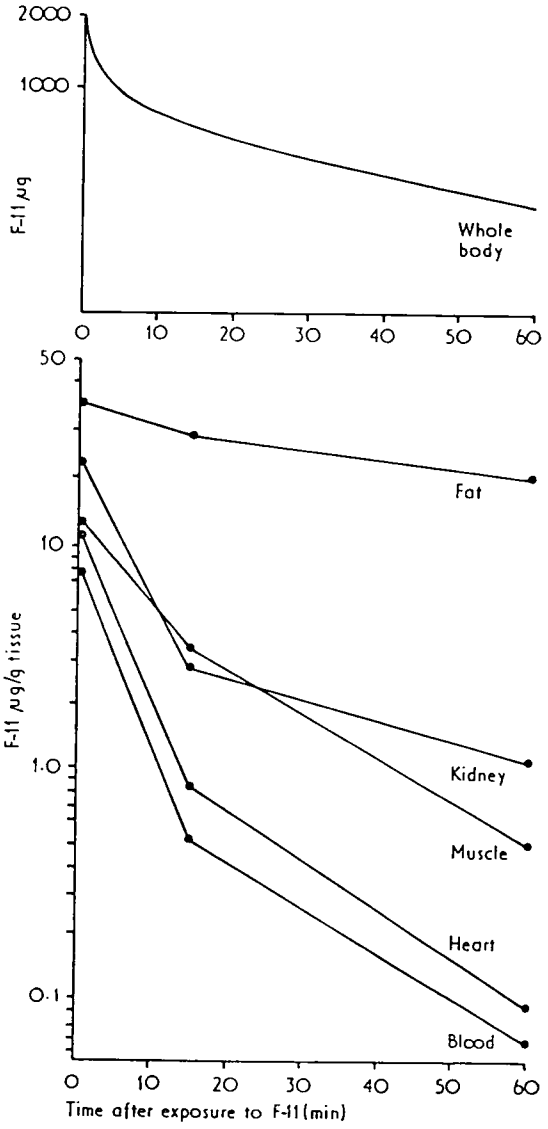

FIG. 1. *Decline of fluorocarbon-11 concentration from whole body and individual organs of rats in air, after breathing F-11, 0·3% vol/vol, for 6 minutes.*

Expired fluorocarbon was removed by enclosing the volunteer's head in a Perspex hood which was exhausted by a vacuum cleaner.

After the volunteer had inhaled one puff from the canister, he held his breath for five seconds, during which time the canister was removed from the room and the vacuum cleaner was switched on. The whole body counter was switched on before the study and the gamma camera immediately after the canister had left the room. Volunteers were seated with back to camera, with either lungs or neck region in the field of view, or with side to the camera and neck region in the field. The volunteer remained stationary in the hood for two minutes during which time the gamma camera was in operation. After this time the volunteer relaxed within the hood but maintained a constant position, and whole body measurements were continued for 20 minutes. Frequent background measurements were made with the volunteer removed to check that no expired radioactivity remained in the hood.

Data from the gamma camera were digitalized and recorded on magnetic tape and subsequently processed on a CDC 6600 computer (Vernon and Glass, 1971). On the processed gamma camera pictures, areas were delineated and the activity/time curves were obtained for each area. The areas delineated were in the lung and mouth regions.

Data from the whole body NaI (Tl) detector measured in counts per one second interval were stored in a multichannel analyser and corrected for background and decay. From a water phantom calibration the whole body content of fluorocarbon-11 could be determined.

RESULTS

FATE OF ^{18}F FLUOROCARBON-11 IN THE RAT The levels of fluorocarbon-11 were measured in whole blood, heart muscle, psoas muscle, liver, kidney, spleen, lung, brain, adrenal, and fat. The levels of fluorocarbon in tissues at 0, 15, and 60 minutes after 6 minutes' rebreathing fluorocarbon (0·3% v/v) are shown in Figure 1. The rate of elimination of fluorocarbon from the heart and blood was similar, with a constant ratio of 1·8 to 1. Fluorocarbon-11 was also rapidly eliminated from the other high blood flow organs, kidney, liver, spleen, lung, and brain. The level in fat was greater than in other tissues. The slow elimination of fluorocarbon from the fat was similar to the fall in whole body count rate (Fig. 2). It is of interest that a high concentration of fluorocarbon-11 was present in the adrenal at 0 and 15 minutes but this had declined by 60 minutes.

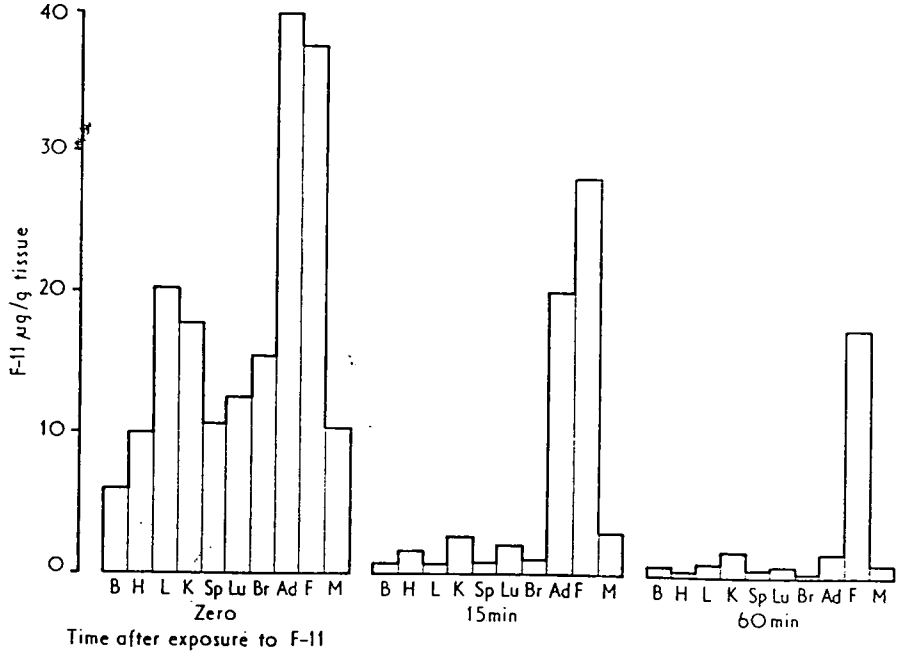

FIG. 2. *Histogram showing the decline in individual organs in the same group of rats as in Figure* 1.
B=blood, H=heart, L=liver, K=kidney, S=spleen, Lu=lung, Br=brain, Ad=adrenal, F=fat, M=skeletal muscle.

carbon concentration fell more slowly but had reached a low value by 60 minutes. Elimination from fat was very slow and had not reached half the initial value by one hour. The slow rate of elimination from fat must reflect a high tissue: blood partition coefficient and a low blood flow per unit mass of tissue. The blood: heart muscle ratio, 1:1·8, agrees well with that found *in vitro* using dog heart muscle (Dollery *et al.*, 1974). Cox, King, and Parke (1972) found that 97% of a single dose of fluorocarbon-11 given to a rat was expired unchanged within six hours, indicating that the radioactivity measured in our studies represents unchanged fluorocarbon.

The whole body count rate in man initially fell quickly. The final phase in our studies ($t\frac{1}{2}$ range 12 to 20 minutes) was shorter than that observed by Morgan *et al.* (1972), who measured expired ^{38}Cl fluorocarbon-11 ($t\frac{1}{2}$ approximately 100 minutes).

The profile of fluorocarbon elimination from the lung indicated an initial transfer of the dose to the blood stream and uptake by tissues and later pulmonary excretion of fluorocarbon released from the tissues and fat. The time course of elimination from the lung observed using the gamma camera was similar to the elimination from alveolar gas measured by mass spectrometry (Draffan *et al.*, 1974). The absence of an early peak and initial fall in count rate in the mouth region suggests that fluorocarbon-11 was not deposited in the mouth as droplets. If droplets had formed one would expect to see a rapid fall in count rate with the first breath as the droplets were volatilized and washed directly out of the mouth.

The main factor influencing the elimination of fluorocarbon-11 from the body is concentration in fat depots. The slow release of fluorocarbon from fat into blood should not prove any hazard to the heart of man. The high concentration in the adrenal gland must also reflect its lipid content. Perfluro-n-hexane (C_6F_{12}) can bind to microsomes and *in vitro* can act as an inhibitor of oxidation (Ullrich and Diehl, 1971). Fluorocarbon-11 (CCl_3F) will probably act in a similar manner. However, it is improbable that a high concentration would persist for long enough in man, after normal use of an aerosol inhaler, significantly to inhibit the formation of adrenal steroids.

REFERENCES

Clark, J. C., Goulding, R. W., and Palmer, L. A. J. (1973). The preparation of ^{18}F labelled fluorocarbons for use in pharmacodynamic studies. In *New Developments in Radiopharmaceuticals and Labelled Compounds*. IAEA, Vienna STI/PUB/344.

Cox, P. J., King, L. J., and Parke, D. V. (1972). A study of the possible metabolism of trichlorofluoromethane. *Biochemical Journal*, **130**, 13P.

Dollery, C. T., Draffan, G. H., Davies, D. S., Williams, Faith M., and Conolly, M. E. (1970). Blood concentrations in man of fluorinated hydrocarbons after inhalation of pressurised aerosols. *Lancet*, **2**, 1164.

—— Williams, F. M., Draffan, G. H., Wise, G., Sahyoun, H., Paterson, J. W., and Walker, S. R. (1974). Arterial blood levels of fluorocarbons in asthmatics following use of pressurised aerosols. *Clinical Pharmacology and Therapeuatics*, in press.

Draffan, G. H., Dollery, C. T., Williams, Faith M., and Clare, R. A. (1974). Alveolar gas concentrations of fluorocarbons-11 and -12 in man after use of pressurised aerosols. *Thorax*, **29**, 95.

Morgan, A., Black, A., Walsh, M., and Belcher, D. R. (1972). The absorption and retention of inhaled fluorinated hydrocarbon vapours. *International Journal of Applied Radiation and Isotopes*, **23**, 285.

Paterson, J. W., Sudlow, M. F., and Walker, S. R. (1971). Blood-levels of fluorinated hydrocarbons in asthmatic patients after inhalation of pressurised aerosols. *Lancet*, **2**, 565.

Ullrich, V. and Diehl, H. (1971). Uncoupling of monooxygenation and electron transport by fluorocarbons in liver microsomes. *European Journal of Biochemistry*, **20**, 509.

Vernon, P. and Glass, H. I. (1971). An off-line digital system for use with a gamma camera. *Physics in Medicine and Biology*, **16**, 405.

Progress in Respiration Research
Editor: H. Herzog, Basel
Publishers: S. KARGER, Basel
SEPARATUM (Printed in Switzerland)

Free Communications

Prog. Resp. Res., vol. 9, pp. 249–253 (Karger, Basel 1975)

An External Counting Method for Regional Measurements of Extravascular Lung Water[1]

F. FAZIO[2], J. C. CLARK, P. D. BUCKINGHAM, C. G. RHODES, F. R. HUDSON, HAZEL A. JONES, T. JONES and J. M. B. HUGHES

Departments of Medicine, Medical Physics and MRC Cyclotron Unit, Hammersmith Hospital, London

Introduction

An estimation of extravascular lung water volume (ELWV) can be made *in vivo* by the standard double indicator technique of CHINARD and ENNS [1]. This technique requires an injection in the venous side of the circulation of a mixture of tracers, one non-diffusible indicator (NDI) or intravascular reference tracer and the other freely diffusible in the interstitial spaces (DI), and arterial sampling of the downstream dilution curves.

The downslope of each curve is then extrapolated in order to eliminate recirculation, and mean transit time (MTT) is calculated.

The ELWV is calculated as:

$$ELWV = (\bar{t}_{DI} - \bar{t}_{NDI})F,$$

where F is the water flow through the lungs (i.e. the water content of the cardiac output) and $\bar{t}_{DI}$ and $\bar{t}_{NDI}$ are, respectively, the MTT for the DI and for the NDI.

Indicators labelled with γ-emitting radioisotopes have already been used as intravascular tracers. On the other hand, the water tracer which is commonly used is THO (tritiated water), a β-emitter which cannot be detected externally. For this reason, it requires arterial sampling and time-consuming laboratory procedures for liquid scintillation counting. Our aim was to

1 Supported in part by grant 73.00490.04 of the Italian National Research Council.

2 On leave from CNR Laboratory of Clinical Physiology, Pisa, Italy. Recipient of a Wellcome Trust Fellowship.

develop a non-invasive method for the estimation of lung water by external recording of dilution curves over the chest.

Therefore, we decided to substitute a γ-emitting radioisotope for THO. The γ-emitting water tracer with the longest half-life $H_2{}^{15}O$ (2.05 min half-life, 511 keV energy) was chosen as the DI. Red blood cells labelled with C^{11} monoxide (20.3 min half-life, 511 keV energy) were used as intravascular tracers. Both isotopes were prepared in the MRC Cyclotron at Hammersmith Hospital.

Methods and Results

Dogs anaesthetized with chloralose were studied in the supine and erect postures. Injections of $H_2{}^{15}O$ and $C^{11}O$ red cells were made via a catheter placed in the superior vena cava, with an interval of approximately 5 min between injections. Blood was withdrawn by a Harvard pump via two identical catheters simultaneously from the aorta (Ao) and the pulmonary artery (PA) and allowed to flow through a coil in front of a scintillation crystal. Time-activity curves, representing the input (PA) and the output (Ao) of the pulmonary circulation, were recorded on a multi-channel analyser. Time-activity curves for two regions of the right lung (apex and base) were also recorded externally by means of probes collimated over the chest. To assess regional distribution of blood flow, ^{125}I-labelled albumin microspheres were injected. The animal was killed, the lungs excised, dried, and sliced. Slices were counted and blood flow distribution from base to apex expressed in counts per gram of dry lung.

Figure 1 shows regional time-activity curves for $H_2{}^{15}O$ and ^{11}CO-RBC in a supine dog. The count rates and definition of these curves are sufficiently good for regional lung water to be measured not only with the double extrapolation technique, but also with the more sophisticated deconvolution procedures [2] required for the determination of the true frequency function of transit times (and consequently the true MTT) for water in the extravascular spaces of the lung.

Figure 2 shows curves from similar regions in a dog tilted head up for about 3 h. Whereas the curves obtained from the bottom of the lung show a steep downslope followed by a recirculation phase, the shape of the curves recorded from the top are very shallow with recirculation poorly defined. The latter resemble arterial dilution curves obtained from heart patients with very low cardiac output [3]. In fact, the erect anaesthetized dog presents a very large gradient of perfusion from apex to base of the lung. Figure 3 shows the distribution of blood flow per gram of dry lung in one erect and one supine dog. Whereas the horizontal dog presents a reasonably uniform

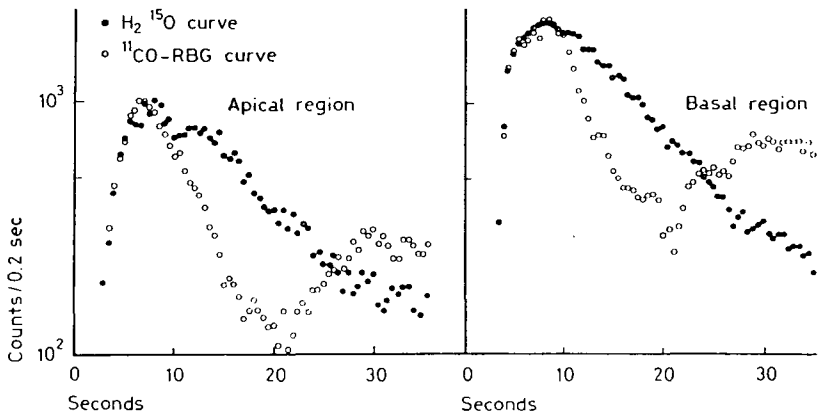

1

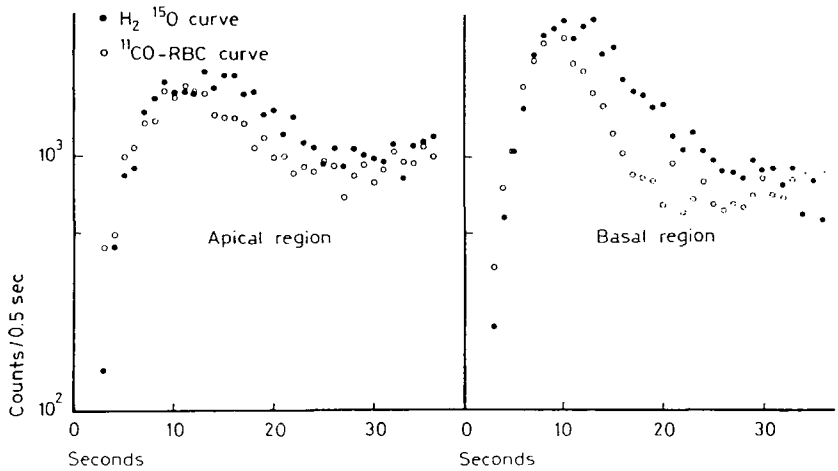

2

Fig. 1. Semilogarithmic plot of time activity curves recorded externally over the chest in a supine dog after injection of tracers in the superior vena cava. On the right: curves from a probe collimated over the base of the right lung. On the left: curves from a probe collimated on the right apex. For each region two curves are shown: one obtained after injection of the non-diffusible tracer, ^{11}CO-RBC (open circles), and one obtained after injection of labelled water (dots). In the supine position, both regions are at the same gravity level and no gross regional differences are evident in MTT for each tracer.

Fig. 2. Same curves as in figure 1 but in an erect dog. The curves recorded from the base (on the right) show a steep downslope followed by a recirculation phase, but the curves recorded from the top (on the left) are shallow with recirculation poorly defined. Estimation of extravascular lung water from the latter using the standard double extrapolation technique can lead to gross errors.

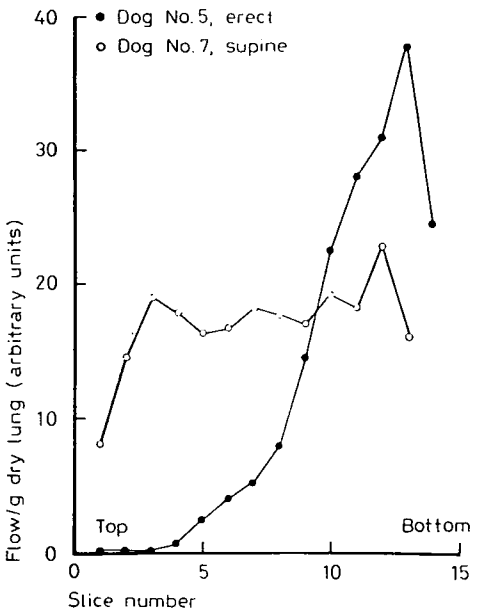

Fig. 3. Distribution of blood flow per gram of dry lung from base to apex in a supine and in an erect dog, obtained by ^{125}I microspheres injection and postmortem counting of dried lung slices. No significant differences of flow are present between base and apex in the supine dog, whereas the erect dog has almost no perfusion in the upper half of the lung.

distribution of blood flow per gram of dry lung, almost all the flow in the vertical dog is confined to the lower third of the lung. This means that most of the tracer is routed through those regions; therefore, the MTT of the downstream arterial dilution curve reflects principally these high flow areas, misrepresenting the MTT through low flow zones. This is, in our opinion, one of the reasons for the variable underestimation of the actual content of water with the standard technique which relies on arterial sampling and double extrapolation [4]. To resolve the true spectrum of transit times from the lung for different tracers, the regional data should be deconvoluted by the input function (PA curve) in the pulmonary circulation.

References

1 CHINARD, F. P. and ENNS, T.: Transcapillary pulmonary exchange of water in the dog. Am. J. Physiol. *178:* 197–202 (1954).

2 GIUNTINI, C. and FAZIO, F.: Extravascular lung water: its measurement by simultaneous pulmonary and aortic sampling and iterative convolution. IAEA Symp.

Dynamic Studies with Radioisotopes in Clinical Medicine and Research, Knoxville 1974.

3 GIUNTINI, C.; FAZIO, F., and MANCINI, P.: Determination of transit time distribution of extravascular lung water; in Central hemodynamics and gas exchange, edited by C. GIUNTINI, pp. 459–472 (Minerva Medica, Torino 1971).

4 PEARCE, M. L.; YAMASHITA, J., and BEAZELL, J.: Measurement of pulmonary edema. Circulation Res. *17:* 414–426 (1965).

Dr. F. FAZIO, Departments of Medicine, Hammersmith Hospital, *London W12 OHS* (England)

Short-lived Radioactive Gases for Clinical Use

J. C. CLARK, BSc

and

P. D. BUCKINGHAM, AIST

Medical Research Council, Cyclotron Unit, Hammersmith Hospital, London

BUTTERWORTHS
London and Boston

Medical and Biological Eng.

book reviews

cc. Prof Davies for circulation 20.1.76

Shortlived radioactive gases for clinical use by J. C. Clark and P. D. Buckingham. *Butterworths*, London), 1975, 353 pp., £9·50

A considerable number of cyclotrons, in many parts of the world, are now being used in the regular production of radioisotopes for medical work, and when these cyclotrons are sited within a hospital complex, one of the anticipated applications is in the use of short-lived radioactive gases. This monograph, with nine chapters, seven appendixes, 36 tables and 128 illustrations, provides an exhaustive technical account of methods developed for the production of ^{15}O, ^{13}N, ^{11}C and radioisotopes of the rare gases. The work described derives largely from the authors' extensive experience with the Medical Research Council Cyclotron Unit at Hammersmith Hospital, but for completeness there is a short description of the techniques used elsewhere for the preparation of ^{133}Xe from the fission products of ^{235}U.

The first four chapters are concerned with general techniques, such as target design, gas handling and the types of facilities used for clinical measurements; four chapters deal with individual radionuclides and a final chapter with hazards and precautions. The monograph is intended primarily for the radioisotope producer and cyclotron operator; detailed critical and comparative accounts are given of techniques of preparation and constructional details of apparatus and of measuring systems with, in essence, operating manuals for particular recommended procedures. The hazards that can arise are described fully; they include the apposite and alarming item that there is no internationally agreed colour code for gas cylinders and on the very practical level a recommended method for making up and storing 5N NaOH solution. The authors also comment, in relation to hazards to the patient (p. 317) 'while it is the responsibility of the clinician in charge to ensure that no patient inhales any dangerous quantity of toxic or inflammable gas, it behoves all concerned with the use of such gases to be aware of the risks involved' and points out the dangers that can arise from CO, HCN, ozone and oxides of nitrogen, and from mixtures of H_2 and air. They remark that 'the clinical application of ^{81m}Kr requires a certain amount of ingenuity' and the book is a tribute to the authors' own ingenuity in designing and commissioning so many techniques for the production and use of these short lived gases. However, it should be noted that those who wish to gain an overall critical impression of the present scope of the clinical applications and the role of the gases in diagnosis, clinical investigation or physiological research, will not find the answers in this book: they are directed to the journal literature and numerous references are provided.

It is a pity that so much skill and ingenuity cannot for the present find many applications in the United Kingdom, outside of the Hammersmith Hospital. Although the book must be a warning to prospective cyclotron users not to underestimate the complexity of the techniques needed to exploit their potential in the manufacture of the short-lived radioactive gases, nevertheless with such a detailed guide now available it is clear that many such users will find the path smoothed for them by the pioneering work reported here. The book is well produced and copiously illustrated. In relation to the cost of a cyclotron, or indeed of any one sample of radioactive material, the price is reasonable.

N. G. TROTT

Active filters for integrated circuits by Walter E. Heinlein and W. Harvey Holmes. *Prentice-Hall International*, 1974, 668 pp., £21

The subtitle of this volume is 'Fundamentals and design methods'. It is a textbook on the theory of, the design of, the synthesis of and practical problems with active filters, both discrete and integrated. Most of it is devoted to linear active *RC* filters and it is aimed at advanced students and practising engineers. Although basically a textbook it has good cross-references and a subject

Short-lived Radioactive Gases for Clinical Use. By J. C. Clark and P. D. Buckingham, pp. xii + 353, 1975 (London, Butterworth), £9·50.

This excellent monograph sets out in a clear and orderly format the detailed technology for producing gaseous radionuclides suitable for pulmonary function and other clinical work. Inevitably it is a specialist's book, since most doctors and physicists using radioactive gases are more concerned with the clinical aspects of the subject than with details of manufacture, yield, and design of processing systems for radiopharmaceuticals. Furthermore a large proportion of the book is devoted to the really "short-lived" gases, $^{13}N_2$, $^{15}O_2$, ^{11}CO and $^{11}CO_2$, which are of only academic interest to those not in close proximity to a cyclotron. The authors devote little space to ^{133}Xe, presumably because its technology is well known, but do give useful sections on ^{127}Xe and ^{135}Xe, and the radionuclides of krypton, of which $^{81}Kr^{m}$ has been shown to be of promise for regional ventilation studies. A section on dispensing and clinical facilities brings the subject closer to the hospital department, but if a multiprobe detector system is to be described in such detail, is not a scintillation camera worthy of mention also? For such a specialist book it seems unnecessary to fill even a small chapter with the elements of nuclear physics, but this happens too often in books concerned primarily with the application of radioactive substances to medicine.

With its attention to detail, clear illustrations, and inclusion of useful appendices on mathematical analysis this book is of direct benefit to those working in a cyclotron unit dedicated to clinical investigation. To those of us less fortunate it provides a comprehensive background to the subject, and leads to a better understanding of the problems of supplying hospitals with clinical radioactive gases.

D. M. Ackery.

Short-lived Radioactive Gases for Clinical Use. By J. C. CLARK and P. D. BUCKINGHAM (London: Butterworths, 1975) [Pp. xii+353] £9·50

When the decision was taken some 25 years ago to set up a medical cyclotron at Hammersmith Hospital it was envisaged that one of its useful functions would be the production of radioactive nuclides for medical research which could not be produced in a reactor. This promise was amply fulfilled as evidenced by the construction of similar cyclotrons and accelerators in medical institutes in many other countries. The short-lived gases (^{11}C, ^{13}N, ^{15}O and various isotopes of Kr and Xe) provided the tools for some spectacular advances in clinical physiology, and it is with the production of these nuclides that this monograph is concerned.

The authors have condensed their considerable expertise and experience into a single volume which covers in minute detail every step of the target preparation, bombardment, separation, purification, assay and dispensing of the various gases listed and some of their simple compounds. The handling techniques, the equipment (much of it original and highly ingenious) and above all the plumbing, are described in equal detail. There can be no doubt that the proud owner of a new cyclotron or other particle accelerator will find this book invaluable. Unfortunately, the paucity of such individuals means that the book will never achieve a mass market, though workers in related fields may be able to profit by a spin-off process if they are prepared to work through a lot of material which may not be immediately relevant to their problem. For example, the 20-minute ^{11}C, at present available as CO_2 or CO, could in theory be used in centres a few kilometres away from the cyclotron for the synthesis of a range of important organic compounds, and there may well be scope for a separate monograph on this subject in the near future. If so, it will draw to a large extent on the techniques described in the present volume.

Although the authors are concerned primarily with the production of short-lived radioactive gases, the increasing number of off-site users of some of these materials will find the volume to be a useful reference source, particularly when it comes to quality control and measurement. The standard of production of the book is high, particularly the illustrations, and the price is modest by today's standards.

N. VEALL

Atomic Power Industry in Japan
Vol 21 No 11 Nov 1975 p8

Short-lived Radioactive Gases for Clinical Use

J. C. Clark and P. D. Buckingham

B 5, 353 p, Butterworth, 1975；定価9ポンド50シリング

サイクロトロンなどによる短寿命核種の医学的利用は最近めざましいものがあり，この方面で10数年来パイオニアの役割を果たしてきたのが，英国の MRC Cyclotron Unit, Hammersmith Hospital である．

本書は，ここの中心的メンバーの2人の協力になるもので，まさにこの方面の要望をみたす最初の，そしておそらく他に追随を許さない好著といえよう．

本書を手にして，時のたつのも忘れてみほれてしまったことは，最近にない筆者の経験である．というのは，いたるところに彼らが経験し開拓してきた技術的な集積が惜し気もなく展開されているからである．

したがって，サイクロトロンを使おうという人にとってはもち論のこと，どちらかといえば縁遠いと思われる人にとってさえ，実験の手順，準備，照射，生成，プロセッシングの詳細がのみこめよう．現状では，どちらかといえば物理，化学，薬学，医学などと分業的になっていて大変に思われる短寿命核種の生産利用がその気になって手がけるならば，経験のない人でも本書のとおりやるなら，運転は別として1人の人で容易にその目的を達しうるほど細かいところまで体験が示されている．

これもこのグループの10数年以上におよぶ経験をきずいてきたアカデミックサイドの Clark 氏とエンジニアの Buckingham 氏との協力によってこそ，はじめてそれが具現されたのである．

本書は9章に分かれており，巻末には用語解説とおそらく800項目はるかに超えるていねいな索引とがある．

8

る，初心者，門外漢を意識した編成である．第1章は放射能，アイソトープの特性などの基本的な解説で，この方面になじみの少ない人々のよい導入である．第2章はサイクロトロンによるアイソトープ生産についてであり，ターゲットのつくり方や冷却法，ビームエネルギーの選定，ビームの分布，生成したガス状 RI の補集のしかたなど，サイクロ利用にかかせない実際的知識といろいろの注意すべき問題点を述べている．つづいて第3章では副生成核種とそれらの検出方法の詳細，生成したガスの移送，沪過，圧力と流速，比放射能濃度の問題，収率の測定などに加え，著者のつくったガス移送系のデザインとつくり方はまさに圧巻といえよう．彼らの深い体験にもとづく成果が，豊富な表と図を入れて述べられており，現場をみている筆者には，ここに到達した苦心の息吹きが紙面から感じられる．第4章は臨床に用いるための消毒，殺菌から，病院におけるレイアウトから必要な設備を述べている．

ここまで本書の約4割がついやされており，題名の示すごとく臨床利用の人々に限らず，まさにサイクロ利用を志向する一般の人のきわめてていねいな入門書として推奨に値することを明記しておきたい．

つぎの4割は著者らの独壇場とでもいうべきガス状短寿命核種の ^{15}O, ^{13}N, ^{11}C に第4～6章があてられている．いずれも，まずこれらの RI の特性，生成上の諸問題，ついでターゲットの問題とガス取扱い真空系が詳しく提供されている．しかもこの真空系は ^{15}O の例をあげると，^{15}OO, $C^{15}OO$, 窒素中の ^{15}OO(4%)，窒素中の $C^{15}OO$(2.5%)，$H_2{}^{15}O$, 赤血球の ^{15}OO 標識用などと目的にあった工夫と詳細なパラメーターを入れた手がきの8つの系統図が入っているほどである．もち論ターゲットからプロセシング装置まで含んだ真空系である．

残りの2割は他のガス状放射性核種の ^{79}Kr, ^{85m}Kr, ^{81m}Kr, ^{135}Xe と ^{127}Xe について上と同じような体裁で述べられている．終りの10頁ばかりの放射性，化学上，電気的な危険，ガス洩れとその防止など安全取扱い上の注意をうながしている．

一読して感じたことは，本書は題名の示すように臨床医家のみが対象だというわけでなく，むしろ広くサイクロトロン，放射性ガスを扱う人にとって実に導入から研究レベルまで引上げてくれる好著ということを再度強調したい．これは著者の経験にもとづくデータの表と手がきの図がいたるところにある貴重さのためである．ちょっといたずら気を出して文字だけのページを数えてみるとやはり印象どおり，全ページの半分以下にしかならず，いかに著者が豊富な体験と独創的なアイデアを蓄積してきたかがよくわかり，この方面の研究者，技術者の広い共感を集めることであろう．

コンパクトなサイクロトロンがわが国にも2つ，さらに ^{11}C, ^{15}O などを対象としたベビー・サイクロがわが国で開発され近く動き出す情勢であり，本書は大いにこの方面に加速効果をおよぼすことであろう．

（東京都立大学理学部　村上悠紀雄）

RADIOCHEM. RADIOANAL. LETTERS 25(4) 245-254 (1976)

KRYPTON-81m GENERATORS

J. C. Clark, P. L. Horlock, I. A. Watson

Medical Research Council, Cyclotron Unit, Hammersmith Hospital, Ducane Road, London W12 OHS, U. K.

Received 5 March 1976
Accepted 11 March 1976

Methods for the production of rubidium-81 and subsequent preparation of Krypton 81m gas and solution phase generator systems are briefly reviewed. Some aspects of zirconium phosphate generator operation and clinical application are discussed.

INTRODUCTION

Krypton-81m decays with a 13 sec half-life and emits 190 keV photons in 65% of its disintegrations. It is the daughter of ^{81}Rb which has a half-life of 4.58 hours.

Recent clinical interests have led to the exploitation of the very short half life of ^{81m}Kr to obtain functional images of various organs directly from the scintillation camera during the continuous administration of ^{81m}Kr at constant concentrations[1-3].

Generators have been developed for producing ^{81m}Kr in solution for intravenous and intraarterial infusion as well as for producing gas for use in lung ventilation studies.

The main factors to be considered in the preparation of these generators are:

1) Cyclotron production of useful quantities of the ^{81}Rb parent

2) Generator design

3) Chemical separation of ^{81}Rb from the target material

4) Loading the generator with ^{81}Rb

5) Procedures for testing the generator

In this paper these points will be considered, together with some practical aspects of generator operation.

THE PRODUCTION OF RUBIDIUM-81

There are several reported methods for producing ^{81}Rb and these are shown in Table 1.

Both the ^{79}Br(α, 2n)^{81}Rb and the ^{81}Be(α, 4n)^{81}Rb reactions are seen to proceed in good yield for the alpha particle energies shown. Sodium bromide and cuprous bromide have been used as target materials. The yield for the 21 MeV helium-3 reaction with bromine is not high enough for useful generator production. The use of ^{3}He at higher energies is being investigated[4]. By using an enriched ^{80}Kr(37%) target both 20 MeV ^{3}He and 8 MeV deuterons have been used to produce practical quantities of ^{81}Rb the latter particle providing samples particularly low in ^{82m}Rb. The ^{82}Kr(p, 2n)^{81}Rb reaction does not appear to have been investigated.

All these methods of producing ^{81}Rb simultaneously produce other rubidium radionuclides which are of importance only when considering the whole body radiation dose due to rubidium breakthrough from solution generators.

GENERATOR DESIGN

The chemical aspects of generator design only are considered here.

Two types of ^{81m}Kr generators have been reported and some of their characteristics are shown in Table 2.

They both use a cation exchange material to retain the ^{81}Rb whilst allowing the ^{81m}Kr to be recovered in either the solution or gas phase. However, they have quite different rubidium loading characteristics.

TABLE 1

Production routes for ^{81}Rb

Nuclear reaction	Target material	Projectile energy (MeV)	Practical beam current μA	^{81}Rb yield at EOB mCi μAhr^{-1}	Institution	Reference
$^{79}Br(\alpha, 2n)^{81}Rb$	NaBr (thick)	30	50	2-2.5	MRC Cyclotron Unit Hammersmith Hospital, London	11, 9
$^{79}Br(\alpha, 2n)^{81}Rb$	Cu_2Br_2 (thick)	30	50	2	Argonne Cyclotron Argonne National Lab. USA	7
$^{81}Br(\alpha, 4n)^{81}Rb$	NaBr(thin)	50→30	15	2.9	Lawrence Radiation Lab. 88" Cyclotron, Berkeley	6
$^{81}Br(^3He, 3n)^{81}Rb$ $^{79}Br(^3He, n)^{81}Rb$	NaBr(thick)	21	25	0.035	Sloane Kettering Institute New York, USA. CS-15 Cyclotron	10
$^{80}Kr(^3He, pn)^{81}Rb$	37% enriched ^{80}Kr	20	5	0.226	Franklin McLean Memorial Research Institute, Chicago. CS-15 Cyclotron	8
$^{80}Kr(d, n)^{81}Rb$	37% enriched ^{80}Kr	8	5(75)	0.7	Franklin McLean Memorial Research Institute, Chicago. CS-15 Cyclotron	8

TABLE 2

^{81m}Kr Generator system

Delivery phase	Generator type		Generator loading criteria	Elution efficiency	References
Gas or solution	Inorganic ion exchanger column	6x30 mm zirconium phosphate Bio Rad ZP1 50-100 mesh	Rapid loading at high NaBr concentrations possible	70 %	5 11
Gas or solution	Organic ion exchange column	11x60 mm Bio Rad AG50 x4, 200-400 mesh	Slow loading at low NaBr concentrations	10 %	6
Gas or solution	Organic ion exchange column	2.5 x 22 mm Dowex 50 x 8 200-400 mesh	^{81}Rb chemically separated from Cu_2Br_2 loaded "carrier-free"	80 %	7

The first type developed in our laboratory[5] incorporates a column of the inorganic ion exchange material zirconium phosphate while the second type of generator developed in the Donner laboratory[6] and subsequently improved in the Veterans Administration Hospital, Hines Illinois[7] uses a cation exchanger of the organic type, a sulphonated polystyrene-divinyl benzene copolymer eg. Dowex 50 x 8.

CHEMICAL SEPARATION OF ^{81}Rb AND GENERATOR LOADING

Zirconium phosphate is an insoluble crystalline material with a high affinity for rubidium even in the presence of high concentrations of sodium ions. This property enables one to load ^{81}Rb onto the zirconium phosphate generator rapidly at high efficiency using the irradiated 2.5 gram sodium bromide target dissolved in 20 ml water. A wash with 100 ml water to remove the unwanted sodium bromide is all that remains to complete the generator preparation. The whole procedure is accomplished in approximately 10 min and readily carried out by remote control.

The organic cation exchanger used in the second type of generator will only retain rubidium when it is applied to the column in solutions of low ionic strength. Thus, if a sodium bromide target is used, the target solution must be diluted to give a concentration of less than 0.5% and the resulting volume of 200-500 ml must be loaded slowly if large losses of ^{81}Rb are to be avoided[6]. Alternatively the ^{81}Rb must be chemically separated from the target material and loaded on to the column essentially carrier free[7]. Both of these procedures are extremely time consuming and the resulting generators appear to offer no advantages over the zirconium phosphate type, both types having elution efficiencies of 70-80% and similar rubidium breakthrough values.

GENERATOR TESTING

The zirconium phosphate generators produced in our laboratory are routinely tested for eluted activity at steady state. Rubidium breakthrough in solution generator eluates is also estimated.

The rubidium breakthrough is usually expressed in microcuries of rubidium eluted per minute. For a generator yielding 20 mCi of ^{81m}Kr at steady state a typical rubidium breakthrough per minute would be 0.04 μCi ^{81}Rb, 0.01 μCi ^{82m}Rb, 1.6×10^{-4} μCi ^{83}Rb and 4×10^{-5} μCi ^{84}Rb. During an infusion procedure the above quantities of rubidium radionuclides infused each minute would give a whole body radiation dose to the subject of approximately 10 microrads. The radiation dose was calculated using data contained in ref. [8]

SOME ASPECTS OF ZIRCONIUM PHOSPHATE GENERATOR OPERATION

The infusion generator must only be eluted with water and its elution with physiological saline is not recommended as this has been shown to increase the breakthrough values by at least an order of magnitude. Additionally ^{24}Na and ^{22}Na become detectable in the generator eluate. In order to render the infusate isotonic the generator eluate is mixed with an equal flow of 1.8% sodium chloride solution. The resulting solution is terminally sterilised using a milipore Millex disposable 0.22 micron filter unit as shown schematically in Fig. 1.

When a generator is used for ventilation studies it is eluted using air or physiological gas mixture. It is essential to ensure that the eluting gas flow is saturated with water vapour before passing through the column as shown in Fig. 2. Dry gas causes the column to dry out and it is found that little ^{81m}Kr can then be recovered. Should a generator accidentally become dry it is possible to re-wet it again and regain the normal high elution efficiency.

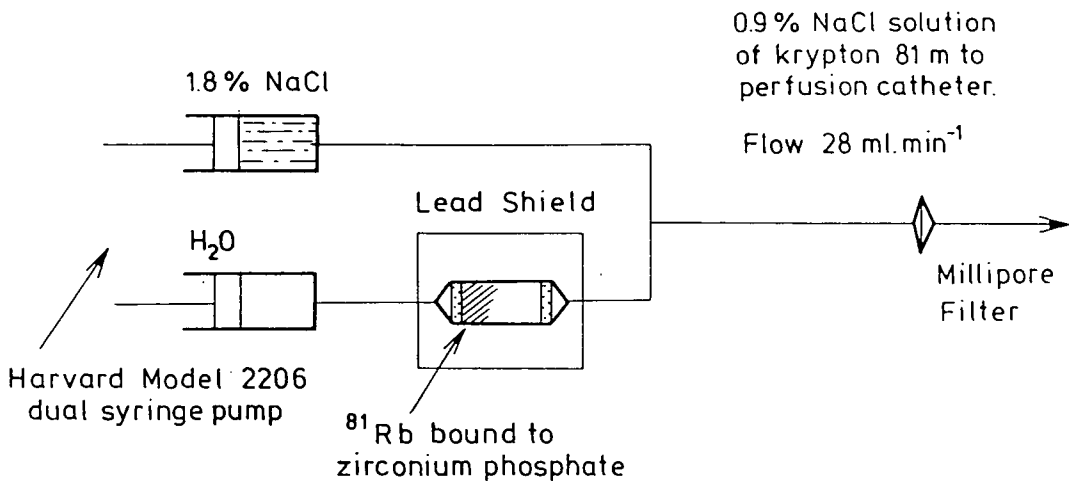

Fig. 1. Recovery of ^{81m}Kr solution for perfusion studies.

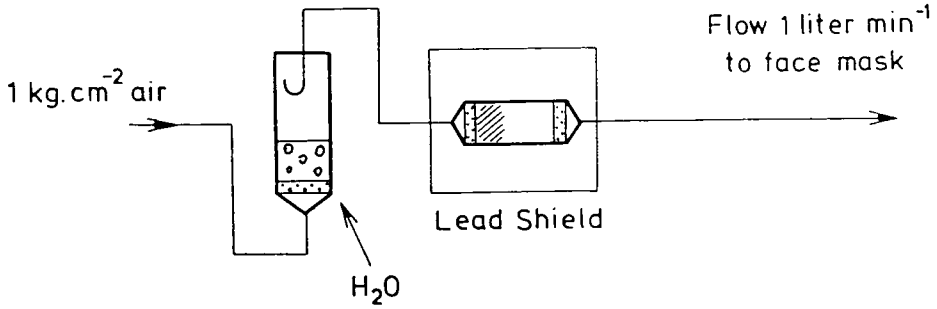

Fig. 2. Recovery of ^{81m}Kr in the gas phase for ventilation studies.

When using these generators clinically it is essential to minimise losses of ^{81m}Kr decay during its passage from the generator to the subject.

This is usually achieved by keeping the diameters and lengths of the delivery tubing and catheters to a minimum and operating at flow rates consistent with their volume and the 13 sec half life of ^{81m}Kr.

CLINICAL USE OF THE MRC KRYPTON-81m GENERATOR

We have developed a simple, reliable and rapid generator production system that enables us to prepare gas phase generators and to distribute

them to many centres in the United Kingdom at distances of up to 600 kilometres by road, rail and air within a few hours.

Solution generators have only been prepared for on site use up to the present time as the present design requires a high standard of technical expertise to ensure its safe assembly and final testing before use in human infusion investigations. An integrated generator system is under construction which has been designed to deliver both sterile solutions for infusion and ^{81m}Kr in the gas phase for ventilation. This development should make lung ventilation and perfusion investigations with ^{81m}Kr a practical proposition as well as making a safe infusion available for off site use.

REFERENCES

1. F. Fazio, T. Jones, British Medical Journal, 265 (1975) 673.

2. E. Kaplan, L. W. Mayron, W. E. Barnes, L. G. Colombetti, A. M. Friedman, J. E. Gindler, J. Nucl. Med., 15 (1974) 874.

3. J. H. Turner, A. P. Selwyn, T. Jones, T. R. Evans, M. J. Raphael, J. P. Lavender. Cardiovascular Research (1976) (in press).

4. J. H. Fremlin, Dept. of Physics, University of Birmingham. U. K. (Personal communication).

5. J. C. Clark, T. Jones, A. Mackintosh. ^{81m}Kr an Ultra Short Lived Inert Gas Tracer for Lung Ventilation and Perfusion studies with the Scintilation Camera. Radioaktive Isotope in Klinik und Furschung, 444 (Urban and Schwarzenberg- München - Berlin, Wien, 1970)

6. Y. Yano, J. McRae, H. O. Anger, J. Nucl. Med., 11 (1970) 674.

7. L. G. Colombetti, L. W. Mayron, E. Kaplan, A. M. Friedman, J. E. Gindler, J. Nucl. Med., 15 (1975) 868.

8. B. Rich, N. Lembares, P. V. Harper, K. A. Lathrop, F. Atkins. Radiopharmaceuticals, 174 (Society of Nuclear Medicine Inc. New York, 1975)

9. S. L. Waters, D. J. Silvester, I. W. Goodier, Phys. Rev., C. 2. (1970) 2441.

10. I. A. Watson. Radiochem. Radioanal. Lett., 4 (1970) 7.

11. J. C. Clark, P. D. Buckingham., Capt. 8, Radionuclides of the Rare Gases in "Short Lived Radioactive gases for Clinical Use". (Butterworths, London, 1975).

THE NON-INVASIVE USE OF OXYGEN-15 FOR STUDYING REGIONAL BRAIN FUNCTION IN PATIENTS WITH CEREBRAL TUMOURS

T. Jones, C.G. McKenzie, S. Moss, P.D. Buckingham & J.C. Clark

Introduction

Oxygen-15, which is the longest lived γ-emitting radioisotope of oxygen (2.1 min $T\frac{1}{2}$), has been used to study the regional cerebral function of patients who have brain tumours being treated with radiotherapy. The method of investigation has been to continuously inhale Oxygen-15 while it is being produced at a constant rate by the cyclotron (1). Following six minutes of constant inhalation the radioactivity within the brain reaches an equilibrium level. Most of this activity is contained within the brain tissue itself, and has been shown that it is due principally to the tissue's production of Oxygen-15 labelled water of metabolism ($H_2{}^{15}O$ met.) (2). During this procedure the level of radioactive water contained within the cerebral tissue is theoretically proportional to the tissue's extraction of oxygen from the blood. Within the normal perfusion range it is fairly independent of flow. However it has a linear dependance with flow at low values of perfusion:

$$H_2{}^{15}O \text{ met} \propto \text{E.R.} \frac{F}{F/V + \lambda}$$

where E.R. = tissue's oxygen extraction ratio :
F " blood flow
V " volume
λ " radioactive decay constant of $^{15}O_2$ (0.335 min^{-1})

It was thought that the cerebral image of oxygen uptake in the brain may provide a means to assess the effectiveness of radiotherapy for the treatment of cerebral tumour. In particular the uptake of Oxygen-15 within the tumour and the surrounding cerebral tissue has been studied as well as changes resulting from radiotherapy.

Procedure

A series of patients with various types of cerebral tumours have been studied. In some cases the tumour had been partially removed by surgery, while in others only a biopsy had been performed. The pattern of cerebral ^{15}O uptake was studied prior, during and following radiotherapy of the tumour. An Anger γ-camera with a $4\frac{1}{2}$ inch thick lead collimator (3) was used to view the lateral aspect of the patient's head. The subject continuously inhaled Oxygen-15 through a mouth piece connected to a two way Rubins valve. The radioactive gas was piped from the Cyclotron which was some 700 feet away and fed continuously into the input of the valve at a flow rate of $\frac{1}{2}$ a litre per minute. The activity levels used were between two to four milli curies per litre. An equilibrium level was normally reached in the brain following 6 minutes of continuous inhalation of the constant supply of radioactivity. During the condition of equilibrium, a 4 minute record was made of the steady state distribution of ^{15}O in the head. This recording, which typically contained 250,000 counts, was stored in an on-line computer where it could be corrected for the camera's non-uniformity of

response. During radiotherapy (4 - 6 weeks duration) weekly Oxygen-15 measurements were carried out on the patient, and then at various times after treatment. The individual uniformity corrected records for each patient were normalised to each other and photographed to provide a pictorial sequence of any regional changes of Oxygen-15 uptake in the brain.

Results

The Oxygen-15 uptake in the left lateral view of a control subject is shown in figure 1:

It is clear that this type of cerebral image does in fact reflect the distribution of cerebral tissue itself. This is unlike such conventional isotopic procedures for brain as ^{99m}Tc where the activity is principally confined to the tissue peripheral to the brain. The Oxygen-15 procedure does in fact provide a true scan of the brain. In general the uptake pattern is symmetrical with a central high uptake area corresponding to the basal ganglian. The image possess a structure which may be related to specific functioning zones within the cerebral cortex. This pattern was fairly general to all the controls subjects studied.

Fig. 2.

^{99m}Tc $^{15}O_2$

This shows the result of a ^{99m}Tc and $^{15}O_2$ investigation in a patient with clinical evidence of cerebral metastases arising from a primary carcinoma of the lung. The multiple uptake defects shown in the $^{15}O_2$ image correlate more closely with the clinical evidence on this patient than did the ^{99m}Tc brain data. This example draws attention to the fundamental concept of detecting lesions as negative rather than positive uptake of tracer. The latter approach although having specific physical advantages (Signal: noise), is dependent on there being a breakdown of the blood brain barrier and the lesion having an adequate blood supply. The negative uptake approach does not have these restraints but is limited by the contribution to the signal from the surrounding healthy cerebral tissue. In order to determine whether or not these defects reflect either areas of low oxygen extraction or poor blood supply, some patients were in addition studied while inhaling Oxygen-15 labelled carbon dioxide ($C^{15}O_2$). This procedure results in the continuous labelling of the pulmonary blood with $H_2{}^{15}O$ (4). The resulting brain signal is $\propto \frac{F}{F/V + \lambda}$ (2). It can be seen that this provides the flow dependent component of the $H_2{}^{15}O$ met signal produced by inhaling Oxygen-15. Thus it may be possible to resolve the reasons for a region of decreased uptake being observed over the area of cerebral tumour. The possibilities are either poor metabolism or poor blood flow.

Fig. 3.

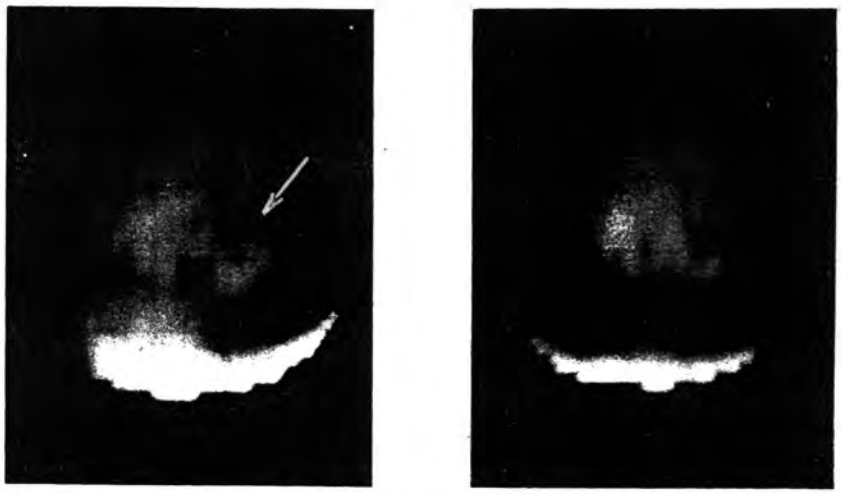

$^{15}O_2$ $C^{15}O_2$

This shows prior to radiotherapy an $^{15}O_2$ and $C^{15}O_2$ image in a patient with a brain tumour diagnosed by arterial angiography. The defect as illustrated in Fig. 3 appears common to both the $^{15}O_2$ and $C^{15}O_2$ procedures. This indicates that the defects of uptake is due primarily to low perfusion at that tumour site. Fig. 4 shows from the same patient the $^{15}O_2$ and $C^{15}O_2$ images following a course of radiotherapy:

$^{15}O_2$ $C^{15}O_2$

The image produced by $C^{15}O_2$ inhalation is fairly normal whereas the $^{15}O_2$ uptake in the lesion although somewhat improved still shows some decrease in uptake. This indicates that there is still a metabolic defect at the site. This patient showed a clear improvement clinically as a result of the radiotherapy.

Discussion

Preliminary results of using Oxygen-15 to produce a positive image of the active cerebral tissue have shown that tumours tend to be exhibited as areas with low uptake of activity. In some cases such defects have been related to poor perfusion of that region which is affected by the lesion. This zone of low uptake has often appeared larger than would have been predicted from the angiographic study, and this is due presumably to local hydrostatic pressure caused by edema formation peripheral to the tumour. Defects located at the site of a tumour have been shown to improve with radiotherapy. In certain cases a regrowth of the tumour has had correlated with it a return of the defect in the Oxygen-15 brain image. This work is still at the preliminary stage, however it does appear that we have a method to monitor local functional changes in the brain. This could provide an objective physiological feed-back to the therapist who may in turn be able to adjust the therapeutic regime.

REFERENCES

1) CLARK, J.C., BUCKINGHAM, P.D. (1975);
Short Lived Radioactive Gases for Clinical Use: pp 136-170.
Butterworths (London).

2) JONES, T., CHESLER, D.A., TER-POGOSSIAN, M.M. (1976):
The continuous inhalation of oxygen-15 for assessing regional oxygen extraction in the Brain of Man.
Accepted for publication: British J. Radiology.

3) WESTERMANN, B.R., GLASS, H.I. (1968): Physical Specifications of a Gamma Camera. J. Nucl Med. 9, 1.24.

4) WEST, J.B., and DOLLERY C.T. (1962): Uptake of Oxygen-15 labelled Co_2 compared with carbon-11 labelled Co_2 in the lung.
Journal of applied physiology 17: 9.

Address

Medical Research Council, Cyclotron Unit and
Departments of Radiotherapy & Medical Physics,
Hammersmith Hospital,
Ducane Road,
London W12.

Abstract

The continuous inhalation of Oxygen-15 which has a half life of 2.1 minute results in the radioactivity within the tissue reaching a state of "dynamic equilibrium". The distribution of tracer in the brain during such a steady state procedure reflects directly the functioning cerebral tissue unlike the conventional brain scan. The inhalation of molecular Oxygen-15 produces a cerebral distribution of radioactivity which is related to oxygen utilisation and blood flow. This can be compared to the distribution obtained while inhaling Oxygen-15 labelled carbon dioxide which has a sole dependance on blood flow. These techniques have been applied to patients with cerebral tumours who are undergoing treatment with radiation. Investigations have been carried out with the object of obtaining information on blood flow and oxygen utilisation rates to the lesions relative to the normal tissue. Serial measurements have helped to understand how these relationships change during and following treatment.

Extrait

L'inhalation continue d'oxygène-15, qui a une demi-vie de 2,1 minutes, conduit à une radioactivité tissulaire qui atteint un état "d'équilibre dynamique". A la différence du scan cérébral conventionnel la distribution du traceur dans le cerveau durant un tel steady state reflète directement le tissu cérébral fonctionnel. L'inhalation d'oxygène-15 moléculaire produit une distribution cérébrale de la radioactivité qui est reliée à l'utilisation de l'oxygène et au débit sanguin. Ces techniques ont été employées chez des malades porteurs de tumeurs cérébrales soumis à un traitement par irradiation. Des études ont été conduites visant à obtenir des informations sur le débit sanguin et l'utilisation d'oxygène des lésions par rapport au tissu normal. Des mesures en séries ont permis de comprendre comment ces relations se modifient durant et après le traitement.

Auszug

Die kontinuierliche Inhalation von ^{15}O mit einer Halbwertszeit von 2,1 min führt im Gewebe zu einer Aktivitätsanreicherung mit dynamischem Gleichgewicht. Die Verteilung des Tracers im Gehirn unter solchen Study State Verhältnissen entspricht, anders als bei der konventionellen Gehirnszintigraphie, direkt der funktionierenden Gehirnsubstanz. Die Inhalation molekularen ^{15}O führt zu einer Radioaktivitätsverteilung im Gehirn, die zum Sauerstoffverbrauch und zur Durchblutung des Gehirns in Beziehung steht. Solche Ergebnisse können zu Verteilungsstudien in Beziehung gesetzt werden, die durch Inhalation von ^{15}O markierten Kohlendioxyd gewonnen werden und die ausschließlich von der Durchblutung abhängen. Diebeschriebenen Techniken wurden bei Patienten angewendet, die wegen eines Hirntumors einer Strahlentherapie unterzogen wurden. Ziel der Unter-

suchungen war Informationen über Durchblutung und Sauerstoffutilisation in den Läsionen im Vergleich zum Normalgewebe zu erhalten. Serienmessungen wurden zum besseren Verständnis von Durchblutung und Sauerstoffverbrauch während und nach der Strahlenbehandlung durchgeführt.

Prog. nucl. Med., vol. 4, pp. 140–145 (Karger, Basel 1978)

The Medical Research Council Cyclotron at Hammersmith Hospital

A Status Report, March 1976

JOHN C. CLARK

Medical Research Council, Cyclotron Unit, Hammersmith Hospital, London

Introductory Overview

The Facility

The Hammersmith cyclotron is of classical design and accelerates α-particles to 32 MeV, deuterons to 16 MeV and protons (via H_2^+) to 8 MeV. Irradiations of targets may be carried out either internally or externally. Four external beam lines are installed at the present time, two of which are available for neutron therapy and radiobiology the remaining two being dedicated to radionuclide production. Both internal and external targets may be removed or replaced remotely without interrupting the cyclotron's running schedule. Additionally a remote-controlled actuator, installed on an external beam line, is able to present any one of eight preloaded targets to the charged particle beam thus facilitating rapid changes between on-line products during a busy clinical program [1, 2]. One of the radionuclide production beam lines is scheduled to be withdrawn from service (October 1976) to be replaced by three beam lines that will be capable of effectively simultaneous operation using a beam-sharing technique [3]. Ancillary facilities around the cyclotron include a shielded room where neutron radiotherapy and radiobiology takes place and a radiochemistry laboratory equipped with hot cells where radionuclides are processed to radiopharmaceutical standards. The cyclotron building also houses an animal investigation and a clinical application facility. Other clinical areas on the hospital site are supplied with most of the short half-lived gaseous products by pipeline.

Table I. Cyclotron running schedule, week commencing 15 March, 1976

Date	Beam	Priority	Scheduled Run	User
Monday, 15 March				
0000–0045	–	–	remove gas targets, load ^{43}K insert	D.A. Cans
0045–0200	III	B	α – As – ^{77}Br	ADN
0200–0430	IV	B	α – A – ^{43}K	PJS
0430–0600	Int.	B	α – Sb – ^{123}I	PLH
0600–0900	III	B	α – NaBr – ^{81}Rb	MLP
0900–0915	–	–	remove ^{43}K	PJS/IAW
0915–1045	I	D	physics	DEB
1045–1100	–	–	actuator set-up	IAW
1100–1730	I/IV/IV	A/A/A	therapy/^{13}N/^{15}O	BCP/JCC
1730–1930	Int.	–	beam line-up	GB
1930–2200	IV	B	α – A – ^{43}K	MLP
Tuesday, 16 March				
0700–0745	III	B	α – NaBr – ^{81}Rb	PLH
0745–0800	IV	B	α – O – ^{18}F	SLW
0800–0815	–	–	remove ^{43}K, ^{18}F, Load ^{18}F (Ne)	
0815–0830	Int.	C	α – Ni – ^{61}Cu	ADN
0830–1000	III	B	α – NaI – ^{129}Cs	SLW
1000–1030	I	D	physics	BCP
1030–1115	I	A	activation	TJS
1115–1145	I	D	physics	DEB
1145–1245	I	C	biology	KRB/WAC
1245–1445	I	C	biology	KRB/SH
1445–1530	IV	B	p – N – ^{11}C	CGR
1530–1700	IV	A	d – N – ^{15}O	CGR
1700–2115	III	B	d – Tl – ^{203}Pb	IAW
2115–2200	–	–	filament change	
Wednesday, 17 March				
0700–0900	Int.	B	α – Sb – ^{123}I	PLH
0900–1030	III	B	α – NaBr – ^{81}Rb	MLP
1030–1100	I	A	activation	TJS
1100–1730	I/IV/IV	A/A/A	therapy/^{13}N/^{15}O	BCP/JCC
1730–1900	I	C	biology	KRB/CND
1900–2045	–	–	P.A. engineering	
2045–2130	III	D	α – As – ^{77}Br	SLW
2130–2200	–	–	remove and load targets	

Thursday, 18 March				
0700–0800	III	B	α – NaBr – ^{81}Rb	PLH
0800–1000	Int.	B	α – Cr – ^{52}Fe	MLP
1000–1100	IV	C	d – Ne – ^{18}F	RWG
1100–1300	I	C	biology	BCP/BC
1300–1400	I	C	biology	BCP/SM
1400–1430	I	D	activation	TJS
1430–1530	III	C	α – NaBr – ^{81}Rb	JCC
1530–1730	IV	A	d – N – ^{15}O	CGR
1730–1830	I	C	activation	GJB
1830–2200	IV	C	d – C – ^{13}N	JCC
Friday, 19 March				
0700–0830	III	B	α – NaBr – ^{81}Rb	MLP
0830–0845	Int.	D	α – Ni – ^{61}Cu	ADN
0845–1000	III	B	α – NaBr – ^{81}Rb	MLP
1000–1630	I/IV/IV	A/A/A	therapy/^{13}N/^{15}O	BCP/JCC
1630–2200	–	–	maintenance	WE

Operators: Monday:

0000–0700	W. Edwards, P. Lewis
0700–1430	E. Watson, M,Th
	P.M. Byrne, T,F
	P. Lewis, W
1430–2200	J.F. Lucas, M,W,F
	J. Lawler, T,Th

Tuesday–Friday:

0700–1430	1430–2200
E. Watson, M,Th	J.F. Lucas, M,W,F
P.M. Byrne, T,F	J. Lawler, T,Th
P. Lewis, W	

A On-line clinical use, i.e. with patients undergoing treatment or tests requiring operation of the cyclotron during their attendance, e.g. therapy, clinical use of short-lived isotopes, whole body or partial body neutron activation analysis.

B Off-line clinical use, i.e. production of clinical radiopharmaceuticals for use in clinics on or off site.

C High priority experimental work or engineering, e.g. radiobiological experiments requiring precise timing or involving preparation and/or follow-up time, neutron activation analysis of clinical samples, important physics experiments, important engineering work.

D Low priority experimental work or engineering.

Table II.

Radionuclide	Application	Reference
^{18}F	bone blood flow	4
^{18}F	radiopharmaceutical development	5
^{11}C	pharmacological studies	6
^{11}C	radiopharmaceutical development	7
$^{15}O_2 + C^{15}O_2$	noninvasive brain metabolism studies	8
$H_2{}^{15}O$	extravascular lung water estimation	9, 10
$C^{15}O$	detection of intrapulmonary hemorrhage	11
$^{81}Kr^m$	pulmonary ventilation and perfusion studies	12–14
$^{81}Kr^m$	myocardial blood flow studies	15, 16
^{129}Cs	myocardial imaging	–
^{52}Fe	bone marrow function studies	–
Neutrons	radiotherapy	17, 18
$^{13}N_2$	respiratory physiology research and clinical diagnosis	19–21

Operating Schedules

The cyclotron operates from 07.00 to 22.00 h 5 days per week. A typical weekly schedule, normally planned on the previous Friday, is shown in table I. It will be seen that neutron radiotherapy is carried out on three afternoons a week. Generally the medium half-life products required for use that day are prepared in the early morning followed by fulfillment of on-line requirements which may continue throughout the day even when radiotherapy is taking place, rapid beam switching being employed to make good use of intertherapy patient set-up time. All irradiations have a predetermined priority as explained in the footnote to table I. Evening sessions are usually devoted to the production of longer-lived radionuclides, machine maintenance and development or preclinical investigations using animals.

The routine nature of the cyclotron operation ensures that most on-site requirements can be met each week and additional capacity is devoted to supplying other UK hospitals with a variety of cyclotron-produced radiopharmaceuticals that are not commercially available. Research and development into new production routes and radiopharmaceutical preparation methods continue.

Table II lists some of our ongoing activities involving both on-site and off-site co-workers.

References

1 SILVESTER, D.J.: Biomedical cyclotron in a medical center: capabilities and problems; in Radiopharmaceuticals, p. 157 (Society of Nuclear Medicine, New York 1975).

2 VONBERG, D.D.; BAKER, L.C.; BUCKINGHAM, P.D.; CLARK, J.C.; FINDING, K.; SHARP, J., and SILVESTER, D.J.: Target systems for radioisotope production on the Medical Research Council cyclotron; in Uses of cyclotrons in chemistry, metallurgy and biology, pp. 258–269 (Butterworths, London 1970).

3 BURTON, G.: Cyclotron beam sharing for multiple target irradiations. Proc. 5th Int. Cyclotron Conf. 1969, pp. 250–253 (Butterworths, London 1970).

4 WOOTON, R.; REEVE, J., and VEAL, N.: The clinical measurement of skeletal blood flow. J. clin. Sci. molec. Med. *50:* 261–268 (1976).

5 GOULDING, R.W.: Fluorine-18 labelled L-*p*-fluorophenylalanine. Int. J. appl. Radiat. Isotopes *26:* 561–564 (1975).

6 PALMER, A.J.: The preparation of ^{11}C-methyl labelled 1,1'-dimethyl-4,4'-dipyridinium diiodide. J. Lab. Cpds. Radiopharm. (in press, 1977).

7 GOULDING, R.W.: Liquid chromatography of sugars and related polyhydric alcohols on cation exchangers. J. Chromat. *103:* 229–239 (1975).

8 JONES, T.; MCKENZIE, C.G.; MOSS, S.; BUCKINGHAM, P.D., and CLARK, J.C.: The assessment of regional cerebral function in brain tumour patients by continuous inhalation of oxygen-15. Br. J. Radiol. *50:* 158 (1977).

9 FAZIO, F.; JONES, T.; MACARTHUR, C.G.C.; STEINER, R.E., and HUGHES, J.M.B.: Measurement of regional pulmonary oedema in man using radioactive water $H_2{}^{15}O$. Br. J. Radiol. *49:* 393–397 (1976).

10 JONES, T.; JONES, H.A.; RHODES, C.G.; BUCKINGHAM, P.D., and HUGHES, J.M.B.: Distribution of extravascular fluid volumes in isolated perfused lungs measured with $H_2{}^{15}O$. J. clin. Invest. *57:* 706–713 (1976).

11 EWAN, P.W.; JONES, H.A.; RHODES, C.G., and HUGHES, J.M.B.: Detection of intrapulmonary haemorrhage in man with carbon monoxide uptake: application in Goodpastures' syndrome. New Engl. J. Med. *295:* 1391–1396 (1976).

12 FAZIO, F. and JONES, T.: Assessment of regional ventilation by continuous inhalation of radioactive krypton-81m. Br. med. J. *iii:* 673–676 (1975).

13 HARF, A.; PRATT, T., and HUGHES, J.M.B.: Regional ventilation perfusion ratios at rest and on exercise using krypton 81m. Bull. Eur. Physiophath. Resp. *12/6:* 1–195 (1976).

14 CLARK, J.C.; HORLOCK, P.L., and WATSON, I.A.: Krypton-81m generators. Radiochem. radioanal. Lett. *25:* 245–254 (1976).

15 TURNER, J.H.; SELWYN, A.P.; JONES, T.; EVANS, T.R.; RAPHAEL, M.J., and LAVENDER, J.P.: Continuous imaging of regional myocardial blood flow in dogs using krypton-81m. Cardiovasc. Res. *10:* 398–404 (1976).

16 SELWYN, A.P. and SHILLINGFORD, J.P.: Continuous assessment of regional myocardial perfusion using krypton-81m in dogs and man: effects of nitroglycerine and stress in acute ischaemia. Circulation *54:* suppl. (1976).

17 CATTERALL, M.; SUTHERLAND, I., and BEWLEY, D.K.: First results of a randomised clinical trial of fast neutrons compared with X-rays or gamma

rays in treatment of advanced tumours of the head and neck. Br. med. J. *ii*: 653–656 (1975).

18 Field, S.B.: An historical survey of radiobiology and radiotheraphy with fast neutrons. Curr. Top. Radiat. Res. Q. *11*: 1–86 (1976).

19 Eiser, N.M.: Local perfusion and ventilation in chronic bronchitis and emphysema. Thorax *30*: 596 (1975).

20 Godfrey, S.; Ronchetti, R.; Stocks, J., and Hallidie-Smith, K.: Generalised pulmonary hyperinflation and Fallot's tetralogy in a neonate investigated by pulmonary physiology and radioisotope methods. Thorax *30*: 452 (1975).

21 Sykes, M.K.; Arnot, R.N.; Clark, J.C., and Hering, A.N.: Studies of ventilation at different inspiratory flow rates using krypton-81m and nitrogen-13. Bull. Eur. Physiopath. Resp. *12*: 1–206 (1976).

Dr. J.C. Clark, MRC Cyclotron Unit, Hammersmith Hospital, *London* (England)

nasal mucosa with clock-like regularity. This area may be associated with the respiratory centre in the medulla as changes in arterial P_{CO_2} cause changes in nasal resistance (Principato & Ozenberger, 1970; Dallimore & Eccles, 1977), although there is some evidence that the hypothalamus regulates the sympathetic outflow to the nasal mucosa of the cat (Malcomson, 1953).

The work was carried out at the V.P. Chest Institute, University of Delhi, and I would like to thank Professor A. S. Paintal, Dr S. K. Jain and Mr A. Kumar for their help and encouragement.

REFERENCES

DALLIMORE, N. S. & ECCLES, R. (in press). *Acta oto-lar.*
HEETDERKS, D. R. (1927). *Am J. Med. Sci.* **174**, 231–244.
MALCOMSON, K. G. (1959). *J. Lar. Otol.* **73**, 73–98.
PRINCIPATO, J. J. & OZENBERGER, J. M. (1970). *Archs Otolar.* **91**, 71–77.
STOKSTED, P. (1953). *Acta oto-lar.* Suppl. 109, 159–175.

C. 61

Effect of posture on distribution of pulmonary ventilation and perfusion studied with ^{81m}Kr and ^{85m}Kr

BY T. C. AMIS, G. CIOFETTA, J. C. CLARK, J. M. B. HUGHES, HAZEL A. JONES and T. A. PRATT. *Departments of Medicine and Diagnostic Radiology, Royal Postgraduate Medical School, and M.R.C. Cyclotron Unit, Hammersmith Hospital, London, W12 0HS*

Using radioactive gases, West & Dollery (1960) and Kaneko, Milic-Emili, Dolovich, Dawson & Bates (1966) have suggested that the effect of posture on the distribution of ventilation and perfusion in the lung is mediated by gravity.

With the introduction of the short half-life (13 sec) isotope ^{81m}Kr ($E\gamma$ 190 keV), distributions of ventilation and perfusion can be measured in the steady state during spontaneous breathing. Using a gamma camera, continuous inhalation of an air–^{81m}Kr mixture, gives regional counts which reflect regional ventilation (Fazio & Jones, 1975). Similarly, continuous intravenous infusion of ^{81m}Kr produces regional counts reflecting local pulmonary perfusion. Division of images constructed from the accumulated counts produces a distribution of ventilation–perfusion ratios ($\dot{V}A/\dot{Q}$). With this technique Harf, Pratt & Hughes (1976) found that $\dot{V}A/\dot{Q}$ in seated subjects decreased from high values at the apex (mean 1·8) to lower values at the base (0·8–0·9).

We have extended these measurements to the supine, right and left lateral decubitus and prone suspended (on all fours) postures and corrected ventilation and perfusion images for local alveolar volume by rebreathing

a longer half-life (4·4 hr) isotope, ^{85m}Kr ($E\gamma$ 150 keV). The $\dot{V}A/\dot{Q}$ ratio decreased from superior to inferior in the prone suspended posture and in the uppermost lung in the lateral decubitus position. This gradient was reversed in the superior–inferior axis in the supine posture and in the lowermost lung in the lateral decubitus posture. Reversal of the $\dot{V}A/\dot{Q}$ gradient might be related to smaller resting lung volumes seen in the latter postures (Kaneko *et al.* 1966) and their effect on blood flow distribution (Hughes, Glazier, Maloney & West, 1968).

Volume correction showed that the decreasing $\dot{V}A/\dot{Q}$ gradient in larger volume situations was due to the gradient of increasing blood flow being greater than that for ventilation. In smaller volume situations blood flow tended to be uniform in the vertical direction but ventilation per unit alveolar volume continued to increase, so reversing the $\dot{V}A/\dot{Q}$ gradient.

In horizontal postures $\dot{V}A/\dot{Q}$ tended to increase, approaching the diaphragm along a cranio-caudal isogravity line. This was more marked in larger resting volume situations and appeared to be related more to decrease in blood flow per unit alveolar volume than increase in ventilation.

We conclude that changes in posture influence local lung expansion which in turn modifies the gravity determined distribution of blood flow, and consequently the distribution of gas exchange within the lung.

REFERENCES

FAZIO, F. & JONES, T. (1975). *Brit. Med. J.* ii, 673–675.

HARF, A., PRATT, T. & HUGHES, J. M. B. (1976). *Bull europ. Physio-path. Resp.* **12**, 195 p.

HUGHES, J. M. B., GLAZIER, B., MALONEY, J. E. & WEST, J. B. (1968). *Respir. Physiol.* **4**, 58–72.

KANEKO, K., MILIC-EMILI, J., DOLOVICH, M. B., DAWSON, A. & BATES, D. V. (1966). *J. appl. Physiol.* **21**, 767–777.

WEST, J. B. & DOLLERY, C. T. (1960). *J. appl. Physiol.* **15**, 405–410.

C. 62

Some properties of the non-chemical drive to breathe at the breaking-point of breath-holding

BY A. J. GUY and J. M. PATRICK. *Department of Physiology and Pharmacology, University Hospital and Medical School, Nottingham, NG7 2UH*

The drive to breathe at the breaking-point of breath-holding can be described in terms of the interaction between a chemical component and a time-dependent non-chemical component that is related inversely to lung volume (Patrick & Reed, 1969). In five young adult subjects we have investigated the dissipation of the non-chemical drive following the breaking-point, and its effect on the subsequent breathing pattern.

Abstract Reproduction Form

Society of Nuclear Medicine 24th Annual Meeting

With the Clinical Radioassay Society

J Nucl Med June '77

CIRCLE *only one preferred subject classification*

- Bone/joint
- Cardiovascular
- Computer/data analysis
- Computed tomography
- Dosimetry
- Endocrine, metabolism
- Gastroenterology
- Hematology
- Hypertension
- Instrumentation
- In vitro studies
- Neurology
- Oncology
- Pediatrics
- (Pulmonary)
- Radioassay
- Radiopharmaceutical science
- Renal/electrolytes

DEADLINE

Abstracts must be *received* (not postmarked) by February 15, 1977.

IMPORTANT

This year all abstracts accepted for the program of the Society of Nuclear Medicine Annual Meeting will be printed directly from the typed copy on this sheet. **To insure printing quality, the instructions on the reverse side must be followed *completely* for all abstracts.** Abstracts that do not conform either will be retyped by the publisher at a cost of $25 to the author or will be rejected.

PLEASE CHECK ABSTRACT CAREFULLY FOR APPEARANCE BEFORE MAILING

TYPE ABSTRACT HERE
(BE SURE TO STAY *WITHIN* BORDER)

PULMONARY VENTILATION AND PERFUSION MEASUREMENTS USING Kr-81m; BASIC METHODOLOGY. Peter J. Kenny, Denny D. Watson, John C. Clark, Ronald D. Finn and Albert J. Gilson. Mount Sinai Medical Center, Miami Beach, FL.

Kr-81m from a Rb-81→ Kr-81m generator has been used to measure changes in regional ventilation ($\dot{V}/V$), regional perfusion ($\dot{Q}/V$) and regional ventilation perfusion ratio ($\dot{V}/\dot{Q}$) in 20 dogs in the control state and following lobar occlusion and/or drug intervention. Data from this work were analyzed to provide a basis for the use of Kr-81m for similar measurements in pulmonary function studies in humans. Serial quantitative images were obtained during the equilibrium and washout phases for both ventilation and perfusion studies using a scintillation camera-computer system. A method was developed for measuring $\dot{Q}/V$ and $\dot{V}/\dot{Q}$ by constant intravenous infusion of Kr-81m in a dextrose solution. In this case, the equilibrium concentration of Kr-81m in any region depends on the values of $\dot{Q}/V$ and $\dot{V}/V$ in that region. $\dot{V}/V$ was measured from ventilation washout studies. From this, separate quantitative determinations of $\dot{Q}/V$ and $\dot{V}/\dot{Q}$, as well as $\dot{V}/V$, for the whole lung and selected regions were made. Because of the short half-life and short equilibration times for Kr-81m distribution in the lungs, it was possible to make repeated determinations of these quantities at intervals of a few minutes to assess the effects of intervention. For example, within minutes of lobar occlusion, perfusion reduction averaging 50% was shown to have occurred in the hypoxic region, as expected, presumably due to reflex vasoconstriction. The techniques developed provide a basis for the use of Kr-81m in combined ventilation and perfusion studies for the measurement of $\dot{V}/V$, $\dot{Q}/V$ and $\dot{V}/\dot{Q}$ in humans.

TYPE FULL NAME OF AUTHOR PRESENTING PAPER:

Peter J. Kenny

EXAMPLE

TECHNETIUM-99m POLYPHOSPHATE BONE IMAGING IN LEGG-PERTHES DISEASE. James A. Danigelis, Robert L. Fisher, and Maer B. Ozonoff. Newington Children's Hospital, Newington, Conn.

This investigation was undertaken to compare the diagnostic usefulness of radionuclide bone imaging techniques to standard radiographic

In both cases, the curves are similar, and reach equilibrium in approximately one minute.

3. Calculation:

Ten sequential quantitative images (one every 3 sec.) taken during last 30 sec. of equilibrium phase. Kr-81m then shut off abruptly and a further ten images taken during first 30 sec. of washout phase. Computed least squares fits to both these curves determine C^{v}_{∞} and $(\dot{v}/v+\lambda)$. Gives $\dot{v}/v$.

For perfusion, multiply $(\dot{v}/v+\lambda)$ of perfusion study by C^{p}_{∞} to obtain ventilation corrected perfusion $C^{p}_{o}\dot{Q}/v$.

$$\dot{v}/\dot{Q} = C^{v}_{\infty}/C^{p}_{\infty} = C^{v}_{o}\,\dot{v}/C^{p}_{o}\dot{Q}$$

In summary, ventilation and perfusion are determined by measuring the local accumulation of ^{81m}Kr when the local rate of inflow through ventilation or perfusion respectively is in equilibrium with the rate of loss through decay and ventilation.

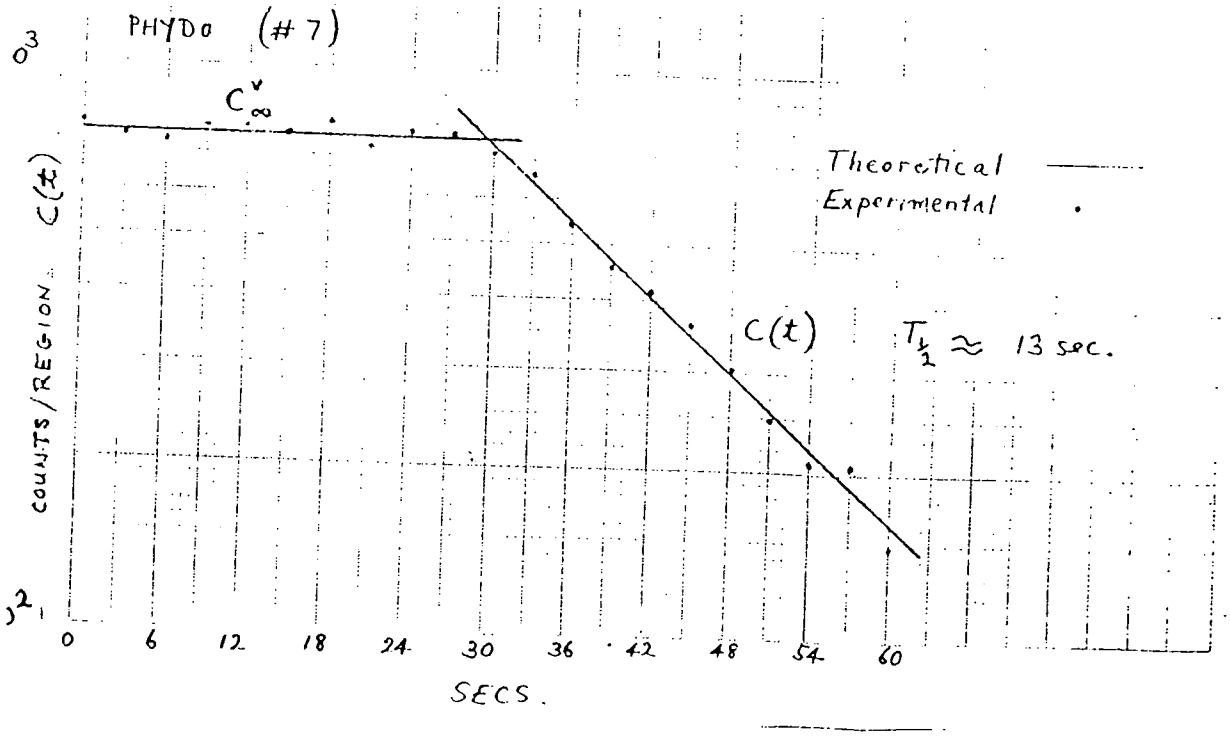

Semilog plots of ventilation equilibrium and washout curves for balloon occluded right lower lobe. Because there is very little ventilation in this region, the Kr-81m washout half-time is the physical half-time for Kr-81m decay. ($\dot{v}/v$ = 0.0017 vol./sec./unit vol.)

MATHEMATICAL BASIS FOR MEASUREMENT OF

$\dot{V}/V$, $\dot{Q}/V$ and $\dot{V}/\dot{Q}$ BY Kr-81m VENTILATION AND PERFUSION

1. Ventilation:

Patient breathes Kr-81m continuously. Input specific activity, C_o^v, is constant. Specific activity C(t) in a volume V with ventilation $\dot{V}$ is given by

$$\frac{dC(t)}{dt} + \left(\frac{\dot{v}}{v} + \lambda\right) C(t) - \frac{\dot{v}}{v} C_o^v = 0$$

giving $$C(t) = \frac{\dot{v}/v}{\dot{v}/v+\lambda} C_o^v \{1-e^{-(\dot{v}/v+\lambda)t}\}$$

For equilibrium, $C_\infty^v = \frac{\dot{v}/v}{\dot{v}/v+\lambda} C_o^v$

where $\lambda = 0.053$ sec^{-1}. for Kr-81m

For washout, $C_o^v = 0$

$$C(t) = \frac{\dot{v}/v}{\dot{v}/v+\lambda} C_o^v e^{-(\dot{v}/v+\lambda)t}$$

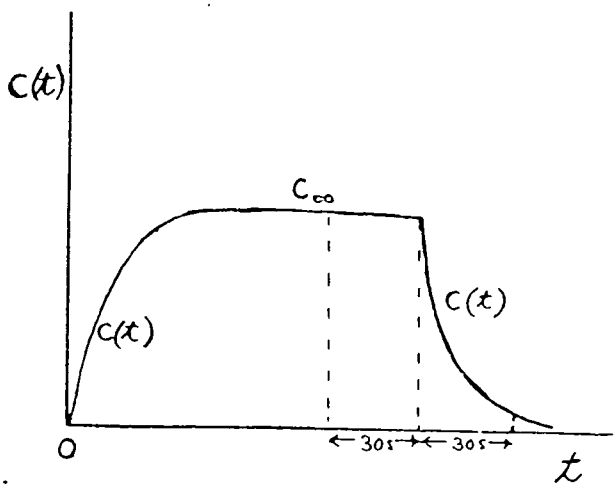

2. Perfusion:

Infuse at constant specific activity C_o^p.

For equilibrium, $C_\infty^p = \frac{\dot{Q}/v}{\dot{v}/v+\lambda} C_o^p$

For washout, $C(t) = \frac{\dot{Q}/v}{\dot{v}/v+\lambda} C_o^p e^{-(\dot{v}/v+\lambda)t}$

where $\dot{Q}$ = cardiac output.

TYPICAL RESULTS OF EFFECT OF BALLOON

OCCLUSION OF RIGHT LOWER LOBE

(Data normalized to equal numbers of image cells)

DOG PHYDO (#7)

Control	$\dot{V}$	$\dot{Q}$	$\dot{V}/\dot{Q}$	$\dot{V}/V$
RL	0.94	1.11 *	0.85	2.6
LL	1.06	0.89	1.19	2.2
RLL	0.88	0.93	0.99	1.9
LLL	0.69	0.73	0.95	2.2
BALLOON OCCLUSION				
RL	0.42	0.66	0.64	1.3
LL	2.01	0.93	2.16	2.2
RLL	0.10	0.54	0.19	0.1
LLL	1.95	0.98	1.99	2.5

RL = Total right lung

LL = Total left lung

RLL = Right lower lobe (balloon occluded)

LLL = Left lower lobe (control area)

$\dot{V}$ = ventilation (relative value)

$\dot{Q}$ = perfusion (relative value)

$\dot{V}/\dot{Q}$ = ventilation perfusion ratio (relative value)

$\dot{V}/V$ = absolute ventilation expressed as volumes/min/unit volume

* $\dot{V}$ and $\dot{Q}$ are normalized so that the average of $\dot{V}$ and $\dot{Q}$ for both lungs taken together = 1.00

International Journal of Applied Radiation and Isotopes, 1977, Vol. 28, pp. 53–65 . Pergamon Press. Printed in Northern Ireland

The Preparation of Fluorine-18 Labelled Radiopharmaceuticals

A. J. PALMER, J. C. CLARK and R. W. GOULDING
MRC Cyclotron Unit, Hammersmith Hospital, Ducane Road, London W12 0HS, U.K.

(*Received* 3 *April* 1976)

Progress in the preparation of fluorine-18 labelled radiopharmaceuticals is reviewed. The pharmacology and design of ^{18}F-labelled organic compounds of biomedical interest, production of the radionuclide and methods of labelling which have been used to date are discussed. Emphasis has been placed on the practical chemical problems encountered, together with the important fields of product purification and quality control.

INTRODUCTION

IN THE past three decades the study of fluorine compounds has become a major branch of organic chemistry, concerning both highly fluorinated systems and those in which fluorine may replace only one or two hydrogen atoms in an organic molecule. Many fluorine-containing compounds have found use in medicine and in recent years some research has been directed towards the preparation of radiopharmaceuticals incorporating the only radionuclide of fluorine with a useful half life, ^{18}F ($T_{1/2}$ 110 min β^+). This article is concerned with the preparative aspects of incorporating ^{18}F into organic molecules of potential biomedical interest, together with the design of such compounds. ROBINSON has recently reviewed their potential applications[1] while the use of ^{18}F as fluoride ion for bone scanning and dental studies is well known.

For labelling organic molecules ^{18}F is usually considered in conjunction with three other common cyclotron produced β^+ emitters, ^{11}C, ^{13}N and ^{15}O. The *in vivo* detection of these nuclides requires specialized detectors and electronics if their full potential is to be realized, but using modern positron imaging devices[2–4] it is possible to obtain more detailed positional information than is obtainable from a γ-emitter. From the biochemical point of view ^{11}C, ^{13}N and ^{15}O are ideal for labelling an organic radiopharmaceutical since no "foreign" atom is introduced. However, they all have very short half-lives, and if this factor proves unacceptable then ^{18}F may offer an alternative. Since, with minor exceptions fluorocarbon compounds do not occur in nature, they are wholly artificial and consequently the electronic properties and size of fluorine relative to hydrogen (which it usually replaces in an organic molecule) must be considered together with the related pharmacological effects.

Superficially ^{18}F would appear to be an ideal label from the radiochemical point of view. It may be produced in a reactor or on a cyclotron using a variety of nuclear reactions. Times of up to 4 hr ($2 \times T_{1/2}$) have been considered acceptable for chemical syntheses. As stated previously fluorine usually replaces hydrogen, consequently a large number of possible positions of labelling are frequently available, and the very high dissociation energy of the C–F bond means that these compounds may be expected to have improved *in vivo* stability when compared for example with similar iodine compounds.

Many fluorination reactions give a low yield based on fluorine, and classical methods of introducing fluorine use extreme reaction conditions and very reactive or corrosive reagents. Often simple compounds have been fluorinated and then transformed into more biologically interesting compounds by a series of time consuming reactions. The aim in ^{18}F chemistry is to avoid such reactions and procedures and where possible adopt the most direct and rapid high yield method. It is always desirable to optimize the yield with respect to the ^{18}F in the starting material. Biosynthetic techniques,[5,6] which are frequently used for preparing other radiopharmaceuticals and have the advantage that they yield high specific activity products, cannot

be used for the direct introduction of inorganic ^{18}F although they may of course be used for subsequent transformations.

Up to the present time one of the principal problems in the preparation of ^{18}F labelled compounds has been that it has proved difficult to prepare them in specific activities comparable with those of other radiopharmaceuticals. This may lead to toxicity problems and a general lack of pharmacological data may be an additional handicap in this respect.

Pharmacology of fluoro-compounds

1. C–F *in place of* C–H. Fluorine is of comparable size to hydrogen and both form strong bonds to carbon, but the chemical reactivities are very different. The enzymic effect of this is that the analogue with fluorine at the reaction centre will very often act as inhibitor rather than substrate. With a fluorine adjacent to the reaction centre the "normal" reaction may still occur but at a greatly changed rate. A remote fluorine atom usually has no effect on the process. Thus the introduction of a halogen atom into an aromatic ring system often prevents biochemical reaction at that position, an effect described as "obstructive halogenation".[7] The effect is very pronounced for fluorine especially at the para position of simple phenyl groups when the metabolically important enzymatic hydroxylation can be severely inhibited.[8] If hydroxylation cannot occur then neither can subsequent conjugation, and the tissue distribution is affected. As an example, Fig. 1 outlines the possible *in vivo* fates of three selected fluoroamino acids. The tissue distribution of ^{18}F at any time may be seen to be due to a range of metabolites in addition to the administered compound (I, II, III).

These considerations are important when it is desired to produce γ-emitting labelled molecules which have known biochemical properties and may tend to localize in specific tissues. For this purpose a single fluorine atom should be placed in a site remote from functional groups. It is useful to synthesize as many isomers of the ^{18}F-labelled compound as possible so that the differences can be evaluated.

2. CF_3 *in place of* CH_3, Br *or* NO_2. When a CF_3 group replaces a CH_3 group in a molecule the change in properties is usually fairly pro-

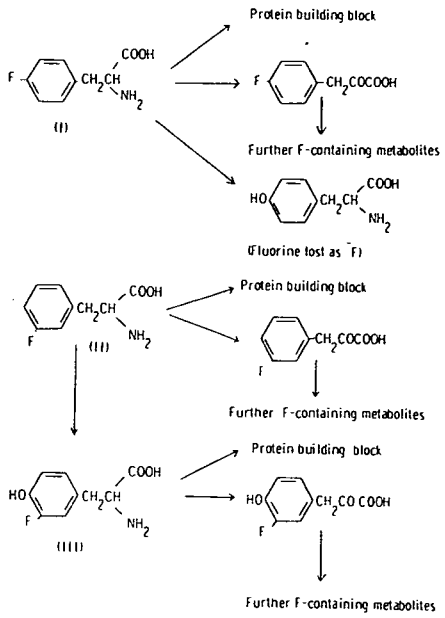

FIG. 1. *In vivo* transformations of *p*-fluorophenylalanine (I) *m*-fluorophenylalanine (II) and 3-fluorotyrosine (III).[8,9]

nounced. The former has significant steric crowding effects and is very strongly electron withdrawing. In aliphatic systems a remote CF_3 group can be reasonably inert (mimicking CH_3) for example in the leucine analogue (IV)[10].

In aromatic systems the CF_3 group normally resembles the NO_2, CN and SO_2–R groups in electronic effects, and in particular activities ortho and para positions to nucleophilic attack. In more complex aromatic systems the effect of the CF_3 group is usually not so pronounced, when it may resemble Br, Cl or even CH_3 in biological behaviour.[8,11]

Therefore a labelled CF_3 group could be introduced to make a ^{18}F-labelled analogue of a CH_3, Cl, Br or NO_2 parent compound under favourable circumstances.

3. C–F *in place of* C–OH. A fluorine atom can

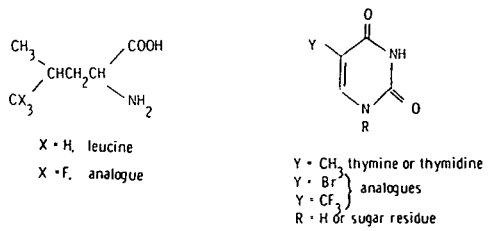

FIG. 2. Trifluoromethyl analogues of leucine (IV)[10] and thymine (V).[12]

also be introduced as the analogue of a hydroxyl group. Pharmacological application has been concentrated on polyhydroxy compounds such as carbohydrates. The fluorine atom can only act as a hydrogen bond acceptor, whereas the hydroxyl group can act as donor and acceptor. It is best to introduce a single fluorine atom because polyfluoro compounds have a different pharmacology. It has been shown that one monofluoro analogue of glucose out of all the possible isomers is transported in the same manner as glucose itself.[13] This is because only in this isomer can the same H-bonding occur in the receptor site of the transport molecule.

4. $-C_6H_4{}^{18}F$ *as a protein label.* Various hapten groups have been used for tagging proteins and enzymes for non-radioactive tracer work. Proteins have been labelled directly with radioiodine, or with ^{111}In *via* covalently bound EDTA groups[14] (these are often not very stable *in vivo*). It would appear that a perfect radio-label would have a half-life of 2–24 hr and would be covalently bound to the protein *via* a spacer group. Proteins have been usefully labelled with ^{11}C-methyl groups despite the short half life.[15,16] ^{18}F labelled fluorophenol, fluoroaniline and fluorobenzoic acid are readily prepared (see under reaction scheme 1) and could be used to label proteins by established procedures.

Up to the present time only ^{18}F-labelled compounds of the type described in section (1) have been reported.

Stereochemical effects

Biological activity is closely related to the stereochemistry of the substrate molecule, and when such a molecule exists in two or more isomeric forms (geometrical or optical) the biological activity of each of these forms can be very different. This isomerism may already be present in the molecule or it may be generated when a foreign atom (the label) is introduced.

In those cases where a single stereo-isomer of a labelled compound is required it may be possible to use a synthetic sequence in which the precursor to be labelled is available as a single stereo-isomeric form and can be converted to the final product via stages which proceed with effectively 100% stereospecificity. Alternatively an epimeric or racemic mixture may be generated during or after the labelling stage (cf. the amino acids below) and this may be followed by a procedure for resolution. The consequent loss of time and material must be offset against the fact that this may be an easier technique than a stereospecific synthesis.

Strategy of ^{18}F labelled synthesis

Because of the short half life it is essential to introduce the ^{18}F label at the latest stage possible. Usually a suitable precursor is prepared in bulk and stored for future use. Most reactions used for ^{18}F labelling have to be completed in less than the optimum times and using other than the optimum relative amounts of reactants. Consequently mixtures of labelled and/or unlabelled products are often obtained. Preparative gas (gc) or liquid chromatography (lc) are especially useful separation techniques since they can be carried out rapidly. Solvent extraction and sublimation may also be useful. Conversely, preparative thin layer chromatography is not so useful because spotting, zone identification and elution are relatively lengthy processes.

^{18}F labelled compounds for *in vivo* use are preferably administered in approximately isotonic solutions. Because of the short half-life, lengthy de-salting or solvent removal stages are not practicable. The best approach is to either be able to isolate a non-polar compound from a volatile organic solvent such as ether, or to carry out reactions in aqueous solutions of low ionic strength. Immobilized reagents are especially useful (e.g. H^+-form ion exchange resin in place of acids, or F^--form resin for fluorination[17]). If any final liquid chromatographic purification is required the preferred eluant is water or an approximately isotonic, non-toxic buffer.

Analytical considerations

It is necessary to establish the identity and homogeneity of any starting materials one may synthesize for subsequent ^{18}F-labelling. Infrared and nuclear magnetic resonance (nmr) are useful for the former, and thin layer (tlc) or gas (gc) chromatography for the latter.

Since the range of compounds that have been labelled with ^{18}F is not very extensive new reactions attempted in future will present new problems to be solved. Development work

normally requires a lengthy series of trial reactions which are followed by various standard radio-chromatographic techniques e.g. tlc/ autoradiography. The technique of coupled glc-mass spectrometry is valuable for the analysis and identification of mixtures that are volatile or can be made volatile by derivatization.

When a complete synthesis of the required ^{18}F-compound has been achieved it is often not possible to perform an extensive chromatographic analysis before the *in vivo* use because of the short half-life of the label. Therefore, in a series of preliminary experiments employing stable or active fluorine and using the projected procedure, the identity and homogeneity of the product should be ascertained. Then a standardized experimental procedure is established and the final product may be analysed by a shortened procedure concurrently with its utilization. In order to determine the specific activity of the solution to be administered, measurement of the u.v. absorbance at a selected wavelength is often a valuable and rapid method.

The points mentioned in this section may appear to be self evident, but failure to appreciate them will invariably give misleading results. Much information in the literature concerning short-lived labelled compounds is unsatisfactory because adequate product analysis is not described. Certain claimed preparations do not quote any method of analysis and the phrase "analysed by tlc" has appeared without a description of the stationary or mobile phase used. Even when exchange processes are used compound degradation may occur and so the identity of the labelled "product" can never be assumed without proof.

PRODUCTION OF THE RADIONUCLIDE

Some nuclear reactions which lead to the production of fluorine-18 are listed in Table 1. The excitation curves for these nuclear reactions together with the thick target saturation activities for deuterons and tritons of up to 24 MeV, and ^3He and ^4He up to 42 MeV have been measured by NOZAKI[18].

TABLE 1. Some nuclear reactions for the production of Fluorine-18

No.	Target	Projectile	Reaction
1	O	^3H	$^{16}O(^3H, n)^{18}F$
2	O	^4He	$^{16}O(^4He, pn)^{18}F$
3	O	^3He	$^{16}O(^3He, p)^{18}F$
4	Ne	d	$^{20}Ne(d, \alpha)^{18}F$
5	Ne	^3He	$^{20}Ne(^3He, \alpha p)^{18}F$

Reaction 1 has been in use for many years using the 2.73 MeV (max) tritons generated in a nuclear reactor by the $^6Li(n, \alpha)^3H$ reaction.[19] The target material is usually Li_2CO_3 with a ^6Li enrichment of at least 90%. Fluorine-18 is recovered as $^{18}F^-$ without the addition of carrier by HF distillation into aqueous alkali,[20–22] or by ion exchange.[23,24] Partial removal of the undesirable impurity tritium (typically 750 mCi ^3H to 2.5 mCi ^{18}F[23]) as water and $^3H_2$ is achieved by repeated evaporations to dryness. The traces of tritium that remain after this treatment have been identified as ^3H-acetate and ^3H-formate.[25]

The recovery of anhydrous $H^{18}F$ from reactor irradiated Li_2CO_3 by distillation of HF onto ion exchange resin which is subsequently dried and eluted with HF has been described.[26] However, as up to 1.5 g of HF was used to achieve a 90% recovery from the resin, the resulting $H^{18}F$ was of low specific activity.

Improvements relating to the Li_2CO_3 target design have been described which enable high neutron fluxes to be used more effectively and batches of 65–75 mCi of fluorine-18 to be prepared.[22]

Reactions 2 and 3 employing oxygen[26] or water[27–30] as target materials have been extensively used for ^{18}F production. Aqueous solutions of ^{18}F from water targets have been used to label aromatic diazonium fluoroborates by exchange.[31,32] Fluoride has been recovered from aqueous solutions using a fluoride form anion exchange resin column which after careful drying has been used in anhydrous interhalogen exchange reactions to label a variety of aliphatic compounds with fluorine-18.[17] The use of an oxygen gas target to produce anhydrous HF has been demonstrated.[26] Here the ^{18}F trapped heterogenously by the silver plated target walls during irradiation is subsequently recovered by exchange with ~1 g of anhydrous HF carrier.

Reactions 4 and 5 have received a great deal of attention in recent years, particularly under anhydrous conditions. Here the aim has been to produce a variety of high specific activity

fluorinating agents. The investigations have followed three main approaches.

1. *Homogeneous scavenging of ^{18}F with recovery during irradiation*

The mixing of nitric oxide, hydrogen or chlorine with neon before irradiation has yielded $NO^{18}F$[33], $H^{18}F$[34] and $Cl^{18}F$[34] reportedly carrier-free from nickel targets preconditioned with F_2. A recovery of 60% is reported for $NO^{18}F$ but the data for $H^{18}F$ and $Cl^{18}F$ suggest large losses of ^{18}F to the target walls. The addition of F_2 to the neon resulted in the recovery of $^{18}F_2$ with 30% efficiency.[34] However, these preliminary results provide encouragement for further development of the technique.

2. *Heterogeneous scavenging with post irradiation recovery*

The losses of ^{18}F in the homogeneous scavenging approach are largely to the walls of the target vessel. There are several reports of the recovery of carrier-free ^{18}F by the washing of glass-lined target vessels with normal saline[35] or water[36,37] with recovery efficiencies of around 60–90%. The washing of a glass-lined target with dilute solutions of AgF, BF_3 and aromatic fluoroborates in anhydrous organic solvents with 50–80% recoveries described by Ido (1974) appears to have some attractive features although the specific activity of the fluorinating agent is reduced by the introduction of carrier.[38]

A further heterogeneous approach to ^{18}F recovery has been to coat the target walls with a thin layer of the organic compound to be labelled. After irradiation the organic material is recovered in solution by washing the target walls. Inorganic ^{18}F is removed by ion exchange and the labelled product separated from the starting material by ion exchange chromatography.[39]

The fluorinating agents AgF, KF and SbF_3 (100 mg–1 g) have been labelled by a similar technique.[18] A variation of the technique has been described where a target lined with AgF or AgF_2 was used. After irradiation the neon was removed and the vessel used as a reactor for the synthesis of CCl_3F and CCl_2F_2.[40] This technique is in principle applicable to many fluorinations involving volatile organic substrates.

3. *Heterogeneous scavenging during irradiation remote from the target*

The recovery of ^{18}F by exchange labelling of a small quantity of a simple or complex fluoride placed remote from the target has been demonstrated.[41] The neon is circulated during irradiation through a glass-lined target vessel, and the effluent gas is led through PTFE tubing to a filter holder where a glass fibre element, previously coated with a 5–50 mg of an ionic fluoro-compound, e.g. KF, $NaBF_4$, SbF_3, or an aromatic diazonium fluoroborate is supported. A reactor containing dry fluoride-form ion exchange resin (Dowex 1, ~2 gm) may also be used.

The volatile ^{18}F-labelled intermediate which is continuously swept from the target during irradiation is removed almost quantitatively by the coated filter. The filter element or ion exchange resin can often be used directly in the chemical syntheses that follow. This technique is useful for fluorinations involving non-volatile organic substrates.

Methods of ^{18}F Labelling

The Balz–Schiemann reaction has been used extensively for making aryl fluoro-substituted compounds. Nucleophilic displacement reactions have been used for the preparation of aliphatic fluoro-compounds. Additionally various other methods have been employed in special cases.

PREPARATION OF AROMATIC FLUORO-CARBONS VIA THE BALZ–SCHIEMANN REACTION

Compounds which are monofluorinated in an aromatic ring system often show biological activity related to the corresponding unfluorinated or phenolic compound. Hence methods of

preparing such compounds in labelled form are of immediate interest. Direct mono-fluorination of aromatic rings is only possible in very special circumstances, but the Balz–Schiemann reaction[42] allows the ready conversion of an aryl nitro compound, via the amine and diazonium salt, to the corresponding fluoro-compound (Fig. 3, general reaction scheme).

The tetrafluoroborate anion of the diazonium salt may be labelled by exchange and the C–^{18}F bond is formed when the diazonium fluoroborate is decomposed thermally. Many simple ^{18}F-aryl fluoro-compounds have been prepared by this method[43] and of these, amines, phenols and carboxylic acids could be used as starting materials for the preparation of other labelled compounds. The chemical yield in the Balz–Schiemann reaction is often low, and a large amount of side-products may be produced. Also, since the fluorine is introduced as the labelled fluoroborate anion, the maximum possible radiochemical yield is 25% and in practical examples it is ~2–15%.

A further complication is introduced because other reactive groups present in the molecule can prevent any of stages I, II or III from proceding. In such cases (in fact with almost all the compounds of biological interest) it is necessary to use "protected" derivatives of such groups, prepared either by a direct protection reaction or by synthesis from simpler compounds. After stage III the protecting group(s) are removed by suitable deprotection reactions. The reported chemistry of protecting groups is very extensive especially in the peptide, steroid and carbohydrate fields,[44] but so far only the simplest protecting groups have been employed during ^{18}F-syntheses.

The diazonium fluoroborates may be labelled by exchange with carrier-free ^{18}F in water[32] or water/acetone[31] or by heterogenous exchange between the solid supported in an inert matrix and carrier-free fluorine-18 extracted from a recirculatory neon gas target.[41] The last method is far superior since exchange is instantaneous and much higher specific activities may be achieved. The labelled diazonium fluoroborate may be decomposed dry or in an inert solvent. A mixture of products is always obtained as shown by tlc (silica gel, 10% ethyl acetate in chloroform) and the ratio of various components varies with the decomposition solvent used. Biphenyl, tetrahydronaphthalene and phenanthrene give good yields, whereas dichlorobenzene and malononitrile give poor yields of the desired protected fluoro-compound.[41,45] Purification of the mixture may be effected by preparative tlc or lc when the diazonium salt is decomposed dry, but lc is the best method when a solvent is used.

1. *Aromatic amino acids and catecholamines*

Fluorine-18 labelled analogues of four naturally occurring aromatic amino acids have been prepared. These are phenylalanine, tyrosine, tryptophan and 3,4-dihydroxyphenylalanine (DOPA). The first three are utilized in the production of enzymes and proteins and the ^{18}F-labelled analogues are being investigated as potential pancreas scanning agents[46] since this organ is a site of rapid utilization of amino acids for protein production. DOPA is associated with melanin-formation and Parkinsonism. All of the ^{18}F-amino acids have been evaluated as potential melanoma localising agents[47] and fluoro-DOPA.

Abnormalities in the quantities and metabolism of catecholamines are associated with hypertension, Parkinsonism, chromaffin tissue tumours and other pathological conditions.[49] ^{18}F-6-Fluoro-dopamine is being evaluated as an adrenal scanning agent.[50] Fluorine-18 labelled derivatives of amino acids and catecholamines which have been prepared are listed in Tables 2–4.

Labelled *p*- and *m*-fluorophenylalanine may be prepared by a published method[51] used for the inactive compounds essentially without modification. A diethyl acetomidomalonate derivative of the corresponding diazonium tetrafluoroborate (Table 2) is first prepared and labelled. After the decomposition the protecting groups (ester and amide) may be removed by vigorous acid hydrolysis when the *dl*-amino acid is obtained.[31,52] Alternatively it is possible to prepare the *dl*-acylamino acid which may be stereoselectively deacetylated using the fungal enzyme amino acylase to give the *l*-amino acid.[53,53]

A mixture of the enzyme, *d*-acylamino acid and *l*-amino acid is obtained and the required *l*-amino acid can be recovered efficiently by lc

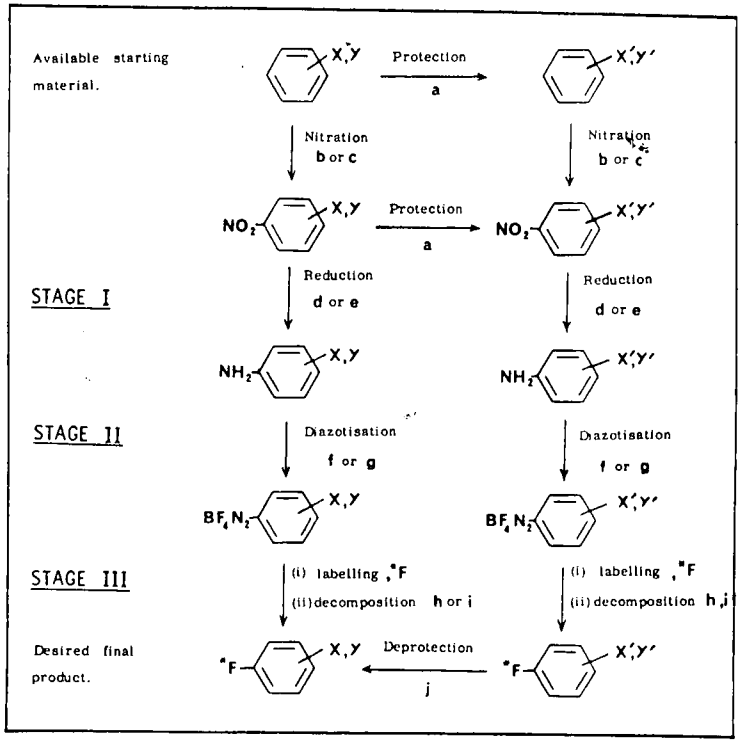

GENERAL REACTION SCHEME.

X,Y general substituents. X′,Y′ protected substituents.

Reagents : a see table below. b HNO_3/H_2SO_4. c HNO_3/CH_3COOH. d $Na_2S_2O_4$. e H_2, Pd/C, CH_3COOH. f HNO_2/HBF_4. g $NOBF_4$. h Δ(130-200°, heat alone). i Δ(130-200°, in inert solvent). j see table below.

PROTECTING GROUPS:

Group (X,Y)	Protected Group (X′,Y′)	Deprotection
$-NH_2$ (aryl, alkyl)	acetamido-, formamido- phthalimido -	strong acid or alkali hydrazine
-OH (aryl)	methyl ether	HBr, HI or BBr_3
-COOH (alkyl)	ethyl ester	alkali
amino acid	diethyl acetamido -malonate	strong acid or alkali OR (i)alkali (ii) acid (iii) enzyme

^{18}F- LABELLED COMPOUNDS PREPARED:

(a) Potential Synthetic Precursors.

Fluoro-aniline(ex $FC_6H_4NHCOCH_3$)
Fluorophenol (ex $FC_6H_4OCH_3$)
Fluorobenzoic acid
o - Fluorobenzyl chloride

References 43, 52.

(b) Biologically Important Compounds.

p-Fluorohippuric acid
o/m/p-Fluorophenylalanine (L , DL)
3-Fluorotyrosine (DL)
5-Fluoro-DOPA (DL)
5/6-Fluorotryptophan (L , DL)
6-Fluorodopamine
Haloperidol (TM)

For references see tables 2 - 4.

FIG. 3. Application of the Balz–Schiemann reaction.

TABLE 2. O/m/p-Fluorophenylalanines

Compound	Starting Material	Protected NO_2 - Compound	Ref
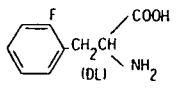	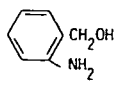	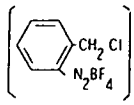	52
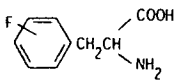 m, p (L, DL)	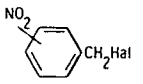	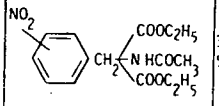	31, 41, 52, 53

TABLE 3. 3-Fluorotyrosine, 5-Fluoro-DOPA and 6-Fluorodopamine

Compound	Starting Material	Protected NO_2 - Compound	Ref
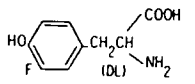	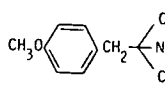	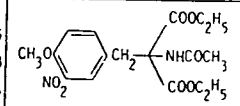	36, 41
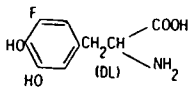	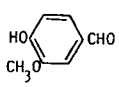	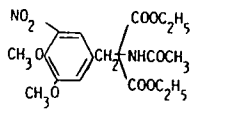	48, 55
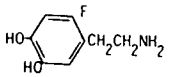	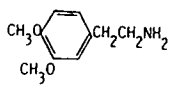	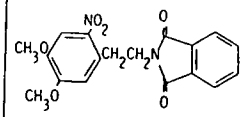	50

TABLE 4. 5/6-Fluorotryptophan

Compound	Starting Material	Protected NO_2 - Compound	Ref
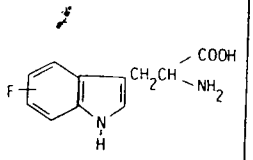 (L, DL)	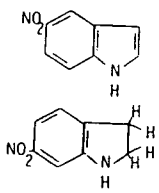	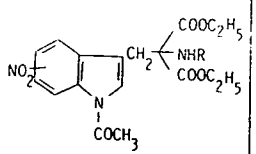 (L, R = $COCH_3$) (DL, R = CHO)	32, 41, 45

using Biogel-P2.[53] Fluorine-18 labelled *dl*-*o*-fluorophenylalanine cannot be prepared by the above route but has been synthesized by a longer method.[52]

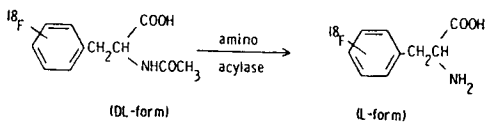

FIG. 4. Preparation of ^{18}F-labelled *L-p-* and *m*-fluorophenylalanine.

In the case of *dl*-3-fluorotyrosine[36] and *dl*-5-fluoro-DOPA[55] the amino acid function is generated from the diethyl acetamidomalonate group, and the phenolic OH function from methyl ether groups. The nitro-compounds shown (Table 3) can be converted into diazonium fluoroborates, labelled and decomposed to give the corresponding fluoro-compounds. These in turn (after purification) may be completely deprotected to give the *dl*-amino acid by treatment with constant boiling HBr or HI. In the

case of fluoro-DOPA care is required to avoid loss of the product through oxidation and polymerization. So far it has not been possible to prepare these amino acids in the *l*-form because of chemical problems encountered.[45]

The preparation of ^{18}F-labelled *dl*-5- and 6-fluorotryptophan has been reported.[32] The 4- and 7-isomers could be prepared by similar procedures if they aroused any interest in the future. Indoles in which a free ring (1−) NH group is present cannot be diazotized without self-reaction occurring. However successful diazotizations and subsequent decompositions have been effected through the use of ring (1−) N-acetylindoles,[56,57] and the nitro-compounds shown (Table 4) may thus be employed. After the thermal decomposition reaction, purification is again carried out by preparative tlc or lc.

Indoles with a free ring (1−) NH group present such as tryptophan are also unstable to to mineral acids and air oxidation. To avoid all of these problems the diethyl formamidomalonate (R = CHO, Table 4) is used in the preparation of labelled *dl*-fluorotryptophans, when the two stage (dilute alkali followed by very dilute acid) hydrolysis gives the free *dl* amino acid directly[32,58] (compare with fluorophenylalanine above). If the diethyl acetamidomalonate (R = $COCH_3$, Table 4) is used the product is the α-*N*-acetyltryptophan derivative[58] which can be treated with the enzyme to give the labelled *l*-amino acid.[45] It should be noted the acetyl group is a very good protecting group for the ring (1 −)NH group because it is readily lost in the hydrolyses.

^{18}F-labelled 6-fluorodopamine has been prepared from the corresponding protected nitrocompound[50] by the standard stages. The catechol group was protected as the bis-methyl ether, and the amino group by phthaloylation. Deprotection was effected by hydrazinolysis followed by treatment with hydrobromic acid or boron tribromide (Table 3).

2. *Other compounds of biomedical interest*

The syntheses of ^{18}F-labelled 4-[4-(*p*-chlorophenyl)-4-hydroxypiperidino]-4′ - fluorobutyrophenone (VI)[59] (the neuroleptic drug "Haloperidol") and ^{18}F-*p*-fluorohippuric acid (VII)[38] have been reported. The former was for use in investigations of its tissue distribution and pharmacokinetics. Both these compounds were prepared directly from the corresponding diazonium tetrafluoroborates, protecting groups being unnecessary.

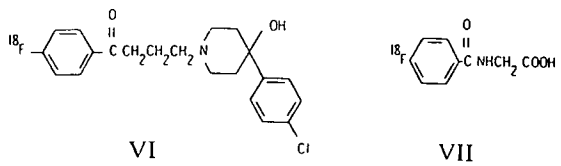

VI VII

FIG. 5. ^{18}F-labelled "haloperidol" (VI)[59] and *p*-fluorohippuric acid (VII).[38]

METHODS EMPLOYING NUCLEOPHILIC DISPLACEMENT

1. *Alkali metal and related fluorides*

A wide range of aliphatic fluoro-compounds have been prepared by nucleophilic displacement of a good leaving group, i.e. bromide, iodide, tosylate (−OTs) or an ammonium salt ($-NMe_3^+X^-$). Often a very large molar excess of the fluoride is necessary to achieve reasonable yields of organic fluoride.

The nature of the solvent used is of critical importance. It should be highly polar and ionizing, and have very low nucleophilicity[60] (in order not to compete with fluoride). It is desirable to have good solvation of the inorganic cation but poor or (preferably) no solvation of the anion. In the aprotic solvents DMA. DMSO or HMPA* the large cations K^+, Rb^+, Cs^+, Tl^+ and Bu_4N^+ are highly solvated but the fluoride ion is essentially "naked". Thus compared with other solvents, e.g. glycol, the rate of reaction is greatly increased (up to 10^6 times). A further improvement is to use catalytic amounts of a crown ether[61] (very effective solvation of cations) or a phase transfer catalyst e.g. cetyl tributyl phosphonium bromide.[62]

In order to obtain useful amounts of ^{18}F-labelled compounds (say > 500 μCi at > 1 mCi/mg) it is essential to take full account of the above considerations. The salts KF, Bu_4NF etc. are extremely difficult to render completely anhydrous especially on the small scale. The presence of traces of water will cause failure of the reaction. In view of the problems involved it

* Dimethyl acetamide, dimethyl sulphoxide and hexamethyl phosphoramide, ($PO(NMe_2)_3$).

is not surprising that relatively little use has been made of these reagents for ^{18}F- labelling.

ROBINSON[17] has developed a novel alternative technique in which fluoride-form ion exchange resin (Dowex-1) is used as the fluorinating agent

$$\text{Resin}\,[CH_2NMe_3 + F^-]_n,$$

which is labelled by exchange with carrier-free fluorine-18 in neon[45] or water.[17] The success of this particular reagent may be due to the ease with which it can be rendered anhydrous (1 hr/150°C *in vacuo*). It has a certain formal similarity to the phase transfer catalysts, and, as an immobilized reagent, facilitates very rapid work up after the reaction.[63] The mixture of alkyl bromide and fluoride obtained can be separated by preparative gas chromatography. Various ^{18}F-2-fluorocarboxylic acids (protected as ethyl esters) have been prepared by the method, and from these, by reduction, the corresponding 2-fluoroalkanols. These compounds have been used for brain and heart studies and also investigation of ethanol metabolism.[64]

2. *Silver fluorides*

Silver (I) fluoride is much more versatile than the alkali metal fluorides in that it can be used to prepare *pri*-, *sec*- and *tert*-alkyl fluorides[65] and heteroaromatic compounds. The reactions are relatively rapid and the reagent is often used without solvent with both liquid and gaseous substrates (at 25–200°C). High yields of the organic fluoro-compound are obtained even with ^{18}F-labelled material (up to 50% radiochemical yield, X = Br or I):

$$RX + 2AgF \rightarrow RF + AgF \cdot AgX$$

However silver fluoride is awkward to handle because it is extremely hygroscopic and corrosive (it normally cannot be used in glass). It has been employed to prepare labelled freon-11 (CCl_3F),[41] 6-fluoro-9-benzyl purine[38] and 3-fluoro-cholestene[38] (Table 5).

Silver difluoride, AgF_2, can occasionally act as nucleophilic fluorinating agent and is more reactive than the monofluoride. It is instantly hydrolysed by water. See also electrophilic fluorinations below. Mercury (I) and (II) fluorides have been used in similar way.[66,67] One fluorine-18 reaction has been reported (Table 5) with $Ag^{18}F_2$. Pratical details concerned with the small scale handling of fluorine gas and silver fluorides have been published.[40]

TABLE 5. Preparation of ^{18}F-labelled compounds by halogen displacement

Reagent	Substrate	Product	Ref
$^{18}F^-$ Ion exchange resin	$BrCH_2CH_2OH$	$^{18}FCH_2CH_2OH$	74
$^{18}F^-$ Ion exchange resin	Ethyl halocarboxylates	Ethyl ^{18}F-fluorocarboxylates, acids and alcohols (by subsequent transformation)	17, 74, 75
$Ag^{18}F$	CCl_4	$C^{18}FCl_3$	40
$Ag^{18}F_2$	$CFCl_3$	$C^{18}F_2Cl_2$	40
$Ag^{18}F$	3-Iodocholestene	^{18}F-3-Fluorocholestene	38
$Ag^{18}F$	6-Chloro-9-benzyl purine	^{18}F-6-Fluoro-9-benzyl purine	38
$K^{18}F$ /COOH	2, 4, Di-iodoestrone	^{18}F-2, 4-Difluoroestrone	76
$K^{18}F$ /COOH	3, 5-Di-iodotyrosine	^{18}F-3, 5-Difluorotyrosine	76
$K^{18}F$	21 - Iodopregnolone - 3 - acetate	^{18}F-21-Fluoropregnolone-3-acetate	77

3. *Antimony and bismuth fluorides*

SbF_3, BiF_3, SbF_3Cl_2, SbF_5 and BiF_5, have been used to affect the transformation $RCCl_3 \rightarrow RCF_3$. The group R may be an alkyl, aryl or heteroaromatic group, but very few compounds of type $RCCl_3$ have been prepared and hence are available to be used as substrates. This is unfortunate since good yields of product are obtained even with 10–100 mg amounts of ^{18}F-labelled SbF_3 (R=CH_3, C_6H_5).[45] Antimony trifluoride may be labelled by exposure to carrier-free fluorine-18 in neon.[18,41] It undergoes partial hydrolysis by exposure to moisture during handling but may afterwards be completely reactivated (as SbF_3Cl_2) by treatment with $SbCl_5$.[66]

Some compounds which have been reported to have been prepared by methods employing nucleophilic displacement are listed in Table 5.

PREPARATION BY DIRECT FLUORINATION AND OTHER ELECTROPHILIC FLUORINATING AGENTS

The past few years has seen the introduction of some novel methods of fluorination which seem likely to lend themselves to the preparation of ^{18}F labelled radiopharmaceuticals. Perchloryl fluoride ($FClO_3$) and fluoroxytrifluoromethane (CF_3OF) have been used extensively as a source of electrophilic fluorine to fluorinate activated alkenes. CF_3OF and

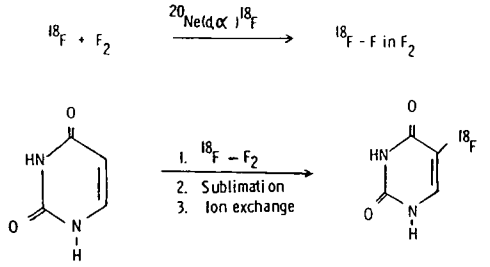

FIG. 6. Preparation of ^{18}F-5-fluorouracil.[70]

molecular fluorine have also been used for the direct electrophilic fluorination of 2,4-dioxopyrimidines to produce the 5-fluoro-derivatives.[68,69] This reaction has been employed in ^{18}F-labelling—when 5-fluorouracil was prepared from uracil and $^{18}F-F_2$ 5-fluorouracil is a cytoxic analogue of uracil which finds some application in cancer chemotherapy,[71] while the active material is a potential tumour localizing agent and may also be used to investigate the pharmacokinetics of the stable compound.[72]

This is a rapid procedure which is well suited to labelling, being capable of yielding high specific activity material. Although specialized targetry is required, elemental fluorine is prepared quite easily in the laboratory.[40] Syntheses using labelled CF_3OF have not so far been reported. Other reactions of this type which have been reported in the chemical literature include the preparation of 5-fluorocytosine, 5-fluoro-orotic acid and 5-fluorobarbituric acid.[68]

MISCELLANEOUS REACTIONS

Several labelled fluorinating agents are currently available but there have been no reports of their applications. These include nitrosyl fluoride, fluoroxytrifluoromethane and chlorine monofluoride. Labelled hydrogen fluoride, which may be prepared by several different methods, has been available for some time but appears so far to have found only very limited use. Cleavage of an epoxide by this reagent or boron trifluoride is a promising method in view of its rapidity and possible use on unprotected substrates, particularly in the preparation of labelled fluoro-steroids.[38,73] STRAATMANN and WELCH[78] have recently prepared ^{18}F-labelled diethylamino sulphur trifluoride (DAST) a reagent which can be used to effect the following transformations:[79,80]

$$RR'CO \rightarrow RR'CF_2.$$
$$RCOOH \rightarrow RCF_3$$
$$ROH \rightarrow RF.$$

CONCLUSION

Several ^{18}F-labelled organic compounds have been prepared and are being evaluated in animals with the ultimate aim of clinical application. However, as this article has attempted to show, the difficulties encountered in designing and preparing ^{18}F-labelled compounds of radiopharmaceutical quality are considerable.

The Balz–Schiemann reaction is relatively easy to apply but is only applicable to aromatic compounds and gives low yields. Fluorinations using silver or antimony fluorides give high yields but there are special problems to be overcome, while the F^- form ion exchange method appears to offer promise for certain aliphatic compounds. The use of elemental fluorine is at present limited to one class of compound, and other methods are a long way from regular utilization. However, radiopharmaceuticals labelled with ^{18}F may offer many potential advantages of *in vivo* stability and improved detection, both in those cases where the pharmacology is already known, for example fluorosteroids and fluorocarbohydrates, and also other classes of compounds in which development is at a very early stage.

Acknowledgement—The authors wish to express their thanks for Dr. D. A. WIDDOWSON, Dept. of Chemistry, Imperial College, London SW7 for many helpful discussions.

REFERENCES

1. ROBINSON G. D. Prospects for ^{18}F radiopharmaceuticals. In *Radiopharmaceuticals*, p. 141. Soc. Nucl. Med., New York (1975).
2. BROWNELL G. L., BURNHAM C. A., HOOP B. and KAZEMI H. Positron Scintigraphy with short-lived cyclotron produced radiopharmaceuticals and a multi-crystal positron camera. In *Medical Radioisotope Scintigraphy*, p. 313. IAEA, Vienna (1973).

3. Ter-Pogossian M. M., Phelps M. E., Hoffman E. J. and Mullani N. A. *Radiology* **114**, 89 (1975).
4. Muehllehner G. *J. nucl. Med.* **16**, 653 (1975).
5. Lifton J. F. and Welch M. J. *Radiat. Res.* **45**, 35 (1971).
6. Cohen M. B., Spolter L., Chang C. C., MacDonald N. S., Takahashi J. and Bobinet D. D. *J. nucl. Med.* **15**, 1192 (1974).
7. Chenoweth M. D. and McCarty L. P. *Pharmacol. Rev.* **15**, 673 (1963).
8. Smith F. A. Chem. Tech. U.S. **3**, 422 (1973).
9. Fowden L. Fluoroamino acids and protein synthesis. In *Carbon-Fluorine Compounds* (A Ciba Foundation Symposium), p. 141. Associated Scientific Publishers, Amsterdam (1972).
10. Rennert O. M. and Anker H. S. *Biochemistry* **2**, 471 (1963).
11. Smith F. A. Handbook of Experimental Pharmacology, (Edited by Smith F. A.), Vol. 20, Part 2, p. 351. Springer-Verlag, New York (1970).
12. Heidelberger C. Fluorinated pyridine nucleotides. In *Carbon-Fluorine Compounds*. (A Ciba Foundation Symposium), p. 125. Associated Scientific Publishers, Amsterdam (1972).
13. Barnett J. E. G. Fluorine as a substitute for oxygen in biological systems: examples in mammalian membrane transport and glycosidase action. *ibid* p. 95.
14. Goodwin D. A., Sundberg M. W., Diamanti C. I. and Meares C. F. ^{111}In-labelled radiopharmaceuticals and their clinical use. In *Radiopharmaceuticals*, p. 80. Soc. Nucl. Med., New York (1975).
15. Straatmann M. G. and Welch M. J. *J. nucl. Med.* **16**, 425 (1975).
16. Marche P., Marazano C., Maziere M., Morgat J. L., de la Losa P., Comar D. and Fromageot P. *Radiochem. Radioanal. Lett.* **21**, 53 (1975).
17. Robinson G. D. Biologically active ^{18}F-fluoro-organic compounds: Rapid high activity synthesis of ^{18}F-fluorocarboxylates and derivatives. In *Radiopharmaceuticals and Labelled Compounds*, Vol. 1, 423. IAEA, Vienna (1973).
18. Nozaki T., Iwamoto M. and Ido T. *Int. J. appl. Radiat. Isotopes* **25**, 393 (1974).
19. *Radioisotope Production and Quality Control*, IAEA Technical Report Series No. 128, p. 589. IAEA, Vienna (1971).
20. Thomas C. C., Sondel J. A. and Kerns R. C. *Int. J. appl. Radiat. Isotopes* **16**, 71 (1965).
21. Helus F., Krauss D. and Maier-Borst W. *Radiochem. Radioanal. Lett.* **15**, 225 (1973).
22. Chan P. K. H., Firnau G. and Garnett E. S. *ibid* **19**, 237 (1974).
23. Beg K. and Brown F. *Int. J. appl. Radiat. Isotopes* **14**, 137 (1963).
24. Scholz K. L. and Sodd V. J. *ibid* **23**, 465 (1972).
25. Collins C. H., Collins K. E., Ackerhalt R. E. and Blau M. *ibid* **26**, 571 (1975).
26. Nozaki T., Tanaka Y., Shimamura A. and Karasawa T. *ibid* **19**, 27 (1968).
27. Clark J. C. and Silvester D. J. *ibid* **17**, 151 (1966).
28. Tilbury R. S. and Dahl R., Mamacos J. P. and Laughlin J. S. *ibid* **21**, 277 (1970).
29. Hinn G. M., Nelp W. B. and Weitkamp W. G. *ibid* **22**, 699 (1971).
30. Lindner L., Suer T. H. G. A., Brinkman G. A. and Veenboer J. T. *ibid* **24**, 124 (1973).
31. Goulding R. W. and Palmer A. J. *ibid* **23**, 137 (1972).
32. Atkins H. L., Christman D. R., Fowler J. S. Hauser W., Hoyte R. M., Klopper J. F., Linn S. S. and Wolf A. P. *J. nucl. Med.* **13**, 713 (1972).
33. Welch M. J., Lifton J. F. and Gasper P. P. *ibid* **12**, 405 (1971) Abstract.
34. Lambrecht R. M. and Wolf A. P. Cyclotron and short lived halogen isotopes for radiopharmaceutical applications. In *Radiopharmaceuticals and Labelled Compounds*, Vol. 1, p. 275. IAEA, Vienna (1973).
35. Harper P. V., Lembares N. and Krizek H. *J. nucl. Med.* **12**, 362 (1971) Abstract.
36. Palmer A. J., Clark J. C., Goulding R. W. and Roman M. The preparation of ^{18}F-labelled DL-3-fluorotyrosine. In *Radiopharmaceuticals and Labelled Compounds*, Vol. 1, p. 291. IAEA, Vienna (1973).
37. Wolber G., Hartmann G., Helus F., Hover K. H. and Lorenz W. J. Applications of the compact cyclotron of the German Cancer Research Centre in nuclear medicine, neutron therapy and radiation biophysics. *7th Int. Conf. Cyclotrons and their Applications*, p. 444. Birkhauser Verlag, Basel (1975).
38. Ido T. Synthesis and *in vivo* distribution patterns of ^{18}F-organic compounds. *Proc. 1st World Cong. Nucl. Med.*, p. 901. World Federation of Nuclear Medicine and Biology (1974).
39. Lebowitz E., Richards P. and Baranowsky J. *Int. J. appl. Radiat. Isotopes* **23**, 392 (1972).
40. Clark J. C., Goulding R. W. and Palmer A. J. Preparation of ^{18}F-labelled fluorocarbons for use in pharmacodynamic studies. In *Radiopharmaceuticals and Labelled Compounds*, Vol. 1, p. 411. IAEA, Vienna (1973).
41. Clark J. C., Goulding R. W., Roman M. and Palmer A. J. *Radiochem. Radioanal. Lett.* **14**, 101 (1973).
42. Suschitzky H. The Balz-Schiemann reaction In *Advances in Fluorine Chemistry* (Edited by Stacey M., Tatlow J. C. and Sharpe A. G.), Butterworths, Washington (1965).

43. NOZAKI T. and TANAKA Y. *Int. J. appl. Radiat. Isotopes* **18,** 111 (1967).
44. MCOMIE (Editor) *Protective Groups in Organic Chemistry*. Plenum, London (1973).
45. GOULDING R. W. Ph.D. Thesis, University of London (1976).
46. TAYLOR D. M. and COTTRALL M. F. The evaluation of amino acids labelled with ^{18}F for pancreas scanning. In *Radiopharmaceuticals and Labelled Compounds*, Vol. 1, p. 405. IAEA , Vienna (1973).
47. DAMPURE H. J., OSMAN S. and SOMAIA S. To be published.
48. GARNET E. S. and FIRNAU G. ^{18}F-5-Fluoro-DOPA as a new brain scanning agent. In *Radiopharmaceuticals and Labelled Compounds*, Vol. 1, p. 405. IAEA, Vienna (1973).
49. AXELROD J. and WEINSHILBOUM R. *N. Engl. J. Med.* **287,** 237 (1972).
50. MACGREGOR R. R., ANSARI A. N., ATKINS H. L., CHRISTMAN D. R., FOWLER J. S. and WOLF A. P. *J. nucl. Med.* **15,** 513 (1974) Abstract.
51. OKUDA T. and TATSUMI S. *J. Biochem.* **44,** 631 (1957).
52. HOYTE R. M., LIN S. S., CHRISTMAN D. R., ATKINS H. L., HAUSER W. and WOLF A. P. *J. nucl. Med.* **12,** 280 (1971).
53. GOULDING R. W. and GUNASEKERA S. W. *Int. J. appl. Radiat. Isotopes* **26,** 561 (1975).
54. TOSA T., MORI T., FUSE N. and CHIBATA I. *Enzymologia* **31,** 214 (1968).
55. FIRNAU G., NAHMIAS C. and GARNETT S. *Int. J. appl. Radiat. Isotopes* **24,** 182 (1973); *J. Med. Chem.* **16,** 416 (1973).
56. HYDORN A. E. *J. org. Chem.* **32,** 4100 (1967).
57. IKAN R., HOFFMANN E., BERGMAN E. D. and GAHIN A. *Israel J. Chem.* **2,** 32 (1964).
58. BERGMAN E. D. and HOFFMAN E. *J. Chem. Soc.* 2827 (1962).
59. KOOK C. S., REED M. F. and DIGENIS G. A. *J. med. Chem.* **18,** 533 (1975).
60. SCHADT F. L. and SCHLEYER P. R. *Tetrahedron Lett.* 2335 (1974).
61. LIOTTA C. L., HARRIS H. P., MCDERMOTT M., GONZALES T. and SMITH K. *Tetrahedron Lett.* 71 (1975).
62. LANDINI D., QUICI S. and DOLLA F. *Synthesis* 430 (1975).
63. CAINELLI G. and MANESCALCHI F. *ibid.* 472 (1976).
64. ROBINSON G. D., USZLER J. M. and BENNETT L. R. *J. nucl. Med.* **16,** 561 (1975) Abstract.
65. BHANDARI K. S. and PINCOCK R. E. *Synthesis,* 655 (1975).
66. HUDLICKY M. *Chemistry of Organic Fluorine Compounds*, pp. 51; 59. Pergamon Press, Oxford (1961).
67. CHAMBERS R. D. *Fluorine in Organic Chemistry*, p. 39. Wiley, New York (1973).
68. BARTON D. H. R., BUBB W. A., HESSE R. H. and PECHET M. M. *J. Chem. Soc. Perkin I.* 2095 (1974).
69. BARTON D. H. R., HESSE R. H., TOH H. T. and PECHET M. M. *J. org. Chem.* **37,** 329 (1972).
70. FOWLER J. S., FINN R. D., LAMBRECHT R. M. and WOLF A. P. *J. nucl. Med.* **14,** 63 (1973).
71. BUSCH H. *An Introduction to the Biochemistry of the Cancer Cell* p. 139. Academic Press, New York (1962).
72. WOLF W., BERMON J. A. and SHANI J. *J. nucl. Med.* **16,** 582 (1975) Abstract.
73. PALMER A. J. Unpublished results.
74. ROBINSON G. D. *J. nucl. Med.* **14,** 446 (1973) Abstract; *ibid* **16,** 561 (1975) Abstract.
75. DE KLEIJN J. P., MEEUWISSEN H. J. and VAN ZANTEN B. *Radiochem. Radioanal. Lett.* **23,** 139 (1975).
76. MANTESCU C., GENUNCHE A. and SIMONESCU L. ^{18}F-labelling of bioactive molecules using $K^{18}F$–CH_3 COOH solutions as fluorinating agent. In *Radiopharmaceuticals and Labelled Compounds*, Vol. 1, p. 395. IAEA, Vienna (1973).
77. ENG R. *J. nucl. Med.* **16,** 526 (1975) Abstract.
78. STRAATMANN M. G. M.Sc. Thesis, Washington University, St. Louis (1976).
79. MARKOVSKIJ L. N., PASHINNIK V. E. and KIRSANOV A. V. *Synthesis* 787 (1973).
80. MIDDLETON W. J. *J. org. Chem.* **40,** 574 (1975).

Journal of Neurology, Neurosurgery, and Psychiatry, 1978, 41, 1–10

Study of regional cerebral metabolism and blood flow relationships in man using the method of continuously inhaling oxygen-15 and oxygen-15 labelled carbon dioxide

G. L. LENZI[1], T. JONES[2], C. G. McKENZIE, P. D. BUCKINGHAM, J. C. CLARK, AND S. MOSS

From the Medical Research Council Cyclotron Unit, Departments of Radiotherapy and Medical Physics, Hammersmith Hospital, London

SUMMARY A new technique for assessing regional oxygen use and blood flow has been applied to a wide range of neurological patients. The method couples the brain's high metabolic demand for oxygen with a shortlived radioactive form of this metabolite, namely oxygen-15 (half life: 2.1 min). This combination produces, during the continuous inhalation of either molecular oxygen-15 or labelled carbon dioxide, steady state functional images of the brain which are relatively free of contribution from extracerebral tissues. These are complementary images in that they relate to regional oxygen uptake and blood flow and hence offer a direct insight to the regional demand-to-supply relationships within the brain in physiological and pathological conditions. In the clinical groups studied, metabolic and circulatory defects were observed and instances of cerebrovascular insufficiency and relative luxury perfusion were defined which hitherto have been deduced from indirect methods. The clinical acceptability of this non-invasive approach allowed us to study those categories of patients which normally do not warrant invasive examination.

The function of the cerebral tissue depends critically on the use of oxygen, its energy turnover being mainly based on glycolytic aerobic metabolism. An impairment in the rate of consumption, because of a failure of either supply or use, often constitutes a pathological condition. It follows that a study of the cerebral blood flow (CBF) and the cerebral oxygen consumption ($CMRO_2$) at a regional level is a direct and rational method of investigating cerebral physiology and pathology. The first clinical study of $CMRO_2$ and CBF was presented by Kety and Schmidt (1948). Their technique required continuous sampling of arterial and jugular bulb blood, and provided an average measurement of $CMRO_2$ and CBF for the hemisphere investigated. This method has been used extensively in clinical research but has a limited resolution for investigating focal disease.

While a large number of regional CBF studies have been presented over the last 20 years, the first regional assessment of $CMRO_2$ in man was published by Ter-Pogossian *et al.* in 1970. This method involves a carotid artery injection of oxygen-15 (2.1 min $T_{\frac{1}{2}}$) labelled red cells to provide the single passage extraction of oxygen, followed by a similar injection of labelled water for the regional CBF determination. This technique requires the use of heavily shielded single probes for external recording and so limits the spatial resolution that can be achieved. These methods, although they provide absolute values of $CMRO_2$, have limited application because of their invasiveness.

A non-invasive approach to studying regional metabolism and flow has recently been published by Jones *et al.* (1976a). The steady state distribution of radioactivity within the brain achieved during the continuous inhalation of oxygen-15 is recorded with a gamma ray imaging device. This distribution is related to the regional oxygen uptake, while a repeat procedure using oxygen-15 labelled carbon dioxide produces a distribution related to regional cerebral circulation. The ratio between the oxygen

[1] Present address: Department of Neuropsychiatry, Institute of Neurology, University of Siena, Italy.
[2] Address for reprint requests: Dr T. Jones, MRC Cyclotron Unit, Hammersmith Hospital, Ducane Road, London W12 0HS, England.

Accepted 14 July 1977

use and circulation images theoretically provides the distribution of the oxygen extraction ratios. The non-invasiveness of this approach, and the indication that relationships between regional oxygen use and flow may be obtained, stimulated us to apply the technique to a series of normal subjects and neurological patients.

This paper summarises the main observations obtained in a group of 25 normal subjects and over 100 neurological patients who were investigated over a six month period, and serves to provide a general insight into the value of this approach.

Theory

The theory underlying the $^{15}O_2$—$C^{15}O_2$ inhalation method was described by Jones *et al.* (1976a). Inhalation of $^{15}O_2$ results in the formation of labelled oxyhaemoglobin. In the tissues, the oxyhaemoglobin dissociates, and the oxygen-15 is presented to the cytochrome systems and becomes coupled with H^+ to form water of the metabolism labelled with oxygen-15 ($H_2{}^{15}O$ met.):

$$2 \text{ Cyt. oxidase } Fe^{++} + \tfrac{1}{2}{}^{15}O_2 + 2H^+ \rightarrow 2 \text{ Cyt. oxidase } Fe^{+++} + H_2{}^{15}O$$

It has been confirmed experimentally that this is the principal fate of the extracted oxygen-15 (Ter-Pogossian *et al.*, 1970), and that contributions to the head signal arising from the presence of oxygen-15 labelled red cells and recirculating $H_2{}^{15}O$ metabolism amount to less than 30% of the total (Jones *et al.*, 1976a). The continuous inhalation of oxygen-15 results in the radioactivity in the tissue reaching a point of equilibrium. This steady state represents the balance between the continuous formation of $H_2{}^{15}O$ metabolism, due to the aerobic glycolytic activity of the brain, and the removal of $H_2{}^{15}O$ metabolism through radioactive decay and perfusion washout (Jones *et al.*, 1976a). When equating these dynamic processes, the regional $H_2{}^{15}O$ metabolism signal is given as:

$$\cdot H_2{}^{15}O \text{ met.} = \frac{Ca - Cv}{Cv} \cdot Ca^* \cdot \frac{(F)}{(\lambda + F/V)} \qquad (1)$$

where λ is the radioactive decay constant of oxygen-15 (0.335 min^{-1}) and F the blood flow per minute to a region of volume V. The stable oxygen content of the venous blood draining the tissue is denoted as Cv, while Ca and Ca* are the respective stable and radioactive oxygen contents of the arterial blood.

It can be seen that the $H_2{}^{15}O$ metabolism has a linear dependence on $\frac{Ca - Cv}{Ca}$ which is the tissue's oxygen extraction ratio (OER). The signal's dependence on blood flow is non-linear and introduces the need to examine the flow term of this relationship $\frac{(F)}{(\lambda + F/V)}$ independently. This is achieved by repeating the continuous inhalation study using oxygen-15 labelled $C^{15}O_2$. This procedure results in $H_2{}^{15}O$ being continuously produced in the lung capillary blood (West and Dollery, 1962). Thus the steady state head signal due to the circulating $H_2{}^{15}O$ ($H_2{}^{15}O$ circ.) will contain no metabolic component but only the combined blood flow and radioactive decay terms that are present in the $H_2{}^{15}O$ metabolism signal:

$$H_2{}^{15}O \text{ circ.} = \frac{(F)}{(F/V + \lambda)} c \qquad (2)$$

where c is the arterial concentration of circulating $H_2{}^{15}O$. Although non-linear with flow the $H_2{}^{15}O$ circulation signal does exhibit a certain sensitivity to flow as shown in Fig. 1.

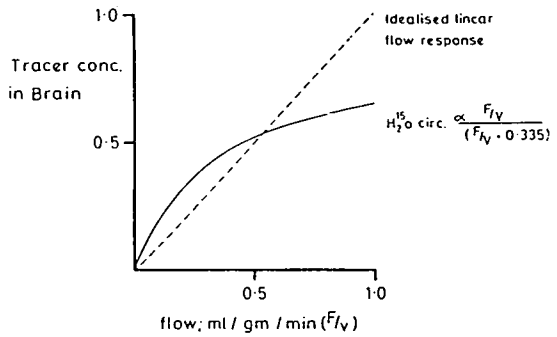

Fig. 1 *Theoretical relationship between blood flow and the equilibrium brain tissue concentration of $H_2{}^{15}O$ ($H_2{}^{15}O$ circulation) which results during the continuous inhalation of $C^{15}O_2$, the arterial blood concentration being taken as unity.*

This shows the theoretical change in the brain $H_2{}^{15}O$ circulation concentration plotted against CBF (F/V) as compared to the ideal linear flow response. For this comparison the two responses have been normalised to the normal average CBF value of 0.53 ml/min/g. Between zero and normal CBF values the $H_2{}^{15}O$ circulation concentration is fairly sensitive to change, while at higher values there is a general tendency to underestimate CBF. Thus the regional $H_2{}^{15}O$ circulation cerebral signal does have a place in estimating the distribution of CBF; however, its most important role lies in obtaining from the $H_2{}^{15}O$ metabolism signal the distribution of the tissue oxygen extraction ratio. This can be realised simply by dividing the $H_2{}^{15}O$ metabolism distribution by that due to $H_2{}^{15}O$ circulation:

$$\frac{H_2{}^{15}O \text{ met.}}{H_2{}^{15}O \text{ circ.}} = \frac{(Ca - Cv)}{(Cv)} \frac{Ca^*}{c} \qquad (3)$$

Ca*/c will be a constant for all cerebral regions and hence this normalisation procedure will produce a distribution which represents the regional oxygen extraction ratio. It should be stated that OER is an expression of the balance between the metabolic demand of the cerebral tissue ($CMRO_2$) and nutritional supply (CBF). In physiological and pathological terms this balance may be of more interest than regional $CMRO_2$ or CBF.

Methods

The Medical Research Council's cyclotron was used as a source of oxygen-15. A constant 25 μA deuteron beam was used to produce $^{15}O_2$ (target gas: $N_2 + 1\%O_2$) and $C^{15}O_2$ (target gas $N_2 + 1\%CO_2$) (Clark and Buckingham, 1975). The radioactive gases were piped some 210 m from the cyclotron to the clinical investigation area where the gamma camera was situated. At this location an operator monitored the specific activity of the gas and made dilution adjustments to ensure a constant administration rate to the patient of 1.5 millicuries per minute of oxygen-15 and 0.75 millicuries per minute of oxygen-15 labelled carbon dioxide. In both cases the total flow rate approximated to 0.5 l/min. The radioactive gases were in turn administered into a standard oxygen mask worn by the patient who breathed mainly room air through the side holes in the mask. Radioactivity exhaled through the side holes was disposed to waste using an exhaust fan withdrawing air over and around the face mask. Cotton wool was inserted into the patient's nostrils to encourage inhalation through the mouth and minimise the contribution to the radioactivity in the antero-inferior parts of the brain from radioactive gas in the upper airways. During the study the patient lay supine with eyes closed and in a quiet room. The distributions of radioactivity contained within the head were recorded using an Anger camera collimated with a 99 mm (4½ inch) thick lead multihole collimator. The performance of this collimator for detecting 511 keV annihilation radiation has been reported previously by Westerman and Glass (1968). The radioactivity within the brain usually attained equilibrium after six minutes of constant inhalation, (Jones *et al.*, 1974) whereupon a four minute steady state image containing between 250.10^3 and 350.10^3 counts was recorded on-line with a computer (HP2100A). The typical time delay between recording the $H_2{}^{15}O$ metabolism image and the $H_2{}^{15}O$ circulation image was 15 minutes. A total of 15 millicuries of $^{15}O_2$ and 7.5 millicuries of $C^{15}O_2$ were administered for each paired study. This represents a radiation absorbed dose of 190 millirads and 120 millirads respectively to the lung tissue (critical organ). The corresponding absorbed doses to the blood are 70 millirads and 110 millirads, and to the gonads 15 and 25 millirads. The computer-stored images were then corrected for the non-uniformity of the Anger camera, smoothed, and displayed for photography. In addition the regional counts were normalised to the counts contained within the area of maximal uptake and printed out in matrix form for subsequent digital analysis.

Results

The study was performed on 127 subjects, 25 normal volunteers and 102 patients. The Table summarises the two groups, with respect to mean age and sex ratio. Neurological patients were further divided into three main subgroups: tumours, cerebrovascular diseases, and extrapyramidal diseases. A few other miscellaneous conditions, including some psychiatric disorders, were investigated.

Table *Summary of mean age and sex ratio of subjects studied*

	Number	*Mean age (yr)*	*Male:female ratio*
Normal volunteers	25	39.9	2:1
Patients			
Cerebrovascular disease	33	57.7	1.6:1
Brain tumours	38	48.7	1.6:1
Extrapyramidal disorders	18	58.0	1.8:1
Other	14	47.4	0.6:1

NORMAL VOLUNTEERS

The distributions of radioactivity recorded in two normal subjects during continuous inhalation of $^{15}O_2$ and $C^{15}O_2$ are shown in Fig. 2. In both subjects the left dominant hemisphere was nearest to the gamma-camera. The pictures clearly show positive images of the brain, due to $H_2{}^{15}O$ metabolism when the subjects inhale $^{15}O_2$, and to $H_2{}^{15}O$ circulation when $C^{15}O_2$ is inhaled. It can be seen that the extracerebral structures contribute little to the head image. This could be predicted from the theory (see Fig. 1), when considering the relatively low blood flow and volumes of these tissues. Some degree of contamination was observed in the antero-inferior regions of the brain, because of the gaseous $^{15}O_2$ and $C^{15}O_2$ contained in the upper airways. This interference was greatest with $^{15}O_2$, because of its lower extraction in the lungs. The distributions of $H_2{}^{15}O$ metabolism and $H_2{}^{15}O$ circulation are not uniform throughout the brain. The geometrical shape of the brain has to be taken into account, the maximal activity being recorded in the inferior parts, where in transverse

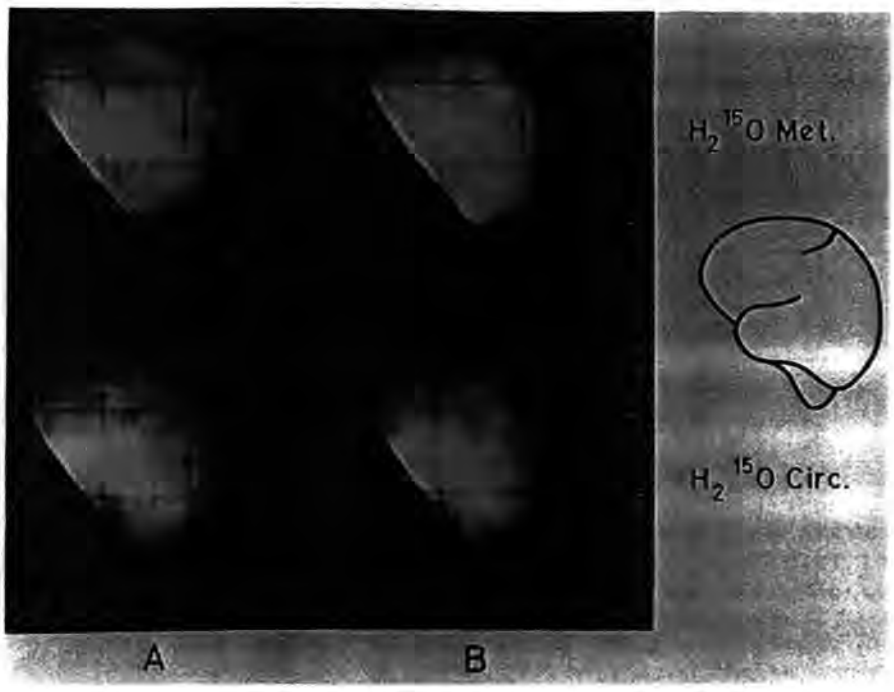

Fig. 2 *Equilibrium distributions of $H_2{}^{15}O$ metabolism and $H_2{}^{15}O$ circulation as recorded in the left lateral views of two normal brains during the continuous inhalation of $^{15}O_2$ and $C^{15}O_2$ respectively.*

projection there is more cerebral tissue. In addition to the shape-dependence, a definite uptake pattern is superimposed which was largely similar in all the normal subjects investigated under the age of 50 years. The inferior part of the brain had two regions of maximal $H_2{}^{15}O$ metabolism activity, one in the supratentorial region, in the middle part of the temporal lobe, the other in the posterior fossa, at mesencephalic—pontine level. Although the distribution of $H_2{}^{15}O$ circulation activity is similar, these two regions are less prominent. In the superior part of the brain, regions with lower activity are intermingled with regions of greater activity in both the $H_2{}^{15}O$ metabolism and $H_2{}^{15}O$ circulation distributions. This aspect must be referred to the presence of "areas containing white matter and ventricles" (Jones *et al.*, 1976a). Furthermore, there is a suggestion of a contribution to physiological activity of the different cortical regions, a finding also observed by other authors (Wilkinson *et al.*, 1969; Risberg *et al.*, 1975). In addition to the analogue picture obtained from the computer, the corresponding numerical matrices were used for an objective analysis of regional cerebral uptake. In both the $H_2{}^{15}O$ metabolism and $H_2{}^{15}O$ circulation distributions, six regions, each approximately 6 cm^2 in area, were selected (frontal, motor, parietal, occipital, temporal, and pontomesencephalic). The average matrix count within each region was ratioed to the average matrix count contained within the region of maximal uptake, which was usually the middle temporal lobe or the pontomesencephalic region. These regional ratios have been designated as Metabolic Ratios (MRs) and Perfusion Ratios (PRs) for the $^{15}O_2$ and $C^{15}O_2$ studies respectively. In turn, the six regions evaluated within the $H_2{}^{15}O$ metabolism distributions (Metabolic Ratios) were normalised to the corresponding regions in the $H_2{}^{15}O$ circulation distributions (Perfusion Ratios). This theoretically provides a distribution of the OER which is largely independent of geometrical factors (see equation 3 in Theory Section). Although quantitative, there will be a background superimposed on the regional Perfusion, Metabolic, and Oxygen Extraction Ratios of the ipsilateral hemisphere because of radioactivity in the contralateral hemisphere. This contribution will be variable and will tend to reduce the sensitivity which these ratios have for detecting perturbations from the normal.

Figure 3 illustrates the results of applying this analysis to data obtained in the normal subjects. The mean value and the standard deviation from the mean for these indices in the six regions chosen for the analysis are shown. Since the age of the normal subjects ranged from 22 to 71 years, an increase in the variability was to be expected because of the CBF and $CMRO_2$ decrease in aging (Scheinberg *et al.*, 1953). In fact, subjects over 50 years of age had slightly increased OERs and decreased MRs and PRs in comparison to the younger subjects (Lenzi *et al.*, in

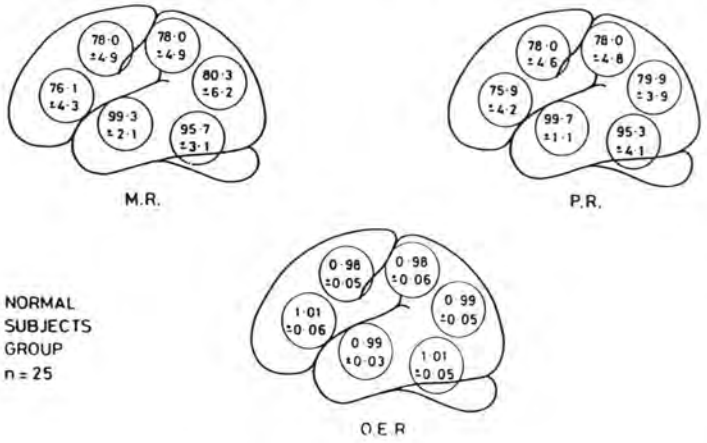

Fig. 3 *Quantitative distribution of the Metabolic Ratios (MR) and Perfusion Ratios (PR) in 25 normal subjects as determined for six representative cerebral regions. The distribution of the Oxygen Extraction Ratios obtained by normalising the Metabolic Ratios to the corresponding Perfusion Ratios is also shown.*

preparation). The OER shown in this figure demonstrates the close relationship between the distribution of oxygen uptake and flow, as observed by Raichle *et al.* (1976) with the intracarotid injection method.

NEUROLOGICAL DISORDERS

Over 100 neurological patients were investigated during a six month period. The different neurological groups studied are listed in the Table. A more detailed evaluation of the three major groups—cerebrovascular disease, brain tumours, and extrapyramidal disorders—will be presented in subsequent publications. In this report we will confine ourselves to describing the main perturbations in the distributions of the $H_2{}^{15}O$ metabolism and $H_2{}^{15}O$ circulation observed within the neurological group.

In general we expect that the present technique would detect a regional decrease in metabolism and circulation, a regional increase in metabolism and circulation, and an imbalance between the regional metabolism and circulation.

Regional decrease in metabolism and circulation

The most common instances of a parallel decrease in the $H_2{}^{15}O$ metabolism and $H_2{}^{15}O$ circulation uptakes were seen in stroke patients who had a permanent occlusion of the affected cerebral arteries, and in patients with primary malignant and secondary brain tumours. All these pathological processes produce gross variations in both the neuronal activity and cerebral function. The parallel circulatory decrease observed was either the primary cause of the disease, as in the strokes, or signified a lower metabolic demand from the tumour's cells relative to the neurones. Figure 4 shows the results obtained in a patient in whom computerised axial tomography

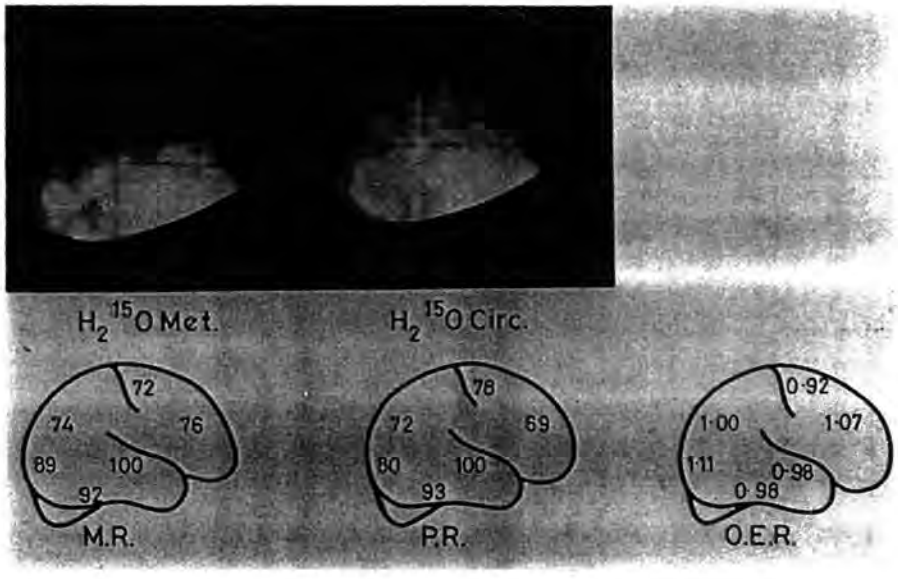

Fig. 4 *Distribution of $H_2{}^{15}O$ metabolism and $H_2{}^{15}O$ circulation in the right lateral view of a patient with diagnosed cerebral atrophy and multiple cerebral infarctions. Although both metabolism and perfusion are regionally reduced the relative balance between the two is near normal.*

demonstrated "a severe cerebral atrophy, with moderate dilatation of ventricles, and numerous cortical translucencies suggesting multiple infarcts". Both $H_2{}^{15}O$ metabolism and $H_2{}^{15}O$ circulation images show an impairment of the radioactivity uptake in the superior region of the brain. Some degree of circulation is observed in the proximity of the middle cerebral artery, as if the process were affecting mainly the smaller arterial branches. Analogue images of the radioactive distribution in the brain are subject to contrast enhancement in the display and photographic process. In all examples the corresponding perfusion and metabolic images were normalised quantitatively to each other in the computer so that the same number of counts were present in the regions of maximal uptake. Thus photographic recordings of the two images were always made under the same conditions of contrast and intensity.

Regional increase in metabolism and circulation

In our series no paralled increases in the $H_2{}^{15}O$ metabolism and $H_2{}^{15}O$ circulation uptakes were observed, such as might be expected within an active epileptic focus as reported by Hougaard *et al.* (1976). We must underline that we have not had the opportunity of studying epileptic patients (only a few patients had had fits, and no fits occurred during an investigation).

Increases of $H_2{}^{15}O$ circulation activity in a lesion were found to parallel the angiographic and neurosurgical findings of increased blood supply. An example of this is shown in Fig. 5 which presents the images obtained in a patient with a highly vascularised meningioma. The position and rich filling of the tumour vessels is shown in the carotid angiogram. The $H_2{}^{15}O$ circulation image endorses these findings while the $H_2{}^{15}O$ metabolism image is within the normal limits. The correlation of the two distributions shows a decreased OER in the region of the meningioma.

Imbalance between regional metabolism and circulation

Examples of imbalance between the metabolic and circulating distributions were also seen in patients without tumours. This uncoupling between flow and metabolism could not have been predicted, and is thus of greater interest with respect to the relevance of these measurements in the interpretation of neurological disorders. The mismatching of the two distributions may reveal a pathological condition that is not actually producing symptoms or anatomically definite lesions. For instance, we were able to

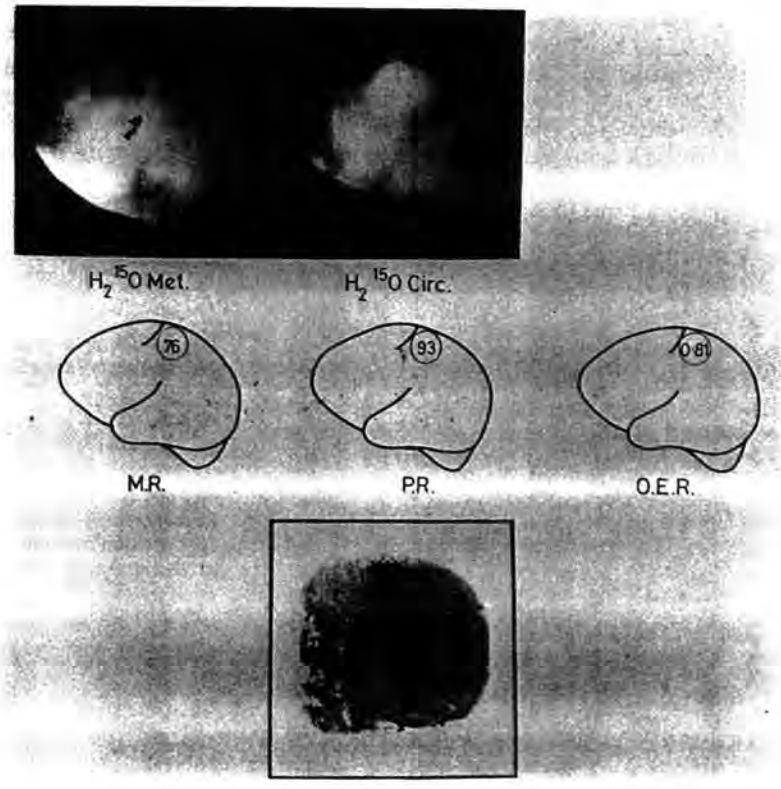

Fig. 5 *Distribution of $H_2{}^{15}O$ metabolism and $H_2{}^{15}O$ circulation in the left lateral view of a patient with a highly vascularised meningioma. The observed area of luxury perfusion correlates anatomically with the tumour's angiographic blush.*

"visualise" areas of clinically silent cerebrovascular insufficiency, where a reduction in circulatory activity was not accompanied by, or was greater than the reduction in metabolic activity. This was observed in asymptomatic cases who had previously presented with transient ischaemic attacks, an example of which is shown in Fig. 6. In this case, the impairment of $H_2{}^{15}O$ circulation activity was larger than that of the $H_2{}^{15}O$ metabolism activity. The slight decrease in metabolic activity in the parietal region indicated that no definite lesion had occurred and this was confirmed by the patient's neurological history. However, an ischaemic region, where there is preserved neuronal activity coupled with a decrease in the blood supply, indicated that the cerebrovascular insufficiency had not caused neuronal damage. Corresponding to the decrease in the PR there was an increase in the OER.

The reverse pattern—that is, unaffected flow but reduced metabolism—was observed in "stroke" patients with a normal angiography. Figure 7 shows the distributions obtained in a patient in whom computerised axial tomography had demonstrated an infarct in the left frontotemporal region. The $H_2{}^{15}O$ metabolism shows a definite triangular area of decrease in the frontal region extending downward to the temporal pole. In contrast, the $H_2{}^{15}O$ circulation image shows no defect, and provides evidence of a relative luxury perfusion situation where there is an excess of blood flow with respect to the metabolic needs of the tissue. In such a situation the reduced use of oxygen points to permanent neuronal damage because of the transient reduction of blood flow. The clear-cut defect in the $H_2{}^{15}O$ metabolism picture also demonstrates that the arterial recirculation of the metabolically produced labelled water does not appear to affect significantly the resolution that this technique has for demonstrating metabolic defects.

The general comparison between the present technique and the other neuroradiological examinations proved it satisfactory in detecting and locating lesions and in assessing their size and shape. However, the important aspect of these studies is not detection of lesions but investigation of the effect of lesions on cerebral metabolism and blood flow. A preliminary report on the use of this method to assess the effect of radiotherapy on cerebral tumours has already been published by Jones *et al.* (1976b). The non-invasiveness of the method allows examination of patients such as those with Parkinson's disease in whom such investigations as carotid catheterisation are usually unjustified. This particular aspect is exemplified in Fig. 8. This patient had a two year history of a very mild right extrapyramidal disease which required only anticholinergic treatment to obtain a good control. Surprisingly, a large impairment particularly in the $H_2{}^{15}O$ metabolism uptake was detected in the left hemisphere which was contralateral to the side presenting the extrapyramidal signs. In this case the right hemisphere study showed fairly normal distributions with no mismatching of metabolism to perfusion (Fig. 8). The frequency of such aspects in extrapyramidal disorders as seen when using this technique is of interest and justifies a more intensive investigation of this particular group of patients.

There was concern that the superimposition of the

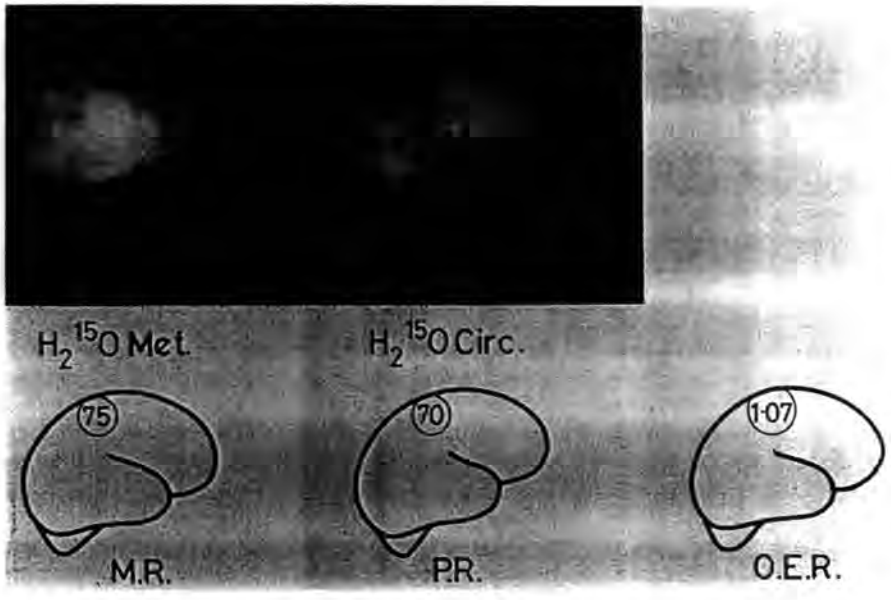

Fig. 6 *Distribution of $H_2{}^{15}O$ metabolism and $H_2{}^{15}O$ circulation in the right lateral view of a patient presenting with symptoms of transient ischaemic attacks. A zone of ischaemia is seen in the parietal region*

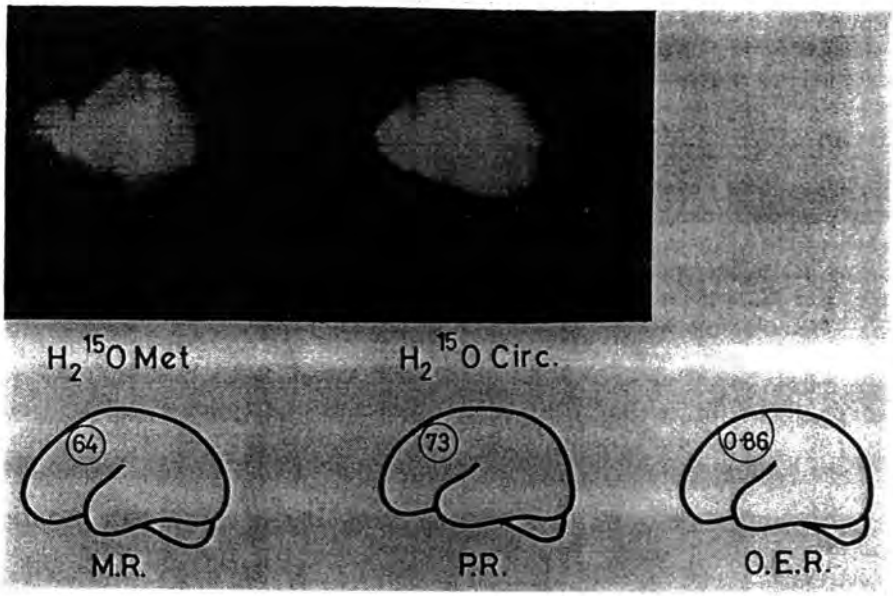

Fig. 7 *Distribution of $H_2{}^{15}O$ metabolism and $H_2{}^{15}O$ circulation in the left lateral view of a stroke patient with a lesion diagnosed in the frontotemporal region from the CAT scan. The isotope study indicates a relative luxury perfusion at this site (which had been found to be normal on angiography).*

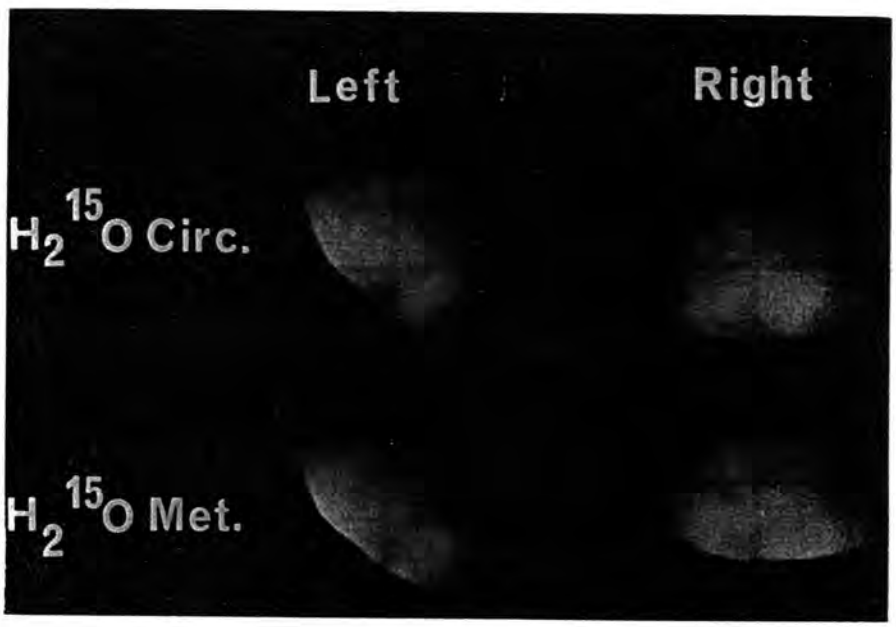

Fig. 8 *Distribution of $H_2{}^{15}O$ metabolism and $H_2{}^{15}O$ circulation in the left and right lateral views of a patient with a two year history of very mild extrapyramidal disease. A decreased metabolic activity is seen in the left parieto-occipital region while the right hemisphere exhibits a normal metabolism/perfusion balance.*

radioactivity in the two hemispheres would significantly impair the focal resolution of this technique. In practice this turned out to be less of a problem than expected as illustrated in Fig. 8 which shows that the defect in the left hemisphere is not detected in the right view. This suggests that the contribution from the contralateral hemisphere does not impair the ability to detect an ipsilateral defect, and can be explained by the fact that most of the radioactivity recorded over the brain arises from the metabolically active cortical grey matter adjacent to the gamma camera. The fall-off of spatial resolution with distance from the camera face and the tissue attenuation of gamma rays emitted from the contralateral hemisphere, calculated as being between 45% and 65% (mean 57%), results in the contralateral signal behaving as a defocused attenuated background superimposed upon the ipsilateral image.

Discussion

The rationale of the present approach rests in coupling the high aerobic metabolic demand of the cerebral tissues with a short half life radionuclide of oxygen. This in effect produces a high differential between the concentration of radioactivity in the brain and extracerebral tissues. Thus it is possible to produce a direct functional image of the brain with a negligible extracerebral contribution, and still administer the labelled oxygen through a general and physiological pathway—namely, inhalation. In addition, repeated investigations showed that these images were reproducible. The study was performed by recording the lateral projection and hence a superimposition of activity from both hemispheres would be expected. However, in detection of focal pathology in the ipsilateral hemisphere, we observed a close agreement with other neuroradiological investigations. This can be explained by the interference from the contralateral hemisphere behaving as a diffuse background, a consequence of the sharp decrease in spatial resolution with distance from the camera and some attenuation of photons (57%) in the interposing tissue. For display purposes the intensity and contrast is adjusted to illustrate any focal mismatching between flow and metabolism. This is legitimate provided both images have been normalised to the counts in the region of maximal uptake, an adjustment which helps to supress the effect of the background due to activity in the contralateral hemisphere. Hence mismatching is more dramatically illustrated in the analogue images than from quantitative ratios which are directly subjected to the background effect.

The interference with the $H_2{}^{15}O$ metabolic cerebral signal due to recirculating $H_2{}^{15}O$ was demonstrated in animals to be less than 30% (Jones *et al.*, 1976a). This low interference was substantiated in those cases in our series which presented a metabolic lesion with preserved blood flow (Fig. 7). The analogue and digital distributions of $H_2{}^{15}O$ metabolism and $H_2{}^{15}O$ circulation obtained are in addition to regional and structural physiological differences dependent on the brain's geometry. In our normal series the regional variations were found to be sufficiently consistent to enable the identification of pathological features. The ratio between the $H_2{}^{15}O$ metabolism distribution and $H_2{}^{15}O$ circulation produces the distribution of the OER which is largely independent of the brain's geometry (equation 3). This ratio represents the balance between the metabolic demand ($CMRO_2$) and the blood supply (CBF), and is, therefore, a direct expression of the physiological condition of the nervous tissue. A striking outcome of the application of this approach to a neurological population has been the positive demonstration of instances of true cerebrovascular insufficiency—that is, a situation of low flow with preserved metabolic activity, and of relative luxury perfusion where there is normal flow but reduced regional metabolism. These situations until now have been only indirectly inferred. In addition, unsuspected impairments have been observed in neurological patients such as those with extrapyramidal disorders which, to date, not being ethically suitable for invasive investigation, were only evaluated with clinical examination. No evident increase in regional metabolism was observed, in contrast to recent experimental observations (Reivich, 1976 unpublished), but it should be emphasised that the present technique detects only aerobic glycolytic metabolism.

The main limitation of this work has been the lack of absolute quantitative measurement of regional $CMRO_2$ or CBF. The theory indicates that such parameters may be extracted from the steady state uptake of $H_2{}^{15}O$ metabolism and $H_2{}^{15}O$ circulation provided quantitative regional uptake measurements are performed and related to the corresponding arterial blood concentrations (Jones *et al.*, 1976a). This is technically difficult when using a conventional Anger camera, and is best performed with imaging devices which employ positron-coincidence detection. Tomographic emission studies of cerebral uptake would eliminate the superimposed position of tissue signals, and hence greatly advance the method by virtue of improved detection contrast. The most practical technical approaches to both quantitation and tomography would appear to be either the PETT system developed by Ter-Pogossian *et al.* (1975) or the Positron camera of Brownell (Brownell and Burnham, 1972; Hoop *et al.*, 1976). It should be emphasised, however, that, even when these sophisticated devices are used, arterial sampling will be necessary to obtain absolute regional $CMRO_2$ or CBF values.

The acceptability of this non-invasive method is underlined by the fact that out of more than 100 patients studied, only one refused to cooperate. Therefore, it seems logical to speculate upon a larger application to the complete spectrum of neurological and psychiatric disorders. The modifications of the distributions observed in old normal subjects indicate that this approach could be relevant in the investigations of aging processes. A logical progression of our approach would be the evaluation of therapeutic agents in neurological disorders (Jones *et al.*, 1976b). In particular, our demonstration of ischaemia is a positive example where an objective assessment of therapy could be obtained.

The continuous support of this work by Mr D. D. Vonberg and Dr R. Morrison is acknowledged. The success of this study has rested closely on the co-operation of those neurologists who referred patients to us from outside our institutes. In particular our colleagues at the following London centres—Hammersmith, Central Middlesex, Royal Free, and National Hospital for Nervous Diseases—are acknowledged for the interest they have shown in these investigations. We are deeply indebted to Professor J. Marshall and to Professor C. Fieschi for their invaluable suggestions and criticisms in the preparation of this manuscript. The technical support of Mr P. J. Sleight and the cyclotron operating team is recognised as having been of utmost importance. Dr Lenzi was supported by NATO and the National Research Council of Italy Grant Number 215.7 (1974).

References

Brownell, G. L., and Burnham, C. A. (1972). MGH positron camera. In *Tomographic Imaging in Nuclear Medicine*. Edited by F. S. Freedman, pp. 154–164. Society of Nuclear Medicine: New York.

Clark, J. C., and Buckingham, P. D. (1975). *Short lived Radioactive Gases for Clinical Use*. Butterworths: London.

Hoop, B., Hnatowich, D. J., Brownell, G. L., Jones, T., McKusick, K. A., Ojemann, R. G., Parker, J. A., Subramanyam, R., and Taveras, J. M. (1976). Techniques for positron scintigraphy of the brain. *Journal of Nuclear Medicine*, **17**, 473–479.

Hougaard, K., Oikawa, T., Sveinsdottir, E., Skinhøj, E., Ingvar, D. H., and Lassen, N. A. (1976). Regional cerebral blood flow in focal cortical epilepsy, *Archives of Neurology (Chicago)*, **33**, 527–535.

Jones, T., Brownell, G. L., and Ter-Pogossian, M. M. (1974). Equilibrium images of short-lived radiopharmaceuticals for dynamic observations. *Journal of Nuclear Medicine*, **15**, 505.

Jones, T., Chesler, D. A., and Ter-Pogossian, M. M. (1976a). The continuous inhalation of oxygen-15 for assessing regional oxygen extraction in the brain of man. *British Journal of Radiology*, **49**, 339–343.

Jones, T., McKenzie, C. G., Moss, S., Buckingham, P. D., and Clark, J. C. (1976b). The non-invasive use of oxygen-15 for studying regional brain function in patients with cerebral tumours. *Proceedings of the 12th Bad Gastein Symposium on Radioactive Isotopes in Clinical Medicine and Research.*

Kety, S. S., and Schmidt, C. F. (1948). The nitrous oxide method for the quantitative determination of cerebral blood flow in man: theory, procedures and normal values. *Journal of Clinical Investigation*, **27**, 476–483.

Raichle, M. E., Grubb, R. L., Gado, M. H., Eichling, J. O., and Ter-Pogossian, M. M. (1976). Correlation between regional cerebral blood flow and oxidative metabolism. In vivo studies in man. *Archives of Neurology (Chicago)*, **33**, 523–526.

Risberg, J., Halsey, J. H., Wills, E. L., and Wilson, E. M. (1975). Hemispheric specialization in normal man studied by bilateral measurements of the regional cerebral blood flow. A study with the 133-Xe inhalation technique. *Brain*, **98**, 511–524.

Scheinberg, P., Blackburn, I., Rich, M., and Saslaw, M. (1953). Effects of ageing on cerebral circulation and metabolism. *Archives of Neurology and Psychiatry (Chicago)*, **70**, 77–85.

Ter-Pogossian, M. M., Eichling, J. O., Davis, D. O., and Welch, M. J. (1970). The measure in vivo of regional oxygen utilization by means of oxyhemoglobin labelled with radioactive oxygen-15. *Journal of Clinical Investigation*, **49**, 381–391.

Ter-Pogossian, M. M., Phelps, M. E., Hoffman, E. J., and Mullani, N. A. (1975). A positron emission transaxial tomograph for nuclear medicine imaging (PETT). *Radiology*, **114**, 89–98.

West, J. B., and Dollery, C. T. (1962). Uptake of oxygen-15 labelled CO_2 compared with carbon-11 labelled CO_2 in the lung. *Journal of Applied Physiology*, **17**, 9–13.

Westerman, B. R., and Glass, H. I. (1968). Physical specification of a gamma camera, *Journal of Nuclear Medicine*, **9**, 24–30.

Wilkinson, I. M. S., Bull, J. W. D., Du Boulay, G. H., Marshall, J., Ross Russell, R. W., and Symon, L. (1969). Regional blood flow in the normal cerebral hemisphere. *Journal of Neurology, Neurosurgery, and Psychiatry*, **32**, 367–378.

Radiochemistry in Medicine

The following are summaries of the seven papers presented at a Meeting of the Radiochemical Methods Group held on May 17th, 1978, in Sutton, Surrey.

Value of *In Vivo* Radionuclide Methods in Clinical Diagnosis

D. O. Cosgrove

Department of Nuclear Medicine, Royal Marsden Hospital, Sutton, Surrey, SM2 5PT

Central to the use of radionuclides in diagnostics is the well tried tracer concept with its implication that the nuclide used is not discriminated by the body mechanisms. The choice of radionuclides for *in vivo* use is greatly influenced by dosimetric considerations, especially the biological $T_{\frac{1}{2}}$ and, for external counting, the degree to which the disintegration pattern approximates to the ideal of a pure γ emitter of medium energy (too low and the tissue dose rises, too high and capture by the sodium iodide crystal falls off). For imaging, the metastable nuclides, especially $^{99}Tc^{m}$, have proved physically ideal (although not without difficulty for the radiochemist) and have allowed the use of larger doses than were acceptable with, for example, ^{131}I, with great improvements in image clarity and with the potential for dynamic imaging.

Dynamic imaging, well established and invaluable in renal work, has become increasingly more important in cardiology. It is much simpler than X-ray angiocardiography and therefore more readily repeatable. Information on the passage of a blood pool agent is collected through several cardiac cycles and displayed in slow motion in order to give a good visual impression of the heart's contractions. Numerical information can be extracted and promises to be useful in providing cardiac output measurements, etc.

Static imaging has improved considerably over the past decade, owing to a combination of better γ-ray cameras and more suitable radiopharmaceuticals. The images are two-dimensional representations of the distribution of the nuclide in the body, but it must be emphasised that they are not simple anatomical images, but show anatomy as revealed by selective organ function. Some specific clinically valuable applications are mentioned and a classification by tracer type is informative.

Chemical Identity

The classic imaging nuclide is ^{131}I for the thyroid, and it is still one of the most valuable. Its action depends upon selective concentration of iodide by functioning thyroid tissue and may be thought of as giving a positive image. In the brain an intact blood - brain barrier excludes most solutes but becomes permeable when damaged. Many tracers are available but the most useful are anionic forms of $^{99}Tc^{m}$ pertechnetate. The normal brain scan thus shows no brain at all; regions of increased activity are abnormalities. Many other examples of this group are less commonly used, *e.g.*, ^{57}Fe for the bone marrow and tagged damaged red cells for the spleen.

Chemical Similarity

In this application the tracer is sufficiently similar to a chemical present in the tissue under examination, although the lack of identity can lead to difficulties in interpretation. The use of ^{18}F as a substitute for chloride as a bone scanning agent is a now superseded example, and one of current interest is the substitution of ^{201}Tl for potassium as a cardiac muscle imaging agent. Selenium-75 can be substituted for sulphur in amino acids used to reveal sites of protein synthesis. Selenomethionine is a useful agent for imaging the pancreas.

Tracers Linked to Metabolites

In this application the nuclide is bonded to a metabolite with a minimum of disturbance of behaviour. Iodoalbumin is the classic example, used for blood pool imaging or volume estimation and iodo- or selenocholesterol are similar substances that are useful in imaging the adrenals. The most valuable example is the use of phosphate-like substances, tagged with $^{99}Tc^{m}$, for bone scanning. A number of similar compounds are available, and these rely on the fact that increased laying down of calcium phosphate occurs whenever bone is diseased so that a hot spot is produced. Thus the scans are non-specific for pathology but they are

TABLE I

SOME TECHNETIUM-99m RADIOPHARMACEUTICALS

Preparation	Organ visualised
Pertechnetate	Brain, thyroid
$^{99}Tc^m$ - sulphur colloid	Liver
$^{99}Tc^m$ - hydrolysed tin colloid	
$^{99}Tc^m$ - bromomercurihydroxypropane	Kidney
$^{99}Tc^m$ - dimercaptosuccinate	
$^{99}Tc^m$ - DTPA	
$^{99}Tc^m$ - glucoheptonate	Kidney, brain
$^{99}Tc^m$ - methylenediphosphonate	Bone
$^{99}Tc^m$ - imidodiphosphonate	Heart
$^{99}Tc^m$ - diethylacetanilidoiminodiacetate	Gall bladder
$^{99}Tc^m$ - dimethylacetanilidoiminodiacetate	
$^{99}Tc^m$ - pyridoxylidineglutamate	
$^{99}Tc^m$ - human serum albumin—native	Blood pool
microspheres	Blood pool
macroaggregates	Lungs
$^{99}Tc^m$ - fibrinogen	Blood clot detection
$^{99}Tc^m$ - plasmin	
$^{99}Tc^m$ - streptokinase	
$^{99}Tc^m$ - urokinase	
$^{99}Tc^m$ - labelled cells—	
red blood cells (heat damaged)	Spleen
leucocytes	
platelets	

The oxidation states of $^{99}Tc^m$ in some of the commonly used radiopharmaceuticals have been studied and the evidence suggests[3] that the diethylenetriamine-*NNN'N"N"*-pentaacetic acid (DTPA) complex contains Tc(III) and the human serum albumin complex Tc(V).

In the development of new $^{99}Tc^m$ radiopharmaceuticals not only is the chemistry of technetium important but so is the choice of the complexing ligand, which must be based on known or predicted biological behaviour. In relation to radiopharmaceuticals based on complex and chelate formation a point that is often unrecognised, or forgotten, is that the formation of the complex can itself change the biological properties of the ligand. This change can result from complexing with groups essential for biological activity, or from changes in lipophilicity or molecular charge. These changes usually lead to radiopharmaceuticals which do not fulfil the intended aim. Occasionally however, alteration in properties may be advantageous. For example, dimethylacetanilidoiminodiacetic acid is a derivative of the drug lidocaine. The parent compound is excreted mainly in the urine whereas the $^{99}Tc^m$ complex is excreted almost exclusively in the bile, making it a useful agent for imaging the gall bladder.[4]

To conclude, $^{99}Tc^m$ is not only the most widely used radionuclide in contemporary nuclear medicine, but it retains great potential for further exploitation. To the chemist the development of new $^{99}Tc^m$ radiopharmaceuticals provides many fascinating challenges, from the basic chemistry of technetium at picomolar concentrations, through the chemistry, biochemistry and pharmacology of $^{99}Tc^m$ complexes, to the problems of developing rapid and reliable methods of preparation and of quality control.

References

1. "Guidelines for the Preparation of Radiopharmaceuticals in Hospitals," British Institute of Radiology Special Report No. 11, British Institute of Radiology, London, 1975.
2. Owunwanne, A., Marinsky, J., and Blau, M., *J. Nucl. Med.*, 1977, **18**, 1099.
3. Richards, P., and Steigman, J., *in* Subramanian, G., Rhodes, B. A., Cooper, J. F., and Sodd, V. J., *Editors*, "Radiopharmaceuticals," Society of Nuclear Medicine, New York, 1975, p. 23.
4. Ryan, J., Cooper, M., Loberg, M., Harvey, E., and Sikorski, S., *J. Nucl. Med.*, 1977, **18**, 997.

Radioactive Gases of Short Half-life for Brain, Heart and Lung Studies

John C. Clark

Medical Research Council, Cyclotron Unit, Hammersmith Hospital, Ducane Road, London, W12 0HS

The application of radioisotopes as *in vivo* probes in order to study organ morphology and function and the measurement of body spaces by radioisotope dilution analysis has been sum-

marised in the preceeding papers. This paper discusses the clinical applications of gaseous species containing radionuclides with short half-lives.

Of the radioisotopes in current practice $^{81}Kr^{m}$ at 13 s has the shortest half-life. It is obtained from a radionuclide generator, the parent radionuclide ^{81}Rb having a half-life of 4.58 h. The chemical separation is simple, the daughter being an inert gas. $^{81}Kr^{m}$ decays to $^{81}Kr^{g}$, which has a half-life of 2.1×10^{5} year and thus poses no further hazard. The krypton generator can be coupled on-line to the patient and after the study a very rapid decay occurs when the generator is switched off. In this respect the almost instant disappearance of radiation resembles the conventional X-ray technique. The use of a short half-life radioisotope provides a new approach to dynamic studies in nuclear medicine. The krypton generators can be shipped readily by air and by using Concorde can reach America, where until recently they were unobtainable, in a usable state. An ultra-safe generator design is essential as the direct coupling to patients precludes intermediate testing.

^{81}Rb is prepared by either the (p,2n) or (d,3n) reactions on ^{82}Kr or, as at Hammersmith, the alternative reaction $^{79}Br(\alpha,2n)^{81}Rb$ using sodium or copper bromides as targets. The gas-phase reaction with a krypton target is the preferred production method. The bombardment of natural krypton with 30 MeV protons yields approximately 10 mCi of ^{81}Rb μA^{-1} h^{-1}. The ^{81}Rb collects on the walls of the gas target pressure vessel. The best ^{81}Rb recovery method reported is the use of a target vessel whose cylindrical stainless-steel walls can be rotated. When water is introduced into the rotating liner an epicyclic rod acts as a squeegee, ensuring good contact with the walls and an 80–90% recovery of ^{81}Rb, which can be absorbed on to a very small cation-exchange column. With sodium bromide targets it is found that a zirconium phosphate inorganic ion exchanger has a high affinity for rubidium even in the presence of a gross excess of sodium ions. At Hammersmith Hospital there is a hot cell where six generators can be made and tested in parallel from one irradiation, all chemistry and target handling being carried out by remote control. Irradiations are carried out between 05.00 and 07.00 hrs, shipment throughout the UK and continental Europe being by road, rail or air.

In operation the column is eluted with humidified air for use in pulmonary ventilation studies. When $^{81}Kr^{m}$ is required in solution a specially prepared column is eluted with 5% dextrose in water. The eluate is passed through a small column of AG50 resin to ensure low ^{81}Rb contamination. Terminal sterilisation is carried out on-line using a Millipore 0.22 μm Swinnex disposable filter unit.

$^{99}Tc^{m}$ microspheres (Eγ 140 keV) can be monitored along with $^{81}Kr^{m}$ (Eγ 190 keV) as a differential test of lung function. The $^{99}Tc^{m}$ microspheres test the blood supply and $^{81}Kr^{m}$ tests the ventilation as this isotope decays so rapidly that a significant decay occurs before a volume distribution can be achieved. Gross mismatching of the two isotopes (monitored at 140 and 190 keV, respectively) indicates abnormal lung function.

Continuous infusion of $^{81}Kr^{m}$ solution by a specially designed aortic root catheter whose tip is placed just above the aortic valve (the region from where the coronary arteries draw their blood supply) allows studies of the blood flow to the myocardium. This technique can give a semi-quantitative estimate of flow on a minute to minute basis. In contrast only one flow estimation can be carried out using $^{99}Tc^{m}$ microspheres. Similarly, arterial infusion of $^{81}Kr^{m}$ enables studies of brain blood flow during drug stimulation.

Radioactive oxygen, ^{15}O, has been available for many years. It has a 2 min half-life and is available as $C^{15}O$, $C^{15}O_2$, $^{15}O_2$ and $H_2{}^{15}O$. Nitrogen is irradiated with deuterons at about 7 MeV. Oxygen-15 atoms are produced by the $^{14}N(d,n)^{15}O$ reaction and react with selected substrates in radiolytic reactions in the target to form, for example, $^{15}O_2$ and $C^{15}O_2$ at radiochemical purities of around 99%. One recent application of $^{15}O_2$ and $C^{15}O_2$ is in the study of regional brain oxygen consumption and blood flow.

If a subject breathes $^{15}O_2$ until a steady-state equilibrium is obtained the body tissues become labelled with $H_2{}^{15}O$ generated by metabolism of $^{15}O_2$. Some background is inevitably present due to the $^{15}O_2$ bound to haemoglobin in the blood but in practice this effect is small. If on the other hand $C^{15}O_2$ is administered under similar conditions the body tissues become labelled with $H_2{}^{15}O$ by the exchange process

$$C^{15}O_2 + H_2O \rightleftharpoons CO_2 + H_2{}^{15}O$$

(catalysed by carbonic anhydrase) and in this instance the labelled water content of the

tissue can be related to blood flow. Thus, by use of a suitable imaging device distributions of water of metabolism and flow can be studied and compared.

Initial studies are being carried out in the brain where mismatching between metabolism and flow can be seen clearly in a variety of disorders. During radiotherapy of brain tumours, for example, brain metabolism and blood flow can be monitored non-invasively, the only co-operation required from the patient is to breath the labelled gas whilst being located in front of the imaging device (γ-ray camera). Small cyclotrons (7–8 MeV deuterons) suitable for dedicated ^{15}O production may at £250 000 become a useful addition to the technological arsenal of the clinical scientist.

Radioactive nitrogen ^{13}N with its 10 min half-life can be produced by the $^{12}C(d,n)^{13}N$ or $^{16}O(p,\alpha)^{13}N$ reactions. If carbon dioxide or methane are irradiated with deuterons $^{13}N_2$ and $^{13}NH_3$ are the major products, respectively. If water is irradiated with protons of 10 MeV or more ^{13}N-labelled nitrate and nitrite are formed which can be reduced readily to $^{13}NH_3$.

$^{13}N_2$ is used in the solution and gas phase for pulmonary function studies whereas $^{13}NH_3$ has found application as a cerebral blood flow marker and in myocardial metabolism studies.

Radioactive carbon-11 is commonly produced by the $^{14}N(p,\alpha)^{11}C$ reaction to yield $^{11}CO_2$, which can be reduced to ^{11}CO by zinc at 400 °C. ^{11}CO can be used to label red blood cells as ^{11}C carboxyhaemoglobin and used to define blood pools, *e.g.* the heart chamber volumes *in vivo*. If approximately 5% H_2 is present during the proton irradiation of nitrogen $^{11}CH_4$ is produced; this can be chemically converted into the useful synthetic precursor $H^{11}CN$ with ammonia by passing over platinum catalyst at 1 000 °C. Several natural and synthetic amino acids have been prepared using $H^{11}CN$ and a modified Strecker synthesis for use in *in vivo* protein metabolism studies, *e.g.*, in the pancreas and tumours.

The radionuclides ^{15}O, ^{13}N and ^{11}C all decay by the emission of positrons. These positrons, on annihilation, give rise to a 180° correlated coincidence pair of 511 keV photons. These photons can, with the aid of recently developed multi-crystal ring detectors using 66 or more sodium iodide (thallium) crystals, be used to generate a quantitative image similar to an *in vivo* autoradiograph using computer assisted reconstructed emission tomography, a technique akin to that used by the now familiar EMI scanner. The positron and EMI studies can be considered as complementary. With suitable labelled radiopharmaceuticals the former provides functional information whereas the latter provides morphological information.

In conclusion, the application of radioactive gases of short half-life is now providing the clinician with useful information previously unobtainable both in the routine and research areas. The transition to the preparation and use of more complex molecules, based on simple gases as precursors has begun, and a challenging but interesting future seems to lie ahead.

Radiopharmaceuticals Containing Fluorine-18

A. J. Palmer

Medical Research Council, Cyclotron Unit, Hammersmith Hospital, Ducane Road, London, W12 0HS

Fluorine-18 (half-life 110 min β^+) found a place in nuclear medicine in the late sixties and early seventies when it was extensively used (in the form of a simple aqueous solution of fluoride) for bone scanning.[1] Since that time it has been largely superseded for this purpose by $^{99}Tc^m$ labelled polyphosphate complexes but its use on a smaller scale for dental studies continues.[2] Interest has also continued in the preparation and applications of organic radiopharmaceuticals labelled with this radionuclide.

Fluorine-18 labelled organic radiopharmaceuticals would appear to have several potential advantages. In fluorinated analogues the fluorine can replace either a hydrogen atom or a hydroxyl group in a normal organic compound, while a third possibility is the introduction of a trifluoromethyl group. In analogues of the first type the Van der Waals radii of the two elements are very similar (r_F = approximately 0.135 nm, r_H = approximately 0.110 nm) and fluorine is the only element that can replace hydrogen without notable steric consequences.[3] The carbon - fluorine bond has a very high dissociation energy and consequently improved *in vivo* stability would be expected for these compounds when compared with, for example, the equivalent iodine-labelled material. Fluorine and hydrogen are however very different in their reactivities. Owing to the very strong electron withdrawing inductive effect of

the hypertensive process in the rat. Circ Res 39: 433–441, 1976
24. Mohring J: High arterial pressure versus humoral factors in the pathogenesis of the vascular lesions of malignant hypertension: The case for humoral factors as well as pressure. Clin Sci 52: 113–117, 1977
25. Bloom DS, Stein MG, Rosendorff C: Effects of hypertensive plasma on the response of an isolated artery preparation to noradrenalin. Cardiovasc Res 10: 268–274, 1976
26. Coleman TG, Granger HJ, Guyton AC: Whole-body circulatory autoregulation and hypertension. Circ Res 28/29 (suppl II): 76–87, 1971
27. Coleman TG, Cowley AW Jr, Guyton AC: Experimental hypertension and long term control of arterial pressure. *In* Cardiovascular Physiology, edited by AC Guyton, CE Jones. Baltimore, University Park Press, 1974, pp 259–299
28. Kalsner S: Steroid potentiation of responses to sympathomimetic amines in aortic strips. Br J Pharmacol 36: 582–593, 1969
29. Abboud FM: Effects of sodium angiotension, and steroids on vascular reactivity in man. Fed Proc 33: 143–149, 1974
30. Reid JL, Zivin JA, Kopin IJ: Central and peripheral adrenergic mechanisms in the development of deoxycorticosterone-saline hypertension in rats. Circ Res 37: 569–579, 1975
31. Haeusler G, Finch L, Thoenen H: Central adrenergic neurons and the initiation and development of experimental hypertension. Experientia 28: 1200–1203, 1972
32. Lewis PJ, Dargie HJ, Dollery CT: Role of saline consumption in the prevention of deoxycorticosterone hypertension in rats by central 6-hydroxydopamine. Clin Sci 48: 327–330, 1975
33. Bevan RD: Effect of sympathetic denervation on smooth muscle cell proliferation in the growing rabbit ear artery. Circ Res 37: 14–19, 1975
34. Fleming WW: Variable sensitivity of excitable cells: Possible mechanisms and biological significance. Rev Neurosci 2: 43–90, 1976
35. Fleming WW, McPhillips JJ, Westfall DP: Postjunctional supersensitivity and subsensitivity of excitable tissue to drugs. Ergeb Physiol 68: 55–119, 1973

Continuous Assessment of Regional Myocardial Perfusion in Dogs Using Krypton-81m

ANDREW P. SELWYN, TERRY JONES, J. HARVEY TURNER, TIM PRATT, JOHN CLARK, AND PETER LAVENDER

SUMMARY Krypton-81m has been continuously eluted in 5% dextrose from a cyclotron-made rubidium-81 generator. The unique physical properties of this inert freely diffusible gas (half-life 13 seconds) have allowed the development of a technique for the constant infusion of this tracer into the aortic sinuses of 25 dogs. Theoretical considerations suggest that an equilibrium of ^{81m}Kr activity in the myocardium is principally dependent on blood flow. Experiments have tested the delivery of this indicator and have recorded quantitative high spatial resolution images of the heart with a gamma camera and digital computer. The systematic error was determined by comparing changes in regional blood flow (in ml/g per min, using an electromagnetic flow probe) and changes in calculated flow (ml/g per min) using the regional activity of ^{81m}Kr ($P = < 0.001$; $r = 0.97$; $y = 908 X + 0.105$; $n = 60$). The random error and uncertainties concerning mixing and streaming of the indicator were tested by repeating measurements with alterations in heart rate, blood pressure, coronary flow, and total myocardial ^{81m}Kr activity using different interventions (reproducibility, $P = 0.001$, $r = 0.982$; $y = 0.982x + -0.257$, $n = 100$ observations). Any quantification of changes in the myocardial activity of ^{81m}Kr must consider the stability of the arterial concentration of this indicator and washout of ^{81m}Kr at high values of myocardial blood flow. This ultra-short-lived radionuclide will, however, provide an assessment of changes in the distribution of regional myocardial perfusion.

IN 1968, Yano and Anger first suggested that ultrashort-lived radionuclides such as krypton-81m could be used to visualize blood vessels and organs.[1] Krypton-81m generators were designed to allow the intermittent elution of this gas indicator from its parent compound, rubidium-81 (^{81}Rb).[2, 3] This was used initially for ventilation and perfusion studies of the lungs and later for studies of cerebral blood flow.[4, 5]

Krypton-81m (half-life 13 seconds) allowed the introduction of a technique for continuous observation and assessment of the distribution of regional myocardial perfusion in dogs.[6] Although the theoretical considerations and initial experiments are of interest, a practical validation of the results by an independent method has not been provided.

It is the purpose of this paper to present an investigation of and validation for the use of ^{81m}Kr for continuous assessment of changes in regional myocardial perfusion (RMP) in 25 dogs.

From the Cardiovascular Research Unit, MRC Cyclotron Unit and Radiology Department, Royal Postgraduate Medical School, Hammersmith Hospital, London, England.

This work was supported in part by the British Heart Foundation.

Address for reprints: Dr. A.P. Selwyn, Cardiovascular Research Unit, R.P.M.S., Hammersmith Hospital, Du Cane Road, London W12 OHS, England.

Received June 20, 1977; accepted for publication February 8, 1978.

Methods

Theoretical Considerations

If ^{81m}Kr is infused constantly into the aortic sinuses, the arterial concentration of this indicator will fluctuate with pulsatile blood flow. If the pattern of mixing and streaming of this freely diffusible gas is stable, then the effect, over minutes, will be that a constant quantity of ^{81m}Kr will reach the coronary circulation per unit of blood flow. Accumulation of ^{81m}Kr in the myocardial water space will

result in an equilibrium of activity within the heart. During a constant infusion the amount of ^{81m}Kr, [Kr], in a volume of myocardium (V) will depend on: (1) blood flow into the myocardium (F); (2) arterial concentration of the indicator (Ca); (3) blood flow out of the myocardium (F); (4) venous concentration of the indicator [Kr]; and (5) disappearance of the indicator by decay (λ)

$$F(ca) \rightarrow \text{Myocardium} \rightarrow \frac{F}{V}[Kr]P + \lambda[Kr].$$

This model assumes that the venous concentration is in equilibrium with the tissue concentration.[7] P represents the partition coefficient of ^{81m}Kr taken to be 1.0.[8]

It is probable that the partition coefficient of ^{81m}Kr will change with different pathophysiologic circumstances. If one uses this ultrashort-lived tracer, as shown in Equations 1 and 4, the partition coefficient is related to the washout of the isotope $\left(\frac{F}{V}\right)$ and therefore takes a secondary role in the myocardial signal of ^{81m}Kr activity. The myocardial equilibrium of ^{81m}Kr in the heart will be influenced by arrival of ^{81m}Kr, by blood flow, and by rapid decay. Small changes in the partition coefficient will not be important. This is quite unlike the circumstances that exist when considering the washout of a long-lived indicator such as xenon-133,[7] this state of dynamic equilibrium can be expressed as:

$$F(Ca) = F\frac{[Kr]P}{V} + [Kr]\lambda$$

therefore

$$[Kr] = \frac{F(Ca)}{P\frac{F}{V} + \lambda} \quad (1)$$

The decay constant for ^{81m}Kr is 3.2/min, and this means that the time constant for observing a change in the equilibrium of ^{81m}Kr activity in the myocardium must be more than 13 seconds and preferably 30 seconds. The magnitude of fluctuation of ^{81m}Kr in the arterial blood with each heart beat will be small in comparison to the quantity of the active indicator in the myocardial water space. The denominator in Equation 1 is influenced by the high value for the decay constant. Hence, the steady state myocardial ^{81m}Kr activity is principally dependent on the arrival of the tracer, i.e., myocardial blood flow (F) rather than its removal.[6]

If the delivery of ^{81m}Kr is such that the mean concentration of the tracer in the arterial blood is constant (when measured at 30-second intervals), it is possible to examine theoretically the change in the myocardial signal, [Kr] which results from changes in myocardial blood flow (F). For any change in myocardial blood flow from F_1 to F_2 we have the following expressions for the corresponding myocardial counts/min of ^{81m}Kr, [Kr].

$$F_1(Ca) = g[Kr_1]\left(\frac{F_1}{V}P + 3.2\right) \quad (2)$$

$$F_2(Ca) = g[Kr_2]\left(\frac{F_2}{V}P + 3.2\right) \quad (3)$$

where g is the relative detection efficiencies between counting the myocardial ^{81m}Kr content, [Kr], and the concentration of ^{81m}Kr in the arterial blood (Ca). If it is assumed that in any single experiment Ca does not change significantly and g remains constant, it is possible to solve for F_2 by dividing Equation 2 by 3

$$F_2 = \frac{3.2F_1}{\frac{[Kr_1]}{[Kr_2]}\left(\frac{PF_1}{V} + 3.2\right) - \frac{PF_2}{V}}$$

This can be written:

$$\frac{F_2}{V} = \frac{3.2\frac{F_1}{V}}{\frac{[Kr_1]}{[Kr_2]}\left(P\frac{F_1}{V} + 3.2\right) - P\frac{F_2}{V}} \quad (4)$$

It follows that given a known value of $\frac{F_1}{V}$, as measured by a reference technique, and the corresponding myocardial ^{81m}Kr signal, [Kr], it should be possible to convert subsequent tissue counts i.e., $[Kr_2]$ into values of $\frac{F}{V}$, simply by insertion into Equation 4. In effect it should be possible to calibrate each preparation in order to convert changes in myocardial ^{81m}Kr activity into absolute changes in $\frac{F}{V}$.

By calibrating the ^{81m}Kr counts in this way it is possible to test: (1) the theoretical considerations, (2) the stability of the arterial concentration, mixing and streaming of the indicator, and (3) whether this technique can detect changes in regional myocardial perfusion.

Experimental Protocol

Mongrel dogs weighing 30–55 kg were anesthetized with intravenous sodium thiopental (12 mg/kg). Ventilation was provided via a cuffed endotracheal tube and a mechanical ventilator. Anesthesia was maintained by the intermittent intravenous injection of pentobarbital (1.5 mg/kg). Care was taken that with each administration the eyelash reflex was not abolished and the heart rate and blood pressure did not change by more than 5%. A left thoracotomy was performed and the heart supported in a pericardial cradle. A reversible snare was placed around the left anterior descending coronary artery (LAD) or a major branch of this vessel (Fig. 1). This allowed occlusion and release to be effected without interfering with imaging.

A modified Paulin ring cardiac catheter (Cooks Catheter Co.), introduced through a femoral arteriotomy, was seated below the coronary ostia in the aortic sinuses.[9] ^{81m}Kr was eluted continuously in normal saline from a ^{81}Rb generator and infused in 5% dextrose at 10 ml/min by a constant rate infusion pump (Watson-Marlow MHRE200).[6]

The dog's heart was positioned under a wide-field gamma camera (Toshiba GCA 202), and images were recorded on Polaroid or 35-mm film with the dog in the left lateral position. The resolution of this camera plus

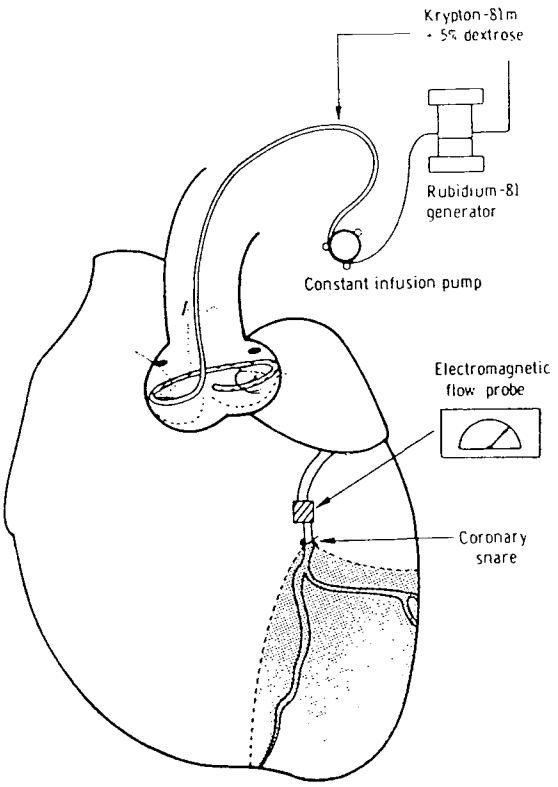

FIGURE 1 *The experimental diagram shows the ^{81}Rb generator, infusion pump, and the aortic sinus catheter. Regional coronary flow was measured using an electromagnetic flow probe. The LAD snare is shown.*

collimeter for ^{81m}Kr was 7 mm, using a line spread function. Quantitative high spatial resolution images of total and regional myocardial counts/min of ^{81m}Kr were recorded with the gamma camera and a digital computer (Deltron-Nova 1220). These quantitative images were recorded on a magnetic disc at 30-second intervals throughout the experiments. The digital computer was programmed to recall and display images recorded on an oscilloscope screen within a 64 × 64 matrix of squares. An electronic light pen was available to enclose up to seven areas of interest within the matrix, and the computer was capable of displaying the counts recorded in each area of interest for each 30-second interval of the experiments. Corrections were made for the decay of ^{81}Rb. A cannula was inserted into the second femoral artery, and thoracic aortic pressure was measured with Statham P23Db pressure transducer. The ECG (standard lead 2) was continuously monitored, and these variables were recorded on a multichannel instrument (Hewlett-Packard, 7788A).

A suitably sized standard error electromagnetic flow probe was fitted to the coronary vessel immediately proximal to the snare. The probe diameter varied between 3 and 5 mm. Pulsatile regional coronary flow was recorded by connecting the probe to a standard error flowmeter (SEM 275). The flowmeter system has a carrier frequency of 285 Hz and the output is nominally flat (down less than 3 dB) to 80 Hz. Numerous mechanical occlusions of the LAD were made by a distally placed snare to ensure an accurate zero level throughout the studies. Recordings were selected for analysis only if, in adjacent zero determinations, there was a change in zero level of less than 5% of peak flow. The flow probes were calibrated in situ at the end of the experiments by cannulating the main left coronary artery, tying off all the branches except the one of interest, and perfusing that artery with the dog's own blood from a continuous infusion pump. The areas under the systolic and diastolic portions of the phasic flow tracings were analyzed by planimetry and were calculated by using the calibration data flow in milliliters per minute (ml/min). The mean of six measurements of flow in ml/min for each control period and each intervention was used. The dicrotic notch of the arterial pressure wave was taken as the beginning of diastolic coronary flow.

Each experiment was started by positioning the dog's heart under the gamma camera. ^{81m}Kr in 5% dextrose was delivered by constant infusion into the aortic sinuses. The total and regional myocardial activities of the indicator were recorded for 20 minutes while heart rate, aortic pressure, and phasic regional coronary flow were stable. The LAD was occluded for 30 seconds and a region on the heart on the visual display showing diminished ^{81m}Kr activity was identified. The camera was rotated in relation to the heart so that the area of interest was positioned on the edge of the image. This minimized the effects of counts from the opposite side of the heart when investigating regional counts/min (CPM) in the area under study.

A variety of interventions was used to change total or regional myocardial blood flow.

1. The atria were placed at rates of 150 to 225 beats/min (n = 25 dogs).
2. Intravenous isoproterenol was given at between 0.15 and 0.4 μg/kg per min (n = 25 dogs).
3. Temporary LAD occlusion was used to produce 2.0 and 5.0 minutes of regional ischemia followed by reperfusion (n = 25 dogs).
4. Pentobarbital (3.0 mg/kg, iv) was used to produce decreases in coronary flow (n = 20 dogs).

Regional coronary flow (electromagnetic flow probe) and total and regional myocardial CPM of ^{81m}Kr were recorded before, during, and after each intervention, when heart rate, blood pressure, and phasic regional coronary flow were stable.

The reproducibility of changes in ^{81m}Kr myocardial CPM was tested in three ways.

1. Total CPM of ^{81m}Kr was recorded for 20 minutes before the interventions were initiated and while heart rate, blood pressure, and regional coronary flow (electromagnetic flow probe) were stable (n = 25 dogs).
2. In each experiment, the total and regional myocardial CPM of ^{81m}Kr were recorded before, during, and after interventions affecting the whole heart (i.e., atrial pacing, pentobarbital and isoproterenol) and in those producing local changes (i.e., LAD occlusion). The dogs were allowed to recover so that heart rate, blood pressure, and coronary flow returned to control. At least four interventions were used in each experiment and at least two of these were repeated. The initial control myocardial ^{81m}Kr activity and the controls after the interventions were compared. The effects of the same intervention delivered

twice on total and regional myocardial ^{81m}Kr CPM were compared (n = 25 dogs).

3. In each dog, the quantitative images of myocardial ^{81m}Kr recorded before, during and after those interventions that affected the whole heart, were divided into six areas with an electronic light pen, using the visual display. The activity in each area was expressed as a ratio of the total myocardial activity. Six ratios from each heart were calculated before, during, and after each intervention (n = 25 dogs; 125 observations). A two-way analysis of variance was used to test whether the control or intervention ratios changed during the experiments.

After the interventions, the heart remained in position under the gamma camera and the LAD carrying the flow probe was occluded for 45 seconds. The regional decrease in activity of ^{81m}Kr was recorded with the gamma camera and digital computer and was outlined on the visual display with an electronic light pen. The position of each heart and region of interest were checked by comparing this area to the one outlined at the beginning of the experiments. The background activity was estimated by the simultaneous recording of CPM from an area around the image in the field of the gamma camera. This area was the same size as the heart image. Total myocardial CPM

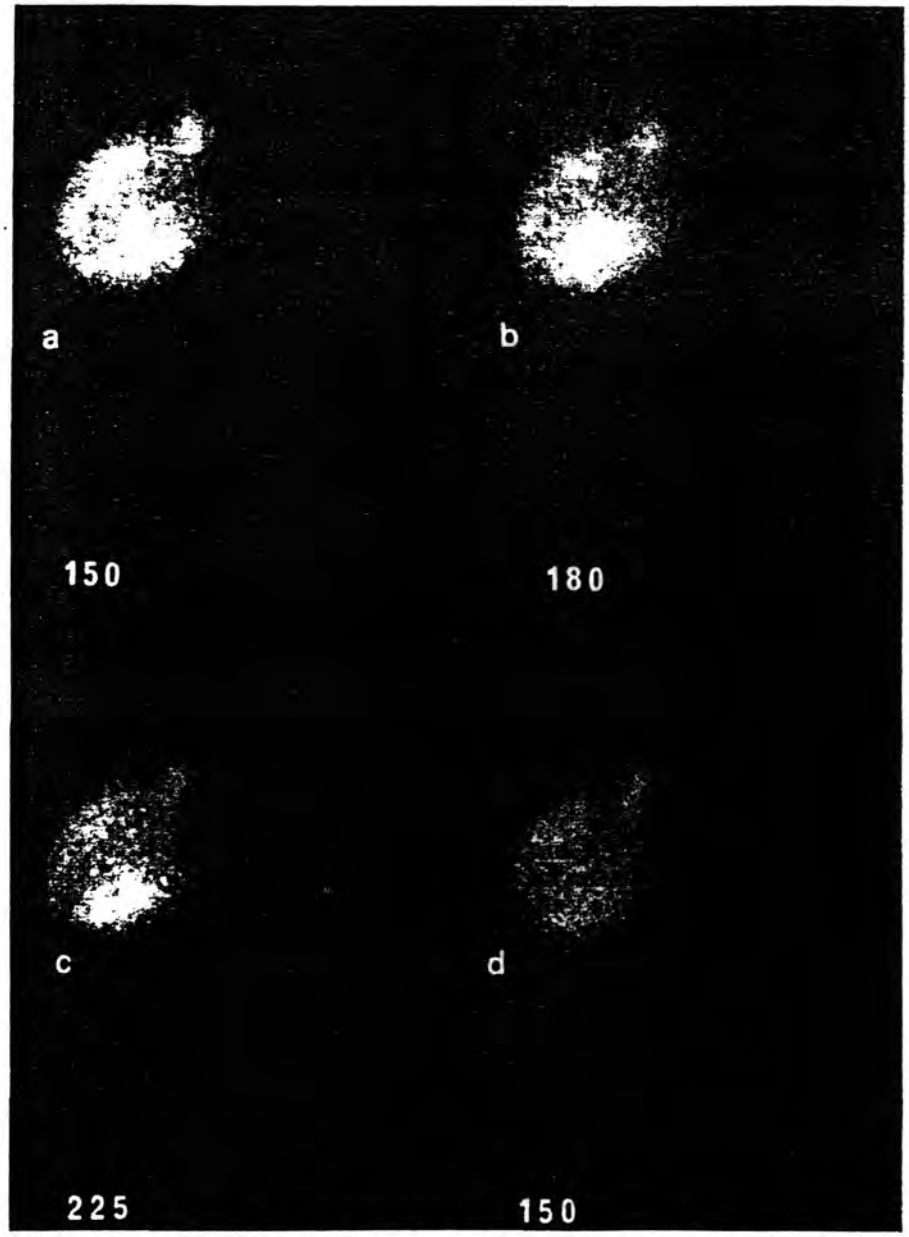

FIGURE 2 *The four images show the myocardial distribution of ^{81m}Kr during the aortic sinus infusion. The distribution did not change when heart rate, aortic pressure, and coronary flow were altered by interventions affecting the whole heart. This suggested stability of catheter position, also mixing and streaming of the indicator. a = control heart rate 150/minute; b = IVI isoproterenol given, heart rate 180/minute; c = heart rate 220/minute; d = control, 150/minute, after infusion.*

were analyzed by constructing an area of interest including the whole heart and excluding the aortic root. The background activity was typically less than 3% of the myocardial activity. The edge of the image of myocardial activity was therefore clearly delineated when constructing the areas of interest with an electronic light pen.

At the end of each experiment, patent blue 5 dye was selectively injected into the vessel carrying the flow probe. The heart was stopped within 3 seconds with intra-arterial potassium chloride.[10] This outlined the area of supply for dissection. The heart was removed and the myocardium supplied by the coronary vessel carrying the probe was dissected out and weighed. Paired *t*-tests and linear regression analysis were used to examine the systematic and random errors using krypton-81m.

Results

The arterial tension of oxygen and carbon dioxide did not vary beyond the normal ranges (Po_2, 95–125 mm Hg, and Pco_2, 36–42 mm Hg) in all the dogs. The arterial pH was maintained between 7.41 and 7.48. The measured background activity did not exceed 2.5% of the total myocardial activity of ^{81m}Kr in any of the experiments. There was no detectable activity in the lung fields (i.e., no more than 2% of the total myocardial ^{81m}Kr CPM counting areas of equivalent size.

Figure 2 shows four images of the myocardial distribution of ^{81m}Kr. This typical example from one experiment shows images recorded before, during, and after intravenous isoproterenol was administered. Each image was composed by recording 100,000 counts. The regional activity in six selected areas of interest was expressed as a ratio of the total ^{81m}Kr myocardial CPM. These ratios did not change by more than ±4% in any of the experiments (a two-way analysis of variance was used to show that the changes were insignificant in 125 observations). The myocardial distribution of ^{81m}Kr was tested in this way by using interventions that altered regional coronary flow, heart rate, and aortic blood pressure. The myocardial distribution was changed if the ring catheter was withdrawn into the ascending aorta.

Quantitative images recorded at 30-second intervals showed no evidence of beat-to-beat fluctuations in myocardial ^{81m}Kr activity that may have been present due to the pulsatile nature of the coronary arterial circulation. Occlusion of a major branch of the LAD resulted in images showing regional defects in activity (Fig. 3c). On release of the coronary snare, a regional reactive increase in activity was seen (Fig. 3, d and e), and after 20 minutes the images returned to control (Fig. 3f).

Areas of interest were constructed around the region supplied by the snared coronary vessel and the rest of the

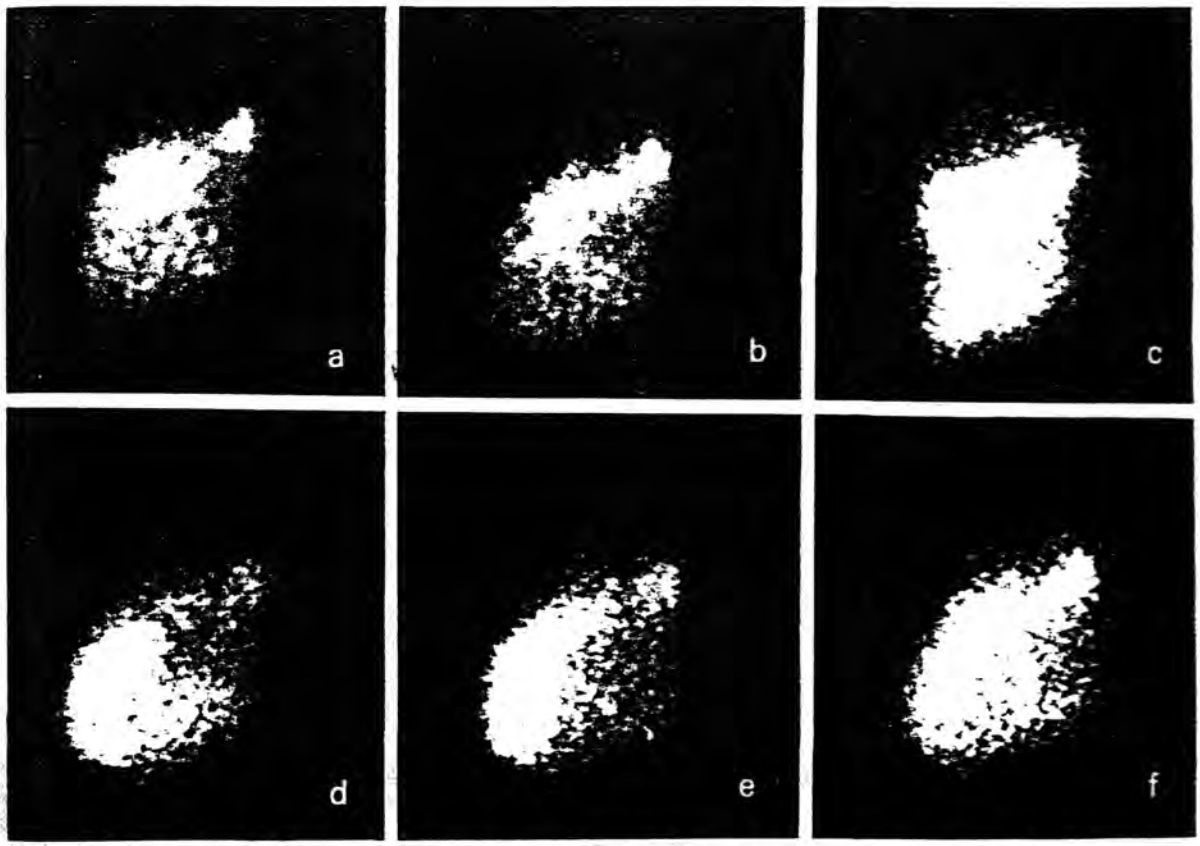

FIGURE 3 *A typical example of the myocardial distribution of ^{81m}Kr activity during a continuous aortic sinus infusion. Panels a and b show the control period; c shows the distribution of ^{81m}Kr 2 minutes after LAD occlusion; d and e show the myocardial distribution at 30 seconds and 3 minutes after LAD release. The regional reactive increase in activity is shown. Panel f shows recovery at 20 minutes after LAD occlusion.*

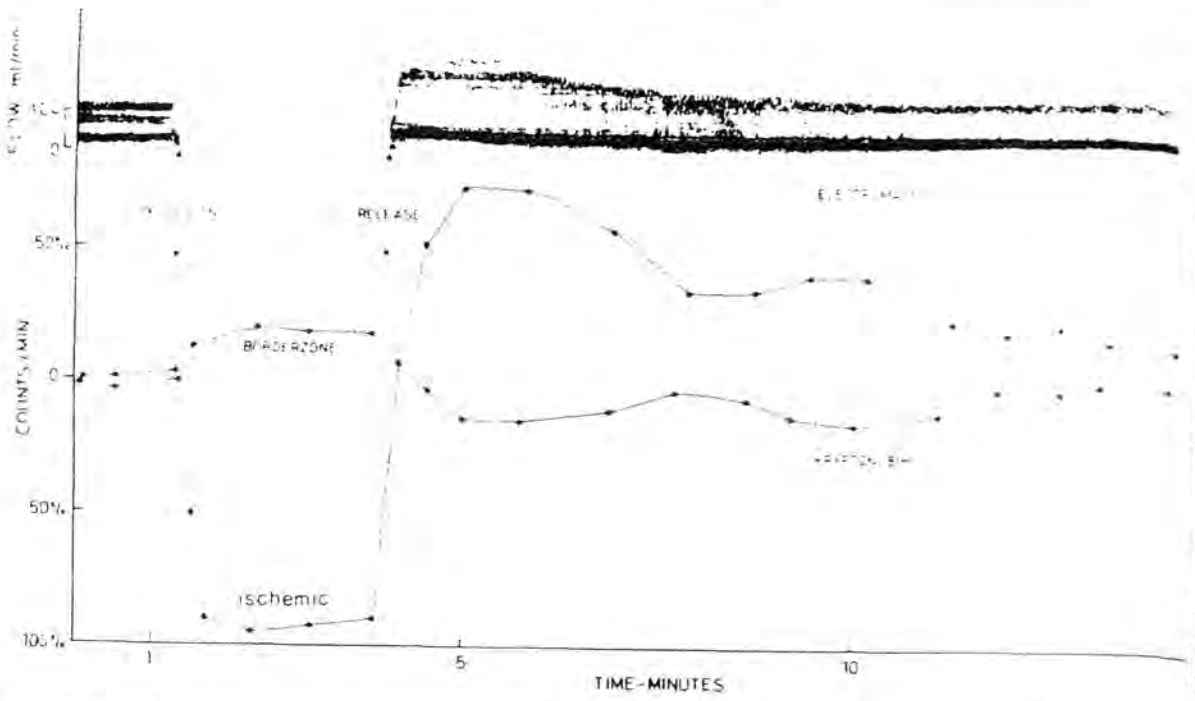

FIGURE 4 *Typical individual data recorded during the imaging shown in Figure 3. The control period shows a stable baseline of regional coronary flow [electromagnetic flow (e.m.f.) probe] and regional activity of ^{81m}Kr. Regional myocardial diminution in ^{81m}Kr activity and zero coronary flow follows occlusion of the LAD. Reactive hyperemia and recovery of both parameters is shown after LAD release.*

myocardium. Figure 4 shows a typical example of the time course for the changes in regional phasic coronary flow (electromagnetic flow probe) and the regional changes in myocardial ^{81m}Kr activity.

Reproducibility

The total myocardial activity of ^{81m}Kr varied by no more than ±4% in each dog during the 20-minute control period while heart rate, blood pressure, and regional coronary flow (electromagnetic flow probe) were stable (n = 25 dogs).

In each dog, control values for regional and total ^{81m}Kr CPM before and after interventions were compared. The effects of identical interventions given twice on ^{81m}Kr CPM were also compared (total observations = 100). The return to control and the changes in regional and total myocardial activity produced by repeating interventions were highly reproducible ($P = < 0.001$; $r = 0.982$; y = 0.982X + −0.257; linear regression).

In each dog, the resting reference control regional coronary flow in ml/g per min was calculated using the flowmeter data. The specific gravity of myocardium (1.05) was used to convert this to flow per unit volume (F_1/V). This was related to the resting control regional CPM of ^{81m}Kr in that area [K_1]. During each intervention, a new value for flow per unit volume (F_2/V) was calculated using the new regional CPM of ^{81m}Kr, [K_2], and Equation 4. This result was converted to ml/g per min and compared to the new regional coronary flow measured using the electromagnetic flow probe and weight of myocardium

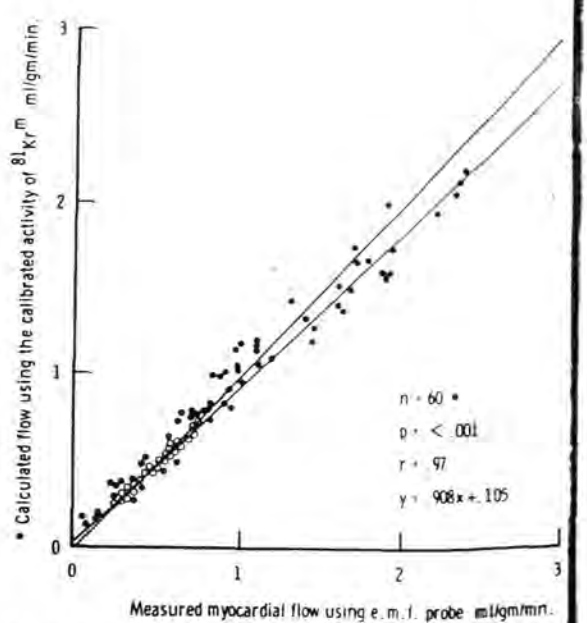

FIGURE 5 *The relationship between measured regional myocardial blood flow (electromagnetic flow probe and weight of segment) and calculated regional myocardial blood flow using the changes in the regional activity of ^{81m}Kr in the same segment. The open circles represent the initial values of regional blood flow measured with the probe and used to calibrate subsequent changes in myocardial ^{81m}Kr activity.*

supplied. The relationship shown in Figure 5 was statistically significant.

Discussion

Krypton-81m emits a monoenergetic 190 keV gamma ray. The gas is biologically and chemically inert and diffuses freely. This indicator can be eluted continuously from the cyclotron-produced radioactive parent, rubidium-81, contained in a portable generator.[3]

Kaplan and Mayron[11] have shown that when ^{81m}Kr was infused into the coronary circulation there was no significant detectable activity in the lung fields.

The major disadvantage of using ^{81m}Kr is the delivery of the indicator which requires an invasive technique. The use of radiopotassium and related radionuclides is much less invasive but makes certain assumptions about myocardial cell membrane metabolism.[12] The energies emitted by ^{43}K, ^{201}TL, ^{80}Rb, and ^{131}Cs can impair image resolution seriously.[13]

The clearance of ^{133}Xe from the heart is a function of myocardial blood flow.[7] The partition coefficient must be considered because of the accumulation of this gas in fat. Also, these techniques generally do not provide images of high spatial resolution. Radioactive microspheres must be injected into the left atrium to assess myocardial blood flow and can provide detailed quantitative measurements separating endocardial and epicardial events. This cannot be done in man; the measurements are not dynamic and problems of uneven vascular distribution must be considered.[14]

In these experiments the systematic error was tested within a segment of ventricular myocardium. A different experimental design will be necessary if this technique is required to assess changes in overall or total myocardial perfusion.

The gamma camera used in this way cannot record the regional myocardial distribution of ^{81m}Kr in three dimensions. This can be overcome partially by observing the region of interest on the edge of the image of myocardial activity. This minimizes interference from ^{81m}Kr CPM from the opposite side of the heart. In its present form, this technique cannot separate endocardial and epicardial CPM of ^{81m}Kr. Pinhole collimation of transaxial emission scanning may be of help in the future.

Changes in the regional distribution of activity could occur if the delivery, mixing, or streaming of the indicator were unstable. These experiments showed that when the position of the catheter was stable and a constant infusion was delivered into the aortic sinuses, a stable baseline of total myocardial CPM of ^{81m}Kr could be recorded. Six selected areas of myocardium in each dog received the same proportion of ^{81m}Kr activity when heart rate, blood pressure, and coronary flow were altered by interventions that affect the whole heart. This suggested that, in these experiments, mixing and streaming of the indicator in the aortic sinuses and coronary circulation were stable. The myocardial distribution of radioactively labeled microspheres and ^{81m}Kr were identical when both were administered in the same way using the ring catheter.[6]

It is necessary to consider that as blood flow increases the effects of washout of ^{81m}Kr on the relationship between regional CPM of the tracer and blood flow become more important. In this study, a reference technique was used to determine this relationship. Using theoretical considerations, it was possible to calibrate the regional myocardial activity of ^{81m}Kr. Figure 5 demonstrates the systematic error and shows a significant relationship between measured and calculated myocardial blood flow.

If regional CPM of ^{81m}Kr are used in this way to calculate changes in myocardial perfusion, the concentration of the indicator in blood delivered to the coronary circulation must be stable or measured and incorporated in the calculations. In these experiments, the relationship between calculated and measured regional myocardial perfusion suggested that the arterial concentration did not change enough to invalidate the theoretical considerations or the comparison with a reference technique. If arterial concentration of ^{81m}Kr altered, but mixing and streaming were stable, then regional activity could be used to assess relative changes in the regional perfusion of one area in relation to the surrounding myocardium. In conclusion, investigations of the systematic and random errors have shown that the indicator must be delivered into the aortic sinuses and that the myocardial distribution of ^{81m}Kr during a constant infusion is stable. Absolute quantitation of flow is difficult because the geometrical relationship between a heart and the gamma camera is complex, the arterial concentration of the indicator must be stable, and washout of ^{81m}Kr at high values for flow unit volume must be considered. The theoretical considerations and these experiments have shown that the unique physical properties of ^{81m}Kr can be used to assess changes in regional myocardial perfusion.

Acknowledgments

We thank Aviva Petrie (consultant statistician) for advice, T. Pratt for technical assistance, and P. Horlock for preparation of generators.

References

1. Yano Y, Anger HO: Ultrashort lived radioisotopes for visualizing blood vessels and organs. J Nucl Med **9:** 2-6, 1968
2. Yano Y, McRae J, Anger HO: Lung function studies using short lived radionuclides and the scintillation camera. J Nucl Med **11:** 674-679, 1970
3. Clark JC, Horlock PL, Watson IA: Krypton-81m generators. Radiochem Radioanalyt Letters **25:** 245-248, 1976
4. Anrot RN, Glass HI, Clark JC: Radioaktive Isotope. *In* Klinik und Forshung, vol 9, pp 76-78, 1970
5. Jones T, Clark JC: A cyclotron produced ^{81}Rb-^{81m}Kr generator and its uses in gamma camera studies (abstr). Br J Radiol **42:** 237, 1969
6. Turner JH, Selwyn AP, Jones T, Evans TR, Raphael MJ, Lavender JP: Continuous imaging of regional myocardial blood flow in dogs using Krypton-81m. Cardiovasc Res **10:** 398-404, 1976
7. Kety SS: The theory and applications of the exchange of inert gas at the lungs and tissues. Pharmacol Rev **3:** 1-41, 1951
8. Ross RS, Ueda K, Litchtlen P, Rees R: Measurement of myocardial blood flow in animals and man by selective injection of radioactive inert gas into the coronary arteries. Circ Res **15:** 28-41, 1963
9. Paulin S: Coronary Angiography. Acta Radiol [Diagn] (Stockh) **233:** 1-180, 1964
10. Eckenhoff JE, Hafkenshiel JH, Landmesser CM: The coronary circulation in the dog. Am J Physiol **148:** 582-596, 1947
11. Kaplan E, Mayron LW: Evaluation of perfusion with the ^{81}Rb-^{81m}Kr generator. Semin Nucl Med **6:** 163-190, 1976
12. Poe ND: Comparative myocardial uptake and clearance characteristics of potassium and cesium. J Nucl Med **13:** 551-560, 1974
13. Martin ND, Zaret BL, Strauss WH, Wells HP, Albes J: Myocardial imaging using ^{43}K and the gamma camera. Radiology **112:** 446-448, 1974
14. Buckberg GD, Luck JC, Payne B, Hoffman JIE, Archie JP, Fixler DE: Some sources of error in measuring regional blood flow with radioactive microspheres. J Appl Physiol **31:** 598-604, 1971

KRYPTON 81m GENERATORS FOR VENTILATION AND PERFUSION

J. C. Clark, P. L. Horlock and I. A. Watson

Krypton 81m decays with a 13 second half-life and emits 190 keV photons in 65% of its disintegrations. It is the daughter of rubidium 81 which has a half-life of 4·58 hours.

Recent clinical interests have led to the exploitation of the very short half-life of $^{81}Kr^{m}$ to obtain functional images of various organs directly from the scintillation camera during the continuous administration of $^{81}Kr^{m}$ at constant concentrations (Kaplan *et al.*, 1974a; Fazio and Jones, 1975; Turner *et al.*, 1976b; Kaplan *et al.*, 1976). Generators have been developed for delivering constant concentrations of $^{81}Kr^{m}$ solution for intravenous and intra-arterial infusion as well as in the gas phase for use in lung ventilation studies.

The main factors to be considered in the preparation of these generators are:

(1) Cyclotron production of useful quantities of the ^{81}Rb parent.
(2) Generator design.
(3) Chemical separation of ^{81}Rb from the target material and generator loading.
(4) Procedures for generator testing.

In this paper these points will be considered, together with some practical aspects of generator operation, with particular reference to generators produced and distributed by the Medical Research Council, Cyclotron Unit.

THE PRODUCTION OF RUBIDIUM 81

There are several reported methods for producing ^{81}Rb and these are shown in Table 1–I. Both the $^{79}Br(\alpha, 2n)^{81}Rb$ and the $^{81}Br(\alpha, 4n)^{81}Rb$ reactions proceed in good yield with 30 and 50 MeV alpha particles respectively. Sodium bromide and cuprous bromide have been used as target materials. The yield for the 21 MeV helium 3 reaction with bromine is not high enough for useful generator production. The use of ^{3}He at 29 MeV has recently been investigated (Guillaume, 1978) using sodium bromide and cupric bromide targets and ^{81}Rb yields of practical proportions achieved.

TABLE 1.1

Production routes for ^{81}Rb

Nuclear reaction	Target material	Projectile energy (MeV)	Practical beam current (μA)	^{81}Rb yield at EOB ($mCi\,\mu A^{-1}\,h^{-1}$)	Institution	Authors
$^{79}Br(\alpha, 2n)^{81}Rb$	NaBr (thick)	30	50	2	MRC Cyclotron Unit, Hammersmith Hospital, London	Clark *et al.*, 1970; Clark and Buckingham, 1975
$^{79}Br(\alpha, 2n)^{81}Rb$	Cu_2Br_2 (thick)	30	50	2	Argonne Cyclotron, Argonne Nat. Lab., USA	Colombetti *et al.*, 1974
$^{81}Br(\alpha, 4n)^{81}Rb$	NaBr (thin)	50 → 30	15	2·9	Lawrence Radiation Lab., 2·2 m Cyclotron, Berkeley, USA	Yano *et al.*, 1970
$^{81}Br(^3He, 3n)^{81}Rb$ and $^{79}Br(^3He, n)^{81}Rb$	NaBr (thick)	21	25	0·035	Sloane Kettering Inst., New York, USA, CS-15 Cyclotron	Watson, 1970
	NaBr or $CuBr_2$ (thick)	29	—	1·5	Liège Univ., Thompson CSF 520 Cyclotron	Guillaume, 1978
$^{80}Kr(^3He, pn)^{81}Rb$	37% enriched ^{80}Kr	20	5	0·226	Franklin McLean Memorial Research Inst., Chicago, USA, CS-15 Cyclotron	Rich *et al.*, 1975
$^{80}Kr(d, n)^{81}Rb$	37% enriched ^{80}Kr	8	5 (75)	0·7	CS-15 Cyclotron	Rich *et al.*, 1975
$^{82}Kr(p, 2n)^{81}Rb$	11% (natural) ^{82}Kr	26·5 → 22	15	3·5 4	Mt. Sinai Medical Center, Miami, CS-30 Cyclotron	Clark *et al.*, 1977
$^{82}Kr(p, 2n)^{81}Rb$	70% enriched ^{82}Kr	22 → 14		15	Medi-Physics CS-22 Cyclotron	Lamb *et al.*, 1978
$^{82}Kr(d, 3n)^{81}Rb$	70% enriched ^{82}Kr	21 22	40	1	Argonne Cyclotron, Argonne National Lab., USA	Gindler *et al.*, 1976
$^{85}Rb(p, 5n)^{81}Sr$ $^{81}Sr \xrightarrow{25\ min.} {}^{81}Rb$	RbCl	65		0·4	Crocker Nuclear Lab. Univ. of California Davis, USA	Peek *et al.*, 1976; Schneider and Goldberg, 1976
$^{85}Rb(p, p4n)^{81}Rb$	RbCl				Note: only low specific activity ^{81}Rb possible	
$^{84}Sr(p, \alpha)^{81}Rb$	70% enriched ^{84}Sr	8 10				Cann, 1973

By using a 37% enriched krypton 80 target both 20 MeV ^{3}He and 8 MeV deuterons have been used to produce useful quantities of rubidium 81. Natural and 70% enriched ^{82}Kr* have been irradiated with protons and deuterons to produce clinically useful generators (Clark *et al.*, 1977; Gindler *et al.*, 1976; and Lamb *et al.*, 1978). In all target systems using krypton the ^{81}Rb product must be recovered from a large area of target wall and no particularly attractive method of achieving this has yet been reported. A remotely controlled target with a rotating glass or stainless steel liner may offer a practicable solution if suitable conditions can be found to effect an efficient recovery of ^{81}Rb from the walls (Palmer *et al.*, 1973; Guillaume, 1976). Alternatively, a target whose walls can be remotely steam treated may be considered (McDonald, 1977; Friedman, 1976). If enriched krypton is to be used a highly reliable containment system should be employed.

The irradiation of rubidium targets with about 65 MeV protons has been described primarily as a source of high purity ^{81}Rb via ^{81}Sr for *in vivo* generator studies, but higher production rates may be possible if lower purities and specific activities are acceptable for *in vitro* generator applications. The proton irradiation of enriched ^{84}Sr was proposed by Cann (1973) but no practicable applications have been described.

Most methods of producing ^{81}Rb simultaneously produce other rubidium radionuclides which are of importance primarily when considering the whole body radiation dose due to rubidium breakthrough from solution generators. Of secondary concern is the provision of lead shielding for the generator assembly as ^{82}Rb^{m} emits particularly hard gamma-rays.

GENERATOR DESIGN

Two types of ^{81}Kr^{m} generators have been reported and some of their characteristics are shown in Table I–II. Both use a cation exchange material to retain the ^{81}Rb whilst allowing the ^{81}Kr^{m} to be recovered in either the solution or gas phase. However, they have quite different rubidium loading characteristics (see next section).

The first type developed in our laboratory (Clark *et al.*, 1970) incorporates a column of the inorganic ion exchange material zirconium phosphate. The second type of generator developed in the Donner laboratory (Yano *et al.*, 1970) and subsequently improved in the Veterans Administration Hospital, Hines, in collaboration with the Argonne National Laboratory (Colombetti *et al.*, 1974) uses a cation exchanger of the organic type, e.g. Dowex 50 × 8.

Neither generator system may be eluted with isotonic (0·9%) NaCl

* 70% enriched ^{82}Kr, $7300 per litre (Nov., 1976), Mound Laboratory, Miamisburg, Ohio 45342, USA.

TABLE 1-II
$^{81}Kr^{m}$ Generator system

Delivery phase	Generator type		Generator loading criteria	Elution efficiency	References
Gas or solution	Inorganic ion exchanger column	6 × 30 mm zirconium phosphate Bio Rad ZPI 50–100 mesh	Rapid loading at high NaBr concentrations possible	70%	Clark *et al.*, 1970; Clark and Buckingham, 1975
Gas or solution	Organic ion exchange column	11 × 60 mm Bio Rad AG50 × 4, 200–400 mesh	Slow loading at low NaBr concentrations	10%	Yano *et al.*, 1970
Gas or solution	Organic ion exchange column	2·5 × 22 mm Dowex 50 × 8, 200–400 mesh	^{81}Rb chemically separated from Cu_2Br_2 loaded "carrier-free"	80%	Colombetti *et al.*, 1974
Gas	Organic ion exchange column	2 mg Bio Rad AG MP50	^{81}Rb recovered "carrier-free" from proton irradiated 70% enriched krypton	~90%	Lamb *et al.*, 1978

solutions without incurring significant losses of rubidium. Elution with water or isotonic dextrose, however, may be carried out at high flow rates (5–10 ml min^{-1}) with little loss of rubidium (see below). As the half-life of the eluted product is only 13 seconds the ion exchange column bed volumes are kept as small as is practicable consistent with maintaining adequate safety levels for rubidium breakthrough or leakage.

CHEMICAL SEPARATION OF RUBIDIUM 81 AND GENERATOR LOADING

Zirconium phosphate is an insoluble crystalline material with a high affinity for rubidium even in the presence of high concentrations of sodium ions. This property enables one to load ^{81}Rb on to the zirconium phosphate generator rapidly at high efficiency using the irradiated 2·5 g sodium bromide target dissolved in 20 ml water. A wash with 100 ml water to remove the unwanted sodium bromide is all that remains to complete the generator preparation. The whole procedure is accomplished in approximately ten minutes and readily carried out by remote control.

The organic cation exchanger used in the second type of generator will only retain rubidium when it is applied to the column in solutions of low ionic strength. Thus if a sodium bromide or cuprous bromide target is used, the ^{81}Rb must be chemically separated from the target material before being loaded on to the column essentially carrier free (Colombetti *et al.*, 1974). These procedures are time-consuming and difficult to carry out by remote control and the resulting generators offer few advantages over the zirconium phosphate type, both types having elution efficiencies of 70–80% and similar rubidium breakthrough values.

If carrier-free ^{81}Rb is recovered in neutral ion-free solution after krypton irradiation the AG 50 × 8 material may be loaded rapidly with high efficiency.

PROCEDURES FOR GENERATOR TESTING

The zirconium phosphate generators produced in our laboratory are routinely tested for eluted activity at steady state. Rubidium breakthrough values for eluates of both gas and solution generators are also estimated.

The elution test is carried out using water at a standard flow rate of 10 ml min^{-1} and the steady state eluted $^{81}Kr^{m}$ is monitored in a 15 ml coiled tube placed in a calibrated re-entrant ionization chamber. A 25 ml sample of this eluate is collected for subsequent assay for rubidium breakthrough using a calibrated Ge/Li gamma-ray spectrometer.

Solution generators intended for human use are assembled a few hours before loading from cleaned, sterilized and dried components. The assembly is then washed through with sterile pyrogen-free water which is also used throughout the loading and washing procedure. Pyrogen testing of eluates from generators taken at random are carried out by the standard rabbit test or the *in vitro* Limulus test.

SOME ASPECTS OF ZIRCONIUM PHOSPHATE GENERATOR OPERATION

The infusion generator may be eluted with water or isotonic dextrose. In order to render the infusate isotonic when water is used, the generator eluate is mixed with an equal flow of 1·8% sodium chloride solution as shown in Fig. 1–1. A simplified infusion generator arrangement using isotonic dextrose

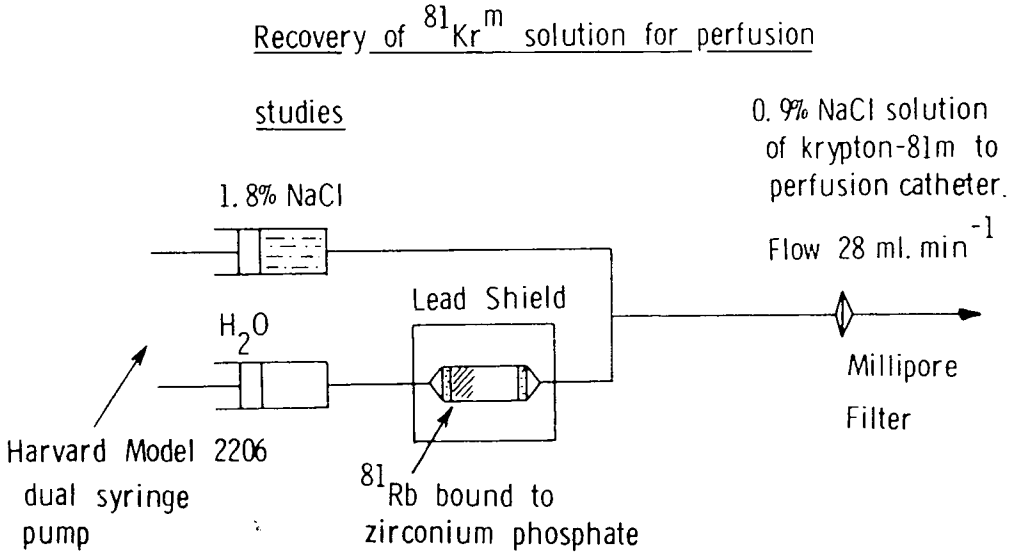

Fig. 1–1. Schematic diagram of the $^{81}Kr^{m}$ solution generator using a water eluant.

as the eluant is shown in Fig. 1–2A. The small rubidium trap column of AG 50 × 8 (H^+) resin is introduced into the system, after the generator has been loaded and washed, to control the small but significant increased Rb breakthrough that occurs with zirconium phosphate when eluted with isotonic dextrose. The eluant is in both cases terminally sterilized using a Millipore Millex disposable 0·22 μm filter unit with the inevitable introduction of its 1·5 ml dead volume. The filter should be preloaded with eluant and the generator system purged well to remove air bubbles before the filter unit is installed to avoid the risk of "gas-locking" with the attendant

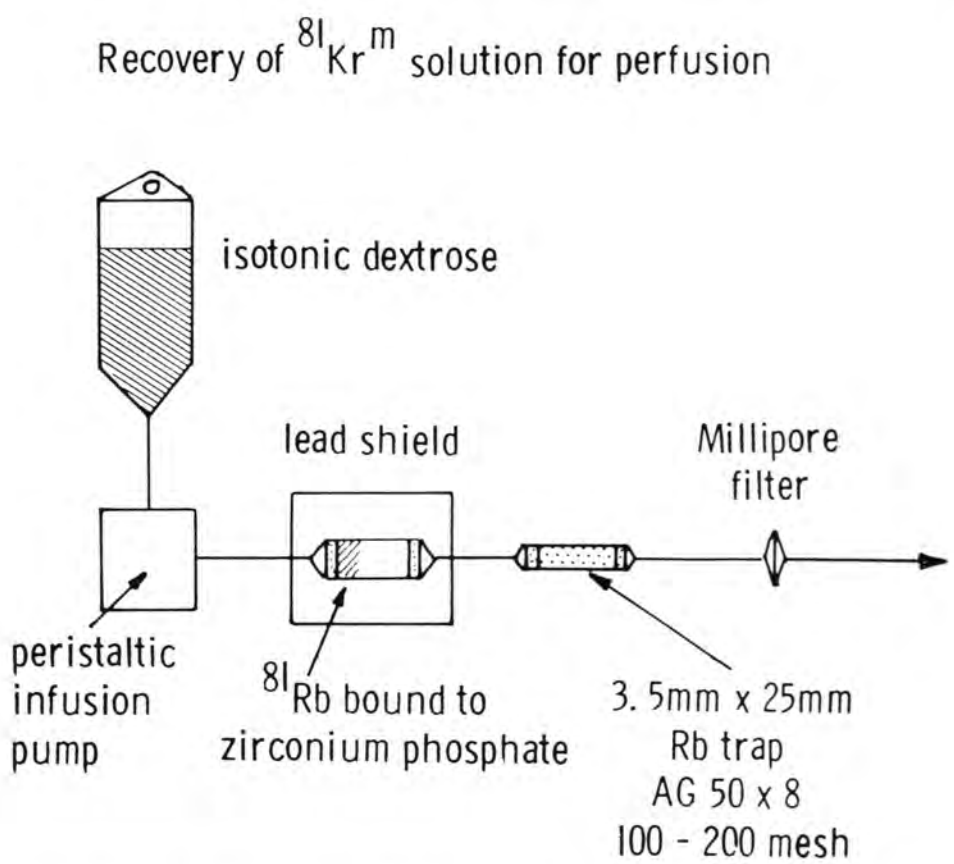

Fig. 1–2A. Schematic diagram of the $^{81}Kr^{m}$ solution generator using an eluant of isotonic dextrose in water.

Fig. 1–2B. The MRC $^{81}Kr^{m}$ solution generator for use with an isotonic dextrose eluant. Shown with the zirconium phosphate column (white) out of the lead shield and the series rubidium trap column.

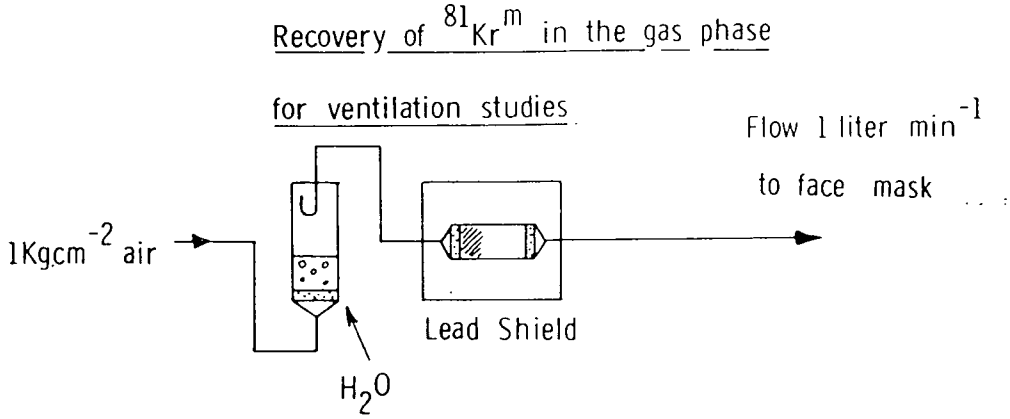

Fig. 1–3A. Schematic diagram of the $^{81}Kr^{m}$ gas generator

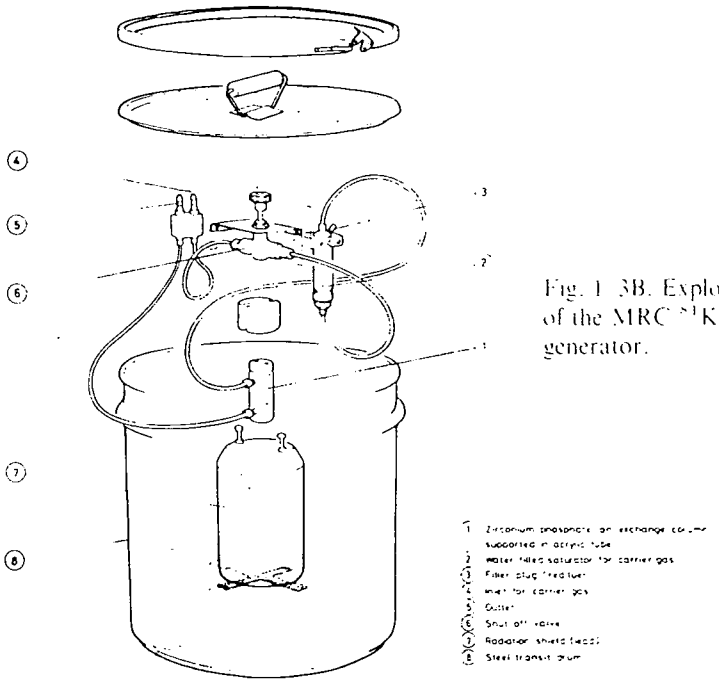

Fig. 1–3B. Exploded view of the MRC $^{81}Kr^{m}$ gas generator.

risk of membrane fracture. A new filter unit should be used for each subject studied. Figure 1–2B shows the MRC solution generator with its column exposed.

When a generator is used for ventilation studies it is eluted using air or a physiological gas mixture. It is essential to ensure that the eluting gas flow is saturated with water vapour before passing through the column as shown in Fig. 1–3A. Dry gas causes the column to dry out and little $^{81}Kr^{m}$ can then be recovered. Should a generator accidentally become dry it is possible to re-wet it and regain the normal high elution efficiency. Figure 1–3B shows the salient features of the MRC gas generator as currently distributed.

When using $^{81}Kr^{m}$ generators it is essential to minimize losses of $^{81}Kr^{m}$ by decay during its passage from the generator to the subject. This is achieved by keeping the diameters and lengths of the delivery tubing and catheters to a minimum and operating at flow rates consistent with their volume and the 13 second half-life of $^{81}Kr^{m}$.

Delivery of $^{81}Kr^{m}$ in the gas phase is normally accomplished using a disposable face mask as for oxygen administration but there may be occasions when the inhomogeneous inhaled mixture delivered by this method has disadvantages. In these cases it may be necessary to provide some suitable premixing system to cope with breath by breath administration. Occasionally small droplets of liquid may be found in the gas delivery tube and they may be found to contain small amounts of ^{81}Rb. They are due to operating the generator with too much water in the saturator or at too high a flow rate. They may readily be prevented from reaching the face mask by the insertion of a small trap in the delivery tube close to the generator.

CONCLUSION

Krypton 81m generators for infusion and ventilation studies have been developed for use in routine clinical investigations. Their widespread application will depend largely on a highly organized production and distribution system.

New applications continue to be found particularly for the infusion generator and the results reported so far seem to match the ingenuity of the investigators in tackling the problems of working with a 13 second half-life radionuclide in clinical research.

COMBINED USE OF KRYPTON 81m AND 85m IN VENTILATION STUDIES

T. Jones, J. C. Clark, C. G. Rhodes, J. Heather and P. Tofts

The continuous inhalation of krypton 81m gas provides a sensitive means for detecting focal defects in lung ventilation (Fazio and Jones, 1975). Although of clinical value the lung ventilation images obtained have a limited functional interpretation. This is due to the regional lung counts being representative of the total ventilation $\dot{V}$ to that area and not ventilatory turnover $\dot{V}$/vol which is the basic quantitative measure of ventilation and of which absolute values are required. Furthermore, the relationship between the content of $^{81}Kr^{m}$ in the lung and ventilation is non-linear with a tendency to underestimate $\dot{V}$ as ventilatory turnover $\dot{V}$/vol increases. This is a particular problem when assessing ventilation images obtained in young children and certain disease states where high values of $\dot{V}$/vol are experienced. The goal then is to be able to analyse the semi-quantitative $^{81}Kr^{m}$ lung ventilation images to obtain absolute values of regional $\dot{V}$/vol. In turn, this could be used to obtain the true distributions of both $\dot{V}$, on the $^{81}Kr^{m}$ inhalation image, and regional lung blood flow from the image obtained during the continuous intravenous infusion of $^{81}Kr^{m}$ solution (Harf *et al.*, 1978; Ciofetta *et al.*, 1977). As discussed in the earlier paper on the theoretical use of $^{81}Kr^{m}$, one approach to achieving quantitation would be to repeat the inhalation procedure using a krypton isotope with a different radioactive half-life to that of $^{81}Kr^{m}$. For this purpose we have elected to use cyclotron produced $^{85}Kr^{m}$ (Clark and Buckingham, 1975) which has a half-life of 4·4 hours. This follows the initial use of this tracer as an internal standard in brain blood-flow studies with $^{81}Kr^{m}$ by Arnot *et al.* (1970). Figure 6–1 shows the time-activity curve one would theoretically expect to record over the lung during the continuous inhalation of (a) $^{81}Kr^{m}$ and (b) a long-lived krypton isotope such as $^{85}Kr^{m}$. These curves have been calculated for a $\dot{V}$/vol of 1·7 litre min^{-1} litre^{-1} (typical values in erect normal man) with the lung concentration of tracer being expressed as a percentage of that in the inspired gas. With the long-lived krypton the lung concentration will build up to reach that of the concentration in the inspired gas. The 13 second half-life of $^{81}Kr^{m}$ causes the equilibrium concentration in the lung to be appreciably less than that in the

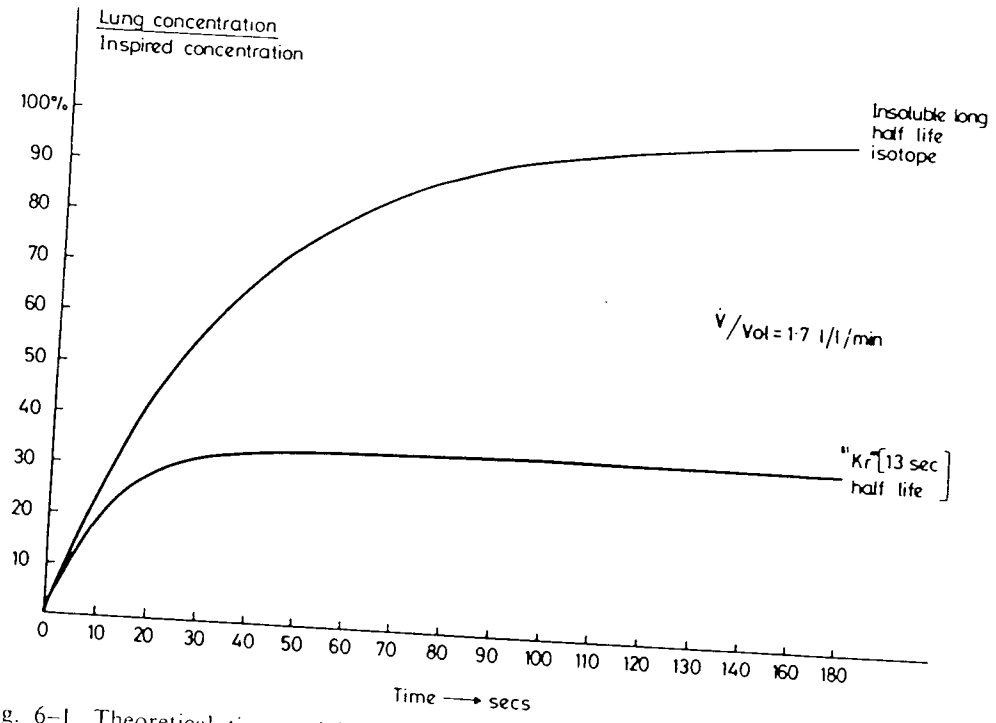

Fig. 6–1. Theoretical time activity curves that would be recorded over the lung, with a ventilatory turnover rate of 1·7 $l l^{-1}$ min^{-1}, during the continuous inhalation of (a) a long-lived insoluble radioactive gas and (b) krypton 81m.

inspired gas. Thus by comparing the equilibrium level reached by $^{81}Kr^{m}$ with that of $^{85}Kr^{m}$ it is possible to determine how nearly the short half-life isotope has reached equilibrium with the inspired concentration. In effect one is providing the lung with a challenge (radioactive decay) in an attempt to reach true equilibrium. From the measured response to this challenge it is possible to determine the rate of ventilatory turnover $\dot{V}$/vol. This process of challenge and observation of the consequence of introducing a tracer is not unlike that of challenging the lung with a delta function of activity, a procedure commonly used in the differentiation approach to measuring tissue flow rates. With continuous administration of $^{81}Kr^{m}$, the challenge (half-life of the tracer) is known precisely. In writing the basic formulae for the equilibration levels of $^{81}Kr^{m}$ and $^{85}Kr^{m}$ in the lung, ($^{81}Kr^{m}$) and ($^{85}Kr^{m}$), we have:

$$(^{81}Kr^{m}) = \frac{g\dot{V}Ca(81m)}{\dot{V}/vol + 3{\cdot}2} \qquad (1)$$

and

$$(^{85}Kr^{m}) = \frac{g\dot{V}Ca(85m)}{\dot{V}/vol + 0{\cdot}0026} \qquad (2)$$

where $Ca(81m)$ and $Ca(85m)$ are the respective inspired concentrations of $^{81}Kr^{m}$ and $^{85}Kr^{m}$.

For $^{85}Kr^m$ the emitted γ ray used in detection has an energy of 150 keV which is sufficiently close to the 190 keV photons from $^{81}Kr^m$ for q to be the same for both tracers. The radioactive decay rate of $^{85}Kr^m$ (0·0026 min^{-1}) is negligible relative to the typical value of $\dot{V}$/vol. Hence by dividing the two lung signals we have:

$$\dot{V}/\text{vol} = \frac{3{\cdot}2}{\left(\frac{^{85}Kr^m}{^{81}Kr^m}\right)\frac{Ca(81m)}{Ca(85m)} - 1} \qquad (3)$$

This expression takes the same form as that of equation (3) derived in the earlier theoretical paper. The relationship between the $^{85}Kr^m$ lung signal and the concentration of this tracer in the inspired air provides the transposition between the detection efficiencies for monitoring the inspired concentration and the lung concentration.

EXPERIMENTAL PROCEDURE

The experimental procedure is to administer sequentially $^{81}Kr^m$ and $^{85}Kr^m$ from a well-mixed reservoir. The resulting pulmonary distributions at equilibrium measured by the gamma camera are recorded in turn as numerical matrices, so providing values of regional $^{81}Kr^m$ and $^{85}Kr^m$. On both occasions the tracers are pumped from the reservoir, which is at atmospheric pressure, through a thin bore tube which delivers the isotopes to a disposable face mask. At equilibrium the content of tracer in the tube is recorded with a scintillation counter viewing a short section of tube to give the ratio: $Ca(81m)/Ca(85m)$ necessary for equation (3). This is used to operate on the regional $(^{85}Kr^m)/(^{81}Kr^m)$ ratios determined for each of the matrix points and the computer is set to calculate expression (3) and so obtain a matrix of $\dot{V}$/vol values. Before this is done it is necessary to correct for possible differences in photon energy window setting on the camera and scintillation probe. This is done by piping in turn the two tracers to a short tube placed in front of the gamma camera. In addition, the appropriate amount of absorber, equivalent to the chest wall, is placed between the tube and the camera face in order to simulate the differential absorption of the two tracers. Figure 6–2 shows how important this is, due to the spill-over in the 150 keV photo peak (74% abundant) from the 315 keV photons also emitted by $^{85}Kr^m$ (13% abundant). This energy spectrum was recorded with the gamma camera placed over the chest of a normal subject during the continuous inhalation of $^{85}Kr^m$. This calibration procedure allows for the additional counts falling into the 150 keV windows of the camera and probe.

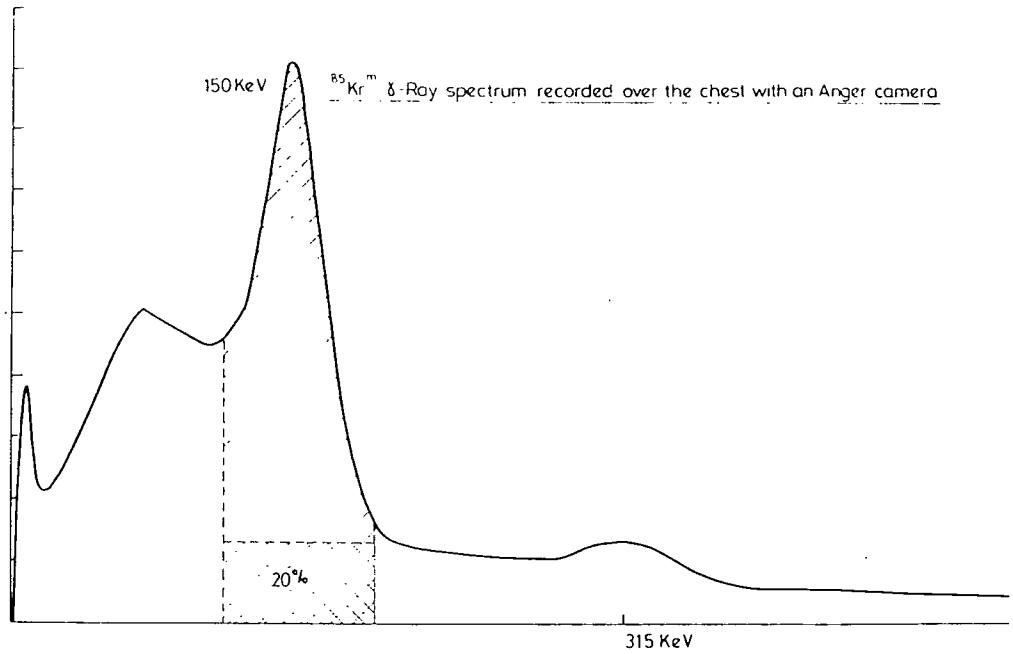

Fig. 6–2. Gamma ray spectrum from an Anger Camera viewing the chest of a normal erect subject recorded at equilibrium during the continuous inhalation of $^{85}Kr^{m}$.

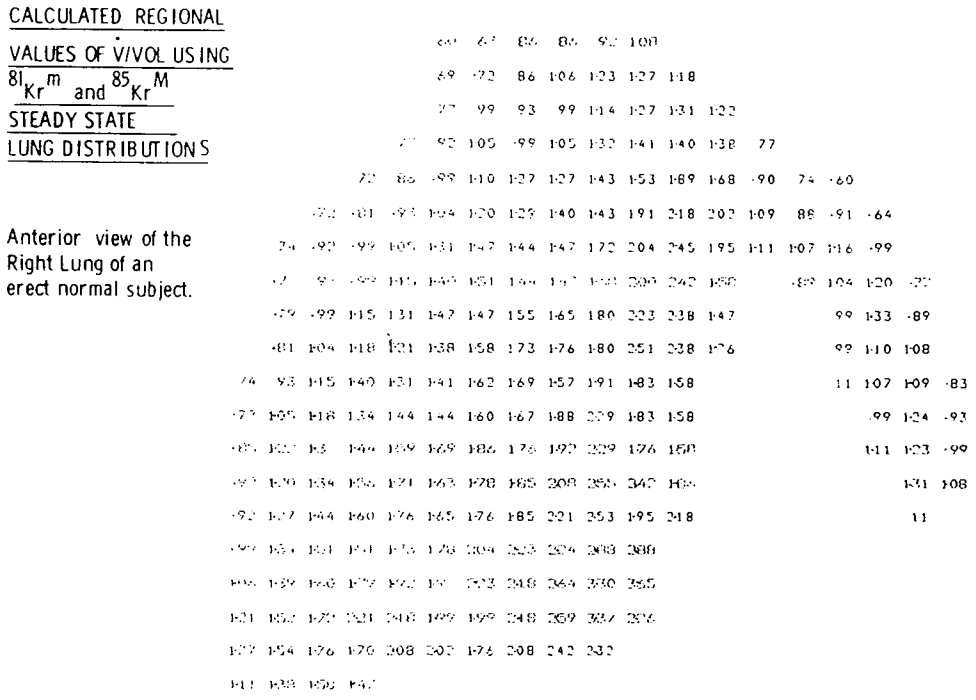

Fig. 6–3. Regional values of ventilation per unit lung volume $\dot{V}$/vol ($l\,l^{-1}\,min^{-1}$) for the anterior view of the erect right lung of a normal subject. These were calculated from the steady state inspired concentrations and lung distributions of $^{81}Kr^{m}$ and $^{85}Kr^{m}$.

RESULTS

Figure 6–3 shows the result of applying this method to the right lung of a normal subject. A matrix of numbers representing the regional values of $\dot{V}$/vol is obtained, demonstrating that it is possible to achieve quantitative values of regional lung ventilation using $^{81}Kr^{m}$. In the mid region of the lung the values are between 1·5 and 2·0 litre min^{-1} $litre^{-1}$ which is the range expected for normal erect man. However, in the periphery of the lung near the heart the values become higher than would be expected and in the outer periphery they are lower. This is attributed to a slight movement of the subject between the two measurements and serves to emphasize the need for immobility when carrying out these dual isotope studies. An additional limitation to this quantitative approach is that the assumption of true equilibration during the $^{85}Kr^{m}$ procedure may not be correct. This may particularly be the case in conditions of lung disease where $\dot{V}$/vol is low.

CONCLUSION

This added isotopic procedure clearly adds to the complexity of the $^{81}Kr^{m}$ method. However, it does offer the possibility of obtaining high quality quantitative regional distributions of lung ventilation.

DISCUSSION III

Chairman: Phillip Hugh-Jones

PHILLIP HUGH-JONES: I would like a chance of asking you about the changing ratio between $^{81}Kr^{m}$ and $^{85}Kr^{m}$ being solely due to movement of the patient.

TERRY JONES: We did identify movement by looking at the qualitative profile and also we were able to superimpose the images by moving one of them. There was then a uniform gradient of values across the lung in the way that you might have predicted.

MICHAEL HUGHES: I think normalizing to the inspired concentrations of two gases is technically a little bit messy. It means introducing an extra counting channel and may not be a very useful tool for respiratory physicians because you are now going to end up with the distribution of total ventilation. The trouble is that the dead space of the lungs, that is the trachea and bronchi, have a volume which is only about one-twentieth of the alveolar compartment, and therefore when you compute ventilation per unit volume you will get very high values in the centre of the lung. This would not be so bad, but in the centre of the lung you would have the major bronchi with a high $\dot{V}$/vol and the surrounding lung with a very low $\dot{V}$/vol and the result is a rather confusing mixture.

TERRY JONES: Yes, I am sure that is right but it is a matter of which way the signal is weighted. Where are the counts coming from? Are they coming mainly from the bronchi or the alveoli? There is a big weighting factor for the high volume areas.

USE OF KRYPTON 81m AND 85m FOR MEASUREMENT OF VENTILATION AND PERFUSION DISTRIBUTION WITHIN THE LUNGS

T. C. Amis, G. Ciofetta, J. C. Clark, J. M. B. Hughes, Hazel A. Jones and T. A. Pratt

The use of $^{81}Kr^{m}$ for measurement of pulmonary ventilation and perfusion distributions (Fazio and Jones, 1975; Harf *et al.*, 1978) is subject to certain limitations because of the influence of regional lung volume and ventilatory washout of the radioactive gas.

As part of a general study into the effect of posture on regional distribution of ventilation and perfusion within the lung we have used information obtained during equilibration and clearance of the longer half-life (4·4 hours) isotope krypton 85m ($^{85}Kr^{m}$) to correct that obtained with $^{81}Kr^{m}$ for local alveolar volume and ventilatory washout. In order to demonstrate the application of this technique, results for two normal subjects in a lateral decubitus posture will be presented.

THEORY

During steady state inhalation of $^{81}Kr^{m}$ counts are obtained from particular regions which reflect the balance between arrival of the radioactive gas, representing ventilation, and its removal due to ventilatory washout and radioactive decay (Fazio and Jones, 1975). Removal, except at high ventilatory rates, tends to be dominated by the high value (3·2 min^{-1}) for the decay constant (λ) of $^{81}Kr^{m}$. Thus:

$$^{81}N_R = \dot{V}_R C_1 k'_R / [(\dot{V}/VA)_R + \lambda] \quad (1)$$

where $^{81}N_R$ is the regional counts obtained with $^{81}Kr^{m}$, $\dot{V}_R$ is regional ventilation, C_1 is inspired concentration of $^{81}Kr^{m}$, VA is alveolar volume and k'_R the regional geometric factor. As the inspired concentration is not measured, regional counts are expressed as a fraction of the total counts for the lung field. That is:

$$\frac{^{81}N_R}{^{81}N_T} = \frac{\dot{V}_R}{\dot{V}_T}\left[\frac{(\dot{V}/VA)_T + \lambda}{(\dot{V}/VA)_R + \lambda}\right]\frac{k'_R}{k'_T} \quad (2)$$

The subscript T refers to values for the total lung field.

After equilibration with the longer half-life isotope $^{85}Kr^m$, regional count rates reflect local lung volume.

$$^{85}N_R = (VA)_R C_2 k''_R \tag{3}$$

where $^{85}N_R$ refers to the regional count rate for $^{85}Kr^m$, C_2 the concentration of $^{85}Kr^m$ throughout the lung and k''_R the regional geometric factor for $^{85}Kr^m$ equilibration.

Local counts are expressed as a fraction of those for the total field:

$$\frac{^{85}N_R}{^{85}N_T} = \frac{(VA)_R}{(VA)_T}\frac{k''_R}{k''_T} \tag{4}$$

An arbitrary index for ventilation per unit alveolar volume is obtained by division of equations (2) and (4):

$$\left(\frac{^{81}N_R/^{81}N_T}{^{85}N_R/^{85}N_T}\right)_{\text{inhaled 81}} = \frac{(\dot{V}/VA)_R}{(\dot{V}/VA)_T}\left[\frac{(\dot{V}/VA)_T+\lambda}{(\dot{V}/VA)_R+\lambda}\right] \tag{5}$$

Similarly, an intravenous infusion of $^{81}Kr^m$ combined with equilibration and clearance of $^{85}Kr^m$ gives:

$$\left(\frac{^{81}N_R/^{81}N_T}{^{85}N_R/^{85}N_T}\right)_{\text{infused 81}} = \frac{(\dot{Q}/VA)_R}{(\dot{Q}/VA)_T}\left[\frac{(\dot{V}/VA)_T+\lambda}{(\dot{V}/VA)_R+\lambda}\right] \tag{6}$$

where $\dot{Q}/VA$ refers to perfusion per unit alveolar volume.

In equations (5) and (6) it has been assumed that the ratio of regional and total geometric factors (k_R/k_T) is the same for both isotopes. This assumption is based on the similar principal gamma-ray energies of the two isotopes (190 keV for $^{81}Kr^m$ and 150 keV for $^{85}Kr^m$). In addition, errors associated with the relative counting efficiency of the detector for both isotopes are minimized by dealing with ratios of counts in this manner.

In the case of regional ventilation it is possible to solve equation (5) for regional ventilation per unit alveolar volume in litre min^{-1} $litre^{-1}$.

$$(\dot{V}/VA)_R = \lambda \Big/ \left[\frac{^{85}N_R/^{85}N_T}{^{81}N_R/^{81}N_T}\{1+\lambda/(\dot{V}/VA)_T\}-1\right] \tag{7}$$

$(\dot{V}/VA)_T$ is obtained from an initial slope analysis (Lassen, 1967) of the clearance of $^{85}Kr^m$ from the total lung field.

In addition, $(\dot{V}/VA)_R$ has been estimated from the local clearance of $^{85}Kr^m$ for comparison with the results obtained from equation (7). Calculated $(\dot{V}/V)_R$ values are used to correct the $\dot{Q}/VA$ index obtained with equation (6).

METHODS

For the $^{81}Kr^m$ ventilation and perfusion study krypton is continuously eluted from a generator containing its parent ^{81}Rb (Jones *et al.*, 1970) and administered as described by Harf *et al.* (1978), except that the subject breathes through a mouth piece.

Immediately following the perfusion study the subject is switched into a rebreathing circuit containing a spirometer filled with oxygen and sufficient $^{85}Kr^m$ to provide a concentration at equilibration of 1 mCi per litre. $^{85}Kr^m$ is prepared in the Medical Research Council cyclotron by 16 MeV deuteron irradiation of krypton (Clark and Buckingham, 1975).

The subject takes a few deep breaths to speed equilibration and then breathes quietly until a satisfactory plateau of counts is obtained and an image representing alveolar volume is accumulated. The subject then breathes room air while clearance of the radioactive gas from the lungs is monitored.

Count rates are recorded with a large field gamma camera (Jumbo, Toshiba Corp.) using a low energy, high resolution collimator. The camera is linked to a computer (Nova 1220, Medical Data System) which displays the information as an image on a 64 × 64 matrix.

Areas of interest are selected and normalization and division undertaken as described previously. Washout curves are plotted for the total lung field and for regions within the lung. Rate constants are calculated from the initial slopes of these curves.

The total radiation dose to the lungs for a $^{81}Kr^m$ ventilation and perfusion study lasting approximately four minutes is 40 mrad, while rebreathing for three minutes at a lung concentration of 1 mCi $^{85}Kr^m$ per litre involves a dose to the lungs of 100 mrad.

RESULTS

Ventilation, perfusion and alveolar volume images obtained for a normal subject in the left lateral decubitus posture are shown in Fig. 7–1. Ventilation, as measured by count density, appears evenly distributed between the upper and lower lungs. The volume distribution obtained with $^{85}Kr^m$ is heavily weighted to the upper lung.

Despite the uniform ventilation image, ventilation per unit alveolar volume is greater in the lower lung (2·23 litre min^{-1} $litre^{-1}$) than in the upper lung (0·94 litre min^{-1} $litre^{-1}$) as demonstrated by the clearance of $^{85}Kr^m$ (Fig. 7–2).

Ventilation per unit alveolar volume was found to increase from superior to inferior for a vertical slice taken across both lungs in a subject in right

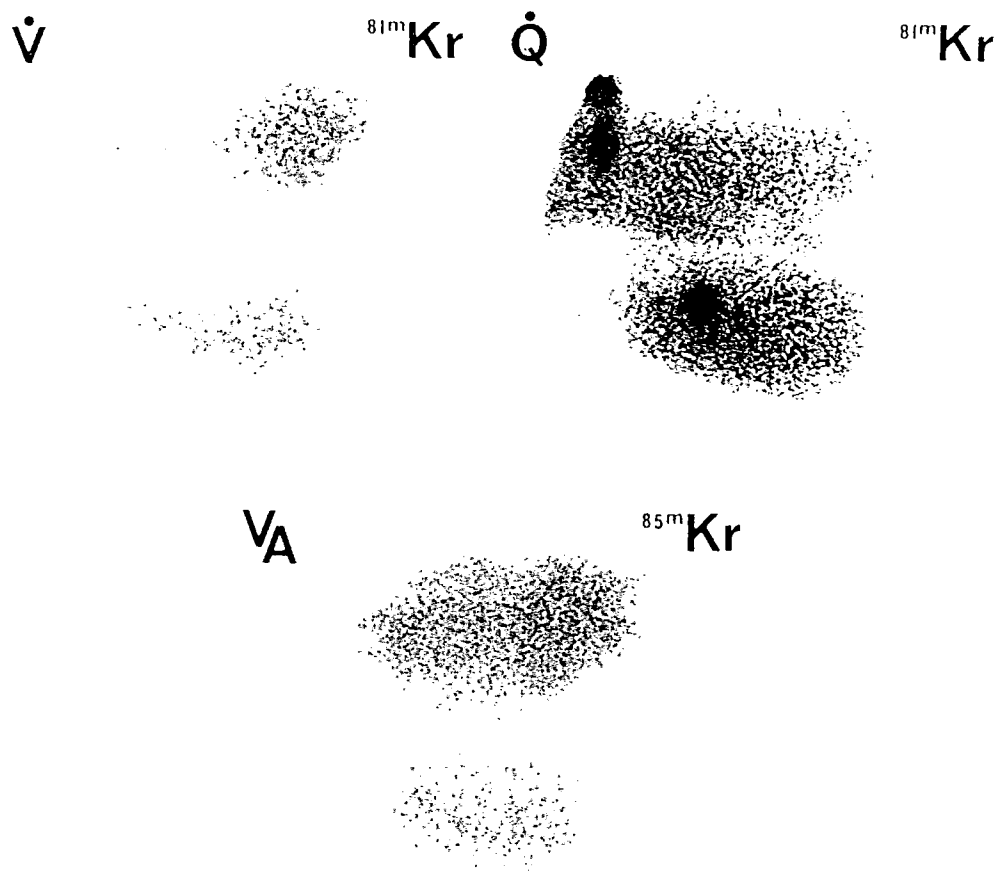

Fig. 7-1. Ventilation, perfusion and alveolar volume images for a subject in left lateral decubitus. Note the apparent uniform count density on the ventilation image while the volume distribution is heavily weighted to the upper lung. The perfusion scan contains the artifact produced by activity entering via the subclavian vein.

lateral decubitus with the gradient being more marked in the lower lung. Similar values were obtained from both equation (7) and the regional $^{85}Kr^{m}$ clearance (Fig. 7–3).

Perfusion per unit alveolar volume was also found to increase from superior to inferior after correction for ventilatory washout (Fig. 7–4).

DISCUSSION

$^{81}Kr^{m}$ possesses a number of advantages for assessment of regional pulmonary ventilation and perfusion. These include its gamma energy (190 keV) which is ideal for use with the scintillation camera, its short physical and biological half-life, and the low radiation dose associated with its use (Jones *et al.*, 1970).

Clinically, the technique is useful in detecting defects in ventilation (Fazio and Jones, 1975). Recently Harf *et al.* (1978) have quantitated results from $^{81}Kr^{m}$ images in terms of ventilation–perfusion ratio ($\dot{V}A/\dot{Q}$). However, separate assessment of $\dot{V}A$ and $\dot{Q}$ distributions requires measurement of ventilation and perfusion per unit lung volume. Typically a long half-life

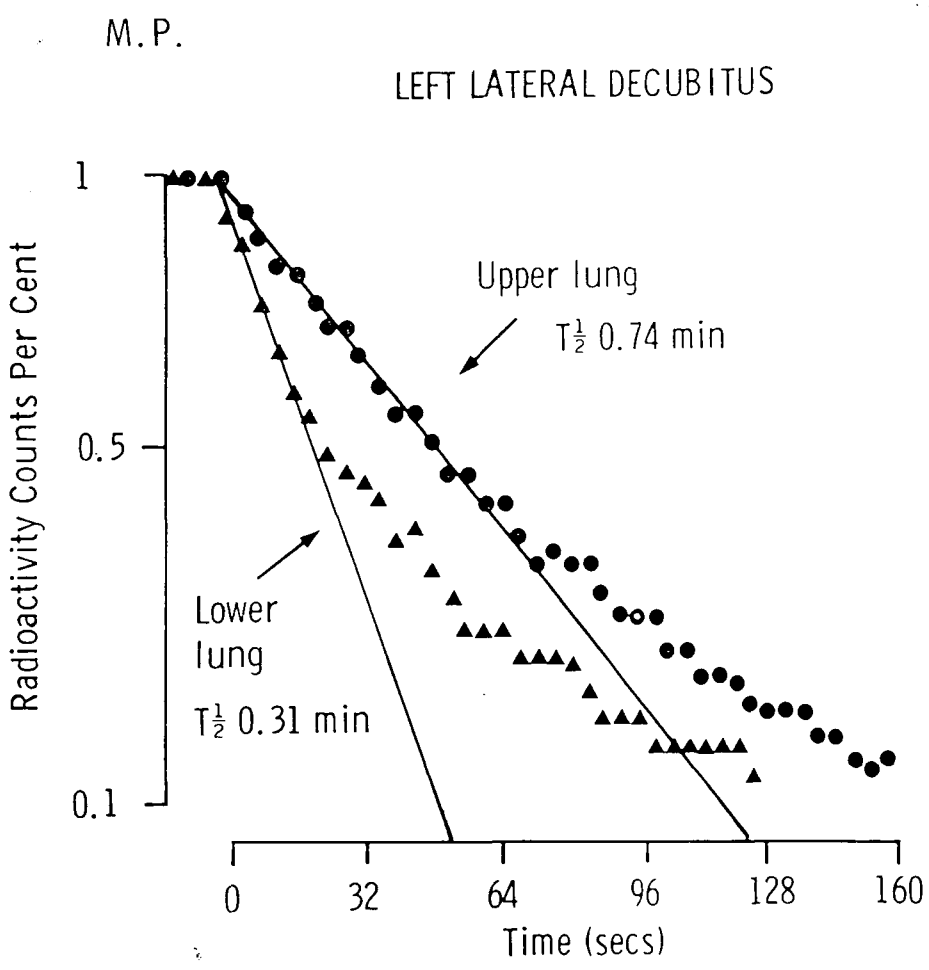

Fig. 7–2. Clearance of $^{85}Kr^{m}$ from upper and lower lungs for a normal subject in left lateral decubitus posture. Initial slope analysis for the upper lung yielded a rate constant of 0·94 litre min^{-1} $litre^{-1}$ and for the lower lung 2·23 litre min^{-1} $litre^{-1}$. Counts per 4 sec are plotted against time on a semilogarithmic scale.

radioactive gas, such as ^{133}Xe with 80 keV γ-ray energy, has been used to estimate local lung volume (Milic-Emili *et al.*, 1966), but for comparison of $^{81}Kr^{m}$ ventilation and perfusion images with an image of regional lung volume an energy similar to the 190 keV γ ray of $^{81}Kr^{m}$ is required. This may be provided by the 150 keV γ ray of $^{85}Kr^{m}$.

At high ventilation rates the relation between local radioactivity and regional ventilation during $^{81}Kr^{m}$ administration becomes curvilinear as the

isotope tends to measure lung volume rather than ventilation (Fazio and Jones, 1975). However, over a useful range of values (e.g. up to $(\dot{V}/VA)_R$ of 5–6 litre min^{-1} $litre^{-1}$ for a $(\dot{V}/VA)_T$ of 2 litre min^{-1} $litre^{-1}$), allowance for ventilatory washout can be made using equation (7) and regional ventilation per unit lung volume calculated.

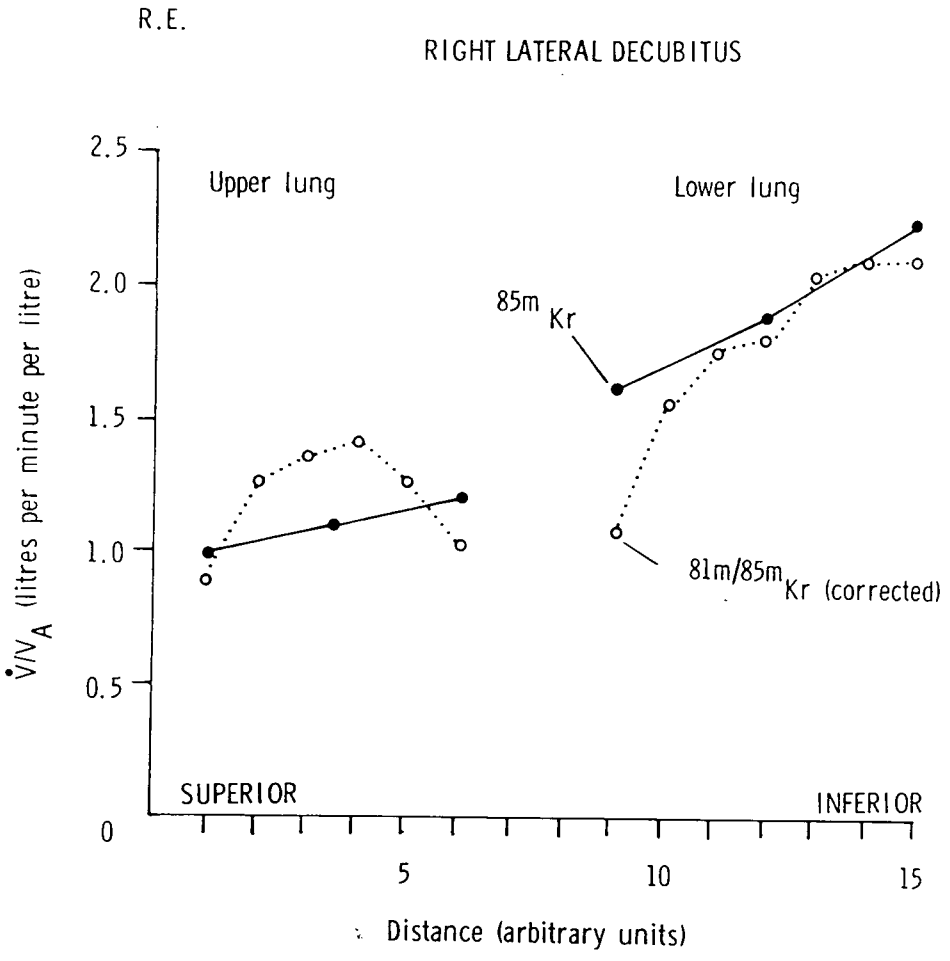

Fig. 7–3. $\dot{V}/VA$ in litre min^{-1} $litre^{-1}$ for a vertical slice through upper and lower lungs in a normal subject in the right lateral decubitus posture. Dotted line indicates calculated $\dot{V}/VA$ while full line indicates values obtained from the clearance of $^{85}Kr^m$. Note that each point on the clearance line refers to an area of lung covered by 2–3 points on the calculated line.

The effect of ventilatory washout of $^{81}Kr^m$ must also be taken into account in the calculation of perfusion per unit lung volume from $^{81}Kr^m$ (infusion) and $^{85}Kr^m$ images. This is particularly so where regional ventilation is high, resulting in a systematic underestimation of perfusion. With the calculation of regional and total field ventilation an allowance can be made for this effect.

In conclusion, ventilation and perfusion images obtained with $^{81}Kr^m$ may

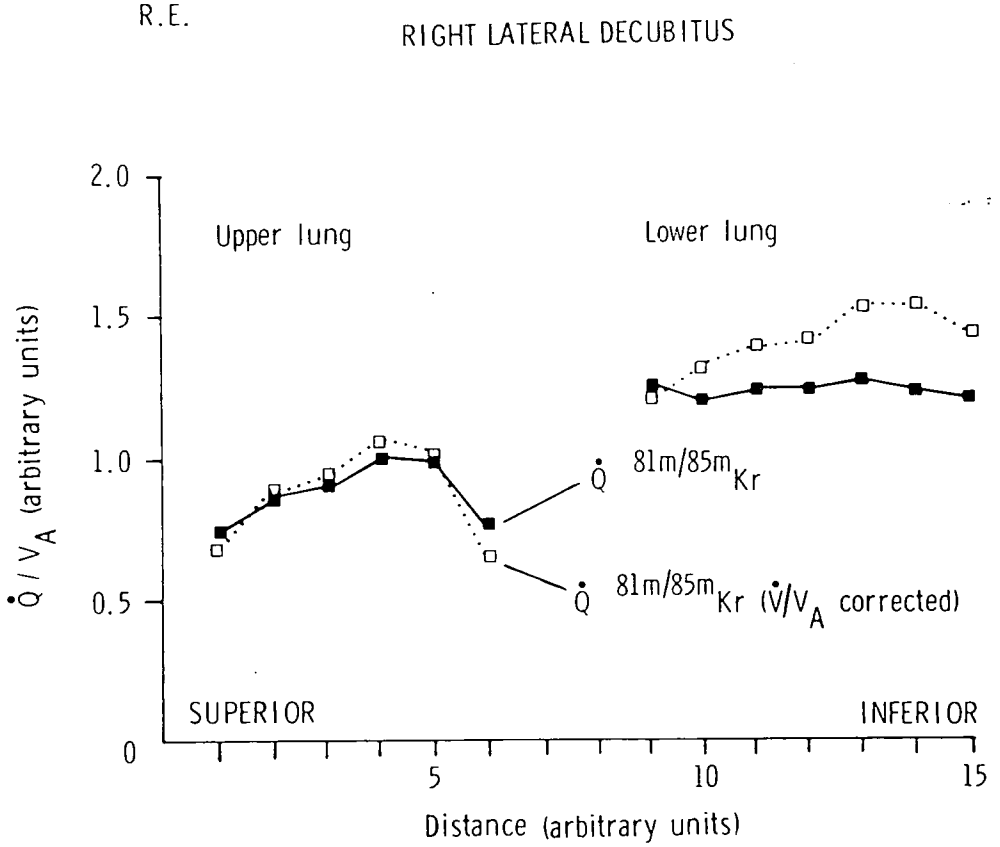

Fig. 7–4. $\dot{Q}/VA$ in arbitrary units before (full line) and after (dotted line) allowance for $\dot{V}/VA$. Note the disclosure of a perfusion gradient in the lower lung not shown on direct normalization and division of the two images.

be misinterpreted if the effects of alveolar volume and ventilatory washout are not considered. The addition of $^{85}Kr^{m}$ to the procedure enables ventilation and perfusion per unit alveolar volume to be measured and permits a correction for ventilatory washout to be applied.

Vertical distributions of ventilation and perfusion in the lateral decubitus posture obtained with this technique are in agreement with those reported by previous workers using ^{133}Xe (Kaneko *et al.*, 1966).

ACKNOWLEDGMENT

The use of $^{85}Kr^{m}$ as a marker of regional lung volume was suggested to us by Mr. Terry Jones of the M.R.C. Cyclotron Unit. We are grateful to Dr. J. P. Lavender for permission to use facilities in the Diagnostic Radiology Department Scanning Unit.

DISCUSSION IV

Chairman: Phillip Hugh-Jones

PHILLIP HUGH-JONES: Thank you very much Dr. Amis. It is interesting that, years ago, people showed by bronchospirometry that the lower lung was the better ventilated but I did not expect to see such a beautiful demonstration of it as you have shown.

TERRY JONES: You were using the washout to give you a calibration, but the washout techniques are not very satisfactory. I wonder whether we could use the same approach, using $^{81}Kr^{m}$ or $^{85}Kr^{m}$, but measuring overall ventilation per unit volume by measurements taken at the mouth. This could result in very accurate values.

TERRY AMIS: It would be very hard to relate these values to the washout you see with a gamma camera. It is possible to obtain a figure for the total washout of the whole field but that can be half of the ventilation as measured at the mouth.

TERRY JONES: What I was suggesting was looking at the end expired $^{81}Kr^{m}$ and therefore getting a measure of actual alveolar turnover, that is tidal volume versus total lung capacity.

Chapter 9

MEASUREMENT OF TOTAL LUNG VENTILATION IN ANAESTHETIZED DOGS USING KRYPTON 81m AND NITROGEN 13

R. N. Arnot, M. K. Sykes, J. C. Clark, A. N. Herring,
M. K. Chakrabarti and P. Buranapong

The use of the radionuclide $^{81}Kr^m$ for the demonstration of regional underventilation in pulmonary disease by means of gamma camera imaging of the lungs during continuous inhalation of the gas was described by Fazio and Jones in 1975. $^{81}Kr^m$ has a half-life of 13 seconds, radioactive equilibrium is obtained rapidly, and the regional count rate depends on the relationship between the ventilation and the rates of wash-out and radioactive decay. In abnormal regions, the rate of wash-out is much less than the rate of radioactive decay (3·2 min^{-1}); hence the regional count rate is highly dependent on the regional ventilation.

An alternative technique for assessing regional ventilation is based on the analysis of regional wash-out curves of an inert gas such as ^{133}Xe or $^{13}N_2$. Although the use of $^{13}N_2$ is restricted to locations where there is a cyclotron or other particle accelerator producing radionuclides, it has the advantage over ^{133}Xe of a lower solubility in blood and tissue which reduces errors due to radioactivity washing out of tissue into the lungs and to radioactivity in the chest wall. $^{13}N_2$ has been used in studies of both normal and abnormal lungs using collimated scintillation counters (Rosenzweig *et al.*, 1970) and gamma cameras (Ronchetti *et al.*, 1975; Ewan *et al.*, 1975; Nosil *et al.*, 1976a).

It is of interest to assess whether the variation of $^{81}Kr^m$ count rate with change in ventilation is in accordance with the theoretical response, and whether the use of $^{13}N_2$ *in vivo* wash-out curves to measure ventilation is valid. Rosenzweig *et al.* (1970) compared $^{13}N_2$ regional wash-out measurements with results derived from curves of the $^{13}N_2$ concentration in expired air during wash-out, but, since the latter provide a measure of total lung ventilation, it was not possible to draw conclusions on the degree of correlation between the two techniques. No quantitative studies of the $^{81}Kr^m$ technique have been described. Using a gamma camera, we have obtained $^{81}Kr^m$ count rates and $^{13}N_2$ wash-out curves in the whole lung field at varied rates of ventilation. Also, curves of $^{13}N_2$ concentration in expired air were obtained by end-tidal sampling, and alveolar ventilation and functional

residual capacity were measured. Comparisons of the results were made, and the use of the techniques in regional ventilation studies considered.

METHOD

The measurements were performed on two supine, anaesthetized, paralysed dogs, ventilation being controlled by a mechanical ventilator at a frequency of 15 breaths/minute and an inspiratory : expiratory ratio of 1 : 2. Ventilation was changed by varying the tidal volume between 200 ml and 1200 ml. Alveolar ventilation ($\dot{V}$) was calculated from tidal volume (measured by spirometer tracings) and anatomical dead space (measured by the Böhr method utilizing end-tidal and mixed expired CO_2 concentrations measured on an infra-red analyser). Functional residual capacity was estimated for each tidal volume using the helium closed-circuit technique. The lung volume, V, was calculated by summing the functional residual capacity and the tidal volume and subtracting the anatomical dead space. This is the lung volume to be considered when calculating $\dot{V}/V$ for comparison with measurements depending on wash-out of an inert gas from the lungs (Fowler *et al.*, 1952).

The breathing circuit used for $^{81}Kr^m$ contained a mixing bag with a volume greater than the largest tidal volume used, which was fed, at a constant rate greater than the largest minute ventilation used, with air containing $^{81}Kr^m$ from a $^{81}Rb/^{81}Kr^m$ generator supplied by the MRC Cyclotron Unit (Clark *et al.*, 1976). From the bag, the mixture of air and $^{81}Kr^m$ was pumped by a ventilator, in which further mixing took place, to the animal via a non-rebreathing valve and an endotracheal tube, the excess gas from the mixing bag being led outside the laboratory. This circuit was designed to supply to the animal a $^{81}Kr^m$ concentration that was constant during the inspiratory period apart from the decrease due to radioactive decay of $^{81}Kr^m$ during that time, and which was close to being constant at all tidal volumes apart from variations due to radioactive decay of the parent radionuclide ^{81}Rb and to changes in generator elution efficiency during the investigation. Input concentration of $^{81}Kr^m$ was monitored by a scintillation detector placed on the input line close to the non-rebreathing valve. The concentration of $^{81}Kr^m$ during inspiration was constant to within $\pm 5\%$, and corrections were made for variation in inspired concentration at each tidal volume, using the average count rate recorded by the monitor detector during each study. For the studies with $^{13}N_2$ (Clark and Buckingham, 1975), a rebreathing circuit with CO_2 absorption was used for four minutes to obtain equilibrium; then room air was inspired during wash-out measurements, the expired gas being led outside the laboratory. End-tidal

samples of expired $^{13}N_2$ were passed through a coil in a well-type scintillation counter whose output was recorded on paper tape for computer processing.

Right lateral gamma camera views of the supine dogs were obtained using a high energy collimator, and data from both $^{81}Kr^m$ and $^{13}N_2$ studies were recorded on magnetic tape for computer processing. Maximum count rates of less than 7000 counts/s were used, avoiding the need to correct for gamma camera dead-time. Non-uniformity corrections were made, and an area covering the whole lung field was chosen (Fig. 9–1), thus minimizing effects

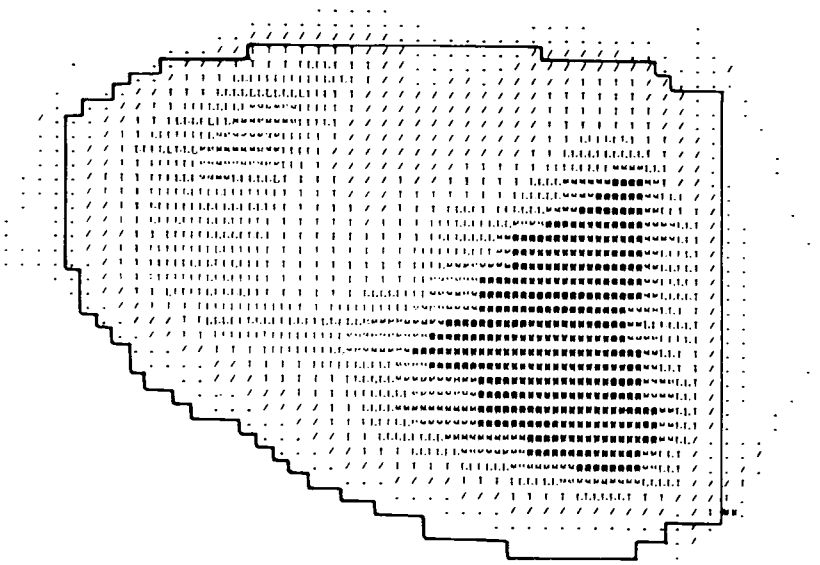

Fig. 9–1. Computer output of the right lateral gamma camera view of the lungs of a dog ventilated with $^{81}Kr^m$. The anterior of the animal is in the upper part of the view and its diaphragm to the right. The shadow of the heart is visible anteriorly. The area used for quantitation is outlined.

due to different detector sensitivities to the 190 keV and 511 keV radiations of $^{81}Kr^m$ and $^{13}N_2$. A modification of the computer program of Vernon and Glass (1971) was used to obtain the total $^{81}Kr^m$ counts accumulated and the $^{13}N_2$ wash-out curves corrected for background and radioactive decay. $^{81}Kr^m$ counts accumulated during the whole breathing cycle were obtained, and $^{13}N_2$ counts accumulated during alternate time intervals of 2 seconds that included the inspiratory phase of the breathing cycle were used to obtain the $^{13}N_2$ wash-out curves. The $^{13}N_2$ wash-out curves were analysed into two exponential components using the SAAM compartment analysis program of Berman *et al.* (1962), and average fractional ventilation ($\dot{V}/V$) was calculated. The expired air concentration curves were analysed similarly to obtain $\dot{V}/V$.

RESULTS

Figure 9–2 shows the correlation between the average fractional ventilation, $\dot{V}/V$, measured using gamma camera wash-out curves and the same quantity measured using expired air concentration curves. Gamma camera estimations are within 5% of those obtained using expired air concentration, as indicated by the regression equation. Figure 9–3 compares $\dot{V}/V$ measured using $^{13}N_2$ with $\dot{V}/V$ calculated from alveolar ventilation ($\dot{V}$) and functional residual capacity + tidal volume − anatomical dead space (V). The $^{13}N_2$ method gives $\dot{V}/V$ values less than the calculated values in one case and greater in the other, the slopes being 0·86 and 1·18 respectively.

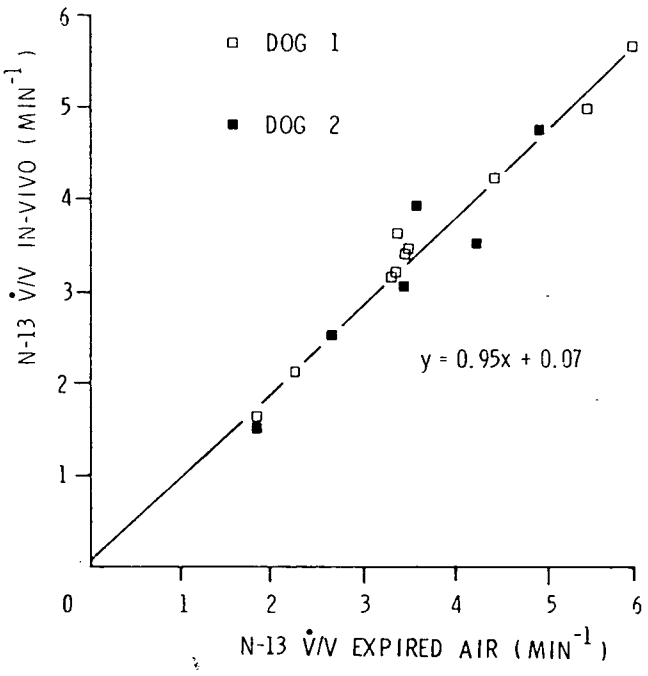

Fig. 9–2. Graph of fractional ventilation $\dot{V}/V$ obtained from gamma camera $^{13}N_2$ wash-out curves plotted against $\dot{V}/V$ obtained from expired gas $^{13}N_2$ concentration curves. Data from two dogs are shown and the regression equation is given.

In Fig. 9–4, $^{81}Kr^m$ count rates obtained in one dog are shown plotted against $\dot{V}/(\dot{V}/V + 3{\cdot}2)$ calculated from measured alveolar ventilation, $\dot{V}$, and from lung volume in one case equal to (FRC + tidal volume − anatomical dead space) and in the second case equal to FRC alone. Similar results were obtained in the second dog. The expression $\dot{V}/(\dot{V}/V + 3{\cdot}2)$ is obtained from the equation that holds when a constant activity of $^{81}Kr^m$ is present in the lungs:

$$\text{Rate of inflow} = \text{Rate of outflow}$$

$$\dot{V}c = A(\dot{V}/V + \lambda)$$

where $\dot{V}$ = ventilation (l/min),
c = concentration inspired (μCi/l),
A = activity present (μCi),
$\dot{V}/V$ = fractional rate at which activity is lost due to ventilation (min^{-1}),
λ = fractional rate at which activity is lost due to $^{81}Kr^{m}$ radioactive decay (3·2 min^{-1}).

Thus,

$$A = c\dot{V}/(\dot{V}/V + 3{\cdot}2).$$

Hence, provided the $^{81}Kr^{m}$ count rate is always proportional to the radioactivity present and is corrected for the concentration inspired at each

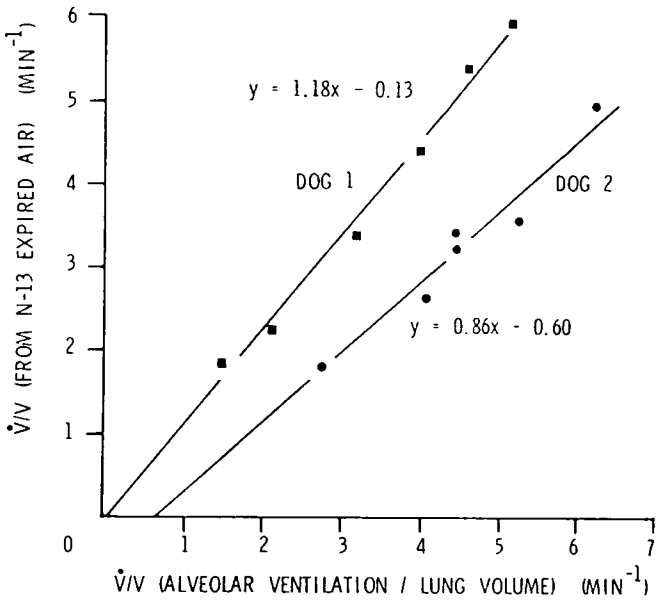

Fig. 9–3. Graph of fractional ventilation $\dot{V}/V$ obtained from expired gas $^{13}N_2$ concentration curves plotted against $\dot{V}/V$ calculated from measured alveolar ventilation, $\dot{V}$, and (functional residual capacity + tidal volume − anatomical dead space), V. Data from two dogs are shown and the regression equations are given.

ventilation rate, then it should be directly proportional to $\dot{V}/(\dot{V}/V + 3{\cdot}2)$, and a straight line passing through the origin should be obtained when $^{81}Kr^{m}$ count rate is plotted against $\dot{V}/(\dot{V}/V + 3{\cdot}2)$. It is seen that when FRC is used to calculate $\dot{V}/(\dot{V}/V + 3{\cdot}2)$, a straight line passing above the origin is obtained, while if a lung volume equal to (FRC + tidal volume − dead space) is used, the relationship appears approximately linear at low ventilation rates but when $\dot{V}/(\dot{V}/V + 3{\cdot}2)$ is greater than about 0·5 ($\dot{V}$ about 2·5 l/min, $\dot{V}/V$ about 2 min^{-1}), the linearity is lost.

DISCUSSION

Correction for $^{13}N_2$ absorbed into blood and tissues during rebreathing and returning to the lungs in venous blood during wash-out measurement was

not made in either the *in vivo* wash-out curves or the expired gas concentration curves. Since removal of $^{13}N_2$ from tissue is slower than its removal from the lungs, the presence of this component in the analysed curves causes average fractional ventilation to be underestimated. This would lead to some disagreement between the $^{13}N_2$ $\dot{V}/V$ and the $\dot{V}/V$ calculated from alveolar ventilation and lung volume. The measurement of anatomical dead space is very inaccurate at high tidal volumes when expired CO_2 concentrations are low. Errors in this measurement and in the

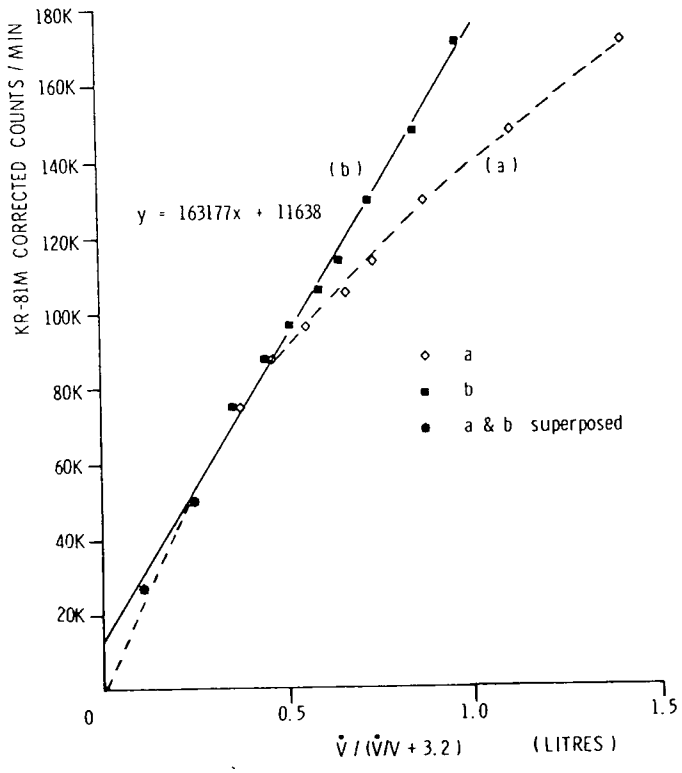

Fig. 9·4. Data from one dog. Graph of $^{81}Kr^{m}$ count rate plotted against $\dot{V}/(\dot{V}/V + 3{\cdot}2)$ calculated from alveolar ventilation, $\dot{V}$, and (a) V = (functional residual capacity + tidal volume − anatomical dead space) and (b) V = functional residual capacity. The regression equation for (b) is given.

measurement of FRC might produce overall errors of up to $\pm 30\%$ in the estimation of $\dot{V}/V$. The 5% underestimation of $\dot{V}/V$ by measurement of *in vivo* wash-out compared with the values obtained by measurement of expired gas concentration may be due to the contribution of slowly washed out radioactivity in the chest wall. Although little $^{13}N_2$ may be expected to be present in the chest wall, sensitivity of the gamma camera to radioactivity in the wall is high since it is close to the detector. Another source of disagreement between the two methods of estimating $\dot{V}/V$ with $^{13}N_2$ may be in the use of end-tidal samples rather than samples of mixed expired gas, and in the possible distortion of gamma camera wash-out curves due to asynchronism between the ventilator period and the data analysis period of two seconds.

Although agreement between the calculated values of $\dot{V}/V$ and the values measured with $^{13}N_2$ was not obtained, Fig. 9–3 shows that the relationship is close to linear. Thus, measurements of $\dot{V}/V$ with $^{13}N_2$ under different physiological conditions may be expected to give the correct *relative* values. This would also apply to measurements of relative regional $\dot{V}/V$ made with a gamma camera since the shapes of wash-out curves should not be affected by the different camera sensitivities to radioactivity in the regions under consideration. Measurements of relative regional ventilation, $\dot{V}$, are also possible using $^{13}N_2$ if measurement of the relative volumes under consideration is made. This may be achieved in multiple studies by obtaining uniform $^{13}N_2$ concentration throughout the lungs by rebreathing and obtaining images of the radioactivity distributions. The count density in any region is dependent on the camera sensitivity to radioactivity in that region, so the relative volumes of regions in any one image cannot be obtained; but when multiple studies are carried out, for example under different physiological conditions, without movement of the subject, then changes in relative regional volume and hence in relative regional ventilation can be obtained since sensitivity factors are then reduced.

The results given in Fig. 9–4 show that the $^{81}Kr^m$ response was in accordance with the predicted response only at the lower ventilation rates used if lung volume was calculated as (FRC + tidal volume – dead space). but that when FRC alone was used as the lung volume, a linear relationship between $^{81}Kr^m$ count rate and $\dot{V}/(\dot{V}/V + 3{\cdot}2)$ held over the whole range of ventilation rates used. This indicates that the lung volume V in the steady state equation for $^{81}Kr^m$ may be close to the FRC alone if counts are accumulated during the entire breathing period when expiration time is longer than inspiration time, as was the case in these experiments. At the lower ventilation rates, the increase in lung volume due to the addition of the tidal volume – dead space was small, resulting in little difference in the values of $\dot{V}/(\dot{V}/V + 3{\cdot}2)$ calculated by the two methods and in little difference between the count rates recorded during inspiration and expiration. At higher ventilation rates, tidal volume – dead space becomes an increasingly higher fraction of lung volume, and the difference between the count rates recorded during inspiration and expiration increases. Thus, using an inspiratory : expiratory ratio of 1 : 2, the number of counts obtained from $^{81}Kr^m$ in the lungs during continuous accumulation was biased towards the measurement of the smaller volume. This finding may be of importance in techniques that involve measurement of high ventilation rates using both $^{81}Kr^m$ images and estimations of $\dot{V}/V$ from wash-out curves (Amis *et al.*, 1978; Spaventi *et al.*, 1978), since $\dot{V}/V$ obtained from wash-out curves refers to a lung volume equal to (FRC + tidal volume – dead space) and the $\dot{V}/V$ in the steady state equation for $^{81}Kr^m$ may not.

The use of $^{81}Kr^m$ images alone for investigating ventilation is limited owing to the non-linear relationship of count rate or count density with either $\dot{V}$ or $\dot{V}/V$. The $^{81}Kr^m$ response is proportional to $\dot{V}/(\dot{V}/V + 3{\cdot}2)$. Thus, except at very low values of $\dot{V}/V$ (< 1) such as may be found in diseased lung, the response never approaches proportionality with $\dot{V}$. In the human, the normal value of $\dot{V}/V$ is approximately half of that in the dog, hence the non-linearity of the relationship between $^{81}Kr^m$ count rate and ventilation $\dot{V}$ up to the normal range of ventilation is probably less pronounced in the human than in the dog. Nevertheless, even in this range, measurements of relative ventilation of the whole lung or of changes in relative regional ventilation under several different physiological conditions can be considered to indicate only the direction of change and not its magnitude. Values of relative regional ventilation in a single image cannot be obtained owing both to the non-linearity of the response of the technique and to the dependence of the count densities in different regions on different camera sensitivities to radioactivity in those regions. Additional measurements, such as those described by Spaventi *et al.* (1978), Amis *et al.* (1978) or Jones (1978) are necessary to obtain more precise data on ventilation from $^{81}Kr^m$ images. As outlined above, care in the use of such techniques may be necessary under certain ventilatory conditions.

A final point should be considered in assessing the usefulness of $^{81}Kr^m$ images in studies of regional ventilation. The distribution of count density in the lung field may also depend on the variation of $^{81}Kr^m$ concentration in the gas taken into the alveoli during inspiration. It has been found in the conscious human that the first part of the breath inhaled from residual volume is distributed preferentially to the upper (non-dependent) part of the lungs (Milic-Emili *et al.*, 1966; Jones *et al.*, 1970; Grant *et al.*, 1974). Therefore, if the inhaled $^{81}Kr^m$ is not of constant concentration, artefacts in count density distribution may occur. Some radioactive decay during inspiration is inevitable but may be of less consequence than the inhalation during the first part of the breath of dead-space gas in which $^{81}Kr^m$ concentration may be only 50% of that in the remainder of the tidal volume. In the dog the dead-space constitutes about 40% of the normal tidal volume. It is less in the human, but its possible effect requires consideration.

CONCLUSION

Using the described breathing circuits and data analysis techniques on whole immobilized lungs, the predicted relative responses of the $^{81}Kr^m$ and $^{13}N_2$ techniques to changes in alveolar ventilation are obtainable, over a wide range in the case of $^{13}N_2$ and over a range of ventilation rates from below

normal to normal in the case of $^{81}Kr^m$. With $^{13}N_2$, measurements of $\dot{V}/V$ in repeated studies of the whole lung and in either a single image or repeated studies of regions of the lung can be expected to give the correct relative values. Measurements of changes in relative $\dot{V}$ in repeated studies can be made with $^{13}N_2$ if the relative volumes being investigated are also measured. Using $^{81}Kr^m$ imaging alone, values of relative regional ventilation in a single image cannot be found, but in repeated studies of the whole lung or of regions, the direction of change in relative ventilation should be obtainable, provided artefacts due to non-constant $^{81}Kr^m$ concentration during inspiration are not introduced. To obtain the magnitude of relative ventilation, measurements in addition to count densities are required. When repeated studies are carried out, whether with $^{81}Kr^m$ or $^{13}N_2$, it is important that there be no movement of the subject between studies.

Measurements of $\dot{V}/V$ using $^{13}N_2$ gamma camera wash-out curves correlated well with those made using $^{13}N_2$ expired gas concentration curves. Good agreement between these $^{13}N_2$ measurements and the values of $\dot{V}/V$ calculated from measured alveolar ventilation, $\dot{V}$, and lung volume (functional residual capacity + tidal volume − anatomical dead space), V, was not obtained; this is considered to be due to errors in the measurements of dead space and functional residual capacity and to non-correction of $^{13}N_2$ data for return of absorbed $^{13}N_2$ from blood to the lungs.

ACKNOWLEDGMENTS

We wish to thank Mr. P. Horlock and Mr. I. A. Watson for supplying the $^{81}Rb/^{81}Kr^m$ generators and Mr. S. C. Choong of the Computer Unit of the Royal Postgraduate Medical School for his assistance in computer programming.

DISCUSSION VI

Chairman: Phillip Hugh-Jones

PHILLIP HUGH-JONES: I didn't quite gather how you measure the dead space and functional residual capacity (FRC) on the animals.

KEITH SYKES: We measured FRC by the helium dilution technique. This increased with tidal volume. We also measured the dead space first by the Bohr and then by the Fowler technique; there were large discrepancies between the two which we are now trying to sort out.

PHILLIP HUGH-JONES: Why I questioned this is that you are using a dead space corrected ventilation per unit volume as your standard and so it is fairly critical.

ROSEMARY ARNOT: Yes indeed.

PHILLIP HUGH-JONES: I think to me the great interest is the curvilinear relation of ventilation ($\dot{V}$) to $^{81}Kr^{m}$ counts. This does seem linear over a useful range but it raises a problem with exercise.

MICHAEL HUGHES: I would like to ask Miss Arnot how she kept the inspired concentration of $^{81}Kr^{m}$ constant unless the bag was emptied with each breath? About the dead space errors: first the gas in the dead space from the previous breath goes preferentially to the apex. That is physiological. The only additional error that you have with $^{81}Kr^{m}$ is the decay that has occurred between one cycle and the next. Normally the oxygen we exhale is re-inhaled with the next breath but nothing happens to it while it is sitting in the dead space. This is not quite the same with $^{81}Kr^{m}$.

ROSEMARY ARNOT: The aim was to achieve constant concentration of $^{81}Kr^{m}$ during each breath. The breaths might vary from each other but during each inspiratory period we think we got constant concentration simply by mixing all ages of gas within the bag and again within the ventilator. When we monitored the concentration there was only about 5% variation during the inspiratory period.

MICHAEL HUGHES: You monitored it over the trachea?

ROSEMARY ARNOT: No, we monitored it just before entering the mouth. We

confirmed your work (with B. J. B. Grant) on the regional distribution of the first part of the breath by looking at the regional distribution of $^{81}Kr^{m}$ using the circuit that I have described and comparing it with the regional distribution of a bolus of $^{81}Kr^{m}$ put into the endotracheal tube at the beginning of each breath. We found a preferential distribution to the upper regions with the bolus.

TERRY JONES: Your relationship of $^{81}Kr^{m}$ counts to theoretical values (Fig. 9–4) does not go through the origin. Do you think that the theory of $^{81}Kr^{m}$ breaks down at very low ventilation rates?

ROSEMARY ARNOT: The reason for its not going through the origin may be a technical error. We plotted the calculated response against the actual counts that we obtained and these had to be processed, corrected for concentration and for the decay of the generator. The calculated expression we plotted it against had to contain calculated measurements including alveolar ventilation and FRC and somewhere between the two there may be room for error. I would expect this to be the case rather than a breakdown in the theoretical equation.

ERVIN KAPLAN: You were using normal animals, but in a clinical situation where, for instance, you are dealing with obstructive pulmonary disease and you have emphysematous areas and bullae in these regions, you may have virtually total decay of the $^{81}Kr^{m}$ at the time of equilibration. Then all you can say about these areas is that the ventilation is so low that the counts which you are getting may be almost undetectable. So this refers back to Terry Jones' comment that the equation may not work at very low ventilatory rates. This will not cause any problems in a clinical situation.

ROSEMARY ARNOT: Of course in the poorly ventilated areas of the lung, because the count rates are so low, statistics are very bad.

Chapter 21

CLINICAL APPLICATIONS OF KRYPTON 81m IN THE ASSESSMENT OF REGIONAL MYOCARDIAL PERFUSION

A. P. Selwyn, R. E. Steiner, J. Clark, M. Raphael and G. Forse

Angina pectoris and acute myocardial infarction are thought to be due to functional disturbances of regional myocardial perfusion in patients with segmental rigid coronary artery stenosis. A dynamic assessment of the distribution of blood flow particularly in relation to the stenotic lesions seen at arteriography may help to rationalize the treatment of angina pectoris and the application of coronary venous bypass graft surgery (CABGS).

The purpose of this paper is to introduce a technique using $^{81}Kr^{m}$ for the dynamic assessment of regional myocardial perfusion in man. The preliminary results are shown, demonstrating the potential of this ultra-short-lived, inert, freely-diffusing indicator.

METHODS

Eighteen patients (all male, aged between 41 and 64 years) were selected for coronary arteriography and left ventricular angiography. All suffered typical anginal chest pain and all had ECG evidence of ischaemic heart disease. These symptoms were disabling and resistent to medical therapy in each patient. Informed consent was obtained in each case.

Ten mg of Diazepam were given intramuscularly 30 minutes before the procedure. A pacing electrode was introduced percutaneously into the right femoral vein and positioned in the right atrium. Selective coronary arteriography and left ventricular angiography were performed via a Seldinger puncture of the right femoral artery and using the Judkins technique.

A number 7 French sheath was introduced into the femoral artery using a guide wire and introducer. This was used to introduce a modified ring catheter (Paulin, 1964). The catheter was heparinized and had a ring diameter approximately equal to the diameter of the aortic root in each patient. The patients were then moved in order to position their chests within the field of the gamma camera (Toshiba GCA 202).

$^{81}Kr^{m}$ was continuously eluted in 5% dextrose from a ^{81}Rb generator and delivered by a constant infusion pump via the ring catheter at between 5 and 10 ml/min into the aortic sinuses. The myocardial activity of $^{81}Kr^{m}$ was recorded on Polaroid or 35 mm film. The camera was rotated in relation to the heart to obtain views in the anterior, left and right oblique positions. Quantitative high spatial resolution images of the total and regional activity of $^{81}Kr^{m}$ in the heart were recorded using a digital computer (Deltron-Nova-1220). The images were recorded on magnetic disc at 30 second intervals throughout each study and corrections were made for the decay of ^{81}Rb.

The total and regional activities of $^{81}Kr^{m}$ in the heart were recorded for 15 minutes during a control period while heart rate, blood pressure and ECG were stable in each patient. Atrial pacing was used to increase heart rate by 10 beats/min at 5 minute intervals. This was continued until the patient complained of chest pain and/or showed ECG changes suggesting myocardial ischaemia.

Atrial pacing was stopped and in seven patients 500 µg of GTN was administered sublingually. Recordings of the $^{81}Kr^{m}$ cardiac scintigrams were acquired for 10 minutes and the catheter was then removed. Haemostasis was ensured by 15 minutes of manual compression.

RESULTS

In four of the 18 patients the ring catheter could not be seated correctly in the aortic sinuses. In a further five patients the myocardial activity of $^{81}Kr^{m}$ was insufficient to record images using the gamma camera.

In nine patients high spatial resolution images of an equilibrium of $^{81}Kr^{m}$ activity in the myocardium was recorded. Figure 21–1 demonstrates the left ventricular angiogram (in the right oblique) at end diastole of a patient who suffered an anterior infarction one year before this study. This shows a large dyskinetic anterior and apical ventricular segment (Fig. 21–1a). The left coronary angiogram demonstrates a blocked left anterior descending coronary artery (LAD) (Fig. 21–1b) and the anterior view of the $^{81}Kr^{m}$ cardiac scintigram shows a large apical defect in perfusion (Fig. 21–1c). This was present at rest, on exercise and following the administration of nitroglycerine.

Figure 21–2 shows four $^{81}Kr^{m}$ cardiac scintigrams from a 46-year-old patient suffering intractable angina. Important stenotic lesions were reported in the proximal third of the LAD and the right main coronary artery. Figure 21–2a shows the myocardial distribution of $^{81}Kr^{m}$ (seen in the left oblique position) in the patient while at rest (heart rate 70/min, blood pressure 160/90 mmHg, V_4 on standard ECG normal). Figure 21–2b shows the

myocardial distribution of $^{81}Kr^{m}$ while the atria were paced at 100/min. The overall changes in the colour ranges indicated a uniform increase in myocardial perfusion. When the atria were paced at 120/min the scintigram showed a defect in activity affecting the anterior portion of the image in the area of distribution of the LAD. This was followed by anginal chest pain and planar ST segment depression in the V_4 ECG (Fig. 21–2c).

Fig. 21–1. (a) Shows the left ventricular angiogram demonstrating anterior and apical dyskinesia. (b) The left coronary arteriogram shows a blocked LAD. (c) The anterior view of the $^{81}Kr^{m}$ scintigram shows an anterior and apical perfusion defect. This patient suffered anterior infarction one year before the study.

The atrial pacing was stopped and nitroglycerine administered sublingually (500 μg). The $^{81}Kr^{m}$ cardiac scintigrams recorded at 30 second intervals showed the disappearance of the regional defect in activity within 2 minutes and a marked increase in activity in the areas surrounding the affected region. This change lasted for 12 minutes and was associated with the relief of chest pain and disappearance of the abnormal ECG changes (Fig. 21–2d).

DISCUSSION

A continuous infusion of $^{81}Kr^{m}$ into the aortic sinuses resulted in an equilibrium count-rate from the myocardial water space. This inert freely

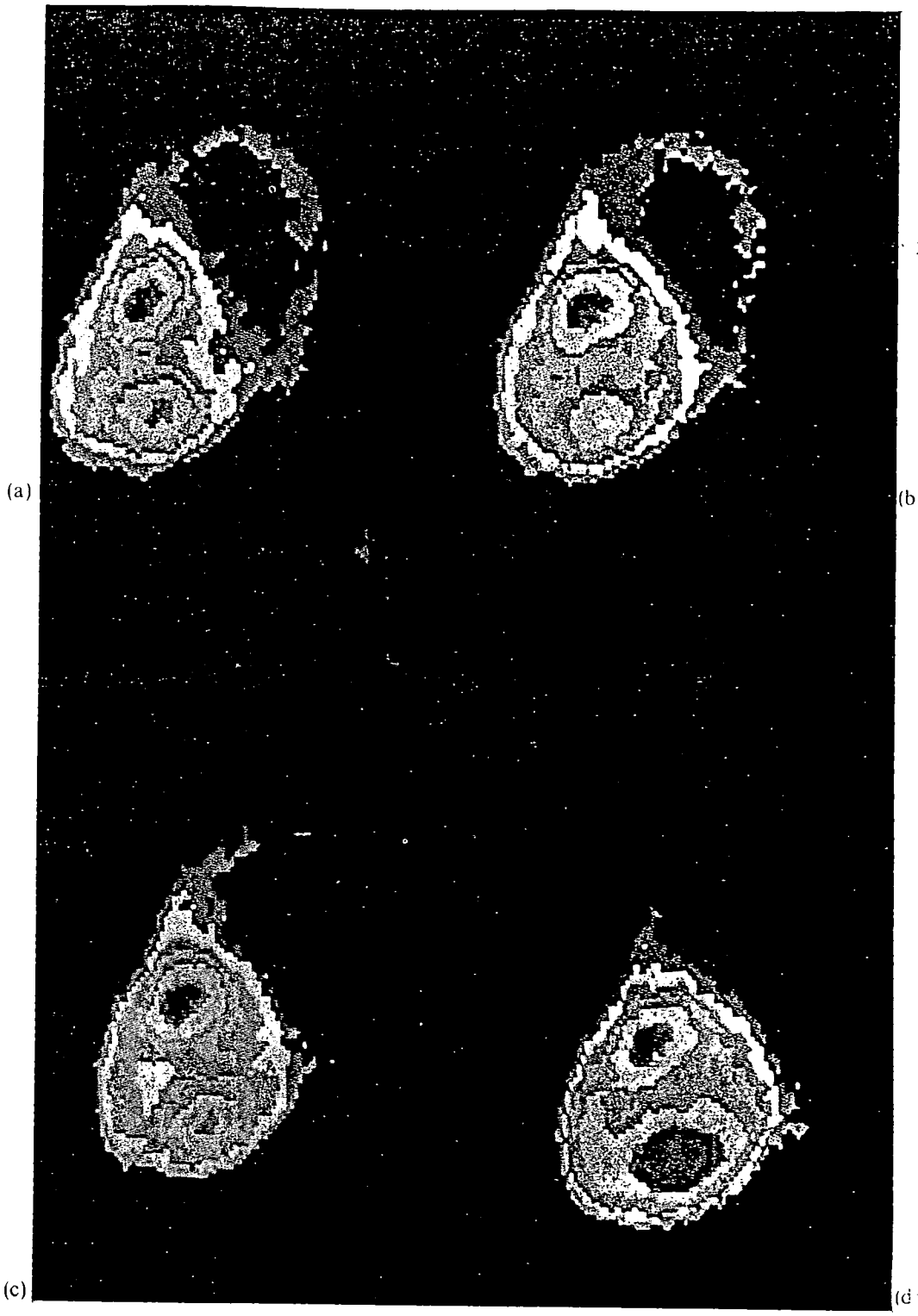

Fig. 21–2. This patient had intractable angina and important stenotic coronary lesions of the LAD and right main coronary artery. (a) $^{81}Kr^{m}$ cardiac scintigram at rest in the left oblique position. (b) Atrial pacing (100/min) produced an overall increase in perfusion. (c) Pacing at 120/min produced pain, ECG change and an anterior defect in perfusion. (d) Atrial pacing was stopped, nitroglycerine given and the regional defect in perfusion disappeared followed by an increase in perfusion in the surrounding area.

diffusing radionuclide emits a single 190 keV gamma ray, ideally suited to high spatial resolution imaging using a gamma camera. The myocardial equilibrium of $^{81}Kr^{m}$ in the heart depends on the arrival of the indicator by blood flow and radioactive decay. Animal studies have shown that moment to moment changes in the regional activity of $^{81}Kr^{m}$ can be used to assess changes in regional myocardial perfusion.

Segmental rigid stenosis of a coronary artery in man interferes with the adaptation of myocardial perfusion necessary to meet the metabolic requirements of working ventricular tissue. Selective coronary arteriography will outline the luminal anatomy of affected vessels. This procedure cannot assess the relative importance of each lesion with respect to the disturbances of blood flow. Techniques using long-lived radionuclides provide information of the situation only at the moment of administration. The singular advantage of $^{81}Kr^{m}$ is that the short half life (13 seconds) allows dynamic studies of right and left coronary circulations and of each coronary venous bypass graft.

This short-lived tracer must, however, be delivered by invasive techniques and is therefore only applicable during angiography or during bypass graft surgery. The geometrical factors relating the heart to a gamma camera are complex and limit the separation of endocardial and epicardial events. Absolute quantitation of myocardial blood flow must assume a stable arterial concentration of the tracer. The ring catheters used in this study were not easily seated in the aortic sinuses, nor did they provide consistently adequate images. Clearly more work is required in order to design a catheter that is easily introduced and reliable when in position.

In conclusion, this preliminary study has shown that a continuous infusion of $^{81}Kr^{m}$ into the aortic sinuses of patients with intractable angina pectoris can provide an assessment of moment-to-moment changes in regional myocardial perfusion. The functional disturbances in myocardial blood flow can be related to the stenotic lesions seen on the angiogram. These dynamic techniques may provide a rational method of investigating the effects of therapies and the application of CABG surgery.